Thermorheological Evaluation of a Bioglass System

By

Eakasit Sritham

A dissertation submitted in partial fulfillment of

the requirements for the degree of

Doctor of Philosophy

(Biological Systems Engineering)

at the

UNIVERSITY OF WISCONSIN-MADISON

2013

Date of final oral examination: February 15, 2013

The dissertation is approved by the following members of the Final Oral Committee:

Sundaram Gunasekaran, Professor, Food Engineering
Roderic S. Lakes, Wisconsin Distinguished Professor, Engineering Physics
Richard W. Hartel, Professor, Food Engineering
Xuejun Pan, Associate Professor, Bioenergy and Bioproducts Engineering
Troy Runge, Assistant Professor, Biomaterials, Bioenergy, Bioprocessing

In Loving Memory of My Beloved Mom and Dad

THERMORHEOLOGICAL EVALUATION OF A BIOGLASS SYSTEM

Eakasit Sritham

Under the supervision of Professor Sundaram Gunasekaran

At the University of Wisconsin-Madison

ABSTRACT

Sucrose and maltodextrin are common ingredients found in various commercial food products. Sucrose can be readily vitrified and has the ability to form hydrogen bonding with different other molecules. Maltodextrin has a higher glass transition temperature (T_g) than sucrose, and it can inhibit crystallization. The aim of this study was to investigate the effect of Na citrate on the properties and behaviors of sucrose-maltodextrin mixture. Thus, amorphous sucrose-maltodextrin-Na citrate systems were prepared and characterized using the modulated differential scanning calorimetry (MDSC), Fourier transform infrared spectroscopy (FTIR), small amplitude oscillatory shear (SAOS) test and scanning electron microscopy (SEM). Samples were formulated with different sucrose/maltodextrin ratios (SC/MD = 7:3, 5:5 and 3:7, by mass), and Na citrate/sucrose ratios (NaCit/SC = 0, 0.1 and 0.2, by mole). Samples in glassy state were studied at two levels of residual moisture content: low (0.27 – 0.35 %wb) and high (2.83 – 4.40 %wb). It was found that moisture and all other components significantly affected glass transition characteristics and enthalpy relaxation behavior of the systems.

On average, glass transition temperatures (T_g) of the systems with SC/MD of 7:3, 5:5 and 3:7 were approximately 77, 84 and 101 °C, respectively. The T_g tended to increase when Na citrate was added, with a noticeable increase in T_g occurring in the system with SC/MD of 7:3 at low-level moisture content. Moisture exhibited a significant plasticization effect lowering the T_g from approximately 106 °C to 67 °C when moisture content increased from low to high level. The DSC data suggested that water molecules may interfere with intermolecular interactions between glass-forming molecules causing changes in molecular mobility of the bioglass matrix. Isothermal aging experiments were carried out on low-moisture samples with the degree of undercooling in a range of approximately 12 – 57 °C and aging times (t_a) of 8, 20, 47 and 71 h. The Kohlrausch-Williams-Watts (KWW) decay function fitted well with enthalpy relaxation data in general. The β values spread over a broad range. The enthalpy relaxation time (τ^{KWW}) and the time required for 50% completion of the theoretical possible maximum enthalpy relaxation at a constant temperature ($t_{\phi(t)=0.5}$) increased with increasing maltodextrin concentration or with decreasing aging temperature (T_a). The greatest apparent activation energy (E_a), and the dramatic increase in τ^{KWW} and $t_{\phi(t)=0.5}$ were observed upon slightly decreasing T_a in the system with highest sucrose and Na citrate concentrations (SC/MD = 7:3 with NaCit/SC = 0.2). These findings suggest that Na citrate modulated the system by primarily interacting with sucrose, possibly forming up large less-mobile clusters, which help improve the T_g and restrict matrix mobility.

Hydrogen bonding interaction in the glass matrices was investigated by analyzing the OH-stretching absorption band in FTIR spectra. There was no noticeable effect of moisture on the FTIR spectra other than the slight shifting down of OH-stretching band. The weak

hydrogen bonding found in the system with high maltodextrin concentration indicates a loosely packed matrix. Although Na citrate could interact with both sucrose and maltodextrin through carboxylic groups, as evidenced by the shifting of $\nu_{as}(COO^{-})$ and $\nu_{s}(COO^{-})$, this salt tended to primarily interact with sucrose. The strongest hydrogen-bonded network was observed in the system with highest concentration of sucrose (SC/MD = 7:3) and Na citrate (NaCit/SC = 0.2).

Rheological data were obtained from samples in the rubbery amorphous state (moisture content of approximately 8.5 – 12.0 %wb). The SAOS tests were conducted in a frequency range of 0.1 – 150 Hz at room temperature. It was found that maltodextrin primarily contributed to the rigidity of the amorphous matrix which is possibly due to the stronger glycosidic linkages as compared to those in sucrose. The system with high sucrose concentration exhibited viscous-dominant relaxation suggesting that the viscoelastic behavior is governed by molecular motions of small molecules—sucrose, and the configurational vibrations of segments. These molecular motions generate heat which dissipates during the sinusoidal deformation. On the other hand, elastic-dominant relaxation was observed in the system with high maltodextrin concentration. Accordingly the viscolelastic nature of this system might be mainly contributed by the stretching and bending of glycosidic linkages in maltodextrin. The downshift of loss peak frequency (f_p) in the system with SC/MD = 7:3 when Na citrate was added indicates the lesser matrix mobility; the higher Na citrate concentration, the lower the molecular mobility. This finding suggested that molecular interaction between Na citrate and sucrose could retard molecular mobility of the bioglass system. The technique was also capable of detecting changes in the molecular process even with a small variation in the matrix composition. SEM images suggested that Na citrate

interfere with molecular interactions in the system with high maltodextrin concentration; such interference made the system more brittle.

ACKNOWLEDGEMENTS

It is with immense gratitude that I acknowledge the guidance, support, encouragement, trust, and persistent help of my advisor, professor Sundaram Gunasekaran. This dissertation would not have been possible without him.

I would like to sincerely acknowledge professor Roderic S. Lakes for his valuable guidance, support, and patience with me during my access to his laboratory.

I also would like to thank professor Richard W. Hartel for his advice and assistance, and for granting me permission to access his laboratory.

I would like to express special thanks to associate professor Xuejun Pan and assistant professor Troy Runge for their valuable time, suggestions, and constructive criticism.

I truly appreciate the assistance and support from the staff at the Department of Biological Systems Engineering, in particular Debby Sumwalt, Harold Bohne, and Bradley A. Brooks.

I would like to thank the Biological and Biomaterials Preparation, Imaging, and Characterization (BBPIC) facility at the University of Wisconsin for the permission to access the SEM facility, and all of the staff for their assistance. The CALS Statistical Consulting Group is also greatly appreciated for their consultancy.

My sincere thanks go to all my Thai friends and colleagues and to my group of Madison friends for having welcomed me into such wonderful and life-long friendships. All of you have made Madison my home away from home.

I owe my deepest gratitude to my family for their support and understanding.

I am greatly indebted to the Ministry of Science and Technology of Thailand for their financial support.

Finally, I would like to express my deepest gratitude to the staffs at the Ministry of Science and Technology of Thailand, the Office of Educational Affairs at the Royal Thai Embassy in Washington, D.C., and the Office of Civil Service Commission of Thailand for their continued direction, support, and understanding.

TABLE OF CONTENTS

LIST OF FIGURES

LIST OF TABLES

CHAPTER 1

INTRODUCTION

1.1 The State of Glass

When a liquid is rapidly cooled the equilibrium crystalline state may be avoid and an amorphous material is obtained. This phenomenon occurs due to an enormous increase in viscosity during the cooling that prevents molecules to rearrange themselves into a crystal lattice. The amorphous material exists as either a high-viscosity supercooled liquid, rubbery or glassy solid, depending on temperature (Elliott et al., 1986; Allen, 1993). The temperature at which a material undergoes the transformation from a rubber to a glass is known as the "glass-transition temperature (T_g)"(Young and Lovell, 1991). Such a process to convert a material into a glassy solid without any crystalline structure is also known as vitrification. A significantly reduced molecular mobility in the glassy state leads to its relative stability against crystallization while the rubbery state is considerably physically unstable (Roos, 1995). The molecular disorder of a glass is characteristic of its liquid state. Glassy materials are strong, brittle, and transparent; they become progressively soft, flexible and pliable when heated. Molecular motions remaining in glass are only vibrational and limited rotational.

Rubbery solids and supercooled liquids exhibit macroscopic flow due to the onset of translational motion (Zallen, 1983). In polymer systems, a general rule is that cross-linked amorphous polymers exhibit rubber elasticity while linear amorphous polymers exhibit flow at temperatures above T_g (Sperling, 1986).

A number of methods may be used to produce amorphous materials (Elliott et al., 1986; Angell, 1995). The location of T_g is dependent on the rate of cooling. Cooling at slower rate leads to lower T_g and a more dense glass. However, the density of glassy materials is slightly lower than crystalline form due to molecular packing in the glassy state is less efficient (Allen, 1993). Various properties of glassy materials depend on temperature and time since they are thermodynamically nonequilibrium. They possess more free energy and entropy compared to their crystalline counterparts at the same temperature and pressure conditions (Sperling, 1986).

Food material like sugars can be readily vitrified upon cooling their concentrated solutions. It is however important to note that the physical behavior of foods may differ from that of polymers (Roos, 1995). Amorphous sugar systems are capable of preserving seeds, spores and living organisms under extreme conditions (Crowe et al., 2001; Buitink and Leprince, 2004). Sugars and some other carbohydrates in the glassy state also help modulate the stability of dry and frozen food and pharmaceutical products (Roos, 1995). The potential of amorphous sugars in protecting biomaterials, in particular labile compounds such as vitamins, flavors, enzymes and other proteins has caught much of attention from researchers.

1.1.1 Significance of glass transition and the state of amorphous

The primary interest in the study of glass transition and amorphous materials may differ among disciplines. Among other issues, polymer scientists are concerned about physical aging since this phenomenon can adversely affect properties and applications of polymers. As for examples, the design, manufacture, and performance of polymer-based composites, automotive applications, adhesive, permeability of packaging materials, curing of graphic film supports (Hodge, 1995; Angell, 1997). Metallurgists focus on properties of metallic glass, for example, very high flow stress, wear and corrosion resistance, and magnetism, which provided variety of engineering applications (Greer, 1995). The excellent protective property of amorphous trehalose in dry state has caught much attention from biologists (Aldous et al., 1995; Crowe et al., 1996; Crowe et al., 1998; Crowe et al., 2001).

Certain behaviors of amorphous foods, pharmaceutical materials, polymers, ceramics, semiconductors, optical glasses and other engineering materials are common. The relaxation time of molecular or ionic constituents of a supercooled liquid can increase in non-Arrhenius fashion by many orders of magnitude within a narrow range of temperature upon cooling. Matters in this state exhibit non-exponential response to an external perturbation (Bohmer et al., 1993; Angell, 1995). In the region near T_g or sub-T_g, the structure of this materials evolves toward the equilibrium on a very long time scale and this is referred to as the so-called “nonlinearity of relaxation.” The nonlinear nature arises from the coupling between thermodynamic and dynamic properties (Angell, 1995; Hodge, 1995). The step change in a specific heat capacity in the glass transition region is another common feature of amorphous materials (Bohmer et al., 1993).

However, food products generally contain a number of ingredients which give rise to the heterogeneity in their chemical compositions and structure. In supercooled state, the effects of heterogeneity on different modes of diffusion, particularly when the temperature is lowered toward T_g, have been reported (Cicerone and Ediger, 1996). Besides, water which prevails in foods plays a prominent role as a plasticizer by increasing the free volume (or the defect concentration) between glass forming molecules (Chan et al., 1986; Champion et al., 2000). Hence predicting the diffusion behavior of amorphous foods becomes very problematic due to numerous variables which could affect its transport properties.

Transport property of amorphous food materials is prime important in a number of applications. These include, for example, encapsulating labile compounds to prevent loss during processing and storage (Schrooyen et al., 2001), or freeze-drying emulsion within an amorphous matrix to inhibit lipid oxidation (Gejl-Hansen and Flink, 1977). Rheological or mechanical properties are also critical for manufacturability (e.g., in extrusion cooking) and stability of amorphous food products. The knowledge of strong/fragile behavior of materials could practically benefit the extrusion, puffing or flaking of products. There has been evidenced that molecular mobility exists at temperatures below T_g, and hence T_g cannot be considered as the sole measure of stability of food products in glassy state. The kinetics of relaxation behavior at temperatures below T_g is fundamental for predicting the loss of stability, which leads to unacceptable textural quality in low-moisture food products (Champion et al., 2000).

1.1.2 The challenge

Questions and unsolved problems about glass transition of matters have arisen since scientists discovered this phenomenon. There has been a lot of effort in search of the answers (Angell, 1996). Even though glass transition has a long and rich history of study and some common properties of glasses are well documented (Angell, 1995; Slade and Levine, 1995; Angell, 1996), the universally acceptable theory that is supported by all evidences from observations and experiments is not yet firmly established (Ediger et al., 1996). The famous quote by Anderson has long been valid until this day:

> "*The deepest and most interesting unsolved problem in solid-state theory is probably the theory of the nature of glass and the glass transition*" (Anderson, 1995).

Besides, new questions continually arise from observations in certain amorphous systems. For instance, why diffusion has a weaker temperature dependence than viscosity or relaxation time τ_α? (Mapes et al., 2006), and why crystals grow too fast in some classes of glass? (Sun et al., 2008). This is why the study of glass transition and amorphous materials is still active, exciting, and, of course, worth pursuing.

Like many other amorphous systems, carbohydrate glass possesses excellent protective property which makes them attractive for numerous food applications. However, materials in the amorphous state are thermodynamically out-of-equilibrium. Their properties change toward equilibrium with time, generally known as "aging". Food technologists are then challenged as how to formulate amorphous carbohydrate with desirable functional properties for the designated applications, and substantial degree of stability. Of course, the knowledge about characteristics and parameters that could affect the formulated system is fundamentally indispensable. The use of T_g as a reference temperature for predicting the rate

of diffusion-controlled process was found to be relevant (Champion et al., 2000), even though not exclusively since certain reactions can still take place at temperatures below T_g (Hancock and Zografi, 1997). The concept of fragility (Bohmer et al., 1993; Hodge, 1996) could be also benefit to process control. However, the time- and temperature-dependent dynamic behavior of any amorphous system is not simple and need to be thoroughly characterized. The complication arises from two reasons: first, the nonlinearity which refers to the change of characteristics respect to time and structure of the glass; and second, the non-exponentiality which refers to the dispersion (or distribution) of relaxation times due to microstructural heterogeneities. It is this non-exponentiality behavior that makes the description using a single relaxation function inadequate (Hodge, 1996; Champion et al., 2000). Although a large dispersion of relaxation time is often found in foods, not much consideration has been placed on it (Champion et al., 2000). Besides, more experimental data of different materials are always needed to bring the theoretical advance into practical usefulness in food technology. In the light of the advancement in innovative scientific techniques, we expect to contribute further to the understanding of some properties and viscoelastic behaviors of the selected carbohydrate system in its glassy state.

1.1.3 Purpose of study and specific objectives

The mechanisms that are responsible for stabilizing biomaterials in amorphous matrix include vitrification and direct interaction (Crowe et al., 1998). Accordingly the desirable protective amorphous matrix in this regard should be highly stable and has the ability to bind with labile/sensitive molecules being protected or encapsulated.

Among glass-forming food materials, sucrose can be readily prepared as amorphous matrix. The primary flavor function of sucrose is generally to sweeten foods. Sucrose also influences the flavor of foods in several ways. The addition of sucrose in small amount below the sweet detection level could improve overall flavor in many types of food products. Interactions between sucrose and some basic tastes including bitter, acid, and salty could suppress these tastes resulting in the smoother flavor of foods. Also, many model studies have shown that sucrose is effective in retaining aromas of dehydrated foods (Godshall, 1995). Sucrose is able to form hydrogen bonds with polymers to a greater extent than other sugars having a higher T_g. This ability of sucrose could be of prime importance for the stabilization of polymers in amorphous sucrose matrix (Taylor and Zografi, 1998; Wolkers et al., 1998; Davidson and Sun, 2001).

The utilization of sugar glasses as an encapsulation matrix could be enhanced by mixing with larger biomolecules such as maltodextrin; this combination could also contribute to certain desirable characteristics. In spray drying, for example, an ideal carrier should have a high degree of solubility, limited viscosity at 30-45% solid content, emulsifying characteristics, good drying properties, bland taste, and non reactivity. Maltodextrin serves well for these purposes (Desobry et al., 1999; Galmarini et al., 2008). In addition, maltodextrin has proven to inhibit crystallization in amorphous sucrose matrix and provide good product stability to dry powder products (Bhandari and Hartel, 2005). It was also found that glasses which is formulated from the mixtures of sucrose and maltodextrin exhibit stronger hydrogen bonding than pure sucrose glasses (Oldenhof et al., 2005). Other interesting functional properties of maltodextrin are the ability to bind flavors and fat, and to

serve as oxygen barrier (Chronakis, 1998). From economic stand point, both sucrose and maltodextrin are considerably cheap and substantially available.

Other than mixing with larger biomolecules, the stability of an amorphous sugar matrix could also be enhanced by the inclusion of small amount of salt. Salts can inhibit crystallization by altering molecular interactions and reducing molecular mobility (Izutsu and Aoyagi, 2005). The result from a sucrose crystallization study suggested that the presence of salts constrained the number of configurations for crystal growth. This could be attributed to the effects of salt on the nucleation mechanism of ion-induced microheterogeneities in the supercooled solutions. It was also found that the crystallization was delayed without affecting the T_g of the system (Longinotti et al., 2002). As a result it was proposed that the salt effect on sucrose crystallization occurs at a molecular level, but in such a dynamic way that the cooperative relaxations that give rise to glass transitions are not affected (Buera et al., 2005). However, for dried glassy amorphous sodium indomethacin, it was reported that the T_g was 121 °C which is around 75 °C higher than that for the glassy indomethacin but the enthalpy relaxation patterns at the same degree of supercooling relative to T_g were similar (Tong and Zografi, 1999). Some recent studies reported the potential of salts to enhance the stability of sugar glasses when residual moisture was less than 2%. It was suggested that the mechanisms that help improve matrix stability are interactions between either ions (You and Ludescher, 2008b) or the functional groups (Kets et al., 2004) of salts and sugar molecules. Na citrate is among salts that has caught much of interest from researchers. This type of salts has been widely used in food products for a number of purposes.

In the light of all evidences found in literature as given above, sucrose, maltodextrin and Na citrate appear to be potential candidates to utilize as amorphous matrix components

for various applications in foods. However efficient formulation and process control would be made possible only after the characteristics and behaviors of the mixture have been thoroughly investigated. This study was aimed at gaining better understanding of the molecular mobility in glassy sucrose-maltodextrin-Na citrate mixture. It was interesting how salt will influence properties and behaviors of the system.

Based on all relevant evidences, we hypothesized that the inclusion of Na citrate into amorphous sucrose-maltodextrin mixture at low moisture content would alter the molecular structure of the system. Na citrate which contains a number of binding sites would make the system more compact and less mobile. To test this hypothesis, aging experiments were carried out to observe a long-term stability of amorphous sucrose-maltodextrin-Na citrate in sub-T_g region. The calorimetric measurements were performed using the modulated differential scanning calorimeter (MDSC) to observe glass transition and enthalpy relaxation. Molecular interactions within the system were investigated using the Fourier transform infrared spectroscopy (FTIR). Molecular mobility was also observed from mechanical relaxation. A dynamic Bohlin C-VOR rheometer was employed to obtain rheological data and mechanical relaxation behavior. Rheological measurements was expected to provide overall viscoelastic behavior of the system in which dynamic heterogeneity prevails over glass matrix as a result of incorporating salt into the system (You and Ludescher, 2008b). Transport properties of amorphous matrix are closely related to its viscosity (or relaxation time). It is these properties that govern the diffusion-controlled processes (Hachisuka et al., 1991). Accordingly parameters obtained with rheological measurements would provide meaningful information as an indication of the stability of the system. In addition,

microstructural aspects of the glass matrix were also studied using the scanning electron microscopy (SEM). The specific objectives include:

Objective 1: Characterize thermal, rheological and microstructural properties as well as molecular interaction of amorphous sucrose-maltodextrin-Na citrate system,

Objective 2: Identify the effects of sucrose, maltodextrin, Na citrate, and residual moisture content on properties, behaviors, and microstructural characteristics of the system, and

Objective 3: Investigate the effect of aging conditions on molecular mobility of the system.

1.2 Review of Literature

1.2.1 Components of the bioglass model system

Experimental treatments of the bioglass model system were formulated from sucrose, maltodextrin, and sodium citrate (for some treatments). Brief information about the selected glass forming materials is given as follows.

1.2.1.1 Sucrose

Sucrose, also know as table sugar, is a disaccharide—a compound in which two monosaccharide units are joined by a glycosidic linkage. In sucrose, one glucose molecule is linked by the 1→2-α,β-glycosidic bond to one fructose molecule (Campbell and Farrell, 2006). According to the International Union of Pure and Applied Chemistry-International Union of Biochemistry (IUPAC-IUB) Commission on Biochemical nomenclature, sucrose is systematically named as α-D-glucopyranosyl-(1→2)-β-D-fructofuranoside with the moelcular formula of $C_{12}H_{22}O_{11}$ and the structural formula as illustrated in Figure 1.1 (Perez, 1995).

A disaccharide can be classified as either reducing or non-reducing. A reducing sugar either has an aldehyde group or is capable of forming one in the solution through isomerism. The aldehyde functional group allows sugar to act as a reducing agent. In the formation of sucrose, the reducing groups of both glucose and fructose molecules are mutually engaged in glycosidic linkage. Since there is no reducing group available, sucrose is classified as a non-reducing sugar (Stacey and Barker, 1960; Perez, 1995). A sucrose molecule contains eight

alcohols groups, three of which are hydroxyls at the primary positions (–CH_2OH) and the remaining five at the secondary positions (–CHOH–). Due to the more exposed positions on D-glucopyranosyl and D-fructofuranoside rings, the hydroxyls at primary positions are of higher reactivity than those at the secondary positions (Kollonitsch, 1970; Hough, 1971).

Sucrose is usually extracted from sugarcane or sugar beets. The primary flavor function of sucrose in foods is as a sweetener. Sucrose also possesses many other characteristics which are important in food manufacture, e.g., increasing sweetness, osmotic pressure, viscosity, boiling point and moisture retention, and enhancing flavour and appearance (Brook, 1971). Some other characteristics, properties and its applications can be found elsewhere (Brook, 1971; Clarke, 1995; Godshall, 1995; Khan, 1995)

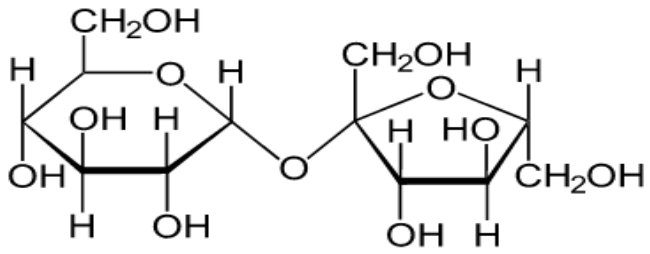

Figure 1.1 The structural formula of sucrose.

Source: http://en.wikipedia.org/wiki/File:Sucrose-inkscape.svg

1.2.1.2 Maltodextrin

Starch can be hydrolysed or digested by different means into numerous products which are described in terms of dextrose equivalent (DE) value. This value is a measure of the total reducing power of all sugars present relative to glucose as 100, based on dry basis,

i.e., 5 DE refers to a 100 g of sample having the same reducing activity as 5 g of glucose. The higher the DE value the greater the degree of starch hydrolysis. Maltodextrins are products from starch hydrolysis with the DE value lower than 20 (the term syrup solids or dextrins is used for DE value higher than 20). They are polymers of D-glucose units primarily linked by the α(1→4) glycosidic bonds. The basic chemical structure of Maltodextrin is illustrated in Figure 1.2. They contain both linear amylose and branched amylopectin degradation products, and hence incorporating a spectrum of saccharides with a broad molecular weight distribution. The ratio of linear amylose chain molecules to branched amylopectin varies depending on the source of starch. Most of starches contain 15% – 35% of amylose. Maltodextrins are of bland flavor and exhibit low viscosity in solution even at high concentrations (Chronakis, 1998; Desobry et al., 1999).

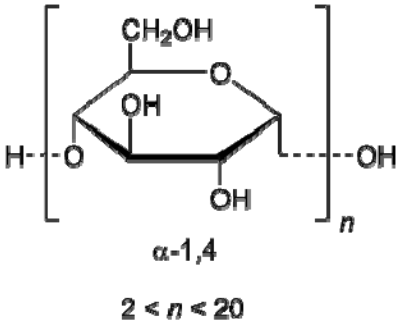

Figure 1.2 D-Glucose unit—a building block of maltodextrin.

Source: http://en.wikipedia.org/wiki/File:Maltodextrin.png

Maltodextrins provide many desirable functions in food systems including bulking, providing resistance to caking, adding texture and body, forming film, binding flavor and fat, substituting for fat, serving as an oxygen barrier, giving surface sheen, aiding dispersibility

and solubility, freezing control and preventing crystallization. They are also helpful in reducing Maillard reaction. The excellent matrix forming property allows them to be used as a major constituent of coating material for microencapsulation of food components such as fat and oil, vitamins, minerals and colorants (Chronakis, 1998). Previous study has found that maltodextrin with DE values between 10 – 20 could be satisfactorily utilized as wall material for flavor encapsulation (Raja et al., 1989). However, the stability of microencapsulation using maltodextrin-based coating could vary depending on the composition of coating or wall material as well as the species of encapsulated entities (Desobry et al., 1999; Galmarini et al., 2008).

1.2.2 Concept of the glass transition

At temperatures below melting point, liquids are in an equilibrium state known as supercooled liquids. A supercooled liquid can be frozen when cooled below its T_g. The state of a supercooled liquid at temperatures just above T_g is called "rubbery" due to its rubber-like character. The event in which a supercooled liquid, specifically in rubbery state, is transformed to a solid-like liquid (or glass), or vice-versa, is known as glass transition. The phenomenon of glass transition is a kinetic event, not a phase transition. It depends upon the crossing of the experimental and the molecular rearrangement time scales (Ediger et al., 1996; Champion et al., 2000). The formation of glass involves the transition in the rate of translational, rotational and vibrational molecular mobility. There are many routes by which amorphous glassy state can be induced, e.g., solid-state diffusion-controlled reaction, *in situ* liquid polymerization reaction, solvent evaporation, cold electrochemical deposition,

hydrolysis of precursor organics and drying, supercooling of melt, vapor deposition, cold compression of crystal, or shock, irradiation, or intense grinding, treatments of crystal (Angell, 1995).

A typical semi-log plot of viscosity vs. temperature that covers glass transition region generally shows two approximately linear sub-regions of different slopes, on glass and liquid sides. The intersection of these lines is designated as a "glass transition temperature" (T_g). There have been also attempts to analyze the glass transition from thermodynamics stand point. Basically for the first-order transition like melting, fundamental thermodynamic properties such as enthalpy (H) or volume (V) will undergo abrupt change. In the second-order transition, only changes of heat capacity (C_p) and volume thermal expansion coefficient (∞) present (Young and Lovell, 1991). These two properties are the first derivative of H and V, respectively, and defined as:

$$C_p = \left(\frac{\partial H}{\partial T}\right)_p \qquad \text{and} \qquad \infty = \frac{1}{V}\left(\frac{\partial V}{\partial T}\right)_p .$$

Since both these properties change abruptly at T_g, some authors consider this phenomenon a second-order thermodynamic transition (Allen, 1993). However, thermodynamic measurements have shown that the glass transition cannot be definitely considered as a thermodynamic event (Young and Lovell, 1991).

Figure 1.3 depicts the schematic variation of enthalpy (H) and specific volume (V) with temperature (Hancock and Zografi, 1997). Upon rapid cooling, H and V of melt follow the equilibrium pathway of liquid into the region of supercooled liquid. The supercooled

liquid has the structural characteristics of a liquid but with much higher viscosity, in the order between 10^{-3} and 10^{12} Pa.s. An average time scale of molecular motions within a supercooled liquid is generally less than 100 s. Since there is no discontinuity of H and V between the liquid and the supercooled regions, the supercooled liquid is considered as an equilibrium state. Further rapid cooling beyond T_g, leads to a change of rate at which H and V change with temperature yielding an out-of-equilibrium glassy amorphous state of higher H and V compared to its crystalline counterpart.

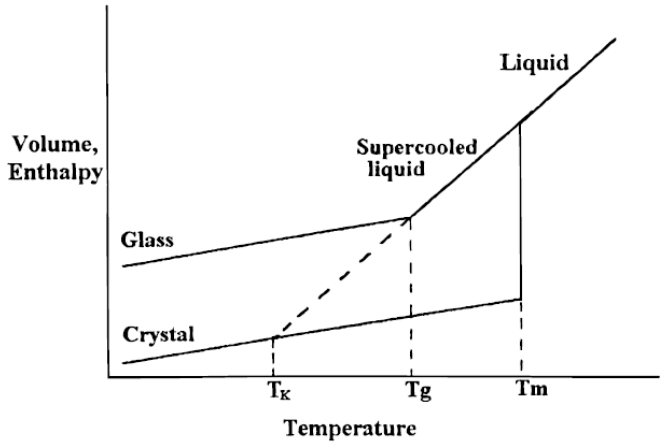

Figure 1.3 Schematic representing the temperature dependence of enthalpy (or volume) (Hancock and Zografi, 1997).

According to Figure 1.3, if the equilibrium line of liquid is extended toward that of crystal, the temperature at which these lines intersect is thought to be a lower limit of experimental T_g, also known as the critical Kauzmann temperature (T_k). At this point it is considered that configurational entropy of the system drops to zero (Ediger et al., 1996). Note that the configuration entropy is the part of entropy due to configurational rather

vibrational degrees of freedom and is equal to the difference between entropy of the supercooled liquid and that of the crystal (Ediger et al., 1996).

While the crystal state is conventionally regarded as the equilibrium state below T_m, the supercooled liquid and glassy state are respectively considered as metastable and unstable (Ediger et al., 1996). The mechanical behavior of supercooled liquid is similar to that of viscoelastic rubber of polymeric materials, and like viscous liquid of low molecular weight materials. Materials in glassy state are more like brittle solid with storage modulus of typically around 10^9 Pa (Champion et al., 2000). Morphologically, the states of rubbery and glassy are collectively called amorphous. The amorphous form is quite common for certain classes of materials including polymeric molecules, large peptides and proteins, and some small organic and inorganic molecules. Unlike crystalline state, the three-dimensional long range of molecular order does not exist in amorphous. The positions of molecules in amorphous matrix are random with the presence of only short-range order (Hancock and Zografi, 1997; Yu, 2001).

The average molecular motions of over 100 s and the viscosity greater than 10^{12} Pa.s are typical in glasses (Angell, 1995). The experimentally observed T_g of any particular system generally varies with several factors, for example, experimental conditions, sample history, sample geometry, and the choice of techniques used. The sensitivities of measurement techniques are dependent on types and speed of molecular motions (Hancock and Zografi, 1997). Even with the same technique, the different T_g values may be observed depending on how the experimental data are analyzed. For instance the T_g value obtained with DSC depends on the definition of T_g - onset, midpoint, or endpoint (offset) (Meste et al., 2002). Accordingly glass transition should be characterized by at least two parameters

indicating the onset or the midpoint and the width of the transition. Also reporting the experimental conditions along with the observed T_g values would make the data more comprehensive (Champion et al., 2000).

1.2.3 Glass transition theories

As theoretical understanding of glass transition is still unclear, a number of theories have been developed to describe the molecular basis of this phenomenon. These include, for example, the free-volume theory (Ferry, 1980), the mode-coupling theory (Ngai et al., 1991; Ngai, 1993), the entropy-controlled cooperative motion (Adam and Gibbs, 1965) and the hierarchical correlated molecular motion (Perez, 1994). Some other theories were reviewed elsewhere (Mansfield, 1993; Ediger et al., 1996; Champion et al., 2000). Of these, the free-volume theory is one of the most useful approaches to analyze glass transition. The concept of free-volume theory was initially applied for the analysis of liquid. Later it was extended to describe the glass transition in polymers. Free volume is basically the empty space in a material and conveniently talked about in terms of fractional free volume, relative to the whole volume of the material. The free volume is supposed to be high in liquid state and so molecular motions can take place easily. A reduction in temperature of a system could lead to two consequences. Firstly, the available thermal energy for molecular motion is lessened; and, secondly, the free volume is reduced. As the temperature is lowered, the free volume will keep continually reduced and eventually there is not enough free volume for the molecular rotation or translation to take place. The temperature corresponding to this point is assigned to as the T_g (Young and Lovell, 1991).

1.2.4 Relaxations process

Relaxation is a recovering process of a material to return to its equilibrium conditions after subjected to perturbation. The process is usually characterized by a relaxation time (τ) or characteristic time of mobility. The relaxation time is defined as the time required for the recovery of equilibrium after perturbation of one property of the material. The sensitivity of relaxation process to temperature is characterized by the apparent activation energy (E_a). The magnitude of E_a reflects the degree of cooperativity of molecular motions. It is believed that glass transition relates to the primary or α-relaxation process of material (Champion et al., 2000). This process is highly cooperative and complex with the E_a value greater than the chemical bond energy (Starkweather, 1988). On the other hand, the transitions at lower temperatures are much less cooperative or even non-cooperative. The lower magnitude of E_a implies that these transitions are very localized (Starkweather and Avakian, 1989; Kalichevsky et al., 1993)

1.2.5 Molecular mobility of amorphous materials

In the context of stability of food products, the term molecular mobility encompasses a number of different types of motions. These include, for example, molecular displacement or deformation, migration of solvent or solute molecules, molecular diffusion, and the rotation of atoms, groups or polymeric branches around covalent bonds (Roudaut et al., 2004).

The kinetics of molecular motions of amorphous matrices could be totally different depending on the state of the matrices—rubbery or glassy. The familiar Arrhenius kinetics

applies only for amorphous materials in the glassy state ($T < T_g$). In the region from melting temperature (T_m) to T_g where the materials are in the supercooled or rubbery state, the kinetics completely changes (see Figure 1.4). Theoretical aspects of molecular kinetics in the region around T_g for amorphous materials are provided as follows.

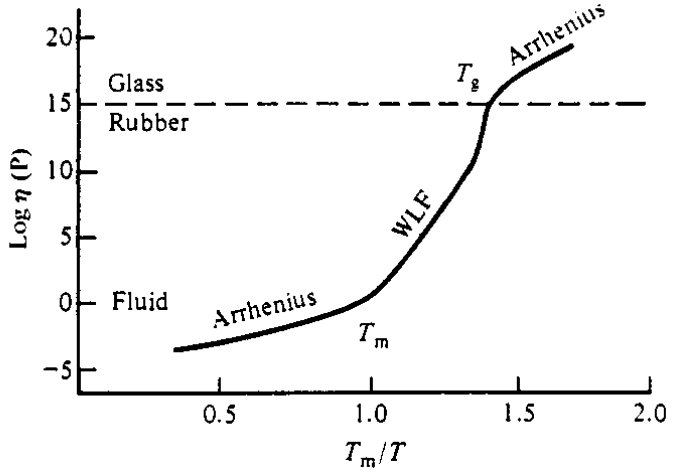

Figure 1.4 Viscosity of glassy and partially crystalline polymers as a function of reduced temperature (T_m/T) (Slade and Levine, 1988).

1.2.5.1 Mobility above glass transition

At the temperature well above T_g, there is enough free volume so that molecules or structural units can move independently from each other. Accordingly the apparent activation energy (E_a) only corresponds to the minimum interaction energy between units, and is independent of the temperature. In a supercooled melt, there is a higher level of interaction energy which induces the cooperative motions of molecules. The E_a is now under the influence of the variation of free volume and the intermolecular interactions with temperature. As a result the temperature dependence is no longer being accurately described

using Arrhenius law. The value of E_a has been reported in the range of approximately 200-500 kJ/mol. E_a increases as the temperature decreases toward T_g (Champion et al., 2000; Meste et al., 2002; Roudaut et al., 2004).

In 1955, William, Landel and Ferry proposed the non-Arrhenius empirical equation (WLF) to describe the effect of increasing temperature (T) on viscosity (η) or relaxation time (τ) in glass-forming systems. This equation is based on the free volume theory and applicable in the temperature region between T_g and T_g +100. It has a form of:

$$\log a_T = \log \frac{\eta(T)}{\eta(T)_{ref}} = \log \frac{\tau(T)}{\tau(T)_{ref}} = -\left[\frac{C_1\left(T - T_{ref}\right)}{C_2 + \left(T - T_{ref}\right)} \right] \qquad (1.1)$$

where a_T is called the shift factor, C_1 and C_2 are constants, and T_{ref} is a reference temperature. The universal values of the constants C_1 and C_2 for polymers are 17.4 and 51.6 K, respectively (Williams et al., 1955). However these constants may fluctuate around those universal values (Ferry, 1980). The T_g is normally used as a reference temperature in the study of glass transition (Slade and Levine, 1988; Angell, 1997). Note here that, the viscosity η is connected to the shear relaxation time τ_s through Maxwell equation:

$$\eta = G_\infty \tau_s \qquad (1.2)$$

where G_∞ is high frequency shear modulus having only a weak temperature dependence (Angell, 1997).

Another expression that is often used to describe the temperature dependence of amorphous material in the region above its T_g was derived from the entropy-based theory. The theory proposed by Adam and Gibbs (Adam and Gibbs, 1965) is one of those and provides a good foundation for treating nonlinearity (Hodge, 1987). By assuming hyperbolic relation between the configurational heat capacity (C_P) and temperature (T), the heuristic nonlinear Adam-Gibbs equation could be obtained as follows:

$$\tau = \tau_0 \exp\left(\frac{B}{T\left(T - T_K / T_f\right)}\right) \tag{1.3}$$

where τ is the characteristic or relaxation time, and B and τ_0 are constants. This equation is frequently used to describe nonlinear relaxation of both polymeric and non-polymeric materials below their T_g (Mao et al., 2006). At equilibrium state above T_g, the material is considered to be in equilibrium liquid state where $T_f = T$, then Eq. 1.3 simplifies to the well-known Vogel-Tammann-Fulcher (VTF) equation. Originally, this equation was empirically obtained from the observed non-Arrhenius behavior of liquid viscosity at the region of temperatures close to the T_g (Mao et al., 2006). Later it was extended to express the molecular relaxation process (Liu et al., 2006). The VTF has the form of:

$$\tau = \tau_0 \exp\left(\frac{B}{T - T_\infty}\right) \tag{1.4}$$

with $T_\infty = T_K$ (Hodge, 1986; Hodge, 1987; Hodge, 1995; Angell, 1996). Note that, if $T_\infty = 0$, then the VTF equation reduces to the Arrhenius equation. When $T_\infty > 0$, the temperature

dependence is non-Arrhenius and the predicted relaxation time becomes infinite at T_∞. The WLF equation normally applied in polymer studies is mathematically equivalent to the VTF equation and is in fact a special case of the VTF equation (Ediger et al., 1996; Hancock and Zografi, 1997).

1.2.5.2 Mobility below glass transition

Glass matrices generally encompass both dense and less dense regions. In literature, the less dense regions may be referred to as defects, heterogeneities, or density fluctuations. These are the locations in a glass matrix where localized motions of the polymers or translational motions of small molecules occur (Roudaut et al., 2004).

From thermodynamic view point, they are the excess entropy and enthalpy frozen-in during glass formation that give rise to molecular motions at the temperature below T_g (Shamblin et al., 1999). The cooperative long range molecular motions of an amorphous material in this temperature region are however restricted. The motions which still exist are mainly local, not involve the surrounding atoms or molecules (Meste et al., 2002). The temperature dependence of the motions is less extreme than above T_g and tends to follow the Arrhenius kinetic. The extent of departure from equilibrium is determined by the conditions at which the glass was formed. As a result the molecular motions in this region are highly dependent on the glass forming process (Hancock and Zografi, 1997).

There are several sub-T_g relaxation processes that can be observed in biopolymers and low molecular weight sugar glass systems. Mechanical or impedance spectroscopies are the two common measurement techniques for observing the processes. They are known as β and γ, named according to their position relative to the primary or α-relaxation. They present

with a low amplitude and cooperativity than that of the α-relaxation process (Champion et al., 2000). However, the secondary or β-relaxation is the only one that has been extensively studied. The origin of β-relaxation process is still unclear and has been widely discussed. Some researchers believe that it may involve the localized high-volume, high-entropy regions within a glass matrix (Chan et al., 1986). In glassy sugar systems, it is related to the motions of -OH group. It has also been reported that β-relaxation could be due to the rotation of the whole molecule of sugar since the relaxation is sensitive to the molecular structure of the system (Champion et al., 2000). The study of sorbitol and maltitol over a wide range of time-temperature suggested that the important part of β-relaxation is probably associated to the intermolecular interactions (Faivre et al., 1999). It was found that the structure of glass-forming molecules could affect the temperature at which β-relaxation occurs (Noel et al., 2000). The β-relaxation process of biopolymers and low molecular weight sugars has been reported with E_a values in the range of 40-70 kJ/mole (Chan et al., 1986; Noel et al., 1996; Noel et al., 2000; Meste et al., 2002) which is considerably lower than that of the primary or α-relaxation at the glass transition (Noel et al., 2000).

In glass transition studies, much interest has been placed on the structural or α-relaxation. It is believed that α-relaxation is associated with glass transition. However, there is also a special class of secondary relaxations that has various properties bearing strong connection with the α-relaxation, and hence the glass transition. This class of relaxations does not involve intramolecular degree of freedom. It originates from local motions of the entire molecules in small molecules system, or local motions of the entire repeat units in polymers system. In fact this class of relaxations presents in all kinds of glass forming

materials. To honor the researchers for their significant discovery and to distinguish from trivial secondary relaxations that possess no connection to the α-relaxation, this special class of relaxations is then named the Johari-Goldstein (JG) β-relaxation (Johari and Goldstein, 1970; Kessairi et al., 2008; Roland, 2010; Capaccioli et al., 2012).

1.2.6 Structural relaxation of glass

When a glassy material is stored at a temperature under its T_g (particularly between T_β and T_g), the remaining molecular motions in the matrix could result in a phenomenon that the microstructure evolves towards the metastable equilibrium over time. The phenomenon occurs with some loss in enthalpy, entropy and volume. This microstructural evolution is also known as the "enthalpy relaxation," "structural relaxation," or "physical aging" (Meste et al., 2002; Liu et al., 2006). The term physical aging was first introduced by Struik (Struik, 1978) and could be regarded as the continuation of α-relaxation (Champion et al., 2000).

The terminologies of structural relaxation are varied among disciplines. The process is known as "annealing" when it occurs by design and "aging" when the occurrence is unwanted. It is preferable in the glass industries and frequently referred to as "stabilization" (Angell, 1995). In inorganic glass literature, it is traditionally referred to as "structural relaxation." This process is generally undesirable for polymers due to its adverse effects on various applications and hence referred to as "aging" (Hodge, 1995). No matter what it is called or referred to, this process reveals that molecular motions do occur below T_g (Hancock and Zografi, 1997).

Structural relaxation is rather common for a wide range of materials including polymers, inorganic glasses, composites, amorphous metal and foodstuffs. It could affect the kinetics of diffusion controlled processes and has been of prime interest in the field of food science and engineering, and pharmaceuticals (Hodge, 1995). This process gives rise to a more compact molecular organization and strengthening of interactions which eventually leads to changes in mechanical and transport properties (Champion et al., 2000). It should be however recognized that even though structural relaxation is common over a wide range of glasses and affects a number of properties, the aging kinetics of different properties for a particular glass material are different (Hodge, 1995). In biological amorphous systems, the temperature- and time-dependent aging effects on glass transition and enthalpy relaxation have been reported. It was found that the T_g and the recovery of enthalpy relaxation of aged lactose increased with aging time (t_a) and temperature (T_a) (Haque et al., 2006). For normal and waxy glassy rich starches, T_g appeared to increase as T_a decreased (Chung and Lim, 2003). Physical aging has been receiving much of attention from food technologists due to its relevance with the stability of low moisture products (Meste et al., 2002).

However, the phenomenon of structural relaxation is considerably complex. It exhibits both nonlinearity, and nonexponentiality, or memory effect. It is believed that the coupling of thermodynamic and dynamic properties gives rise to the nonlinearity which significantly depends on the change of temperature. As a result of their memory effects, the relaxation of glasses from a particular state depends not only on what that state is, but on how the state was reached as well (Hodge, 1995). The loss of enthalpy allows the characteristic or relaxation time of the process to be determined experimentally by means of calorimetric technique.

1.2.6.1 Nonexponentiality

Microstructure of glasses is commonly heterogeneous making the relaxation complicate. As a result, the enthalpy relaxation cannot be simply described using a single relaxation function. The distribution of relaxation time is usually described by the stretch exponential function, also known as the Kohlrausch-Williams-Watts (KWW) decay function (Angell, 1995; Hodge, 1995):

$$\phi(t) = \exp\left[-\left(\frac{t}{\tau^{KWW}}\right)^{\beta}\right] \tag{1.5}$$

where $\phi(t)$ is the property studied as a function of time (t), and τ^{KWW} and β ($0 < \beta \leq 1$) are parameters. The β parameter represents the extent of nonexponentiality and usually considered as the distribution of relaxation time. A single relaxation time with exponential behavior will have $\beta = 1$. The smaller β value corresponds to the more distribution of molecular motion deviates from a single exponential behavior (Shamblin and Zografi, 1998; Haque et al., 2006; Liu et al., 2006). This equation is written in the sense that τ^{KWW} does not depend on aging time (Hodge, 1995)

1.2.6.2 Nonlinearity

The characteristic relaxation time changes with time as it depends on both temperature and the structural state of the glass matrix. This dependence is commonly described by the so called Tool-Narayanaswamy-Moynihan (TNM) expression:

$$\tau = \tau_0 \exp\left(\frac{x\Delta h}{RT_a} + \frac{(1-x)\Delta h}{RT_f}\right) \tag{1.6}$$

where τ_0 is the relaxation time in equilibrium at an infinitely high temperature, Δh is the apparent activation energy in the equilibrium state above T_g, R is the ideal gas constant, T_a is the aging temperature, x is the empirical nonlinearity parameter which defines the contributions of temperature and structure state to τ (the closer to 1, the more dependency of τ on temperature), and T_f is the fictive temperature for a material representing its structural state. The fictive temperature is a hypothetical temperature at which the structure of glass would be in equilibrium and is a function of the sample temperature. It is equivalent to the intersection point of the enthalpy curves for the glassy state and the equilibrium liquid state. It can be calculated from the following relationship:

$$\int_{T_2}^{T_f} (C_{pl} - C_{pg})dT = \int_{T_2}^{T_1} (C_{pt} - C_{pg})dT \tag{1.7}$$

where C_{pl}, C_{pg}, and C_{pt} are the specific heat of the material at the liquid state, glass state, and the glass transition region, respectively. T_1 is a temperature well below the transition region and T_2 is a temperature above the transition region (Liu et al., 2006; Aji and Johari, 2010). The fictive temperature could also be estimated from

$$T_f(T_a, t_a) \approx T_g - \frac{\Delta H}{\Delta C_p} \tag{1.8}$$

where Tg and ΔCp are determined from unaged sample and ΔH is the relaxed enthalpy through aging (Liu et al., 2006).

1.2.7 Factors affecting characteristics of amorphous system

Characteristics of amorphous sugar matrix are affected by various factors. Some important factors, other than storage conditions (temperature and humidity), are —water as plasticizer (Chan et al., 1986; Roos and Karel, 1991; van den Dries et al., 1998; Nowakowski and Hartel, 2002), physical aging due to thermodynamically nonequilibrium nature (Kawai et al., 2005; Haque et al., 2006), species of glass-forming molecules in the system (Roos and Karel, 1991; Gabarra and Hartel, 1998; Nowakowski and Hartel, 2002; Shirke and Ludescher, 2005; Seo et al., 2006), and the presence of other species like salts (Kets et al., 2004; You and Ludescher, 2008b). Details about the effects of these factors are provided hereafter.

1.2.7.1 Species of glass-forming molecules

In amorphous state, molecular weight of glass-forming molecule(s) directly influence characteristics of the system. The T_g of any amorphous polymer and bio-material generally depend on its molecular weight. For homopolymers, the T_g increases with molecular weight of polymers in the form of (Fox and Flory, 1950):

$$T_g = T_{g(\infty)} - \frac{K_g}{M_e} \tag{1.9}$$

where $T_{g(\infty)}$ is glass transition of limiting molecular weight, K_g is a constant, and M_e is the effective molecular weight. The T_g of maltodextrin with different molecular weight was found to be in agreement with this relationship (Roos and Karel, 1991). In multi-components

amorphous systems, for example, a system with two species of molecules, T_g could be estimated based on free-volume theory with the assumption that the two components are miscible, and size and shape of the two components are the same so that the packing fraction remains unchanged, and no interaction takes place between components (Shamblin et al., 1998). This yields the Gordon-Taylor (GT) equation (Gordon and Taylor, 1952);

$$T_{g12} = \frac{w_1 T_{g1} + K w_2 T_{g2}}{w_1 + K w_2} \tag{1.10}$$

where w_1 and w_2 are mass fraction of the first and the second components, and T_{g1} and T_{g2} are their glass transition temperatures. The constant K relates to free volume of the components and can be estimated using the Simha-Boyer rule (Simha and Boyer, 1962),

$$K = \frac{T_{g1}\rho_1}{T_{g2}\rho_2} \tag{1.11}$$

where ρ is the density of each component. In reality, however, the prediction of T_g of multi component systems-sugars mixtures, often deviates from the Gordon-Taylor equation due to the differences in size and shape of components (Seo et al., 2006). In addition, the assumption of ideal mixing associated with the free-volume theory which assumes no interaction takes place between components is practically difficult to achieve. Also for saccharides, the presence of hydrophilic groups usually induces hydrogen bonding formation causing the T_g value calculated with the GT equation to be under predicted (Liu et al., 2006).

Another approach that has been satisfactorily applied to estimate the T_g for a mixture is the Couchman-Karasz (CK) equation in which the second-order phase transition is taken into account. In this approach, the constant K is derived from the heat capacity change at glass transition (Couchman and Karasz, 1978);

$$K = \frac{\Delta C_{p2,GT}}{\Delta C_{p1,GT}} \tag{1.12}$$

where $\Delta C_{p1,GT}$ and $\Delta C_{p2,GT}$ are the heat capacity change at glass transition for the two components. The change of heat capacity is an indicative of changes on rotational, translational, and configuration contributions to heat capacity (Noel and Ring, 1992). Initially, the CK equation had received little attention due to non-availability of accurate value of $\Delta C_{p,GT}$ for individual component. Later, the advancement in calorimetric measurement allows the determination of an accurate $\Delta C_{p,GT}$ value, and then the application of the CK equation has become practical. Even though observations from glass transition study revealed the effect of kinetics, a better fit of the CK equation over the GT equation has been reported (Forster et al., 2003).

In addition to the effect on primary or α-relaxation or glass transition, the structure of glass-forming carbohydrate molecule also significantly affect the nature of secondary or β-relaxation (Noel et al., 1996; Noel et al., 2000). In certain formulation, for example, combining different types of sugar like sucrose and trehalose, not only slightly altered the T_g of the system, but it could also significantly delay or inhibit, depending on mixing ratio,

crystallization in the glass. This may be due to the mechanism of actual linking onto the growth site or by some effects on the mobility (Roe and Labuza, 2005).

1.2.7.2 Water

Water generally prevails in biological amorphous systems at various concentrations. It is known to have adverse effects on the systems include accelerating chemical degradation and crystallization, and plasticization. The roles of water molecules in accelerating chemical degradation might be as reactant, product, or medium. Some physical changes like deterioration, stickiness and collapse of dehydrated amorphous foods are directly relates to their T_g (Karel et al., 1993). The crystallization of amorphous solids can be accelerated by the plasticization effect of water and by the ability of water to build units of hydrated crystals with excipients which then crystallize as hydrates, for example, lactose, trehalose, glucose, and manitol (Shalaev and Zografi, 1996). In food materials, water usually acts as a strong plasticizer (Champion et al., 2000). It is believed that the increase in free volume of the interchain and/or intrasegmental motion leads to the shifting down of T_g (Ferry, 1980; Chan et al., 1986; Roos and Karel, 1991; Roos and Karel, 1991; Noel et al., 1996; van den Dries et al., 1998; Noel et al., 2000). The severity of plasticizing effect also depends on the structure of glass-forming molecules. In glassy carbohydrate system, it has been reported that the addition of 10% water (w/w) resulted in the depression of T_g (in K) by $11 - 18\%$, 24%, and 27% for monosaccharide, disaccharide, and trisaccharide, respectively (Noel et al., 2000). The result from nuclear magnetic resonance (NMR) study suggested that the plasticization effect comes from the disruption of hydrogen-bond network between sugar molecules by

water which then results in the higher mobility of the functional group (van den Dries et al., 1998).

The strong plasticization effect of water could shift the α-relaxation process of glassy carbohydrate to lower temperatures. The evidence from dielectric relaxation measurements indicated that the α-relaxation process was broadened upon the addition of water (Chan et al., 1986; Noel et al., 2000). It is believed that the motion of water molecules within the glass matrix is partly responsible for the presence of β-relaxation process. The addition of water does not only broaden the process but also shift it down to lower temperatures and increase its strength (Noel et al., 1996). However this is not the case for polymer systems where the plasticization effect does not affect the location and the height of β-relaxation peak (Chan et al., 1986).

Even with its adverse effects on amorphous systems, a certain level of moisture content may still be required in some applications. As an example, amorphous capsule-forming materials requires the matrix with some flexibility to provide optimum compression properties (Hancock and Zografi, 1997).

1.2.7.3 Salts

In some aqueous sugar systems, it was found that salts could delay crystallization probably due to ion-water interaction. Water adsorption of these systems was higher when compared to water uptake by each pure component while the T_g remained unaltered. This observation implied that the effect of salts may reflect the dynamic interactions of water-sugar-salt which take place in the molecular level without affecting macroscopic properties (Mazzobre et al., 2001).

Evidences from literature suggest that the stability of amorphous sugar systems could be improved by adding salts. This is possibly by two key mechanisms include the increase in T_g and/or the direct effect of specific interaction between either ions or functional groups with the glass-forming molecules. From the recent study, a clear correlation between the increasing sodium citrate concentration (sodium citrate/sucrose mass ratio from 0 to 2.5) and the rising of T_g value has been observed. An increased average strength of hydrogen bonding in the mixture was evidenced by the results from FTIR analysis. In the absence of moisture, the T_g values of sucrose-citrate mixture exceeded T_g of both pure components. It is believed that such effect arose from hydrogen bonding in that citrate interacts with the sucrose OH via its carboxylate group leading to a more tightly packed molecular structure than that of pure sucrose system (Kets et al., 2004). In a binary mixture glass containing sucrose and NaCl, the results from erythrosin B phosphorescence probe measurements revealed the suppression of matrix mobility upon increasing NaCl/sucrose mole ratio from 0 to 0.46. However, there was no further improvement at higher NaC/sucrose mole ratios. The results also showed a broader distribution of dynamic sites in the glass matrix with NaCl added as compared to that in the matrix of pure sucrose. The overall result led to a conclusion that sodium and chloride ions interact with sucrose OH by ion-dipole interactions, forming a cluster of less mobile molecular within the matrix. The effects of salt on amorphous sugar matrix appeared to be dependent on concentration and type of salts. Excessive amount of NaCl in the matrix would result in a high residual moisture content which may adversely plasticize the system (You and Ludescher, 2008b).

1.2.8 Glass transition measurements

There are a number of techniques available for characterizing the glass transition phenomenon. In general, a choice of techniques is dependent on two criteria: fundamental (e.g., physical property studied, time and distance scale probe), and practical (e.g., availability, sampling requirements, measurement time and sensitivity) (Roos, 1995; Ottenhof et al., 2003). Practically the chosen technique should closely relate to the intended application. For instance, if one's concern is sensory properties of food texture or the dynamic processes like collapse or agglomeration, then the relevant techniques would probably be mechanical spectroscopy or change in Young's modulus or viscosity with temperature (Meste et al., 2002).

Abrupt changes in several physical properties are observed at glass transition region. These include the changes of entropy, heat capacity, rigidity, viscosity and thermal expansion coefficient. Recent study also revealed the change in hydrogen bonding of sugar molecules during glass transition (Wolkers et al., 1998). Accordingly, the measurement of glass transition may be made using different techniques. The concepts of glass transition measurement are briefly reviewed as follows.

1.2.8.1 Calorimetry

Glass transition is accompanied by a change in some physical characteristics of a system. Heat capacity (C_p) is among those which increases as the system transform from the glassy to the liquid state. The change of C_p allows using the calorimetric technique to probe the transformation (Suga and Seki, 1974; Tsukushi et al., 1994). Since such change occurs as

a function of temperature, the use of this technique necessarily involves temperature scanning (Reid et al., 1993).

By far, the differential scanning calorimetry (DSC) has been the most common technique for studying glass transition. In the field of carbohydrate research, there have been a vast number of studies using DSC (Crichton and Moynihan, 1988; Roos and Karel, 1991; Kalichevsky and Blanshard, 1992; Roos, 1993; Shalaev et al., 1996; Gabarra and Hartel, 1998; Shamblin and Zografi, 1998; Noel et al., 1999; Shamblin et al., 1999; Craig et al., 2000; Hancock and Shamblin, 2001; Borde et al., 2002; Borde et al., 2002; Chung and Lim, 2003; Kets et al., 2004; Kawai et al., 2005; Roe and Labuza, 2005; Haque et al., 2006; Seo et al., 2006; Liu et al., 2007; Jiang et al., 2008; Bhandari and Hartel, 2010). The important advantages of DSC include relatively simple sample preparation and brief measurement time (Schawe, 2002). Besides, the measurement can be conducted with good control of hydration and this is particularly important for the study of food materials.

Experimental procedure significantly affects the value of calorimetric T_g (Borde et al., 2002). Most importantly, the calorimetric T_g depends on the rate of temperature change - heating and cooling rates (Crichton and Moynihan, 1988; Surana et al., 2005). The lower the cooling rate, the lower the value of T_g. There is still a debate about whether the limiting value of T_g exists when the cooling rate was low enough (Young and Lovell, 1991).

1.2.8.2 Dynamic mechanical spectroscopy

Dynamic mechanical spectroscopy is particularly useful for measuring glass transition in certain materials. For products containing starch or flour, the DSC is not sensitive enough to detect the glass transition (Nikolaidis and Labuza, 1996). In this case, the

dynamic mechanical spectroscopy can be used to observe the progress of rheological properties through the glass transition region. Such progress of rheological properties is an evidence for the α-relaxation process associated with the glass transition (Champion et al., 2000).

In sub-resonance region, the strain response of linear viscoelastic material under sinusoidally varying stress lags the stress by some phase angle δ due to energy loss. For shear deformation, the ratio of stress amplitude to strain amplitude is shear or the dynamic rigidity modulus (G^*) which is divided into elastic (G') and viscous (G'') components. The relationships among these quantities are as follows:

$$G' = \left(\frac{stress\_amplitude}{strain\_amplitude} \right) \cos\delta \tag{1.13}$$

and

$$G'' = \left(\frac{stress\_amplitude}{strain\_amplitude} \right) \sin\delta \tag{1.14}$$

It could be easily seen that above two equations yield tan $\delta = G''/ G'$ or loss tangent which can be viewed as the ratio of energy loss to energy recovered per cycle. In extension or bending, given the correction for specimen geometry, the ratio of stress amplitude to strain amplitude defines the dynamic Young's modulus (E^*) which can be divided into elastic (E') and viscous (E'') components. Equations 1.13 and 1.14 hold true when substitute G' with E' and G'' with E''. Loss tangent arises due to the presence of some internal motion in the viscoelastic material. The magnitude of loss tangent increases proportionately as more energy

being lost in the frequency range similar to that of the applied stress. The peak of loss tangent can be experimentally obtained from dynamic mechanical technique in either by frequency or temperature scan test (Kalichevsky et al., 1993).

Under sinusoidal perturbation, the maximal energy absorption or the loss modulus (E'' or G'') will be observed when the applied frequency (f) and the average relaxation time (τ) of the system are in the following relationship:

$$\tau = \frac{1}{2\pi f} \tag{1.15}$$

From physical point of view, the location where the maximal viscous or loss modulus presents seems to be logical to designate the corresponding frequency or temperature of the α relaxation (T_α). However, the T_α is conventionally assigned at the peak of loss factor or tan δ (Champion et al., 2000).

Examples of apparatus in this category are the TA Instruments Dynamic Mechanical Analyser (DMA), Polymer Laboratories Dynamic Mechanical Thermal Analyzer (DMTA), Rheometrics Solids Analyzer, Mechanical Spectrometer, Toyo Baldwin Rheovibron Viscoelastometer (Kalichevsky et al., 1993), Advanced Rheometrics Expansion System (ARES) (Kasapis et al., 1999; Kasapis and Sablani, 2005), Bohlin Rheometer, and Broad band Viscoelastic Spectroscopy (BVS).

For a system of small molecules, mechanical spectroscopy may not be applicable for determining T_α since there is no observable peak of loss modulus or loss factor (Champion et al., 2000). Also, specimen preparation, particularly for brittle materials, may limit the use of

this technique. This is the case we found during preliminary work with the BVS. In addition, care must be taken when dealing with data obtained above room temperature on the system containing water as it is difficult to prevent water loss (Kalichevsky et al., 1993).

1.2.8.3 Dielectric spectroscopy

Instead of applying a continuous sinusoidal field, the relaxation process of certain materials can also be observed from the decay in response to an applied pulse. The obtained data can be then converted into a continuous waveform by using the well-known mathematical technique called the Fourier transformation. This is the fundamental of dielectric spectroscopy. Basically, the variations of dielectric constant as a function of temperature or/and frequency are observed (Champion et al., 2000).

Given the relationship of the relaxation time of the α-relaxation process (τ_α) and the loss peak frequency (f_p) as in Equation 1.15, the dielectric T_g is defined as the temperature where τ_α is equal to 100 s. It has been shown that the dielectric T_g is in good agreement with the calorimetric T_g (Shinyashiki et al., 2008) and the mechanical T_g (Huang et al., 1996).

Due to its sensitivity to polar groups like hydroxyl groups, this technique is well suited for measuring the molecular mobility in solid samples containing of polysaccharides (Roudaut et al., 1999). In hydrogen bonded materials, the dipole rotation is manifested in the dielectric relaxation process (Gangasharan and Murthy, 1995). The dielectric spectroscopy has proven to be a very useful tool for studying the relationship of the α-relaxation and the Johari-Goldstein (JG) β-relaxation—the special class of β-relaxation process (Johari and Goldstein, 1970; Shinyashiki et al., 2008). In addition, this technique is also a good alternative to the mechanical spectroscopy for brittle products (Roudaut et al., 1999).

1.2.8.4 Fourier transform infrared spectroscopy (FTIR)

Infrared spectroscopy technique is used to observe the infrared absorption spectrum of materials. The resulting absorption spectrum is considered as a molecular fingerprint with absorption peaks corresponding to the frequencies of chemical bond vibrations in a molecule. For identification purpose, the spectrum has to be compared to the reference spectra from an existing data base. The term FTIR refers to the recent development in that the data is collected and converted from interference pattern—the interferogram—to a frequency spectrum using the Fourier transformation. By incorporating a computer system, current FTIR instruments have become even faster and more sensitive (Coates, 2000; Anonymnous, 2010)

For amorphous matrixes formed by sugars, hydrogen bonds between hydroxyl groups of sugar molecules are responsible for holding the matrixes. Hence, the analysis of the vibration spectrum of hydroxyl groups of sugars would yield more understanding about the glass transition behavior of amorphous sugar matrixes (Imamura et al., 2006). In the study of some sugar glasses using FTIR, Wolkers and co-workers discovered that the peak wave number for the hydroxyl groups of sugar (OH stretching vibration) linearly increased with temperature and, for all sugars measured, there was an abrupt change of the slope of the line at certain temperature. The temperature at the intersection of the two lines was comparable with the calorimetric T_g in the literature. They then defined such temperature as the T_g (Wolkers et al., 1998). This finding formed the basis of determining T_g using FTIR (Wolkers et al., 2004b; Imamura et al., 2006).

1.2.9 Conventional techniques for measuring molecular mobility of amorphous materials

A general practice to estimate the degree of molecular mobility in amorphous materials is by inferring from a relaxation process. A number of measurement techniques can be employed to study the process. This section provides information on the common techniques used for studying the mobility in amorphous matrix.

In the state of glass, molecular mobility has been widely studied using the dynamic excitation techniques include dielectric spectroscopy (Johari and Goldstein, 1970; Chan et al., 1986; Noel et al., 1996; Faivre et al., 1999; Noel et al., 2000) and dynamic mechanical spectroscopy (Wetton, 1984; Kalichevsky et al., 1993; Faivre et al., 1999). Mechanical or dielectric loss peak reflects a large-scale molecular motion conventionally labeled as a primary or α-relaxation. The peak occurs at the highest temperature under constant frequency measurements or at the lowest frequency under constant temperature measurement. This is what underlines the onset of translational motion at the glass transition. Other peaks at temperatures below T_g reflect localized molecular motions within the rigid glassy matrix and is conventionally labeled as the secondary or β-relaxation and/or γ-relaxation if there are more than one (Johari and Goldstein, 1970; Johari and Goldstein, 1971).

Probe measurement is another technique that has been used to monitor molecular mobility. The measurement can be conducted using different types of probe. The accuracy of this type of measurement greatly depends on probe size and shape (Hall et al., 1998) and also it may be affected by the existence of interaction between probe and the amorphous matrix (Hall et al., 1999). The use of phosphorescent probe has been reported by several researchers (Pravinata et al., 2005; Shirke and Ludescher, 2005; You and Ludescher, 2008b). The

strength of specific chemical bonding in the glass matrix can be determined using FTIR (Wolkers et al., 1998; Wolkers et al., 2004b) and NMR (van den Dries et al., 1998) measurements. The calorimetric measurement is also commonly used as a complementary technique to determine thermal properties (Wetton, 1984; Ottenhof et al., 2003). Some more extensive reviews of the techniques are listed elsewhere (Slade and Levine, 1993).

Here we place our attention on the calorimetric measurement and the mechanical spectroscopy. The first has been widely used for investigating "slow" structural relaxation process over an extended period of time. The later has been generally used to study the "temporary" relaxation process from mechanical perturbation generally in much shorter time of experiment. These two techniques provide different aspects of molecular motions. The study on activation energy of enthalpy relaxation process suggested that this process corresponds to the macroscopic mobility of molecules in glassy state – translational diffusion (Kawai et al., 2005). On the other hand, the mechanical spectroscopy can provide information about the β-relaxation process (Kalichevsky et al., 1993) which is believed to reflect local mobility such as the rotational or vibrational movement of the side chain or functional groups (Noel et al., 1996; Noel et al., 2000). So the two techniques are essentially complementary and this is a good reason to choose these techniques for our study to obtain more complete information about the molecular mobility in the bioglass under T_g.

1.2.9.1 Calorimetric measurement

Upon heating through the T_g, endothermic peak, referred to as the recovery of enthalpy that lost due to structural relaxation, results at the end of glass transition process (see Figure 1.5). The size of this peak increases with the increasing of aging time and

temperature (Shamblin and Zografi, 1998; Haque et al., 2006). The enthalpy associated with this endotherm may be quantified by subtracting with the response of an unaged sample with the same thermal history. In general practice, it can be alternatively estimated by extrapolating the supercooled liquid response to be an approximate baseline as illustrated in Figure 1.5. The enthalpy relaxation is an indication of the extent that the sample relaxed under the chosen storage conditions and is related to the average molecular mobility (Hancock and Shamblin, 2001). It is believed that the relaxation occurs as a consequence of local diffusive motion at molecular level which leads to molecular rearrangements. The coefficient of translational diffusion may be predicted by the Stoke-Einstein relationship (Noel et al., 1993). However, it is important to recognize that, in reality; the molecular motions in an amorphous system are heterogeneous and are generally described by a distribution of relaxation times. So, the relaxation times inferred from the data obtained with this type of measurement is considered as an "averaged" relaxation time (Shamblin et al., 1999).

Since the enthalpy relaxation process does not obey a simple exponential decay (Oguni et al., 1990; Williams, 1991), a number of attempts have been made to analyze the process. Among variety of approaches, the stretch exponential or the empirical Kohlrausch-Williams-Watts (KWW) decay function, and the extended Adam-Gibbs (ExAG) have been widely applied. These two approaches originated from different physical models. The empirical KWW assumes the relaxation time as a special type of distribution while the ExAG is based on the thermodynamic concept that the configurational entropy (S_c) decreases with aging (Kawai et al., 2005).

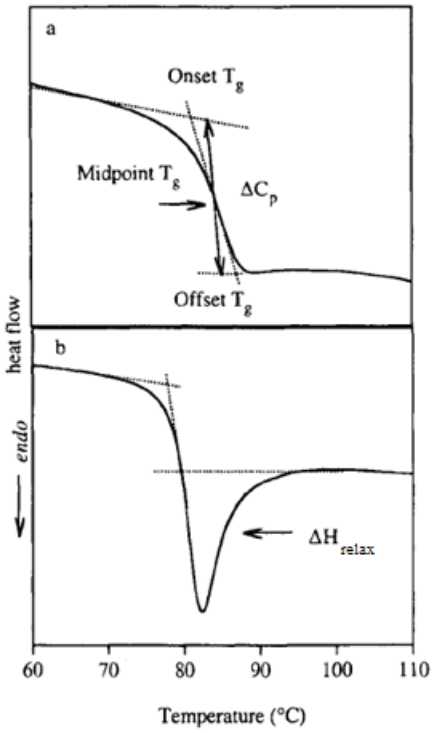

Figure 1.5 A schematic diagram representing the measurement of glass transition using DSC; (a) unaged sample shows no or very small endothermic peak while (b) aged sample clearly shows this peak at the end of glass transition process (Shamblin and Zografi, 1998).

However, the expressions of both approaches fit well with enthalpy relaxation data from calorimetric measurements (Mehl, 1993; Shamblin and Zografi, 1998; Kawai et al., 2005; Haque et al., 2006) and the interpretation of the relaxation times is in good agreement (Kawai et al., 2005). Details of the mentioned approaches are provided as follows.

1) Estimating the average relaxation time using the KWW approach

In order to determine the average relaxation time from the enthalpy change over time during storing or aging using this function, it is necessary to estimate the maximum possible enthalpy recovery at each aging temperature (ΔH_∞). This can be calculated using the following equation:

$$\Delta H_\infty = \Delta C_{p,GT}(T_g - T_a) \tag{1.16}$$

where $\Delta C_{p,GT}$ is the heat capacity change at glass transition and T_a is the aging temperature. According to Eq. 1.5, the function $\phi(t)$ of interest here is the portion of unreleased enthalpy relative to the metastable equilibrium state at T_a which is defined as (Cowie and Ferguson, 1986):

$$\phi(t) = 1 - \frac{\Delta H(t)}{\Delta H_\infty} \tag{1.17}$$

Then Eq. 1.5 can be written as (Shamblin and Zografi, 1998; Hancock and Shamblin, 2001; Kawai et al., 2005; Haque et al., 2006):

$$\frac{\Delta H(t)}{\Delta H_{\infty}} = 1 - \exp\left[-\left(\frac{t}{\tau^{KWW}}\right)^{\beta}\right] \tag{1.18}$$

where $\Delta H(t)$ is the enthalpy associated with the endothermic peak after aging for a time t.

2) Estimating the effective relaxation times using the ExAG approach

This approach describes the enthalpy relaxation based on the cooperative rearrangement region (CRR) model proposed by Adam and Gibbs (Adam and Gibbs, 1965). The model was originally used to describe the temperature dependence of molecular relaxation time in a supercooled liquid. Several assumptions were made in this theorem. It was assumed that at the temperature below T_k the motions requiring diffusion or rotation cease, and S_c vanishes. Another assumption was that glasses at temperatures below T_g have small and constant S_c. These assumptions imply that the molecular motions are constant at all temperatures below T_g but in reality they are not (Hancock and Shamblin, 2001) and this has been explored in many studies (Shamblin and Zografi, 1998; Noel et al., 1999; Shamblin et al., 1999; Cerrada and McKenna, 2000; Chung and Lim, 2003; Kawai et al., 2005; Haque et al., 2006). As a result, the model was later extended to account for the excess configurational entropy which exists in real glasses at different temperatures (Oguni et al., 1990).

In order to account for the excess S_c, which exists in real glasses at different temperatures, it was assumed that the number of molecules involved in the CRR would increase as the enthalpy relaxation proceeds during isothermal aging, and consequently leads to a decrease in the S_c. As a result, the τ increase with enthalpy relaxation during isothermal aging and can be expressed as follows:

$$\frac{d\left[\Delta H_{\infty} - \Delta H(t)\right]}{dt} = -\frac{1}{\tau^{eff}(t)}\left[\Delta H_{\infty} - \Delta H(t)\ \right] \tag{1.19}$$

where $\tau^{eff}(t)$ is defined as the effective enthalpy relaxation time.

It has been found experimentally that $\tau^{eff}(t)$ increased with the decreasing of the excess enthalpy and could be expressed as follows:

$$\ln \tau^{eff}(t) = \ln \tau^{eff}{}_{\infty} + B[\Delta H_{\infty} - \Delta H(t)] \tag{1.20}$$

where B and $\tau^{eff}{}_{\infty}$ are constants. $\tau^{eff}{}_{\infty}$ corresponds to $\tau^{eff}(t)$ when enthalpy relaxation has proceeded up to the equilibrium state. In some study, the initial (or unrelaxed) enthalpy relaxation time, $\tau^{eff}{}_{0}$, was also considered. According to the CCR model proposed by Adam and Gibbs, the $\tau^{eff}{}_{0}$ and $\tau^{eff}{}_{\infty}$ correspond to the relaxation time of minimum and maximum CRR size, respectively, during isothermal aging at a given temperature (Kawai et al., 2005; Haque et al., 2006).

1.2.9.2 Mechanical spectroscopy

This technique is conducted by applying a sinusoidal external field to couple with the specimen so that the natural dynamic behavior of the sample is not seriously perturbed. The dynamic response of sample is then observed as a function of frequency of the applied field (Allen, 1993).

By considering that the motion of atoms or molecules involved in the transition between two energy states over a certain level of energy barrier, the energy barrier or

activation energy (E_a) can be determined from the change of loss peak positions with frequency in temperature scans or such changes with temperature in frequency scans using a well-known Arrhenius relationship:

$$\tau = \tau_0 \exp\left(\frac{E_a}{RT}\right) \tag{1.21}$$

where R is gas constant, T is absolute temperature and τ_0 is reciprocal frequency of vibration (Kalichevsky et al., 1993).

Under isothermal experiments, the dynamic mechanical properties of polymer depend on testing frequency. These properties are often related to certain types of molecular motion in the polymer. The peaks of loss (or viscous) modulus and tan δ are also regarded as a damping effect and present at the frequency of molecular motion in the polymer. When the applied test frequency equals the natural frequency for the main chain rotation, significant damping occurs. The polymer tested at higher frequency will appear to be stiff since there is insufficient time for the chain to uncoil. In contrast, the polymer will appear to be soft and rubbery when tested at lower frequency due to the chain has plenty of time to move. There may also be other types of molecular motion such as side group rotation which usually results in weaker damping at different frequencies (Young and Lovell, 1991).

The instruments for conducting dynamic mechanical measurement on solid materials may be categorized into two classes. The first class employs resonance techniques, for example, the Torsiomatic Zwick 5204 torsion pendulum, the Plastics Analysis Instruments torsion braid analyzer (TBA) (Kalichevsky et al., 1993), and resonant ultrasound

spectroscopy (RUS) (Migliori and Sarrao, 1997; Lee et al., 2000; Wang and Lakes, 2003; Lakes, 2004). G′ and loss tangent can be obtained from the natural frequency and the decay rate of free torsional oscillations. These instruments are not considerably versatile since it is not straightforward to measure material properties as a function of frequency and the frequency change during transition due to limited frequency range (Kalichevsky et al., 1993). The second class is a non-resonance method which operates below resonance frequency. The dynamic moduli and loss tangent are obtained from the amplitude and phase angle between force, or torque in torsion mode, and displacement cycles of the specimen under a sinusoidally varying applied load. Examples of this class of instruments are TA Instrument dynamic mechanical analyzer (DMA), the Polymer Laboratories dynamic mechanical thermal analyzer (DMTA), Rheometrics solids analyzer, Toyo Baldwin Rheovibron viscoelastometer (Kalichevsky et al., 1993), and the Broadband Viscoelastic Spectroscopy (BVS) (Chen and Lakes, 1989; Brodt et al., 1995).

1.2.9.3 Mechanical spectroscopy vs calorimetry

There have been a vast number of glass transition studies on food materials that relied on DSC as a primary or a complementary technique. As noted earlier, the enthalpy relaxation of sugar glasses was also clearly observed using this technique (Kawai et al., 2005; Haque et al., 2006). However, some reports pointed out the failure of DSC in detecting the glass transition of many samples when significant phase separation occurred during storage (Wetton, 1984; Davidson and Sun, 2001). Even though DSC is sensitive to the heat change during first-order thermodynamic transitions (e.g., melting and crystallization), the resolution on second-order transitions is rather poor as compared to mechanical spectroscopy, which is

sensitive to molecular relaxation with a factor of approximately 1000 times higher (Wetton, 1984). Also, a small amount of addition is possible to detect with dynamic mechanical measurement technique while calorimetric technique provides primarily only the mobility of the major component (Kasapis et al., 2003). From DSC measurements on composite complex food like cookies or crackers, Labuza and co-workers suggested that the sample size of 10-20 mg practically used for this type of measurement is too small (Labuza et al., 2004). Another difficulty is that data obtained with the DSC are highly dependent on the experimental conditions, specifically heating and cooling rates, and the result could lead to an ambiguous conclusion (Moynihan et al., 1991). Details of experimental conditions should be provided along with the report of DSC measurement.

Under the category of mechanical spectroscopy, the dynamic mechanical thermal analyzer (DMTA) seems to be common. Monitoring relaxation process may be performed in either frequency scan at constant temperature or temperature scan at constant frequency. The former could provide purer data since structural changes may occur during temperature scan. For commercially available DMTA, the experimentally accessible frequency ranges are considerably limited, approximately 0.01 – 100 Hz in general (Kalichevsky et al., 1993), and even a single relaxation process cannot be conveniently encompassed (Wetton, 1984). A practical solution for such limitation is to perform temperature scan. Yet problems associated with the use of temperature scan practice in DMTA with food materials have been reported. The hygroscopic nature of foods could lead to moisture loss during an extreme temperature scan experiment. In addition, the recorded temperature is not exactly the sample temperature (Nikolaidis and Labuza, 1996).

1.2.10 Modulated differential scanning calorimetry (MDSC)

The principle operation of traditional DSC technique is based on measuring the differential heat flow between an inert reference and a sample. When the sample and the reference are heated at the known rate in a control environment, the increase of their temperature will be dependent on their specific heat. However, when heat related change takes place in the sample, the changes of temperature of the sample and that of the reference will be different, and can be directly related to the differential heat flow. Nevertheless, the traditional DSC encounters three main categories of problems: analysis of complex transitions, need for increased sensitivity, and need for increased resolution. Transitions are complex due to the fact that they involve multiple processes, for example, the enthalpic relaxation that occurs at the glass transition, crystallization prior or during melting. Since traditional DSC measures only the sum of all thermal events taking place in the sample, the multiple transitions that occur in the same temperature range often lead to confusion and misinterpretation of the result. The results obtained with the traditional DSC measurements are always a compromise between sensitivity and resolution. It is due to the fact that high resolution - the ability to separate transitions that occur at a few degrees apart - requires the use of small amount of samples with low heating rate. This requirement leads to a decrease of the magnitude of heat flow signal and consequently results in the reduction of sensitivity.

MDSC technique is capable of extracting more information from a single DSC measurement using the same heat flux DSC cell as the traditional DSC. Other than the same information as obtained with traditional DSC, the MDSC provides additional capabilities including measurement of heat capacity and heat flow in a single experiment, separation of complex transitions into more easily interpreted components, increased sensitivity for

detection of weak transitions, increased resolution of transitions without loss of sensitivity, increased accuracy in the measurement of polymer crystallinity, and direct determination of thermal conductivity. These make the MDSC technique capable to overcome all of the limitations encountered in the traditional DSC measurements. Interpretation of complex transition can be made possible by separating the total heat flow signal into its heat capacity and kinetic components. Problem due to the variations of baseline signal is eliminated by using both heat flow and temperature amplitudes to calculate the heat capacity instead of solely the absolute value of the total heat flow. The resolution can be increased without the expense of sensitivity by having two heating rates. The high resolution is achieved by using the average heating rate at the desired low level while the high sensitivity is maintained by using the high rate of instantaneous heating to create a large heat flow.

The MDSC technique applies a sinusoidal temperature oscillation (modulation) overlaying on the conventional linear temperature ramp. Due to the fact that the underlying heating rate is always positive; the resulting (or actual) heating rate during heating is larger than during cooling. However, the actual variations in heating rate depend on experimental settings including the underlying heating rate, the amplitude of modulation, and the period of modulation. The general equation describing the calorimetric response of the sample may be mathematically represented as follows:

$$\frac{dQ}{dt} = C_p \frac{dT}{dt} + f(t,T) \tag{1.22}$$

where dQ/dt is the total heat flow,

dT/dt is the heating rate,

C_p is the heat capacity the sample,

t is time, and

$f(t,T)$ is a function of time and temperature which governs the kinetic response of the observed transition.

As can be seen from above equation, the total DSC heat flow consists of two components. The first component is heating rate dependent which directly follows the modulated heating rate. The second is a kinetic component which depends on absolute temperature and time, and does not follow the heating rate (Anonymous, 1996).

It may be also considered that the heat capacity of the sample consists of two contributions. The first is the baseline heat capacity resulting from the heat necessary to change the temperature of the sample without changes in the phase or phase distribution, which is considered as reversing in the time scale of the modulation applied. The second contribution is the so called excess heat capacity that arises from other heat-related changes taking place in the sample which can be reversing, nonreversing, or partly reversing (Wurm and Schick, 2003). As compared to Eq. 1.22, all of the reversing contributions go to the first term of the right hand side while the nonreversing contribution is represented by the second term.

Raw data signals (modulated temperature and modulated heat flow) are deconvoluted or separated into the average and amplitude by the discrete Fourier transformation. This computation is executed over one complete cycle of the respective raw modulated signal. The heat capacity signal can be calculated from the amplitudes of those signals by the following equation:

$$C_p = K_{Cp}\left(\frac{Q_{amp}}{T_{amp}}\right)\left(\frac{period}{2\pi}\right) \qquad (1.23)$$

where C_p is the heat capacity,

K_{Cp} is the heat capacity calibration constant,

Q_{amp} is the amplitude of modulated heat flow signal,

T_{amp} is the amplitude of modulated temperature signal, and

period is the modulation period.

The reversing heat flow is calculated by multiplying the C_p by the underlying heating rate. Then the nonreversing heat flow is readily obtained as the difference between the total heat flow and the reversing heat flow (Anonymous, 1996).

1.3 Summary

Certain classes of liquid can be rapidly cooled so that the equilibrium crystalline state is avoided and the resulting materials are in glassy. This process is known as glass transition and is characterized with the temperature T_g. The molecular disorder of glassy state is characteristic of liquid but it physically appears solid-like. Glassy materials are out of equilibrium and gradually change toward equilibrium over time, the so called physical aging. Changes in a number of properties can be observed in the aged glass.

Glass transition phenomenon has long been of interest across various disciplines. Even though this phenomenon is not yet clearly understood, glassy materials have become attractive in various applications. In the field of food technology, the excellent protective

property of glass could be beneficial to the encapsulation of labile compounds, e.g., flavors, vitamins, or the drying of bacterial cultures, enzymes and proteins.

Sucrose and maltodextrin are among high potential food materials to utilize as an encapsulation matrix. They are common ingredients found in various commercial food products. Though the T_g of sucrose is not considerably high, its ability to form a great extent of hydrogen bonding with other kinds of molecules is prominent. On the other hand, maltodextrin possesses a higher T_g and could inhibit crystallization in amorphous sucrose. The strength of hydrogen bonds in sucrose glass could be improved upon mixing with maltodextrin (Oldenhof et al., 2005). Besides, literature has suggested a possible application of salts in amorphous carbohydrate systems. Salts could help increase T_g (Kets et al., 2004) and reduce molecular mobility within amorphous sucrose matrix (You and Ludescher, 2008a; You and Ludescher, 2008b).

In this study, a bioglass model system was formulated with sucrose, maltodextrin and Na citrate. It was aimed at investigating the effects of these components on properties and behavior of the system.

1.4 References

Adam, G. and Gibbs, J. H. (1965). "On the temperature dependence of cooperative relaxation properties in glass-forming liquids." The Journal of Chemical Physics **43**(1): 139-146.

Aji, D. P. B. and Johari, G. P. (2010). "Fictive temperature, structural relaxation, and reality of residual entropy." The Journal of Physical Chemistry B **114**(29): 9578-9585.

Aldous, B. J., Auffret, A. D. and Franks, F. (1995). "The crystallisation of hydrates from amorphous carbohydrates." Cryo Letters **16**: 181-186.

Allen, G. (1993). A history of glassy state. The glassy state in foods. J. M. V. Blanshard and P. J. Lillford. Loughborough, Nottingham University Press**:** 1-12.

Anderson, P. W. (1995). "Through the glass lightly." Science **267**(5204): 1609-1618.

Angell, C. A. (1995). "Formation of glasses from liquids and biopolymers." Science **267**(5206): 1924-1935.

Angell, C. A. (1996). "The glass transition." Current Opinion in Solid State and Materials Science **1**(4): 578-585.

Angell, C. A. (1997). "Why C1 = 16-17 in the WLF equation is physical--and the fragility of polymers." Polymer **38**(26): 6261-6266.

Anonymnous (2010). Fourier transform infrared spectroscopy.

Anonymous (1996). DSC 2920 Differential scanning calorimeter operator's manual. New Castle: TA Instruments Inc.

Anonymous (2008). DMA 8000 Dynamic Mechanical Analyzer, PerkinElmer, Inc.

Bhandari, B. R. and Hartel, R. W. (2005). Phase transitions during food powder production and powder stability. Encapsulated and Food Powder. C. Onwulata and R. P. Konstance. New York, Marcel Dekker**:** 261-292.

Bhandari, B. R. and Hartel, R. W. (2010). Kinetics of enthalpy relaxation in corn syrup–sucrose mixtures. Water properties in food, health, pharmaceutical and biological systems: ISOPOW 10. D. S. Reid, T. Sajjaanantakul, P. J. Lillford and S. Charoenrein. Ames, Wiley-Blackwell**:** 419-428.

Bohmer, R., Ngai, K. L., Angell, C. A. and Plazek, D. J. (1993). "Nonexponential relaxations in strong and fragile glass formers." The Journal of Chemical Physics **99**(5): 4201-4209.

Borde, B., Bizot, H., Vigier, G. and Buleon, A. (2002). "Calorimetric analysis of the structural relaxation in partially hydrated amorphous polysaccharides. I. Glass transition and fragility." Carbohydrate Polymers **48**(1): 83-96.

Borde, B., Bizot, H., Vigier, G. and Buléon, A. (2002). "Calorimetric analysis of the structural relaxation in partially hydrated amorphous polysaccharides. II. Phenomenological study of physical ageing." Carbohydrate Polymers **48**(2): 111-123.

Brodt, M., Cook, L. S. and Lakes, R. S. (1995). "Apparatus for measuring viscoelastic properties over ten decades: Refinements." Review of Scientific Instruments **66**(11): 5292-5297.

Brook, M. (1971). Sucrose and the food manufacturer. Sugar - Chemical, Biological and Nutritional Aspects of Sucrose. J. Yudkin, J. Edelman and L. Hough. London, Butterworth**:** 32-46.

Buera, P., Schebor, C. and Elizalde, B. (2005). "Effects of carbohydrate crystallization on stability of dehydrated foods and ingredient formulations." Journal of Food Engineering **67**(1-2): 157-165.

Buitink, J. and Leprince, O. (2004). "Glass formation in plant anhydrobiotes: survival in the dry state." Cryobiology **48**(3): 215-228.

Campbell, M. K. and Farrell, S. O. (2006). Biochemistry. 5th. Belmont: Thomson Brooks/Cole.

Capaccioli, S., Paluch, M., Prevosto, D., Wang, L.-M. and Ngai, K. L. (2012). "Many-body nature of relaxation processes in glass-forming systems." The Journal of Physical Chemistry Letters **3**(6): 735-743.

Cerrada, M. L. and McKenna, G. B. (2000). "Physical aging of amorphous PEN: Isothermal, isochronal and isostructural results." Macromolecules **33**(8): 3065-3076.

Champion, D., Le Meste, M. and Simatos, D. (2000). "Towards an improved understanding of glass transition and relaxations in foods: molecular mobility in the glass transition range." Trends in Food Science & Technology **11**(2): 41-55.

Chan, R. K., Pathmanathan, K. and Johari, G. P. (1986). "Dielectric relaxations in the liquid and glassy states of glucose and its water mixtures." Journal of Physical Chemistry **90**(23): 6358-6362.

Chen, C. P. and Lakes, R. S. (1989). "Apparatus for determining the viscoelastic properties of materials over ten decades of frequency and time." Journal of Rheology **33**(8): 1231-1249.

Chronakis, I. S. (1998). "On the molecular characteristics, compositional properties, and structural-functional mechanisms of maltodextrins: A review." Critical Reviews in Food Science and Nutrition **38**(7): 599 - 637.

Chung, H.-J. and Lim, S.-T. (2003). "Physical aging of glassy normal and waxy rice starches: effect of aging temperature on glass transition and enthalpy relaxation." Carbohydrate Polymers **53**(2): 205-211.

Cicerone, M. T. and Ediger, M. D. (1996). "Enhanced translation of probe molecules in supercooled o-terphenyl: Signature of spatially heterogeneous dynamics?" Journal of Chemical Physics **104**(18): 7210.

Clarke, M. A. (1995). Technological value of sucrose in food products. Sucrose - Properties and Applications. M. Mathlouthi and P. Reiser. London, Chapman & Hall**:** 223-247.

Coates, J. (2000). Interpretation of infrared spectra, A practical approach. Encyclopedia of Analytical Chemistry. R. A. Meyers. Chichester, John Wiley & Sons**:** 10815-10837.
Couchman, P. R. and Karasz, F. E. (1978). "A classical thermodynamic discussion of the effect of composition on glass-transition temperatures." Macromolecules **11**(1): 117-119.

Cowie, J. M. and Ferguson, R. (1986). "The aging of poly(vinyl methyl ether) as determined from enthalpy relaxation measurements." Polymer Communications **27**: 258-260.

Craig, D. Q. M., Barsnes, M., Royall, P. G. and Kett, V. L. (2000). "An evaluation of the use of modulated temperature DSC as a means of assessing the relaxation behaviour of amorphous lactose." Pharmaceutical Research **17**(6): 696-700.

Crichton, S. N. and Moynihan, C. T. (1988). "Dependence of the glass transition temperature on heating rate." Journal of Non-Crystalline Solids **99**: 413-417.

Crowe, J. H., Carpenter, J. F. and Crowe, L. M. (1998). "The role of vitrification in anhydrobiosis." Annual Review of Physiology **60**: 73-103.

Crowe, J. H., Crowe, L. M., Oliver, A. E., Tsvetkova, N., Wolkers, W. and Tablin, F. (2001). "The trehalose myth revisited: Introduction to a symposium on stabilization of cells in the dry state." Cryobiology **43**(2): 89-105.

Crowe, L. M., Reid, D. S. and Crowe, J. H. (1996). "Is trehalose special for preserving dry biomaterials?" Biophysical Journal **71**(4): 2087-2093.

Davidson, P. and Sun, W. Q. (2001). "Effect of sucrose/raffinose mass ratios on the stability of co-lyophilized protein during storage above the Tg." Pharmaceutical Research **18**(4): 474-479.

Desobry, S. A., Netto, F. M. and Labuza, T. P. (1999). "Influence of maltodextrin systems at an equivalent 25DE on encapsulated β-carotene loss during storage." Journal of Food Processing and Preservation **23**(1): 39-55.

Ediger, M. D., Angell, C. A. and Nagel, S. R. (1996). "Supercooled liquids and glasses." The Journal of Physical Chemistry **100**(31): 13200-13212.

Elliott, S. R., Rao, C. N. R. and Thomas, J. M. (1986). "The chemistry of the noncrystalline state." Angewandte Chemie International Edition in English **25**(1): 31-46.

Faivre, A., Niquet, G., Maglione, M., Fornazero, J., Jal, J. F. and David, L. (1999). "Dynamics of sorbitol and maltitol over a wide time-temperture range." The European Physical Journal B **10**: 277-286.

Ferry, J. D. (1980). Viscoelastic properties of polymers. New York: John Wiley & Sons.

Forster, A., Hempenstall, J. and Rades, T. (2003). "Comparison of the Gordon-Taylor and Couchman-Karasz equations for prediction of the glass transition temperature of glass solutions of drug and polyvinylpyrrolidone prepared by melt extrusion." Die Pharmazie **58**(11): 838-839.

Fox, T. G. and Flory, P. J. (1950). "Second-order transition temperatures and related properties of polystyrene. I. Influence of molecular weight." Journal of Applied Physics **21**(6): 581-591.

Gabarra, P. and Hartel, R. W. (1998). "Corn syrup solids and their saccharide fractions affect crystallization of amorphous sucrose." Journal of Food Science **63**(3): 523-528.

Galmarini, M. V., Zamora, M. C., Baby, R., Chirife, J. and Mesina, V. (2008). "Aromatic profiles of spray-dried encapsulated orange flavours: influence of matrix composition on the aroma retention evaluated by sensory analysis and electronic nose techniques." International Journal of Food Science & Technology **43**(9): 1569-1576.

Gangasharan and Murthy, S. S. N. (1995). "Nature of the relaxation processes in the supercooled liquid and glassy states of some carbohydrates." The Journal of Physical Chemistry **99**(32): 12349-12354.

Gejl-Hansen, F. and Flink, J. M. (1977). "Freeze-dried carbohydrate containing oil-in-water emulsions: Microstructure and fat distribution." Journal of Food Science **42**(4): 1049-1055.

Godshall, M. A. (1995). Role of sucrose in retention of aroma and enhancing the flavor of foods. Sucrose - Properties and Applications. M. Mathlouthi and P. Reiser. London, Chapman & Hall**:** 248-263.

Gordon, M. and Taylor, J. S. (1952). "Ideal copolymers and second-order transitions in synthetic rubbers. I. Non-crystalline polymers." Journal of Applied Chemistry **2**: 493-500.

Greer, A. L. (1995). "Metallic Glasses." Science **267**(5206): 1947-1953.

Hachisuka, H., Takizawa, H., Tsujita, Y., Takizawa, A. and Kinoshita, T. (1991). "Gas transport properties in polycarbonate films with various unrelaxed volumes." Polymer **32**(13): 2382-2386.

Hall, D. B., Deppe, D. D., Hamilton, K. E., Dhinojwala, A. and Torkelson, J. M. (1998). "Probe translational and rotational diffusion in polymers near Tg: roles of probe size, shape, and secondary bonding in deviations from Debye-Stokes-Einstein scaling." Journal of Non-Crystalline Solids **235-237**: 48-56.

Hall, D. B., Hamilton, K. E., Miller, R. D. and Torkelson, J. M. (1999). "Translational and rotational diffusion of probe molecules in polymer films near Tg: Effect of hydrogen bonding." Macromolecules **32**(24): 8052-8058.

Hancock, B. C. and Shamblin, S. L. (2001). "Molecular mobility of amorphous pharmaceuticals determined using differential scanning calorimetry." Thermochimica Acta **380**(2): 95-107.

Hancock, B. C. and Zografi, G. (1997). "Characteristics and significance of the amorphous state in pharmaceutical systems." Journal of Pharmaceutical Sciences **86**(1): 1-12.

Haque, M. K., Kawai, K. and Suzuki, T. (2006). "Glass transition and enthalpy relaxation of amorphous lactose glass." Carbohydrate Research **341**(11): 1884-1889.

Hodge, I. M. (1986). "Adam-Gibbs formulation on nonlinearity in glassy-state relaxations." Macromolecules **19**: 936-938.

Hodge, I. M. (1987). "Effects of annealing and prior history on enthalpy relaxation in glassy polymers. 6. Adam-Gibbs formulation of nonlinearity." Macromolecules **20**(11): 2897-2908.

Hodge, I. M. (1995). "Physical aging in polymer glasses." Science **267**(5206): 1945-1947.

Hodge, I. M. (1996). "Strong and fragile liquids -- a brief critique." Journal of Non-Crystalline Solids **202**(1-2): 164-172.

Hough, L. (1971). The chemical reactivity of sucrose. Sugar - Chemical, Biological and Nutritional Aspects of Sucrose. J. Yudkin, J. Edelman and L. Hough. London, Butterworth**:** 49-59.

Huang, V. T., Haynes, L., Levine, H. and Slade, L. (1996). "Glass transitions in starch, gluten and bread as measured." Journal of Thermal Analysis and Calorimetry **47**(5): 1289-1298.

Imamura, K., Sakaura, K., Ohyama, K.-i., Fukushima, A., Imanaka, H., Sakiyama, T. and Nakanishi, K. (2006). "Temperature scanning FTIR analysis of hydrogen bonding states of various saccharides in amorphous matrixes below and above their glass transition temperatures." The Journal of Physical Chemistry B **110**(31): 15094-15099.

Izutsu, K.-i. and Aoyagi, N. (2005). "Effect of inorganic salts on crystallization of poly(ethylene glycol) in frozen solutions." International Journal of Pharmaceutics **288**(1): 101-108.

Jiang, B., Liu, Y., Bhandari, B. and Zhou, W. (2008). "Impact of caramelization on the glass transition temperature of several caramelized sugars. Part I: Chemical analyses." Journal of Agricultural and Food Chemistry **56**(13): 5138-5147.

Johari, G. P. and Goldstein, M. (1970). "Viscous liquids and the glass transition. II. Secondary relaxations in glasses of rigid molecules." The Journal of Chemical Physics **53**(6): 2372-2388.
Johari, G. P. and Goldstein, M. (1971). "Viscous liquids and the glass transition. III. Secondary relaxations in aliphatic alcohols and other nonrigid molecules." The Journal of Chemical Physics **55**(9): 4245-4252.

Kalichevsky, M. T. and Blanshard, J. M. V. (1992). "A study of the effect of water on the glass transition of 1:1 mixtures of amylopectin, casein and gluten using DSC and DMTA." Carbohydrate Polymers **19**(4): 271-278.

Kalichevsky, M. T., Blanshard, J. M. V. and Marsh, R. D. L. (1993). Applications of mechanical spectroscopy to the study of glassy biopolymers and related systems. The Glassy State in Foods. J. M. V. Blanshard and P. J. Lillford. Loughborough, Nottingham University Press**:** 133-156.

Karel, M., Buera, M. P. and Roos, Y. (1993). Effects of glass transitions on processing and storage. The Glassy State in Foods. J. M. V. Blanshard and P. J. Lillford. Loughborough, Nottingham University Press.

Kasapis, S., Al-Marhoobi, I. M. and Mitchell, J. R. (2003). "Testing the validity of comparisons between the rheological and the calorimetric glass transition temperatures." Carbohydrate Research **338**(8): 787-794.

Kasapis, S., Al-Marhoobi, I. M. A. and Giannouli, P. (1999). "Molecular order versus vitrification in high-sugar blends of gelatin and k-carrageenan." Journal of Agricultural and Food Chemistry **47**(12): 4944-4949.

Kasapis, S. and Sablani, S. S. (2005). "A fundamental approach for the estimation of the mechanical glass transition temperature in gelatin." International Journal of Biological Macromolecules **36**(1-2): 71-78.

Kawai, K., Hagiwara, T., Takai, R. and Suzuki, T. (2005). "Comparative investigation by two analytical approaches of enthalpy relaxation for glassy glucose, sucrose, maltose, and trehalose." Pharmaceutical Research **22**(3): 490-495.

Kessairi, K., Capaccioli, S., Prevosto, D., Lucchesi, M., Sharifi, S. and Rolla, P. A. (2008). "Interdependence of primary and Johari-Goldstein secondary relaxations in glass-forming systems." The Journal of Physical Chemistry B **112**(15): 4470-4473.

Kets, E. P. W., Ijpelaar, P. J., Hoekstra, F. A. and Vromans, H. (2004). "Citrate increases glass transition temperature of vitrified sucrose preparations." Cryobiology **48**(1): 46-54.

Khan, R. (1995). Sucrose: its potential as a raw material for food ingredients and for chemicals. Sucrose - Properties and Applications. M. Mathlouthi and P. Reiser. London, Chapman & Hall**:** 264-278.

Kollonitsch, V. (1970). Sucrose chemicals. Ipswich: The International Sugar Research Foundation.

Labuza, T., Roe, K., Payne, C., Panda, F., Labuza, T. J., Labuza, P. S. and Krusch, L. (2004). Storage ability of dried food systems: Influence of state changes during drying and storage. The 14th International Drying Symposium, San Paulo, Brazil.

Lakes, R. S. (2004). "Viscoelastic measurement techniques." Review of Scientific Instruments **75**(4): 797-810.

Lee, T., Lakes, R. S. and Lal, A. (2000). "Resonant ultrasound spectroscopy for measurement of mechanical damping: Comparison with broadband viscoelastic spectroscopy." Review of Scientific Instruments **71**(7): 2855-2861.

Liu, Y., Bhandari, B. and Zhou, W. (2006). "Glass transition and enthalpy relaxation of amorphous food saccharides: A review." Journal of Agricultural and Food Chemistry **54**(16): 5701-5717.

Liu, Y., Bhandari, B. and Zhou, W. (2007). "Study of glass transition and enthalpy relaxation of mixtures of amorphous sucrose and amorphous tapioca starch syrup solid by differential scanning calorimetry (DSC)." Journal of Food Engineering **81**(3): 599-610.

Longinotti, M. P., Mazzobre, M. F., Buera, M. P. and Corti, H. R. (2002). "Effect of salts on the properties of aqueous sugar systems in relation to biomaterial stabilization Part 2. Sugar crystallization rate and electrical conductivity behavior." Physical chemistry chemical physics **4**: 533-540.

Mansfield, M. L. (1993). An overview of theories of the glasstransition. The glassy state in foods. J. M. V. Blanshard and P. J. Lillford. Loughborough, Nottingham University Press**:** 103-122.

Mao, C., Chamarthy, S. P. and Pinal, R. (2006). "Time-dependence of molecular mobility during structural relaxation and its impact on organic amorphous solids: An investigation based on a calorimetric approach." Pharmaceutical Research **23**(8): 1906-1917.

Mapes, M. K., Swallen, S. F. and Ediger, M. D. (2006). "Self-diffusion of supercooled o-terphenyl near the glass transition temperature." Journal of Physical Chemistry B **110**(1): 507-511.

Mazzobre, M. F., Longinotti, M. P., Corti, H. R. and Buera, M. P. (2001). "Effect of salts on the properties of aqueous sugar systems, in relation to biomaterial stabilization. 1. Water sorption behavior and ice crystallization/melting." Cryobiology **43**(3): 199-210.

Mehl, P. M. (1993). "Calorimetric investigation of the glass transition and relaxation in 60:40 ethylene glycol: water : Part 1. Isothermal annealing experiments." Thermochimica Acta **213**: 177-197.

Meste, M. L., Champion, D., Roudaut, G., Blond, G. and Simatos, D. (2002). "Glass transition and food technology: A critical appraisal." Journal of Food Science **67**(7): 2444-2458.

Migliori, A. and Sarrao, J. L. (1997). Resonant Ultrasound Spectroscopy. New York: Wiley.

Moynihan, C. T., Crichton, S. N. and Opalka, S. M. (1991). "Linear and nonlinear structural relaxation." Journal of Non-Crystalline Solids **420**: 131-133.

Ngai, K. L. (1993). "Comparisons between coupling model and molecular dynamics simulation for local chain motions in bulk amorphous polymers." The Journal of Chemical Physics **98**(9): 7588-7592.

Ngai, K. L., Rendell, R. W. and Plazek, D. J. (1991). "Couplings between the cooperatively rearranging regions of the Adam--Gibbs theory of relaxations in glass-forming liquids." The Journal of Chemical Physics **94**(4): 3018-3029.

Nikolaidis, A. and Labuza, T. P. (1996). "Glass transition state diagram of a baked cracker and its relationship to gluten." Journal of Food Science **61**(4): 803-806.

Noel, T. R., Parker, R. and Ring, S. G. (1996). "A comparative study of the dielectric relaxation behaviour of glucose, maltose, and their mixtures with water in the liquid and glassy states." Carbohydrate Research **282**(2): 193-206.

Noel, T. R., Parker, R. and Ring, S. G. (2000). "Effect of molecular structure and water content on the dielectric relaxation behaviour of amorphous low molecular weight carbohydrates above and below their glass transition." Carbohydrate Research **329**(4): 839-845.

Noel, T. R., Parker, R., Ring, S. M. and Ring, S. G. (1999). "A calorimetric study of structural relaxation in a maltose glass." Carbohydrate Research **319**(1-4): 166-171.

Noel, T. R. and Ring, S. G. (1992). "A study of the heat capacity of starch/water mixtures." Carbohydrate Research **227**(0): 203-213.

Noel, T. R., Ring, S. G. and Whittam, M. A. (1993). Relaxations in supercooled carbohydrate liquids. The Glassy State in Foods. J. M. V. Blanshard and P. J. Lillford. Loughborough, Nottingham University Press**:** 173-187.

Nowakowski, C. M. and Hartel, R. W. (2002). "Moisture sorption of amorphous sugar products." Journal of Food Science **67**(4): 1419-1425.
Oguni, M., Hikawa, H. and Suga, H. (1990). "Enthalpy relaxation in vapor-deposited butyronitrile." Thermochimica Acta **158**(1): 143-156.

Oldenhof, H., Wolkers, W. F., Fonseca, F., Passot, S. and Marin, M. (2005). "Effect of sucrose and maltodextrin on the physical properties and survival of air-dried *Lactobacillus bulgaricus*: An in situ Fourier transform infrared spectroscopy study." Biotechnology Progress **21**: 885-892.

Ottenhof, M.-A., MacNaughtan, W. and Farhat, I. A. (2003). "FTIR study of state and phase transitions of low moisture sucrose and lactose." Carbohydrate Research **338**(21): 2195-2202.

Perez, J. (1994). The theories of liquid-glass transition. Water in foods. P. Fito, A. Mulet and B. M. McKenna. New York, Elsevier Applied Science**:** 89-114.

Perez, S. (1995). The structure of sucrose in the crystal and in solution. Sucrose - Properties and Applications. M. Mathlouthi and P. Reiser. London, Chapman & Hall**:** 11-32.

Pravinata, L. C., You, Y. and Ludescher, R. D. (2005). "Erythrosin B phosphorescence monitors molecular mobility and dynamic site heterogeneity in amorphous sucrose." Biophysical Journal **88**(5): 3551-3561.

Raja, K. C. M., Sankarikutty, B., Sreekumar, M., Jayalekshmy, A. and Narayanan, C. S. (1989). "Material characterization studies of maltodextrin samples for the use of wall material." Starch - Stärke **41**(8): 298-303.

Reid, D. S., Hsu, J. and Kerr, W. (1993). Calorimetry. The glassy state in foods. J. M. V. Blanshard and P. J. Lillford. Loughborough, Nottingham University Press**:** 123-132.

Roe, K. D. and Labuza, T. P. (2005). "Glass transition and crystallization of amorphous trehalose-sucrose mixtures." International Journal of Food Properties **8**(3): 559 - 574.

Roland, C. M. (2010). "Relaxation phenomena in vitrifying polymers and molecular liquids." Macromolecules **43**(19): 7875-7890.

Roos, Y. (1993). "Melting and glass transitions of low molecular weight carbohydrates." Carbohydrate Research **238**: 39-48.

Roos, Y. (1995). Phase transitions in foods. San Diego: Academic Press.

Roos, Y. and Karel, M. (1991). "Plasticizing effect of water on thermal behavior and crystallization of amorphous food models." Journal of Food Science **56**(1): 38-43.

Roos, Y. and Karel, M. (1991). "Water and molecular weight effects on glass transitions in amorphous carbohydrates and carbohydrate solutions." Journal of Food Science **56**(6): 1676-1681.

Roudaut, G., Maglione, M. and Le Meste, M. (1999). "Relaxations below glass transition temperature in bread and its components." Cereal Chemistry **76**(1): 78-81.

Roudaut, G., Simatos, D., Champion, D., Contreras-Lopez, E. and Le Meste, M. (2004). "Molecular mobility around the glass transition temperature: a mini review." Innovative Food Science & Emerging Technologies **5**(2): 127-134.

Roudaut, G. L., Maglione, M., van Dusschoten, D. and Le Meste, M. (1999). "Molecular mobility in glassy bread: A multispectroscopy approach." Cereal Chemistry **76**(1): 70-77.

Schawe, J. E. K. (2002). "About the changes of heat capacity, glass transition temperature and relaxation time during the polymerization reaction of thermosetting systems." Thermochimica Acta **391**(1-2): 279-295.

Schrooyen, P. M. M., van der Meer, R. and Kruif, C. G. (2001). "Mricroencapsulation: its application in nutrition." Proceedings of the Nutrition Society **60**: 475-479.

Seo, J.-A., Kim, S. J., Kwon, H.-J., Yang, Y. S., Kim, H. K. and Hwang, Y.-H. (2006). "The glass transition temperatures of sugar mixtures." Carbohydrate Research **341**(15): 2516-2520.

Shalaev, E. Y., Franks, F. and Echlin, P. (1996). "Crystalline and amorphous phases in the ternary system water-sucrose-sodium chloride." Journal of Physical Chemistry **100**: 1144-1152.

Shalaev, E. Y. and Zografi, G. (1996). "How does residual water affect the solid-state degradation of drugs in the amorphous state." Journal of Pharmaceutical Sciences **85**: 1137-1141.

Shamblin, S. L., Tang, X., Chang, L., Hancock, B. C. and Pikal, M. J. (1999). "Characterization of the time scales of molecular motion in pharmaceutically important glasses." The Journal of Physical Chemistry B **103**(20): 4113-4121.

Shamblin, S. L., Taylor, L. S. and Zografi, G. (1998). "Mixing behavior of colyophilized binary systems." Journal of Pharmaceutical Sciences **87**(6): 694-701.

Shamblin, S. L. and Zografi, G. (1998). "Enthalpy relaxation in binary amorphous mixtures containing sucrose." Pharmaceutical Research **15**(12): 1828-1834.

Shinyashiki, N., Shinohara, M., Iwata, Y., Goto, T., Oyama, M., Suzuki, S., Yamamoto, W., Yagihara, S., Inoue, T., Oyaizu, S., Yamamoto, S., Ngai, K. L. and Capaccioli, S. (2008). "The glass transition and dielectric secondary relaxation of fructose-water mixtures." The Journal of Physical Chemistry B **112**(48): 15470-15477.

Shirke, S. and Ludescher, R. D. (2005). "Molecular mobility and the glass transition in amorphous glucose, maltose, and maltotriose." Carbohydrate Research **340**(17): 2654-2660.

Simha, R. and Boyer, R. F. (1962). "On a general relation involving the glass temperature and coefficients of expansion of polymers." The Journal of Chemical Physics **37**(5): 1003-1007.

Slade, L. and Levine, H. (1988). "Non-equilibrium behavior of small carbohydrate-water systems." Pure and Applied Chemistry **60**(12): 1841-1864.

Slade, L. and Levine, H. (1993). The glassy state phenomenon in food molecules. The glassy state in foods. J. M. V. Blanshard and P. J. Lillford. Loughborough, Nottingham University Press**:** 35-101.

Slade, L. and Levine, H. (1995). Glass transitions and water-food structure interactions. Advances in Food and Nutrition Research. J. E. Kinsella. San Diego, Academic.

Sperling, L. H. (1986). Introduction to physical polymer science. New York: John Wiley & Sons.

Stacey, M. and Barker, S. A. (1960). Polysaccharides of micro-organisms. London: Oxford University Press.

Starkweather, H. W. and Avakian, P. (1989). "b-Relaxations in phenylene polymers." Macromolecules **22**(10): 4060-4062.

Starkweather, J., H.W. (1988). "Non-cooperative relaxations." Macromolecules **21**: 1798-1802.

Struik, L. C. E. (1978). Physical aging in amorphous polymers and other materials. Amsterdam: Elsevier.

Suga, H. and Seki, S. z. (1974). "Thermodynamic investigation on glassy states of pure simple compounds." Journal of Non-Crystalline Solids **16**(2): 171-194.

Sun, Y., Xi, H., Ediger, M. D. and Yu, L. (2008). "Diffusionless crystal growth from glass has precursor in equilibrium liquid." Journal of Physical Chemistry B **112**(3): 661-664.

Surana, R., Pyne, A., Rani, M. and Suryanarayanan, R. (2005). "Measurement of enthalpic relaxation by differential scanning calorimetry - effect of experimental conditions." Thermochimica Acta **433**(1-2): 173-182.

Taylor, L. S. and Zografi, G. (1998). "Sugar-polymer hydrogen bond interactions in lyophilized amorphous mixtures." Journal of Pharmaceutical Sciences **87**(12): 1615-1621.

Tong, P. and Zografi, G. (1999). "Solid-state characteristic of amorphous sodium indomethacin relative to its free acid." Pharmaceutical Research **16**(8): 1186-1192.

Tsukushi, I., Yamamuro, O. and Suga, H. (1994). "Heat capacities and glass transitions of ground amorphous solid and liquid-quenched glass of tri-O-methyl-β-cyclodextrin." Journal of Non-Crystalline Solids **175**(2-3): 187-194.

van den Dries, I. J., van Dusschoten, D. and Hemminga, M. A. (1998). "Mobility in maltose-water glasses studied with 1H NMR." Journal of Physical Chemistry B **102**(51): 10483-10489.

Wang, Y. C. and Lakes, R. S. (2003). "Resonant ultrasound spectroscopy in shear mode." Review of Scientific Instruments **74**(3): 1371-1373.

Wetton, R. E. (1984). "Dynamic mechanical method in the characterization of solid polymers." Polymer Testing **4**(2-4): 117-129.

Williams, G. (1991). "Molecular motion in glass-forming systems." Journal of Non-Crystalline Solids **131-133**: 1-12.

Williams, M. L., Landel, R. F. and Ferry, J. D. (1955). "The temperature dependence of relaxation mechanisms in amorphous polymers and other glass-forming liquids." Journal of the American Chemical Society **77**(14): 3701-3707.

Wolkers, W. F., Oldenhof, H., Alberda, M. and Hoekstra, F. A. (1998). "A Fourier transform infrared microspectroscopy study of sugar glasses: application to anhydrobiotic higher plant cells." Biochimica et Biophysica Acta (BBA) - General Subjects **1379**(1): 83-96.

Wolkers, W. F., Oliver, A. E., Tablin, F. and Crowe, J. H. (2004b). "A Fourier-transform infrared spectroscopy study of sugar glasses." Carbohydrate Research **339**(6): 1077-1085.

Wurm, A. and Schick, C. (2003). "Reversing and nonreversing contributions to polymer melting " Colloid & Polymer Science **281**(2): 113-122.

You, Y. and Ludescher, R. D. (2008a). "The effect of salts on molecular mobility in amorphous sucrose monitored by erythrosin B phosphorescence." Carbohydrate Research **343**(15): 2641-2649.

You, Y. and Ludescher, R. D. (2008b). "The effect of sodium chloride on molecular mobility in amorphous sucrose detected by phosphorescence from the triplet probe erythrosin B." Carbohydrate Research **343**(2): 350-363.

Young, R. J. and Lovell, P. A. (1991). Introduction to polymers. 2. Cheltenham: Stanley Thornes.

Yu, L. (2001). "Amorphous pharmaceutical solids: preparation, characterization and stabilization." Advanced Drug Delivery Reviews **48**(1): 27-42.

Zallen, R. (1983). The physics of amorphous solids. New York: John Wiley & Sons.

CHAPTER 2

THERMAL EVALUATION OF SUCROSE-MALTODEXTRIN-Na CITRATE BIOGLASS

2.1 Abstract

Sucrose-maltodextrin-Na citrate bioglass model systems were characterized using modulated differential scanning calorimetry (MDSC). Samples were formulated with sucrose/maltodextrin ratios (SC/MD) of 7:3, 5:5 and 3:7 (by mass), and Na citrate/sucrose ratios (NaCit/SC) of 0, 0.1 and 0.2 (by mole). Two levels of residual moisture content, low (0.27 – 0.35 %wb) and high (2.83 – 4.40 %wb), were studied. It was found that moisture content and components of the systems played significant role on their glass transition characteristics and enthalpy relaxation behavior. On average, glass transition temperatures (T_g) of the systems with SC/MD of 7:3, 5:5 and 3:7 were approximately 77, 84 and 101 °C, respectively. T_g values tended to increase when Na citrate was added, with a noticeable increase occurring in 7:3 SC/MD system at low moisture content. The addition of moisture had a significant plasticization effect on the bioglass; T_g decreased from approximately 106 °C to 67 °C when moisture content was increased from low to high level. The analysis of

DSC thermograms suggests that water molecules may interfere with intermolecular interactions between glass-forming molecules causing changes in molecular mobility of bioglass matrix. Isothermal aging experiments were carried out on low-moisture samples with the degree of undercooling in a range of approximately 12 to 57 °C and aging times (t_a) of 8, 20, 47 and 71 h. In general, the Kohlrausch-Williams-Watts (KWW) decay function fit well with the experimental enthalpy relaxation data. The β values spread over a broad range. The enthalpy relaxation time (τ^{KWW}) and the time required for 50 % completion of the theoretical possible maximum enthalpy relaxation at a constant temperature ($t_{\phi(t)=0.5}$) increased with increasing maltodextrin concentration; similar effect on τ^{KWW} and $t_{\phi(t)=0.5}$ was found when the aging temperature (T_a) was lowered. In the system with high sucrose and Na citrate concentration (SC/MD of 7:3 with NaCit/SC of 0.2), a dramatic increase in τ^{KWW} and $t_{\phi(t)=0.5}$ was observed upon slightly decreasing T_a. This system also exhibited the greatest apparent activation energy (E_a). The findings revealed the ability of Na citrate to enhance the stability of low-moisture bioglass. Na citrate may modulate the system by primarily interacting with sucrose and form large less-mobile clusters, which helps to improve T_g and restrict matrix mobility.

2.2 Introduction

A number of common food processes, such as drying, freezing, grinding, extrusion etc. yield products in the form of amorphous or partially amorphous (Liu et al., 2007). This class of products usually faces stability issues. For the most part, glassy products possess

considerably low level of water activity and so their microbial stability is not a significant concern; however, their chemical and structural stabilities are (Poirier-Brulez et al., 2006).

Glass transition temperature (T_g) is an important property of amorphous materials. The T_g has been found to relate with a number of physiochemical changes in dried food products, for instance crystallization, collapse, stickiness. Accordingly, the T_g has become a good indicator of quality changes in food products during storage (Bhandari and Howes, 1999; Le Meste et al., 2002). However, in some cases, temperature and moisture content related changes in food and biomaterial properties were not satisfactorily explained using solely the concept of glass transition (Champion et al., 2000).

The glassy state is thermodynamically out-of-equilibrium. Therefore, glassy materials progressively change over time towards equilibrium when stored in the region of temperature below T_g due to the structural relaxation process. This process is believed to be due to the residual molecular motions which allow glassy materials to evolve to a lower state of energy (Struik, 1976). As a result, this process leads to loss of volume and enthalpy, and a decrease in molecular mobility, which then manifest in to different changes in macroscopic or physical properties—the so called physical aging—such as toughening, lower diffusion, increased density or decreased oxygen permeability (Struik, 1976; Boersma et al., 2003; Surana et al., 2005). Structural relaxation or physical aging is a common phenomenon for all glassy materials, both organic and inorganic glasses. Struik has stated that nearly all aspects of physical aging can be explained using the concept of free volume (Struik, 1976). Note that in literature, the terms structural relaxation, physical aging, or enthalpy relaxation may be used interchangeably (Liu et al., 2007).

In fact, there are several modes of relaxation in a glass matrix, namely, the primary or α- relaxation; the secondary, including β- and γ-, relaxations. However only the α- and β-relaxations have been widely studied. The α-relaxation is associated with the motion of the whole molecule and relates to the structural relaxation. The β-relaxation is believed to primarily correlate with the motions uncoupled to that of the entire molecule, i.e., the intra-molecular motions, such as the rotation of a side chain on a polymer or a localized motion of a small group of atoms on a large molecule (Kawakami and Pikal, 2005). The β-relaxation of this origin is naturally not relevant to the structural relaxation (Kessairi et al., 2008). However, Johari and Goldstein (Johari and Goldstein, 1970) discovered another class of β-relaxation, which originated by the local motions of the entire molecule in rigid molecular glass formers. This type of secondary relaxation was then named the Johari-Goldstein β-relaxation (Ngai and Paluch, 2004) and it is believed to be relevant to the structural relaxation or the glass transition (Kessairi et al., 2008). It is usually the slowest secondary relaxation (Shinyashiki et al., 2008). In polysaccharide systems β-relaxation could also arise from local conformation changes of the main chain (Bidault et al., 2005).

For the most part, however, structural relaxation is generally regarded as a continuation of α-relaxation or glass transition (Champion et al., 2000; Liu et al., 2006). Given their thermal history and degree of non-equilibrium, the evolution of glasses towards equilibrium is usually predictable (Yu, 2001). However, the exact origins of relaxation behavior in complex systems including foods are difficult to define (Liu et al., 2006) and is still be a matter of debate.

The rate of structural relaxation is mainly proportional to the degree of undercooling —the difference between the aging temperature and the T_g. The presence of relaxation in amorphous materials below their T_g values is a clear evidence for the ongoing molecular mobility of materials in their glassy state. The possible range of temperature over which structural relaxation exists is extended from the T_g down to the first secondary relaxation temperature, conventionally designated as T_β, where secondary motions become frozen (Struik, 1976). Structural relaxation can be studied using a number of techniques with different time scales. By observing the time evolution or frequency dependence of material properties, e.g., enthalpy, volume, viscosity, shear modulus, dipole relaxation, depolarization current, or nuclear spin relaxation, the characteristic time can be then obtained (Yu, 2001).

Molecular mobility of amorphous food and biological materials below their T_g is usually investigated by studying their enthalpy relaxation. Differential scanning calorimetry (DSC) has long been used for studying glass transition and enthalpy relaxation, as either the primary or the complementary measurement (Gangasharan and Murthy, 1995; Shamblin and Zografi, 1998; Desobry et al., 1999; Vanhal and Blond, 1999; Craig et al., 2000; Borde et al., 2002; Tong et al., 2002; Kilmartin et al., 2004; Wolkers et al., 2004b; Izutsu et al., 2005; Kawai et al., 2005; Kilburn et al., 2005; Haque et al., 2006; Mao et al., 2006; Liu et al., 2007; Kadoya et al., 2008; Farahnaky et al., 2009). The extent of structural relaxation or the enthalpy relaxation is usually measured as the recovery of the lost enthalpy—the excess enthalpy frozen in when a liquid undergoes glass transition—associated with the glass transition event during the heating cycle of the aged glass. The measurement of enthalpy recovery is generally carried out on a sample which has been aged or stored at a temperature below T_g (Surana et al., 2005; Poirier-Brulez et al., 2006). Previous thermal history of the

sample is practically erased prior to the aging process simply by heating an amorphous sample up to the temperature at least 40 K above its T_g (Urbani et al., 1997; Liu et al., 2007).

In many cases, amorphous compounds with similar T_g exhibit substantially different crystallization tendencies at the same environmental conditions (Mao et al., 2006). This would be due to the difference in molecular relaxation dynamics of the amorphous matrices. Consequently, the information about enthalpy relaxation behavior of food and biological materials along with their T_g is important and necessary for predicting the stability of food products or for designing the products with the desirable functional characteristics.

Even though the mechanisms of molecular processes taking place within a glass matrix have not been well established, the effects of matrix compositions on the properties and behaviors of materials in the glassy state are clearly observed (Poirier-Brulez et al., 2006). Nevertheless, not much information on the enthalpy relaxation of food and biological materials has been published in the past decade. This experiment was aimed at investigating the dependence of calorimetric properties and behaviors of the sucrose-maltodextrin based bioglass systems on sucrose, maltodextrin, Na citrate and moisture content using the modulated DSC technique. It is expected to provide information of both theoretical and practical importance.

2.3 Materials and Methods

2.3.1 Materials

Sucrose (crystalline/NF/EP/BP/JP) and trisodium citrate dihydrate were purchased from Fisher Scientific (Fair Lawn, NJ). Maltodextrin powder (dextrose equivalent, DE

maximum 20 %, total solids min. 90 %, lead 0.5 mg/kg, residue on ignition 0.5 %, sulfur dioxide 10 mg/kg, protein 0.5 %) was purchased from Spectrum Chemical Manufacturing Corporation (Gardena, CA). All ingredients were used as received without further purification.

2.3.2 Experimental design

The experimental factors and their levels in this study are listed in Table 2.1. Details of experimental treatments are provided in Table 2.2. Two replicates were prepared for each treatment, and the order of experiment was completely randomized.

Table 2.1 Factors and their levels in the experimental design

Factors	Levels		
	-1	0	1
Sucrose/Maltodextrin (SC/MD, mass)	7:3	5:5	3:7
Na citrate/Sucrose (NaCit/SC, mole)	0	0.1	0.2
RH of equilibrating atmosphere	Low	-	High

Table 2.2 Experimental design

Treatment code	Equilibrating atmosphere	Na Citrate: Sucrose	Sucrose: Maltodextrin	Sucrose[c]	Maltodextrin[c]	Na Citrate[c]
Trt-7300	Low RH (~1%)	0	7:3	70	30	0
Trt-5500		0	5:5	50	50	0
Trt-3700		0	3:7	30	70	0
Trt-7301		0.1	7:3	66.78	28.62	4.61
Trt-5501		0.1	5:5	48.33	48.33	3.33
Trt-3701		0.1	3:7	29.39	68.58	2.03
Trt-7302		0.2	7:3	63.84	27.36	8.81
Trt-5502		0.2	5:5	46.77	46.77	6.45
Trt-3702		0.2	3:7	28.81	67.22	3.97
Trt-7300	High RH (~11%)	0	7:3	70	30	0
Trt-5500		0	5:5	50	50	0
Trt-3700		0	3:7	30	70	0
Trt-7301		0.1	7:3	66.78	28.62	4.61
Trt-5501		0.1	5:5	48.33	48.33	3.33
Trt-3701		0.1	3:7	29.39	68.58	2.03
Trt-7302		0.2	7:3	63.84	27.36	8.81
Trt-5502		0.2	5:5	46.77	46.77	6.45
Trt-3702		0.2	3:7	28.81	67.22	3.97

c: % mass (dry basis)

2.3.3 Sample preparation

Ingredients were weighed according to the predetermined amount for each formulation as given in Table 2.2 and dissolved with deionized water yielding a total volume of approximately 150 mL. The solutions were then stirred at 150 rpm using a magnetic stirrer for 3 h prior to heat evaporation process. The sample solutions were continuously stirred while heating beginning at 145 °C in the initial stage and gradually increased up to 175 °C to bring the moisture content down to approximately 4.5% – 9%. These temperatures were that if the hot plate setting and the actual temperature of the solution would be lower. The progress of moisture reduction was monitored by weighing. This level of moisture content was the lowest range attainable by heat evaporation process in this experiment. At very low level of moisture content, the samples with high maltodextrin concentration became highly viscous and moisture evaporation was extremely slow. High viscosity of the solution also made it difficult for the magnetic stirrer to function, virtually stopping it at the very end of heat evaporation process. Note that the heating step in this experiment was selected to avoid the decomposition of sucrose, which reportedly occurs near the vicinity of melting of many sugars (Jiang et al., 2008). Sucrose melts at around 186 °C. Once moisture content reached the level mentioned above, the molten mixtures were spread over a flat Teflon surface allowing them to rapidly cool down to room temperature. The samples were then transferred to a desiccator before subsequent grinding process.

Glass samples were ground and sieved through a 170-mesh screen, corresponding to a 90-μm opening, to obtain samples as a fine powder. Samples were spread evenly as a thin layer on aluminum trays, which were then hung underneath the lid of hermetically sealed glass jars. Each of the nine samples in the first group, labeled as “Low RH” equilibrating

atmosphere in Table 2.2, was stored in an individual glass jar containing phosphorus pentoxide (P_2O_5) to maintain the relative humidity (RH) of the enclosed atmosphere at approximately 1 %. Each of the other nine samples in the second group, labeled as "High RH" equilibrating atmosphere in Table 2.2, was stored in individual glass jar containing saturated lithium chloride (LiCl) solution to maintain the RH at around 11 %. Samples were stored for at least three months to allow for equilibration. The moisture content of the samples was continually monitored by weighing and Karl Fischer titration.

2.3.4 Moisture determination

After several months of equilibration, the moisture content of samples was measured via the Karl Fischer titration technique. Measurements were conducted using the Volumetric Karl Fischer titrator—model 795 KFT Titrino (Metrohm Ltd., Herisau, Switzerland) equipped with the 703 Ti Stand and a temperature control unit. The stand provided agitation during the measurement. The temperature control unit supplied controlled-temperature water flowing around the measuring vessel which contained approximately 50 mL of 2:1 MeOH:Formamide solvent. The measurements were done at 50°C as recommended for most confectionary products. Calibration or adjustment factor was determined using deionized (DI) water prior to the measurements on samples. The measurement on DI water was repeated five or six times and the adjustment factor was calculated using Equation 2.1. The sizes of ground sample ranged from 0.07 g to 0.23 g with an average value of 0.15 g. Each weighed sample was directly loaded into the vessel and dissolved for 4 min before starting the measurement. At least two measurements were carried out for each sample. True

moisture content of sample was then determined by multiplying the measured value with the adjustment factor.

$$Adjustment\ \ factor = \frac{100}{Avg.\ moisture\ \ measures\ \ for\ \ DI\ \ water} \tag{2.1}$$

2.3.5 Calorimetric measurements

2.3.5.1 DSC settings

The calorimetric measurements were carried out using a modulated differential scanning calorimeter (MDSC) equipped with a refrigerated cooling system (Model 2920, TA Instruments, New Castle, DE). Nitrogen was used as purge gas to prevent condensation and control the atmosphere within DSC cell at the flow rate of 35 mL/min. It was also used as a cooling medium flowing through the cooling unit at the rate of 150 mL/min. A wide range of temperature scanning rates, from 0.1 K/min to 20 K/min, have been used in studies reported literature. Since calorimetric T_g is sensitive to the temperature scan rate, both during heating and cooling, Angell suggested a rate of 10 K/min to allow more meaningful comparison with the results obtained from spectroscopy techniques such as dielectric ($\tau_{dielectric}$=100 s) or dynamic mechanical (f_{max}=0.001 Hz) (Angell, 1997). This heating rate has also been suggested to minimize the impact of experimental conditions on enthalpy relaxation determination (Liu et al., 2006). Hence, a heating rate of 10 °C/min was selected along with the cooling rate of 15 °C/min for all experiments. The temperature and heat flow calibrations were performed on the MDSC system using indium (melting point of 156.6 °C), tin (melting

point of 231.93 °C), and distilled water (melting point of 0.0 °C). Temperature modulation amplitude was set as ±1 °C with a period of 60 s.

2.3.5.2 DSC sample preparation

Hermetic aluminum pans and lids were weighed prior to be filled with powder samples. The sample filling was done within a glove box flushed with Nitrogen gas. The relative humidity inside the glove box was brought down to approximately 5% before samples were taken out form the storage bottles. Samples were filled into the pans, closed with the pre-paired lid, and tightly sealed using a sample press. The sealed sample pans were then weighed and the sample mass was calculated, which were in the range of 10 to 17 mg.

2.3.5.3 DSC measurements

A sealed empty pan was used as a reference placing it inside the DSC cell along with the pan containing the measurement glass sample. Samples were subjected to two cycles of heating and cooling temperature scans, which covered the range of approximately 40 °C below the onset-T_g up to approximately 40 °C above the offset-T_g of the each sample. The T_g values of were determined from the second cycle.

Aging experiment was conducted on samples which were equilibrated in the atmosphere of P_2O_5. Before aging, samples were subjected to two cycles of heating-cooling and then heated up again to the designated aging temperatures (T_a). This temperature program is schematically represented in Figure 2.1. The first temperature scan was to erase thermal history of the samples. The T_g and the onset, the midpoint, and the offset, as well as

the change in heat capacity at glass transition ($\Delta C_{p,GT}$) values were determined from the second temperature scan. After completing all temperature scans by DSC, samples were transferred to store in glass bottles containing P_2O_5 and isothermally aged in an oven at different T_a for various aging times (t_a) of 8, 21, 47 and 71 h. Since T_g of samples depends mainly on the concentration of sucrose and maltodextrin, the designated T_a for treatments with different SC/MD were not entirely similar. The T_a was considered within a range of approximately T_g – 40 °C for most of the samples. According to this criterion, the T_a values shown in Table 2.3 were chosen. At the end of the aging period, the samples were removed from the oven and subjected to temperature scan again by cooling down to approximately 40 °C below T_g and heating up to approximately 40 °C above T_g (Figure 2.1). The endothermic recovery peak located at the end of glass transition region was analyzed from the DSC thermogram obtained in this temperature scan. This endothermic peak reflects the enthalpy relaxation of sample after aging. The area of endothermic peak or enthalpy recovery (ΔH) was determined by constructing a tangent to the thermogram from the temperature region above T_g and extrapolating backwards to lower the temperature. These methods for determining T_g and ΔH (Figure 1.5) are similar to that of Shamblin and Zografi (Shamblin and Zografi, 1998) and were done using the Thermal Analysis software (TA Instruments Inc., New Castle, DE).

Three measurements were made at each level of T_g and t_a. The whole scheme of aging or enthalpy relaxation experiment is presented in Figure 2.2.

Table 2.3 Aging temperatures (T_a) for treatments with different levels of SC/MD

SC/MD	T_g (°C)
7:3	60, 70, 75
5:5	70, 75, 80
3:7	80, 85, 90

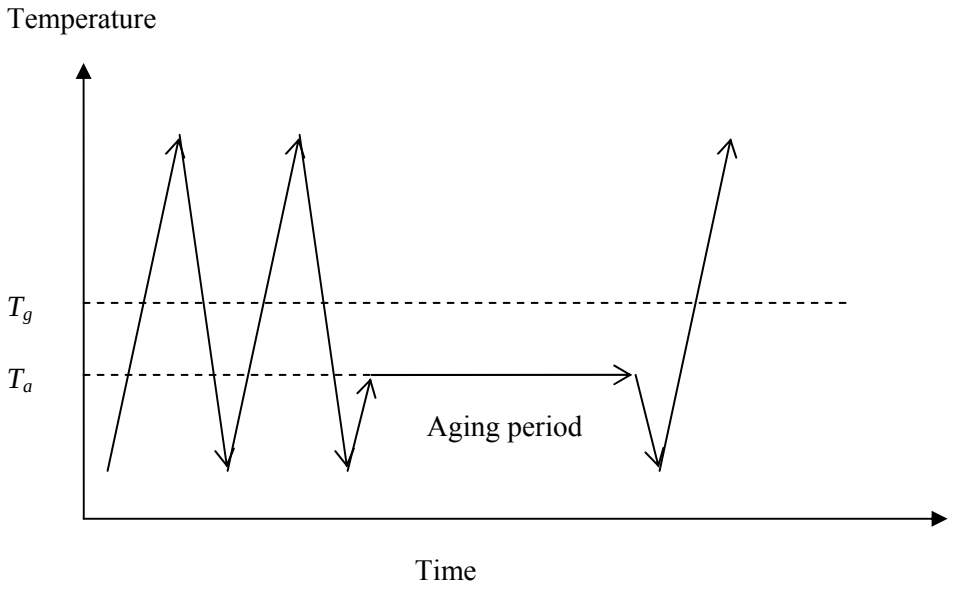

Figure 2.1 Schematic representation of the temperature program used in the measurement of enthalpy relaxation.

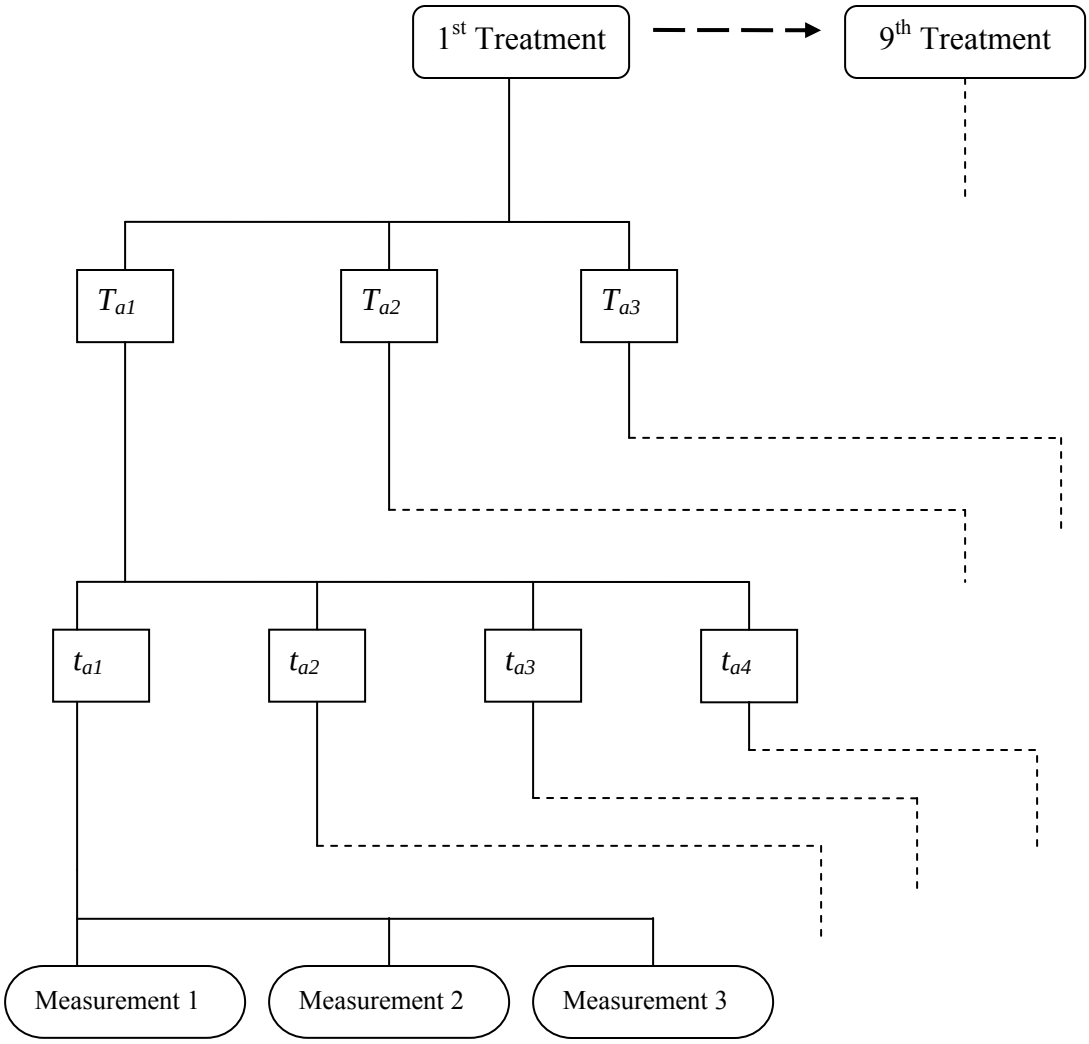

Figure 2.2 The scheme of DSC test runs for aging experiments.

2.3.6 Statistical analysis

The results were statistically analyzed using the IBM SPSS Statistics 19 computer package. The analysis of variance (ANOVA F-test) was first conducted using the general linear model (GLM). A post-hoc analysis was then performed when any significant effect was detected. Comparisons using the Least Significant Difference (LSD) for one pair comparison or the Tukey's range test for simultaneous multiple comparisons were conducted at a significance level (α) of 0.05. The Tukey test is preferable since it helps to control the experimentalwise or family error rate—the overall error rate—at the selected α level (Montgomery, 2005).

2.4 Results and Discussion

2.4.1 Moisture content

The method of sample preparation used in this experiment yielded bioglass samples with considerably low level of residual moisture content. The moisture content of samples equilibrated in low- and high-RH atmosphere were in the range of 0.27 – 0.35 %wb (mean value = 0.31 ± 0.04 %wb) and 2.83 – 4.4 %wb (mean value = 3.64 ± 0.52 %wb), respectively (Figure 2.3). The mean values were significantly different statistically (Appendix. 2.1). The follow-up analysis (Table 2.4) indicated that the moisture contents of samples equilibrated in low-RH atmosphere were not significantly different ($p = 0.906$) while this was not the case for those samples equilibrated in high-RH atmosphere ($p < 0.001$). Additional details of statistical analyses are given in Appendix. 2.1.

Even though the residual moisture contents of the samples equilibrated at high-RH atmosphere were not uniform, the magnitude of difference was only marginal. Besides, this level of moisture content still falls under the same range with that of low moisture commercial food products, e.g., common snacks (Sheppard et al., 1978; AquaLab, 2012) or cereals (Windham et al., 1997; Archibald and Kays, 2000). It was found that amorphous sucrose prepared by freeze drying a solution and hydrating the freeze-dried sample over saturated LiCl solution yielded a comparable level of residual moisture content (Ottenhof et al., 2003).

In large part, the residual moisture content of the samples equilibrated in high-RH atmosphere tended to increase with increasing maltodextrin concentration or Na citrate concentration. The average values of residual moisture content for the samples with SC/MD of 7:3, 5:5 and 3:7 were approximately 3.10, 3.64 and 4.20 %wb, respectively. For samples with NaCit/SC of 0, 0.1 and 0.2, the average values were around 3.39, 3.69 and 3.85 %wb, respectively.

Heat evaporation technique used was primarily to avoid any decomposition of components in the system. During sample preparation, we noticed the increasing viscosity of the melt with the increase of maltodextrin concentration. With the selected heating scheme—time and temperature, the final moisture content of samples with high maltodextrin concentration after heat evaporation did not reach the pre-determined moisture content of 4.5 %wb. Even after long-time equilibration in the atmosphere over saturated LiCl solution, the residual moisture content of the sample did not reach the same level as that of the samples with lower maltodextrin concentration. Maltodextrin consists of glucose polymers with a broad spectrum of chain lengths and molecular weights (McPherson and Seib, 1997;

Chronakis, 1998). These bulky molecules lead to an increased viscosity of a bioglass system. Also, the three-dimensional network of glucose polymers in maltodextrin possesses a high degree of water holding capacity (Chronakis, 1998). Accordingly, high maltodextrin concentration may result in some adverse effects on the application of a bioglass system. Firstly, a high viscosity would cause a systematic difficulty in certain processes such as extrusion cooking. Secondly, the water held inside the matrix of glucose polymers could in turn plasticize the system resulting in a decrease of T_g.

As far as salt is concerned, sodium (Na^+) as an electrolyte ion could strongly bind water molecules, and so the residual moisture content of glass samples was dependent on sodium citrate concentration. A similar result was found in a freeze-dried amorphous of NaCl-sucrose mixture (You and Ludescher, 2008b). Also for the systems formed with larger glass-forming molecules, i.e., amorphous potato and cassava starches prepared by extrusion cooking, freeze-drying and then equilibrating over different super saturated salt solutions, the presence of NaCl made the systems more hygroscopic. The effect of NaCl was more dramatic when the samples were equilibrated at relatively high RH – more than 70% (Farahnaky et al., 2009).

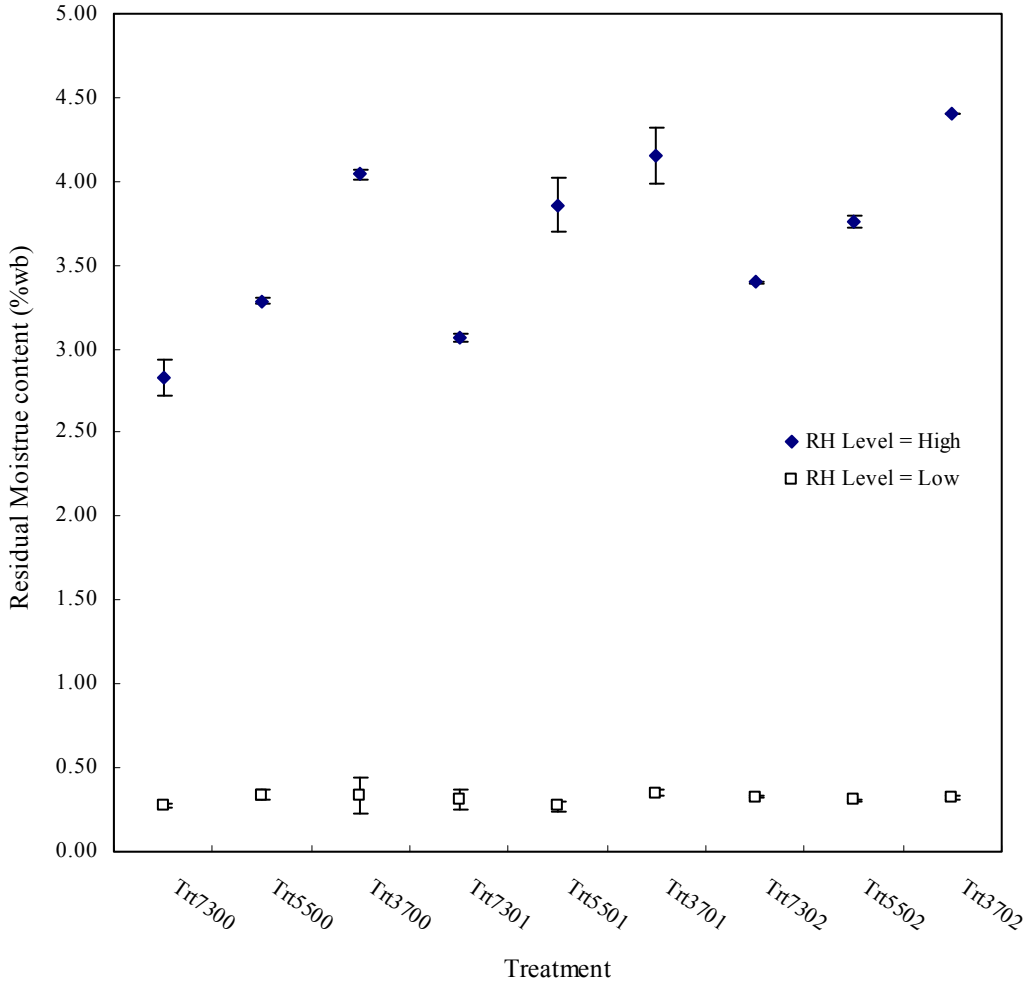

Figure 2.3 Residual moisture content of bioglass samples equilibrated in the atmosphere of low and high RH. Data are means of two replicates, and the error bars reflect standard deviation. The first two figures appearing in the names of treatments indicate SC/MD, e.g., 73 represents a ratio of 7/3; the last two digits indicate NaCit/SC, e.g., 01 represents a ratio of 0.1.

Table 2.4 Summary of the follow-up ANOVA table for residual moisture content analysis

Source	Type III Sum of Squares	df	Mean Square	F	Sig.
Treatment	2.332	8	.291	62.572	.000
RH_Level	99.634	1	99.634	21388.265	.000
Treatment * RH_Level	2.161	8	.270	57.982	.000
Treatment @ RH_Level					
Treatment @ RH_Level=Low	.012	8	.002	0.4	.906
Treatment @ RH_Level=High	4.480	8	.560	112	.000
Error	.084	18	.005		
Corrected Total	104.210	35			

2.4.2 Glass transition temperature

The extent of relaxation is known to affect T_g value of amorphous materials, particularly when measured with conventional DSC (Wungtanagorn and Schmidt, 2001; Surana et al., 2005). Accordingly, representing the T_g values of samples stored at different times and temperatures is inappropriate. Thus T_g values reported here are those collected from samples before aging. In addition, two measuring techniques were applied to obtain more precise values of T_g. First, each sample was heated to around 40 °C above its T_g as suggested in literature (Liu et al., 2006). Second, the MDSC technique used this study allowed the decomposition of the total heat flow into reversing and non-reversing components. This way, the reversible transitions (glass transition, melting) can be observed separately from non-reversible transitions (enthalpy recovery, evaporation) and the T_g values could be determined from the reversing heat flow signal without interferences from the endothermic peak associated with enthalpy recovery, or other peaks induced by thermal history.

A large number of T_g measurements was obtained according to the aging experimental scheme for samples with low moisture (Figure 2.2) which yielded a total of 648 measurements (36 per treatment × 9 treatments × 2 replicates) plus 54 measurements for the high moisture content samples (3 per treatment × 9 treatments × 2 replicates). The T_g values shown in Tables 2.5 and 2.6 represent mean ± standard deviation from two replicates; the value of each replicate was obtained by averaging over a number of measurements mentioned above. Figure 2.4 is a typical of DSC heat flow and the locations of onset-T_g, mid-

T_g, and offset-T_g on a reversing heat flow signal. However, it should be noted that the T_g being discussed in this section are solely the mid-T_g.

The ANOVA revealed that all the main effects from three factors, RH of equilibrating atmosphere (RH_Level), NaCit/SC and SC/MD and all two-way and three-way interaction effects on T_g values were statistically significant ($p < 0.001$; Table 2.7). Additional details of statistical analyses on the T_g are given in Appendix 2.2. The data were further analyzed by considering them according to the levels of equilibrating RH, i.e., the levels of residual moisture content.

From the follow-up analysis (Table 2.7), it could be seen that the interaction effect between NaCit/SC and SC/MD was significant ($p < 0.001$) only for samples with high residual moisture content (2.83 – 4.4 %wb); the effects of NaCit/SC and SC/MD on T_g values were independent.

The T_g values of samples with different levels of residual moisture content were significantly different. On average, increasing the residual moisture content from low (0.27 – 0.35 %wb) to high (2.83 – 4.4 %wb) level resulted in the reduction of T_g from approximately 106 to 67 °C, which indicates a strong plasticization effect of water on bioglass samples.

At high-level moisture content, the T_g was significantly higher with Na citrate, 67 to 69 °C compared to 64 °C for the samples without Na citrate (Table 2.8). However, the T_g values of samples with different NaCit/SC did not differ significantly. As SC/MD decreased, or the concentration of maltodextrin increased, the T_g increased significantly at every level of increase in maltodextrin concentration from approximately 61 to 64 and to 76 °C (Table 2.9). The increase of T_g of a mixture upon the increasing concentration of large glass-forming

molecules was as expected, since T_g strongly depends on molecular weight (Le Meste et al., 2002)

In samples with low-level moisture content, the effects of NaCit/SC and SC/MD could not be considered independently. There was a significant positive correlation between the addition of Na citrate and T_g, which was clearly evidenced when bioglass samples were formulated with higher concentration of sucrose than maltodextrin, i.e., SC/MD of 7:3. Without Na citrate, the T_g was approximately 87 °C. The T_g increased approximately 5 and 12 °C when NaCit/SC values were 0.1 and 0.2, respectively. For the samples containing equal amount of sucrose and maltodextrin, i.e., SC/MD of 5:5 a significant increase in T_g was observed only when NaCit/SC was 0.2. However, the effect of Na citrate was different in the samples that contained more maltodextrin than sucrose, i.e., SC/MD of 3:7; the T_g decreased when Na citrate was added. Interestingly, when NaCit/SC increased from 0.1 to 0.2, the T_g increased from approximately 119 to 123 °C; but it was still lower than that of the system without Na citrate, approximately 137 °C (Table 2.10).

The effect of Na citrate on the T_g value of bioglass samples with low-level residual moisture content depended on SC/MD. The positive dependence of T_g on Na citrate was less pronounced as maltodextrin concentration increased, and the correlation even reversed when maltodextrin concentration was at the highest level. The result suggests that Na citrate might primarily interact with sucrose rather than maltodextrin. Accordingly, in the system dominated by maltodextrin when small amount of Na citrate (NaCit/SC=0.1) was added some Na citrate molecules or their ions might interact with sucrose while some might simply plasticize the system and result in reducing the T_g. When Na citrate concentration was increased (NaCit/SC=0.2), the increased interaction between Na citrate and sucrose which

firmed up the large, less-mobile clusters resulting in less plasticization, and hence the T_g was lowered to a smaller extent. There has been reported that the T_g value of sucrose-Na citrate mixture with low residual moisture content dramatically increased with the addition of Na citrate up to NaCit/SC= 2.5 by mass, or 2.9 by mole (Kets et al., 2004), which was much higher than what was used in this study. The interaction between salt and hydroxyl group of sugar could be in the form of ion-dipole interactions (You and Ludescher, 2008b). This scenario may be similar to what generally found in amorphous polymer systems where side groups could raise the T_g if they are polar or large, and bulky (Young and Lovell, 1991).

The greater tendency for Na citrate to interact with sucrose is likely due to the difference in size and structure between sucrose and maltodextrin molecules. Oldenhof et al. reported that sucrose provided better protection for protein during drying by preventing dehydration-induced conformational changes as it interacted with protein more effectively than did the maltodextrin (Oldenhof et al., 2005). Koster et al. reported that only a small molecule maltodextrin could stabilize dry membranes (Koster et al., 2003). So in general, the effectiveness of carbohydrate to stabilize protein during drying decreases with increasing size (Wolkers et al., 1998).

The effect of salts on T_g value of a system is also dependent on type of salt (Izutsu et al., 2005). It was found from the study on amorphous indomethacin salts that T_g value decreases with the increasing ionic radius of alkaline cation. The decrease in charge density of cation, as the ionic radius increases, may lower electrostatic interaction between the ions causing T_g depression (Tong et al., 2002). From our preliminary experiment (data no shown), the introduction of NaCl into sucrose-maltodextrin mixture caused T_g depression. Farahnaky et al. also reported the T_g depression in amorphous potato and cassava starches upon adding

NaCl up to 6% db. Salts lead to a higher hygroscopicity in starch system, and so the decrease of T_g is due to the plasticization effects of both NaCl itself and the absorbed water, in which the latter showed the greater effect. At constant moisture content, the reduction of T_g due to NaCl at low moisture levels was more evident than that at high moisture level. However, the mechanism of T_g depression by NaCl is still ambiguous. Possibly, NaCl may not dissociate to ions, but simply acts as a plasticizer like other small molecules, or the dissociated atom of NaCl may reduce hydrogen in starch molecule by occupying a number of available sites (Farahnaky et al., 2009).

In this study, T_g of bioglass samples with high moisture level (2.8 to 4.4 %wb) generally increase with the increasing concentration of Na citrate. However, the most dramatic effect of Na citrate was found in the samples with high sucrose content at low moisture level. The result suggests that sucrose and Na citrate ions could efficiently interact only at very low moisture environment. Kets et al. reported a sucrose-citrate mixture with a very high T_g of approximately 105 °C when residual moisture was removed. This enhanced T_g value even exceeds both individual T_g for pure sucrose and citrate. The observation led to a hypothetical explanation that removal of water allows sucrose and citrate to restructure through hydrogen bonding more efficiently (Kets et al., 2004). In other words, water may interfere with hydrogen bonding between sucrose and citrate. Water which usually prevails in food systems is known for its plasticization effect and the effect on molecular mobility of the systems; though the mechanisms are poorly understood (Liu et al., 2006). Another group of researchers (Kilburn et al., 2004) have proposed two complex mechanisms which involve in the plasticization effect of water on carbohydrate systems. The mechanisms include the formation and disruption of intermolecular hydrogen bonds among carbohydrates, and the

changes of free volume in the matrix. In the absence of water, hydrogen bonding among carbohydrate molecules gives rise to the formation of less-mobile large clusters. Once absorbed into glassy carbohydrate matrix, water may either fill up the small voids or disrupt the intermolecular hydrogen bonding which results in a higher degree of freedom for carbohydrate molecules (Liu et al., 2006).

On the whole, it was clearly that the T_g values of bioglass samples primarily depended on SC/MD; the more the concentration of maltodextrin, the higher the T_g value. The dependence of T_g on molecular weight and structure of glass-forming molecules in an amorphous system has been well documented (Orford et al., 1990). The T_g value of a multi-component amorphous system could be estimated using either the Gordon-Taylor (GT) equation (Fox and Flory, 1950; Gordon and Taylor, 1952) or the Couchman-Karasz (CK) equation (Couchman and Karasz, 1978), mentioned in Chapter 1. The GT equation was developed based the free-volume theory with the assumption of ideal mixing, assuming the components are miscible and the free volumes are additive (Shamblin et al., 1998). The CK equation was derived from thermodynamic theory with the assumption that the entropy of mixing is purely combinatorial (Liu et al., 2006). In this experiment, however, the lack of precise molecular weight for maltodextrin did not allow the estimation of T_g value to compare with experimental data.

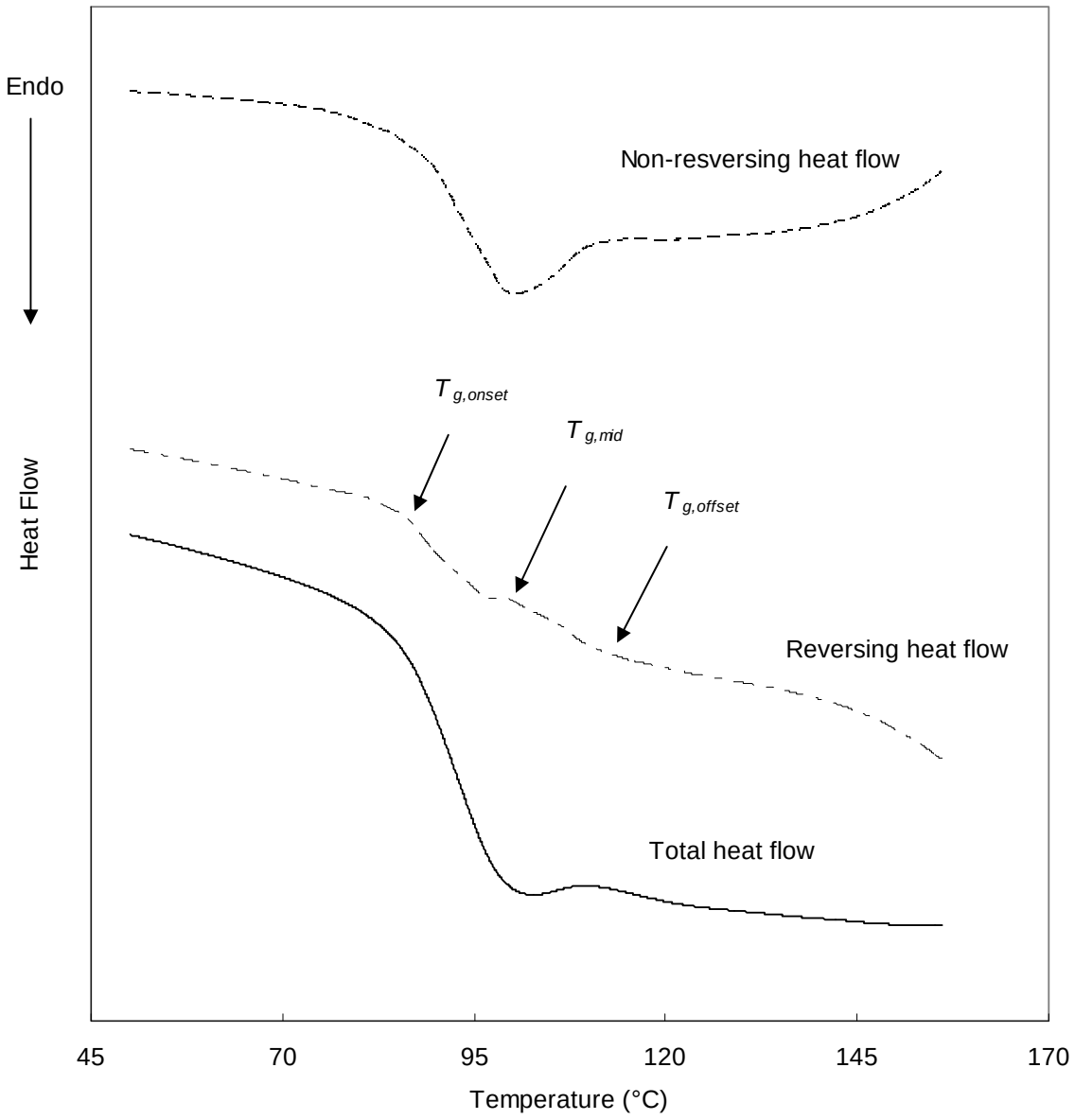

Figure 2.4 Representative MDSC thermograms obtained during the glass transition of a bioglass sample (SC/MD = 5:5, NaCit/SC = 0.1, low-level moisture content). The endothermic peak as a result of enthalpy relaxation can be seen in non-reversing heat flow signal. Locations of T_g including the onset-, mid-, and the offset-values determined from the reversing heat flow signal are illustrated.

Table 2.5 T_g values for the samples equilibrated in the atmosphere over P_2O_5 powder (~1% RH)

SC/ MD	NaCit/ SC	Residual moisture content (%wb)	T_g (°C)			Width of glass transition (°C)
			Onset	Mid	Offset	
7:3	0.0	0.28±0.01	79.3±0.3	86.6±0.3	93.5±0.4	14.2±0.7
7:3	0.1	0.31±0.06	82.6±0.4	91.4±0.3	97.9±0.8	15.3±0.5
7:3	0.2	0.33±0.01	87.8±0.7	98.4±1.0	104.8±0.8	17.0±0.1
5:5	0	0.34±0.03	89.1±1.6	99.2±1.8	110.5±1.1	21.3±0.6
5:5	0.1	0.27±0.03	87.6±0.1	95.2±0.3	104.0±0.1	16.4±0.2
5:5	0.2	0.31±0.01	95.9±0.8	108.1±0.3	115.8±0.3	19.9±0.5
3:7	0.0	0.34±0.11	123.4±1.2	136.9±0.8	146.4±0.4	22.9±0.8
3:7	0.1	0.35±0.01	106.8±9.9	119.0±3.3	133.8±1.6	27.0±8.2
3:7	0.2	0.32±0.01	112.3±0.1	123.3±0.1	134.4±0.1	22.2±0.0

Remarks

The figures represent mean value ± standard deviation

SC: Sucrose

MD: Maltodextrin

GT: Glass transition

Table 2.6 T_g values for the samples equilibrated in the atmosphere over saturated LiCl solution (~11% RH)

SC/ MD	NaCit/ SC	Residual moisture content (%wb)	T_g (°C)			Width of glass transition °C)
			Onset	Mid	Offset	
7:3	0.0	2.83±0.11	53.2±0.1	58.7±0.2	62.5±0.1	9.3±0.2
7:3	0.1	3.07±0.02	55.9±0.1	61.4±0.2	64.6±0.2	8.7±0.1
7:3	0.2	3.40±0.01	57.7±0.2	63.2±0.2	67.2±0.4	9.5±0.2
5:5	0.0	3.29±0.02	55.8±0.3	61.4±0.2	65.2±0.1	9.5±0.2
5:5	0.1	3.86±0.16	58.0±0.1	63.7±0.0	67.9±0.3	9.9±0.2
5:5	0.2	3.76±0.04	59.4±0.1	65.5±0.1	69.8±0.2	10.4±0.1
3:7	0.0	4.04±0.03	64.4±6.6	72.3±5.3	77.0±7.0	12.6±0.4
3:7	0.1	4.15±0.17	70.4±1.9	77.0±1.9	82.3±2.3	11.9±0.4
3:7	0.2	4.40±0.00	69.2±1.3	77.2±0.4	81.8±2.4	12.6±1.1

Remarks:

The figure represents mean value ± standard deviation

SC: Sucrose

MD: Maltodextrin

GT: Glass transition

Table 2.7 Summary of the follow-up ANOVA table for T_g analysis

Source	Type III Sum of Squares	df	Mean Square	F	Sig.
RH_Level	14213.011	1	14213.011	5297.646	.000
NaCit/SC	141.326	2	70.663	26.338	.000
SC/MD	3904.457	2	1952.229	727.658	.000
RH_Level * NaCit/SC	129.819	2	64.909	24.194	.000
RH_Level * SC/MD	617.645	2	308.822	115.108	.000
NaCit/SC * SC/MD	212.527	4	53.132	19.804	.000
RH_Level * NaCit/SC * SC/MD	252.682	4	63.170	23.546	.000
NaCit/SC * SC/MD @ RH_Level					
NaCit/SC * SC/MD @ RH_Level=Low	461.449	4	115.362	42.997	.000
NaCit/SC * SC/MD @ RH_Level=High	3.761	4	.940	.350	.840
NaCit/SC @ SC/MD (RH_Level=Low)					
NaCit/SC @ SC/MD=7:3 (RH_Level=Low)	141.747	2	70.874	26.416	.000
NaCit/SC @ SC/MD=5:5 (RH_Level=Low)	176.242	2	88.121	32.844	.000
NaCit/SC @ SC/MD=3:7 (RH_Level=Low)	350.705	2	175.353	65.357	.000
Error	48.292	18	2.683		
Corrected Total	19519.759	35			

Table 2.8 Effect of NaCit/SC on T_g value for the samples equilibrated in the atmosphere over saturated LiCl solution (RH_Level = High)

NaCit/SC	N	T_g: Subset[abc]	
		1	2
0	6	64.2	
0.1	6		67.4
0.2	6		68.6

Means for groups in homogeneous subsets are displayed. Based on observed means.
The error term is Mean Square (Error) = 2.683.
a) Tukey HSD. b) Uses Harmonic Mean Sample Size = 6. c) Alpha = 0.05.

Table 2.9 Effect of SC/MD on T_g value for the samples equilibrated in the atmosphere over saturated LiCl solution (RH_Level = High)

SC/MD	N	T_g: Subset[abc]		
		1	2	3
7:3	6	61.1		
5:5	6		63.5	
3:7	6			75.5

Means for groups in homogeneous subsets are displayed. Based on observed means.
The error term is Mean Square (Error) = 2.683.
a) Tukey HSD. b) Uses Harmonic Mean Sample Size = 6. c) Alpha = 0.05.

Table 2.10 Effect of NaCit/SC at each level of SC/MD on T_g value for the samples equilibrated in the atmosphere over P_2O_5 (RH_Level = Low)

SC/MD	NaCit/SC	N	T_g: Subset[abc]		
			1	2	3
	0	2	86.6		
7:3	0.1	2		91.4	
	0.2	2			98.4
	0.1	2	95.2		
5:5	0	2	99.2		
	0.2	2		108.1	
	0.1	2	119.0		
3:7	0.2	2		123.3	
	0	2			136.9

Means for groups in homogeneous subsets are displayed. Based on observed means.
The error term is Mean Square (Error) = 2.683.
a) Tukey HSD. b) Uses Harmonic Mean Sample Size = 2. c) Alpha = 0.05.

2.4.3 Width of the glass transition

Glass transition is a kinetic process, depending on cooling rate, and takes place over a range of temperature. Fast cooling rate allows the transition to occur at a higher temperature range than does the slow cooling rate (Roudaut et al., 2004). Food products commonly contain a number of ingredients rendering them the chemically heterogeneous nature. It is this heterogeneity that dictates the width of glass transition zone. The wider transition zone indicates the greater extent of heterogeneity (Ferry, 1980).

In this study, the width of glass transition zone was defined as the temperature range from the onset-T_g to the offset-T_g previously given in Tables 2.5 and 2.6. The ranges of glass transition width for the systems with low and high levels of residual moisture content were 14 to 22 °C, and 9 to 13 °C, respectively. These ranges are comparable to the glass transition width of food saccharides reported in literature which is generally around 5 to 20 °C (Liu et al., 2006; Liu et al., 2007).

The level of moisture content and sucrose/maltodextrin ratio significantly affected the width of glass transition zone ($p < 0.001$ for both). These factors also exhibited a significant interaction effect ($p < 0.05$) on the glass transition width. No significant effect of Na citrate was detected (Table 2.11). The plots of glass transition width constructed according to the significant factors were given in Figure 2.5. Note that, in this case, each data point represents an average of 216 measurements, 2 replicates × 3 levels of NaCit/SC × 36 measurements at each NaCit/SC. The difference in glass transition width could be readily observed from the plots. The width was noticeably greater when the residual moisture content of sample was at low level. Also, the glass transition zone tended to broaden with the increasing concentration

of maltodextrin; a slightly steeper change was found in the set of samples with low level of residual moisture content.

The follow-up analysis showed that glass transition widths of samples with different SC/MD were noticeably different when the residual moisture content was at low level. The width significantly increased from 15.5 °C to 19.2 °C, and to 24.1 °C when SC/MD levels were 7:3, 5:5 and 3:7, respectively. At high level of residual moisture content, the width of glass transition zone of samples with SC/MD of 7:3 (9.2 °C) did not significantly differ from the width obtained from the sample with SC/MD of 5:5 (9.9 °C), but differed from the width obtained from the sample with SC/MD of 3:7 (12.4 °C). However, the widths of glass transition zone for samples with SC/MD of 5:5 and 3:7 were not significant different (Table 2.12). At every SC/MD level, the width of glass-transition zone obtained from the samples having different levels of residual moisture content significantly differed. As the residual moisture content increased from low to high level, the width of glass transition zone decreased by approximately 50%, regardless of SC/MD level (Table 2.13).

In this case, the shrinkage of transition zone should not be interpreted as the decrease of heterogeneity due to the increasing moisture content since there was no substantial chemical alteration of the glass matrix. Instead, the result suggests that water did accelerate the glass transition process. The decrease of glass transition width with the presence of water was also found in amorphous amylopectin (Borde et al., 2002). There were other interesting cases where multi-component matrices showed a narrow glass-transition zone since some component(s) could accelerate the vitrification process (Kasapis et al., 1999). This effect of water on glass transition width of carbohydrate systems is, however, opposite to that of the plasticizer commonly added to synthetic polymers (Bair, 1997).

As could be gleaned from the overall analysis, the heterogeneity of sucrose-maltodextrin-salt bioglass was mainly influenced by maltodextrin. This is readily understandable since maltodextrin encompasses glucose polymers with variety of chain lengths and molecular weights. The onset of translational motions or glass transition of these glucose polymers would occur at slight different temperatures rendering a broad glass transition zone. A similar result was reported in the study of amorphous mixtures containing sucrose where sucrose mixtures exhibited a broader glass transition zone than did the sucrose alone. Accordingly, it was suggested that the mid-T_g represents an "average" value of T_g (Shamblin and Zografi, 1998).

Even though the effect of Na citrate on the heterogeneity of a bioglass was not detectable from DSC measurements, previous study by You and coworkers using a triplet erythrosine B probe revealed the effect of NaCl salt on dynamic site heterogeneity in sucrose glass with low residual moisture content, within approximately 2 % (You and Ludescher, 2008b). Erythrosine B phosphorescence is among the luminescence spectroscopic techniques that could provide direct information about molecular structure and mobility (Ludescher et al., 2001). Due to a number of advantages, e.g., high phosphorescence quantum yield, long life time, site selectivity, and high sensitivity (You and Ludescher, 2008b), erythrosine B phosphorescence has been extensively used to study the molecular motion in amorphous sucrose (Shahs and Ludescher, 1995; Ludescher et al., 2001; Pravinata et al., 2005). Accordingly, there is a possibility that the effect of salt on the heterogeneity of sucrose-maltodextrin glass did exist but the sensitivity of DSC measurement was insufficient to detect.

From the previous studies using a number of spectroscopic techniques, supercooled liquids and amorphous polymers were found to be dynamically heterogeneous through space and time (Ediger, 2000; Richert, 2002). The erythrosine B phosphorescence has provided evidence supporting the existence of spectral heterogeneity in amorphous sugars and alcohols (Pravinata et al., 2005; Shirke and Ludescher, 2005; Shirke et al., 2006), and proteins (Lukasik and Ludescher, 2006; Nack and Ludescher, 2006; Sundaresan and Ludescher, 2008). This information suggests the dynamic site heterogeneity as a characteristic feature of amorphous biomaterials (You and Ludescher, 2008b).

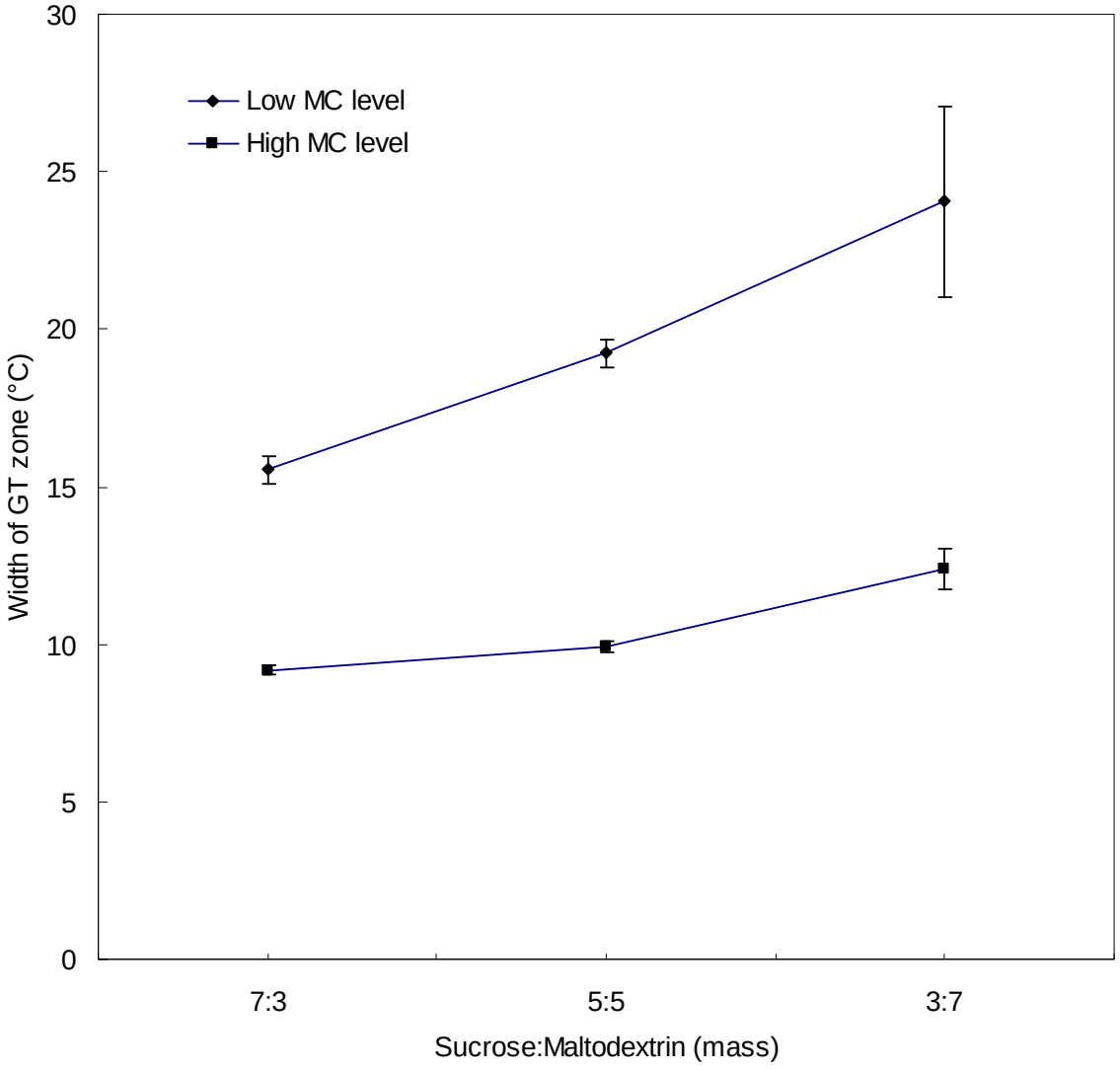

Figure 2.5 The widths of glass-transition (GT) zone of bioglass samples at two levels of moisture content. Data are means of two replicates, and error bars reflect standard deviation.

Table 2.11 Summary of the follow-up ANOVA table for the analysis of the width of glass transition zone

Source	Type III Sum of Squares	df	Mean Square	F	Sig.
RH_Level	747.384	1	747.384	187.714	.000
NaCit/SC	.993	2	.497	.125	.883
SC/MD	210.283	2	105.142	26.408	.000
RH_Level * NaCit/SC	.465	2	.233	.058	.943
RH_Level * SC/MD	42.520	2	21.260	5.340	.015
NaCit/SC * SC/MD	25.993	4	6.498	1.632	.210
RH_Level * NaCit/SC * SC/MD	35.299	4	8.825	2.216	.108
SC/MD @ RH_Level					
SC/MD @ RH_Level=Low	218.959	2	109.480	27.497	.000
SC/MD @ RH_Level=High	33.844	2	16.922	4.250	.031
RH_Level@SC/MD					
RH_Level @ SC/MD=7:3	121.031	1	121.031	30.398	.000
RH_Level @ SC/MD=5:5	260.774	1	260.774	65.496	.000
RH_Level @ SC/MD=3:7	408.100	1	408.100	102.499	.000
Error	71.667	18	3.982		
Corrected Total	1134.605	35			

Table 2.12 Effect of SC/MD at each level of residual moisture content (RH_Level) on the width of glass transition zone

RH_Level	SC/MD	N	Width of glass transition: Subset[abc]		
			1	2	3
Low	7:3	6	15.5		
	5:5	6		19.2	
	3:7	6			24.1
High	7:3	6	9.2		
	5:5	6	9.9	9.9	
	3:7	6		12.4	

Means for groups in homogeneous subsets are displayed. Based on observed means.
The error term is Mean Square (Error) = 3.982.
a) Tukey HSD. b) Uses Harmonic Mean Sample Size = 6. c) Alpha = 0.05.

Table 2.13 Effect of residual moisture content (RH_Level) at each level of SC/MD on the width of glass transition zone

SC/MD	RH_Level	N	Width of glass transition: Subset	
			1	2
7:3	Low	6	15.5	
	High	6		9.2
5:5	Low	6	19.2	
	High	6		9.9
3:7	Low	6	24.1	
	High	6		12.4

Based on estimated marginal means.
The mean difference is significant at the .05 level.
Adjustment for multiple comparisons (for two means): Least significant difference (equivalent to no adjustments).

2.4.4 Change of heat capacity at the glass transition

Glass transition accompanies abrupt changes in several physical properties. As the temperature of a glassy material is raised through the glass transition region, its entropy, heat capacity (C_p), and diffusivity increase, while density, viscosity, and rigidity decrease (Champion et al., 2000). Of these, the change in heat capacity at glass transition ($\Delta C_{p,GT}$) can be readily observed from a DSC thermogram (Figure 2.6).

An early study had suggested that $\Delta C_{p,GT}$ relates to the degree of organization in the glass matrix (Gibbs and DiMarzio, 1958). Accordingly, a glass at the physical state closer to being crystalline would exhibit greater $\Delta C_{p,GT}$ and, hence the magnitude of $\Delta C_{p,GT}$ should decrease with increasing molecular weight. In other words, the quality of hydrogen bonds among glass-forming molecules is manifested in terms of the heat capacity (Avaltroni et al., 2004). The extent of $\Delta C_{p,GT}$ also reflects the magnitude of changes in molecular mobility of amorphous matrix (Borde et al., 2002).

Since glass transition is a kinetic process, the glass-forming condition could strongly affect the $\Delta C_{p,GT}$; a large standard deviation of the observed $\Delta C_{p,GT}$ values may be expected (Orford et al., 1989). Several studies on sugar glasses using FTIR spectroscopy have found that the magnitude of $\Delta C_{p,GT}$ is associated with the strength of hydrogen bonding network in the glass matrix. Sugar glass with higher T_g has a weaker hydrogen bonding network in its structure (Wolkers et al., 2004b), and a smaller $\Delta C_{p,GT}$ (Orford et al., 1990; Wolkers et al., 2004b) than the glass with lower T_g.

The plots of $\Delta C_{p,GT}$ at glass transition as a function of SC/MD for the systems with low and high levels of residual moisture content are shown in Figures 2.7 and 2.8, respectively. The $\Delta C_{p,GT}$ values tended to decrease with the increasing concentration of maltodextrin, and so the increasing T_g, regardless of residual moisture content level, similar to the observation reported in prior studies (Orford et al., 1990; Wolkers et al., 2004b). The analysis of variance showed that all of three factors; level of residual moisture content, NaCit/SC, and SC/MD, significantly affected $\Delta C_{p,GT}$ ($p < 0.001$). Although the 3-way interaction effect was not significant ($p = 0.091$), all the 2-way interaction effects were significant ($p < 0.05$), which made the interpretation of the results rather complicated (Table 2.14). By considering the result from the ANOVA along with visual examination on the profile plots given in Appendix 2.4, the residual moisture content and SC/MD have likely had the most dramatic effect on $\Delta C_{p,GT}$.

A follow-up analysis (Table A2.14), and comparison tests (Tables 2.15 to 2.20) were conducted to elucidate these effects in detail. In general, the $\Delta C_{p,GT}$ value increased with Na citrate concentration. The mean values of $\Delta C_{p,GT}$ for bioglass systems with NaCit/SC of 0, 0.1, and 0.2 were approximately 0.55, 0.61 and 0.68 J/g°C, respectively. The effect of Na citrate on $\Delta C_{p,GT}$ was significant only when the residual moisture content was at high level, where ΔC_p increased at every increasing level of Na citrate concentration (Table 2.15). The $\Delta C_{p,GT}$ was positively dependent on the concentration of Na citrate, but only when SC/MD levels were 7:3 or 5:5. Such dependence was absent in the bioglass system dominated by maltodextrin molecules, i.e., when SC/MD=3:7 (Table 2.16). This result suggests the tendency of interaction between Na citrate and sucrose, rather than maltodextrin, which then

led to stronger hydrogen bonding network—reflected in the $\Delta C_{p,GT}$ values—in a bioglass system having high concentration of sucrose as compared to maltodextrin.

In most samples, the increasing residual moisture content significantly increased the $\Delta C_{p,GT}$. The $\Delta C_{p,GT}$ for systems at low and high levels of moisture content were approximately 0.30 and 0.93 J/g°C, respectively (Tables 2.15 and 2.17). Similarly, the increase of $\Delta C_{p,GT}$ with moisture content in amorphous amylopectin has also been reported (Borde et al., 2002). At every level of NaCit/SC, $\Delta C_{p,GT}$ value of the systems with higher moisture content was significantly greater than that of the systems with lower moisture content (Table 2.18). When considering across the range of SC/MD level, the dependence of $\Delta C_{p,GT}$ on residual moisture content was found only in systems with SC/MD of 7:3 and 5:5, or with sucrose concentration equal to or higher than that of maltodextrin (Table 2.19).

In literature, the $\Delta C_{p,GT}$ values for sucrose in the range of approximately 0.57 to 0.65 J/g°C (Shamblin and Zografi, 1998; Kawai et al., 2005; Mao et al., 2006; Liu et al., 2007), and for maltodextrin (DE19 to DE20) of approximately 0.44 to 0.45 J/g°C (Roos and Karel, 1991; Avaltroni et al., 2004) have been reported. However, the value of $\Delta C_{p,GT}$ for pure water is still a matter of debate. That said, a considerably wide range of reported values has been found, as summarized in another literature (Borde et al., 2002): 0.092 J/g°C for liquid quenched water, 1.94 J/g°C for vapor deposited water. In a mixture, the $\Delta C_{p,GT}$ value of water was found in a range of 0.3 – 1.83 J/g°C. It appears that the value of $\Delta C_{p,GT}$ for water is not much different from that for the glass-forming molecules in sucrose-maltodextrin system.

In this study, by considering the average moisture contents of the system at low and high levels which were respectively around 0.31 and 3.64—only ~3.3% increment, and the

large increase in $\Delta C_{p,GT}$ of the whole system mentioned above, the simple additivity laws may not be legitimate. Also from the evidence that water did modulate the shape of DSC thermogram, specifically narrowed down the glass transition, the introduction of water to sucrose-maltodextrin system would be of a non-ideal type mixing suggesting the existence of molecular interaction between water and carbohydrate molecules. A similar result was also reported in literature (Borde et al., 2002). The non-ideal mixing was evidenced by the failure of the GT equation to predict the T_g of mixtures (Christensen et al., 2002).

Since the moisture content of samples in this study was rather low and there were numerous hydroxyl groups on carbohydrate molecules, it was likely that water was bound to carbohydrates through hydrogen bonding. Such interference by water molecules would then increase the molecular mobility of the matrix and eventually affect the thermal properties.

The mean value of $\Delta C_{p,GT}$ for the samples with SC/MD of 7:3, 5:5, and 3:7 were 0.92, 0.70 and 0.24 J/g°C, respectively (Tables 2.16 and 2.19), suggesting a positive dependence of $\Delta C_{p,GT}$ on sucrose concentration. That is, $\Delta C_{p,GT}$ decreased with the increasing concentration of maltodextrin—the average molecular weight of glass-forming molecules was increased. The result obtained here is in good agreement with that reported in the literature (Avaltroni et al., 2004). At every level of decreasing in sucrose concentration, the $\Delta C_{p,GT}$ value decreased significantly, regardless of NaCit/SC level (Table 2.20). The decrease of $\Delta C_{p,GT}$ with decreasing sucrose concentration was also observed at both low and high levels of residual moisture content (Table 2.17).

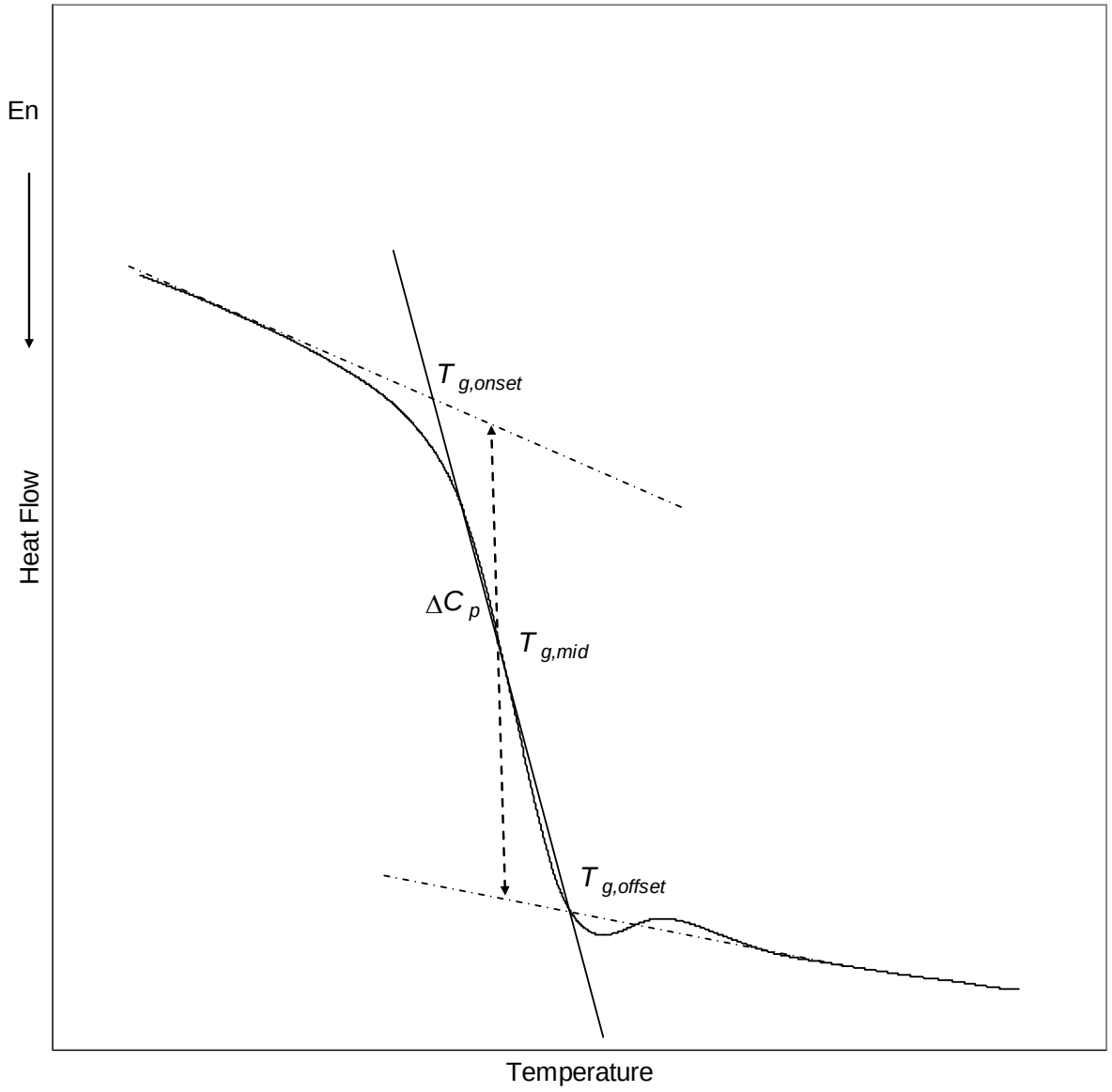

Figure 2.6 Graphical diagram representing the determination of $\Delta C_{p,GT}$ from a DSC thermogram.

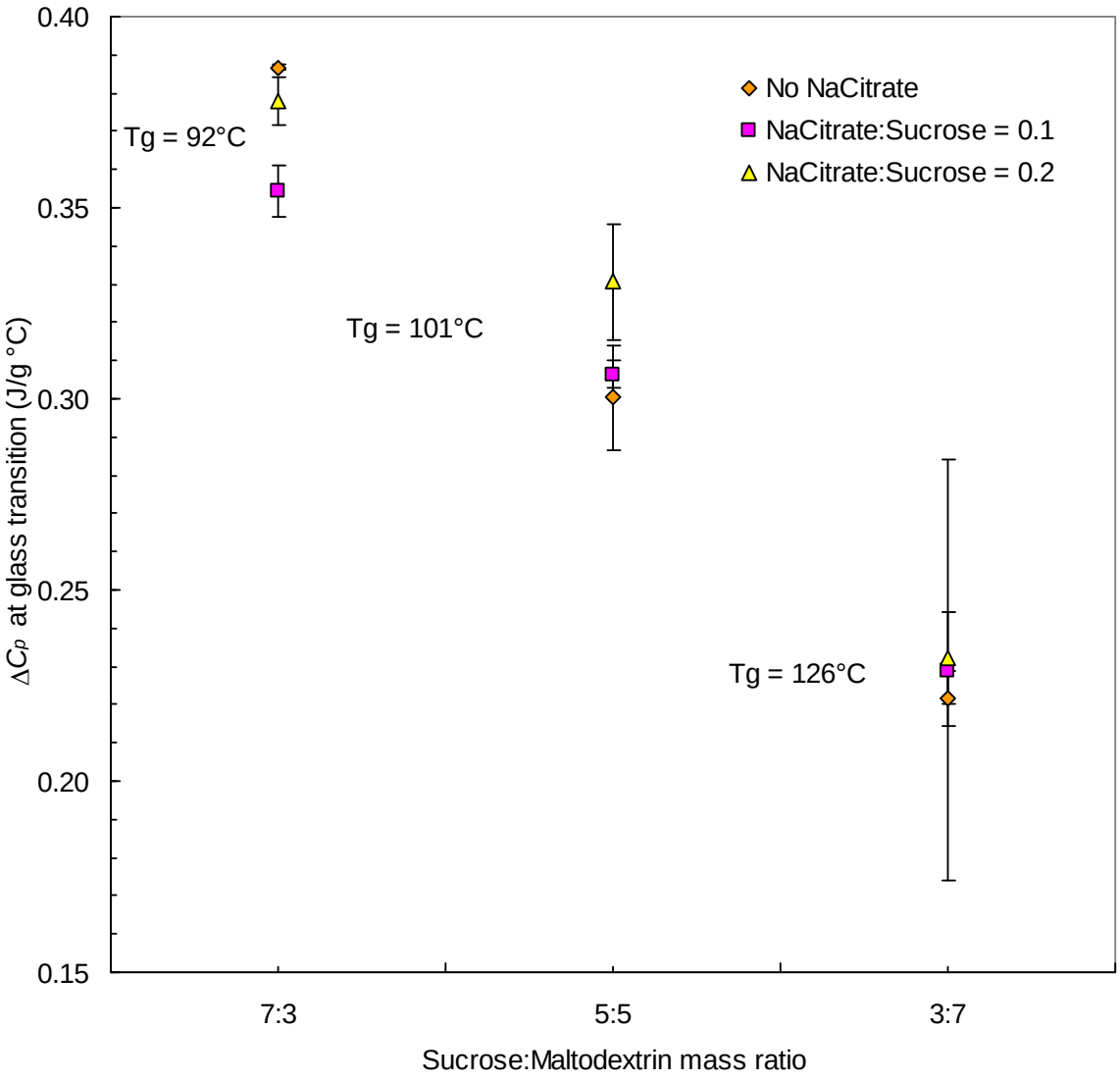

Figure 2.7 Effect of SC/MD on the change of $\Delta C_{p,GT}$. Samples were equilibrated in the atmosphere over P_2O_5 (~1% RH). Data are means of two replicates, and the error bars reflect standard deviation.

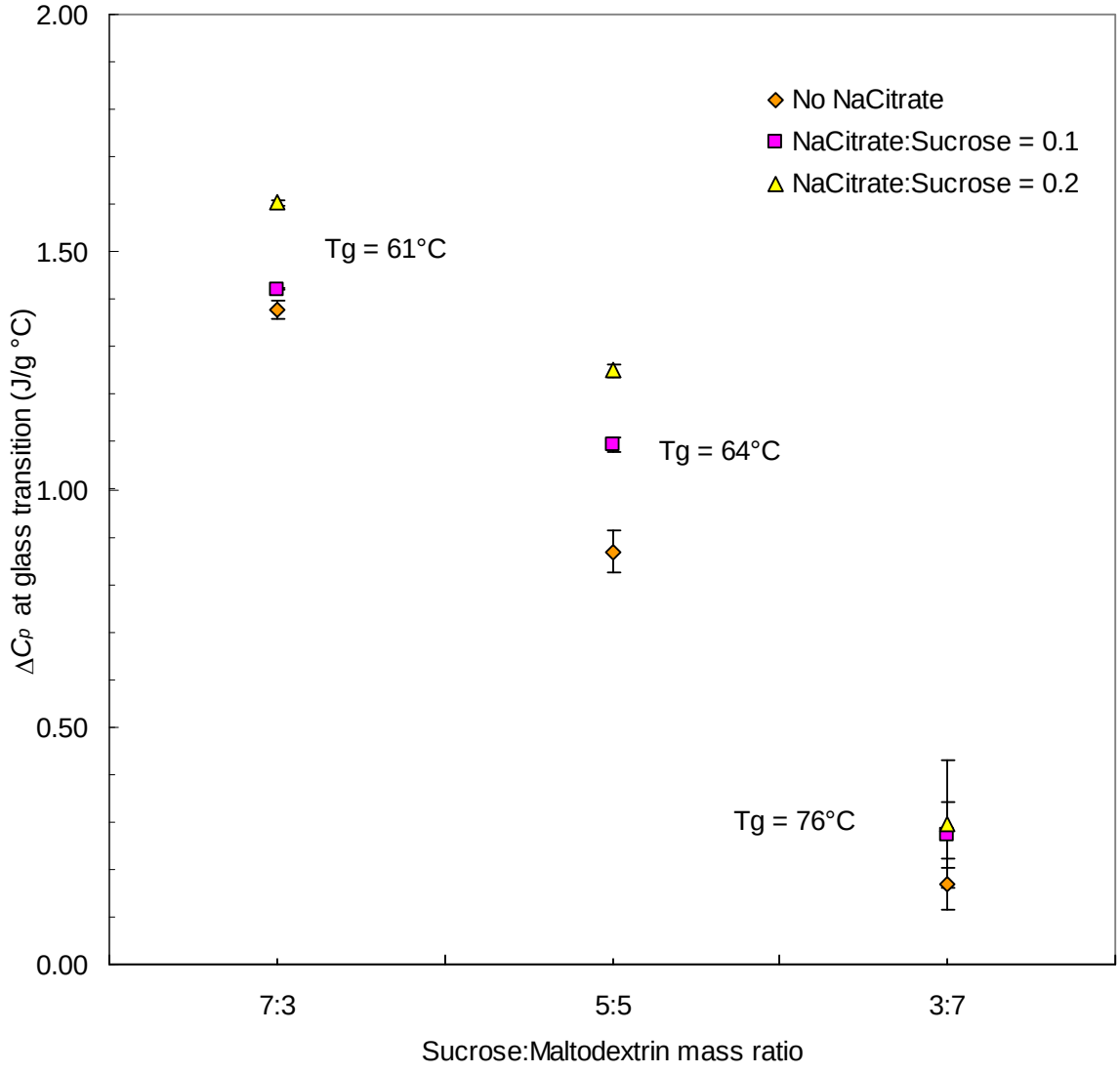

Figure 2.8 Effect of SC/MD on the change of $\Delta C_{p,GT}$. Samples were equilibrated in the atmosphere over saturated LiCl solution (~11% RH). Data are means of two replicates, and the error bars reflect standard deviation.

Table 2.14 Summary of the follow-up ANOVA table for the analysis of $\Delta C_{p,GT}$

Source	Type III Sum of Squares	df	Mean Square	F	Sig.
RH_Level	3.498	1	3.498	1973.312	.000
NaCit/SC	.098	2	.049	27.656	.000
SC/MD	2.910	2	1.455	820.802	.000
RH_Level * NaCit/SC	.082	2	.041	23.256	.000
RH_Level * SC/MD	1.822	2	.911	514.088	.000
Citrate_SC * SC/MD	.028	4	.007	3.916	.019
RH_Level * NaCit/SC * SC/MD	.017	4	.004	2.370	.091
NaCit/SC @ RH_Level					
NaCit/SC @ RH_Level=Low	.001	2	.000	.253	.779
NaCit/SC @ RH_Level=High	.180	2	.090	50.660	.000
RH_Level @ NaCit/SC					
RH_Level @ NaCit/SC = 0	.756	1	.756	426.719	.000
RH_Level @ NaCit/SC = 0.1	1.198	1	1.198	676.068	.000
RH_Level @ NaCit/SC = 0.2	1.625	1	1.625	917.038	.000
SC/MD @ RH_Level					
SC/MD @ RH_Level=Low	.064	2	.032	18.053	.000
SC/MD @ RH_Level=High	4.668	2	2.334	1316.838	.000
RH_Level @ SC/MD					
RH_Level @ SC/MD= 7:3	3.595	1	3.595	2028.259	.000
RH_Level @ SC/MD= 5:5	1.724	1	1.724	972.716	.000
RH_Level @ SC/MD= 3:7	.001	1	.001	.513	.483
SC/MD @ NaCit/SC					
SC/MD @ NaCit/SC = 0	.951	2	.475	268.202	.000
SC/MD @ NaCit/SC = 0.1	.859	2	.430	242.436	.000
SC/MD @ NaCit/SC = 0.2	1.127	2	.564	317.996	.000
NaCit/SC @ SC/MD					
NaCit/SC @ SC/MD= 7:3	.030	2	.015	8.352	.003
NaCit/SC @ SC/MD= 5:5	.086	2	.043	24.155	.000
NaCit/SC @ SC/MD= 3:7	.011	2	.005	2.980	.076
Error	.032	18	.002		
Corrected Total	8.487	35			

Table 2.15 Effect of NaCit/SC at each level of residual moisture content (RH_Level) on $\Delta C_{p,GT}$

RH_Level	NaCit/SC	N	$\Delta C_{p,GT}$: Subset[abc]		
			1	2	3
Low	0	6	0.30		
	0.1	6	0.30		
	0.2	6	0.31		
High	0	6	0.81		
	0.1	6		0.93	
	0.2	6			1.05

Means for groups in homogeneous subsets are displayed. Based on observed means.
The error term is Mean Square (Error) = 0.002.
a) Tukey HSD. b) Uses Harmonic Mean Sample Size = 6. c) Alpha = 0.05.

Table 2.16 Effect of NaCit/SC at each level of SC/MD on $\Delta C_{p,GT}$

SC/MD	NaCit/SC	N	$\Delta C_{p,GT}$: Subset[abc]		
			1	2	3
7:3	0	4	0.88		
	0.1	4	0.89		
	0.2	4		0.99	
5:5	0	4	0.58		
	0.1	4		0.70	
	0.2	4			0.79
3:7	0	4	0.20		
	0.1	4	0.25		
	0.2	4	0.26		

Means for groups in homogeneous subsets are displayed. Based on observed means.
The error term is Mean Square (Error) = 0.002.
a) Tukey HSD. b) Uses Harmonic Mean Sample Size = 4. c) Alpha = 0.05.

Table 2.17 Effect of SC/MD at each level of residual moisture content (RH_Level) on $\Delta C_{p,GT}$

RH_Level	SC_MD	N	$\Delta C_{p,GT}$: Subset[abc]		
			1	2	3
Low	7:3	6	0.37		
	5:5	6	0.31		
	3:7	6		0.23	
High	7:3	6	1.47		
	5:5	6		1.07	
	3:7	6			0.25

Means for groups in homogeneous subsets are displayed. Based on observed means.
The error term is Mean Square (Error) = 0.002.
a) Tukey HSD. b) Uses Harmonic Mean Sample Size = 6. c) Alpha = 0.05.

Table 2.18 Effect of residual moisture content (RH_Level) at each level of NaCit/SC on $\Delta C_{p,GT}$

NaCit/SC	RH_Level	N	$\Delta C_{p,GT}$: Subset	
			1	2
0	Low	6	0.30	
	High	6		0.81
0.1	Low	6	0.30	
	High	6		0.93
0.2	Low	6	0.31	
	High	6		1.05

Based on estimated marginal means.
The mean difference is significant at the .05 level.
Adjustment for multiple comparisons (for two means): Least significant difference (equivalent to no adjustments).

Table 2.19 Effect of residual moisture content (RH_Level) at each level of SC/MD on $\Delta C_{p,GT}$

SC/MD	RH_Level	N	$\Delta C_{p,GT}$: Subset	
			1	2
7:3	Low	6	0.37	
	High	6		1.47
5:5	Low	6	0.31	
	High	6		1.07
3:7	Low	6	0.23	
	High	6	0.25	

Based on estimated marginal means. The mean difference is significant at the .05 level.
Adjustment for multiple comparisons (for two means): Least significant difference (equivalent to no adjustments).

Table 2.20 Effect of SC/MD at each level of NaCit/SC on $\Delta C_{p,GT}$

NaCit/SC	SC/MD	N	$\Delta C_{p,GT}$: Subset[abc]		
			1	2	3
0	7:3	4	0.88		
	5:5	4		0.58	
	3:7	4			0.20
0.1	7:3	4	0.89		
	5:5	4		0.70	
	3:7	4			0.25
0.2	7:3	4	0.99		
	5:5	4		0.79	
	3:7	4			0.26

Means for groups in homogeneous subsets are displayed. Based on observed means.
The error term is Mean Square (Error) = 0.002.
a) Tukey HSD. b) Uses Harmonic Mean Sample Size = 4. c) Alpha = 0.05.

2.4.5 Enthalpy relaxation process

A schematic illustration of changes in enthalpy and specific heat capacity over the entire thermal history is shown in Figure 2.9. Line AB is the liquid or melt line. Line BC is the rubbery or supercooled melt. Line BN represents the isothermal crystallization process at T_m. Line LN is a crystal line. Path ABCDEF represents the cooling process after melting from T_0 to T_1. Path FEDGCBA represents the reheating process of unaged glass. Path EI represents the isothermal aging process at T_a. Path HIJKBA represents the reheating process after aging through which the endothermic peak is observed. T_K and T_f are the critical Kauzmann temperature and the theoretical fictive temperature, respectively.

Sucrose-maltodextrin bioglass samples were isothermally aged at different temperatures (T_a), for aging times (t_a) of 8, 20, 47 and 71 h. Structural relaxation of glass during aging resulted in the loss of enthalpy of which the magnitude depending on the degree of undercooling ($T_g - T_a$) and t_a. Upon reheating, the aged glass rapidly regained the lost enthalpy (ΔH) manifested as the endothermic peak at the end of glass transition process.

Typical DSC thermograms obtained from a sucrose-maltodextrin bioglass sample aged at 70 °C for four t_a ranging from 8 to 71 h are given in Figure 2.10, and those obtained from a bioglass sample aged for 8 h at three different levels of aging temperature (T_a) are given in Figure 2.11. The dependence of the magnitude of endothermic peak can be readily observed from the figures.

In this study, however, the aging experiment could not be conducted with the same degrees of undercooling ($T_g - T_a$) for all samples due to the limitation of available laboratory equipment. As the T_g of bioglass samples primarily depended on SC/MD, a set of three aging

temperatures was selected for each level of SC/MD (Table 2.3) so that the aging temperatures mostly overlapped while the degree of undercooling was within a range of approximately T_g – 40 °C, for most samples. In general, for the expected life time of some products, e.g., pharmaceuticals, studies have found that the molecular mobility from 50 °C below T_g becomes negligible regarding to the stability against crystallization (Hancock et al., 1995; Hancock and Zografi, 1997; Van Den Mooter et al., 1999).

Regardless of the degree of undercooling, at approximately the same aging temperature, it was found that the absolute value of enthalpy relaxation decreased with the increasing concentration of maltodextrin (data not shown). This indicates the suppression of enthalpy relaxation upon the addition of larger glass-forming molecules into the system, which would primarily be due to the increasing T_g. However, a direct comparison among the absolute values of enthalpy relaxation would not be much meaningful since each individual sample was aged at different degree of undercooling. Instead, the characteristic or relaxation time of the enthalpy relaxation process and its kinetics would be more interesting.

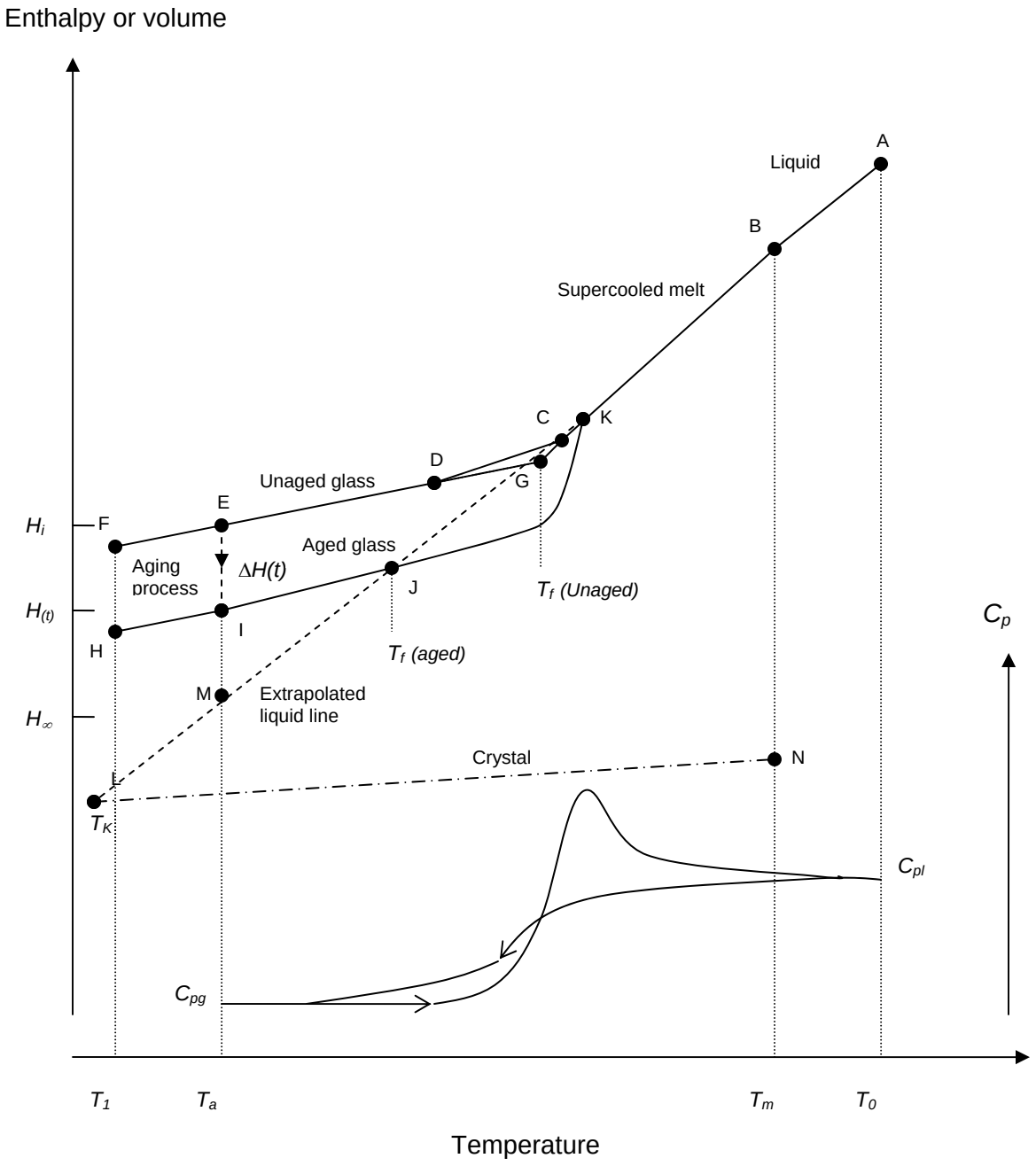

Figure 2.9 Schematic diagram of the change in enthalpy (H) and specific heat capacity (C_p) of a glass subjected to isothermal aging. Adapted from literature (Wungtanagorn and Schmidt, 2001; Liu et al., 2006).

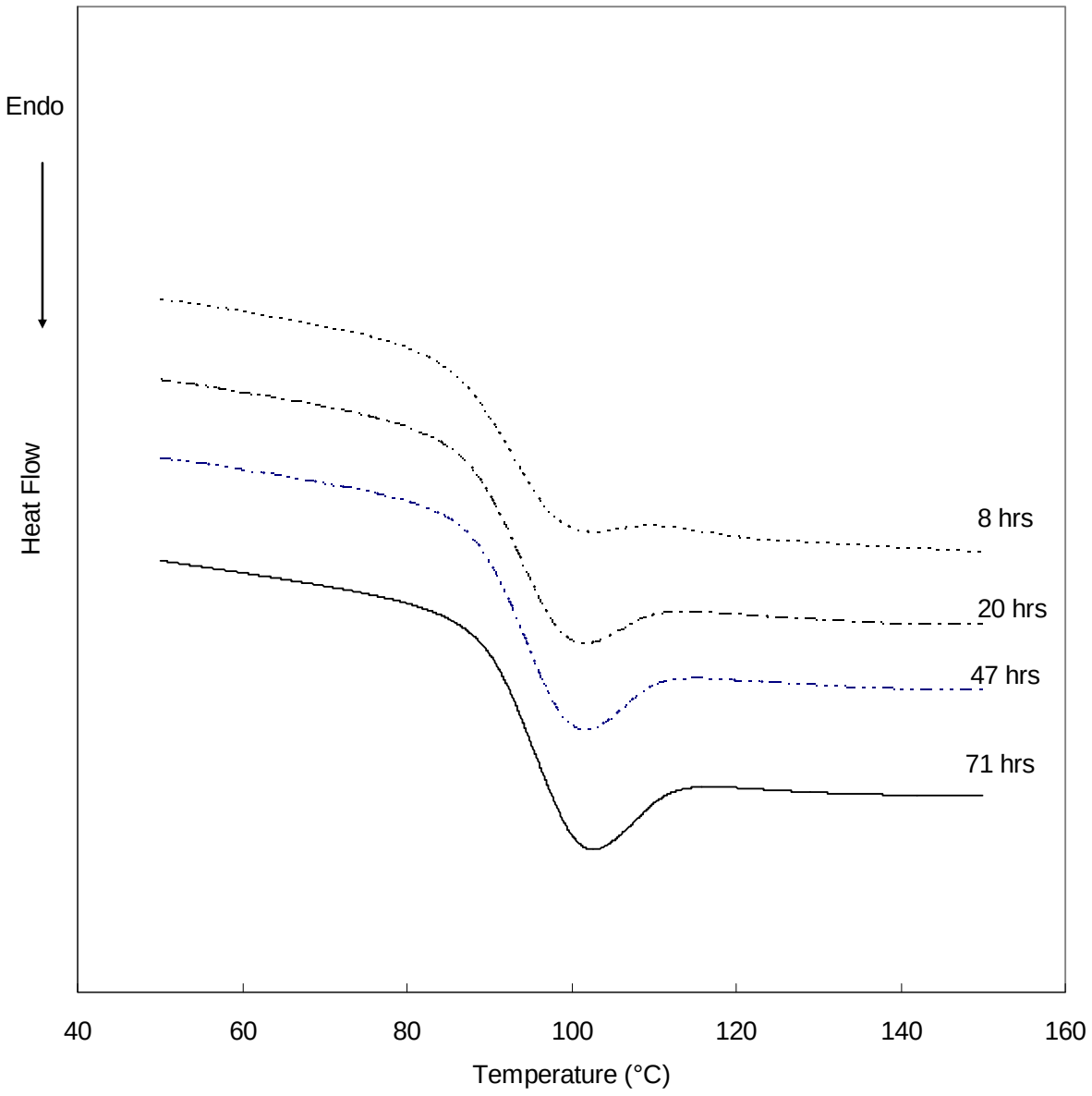

Figure 2.10 DSC thermograms representing the progress of enthalpy recovery obtained from a bioglass sample (SC/MD = 5:5, NaCit/SC = 0.1) after aging for 8 to 71 h at 70 °C. The thermograms were shifted vertically for illustration.

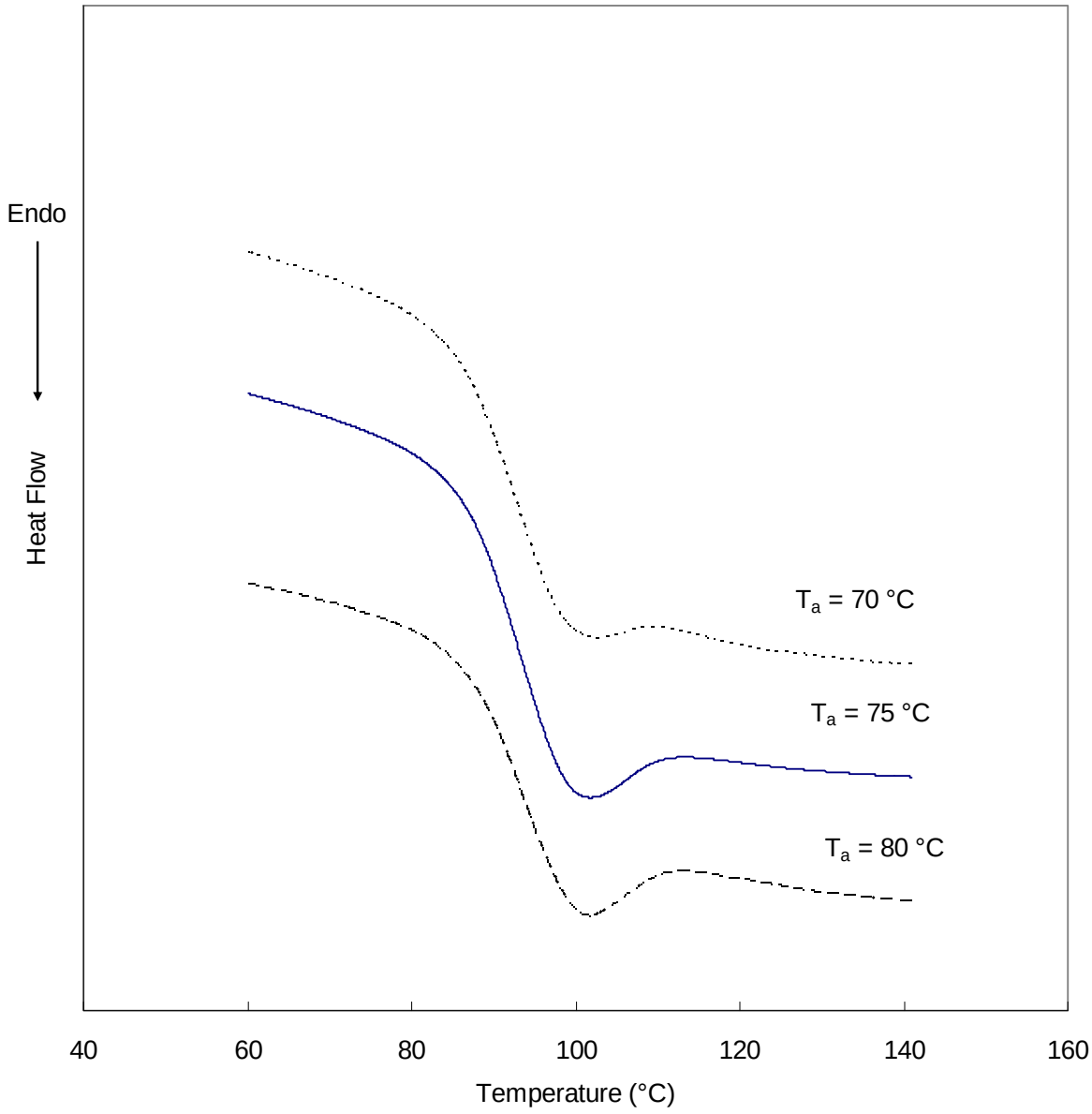

Figure 2.11 DSC thermograms representing the progress of enthalpy recovery obtained from a bioglass sample (SC/MD = 5:5, NaCit/SC = 0.1) after aging for 8 h at three levels of T_a. The thermograms were shifted vertically for illustration.

2.4.5.1 Characteristics of the enthalpy relaxation

For most amorphous systems, particularly those with multiple components, it is believed that their microstructural heterogeneities give rise to non-exponentiality behavior. The structural or enthalpy relaxation process of these systems cannot be satisfactorily described using a simple relaxation function (Liu et al., 2006). In this study, the enthalpy relaxation of bioglass samples was described with the stretch exponential function, commonly known as the Kohlrausch-Williams-Watts (KWW) decay function (Angell, 1995; Hodge, 1995), which yields Equation 1.18 (Chapter 1) for enthalpy relaxation study (Shamblin and Zografi, 1998; Hancock and Shamblin, 2001; Kawai et al., 2005; Haque et al., 2006):

$$\frac{\Delta H(t)}{\Delta H_\infty} = 1 - \exp\left[-\left(\frac{t}{\tau^{KWW}}\right)^{\beta}\right] \tag{1.18}$$

where $\Delta H(t)$ is the magnitude of enthalpy relaxation as a function of time t, and ΔH_∞ is the total possible loss of enthalpy assuming the final enthalpy is at the equilibrium line—the extrapolated liquid line—at the aging temperature T_a (see also Figure 2.9). τ^{KWW} is the characteristic time of mobility which provides an idea about the kinetics of enthalpy relaxation process; the higher value of τ^{KWW} reflects a slower process. It should be noted that the τ^{KWW} obtained with this equation is an "average" value of relaxation times. The constant β, ($0 \leq \beta \leq 1$), represents the width of relaxation time distribution. The smaller value of β indicates the larger distribution of molecular motion. That said, the value of β=1 corresponds

to single relaxation time. Both of the τ^{KWW} and the constant β are of equally important and necessary for describing non-exponential relaxation data using the KWW approach (Shamblin et al., 2000). The KWW decay function has been used in a number of studies on the enthalpy relaxation of food and pharmaceutical materials, e.g., amorphous sugar (Craig et al., 2000; Kawai et al., 2005; Haque et al., 2006), amorphous mixtures with sugar (Shamblin and Zografi, 1998), glassy starch (Jin Kim et al., 2003), and amorphous pharmaceuticals (Hancock and Shamblin, 2001).

In this study, the magnitude of $\Delta H(t)$ was determined from the area of endothermic peak using the Thermal Analysis software (TA Instruments Inc., New Castle, DE) as described in section 2.3.5.3. However, the true equilibrium state of glass is never reachable in the experimental time scale, and so ΔH_∞ is practically estimated using the following equation (Liu et al., 2007):

$$\Delta H_\infty = H_i - H_\infty = \left(C_{pl} - C_{pg}\right) \times \left(T_g - T_a\right) = \Delta C_{p,GT} \times \left(T_g - T_a\right) \qquad (2.1)$$

Where, $\Delta C_{p,GT}$ is the difference between the specific heat of equilibrium liquid (C_{pl}) and that of glass (C_{pg}) determined at the glass transition, assumed to be constant over the temperature range of T_a to T_g (see also Figure 2.9).

The plots of relative enthalpy relaxation [$\Delta H(t)/\Delta H_\infty$] for bioglass samples as a function of aging time are given in Appendix 2.5 (Figures A2.5.1 – A2.5.9). The nonlinearity of the enthalpy relaxation and the dependence of relative relaxation rate on T_a can be observed from the figures. The rate of relative relaxation increased with the increasing T_a

indicating the change of molecular mobility with temperature. The rate was rapid at the beginning of the aging process and this was clearly observed when samples were aged at the highest T_a – the closest temperature to their T_g. In contrast, the relative relaxation rate of samples aged at the lowest T_a was slow and rather constant over the whole range of aging time. The observation suggests that molecular mobility, which could result in an adverse effect on physicochemical changes, in the glass matrix was strongly affected by the initial relaxation time and aging temperature. The larger the distance of aging temperature below the T_g, the lesser the change in molecular mobility over time. Accordingly, storing glassy materials or products at temperatures far below their T_g not only slows down the molecular mobility, but also suppresses the time dynamics of molecular mobility allowing the easier prediction on the stability of amorphous materials (Mao et al., 2006).

Experimental data for sucrose-maltodextrin-salt bioglass samples were fitted with Equation 1.18 using the nonlinear regression tool available in the IBM SPSS Statistics 19 package. The initial values for τ^{KWW} = 100 and β = 0.5 have been reported to give the best fit with experimental data (Hancock et al., 1995; Kawai et al., 2005; Haque et al., 2006). These values were used in this study, and the results are given in Table 2.21. It should be mentioned that the size of this experiment and the availability of equipment did not allow the experiments to be conducted at the same degree of undercooling. Samples with SC/MD of 7:3, 5:5, and 3:7 were aged at a degree of undercooling in the range of approximately 12 to 38 °C, 15 to 38 °C, and 29 to 57 °C, respectively.

Even though the KWW equation has been commonly applied in enthalpy relaxation study, some researchers (Shamblin and Zografi, 1998; Shamblin et al., 2000) mentioned that a simple expression like the KWW equation might not be able to satisfactorily describe the

highly complex relaxation process in multi-component systems. The non-exponential relaxation behavior of the whole system might be due to single "non-exponential" relaxation mechanism or due to the superimposition of individual "exponential" relaxation process of the entities in the amorphous system (Shamblin et al., 2000). Even for single component system, the relaxation process is still considerably complex. For example, the reported β values for amorphous sucrose spans a large range: 0.22 – 0.29 (Christensen et al., 2002), 0.33 (Urbani et al., 1997), 0.4 – 0.8 (Hancock et al., 1995), 0.6 – 0.66 (Liu et al., 2007). Statistical consideration has also been taken into account to elucidate the ability of KWW equation for describing a non-exponential relaxation process. It was found that the KWW equation could not accurately describe the process with extremely broad distribution of relaxation times (Shamblin et al., 2000). In addition, there is generally significant error associated with the non-linear regression algorithm for estimating τ^{KWW} and β values from experimental relaxation data (Shamblin and Zografi, 1998). So, to compare with nonlinear regression technique, the KWW constants were also estimated using the linearised technique in which the KWW equation was rewritten in a linearised form of double logarithm of $\phi(t)$:

$$\ln[-\ln\phi(t)] = \beta \cdot \ln t - \beta \cdot \ln \tau^{KWW} \qquad (2.2)$$

The values of τ^{KWW} and β can be determined using the graphical linear least-square regression methods. Liu et al. used this technique and found a comparable result with literature (Liu et al., 2007). However, with all of uncertainties in mind, one need to exercise caution when interpreting the result of relaxation data using the KWW approach.

It was found in this study that the values of β for several cases were slightly higher than unity (Table 2.21) and so, in such situations, the β values were set to 1, i.e., an exponential behavior was assumed. This instance was also reported in the literature indicating the failure of KWW equation to provide an accurate description for relaxation behavior. It is however not surprising since this is an empirical equation (Williams, 1991; Mao et al., 2006).

The β values did not correlate with the composition of bioglass samples. In all cases, β decreased with increasing T_a indicating the broadening of relaxation time distribution as T_a approached the corresponding T_g. However, there was no common trend of β values upon varying the T_a. The temperature dependence of β reported in the literature has also been inconsistent. Christensen et al. reported increasing β with increasing T_a for sucrose and dry emulsions containing 40% hydroxypropyl methylcellulose, 30% fractionated coconut oil and 30% sucrose; but no explanation was given (Christensen et al., 2002). For some amorphous drugs, e.g., diazepam, temazepam and triazolam, the values of β tend to increase with T_a (Van Den Mooter et al., 1999). In the studies on enthalpy relaxation of amorphous sucrose and tapioca starch syrup solid (Liu et al., 2007) and glassy starch (Kim et al., 2003), no common trend of the β was found. Another group of researchers reported a tendency for β to decrease with increasing t_a (Kawakami and Pikal, 2005). The only agreement among previous reports including this study is the variation of β with T_a, but without a consistent trend. Besides, it was found that β decreases with t_a which suggests the increasing non-exponential behavior as the system continually relaxes (Mao et al., 2006). Therefore, in this study, the effect of T_a on the value of β is not discussed further.

The value of τ^{KWW} varied in a broad range; from less than a hundred up to several thousand hours depending on T_a, in other words, the degree of undercooling, and the composition of a system. In all cases, τ^{KWW} decreased with increasing T_a as has been reported in literature (Kim et al., 2003; Liu et al., 2006; Liu et al., 2007). The result confirms the temperature dependence of molecular mobility within glass matrix of which the molecular motions of relaxation elements are of high magnitude at the temperature close to T_g but become more restricted with increasing distance from T_g.

However, the values of τ^{KWW} obtained in this study can not be directly compared due to several reasons. First, the degree of undercooling was different. Samples with SC/MD of 3:7 were aged at a considerably greater degree of undercooling than the samples with SC/MD levels of 7:3 and 5:5 which experienced similar degree of undercooling. It is important to note that for certain type of materials in the region of glass transition, a small variation in temperature (3 to 5 °C) could result in a substantial change in relaxation rate in the order of one decade (Ediger et al., 1996). The effect of temperature on the evolution of enthalpy relaxation is more pronounced than that of water (Descamps et al., 2009). Second, the relaxation process is very complex, and to describe it with the KWW equation, both the τ^{KWW} and the β parameters are of equally important and necessary. That said, glassy materials that exhibit the same τ^{KWW} values might follow the totally different paths in their molecular motions during aging (Mao et al., 2006). Consequently, a meaningful comparison of τ^{KWW} can only be made if the values of β are comparable, within a range of ±0.1 (Hancock and Shamblin, 2001).

Due to the inconsistent reported β values, the lack of confidence about the precision of determining β value, and the difference in the degree of undercooling, a comparison of τ^{KWW} values would be questionable. Besides, it has been reported in literature that the change in molecular mobility during relaxation could result in changing relaxation time several orders of magnitude (Mao et al., 2006). In such case, the concept of using an "average" relaxation time – the KWW expression – to describe the relaxation process would be insufficient. In fact, until now, the nonlinear and non-exponential nature of relaxation process cannot be adequately described with any particular expression (Mao et al., 2006).

In spite of all uncertainties discussed above, the values of $\ln \tau^{KWW}$ obtained with two different techniques were plotted against degree of undercooling (Figures 2.12 and 2.13) to provide an idea about the magnitude of enthalpy relaxation rate. In general, the figures exhibited similar features. At similar degree of undercooling, τ^{KWW} depended mainly on SC/MD; the higher concentration of maltodextrin, the greater the value of τ^{KWW}. In other words, molecular mobility was suppressed upon introducing large molecules or polymers to the system. Another noticeable observation was found from the system with SC/MD of 7:3, where τ^{KWW} rapidly increased with increasing Na citrate concentration suggesting a tendency of Na citrate to interact with sucrose. The smaller size, the less complex molecular structure and the higher number of available sites on sucrose molecule, as compared to that for maltodextrin molecule, might allow increased interaction between sucrose and Na citrate, which helps to restrict the mobility of glass matrix.

To learn more about the relaxation process of amorphous systems, another quantitative approach using the term "$t_{\phi(t)=0.5}$" has been introduced (Shamblin and Zografi,

1998; Liu et al., 2007). Where, $t_{\phi(t)=0.5}$ is the time required for 50 % completion of the theoretical possible maximum enthalpy relaxation at a constant temperature below T_g. The value of $t_{\phi(t)=0.5}$ can be determined graphically or directly calculated using Equation 1.18. The later method was used in this study by setting the term $\Delta H(t)/\Delta H_\infty = 0.5$ and solving for *t*, the values of $t_{\phi(t)=0.5}$, using the corresponding constants of the KWW equation obtained from the two techniques discussed above. The calculated values of $t_{\phi(t)=0.5}$ based on the KWW are listed in Table 2.21. It should be noted that by considering the $t_{\phi(t)=0.5}$, a bit more meaningful comparison of the stability of amorphous systems could me made since the contribution of the two constants in the KWW expression is manifested in terms of the $t_{\phi(t)=0.5}$ value.

In all cases, $t_{\phi(t)=0.5}$ increased substantially upon reducing the T_a, which indicates that aging process can be dramatically slowed down at a slightly lower T_a. It could be also seen that in general $t_{\phi(t)=0.5}$ increased with the increasing maltodextrin concentration at approximately similar degrees of under cooling. For the system with high sucrose content (SC/MD of 7:3), $t_{\phi(t)=0.5}$ tended to increase with increasing concentration of Na citrate. However, this tendency was not present in other systems. Regarding the concentration of Na citrate, the trend of changes in $t_{\phi(t)=0.5}$ was similar to that for the τ^{KWW}, and this observation is another evidence that Na citrate tends to interact with sucrose rather than with maltodextrin. Sucrose molecules and Na citrate might then form less-mobile larger clusters within glass matrix and lead to lowering the overall mobility of the system.

Though meaningful comparisons of the τ^{KWW}, β, and $t_{\phi(t)=0.5}$ values could not be made, there is still practical usefulness of the information on the relaxation behavior of the sucrose-maltodextrin-salt bioglass. By considering at any particular temperature of interest below T_g,

one could expect a more stable system with high concentration of maltodextrin. Also, the stability of a bioglass can be substantially increased by slightly lowering storage temperature.

Table 2.21 Estimation of τ^{KWW} and β parameters from experimental data and the calculated values for $t_{\phi(t)=0.5}$

SC/ MD	NaCit /SC	$T_g - T_a$ (°C)	T_a (°C)	τ^{KWW} (h)	τ^{KWW*} (h)	β	β*	$t_{\phi(t)=0.5}$ (h)	$t^*_{\phi(t)=0.5}$ (h)
		26.6	60	361	285	0.87	0.97	237	196
7:3	0	16.6	70	169	160	0.42	0.44	71.1	69.6
		11.6	75	153	142	0.32	0.33	47.9	46.9
		31.4	60	305	303	1**	1**	210	210
7:3	0.1	21.4	70	139	111	0.56	0.68	72.2	64.8
		16.4	75	90.3	89.2	0.35	0.35	32.0	31.3
		38.4	60	107	1030	1**	0.99	736	708
7:3	0.2	28.4	70	332	267	0.64	0.71	187	159
		23.4	75	136	136	0.57	0.57	71.5	71.6
		29.2	70	1160	1200	1**	0.98	798	823
5:5	0	24.2	75	594	417	0.84	1.00	385	289
		19.2	80	567	435	0.65	0.72	321	261
		25.2	70	190	165	0.71	0.79	114	104
5:5	0.1	20.2	75	124	116	0.50	0.53	59.3	58.0
		15.2	80	103	99.5	0.46	0.48	46.6	46.4
		38.1	70	940	956	1**	0.98	648	658
5:5	0.2	33.1	75	649	556	0.93	1**	438	385
		28.1	80	520	333	0.80	1**	329	231
		56.9	80	2370	2450	1**	0.98	1630	1690
3:7	0	51.9	85	1680	1660	0.89	0.90	1120	1110
		46.9	90	1010	783	0.81	0.88	639	516
		39.0	80	1720	131	0.70	0.76	1020	807
3:7	0.1	34.0	85	1290	1250	0.66	0.67	743	726
		29.0	90	800	667	0.62	0.66	443	383
		43.3	80	2430	2360	0.1**	0.99	1670	1630
3:7	0.2	38.3	85	1470	1530	0.92	0.91	986	1020
		33.3	90	1100	795	0.83	0.92	707	534

KWW parameters with (*) were obtained with linear regression on the linearised form of double logarithm of $\phi(t)$. The parameter without (*) were obtained with nonlinear regression. $t_{\phi(t)=0.5}$ and $t^*_{\phi(t)=0.5}$ were calculated using the corresponding parameters. ** Exponential behavior was assumed since the solved values of β was a bit higher than unity.

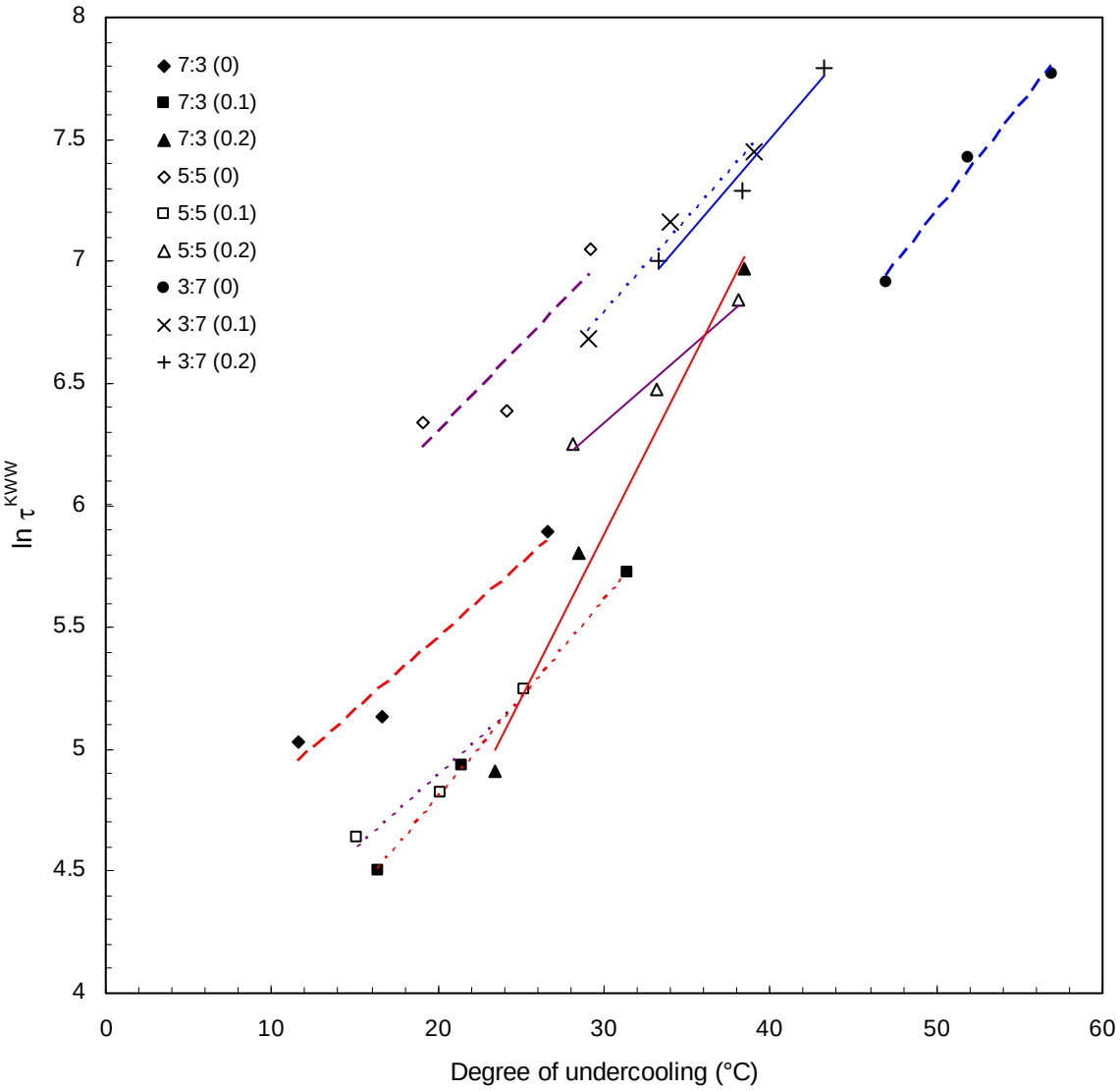

Figure 2.12 Plots for $\ln \tau^{KWW}$ determined using nonlinear regression algorithm as a function of degree of undercooling ($T_g - T_a$). The ratios given in the legend are SC/MD and the figures in parenthesis are NaCit/SC.

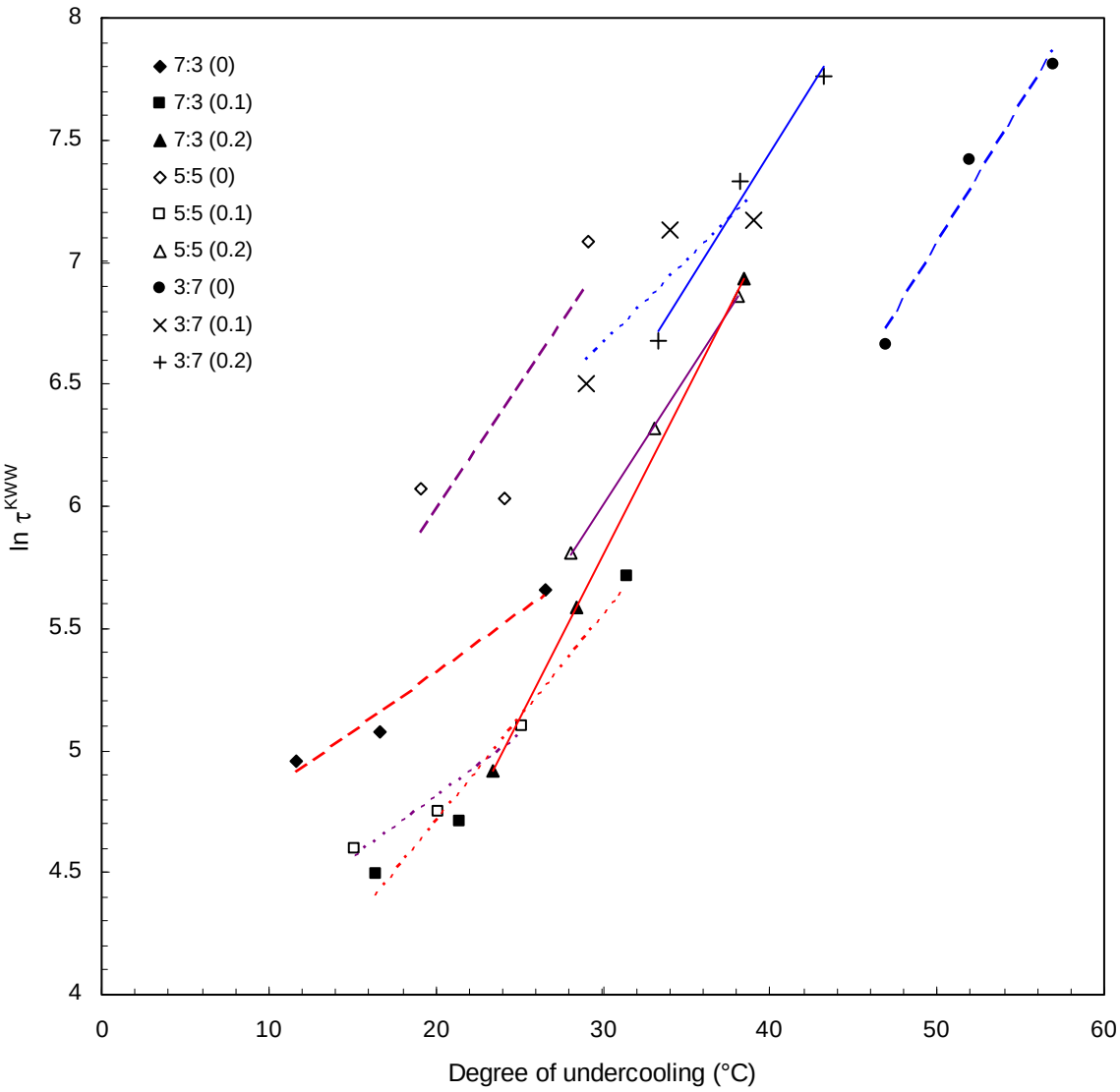

Figure 2.13 Plots for $\ln \tau^{KWW}$ obtained with the linearised technique as a function of degree of undercooling (T_g-T_a). The ratios given in the legend are SC/MD and the figures in parentheses are NaCit/SC.

2.4.5.2 Temperature dependence of the enthalpy relaxation

The temperature dependence or kinetics of enthalpy relaxation process depends on the type of associated molecular motions. This behavior can be characterized with the apparent activation energy (E_a) which corresponds to the minimum interaction energy between molecules (Liu et al., 2006). In other words, E_a represents the degree of cooperativity of molecular motions (Starkweather and Avakian, 1989; Starkweather, 1990). However, E_a could be affected by the temperature-dependence intermolecular interactions and the variation of free volume within the amorphous matrix (Champion et al., 2000; Haque et al., 2006).

In general, the behavior of molecular relaxation in glassy amorphous systems deviates from Arrhenius kinetics due to the strong temperature dependence nature particularly at temperatures around their T_g. The most popular expressions for describing this behavior are the Williams-Landel-Ferry (WLF; Equation 1.1) and the empirical Vogel-Tamman-Fulcher (VTF; Equation 1.4) equations (Liu et al., 2006). In fact, they are mathematically equivalent and the WLF is considered a special case of the VTF equation (Ediger et al., 1996; Hancock and Zografi, 1997). The WLF equation has been commonly applied for studying polymer physics, while the VTF equation for describing the temperature dependence of simple liquid systems (Angell, 1997). From the VTF equation:

$$\tau = \tau_0 \exp\left(\frac{B}{T - T_\infty}\right) \tag{1.4}$$

where B, T_∞ and τ_0 are constant, it is believed that T_∞ corresponds to the theoretical critical temperature at which the configurational entropy of the system reaches zero (Hancock and Zografi, 1997). This temperature is known as the Kauzmann temperature (T_K), graphically illustrated in Figure 2.9. However, in most enthalpy relaxation studies, the value of T_∞ is assumed zero, i.e., assuming Arrhenius-like behavior for τ (Liu et al., 2006). Consequently, Equation 1.4 can be rewritten as (Liu et al., 2007):

$$\tau = \tau_0 \exp\left(\frac{E_a}{R.T_a}\right) \tag{2.3}$$

where R is the ideal gas constant (8.314 J/mol.K). This assumption has been verified with experimental data, e.g., on glassy starch (Kim et al., 2003) and pharmaceutical solids (Hancock et al., 1995).

I applied the same approach to investigate the kinetics of enthalpy relaxation process of bioglass samples subjected to isothermal aging. The Arrhenius plots of τ^{KWW} obtained with two different techniques were constructed as illustrated in Appendix 2.7 and 2.8 and the values of E_a were obtained via linear regression. The resulting E_a values are given in Table 2.22. In general, the assumption of Arrhenius temperature dependence for the enthalpy relaxation process was reasonable; both techniques provided a good fit to experimental data. There were only a few plots that showed the R^2 values of approximately 0.7 to 0.8 indicating deviation from the Arrhenius kinetics, while the majority exhibited considerably high R^2 values (~ 0.98).

The E_a obtained in this study ranged from approximately 50 to 130 kJ/mol which was quite lower than those of sugar and starch systems reported in literature, e.g., 284 kJ/mol for glassy starch (Kim et al., 2003), 212 to 275 kJ/mol for sucrose (Hancock et al., 1995; Kawai et al., 2005; Haque et al., 2006; Liu et al., 2007), 233 kJ/mol for a mixture of 30 % corn syrup and 70 % sucrose, and in the range of 136 to 224 kJ/mol for sucrose and glucose syrup solid mixtures (Liu et al., 2007). As far as the magnitude of E_a is concerned, the possible reason for the low E_a values in this study was not quite clear. However, the obtained E_a values are greater than those for the secondary or β-relaxation process, e.g., 42 to 63 kJ/mol for mixtures of glucose and maltose in glassy state (Noel et al., 1996), 55 kJ/mol for amorphous ethyl cellulose (Bidault et al., 2005), which mainly associated with the local motions of a short sequence of molecules in low-density region with less intermolecular interaction (Liu et al., 2006). A process with higher level of cooperativity requires more energy to activate than does the one associated with lower cooperativity. The greater E_a value of enthalpy relaxation process as compared to that of the β-relaxation process indicates the association with the more cooperative – the translational diffusion – rather than localized molecular motions.

In general, the values of E_a obtained with the linearised technique were slightly higher than those obtained with nonlinear regression. The E_a values tended to increased with increasing concentration of maltodextrin. However, the result became more interesting when sodium citrate was introduced to the bioglass systems. In the system with SC/MD of 7:3, higher E_a values were obtained upon the addition of Na citrate; the higher concentration of Na citrate, the greater the E_a value. This trend was different in the systems with lower concentration of sucrose, i.e., SC/MD levels of 5:5 and 3:7. The addition of small amount of

Na citrate to these systems (NaCit/SC of 0.1) resulted in the decrease of E_a value. However, by increasing Na citrate concentration (NaCit/SC of 0.2), higher E_a values were obtained. It should be noted that the overall trend of change in E_a values upon varying SC/MD and NaCit/SC was similar to that of the change in T_g values of the bioglass systems with low level of residual moisture content (Table 2.5). The molecular interactions between Na citrate and sucrose might be responsible for the increasing of T_g and E_a values. Based on the fact that a number of hydroxyl groups are present in sucrose molecule, and the evidence from FTIR analysis (Kets et al., 2004), it is believed that the interaction between sucrose and Na citrate is in the form of hydrogen bonding. More importantly, similar trends of change in E_a and T_g values might imply a certain level of coupling between the structural relaxation and the glass transition or α-relaxation in bioglass systems. This result agrees with that reported in the literature (Champion et al., 2000), which states that physical aging (or enthalpy relaxation) can be regarded as a continuation of α-relaxation (or glass transition). Nevertheless, the results inferred from enthalpy relaxation data may be considered as suggestive rather than definitive since the experiments were conducted at slightly different degrees of undercooling.

Table 2.22 The E_a values of bioglass samples obtained from Arrhenius plots of the τ^{KWW} values estimated using two different techniques (Appendices 2.7 and 2.8).

SC/MD	NaCit/SC	Nonlinear regression		Linearised technique	
		E_a (kJ/mol)	R^2	E_a (kJ/mol)	R^2
7:3	0	57.7	0.95	46.3	0.97
7:3	0.1	77.8	1.00	93.1	0.98
7:3	0.2	129	0.98	129	1.00
5:5	0	72.2	0.81	103	0.73
5:5	0.1	61.7	0.95	50.8	0.95
5:5	0.2	59.8	0.98	106	1.00
3:7	0	91.3	0.99	122	0.96
3:7	0.1	81.4	0.98	71.4	0.79
3:7	0.2	84.4	0.98	116	0.98

2.5 Conclusions

Moisture and components of sucrose-maltodextrin-salt bioglass model system played significant roles on glass transition characteristics.

Moisture contributed a significant plasticization effect on the system. A slight difference in residual moisture content, between low (0.27 to 0.35 %wb) and high (2.83 to 4.40 %wb) levels, resulted in substantial reduction of T_g from approximately 106 to 67 °C.

The T_g increased with increasing maltodextrin concentration regardless of residual moisture content levels in the range of this study. The average values of T_g for the systems with SC/MD levels of 7:3, 5:5 and 3:7 were 61, 64 and 76 °C at high-level moisture content, and were 92, 101 and 126 °C at low-level moisture content, respectively. The result was as expected since T_g is known to depend on structure and the average molecular weight of glass-forming molecules.

The improvement in T_g value was observed when Na citrate was added to the system. Regardless of SC/MD level, the T_g of systems at high-level moisture content increased slightly upon the addition of Na citrate. The T_g values for the systems with NaCit/SC levels of 0, 0.1 and 0.2 were approximately 64, 67 and 69 °C, respectively. At low-level moisture content, the system with SC/MD of 7:3 showed a dramatic increase in T_g value for approximately 12 °C when NaCit/SC was 0.2. In contrast, T_g values for the systems with SC/MD levels of 5:5 and 3:7 initially decreased when small amount of Na citrate was added (NaCit/SC of 0.1). With an increase in Na citrate concentration (NaCit/SC of 0.2), the T_g of these two systems went up. However, the improvement in T_g value upon the addition of Na

citrate was found only in the system with SC/MD of 5:5. These changes in T_g suggest a tendency of interaction between Na citrate and sucrose, rather than between Na citrate and maltodextrin. Such interaction might create less-mobile large clusters of sucrose and Na citrate, which could raise the T_g of the system.

The width of glass transition zone was under influenced by the SC/MD ratio and residual moisture content. Within the ranges of moisture content in this study, glass transition width increased with the decreasing SC/MD (i.e., the increasing maltodextrin concentration) possibly due to the heterogeneity nature since maltodextrin consists of glucose polymers with broad spectrum of chain lengths and molecular weights. For all the systems with different SC/MD, water did accelerate glass transition so that the glass transition zone narrowed by approximately 50% as moisture content increased from low to high level.

All three factors studied significantly affected $\Delta C_{p,GT}$. In addition to main effects, the interaction effects of the factors rendered the interpretation of the results rather complicated. In general, $\Delta C_{p,GT}$ tended to increase with the increasing concentration of water, sucrose and Na citrate. There was barely detectable change in $\Delta C_{p,GT}$ value of the systems at low moisture content. The dependence of $\Delta C_{p,GT}$ on Na citrate concentration was found in systems with SC/MD levels of 7:3 and 5:5 when residual moisture content was high. The increase of $\Delta C_{p,GT}$ with sucrose and Na citrate concentration suggests the greater degree of organization of the glass matrix, i.e., the more compact system (Gibbs and DiMarzio, 1958), while the increase of $\Delta C_{p,GT}$ values with moisture content would reflect the magnitude of changes in molecular mobility due to the interference of water on the intermolecular interactions between glass-forming molecules (Borde et al., 2002).

The KWW equation was fit with enthalpy relaxation data obtained from aging experiments. There was no correlation between β and composition of the bioglass system. τ^{KWW} decreased with increasing T_a or SC/MD with the magnitude ranging from less than a hundred to several thousand hours. The smaller magnitude of τ^{KWW} at higher T_a indicates more mobility of bioglass at the temperatures closer to its T_g. The greater τ^{KWW} at lower SC/MD (or higher maltodextrin concentration) suggests the ability of large molecules to suppress molecular mobility. In the system with high content of sucrose and Na citrate (SC/MD = 7:3 and NaCit/SC = 0.2), it was found that τ^{KWW} rapidly decreased upon reducing T_a. This observation suggests that the interaction between Na citrate and sucrose is dependent on temperature. The interaction gets stronger at lower temperatures below T_g. In other words, the interaction between Na citrate and sucrose substantially slows down the aging process upon the small reduction in storage temperature. Since, the magnitudes of τ^{KWW} cannot be compared directly due to the broad distribution of β values, the term $t_{\phi(t)=0.5}$ which reflects the combined effect of both τ^{KWW} and β was introduced. It was found that the trend of changes of $t_{\phi(t)=0.5}$ was similar to that of the τ^{KWW}. Though E_a mainly increased with increasing maltodextrin concentration, the highest value of E_a was found in the system with the highest concentration of Na citrate and sucrose (SC/MD = 7:3 and NaCit/SC = 0.2). The noticeable increase in T_g, $t_{\phi(t)=0.5}$, and E_a values with the increasing concentration of Na citrate in the system with high sucrose content suggests that the less-mobile larger clusters of Na citrate-sucrose may be formed, likely by hydrogen bonding, and help restricting the mobility of bioglass matrix. Furthermore, the similar trend of changes in E_a and T_g agree with literature

(Champion et al., 2000) that physical aging can be regarded as the continuation of α-relaxation or glass transition.

2.6 References

Angell, C. A. (1995). "Formation of glasses from liquids and biopolymers." Science **267**(5206): 1924-1935.

Angell, C. A. (1997). "Why C1 = 16-17 in the WLF equation is physical--and the fragility of polymers." Polymer **38**(26): 6261-6266.

AquaLab. (2012). "Snack foods and water activity." Retrieved Dec. 18, 2012.

Archibald, D. D. and Kays, S. E. (2000). "Determination of Total Dietary Fiber of Intact Cereal Food Products by Near-Infrared Reflectance." Journal of Agricultural and Food Chemistry **48**(10): 4477-4486.

Avaltroni, F., Bouquerand, P. E. and Normand, V. (2004). "Maltodextrin molecular weight distribution influence on the glass transition temperature and viscosity in aqueous solutions." Carbohydrate Polymers **58**(3): 323-334.

Bair, H. E. (1997). Thermal analysis of additives in polymers. Thermal Characterization of Polymeric Materials. E. A. Turi. San Diego, Academic Press**:** 205-482.

Bhandari, B. R. and Howes, T. (1999). "Implication of glass transition for the drying and stability of dried foods." Journal of Food Engineering **40**(1-2): 71-79.

Bidault, O., Assifaoui, A., Champion, D. and Le Meste, M. (2005). "Dielectric spectroscopy measurements of the sub-T_g relaxations in amorphous ethyl cellulose: A relaxation magnitude study." Journal of Non-Crystalline Solids **351**(14-15): 1167-1178.

Boersma, A., Cangialosi, D. and Picken, S. J. (2003). "Mobility and solubility of antioxidants and oxygen in glassy polymers II. Influence of physical ageing on antioxidant and oxygen mobility." Polymer Degradation and Stability **79**(3): 427-438.

Borde, B., Bizot, H., Vigier, G. and Buleon, A. (2002). "Calorimetric analysis of the structural relaxation in partially hydrated amorphous polysaccharides. I. Glass transition and fragility." Carbohydrate Polymers **48**(1): 83-96.

Champion, D., Le Meste, M. and Simatos, D. (2000). "Towards an improved understanding of glass transition and relaxations in foods: molecular mobility in the glass transition range." Trends in Food Science & Technology **11**(2): 41-55.

Christensen, K. L., Pedersen, G. P. and Kristensen, H. G. (2002). "Physical stability of redispersible dry emulsions containing amorphous sucrose." European Journal of Pharmaceutics and Biopharmaceutics **53**(2): 147-153.

Chronakis, I. S. (1998). "On the molecular characteristics, compositional properties, and structural-functional mechanisms of maltodextrins: A review." Critical Reviews in Food Science and Nutrition **38**(7): 599 - 637.

Couchman, P. R. and Karasz, F. E. (1978). "A classical thermodynamic discussion of the effect of composition on glass-transition temperatures." Macromolecules **11**(1): 117-119.

Craig, D. Q. M., Barsnes, M., Royall, P. G. and Kett, V. L. (2000). "An evaluation of the use of modulated temperature DSC as a means of assessing the relaxation behaviour of amorphous lactose." Pharmaceutical Research **17**(6): 696-700.

Descamps, N., Palzer, S. and Zuercher, U. (2009). "The amorphous state of spray-dried maltodextrin: sub-sub-Tg enthal relaxation and impact of temperature and water annealing." Carbohydrate Research **344**: 85-90.

Desobry, S. A., Netto, F. M. and Labuza, T. P. (1999). "Influence of maltodextrin systems at an equivalent 25DE on encapsulated β-carotene loss during storage." Journal of Food Processing and Preservation **23**(1): 39-55.

Ediger, M. D. (2000). "Spatially heterogeneous dynamics in supercooled liquids." Annual Review of Physical Chemistry **51**: 99-128.

Ediger, M. D., Angell, C. A. and Nagel, S. R. (1996). "Supercooled liquids and glasses." The Journal of Physical Chemistry **100**(31): 13200-13212.

Farahnaky, A., Farhat, I. A., Mitchell, J. R. and Hill, S. E. (2009). "The effect of sodium chloride on the glass transition of potato and cassava starches at low moisture contents." Food Hydrocolloids **23**(6): 1483-1487.

Ferry, J. D. (1980). Viscoelastic properties of polymers. New York: John Wiley & Sons.

Fox, T. G. and Flory, P. J. (1950). "Second-order transition temperatures and related properties of polystyrene. I. Influence of molecular weight." Journal of Applied Physics **21**(6): 581-591.

Gangasharan and Murthy, S. S. N. (1995). "Nature of the relaxation processes in the supercooled liquid and glassy states of some carbohydrates." The Journal of Physical Chemistry **99**(32): 12349-12354.

Gibbs, J. H. and DiMarzio (1958). "Nature of glass transition and the glassy state." The Journal of Chemical Physics **28**: 373-383.

Gordon, M. and Taylor, J. S. (1952). "Ideal copolymers and second-order transitions in synthetic rubbers. I. Non-crystalline polymers." Journal of Applied Chemistry **2**: 493-500.

Hancock, B. C. and Shamblin, S. L. (2001). "Molecular mobility of amorphous pharmaceuticals determined using differential scanning calorimetry." Thermochimica Acta **380**(2): 95-107.

Hancock, B. C., Shamblin, S. L. and Zografi, G. (1995). "Molecular mobility of amorphous pharmaceutical solids below their glass transition temperatures." Pharmaceutical Research **12**(6): 799-806.

Hancock, B. C. and Zografi, G. (1997). "Characteristics and significance of the amorphous state in pharmaceutical systems." Journal of Pharmaceutical Sciences **86**(1): 1-12.

Haque, M. K., Kawai, K. and Suzuki, T. (2006). "Glass transition and enthalpy relaxation of amorphous lactose glass." Carbohydrate Research **341**(11): 1884-1889.

Hodge, I. M. (1995). "Physical aging in polymer glasses." Science **267**(5206): 1945-1947.

Imamura, K., Sakaura, K., Ohyama, K.-i., Fukushima, A., Imanaka, H., Sakiyama, T. and Nakanishi, K. (2006). "Temperature scanning FTIR analysis of hydrogen bonding states of various saccharides in amorphous matrixes below and above their glass transition temperatures." The Journal of Physical Chemistry B **110**(31): 15094-15099.

Izutsu, K.-I., Fujimaki, Y., Kuwabara, A. and Aoyagi, N. (2005). "Effect of counterions on the physical properties of l-arginine in frozen solutions and freeze-dried solids." International Journal of Pharmaceutics **301**(1-2): 161-169.

Jiang, B., Liu, Y., Bhandari, B. and Zhou, W. (2008). "Impact of caramelization on the glass transition temperature of several caramelized sugars. Part I: Chemical analyses." Journal of Agricultural and Food Chemistry **56**(13): 5138-5147.

Jin Kim, Y., Hagiwara, T., Kawai, K., Suzuki, T. and Takai, R. (2003). "Kinetic process of enthalpy relaxation of glassy starch and effect of physical aging upon its water vapor permeability property." Carbohydrate Polymers **53**(3): 289-296.

Johari, G. P. and Goldstein, M. (1970). "Viscous liquids and the glass transition. II. Secondary relaxations in glasses of rigid molecules." The Journal of Chemical Physics **53**(6): 2372-2388.

Kadoya, S., Izutsu, K. I., Yonemochi, E., Terada, K., Yomota, C. and Kawanishi, T. (2008). "Glass-state amorphous salt solids formed by freeze-drying of amines and hydroxy carboxylic acids: Effect of hydrogen-bonding and electrostatic interactions." Chemical & Pharmaceutical Bulletin **56**(6): 821-826.

Kasapis, S., Al-Marhoobi, I. M. A. and Giannouli, P. (1999). "Molecular order versus vitrification in high-sugar blends of gelatin and k-carrageenan." Journal of Agricultural and Food Chemistry **47**(12): 4944-4949.

Kawai, K., Hagiwara, T., Takai, R. and Suzuki, T. (2005). "Comparative investigation by two analytical approaches of enthalpy relaxation for glassy glucose, sucrose, maltose, and trehalose." Pharmaceutical Research **22**(3): 490-495.

Kawakami, K. and Pikal, M. J. (2005). "Calorimetric investigation of the structural relaxation of amorphous materials: Evaluating validity of the methodologies." Journal of Pharmaceutical Sciences **94**(5): 948-965.

Kessairi, K., Capaccioli, S., Prevosto, D., Lucchesi, M., Sharifi, S. and Rolla, P. A. (2008). "Interdependence of primary and Johari-Goldstein secondary relaxations in glass-forming systems." The Journal of Physical Chemistry B **112**(15): 4470-4473.

Kets, E. P. W., Ijpelaar, P. J., Hoekstra, F. A. and Vromans, H. (2004). "Citrate increases glass transition temperature of vitrified sucrose preparations." Cryobiology **48**(1): 46-54.

Kilburn, D., Claude, J., Mezzenga, R., Dlubek, G., Alam, A. and Ubbink, J. (2004). "Water in glassy carbohydrates: opening it up at the nanolevel." The Journal of Physical Chemistry B **108**(33): 12436-12441.

Kilburn, D., Claude, J., Schweizer, T., Alam, A. and Ubbink, J. (2005). "Carbohydrate polymers in amorphous states: An integrated thermodynamic and nanostructural investigation." Biomacromolecules **6**(2): 864-879.

Kilmartin, P. A., Reid, D. S. and Samson, I. (2004). "Dielectric properties of frozen maltodextrin solutions with added NaCl across the glass transition." Journal of the Science of Food and Agriculture **84**(11): 1277-1284.

Kim, J. Y., Hagiwara, T., Kawai, K., Suzuki, T. and Takai, R. (2003). "Kinetic process of enthalpy relaxation of glassy starch and effect of physical aging upon its water vapor permeability property." Carbohydrate Polymers **53**(3): 289-296.

Koster, K., Maddocks, K. and Bryant, G. (2003). "Exclusion of maltodextrins from phosphatidylcholine multilayers during dehydration: effects on membrane phase behaviour." European Biophysics Journal **32**(2): 96-105.

Le Meste, M., Champion, D., G., R., G., B. and Simatos, D. (2002). "Glass transition and food technology: A critical appraisal." Journal of Food Science **67**(7): 2444-2458.

Liu, Y., Bhandari, B. and Zhou, W. (2006). "Glass transition and enthalpy relaxation of amorphous food saccharides: A review." Journal of Agricultural and Food Chemistry **54**(16): 5701-5717.

Liu, Y., Bhandari, B. and Zhou, W. (2007). "Study of glass transition and enthalpy relaxation of mixtures of amorphous sucrose and amorphous tapioca starch syrup solid by differential scanning calorimetry (DSC)." Journal of Food Engineering **81**(3): 599-610.

Ludescher, R. D., Shah, N. K., McCaul, C. P. and Simon, K. V. (2001). "Beyond Tg: optical luminescence measurements of molecular mobility in amorphous solid foods." Food Hydrocolloids **15**(4-6): 331-339.

Lukasik, K. V. and Ludescher, R. D. (2006). "Effect of plasticizer on dynamic site heterogeneity in cold-cast gelatin films." Food Hydrocolloids **20**(1): 88-95.

Mao, C., Chamarthy, S. P. and Pinal, R. (2006). "Time-dependence of molecular mobility during structural relaxation and its impact on organic amorphous solids: An investigation based on a calorimetric approach." Pharmaceutical Research **23**(8): 1906-1917.

McPherson, A. E. and Seib, P. A. (1997). "Preparation and properties of wheat and corn starch maltodextrins with a low dextrose equivalent." Cereal Chemistry **74**(4): 424-430.

Montgomery, D. C. (2005). Design and Analysis of Experiments. 6th. New Jersey: John Wiley & Sons, Inc.

Nack, T. J. and Ludescher, R. D. (2006). "Molecular mobility and oxygen permeability in amorphous bovine serum albumin films." Food Biophysics **1**(3): 151-162.

Ngai, K. L. and Paluch, M. (2004). "Classification of secondary relaxation in glass-formers based on dynamic properties." Journal of Chemical Physics **120**(2): 857-873.

Noel, T. R., Parker, R. and Ring, S. G. (1996). "A comparative study of the dielectric relaxation behaviour of glucose, maltose, and their mixtures with water in the liquid and glassy states." Carbohydrate Research **282**(2): 193-206.

Oldenhof, H., Wolkers, W. F., Fonseca, F., Passot, S. and Marin, M. (2005). "Effect of sucrose and maltodextrin on the physical properties and survival of air-dried *Lactobacillus*

bulgaricus: An in situ Fourier transform infrared spectroscopy study." Biotechnology Progress **21**: 885-892.

Orford, P. D., Parker, R. and Ring, S. G. (1990). "Aspects of the glass transition behaviour of mixtures of carbohydrates of low molecular weight." Carbohydrate Research **196**: 11-18.

Orford, P. D., Parker, R., Ring, S. G. and Smith, A. C. (1989). "Effect of water as a diluent on the glass transition behavior of malto-oligosaccharides, amylose and amylopectin." International Journal of Biological Macromolecules **11**: 91-96.

Ottenhof, M.-A., MacNaughtan, W. and Farhat, I. A. (2003). "FTIR study of state and phase transitions of low moisture sucrose and lactose." Carbohydrate Research **338**(21): 2195-2202.

Poirier-Brulez, F., Roudaut, G., Champion, D., Tanguy, M. and Simatos, D. (2006). "Influence of sucrose and water content on molecular mobility in starch-based glasses as assessed through structure and secondary relaxation." Biopolymers **81**(2): 63-73.

Pravinata, L. C., You, Y. and Ludescher, R. D. (2005). "Erythrosin B phosphorescence monitors molecular mobility and dynamic site heterogeneity in amorphous sucrose." Biophysical Journal **88**(5): 3551-3561.

Richert, R. (2002). "Heterogeneous dynamics in liquids: fluctuations in space and time." Journal of Physics: Condensed Matter **14**(23): R703-R738.

Roos, Y. and Karel, M. (1991). "Water and molecular weight effects on glass transitions in amorphous carbohydrates and carbohydrate solutions." Journal of Food Science **56**(6): 1676-1681.

Roudaut, G., Simatos, D., Champion, D., Contreras-Lopez, E. and Le Meste, M. (2004). "Molecular mobility around the glass transition temperature: a mini review." Innovative Food Science & Emerging Technologies **5**(2): 127-134.

Shahs, N. K. and Ludescher, R. D. (1995). "Phosphorescence Probes of the Glassy State in Amorphous Sucrose." Biotechnology Progress **11**(5): 540-544.

Shamblin, S. L., Hancock, B. C., Dupuis, Y. and Pikal, M. J. (2000). "Interpretation of relaxation time constants for amorphous pharmaceutical systems." Journal of Pharmaceutical Sciences **89**(3): 417-427.

Shamblin, S. L., Taylor, L. S. and Zografi, G. (1998). "Mixing behavior of colyophilized binary systems." Journal of Pharmaceutical Sciences **87**(6): 694-701.

Shamblin, S. L. and Zografi, G. (1998). "Enthalpy relaxation in binary amorphous mixtures containing sucrose." Pharmaceutical Research **15**(12): 1828-1834.

Sheppard, A. J., Smith, L. M., Hubbard, W. D., Newkirk, D. R. and Dunkley, W. L. (1978). "Individual lipid and proximate analysis of various foods. 3. Potato chips and corn snack foods." Journal of Agricultural and Food Chemistry **26**(2): 346-348.

Shinyashiki, N., Shinohara, M., Iwata, Y., Goto, T., Oyama, M., Suzuki, S., Yamamoto, W., Yagihara, S., Inoue, T., Oyaizu, S., Yamamoto, S., Ngai, K. L. and Capaccioli, S. (2008). "The glass transition and dielectric secondary relaxation of fructose-water mixtures." The Journal of Physical Chemistry B **112**(48): 15470-15477.

Shirke, S. and Ludescher, R. D. (2005). "Dynamic site heterogeneity in amorphous maltose and maltitol from spectral heterogeneity in erythrosin B phosphorescence." Carbohydrate Research **340**: 2661-2669.

Shirke, S., You, Y. and Ludescher, R. D. (2006). "Molecular mobility and dynamic site heterogeneity in amorphous lactose and lactitol from erythrosin B phosphorescence." Biophysical Chemistry **123**(2-3): 122-133.

Starkweather, H. W. (1990). "Distribution of activation enthalpies in viscoelastic relaxations." Macromolecules **23**(1): 328-332.

Starkweather, H. W. and Avakian, P. (1989). "b-Relaxations in phenylene polymers." Macromolecules **22**(10): 4060-4062.

Struik, L. C. E. (1976). "Physical aging in amorphous glassy polymers." Annals of the New York Academy of Sciences **279**(1): 78-85.

Sundaresan, K. V. and Ludescher, R. D. (2008). "Molecular mobility and oxygen permeability in amorphous *b*-lactoglobulin films." Food Hydrocolloids **22**(3): 403-413.

Surana, R., Pyne, A., Rani, M. and Suryanarayanan, R. (2005). "Measurement of enthalpic relaxation by differential scanning calorimetry - effect of experimental conditions." Thermochimica Acta **433**(1-2): 173-182.

Tong, P., Taylor, L. S. and Zografi, G. (2002). "Influence of alkali metal counterions on the glass transition temperature of amorphous indomethacin salts." Pharmaceutical Research **19**(5): 649-654.

Urbani, R., Sussich, F., Prejac, S. and Cesaro, A. (1997). "Enthalpy relaxation and glass transition behaviour of sucrose by static and dynamic DSC." Thermochimica Acta **305**: 359-367.

Van Den Mooter, G., Augustijns, P. and Kinget, R. (1999). "Stability prediction of amorphous benzodiazepines by calculation of the mean relaxation time constant using the

Williams-Watts decay function." European Journal of Pharmaceutics and Biopharmaceutics **48**(1): 43-48.

Vanhal, I. and Blond, G. (1999). "Impact of melting conditions of sucrose on its glass transition temperature." Journal of Agricultural and Food Chemistry **47**(10): 4285-4290.

Williams, G. (1991). "Molecular motion in glass-forming systems." Journal of Non-Crystalline Solids **131-133, Part 1**: 1-12.

Windham, W. R., Kays, S. E. and Barton, F. E. (1997). "Effect of cereal product residual moisture content on total dietary fiber determined by near-infrared reflectance spectroscopy." Journal of Agricultural and Food Chemistry **45**(1): 140-144.

Wolkers, W. F., Oliver, A. E., Tablin, F. and Crowe, J. H. (2004b). "A Fourier-transform infrared spectroscopy study of sugar glasses." Carbohydrate Research **339**(6): 1077-1085.

Wolkers, W. F., van Kilsdonk, M. G. and Hoekstra, F. A. (1998). "Dehydration-induced conformational changes of poly-l-lysine as influenced by drying rate and carbohydrates." Biochimica et Biophysica Acta (BBA) - General Subjects **1425**(1): 127-136.

Wungtanagorn, R. and Schmidt, S. J. (2001). "Thermodynamic properties and kinetics of the physical ageing of amorphous glucose, fructose, and their mixture." Journal of Thermal Analysis and Calorimetry **65**(1): 9-35.

You, Y. and Ludescher, R. D. (2008b). "The effect of sodium chloride on molecular mobility in amorphous sucrose detected by phosphorescence from the triplet probe erythrosin B." Carbohydrate Research **343**(2): 350-363.

Young, R. J. and Lovell, P. A. (1991). Introduction to polymers. 2. Cheltenham: Stanley Thornes.

Yu, L. (2001). "Amorphous pharmaceutical solids: preparation, characterization and stabilization." Advanced Drug Delivery Reviews **48**(1): 27-42.

APPENDIX 2

Appendix 2.1 Statistical analysis of residual moisture content

RH_Level: The levels of relative humidity of the atmosphere used to equilibrate glass samples.
MC: The residual moisture content (%wb) of glass samples after fully equilibrated.

Table A2.1.1 Factors and levels for the analysis of residual moisture contents

Between-Subjects Factors

		Value Label	N
RH_Level	1	Low	18
	2	High	18
Treatment	Trt-3700		4
	Trt-3701		4
	Trt-3702		4
	Trt-5500		4
	Trt-5501		4
	Trt-5502		4
	Trt-7300		4
	Trt-7301		4
	Trt-7302		4

Table A2.1.2 The original ANOVA table for the analysis of residual moisture content

Tests of Between-Subjects Effects

Dependent Variable:MC

Source	Type III Sum of Squares	df	Mean Square	F	Sig.
Corrected Model	104.126[a]	17	6.125	1314.865	.000
Intercept	140.857	1	140.857	30237.711	.000
Treatment	2.332	8	.291	62.572	.000
RH_Level	99.634	1	99.634	21388.265	.000
Treatment * RH_Level	2.161	8	.270	57.982	.000
Error	.084	18	.005		
Total	245.068	36			
Corrected Total	104.210	35			

a. R Squared = .999 (Adjusted R Squared = .998)

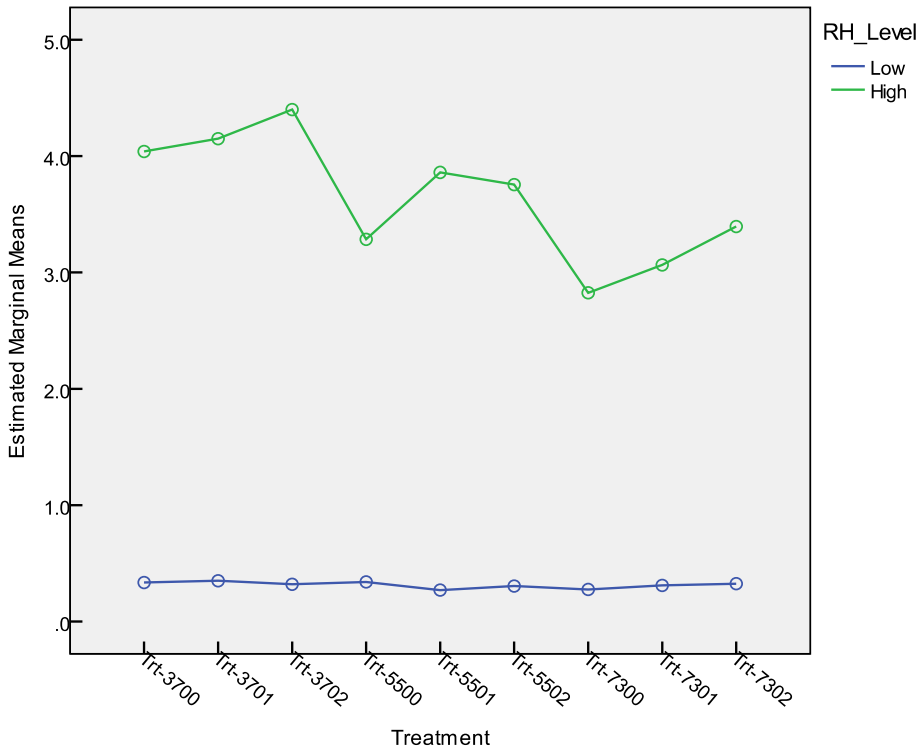

Figure A2.1.1 Residual moisture content of glass samples equilibrated under the atmosphere having different levels of RH.

Appendix 2.2 Statistical analysis of glass transition temperature (T_g)

Table A2.2.1 Factors and levels for the analysis of T_g

Between-Subjects Factors

		Value Label	N
RH_Level	1	Low	18
	2	High	18
Citrate_SC	1	0	12
	2	0.1	12
	3	0.2	12
SC_MD	1	7:3	12
	2	5:5	12
	3	3:7	12

Table A2.2.2 The original ANOVA table for the analysis of T_g

Tests of Between-Subjects Effects

Dependent Variable:Tg

Source	Type III Sum of Squares	df	Mean Square	F	Sig.
Corrected Model	19471.467[a]	17	1145.380	426.920	.000
Intercept	269885.445	1	269885.445	100594.984	.000
RH_Level	14213.011	1	14213.011	5297.646	.000
Citrate_SC	141.326	2	70.663	26.338	.000
SC_MD	3904.457	2	1952.229	727.658	.000
RH_Level * Citrate_SC	129.819	2	64.909	24.194	.000
RH_Level * SC_MD	617.645	2	308.822	115.108	.000
Citrate_SC * SC_MD	212.527	4	53.132	19.804	.000
RH_Level * Citrate_SC * SC_MD	252.682	4	63.170	23.546	.000
Error	48.292	18	2.683		
Total	289405.204	36			
Corrected Total	19519.759	35			

a. R Squared = .998 (Adjusted R Squared = .995)

Profile Plots: SC_MD * Citrate_SC * RH_Level

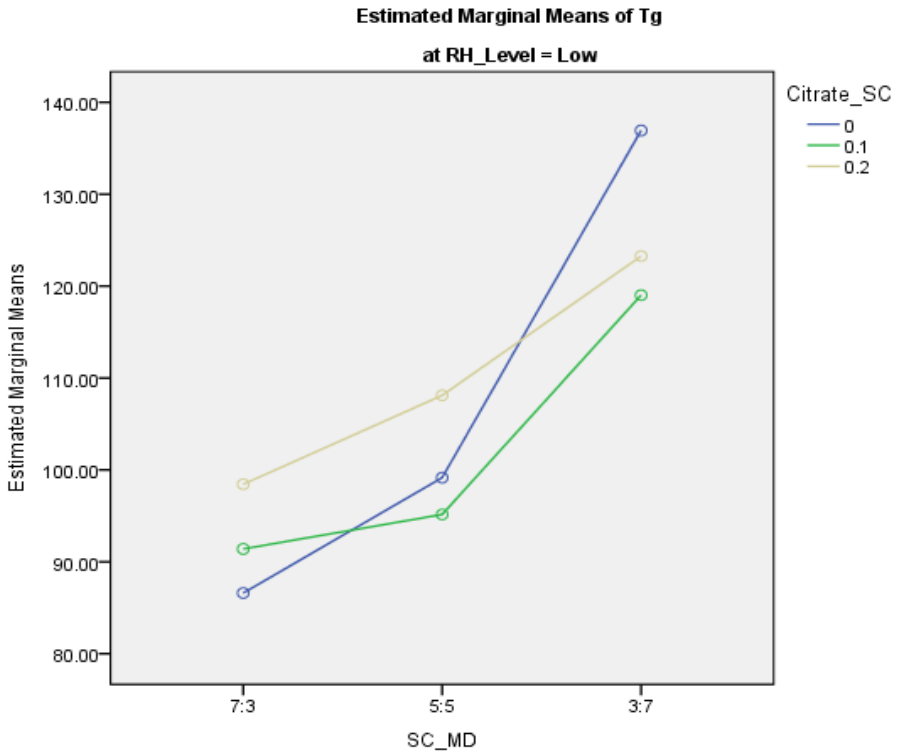

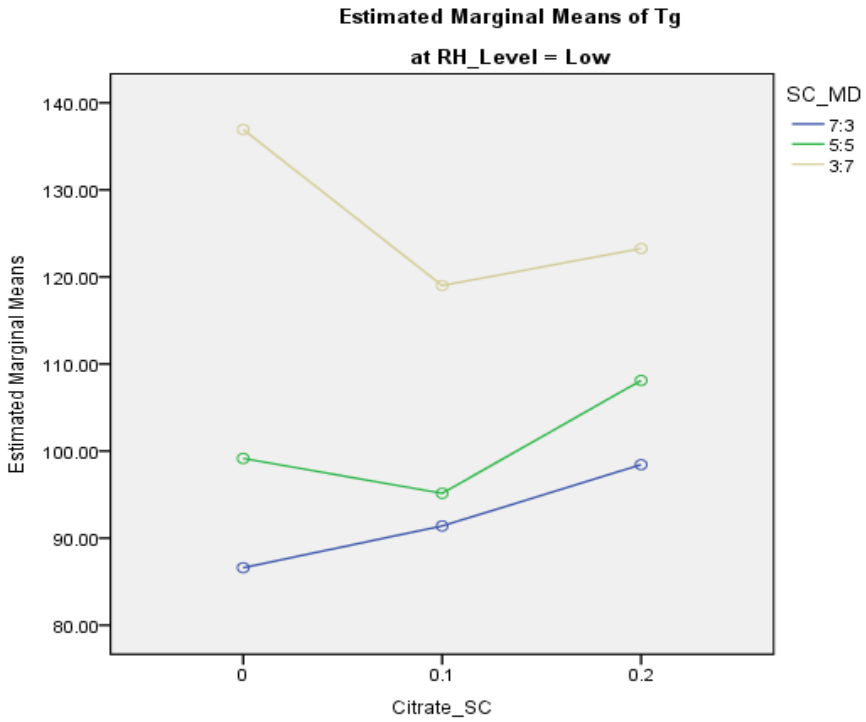

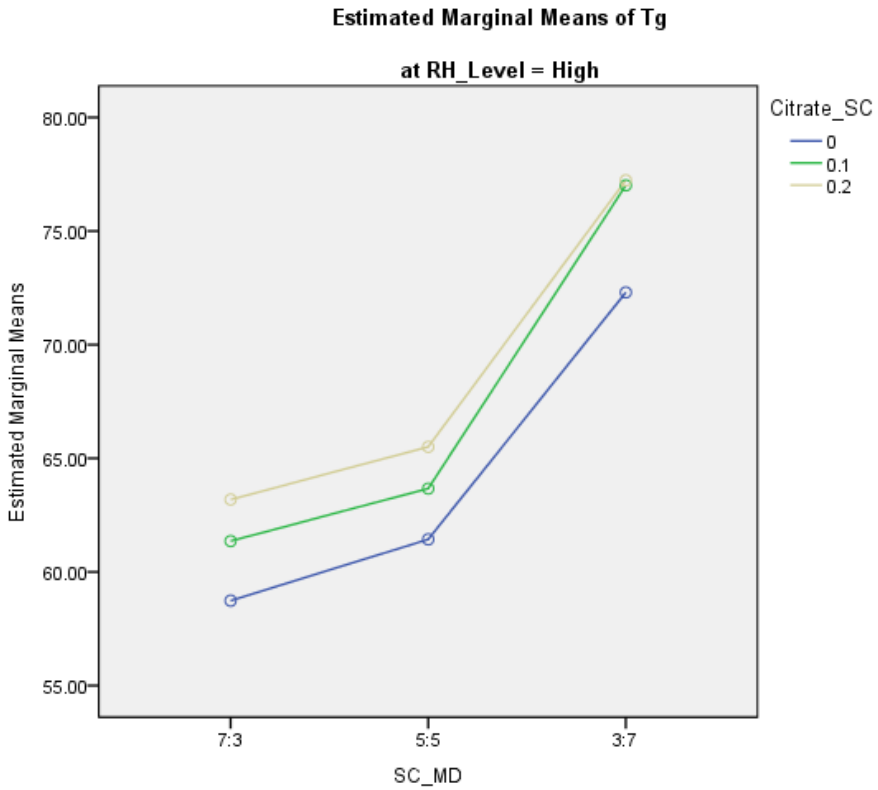
Estimated Marginal Means of Tg
at RH_Level = High
Estimated Marginal Means
80.00
75.00
70.00
65.00
60.00
55.00
7:3
5:5
3:7
SC_MD
Citrate_SC
0
0.1
0.2

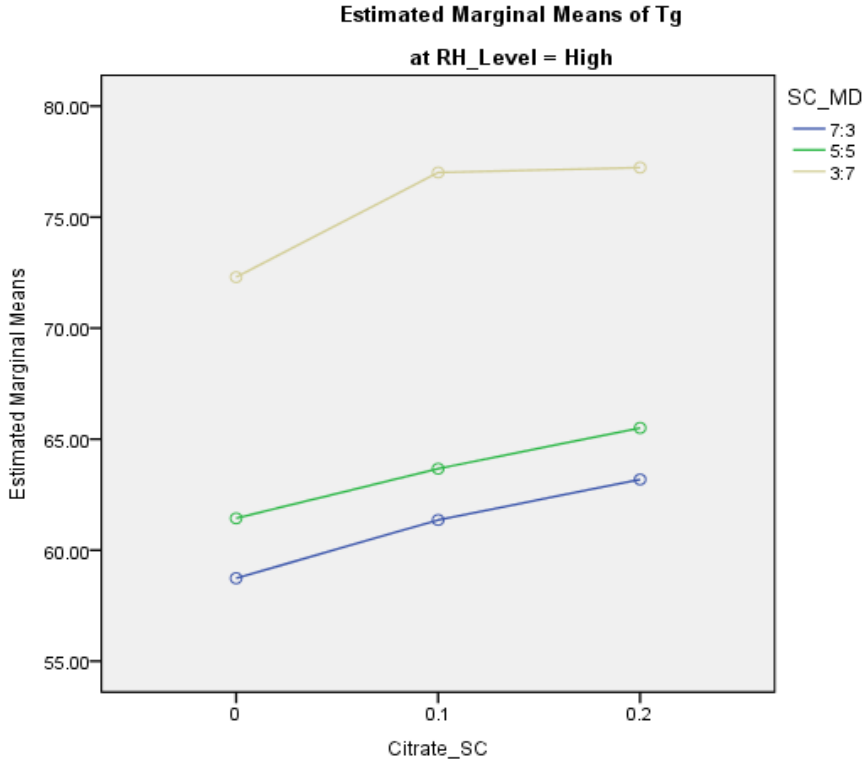
Estimated Marginal Means of Tg
at RH_Level = High
Estimated Marginal Means
80.00
75.00
70.00
65.00
60.00
55.00
0
0.1
0.2
Citrate_SC
SC_MD
7:3
5:5
3:7

Appendix 2.3 Statistical analysis of glass transition width

Table A2.3.1 Factors and levels for the analysis of glass transition width

Between-Subjects Factors

		Value Label	N
RH_Level	1	Low	18
	2	High	18
Citrate_SC	1	0	12
	2	0.1	12
	3	0.2	12
SC_MD	1	7:3	12
	2	5:5	12
	3	3:7	12

Table A2.3.2 The original ANOVA table for the analysis of glass transition width

Tests of Between-Subjects Effects

Dependent Variable:GT_width

Source	Type III Sum of Squares	df	Mean Square	F	Sig.
Corrected Model	1062.938[a]	17	62.526	15.704	.000
Intercept	8150.779	1	8150.779	2047.162	.000
RH_Level	747.384	1	747.384	187.714	.000
Citrate_SC	.993	2	.497	.125	.883
SC_MD	210.283	2	105.142	26.408	.000
RH_Level * Citrate_SC	.465	2	.233	.058	.943
RH_Level * SC_MD	42.520	2	21.260	5.340	.015
Citrate_SC * SC_MD	25.993	4	6.498	1.632	.210
RH_Level * Citrate_SC * SC_MD	35.299	4	8.825	2.216	.108
Error	71.667	18	3.982		
Total	9285.384	36			
Corrected Total	1134.605	35			

a. R Squared = .937 (Adjusted R Squared = .877)

Profile Plots

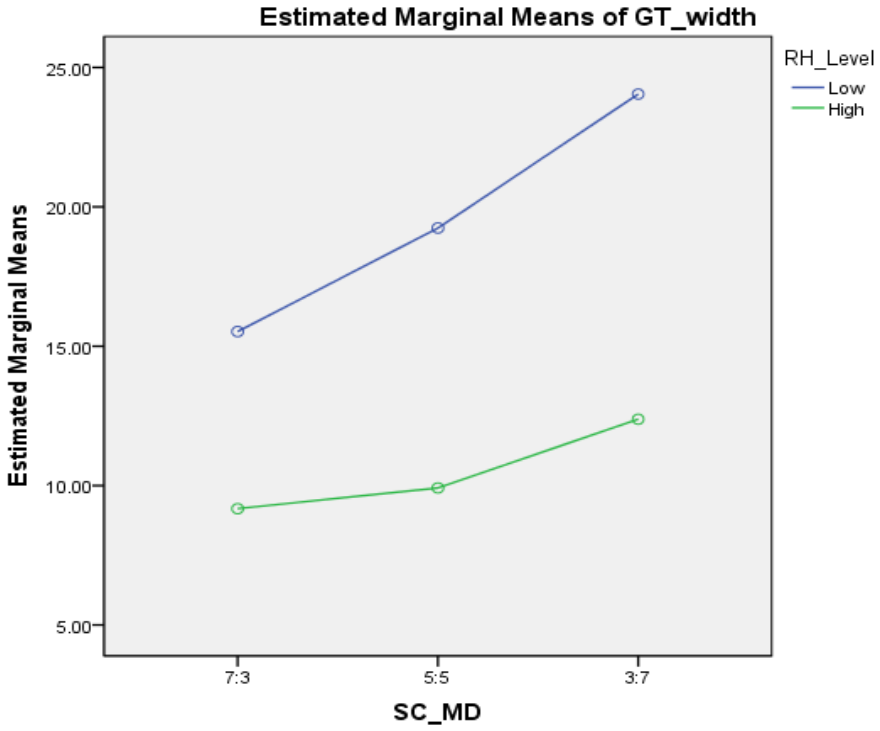

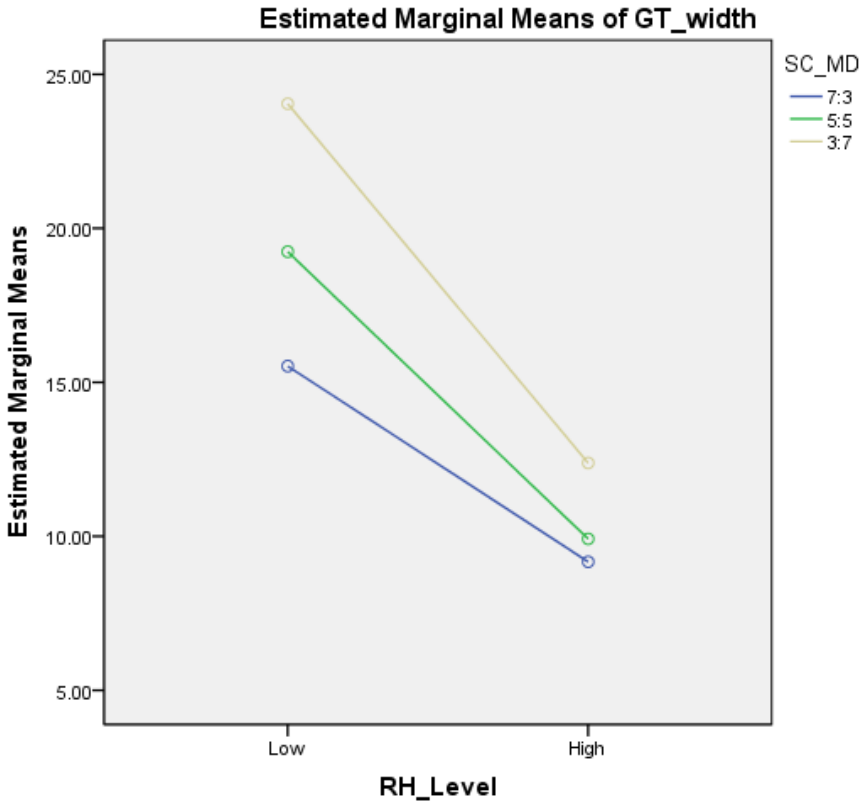

Appendix 2.4 Statistical analysis of specific heat change at the glass transition ($\Delta C_{p,GT}$)

Table A2.4.1 Factors and levels for the analysis of $\Delta C_{p,GT}$

Between-Subjects Factors

		Value Label	N
RH_Level	1	Low	18
	2	High	18
Citrate_SC	1	0	12
	2	0.1	12
	3	0.2	12
SC_MD	1	7:3	12
	2	5:5	12
	3	3:7	12

Table A2.4.2 The original ANOVA table for the analysis of $\Delta C_{p,GT}$

Tests of Between-Subjects Effects

Dependent Variable:DCp_Change

Source	Type III Sum of Squares	df	Mean Square	F	Sig.
Corrected Model	8.455[a]	17	.497	280.592	.000
Intercept	13.661	1	13.661	7707.318	.000
RH_Level	3.498	1	3.498	1973.312	.000
Citrate_SC	.098	2	.049	27.656	.000
SC_MD	2.910	2	1.455	820.802	.000
RH_Level * Citrate_SC	.082	2	.041	23.256	.000
RH_Level * SC_MD	1.822	2	.911	514.088	.000
Citrate_SC * SC_MD	.028	4	.007	3.916	.019
RH_Level * Citrate_SC * SC_MD	.017	4	.004	2.370	.091
Error	.032	18	.002		
Total	22.148	36			
Corrected Total	8.487	35			

a. R Squared = .996 (Adjusted R Squared = .993)

Profile Plots: SC_MD * Citrate_SC * RH_Level

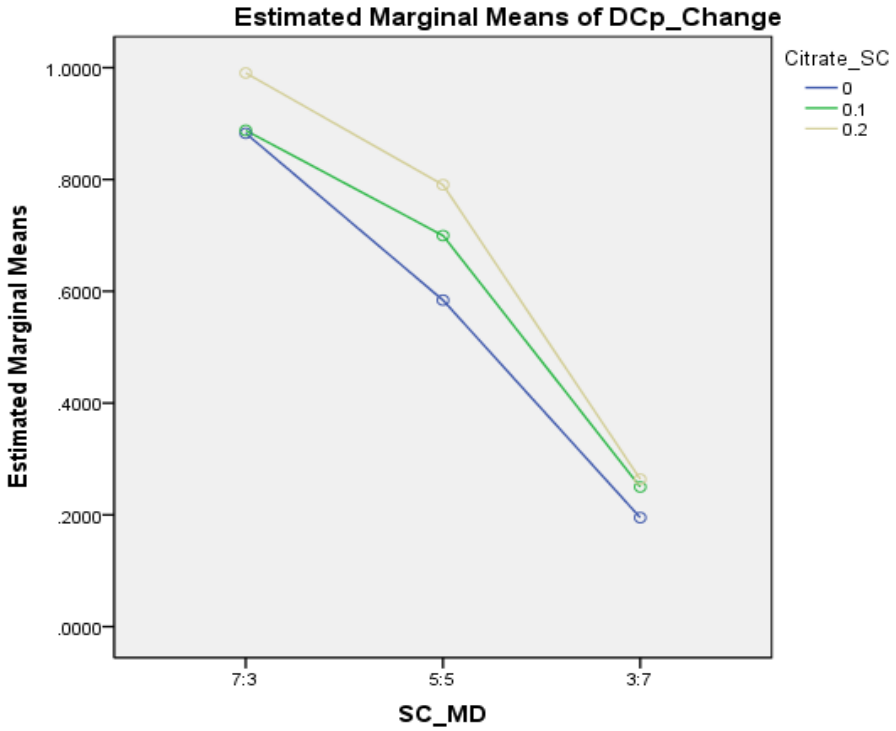

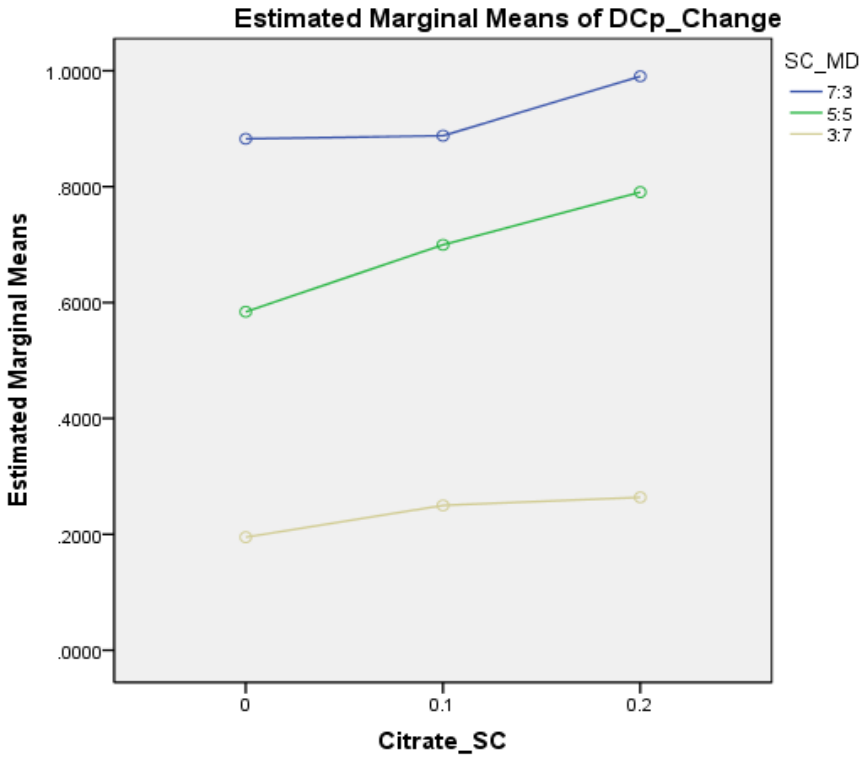

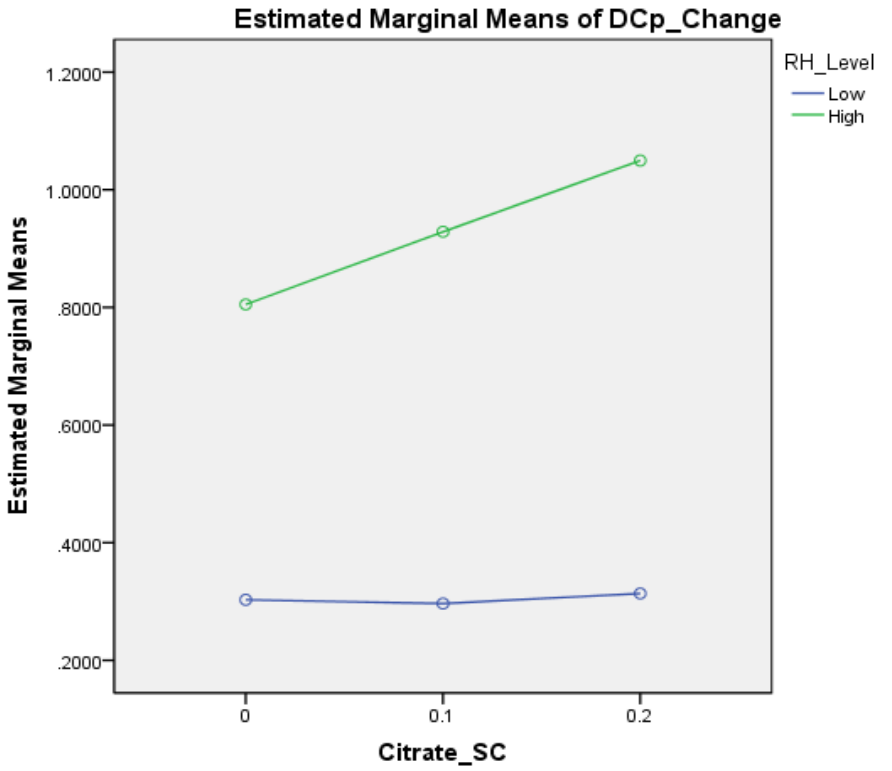
Estimated Marginal Means of DCp_Change
Estimated Marginal Means
1.2000
1.0000
.8000
.6000
.4000
.2000
0
0.1
0.2
Citrate_SC
RH_Level
Low
High

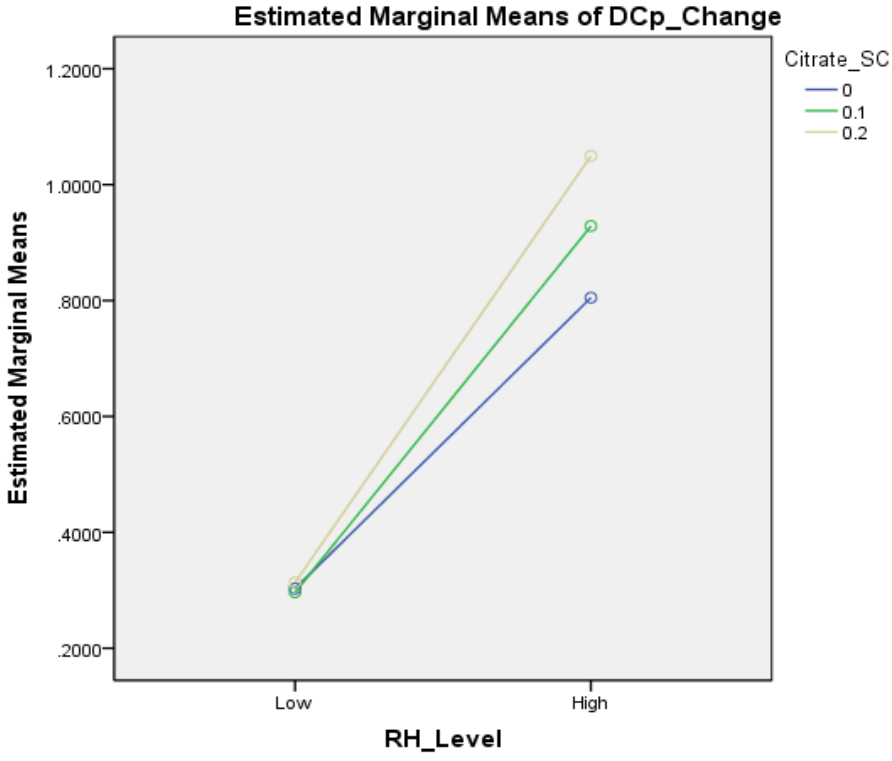
Estimated Marginal Means of DCp_Change
Estimated Marginal Means
1.2000
1.0000
.8000
.6000
.4000
.2000
Low
High
RH_Level
Citrate_SC
0
0.1
0.2

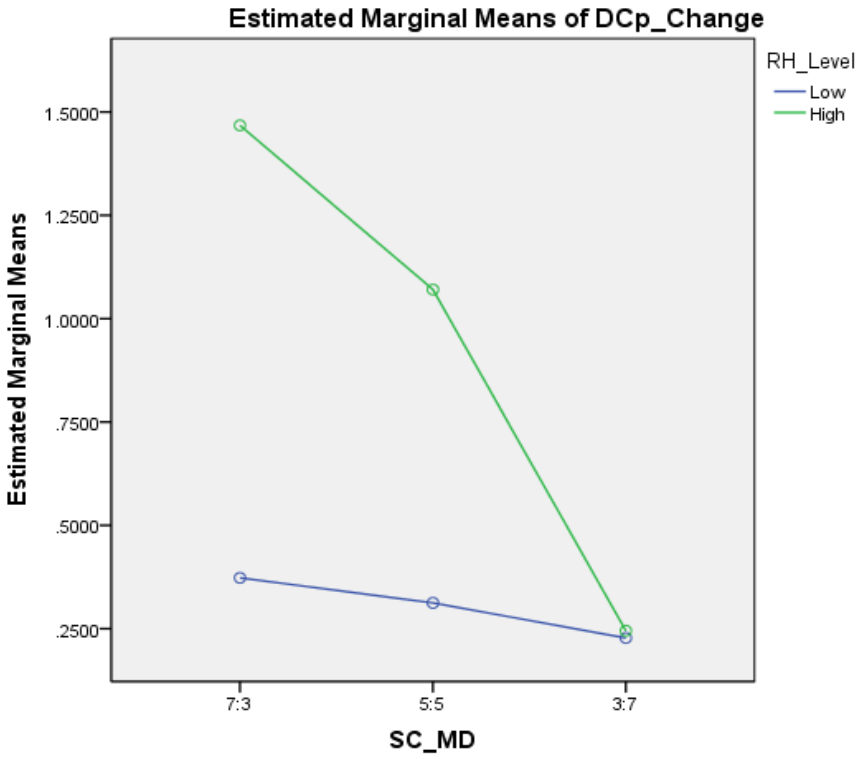
Estimated Marginal Means of DCp_Change
RH_Level
Low
High
Estimated Marginal Means
1.5000
1.2500
1.0000
.7500
.5000
.2500
7:3
5:5
3:7
SC_MD

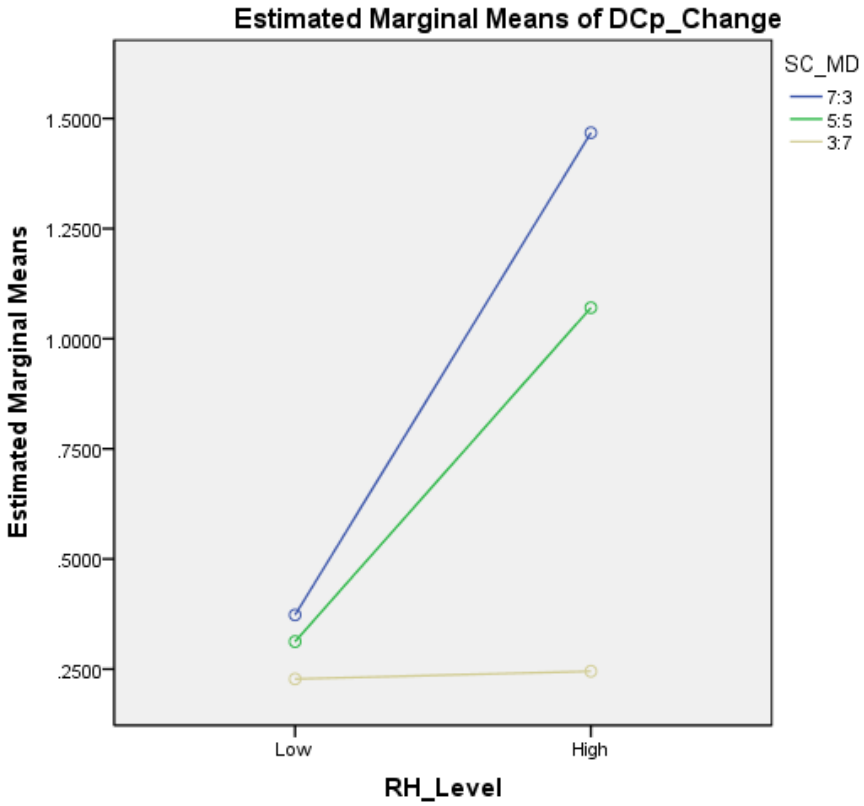
Estimated Marginal Means of DCp_Change
SC_MD
7:3
5:5
3:7
Estimated Marginal Means
1.5000
1.2500
1.0000
.7500
.5000
.2500
Low
High
RH_Level

Table A2.4.3 Summary of the follow-up ANOVA table for the analysis of $\Delta C_{p,GT}$

Source	Type III Sum of Squares	df	Mean Square	F	Sig.
RH_Level	3.498	1	3.498	1973.312	.000
Citrate_SC	.098	2	.049	27.656	.000
SC_MD	2.910	2	1.455	820.802	.000
RH_Level * Citrate_SC	.082	2	.041	23.256	.000
RH_Level * SC_MD	1.822	2	.911	514.088	.000
Citrate_SC * SC_MD	.028	4	.007	3.916	.019
RH_Level * Citrate_SC * SC_MD	.017	4	.004	2.370	.091
Citrate_SC @ RH_Level					
Citrate_SC @ RH_Level=Low	.001	2	.000	.253	.779
Citrate_SC @ RH_Level=High	.180	2	.090	50.660	.000
RH_Level @ Citrate_SC					
RH_Level @ Citrate_SC= 0	.756	1	.756	426.719	.000
RH_Level @ Citrate_SC= 0.1	1.198	1	1.198	676.068	.000
RH_Level @ Citrate_SC= 0.2	1.625	1	1.625	917.038	.000
SC_MD @ RH_Level					
SC_MD @ RH_Level=Low	.064	2	.032	18.053	.000
SC_MD @ RH_Level=High	4.668	2	2.334	1316.838	.000
RH_Level @ SC_MD					
RH_Level @ SC_MD= 7:3	3.595	1	3.595	2028.259	.000
RH_Level @ SC_MD= 5:5	1.724	1	1.724	972.716	.000
RH_Level @ SC_MD= 3:7	.001	1	.001	.513	.483
SC_MD @ Citrate_SC					
SC_MD @ Citrate_SC= 0	.951	2	.475	268.202	.000
SC_MD @ Citrate_SC= 0.1	.859	2	.430	242.436	.000
SC_MD @ Citrate_SC= 0.2	1.127	2	.564	317.996	.000
Citrate_SC @ SC_MD					
Citrate_SC @ SC_MD= 7:3	.030	2	.015	8.352	.003
Citrate_SC @ SC_MD= 5:5	.086	2	.043	24.155	.000
Citrate_SC @ SC_MD= 3:7	.011	2	.005	2.980	.076
Error	.032	18	.002		
Corrected Total	8.487	35			

Table A2.4.4 Homogeneous Subsets for RH_Level*Citrate_SC

A: Effect of Citrate_SC at each level of RH_Level (Tukey HSD[a,b])

RH_Level	Citrate_SC	N	Subset		
			1	2	3
Low	0	6	0.303		
	0.1	6	0.296		
	0.2	6	0.314		
High	0	6	0.805		
	0.1	6		0.929	
	0.2	6			1.050

Means for groups in homogeneous subsets are displayed. Based on observed means.
The error term is Mean Square (Error) = 0.002.
a. Uses Harmonic Mean Sample Size = 6.000.
b. Alpha = .050.

B: Effect of RH_Level at each level of Citrate_SC

Citrate_SC	RH_Level	N	Subset	
			1	2
0	Low	6	0.303	
	High	6		0.805
0.1	Low	6	0.296	
	High	6		0.929
0.2	Low	6	0.314	
	High	6		1.050

Based on estimated marginal means.
The mean difference is significant at the .05 level.
Adjustment for multiple comparisons (for two means): Least significant difference (equivalent to no adjustments).

Table A2.4.5 Homogeneous Subsets for RH_Level*SC_MD

A: Effect of SC_MD at each level of RH_Level (Tukey HSD[a,b])

RH_Level	SC_MD	N	Subset		
			1	2	3
Low	7:3	6	0.373		
	5:5	6	0.312		
	3:7	6		0.228	
High	7:3	6	1.468		
	5:5	6		1.071	
	3:7	6			0.245

Means for groups in homogeneous subsets are displayed. Based on observed means.
The error term is Mean Square (Error) = 0.002.
a. Uses Harmonic Mean Sample Size = 6.000. b. Alpha = .050.

B: Effect of RH_Level at each level SC_MD

SC_MD	RH_Level	N	Subset	
			1	2
7:3	Low	6	0.373	
	High	6		1.468
5:5	Low	6	0.312	
	High	6		1.071
3:7	Low	6	0.228	
	High	6	0.245	

Based on estimated marginal means. The mean difference is significant at the .05 level.
Adjustment for multiple comparisons (for two means): Least significant difference (equivalent to no adjustments).

Table A2.4.6 Homogeneous Subsets for Citrate*SC_MD

A: Effect of SC_MD at each level of Citrate_SC (Tukey HSD[a,b])

Citrate_SC	SC_MD	N	Subset		
			1	2	3
0	7:3	4	0.883		
	5:5	4		0.584	
	3:7	4			0.195
0.1	7:3	4	0.888		
	5:5	4		0.700	
	3:7	4			0.250
0.2	7:3	4	0.990		
	5:5	4		0.791	
	3:7	4			0.264

B: Effect of Citrate_SC at each level of SC_MD (Tukey HSD[a,b])

SC_MD	Citrate_SC	N	Subset		
			1	2	3
7:3	0	4	0.883		
	0.1	4	0.888		
	0.2	4		0.990	
5:5	0	4	0.584		
	0.1	4		0.700	
	0.2	4			0.791
3:7	0	4	0.195		
	0.1	4	0.250		
	0.2	4	0.264		

Means for groups in homogeneous subsets are displayed. Based on observed means.
The error term is Mean Square (Error) = 0.002.
a. Uses Harmonic Mean Sample Size = 4.000. b. Alpha = .050.

Appendix 2.5 Plots of relative enthalpy relaxation obtained from aging experiments

Each data point represents the mean value of relative enthalpy recovery from two replications. Three individual measurements were made for each replication. Error bars reflect the standard deviation.

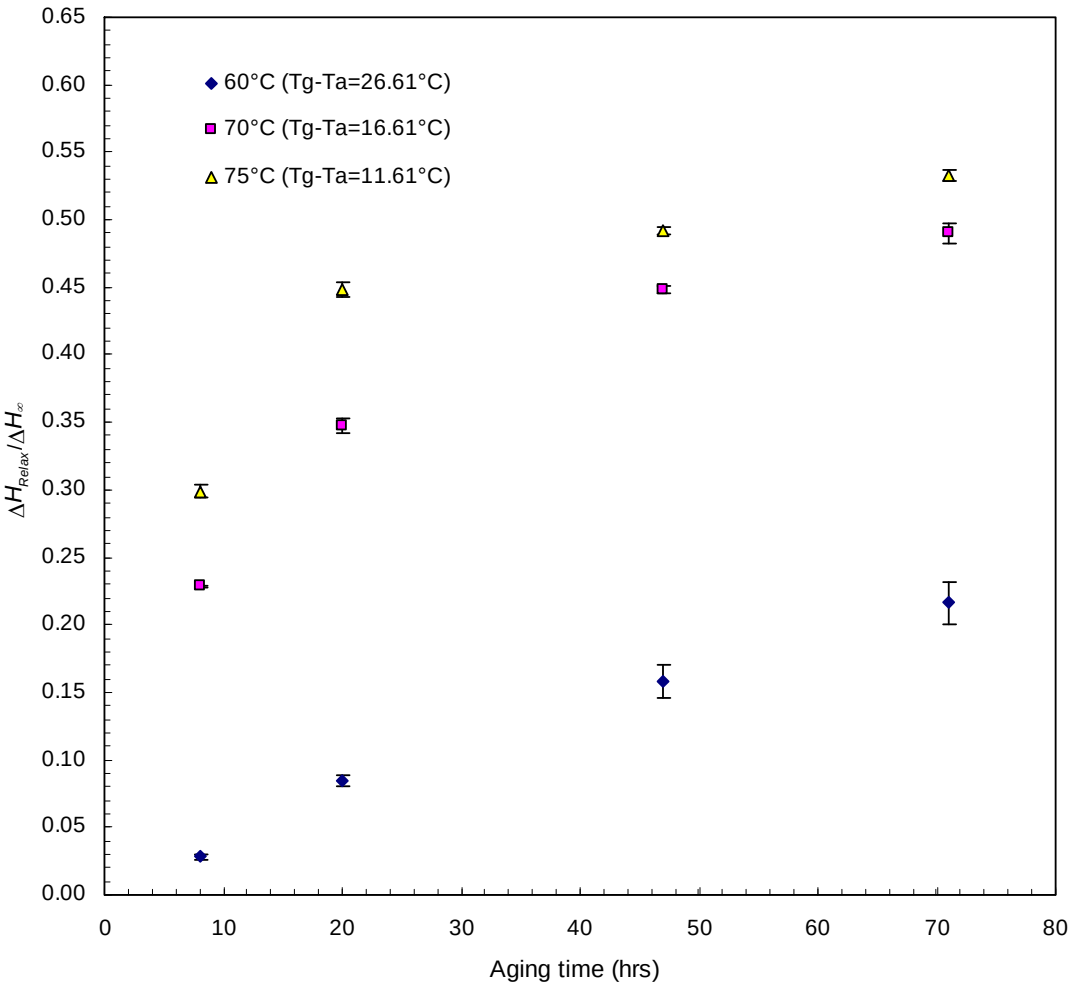

Figure A2.5.1 Relative enthalpy relaxation of a sample consisting of 7:3 S without Na citrate salt obtained at three different aging temperatures.

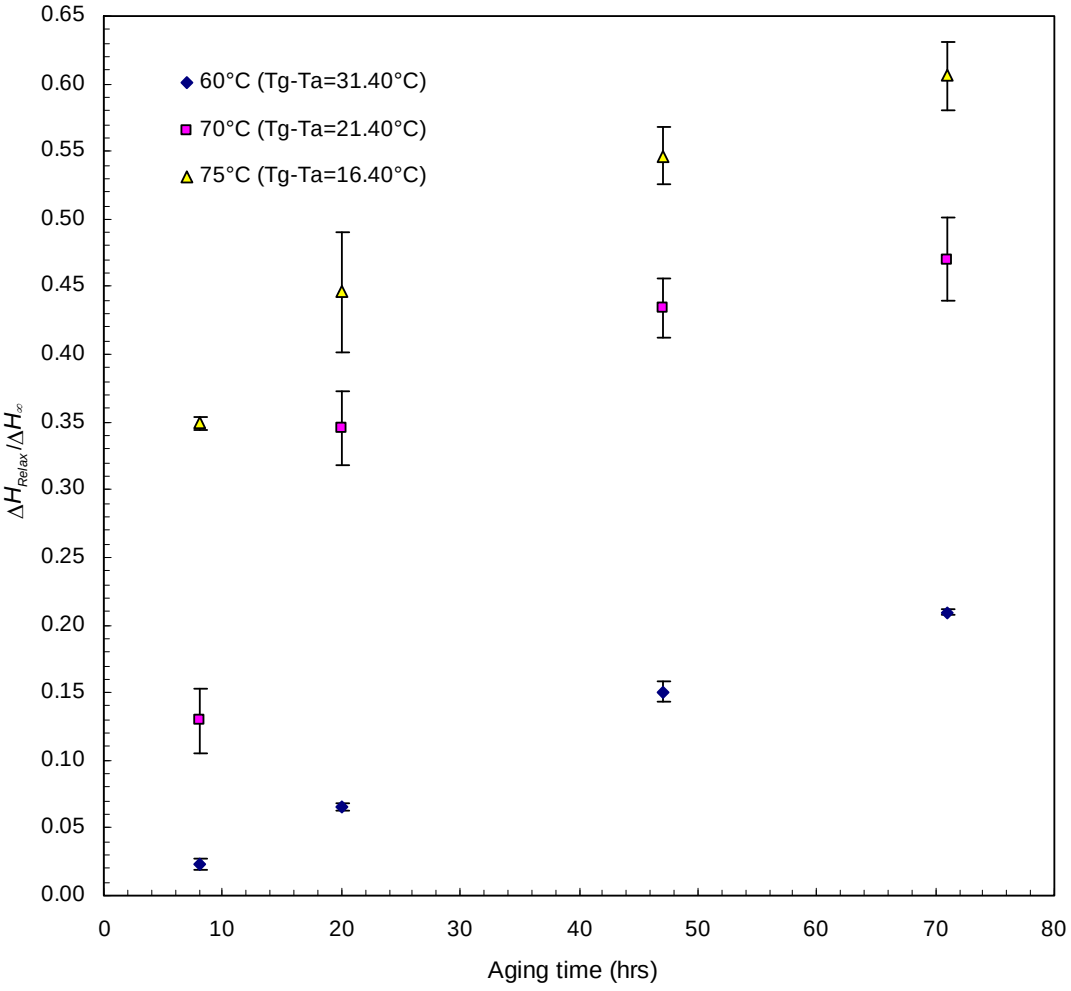

Figure A2.5.2 Relative enthalpy relaxation of a sample consisting of 7:3 sucrose/maltodextrin with Na citrate/sucrose of 0.1 obtained at three different aging temperatures.

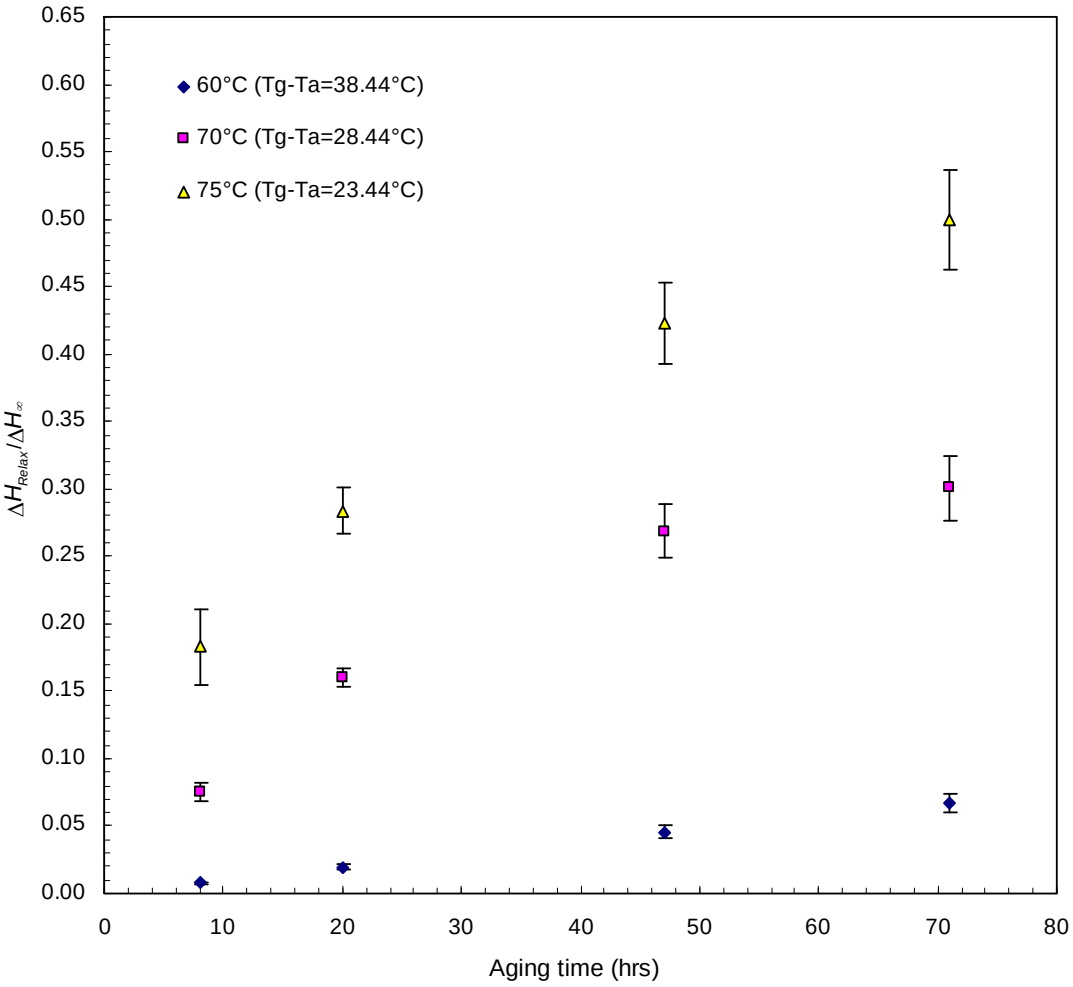

Figure A2.5.3 Relative enthalpy relaxation of a sample consisting of 7:3 sucrose/maltodextrin with Na citrate/sucrose of 0.2 obtained at three different aging temperatures.

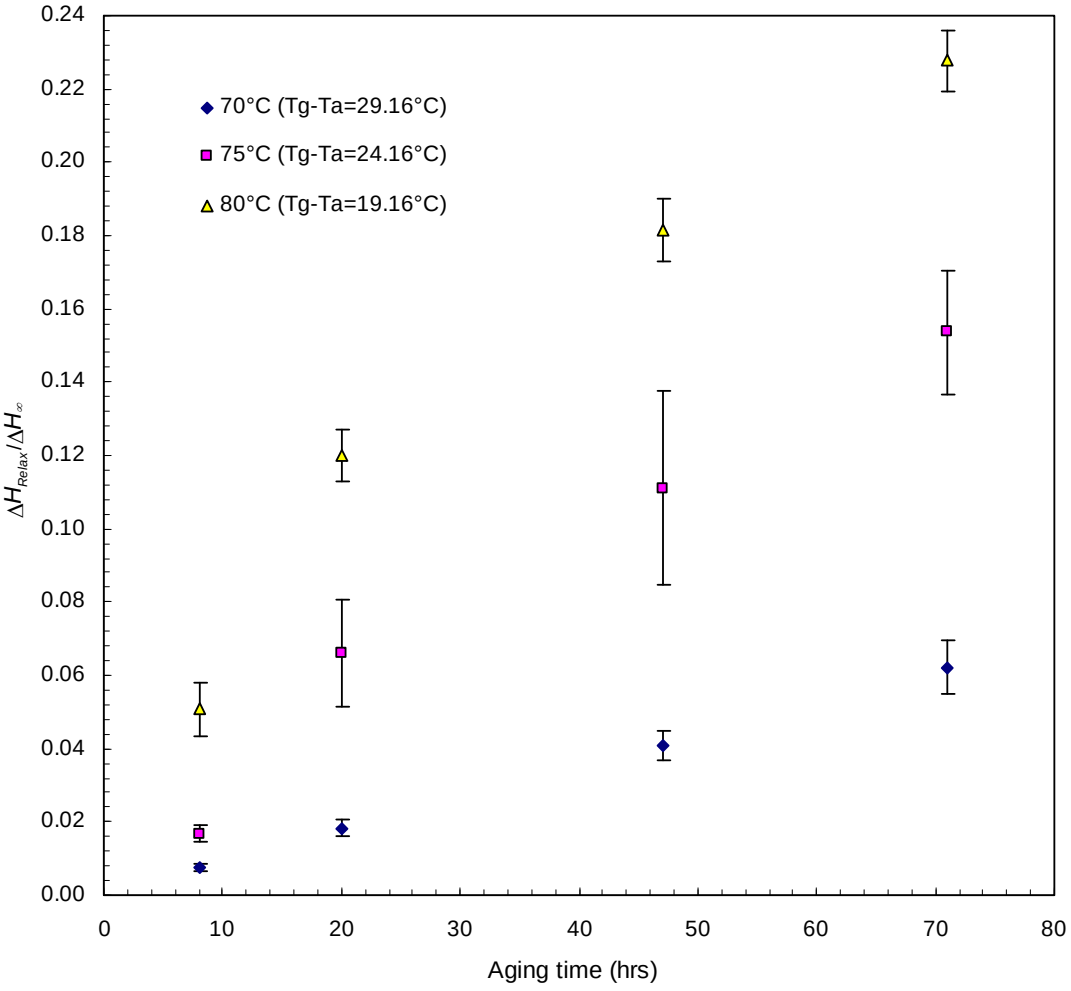

Figure A2.5.4 Relative enthalpy relaxation of a sample consisting of 5:5 sucrose/maltodextrin without Na citrate salt obtained at three different aging temperatures.

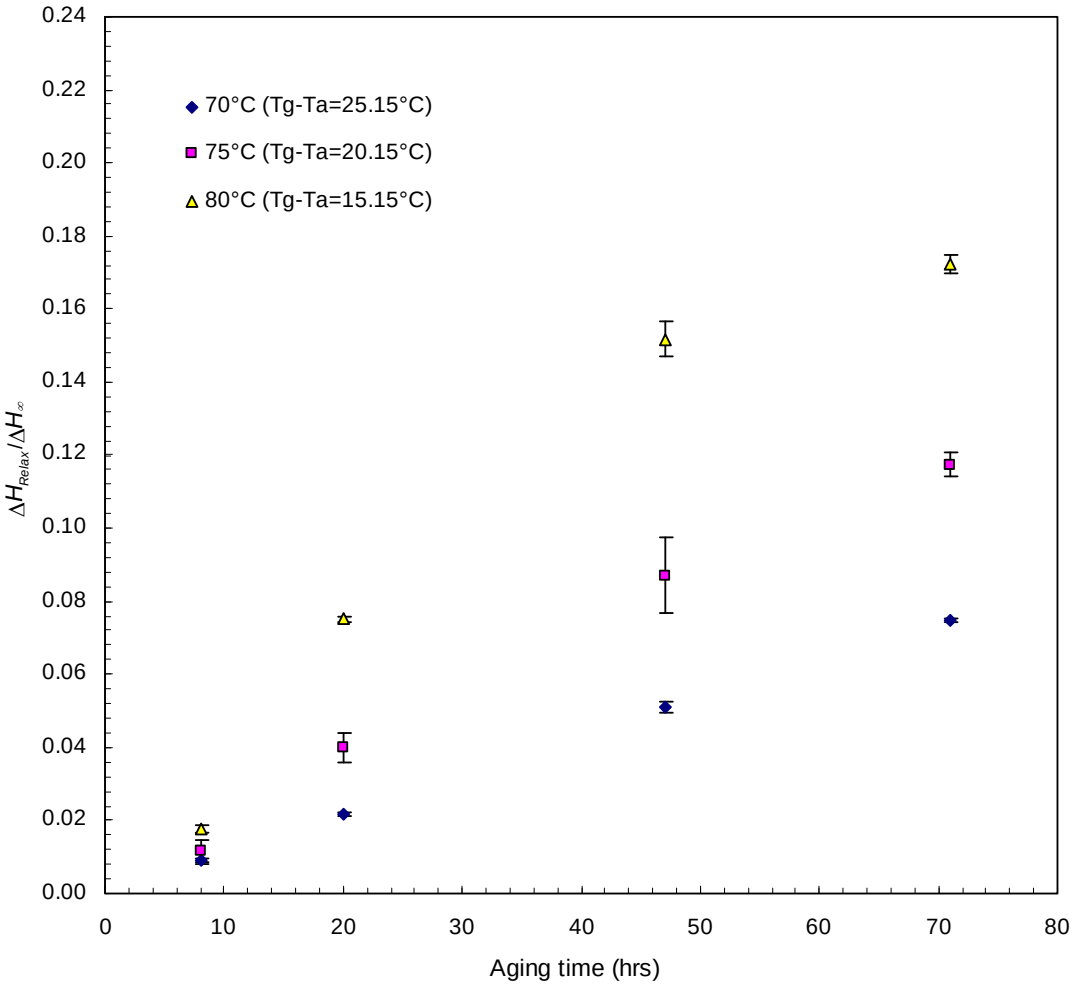

Figure A2.5.5 Relative enthalpy relaxation of a sample consisting of 5:5 sucrose/maltodextrin with Na citrate/sucrose of 0.1 obtained at three different aging temperatures.

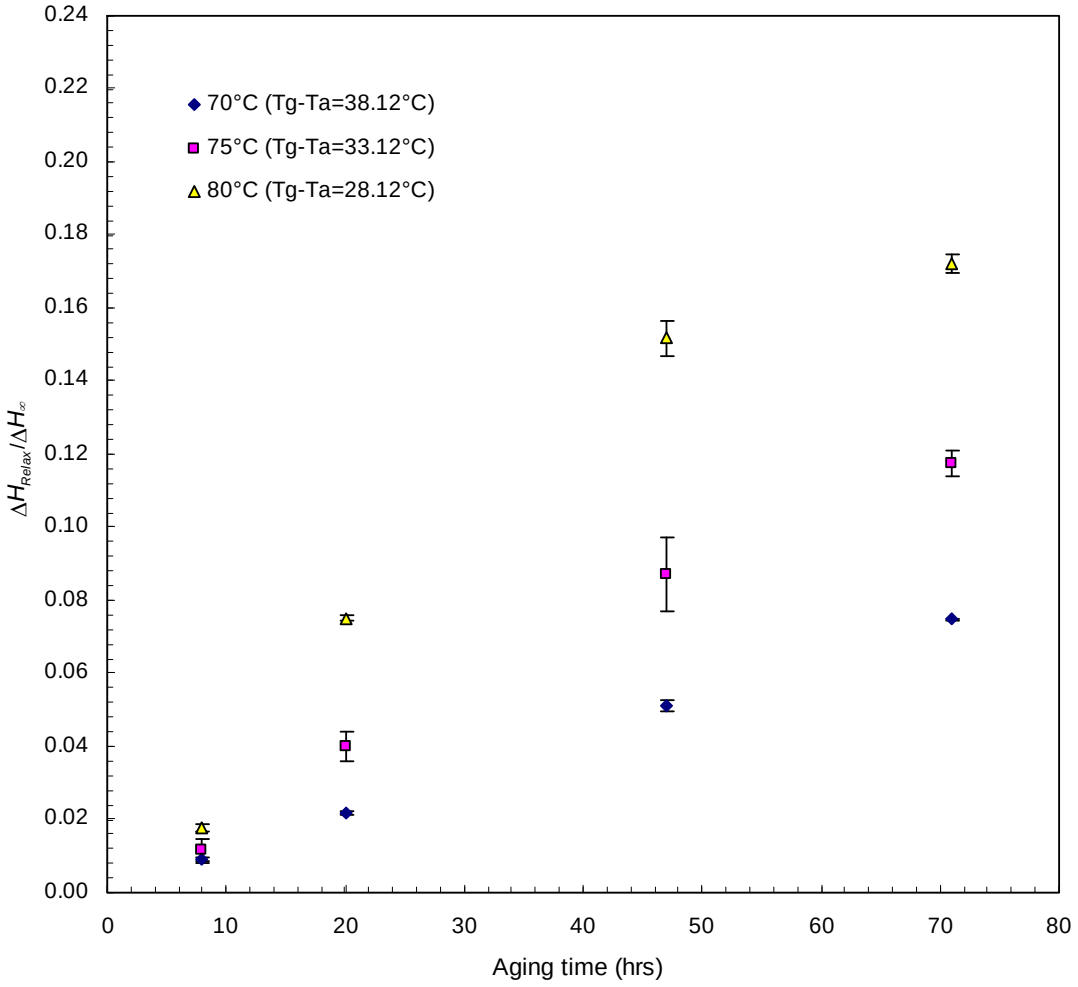

Figure A2.5.6 Relative enthalpy relaxation of a sample consisting of 5:5 sucrose/maltodextrin with Na citrate/sucrose of 0.2 obtained at three different aging temperatures.

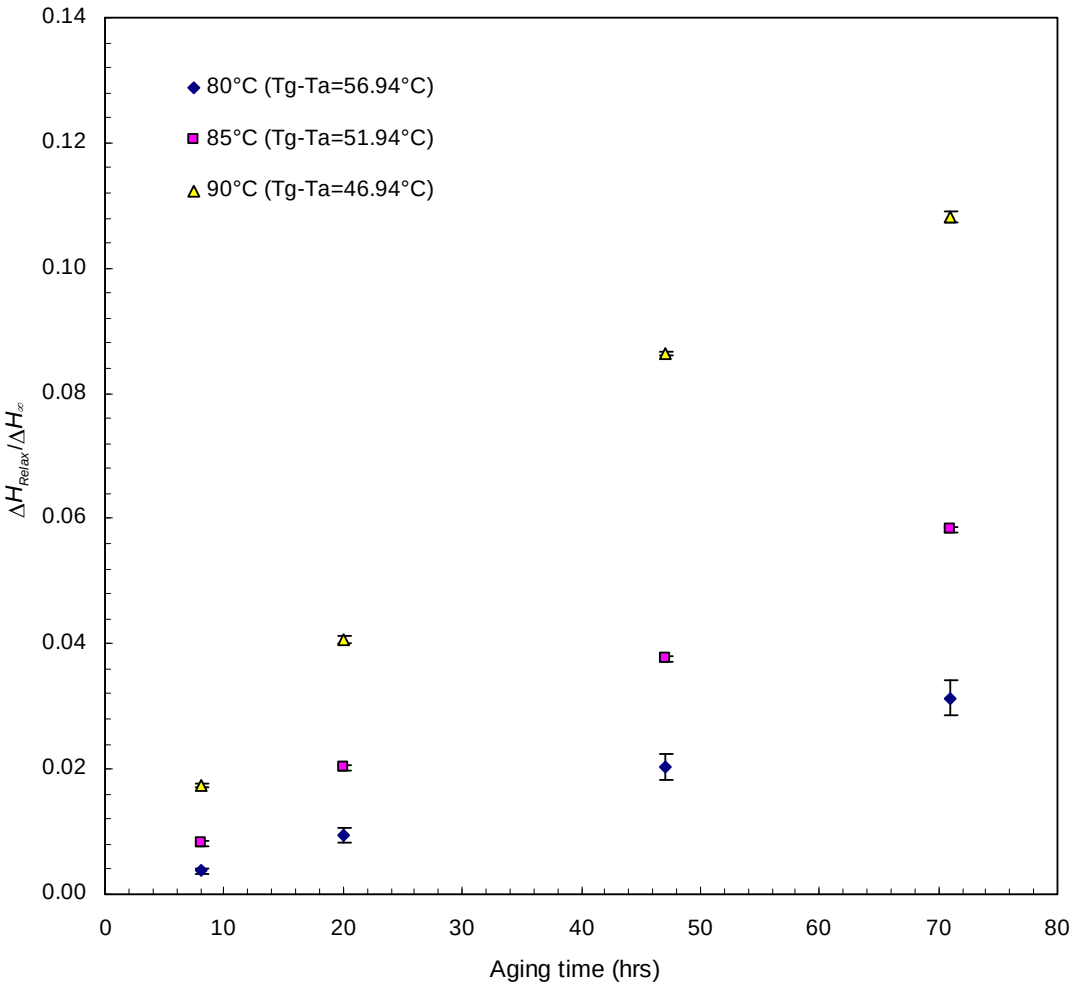

Figure A2.5.7 Relative enthalpy relaxation of a sample consisting of 3:7 sucrose/maltodextrin without Na citrate salt obtained at three different aging temperatures.

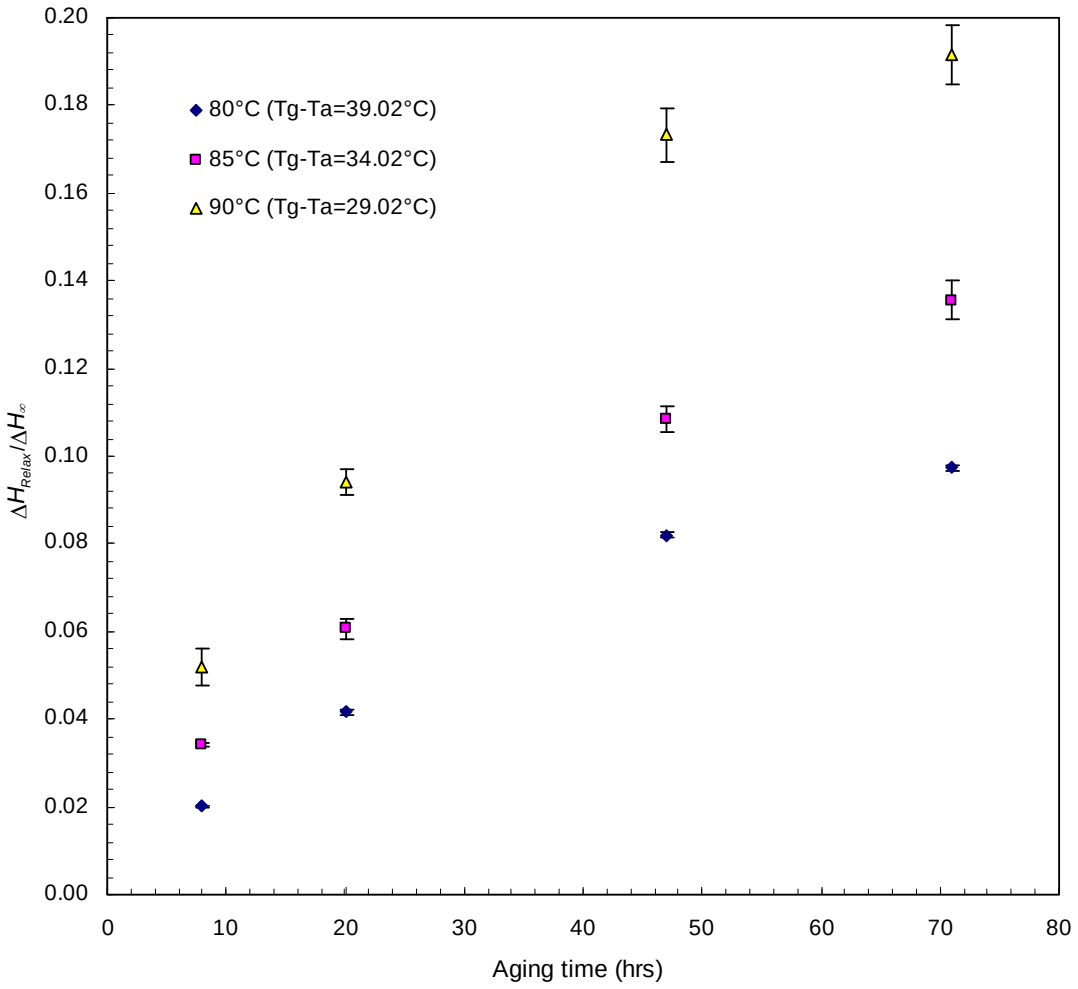

Figure A2.5.8 Relative enthalpy relaxation of a sample consisting of 3:7 sucrose/maltodextrin with Na citrate/sucrose of 0.1 obtained at three different aging temperatures.

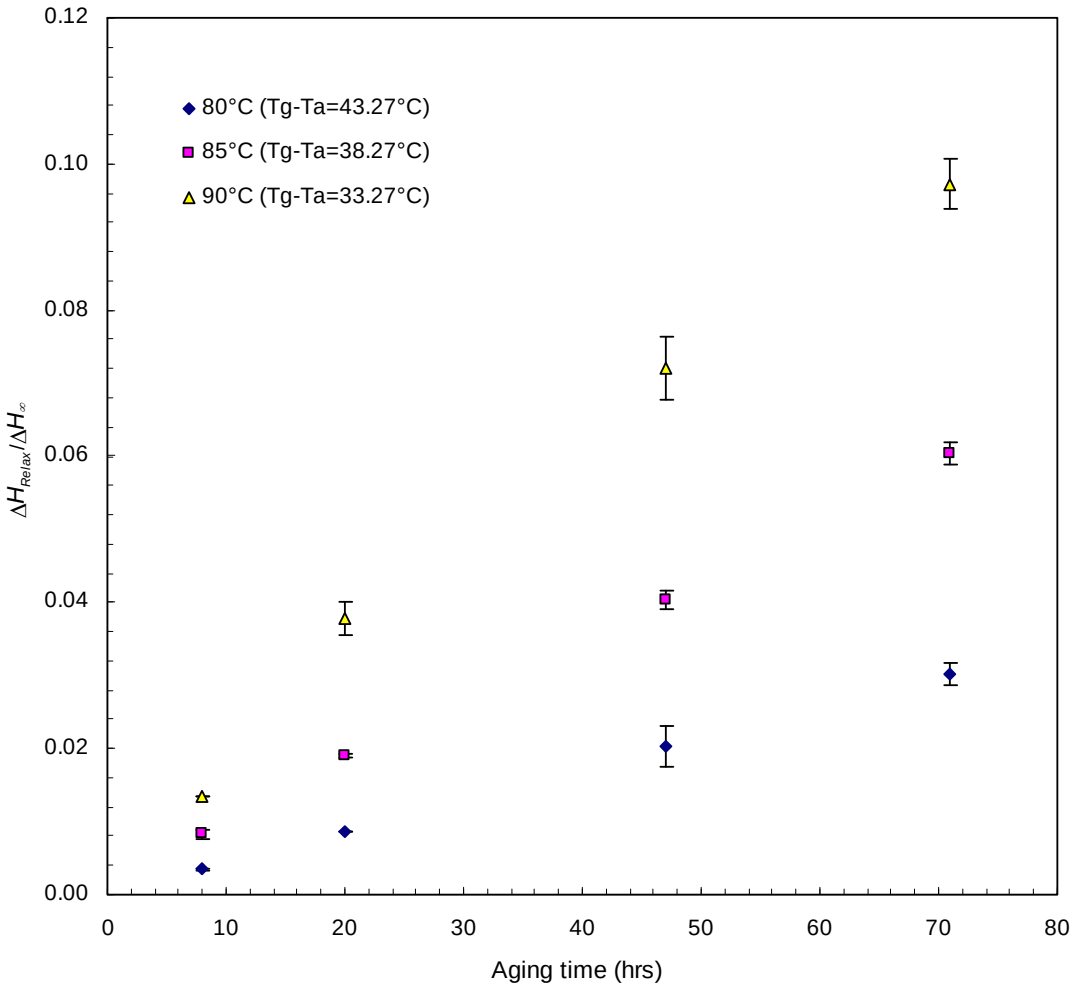

Figure A2.5.9 Relative enthalpy relaxation of a sample consisting of 3:7 sucrose/maltodextrin with Na citrate/sucrose of 0.2 obtained at three different aging temperatures.

Appendix 2.6 Plots for estimating the KWW parameters using the linearised form of double logarithm of $\phi(t)$.

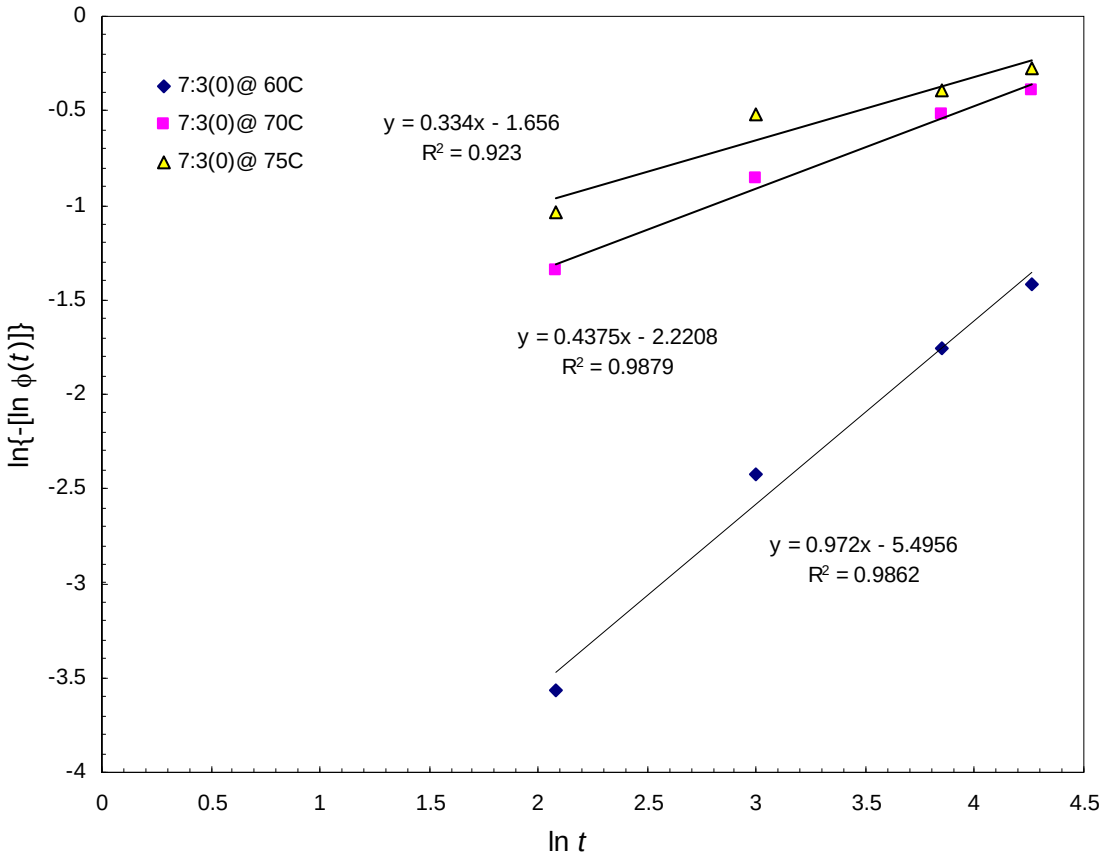

Figure A2.6.1 Plots for linear regression of the KWW parameters for sucrose-maltodextrin based bioglass samples with sucrose/maltodextrin ratio of 7:3, no Na citrate.

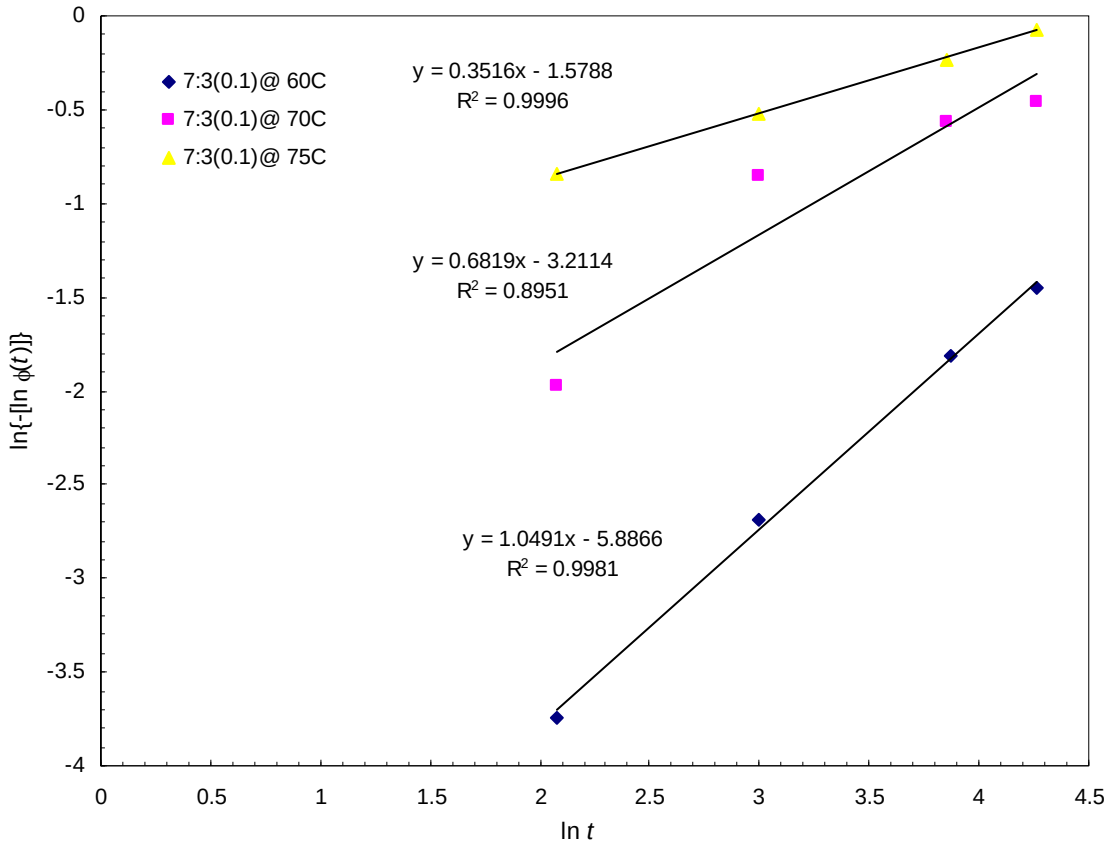

Figure A2.6.2 Plots for linear regression of the KWW parameters for sucrose-maltodextrin based bioglass samples with sucrose/maltodextrin ratio of 7:3, Na citrate/sucrose of 0.1.

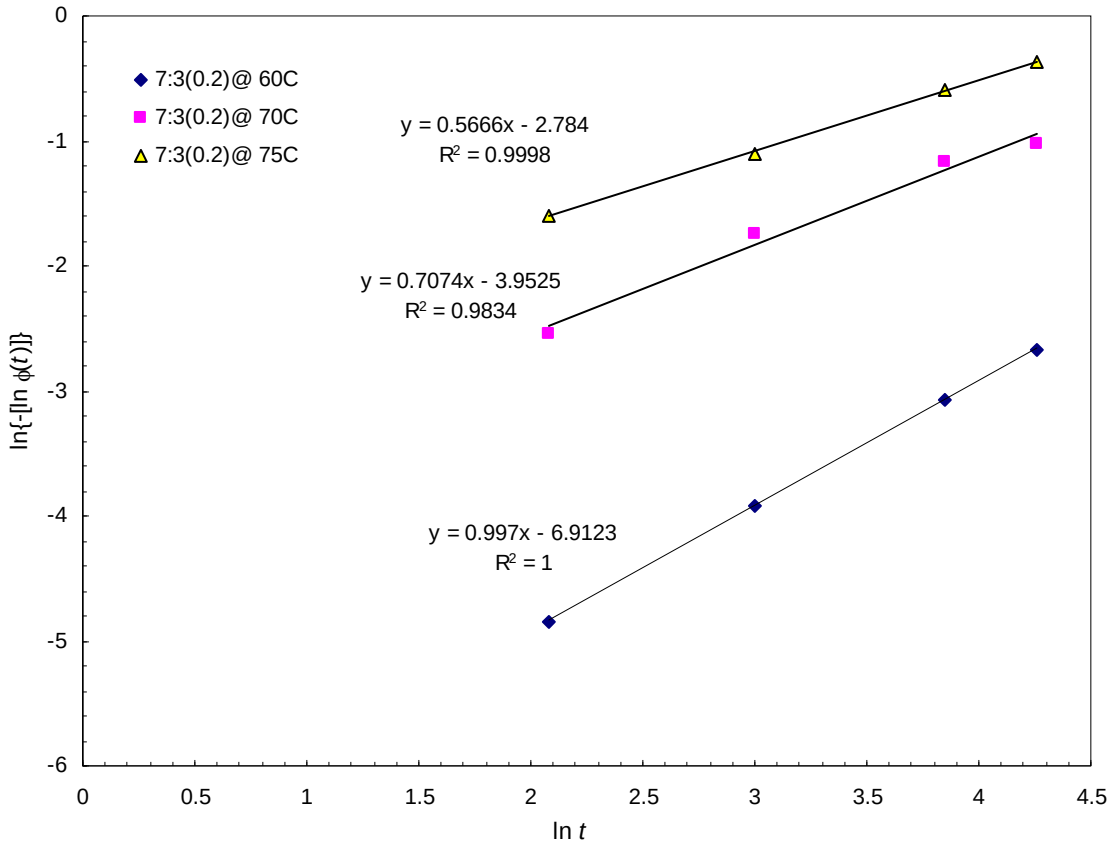

Figure A2.6.3 Plots for linear regression of the KWW parameters for sucrose-maltodextrin based bioglass samples with sucrose/maltodextrin ratio of 7:3, Na citrate/sucrose of 0.2.

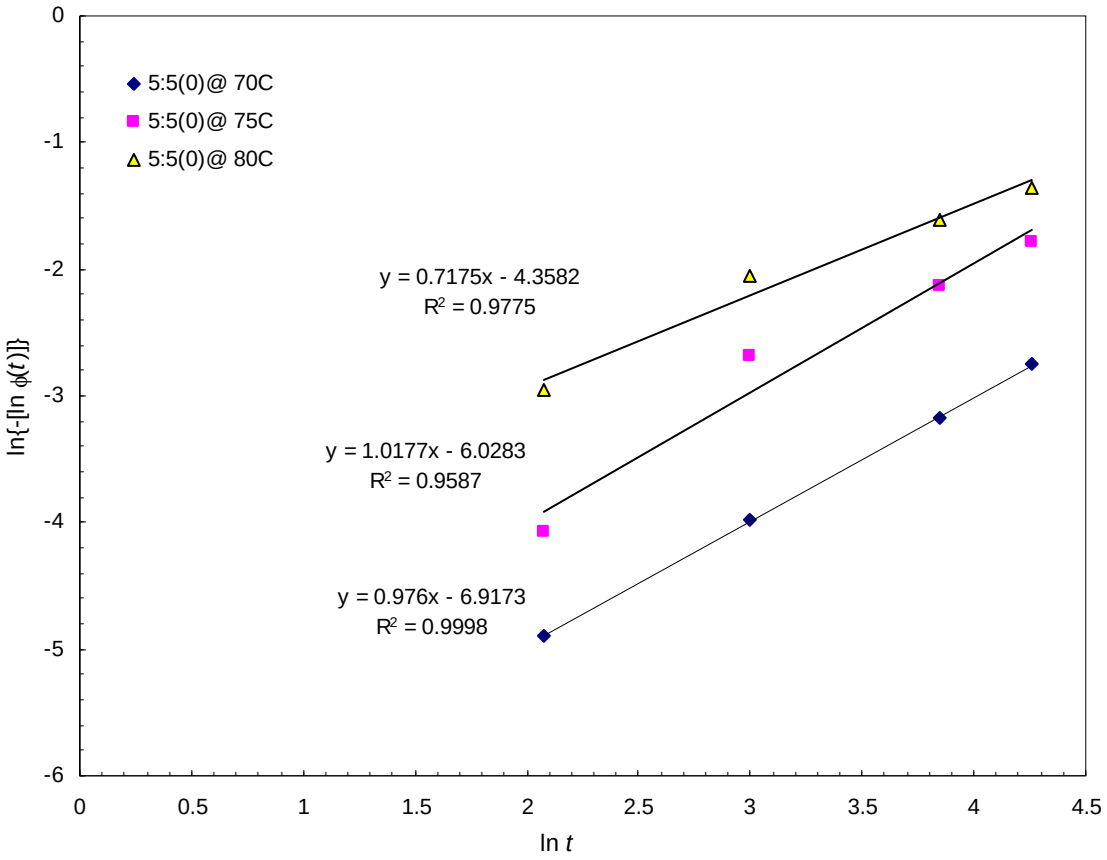

Figure A2.6.4 Plots for linear regression of the KWW parameters for sucrose-maltodextrin based bioglass samples with sucrose/maltodextrin ratio of 5:5, no Na citrate.

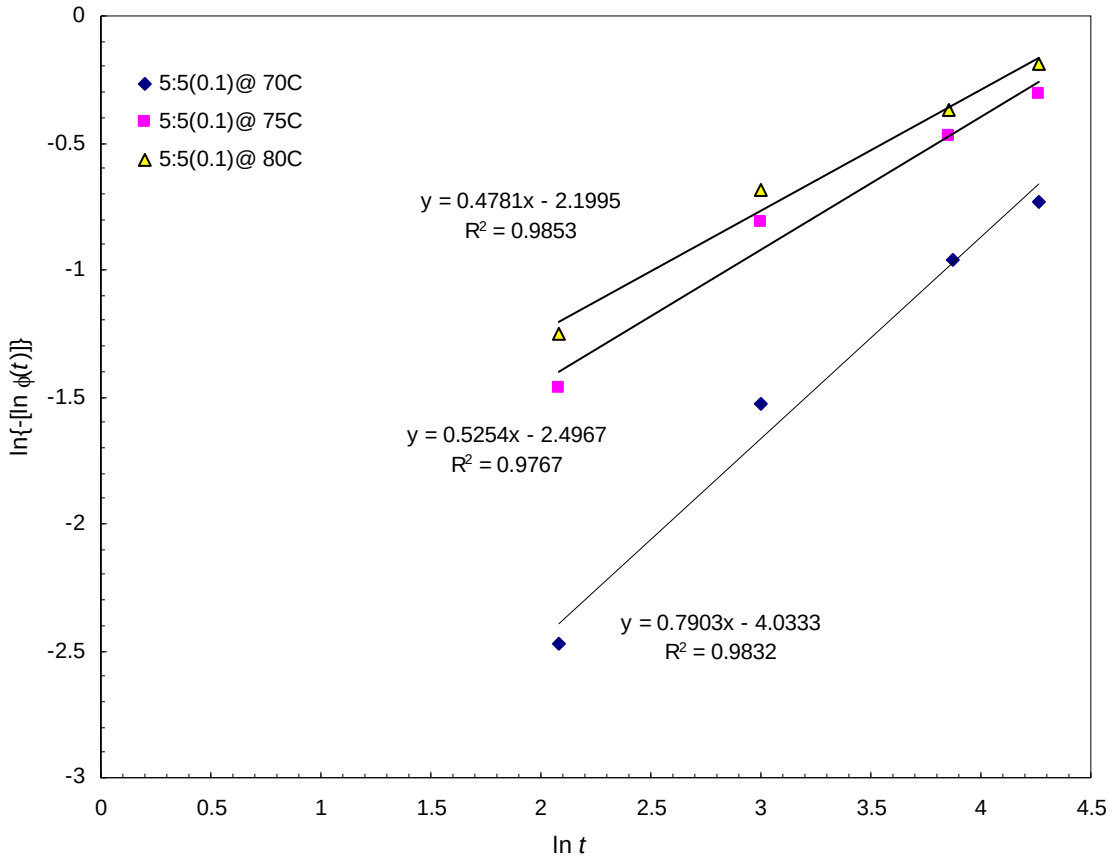

Figure A2.6.5 Plots for linear regression of the KWW parameters for sucrose-maltodextrin based bioglass samples with sucrose/maltodextrin ratio of 5:5, Na citrate/sucrose of 0.1.

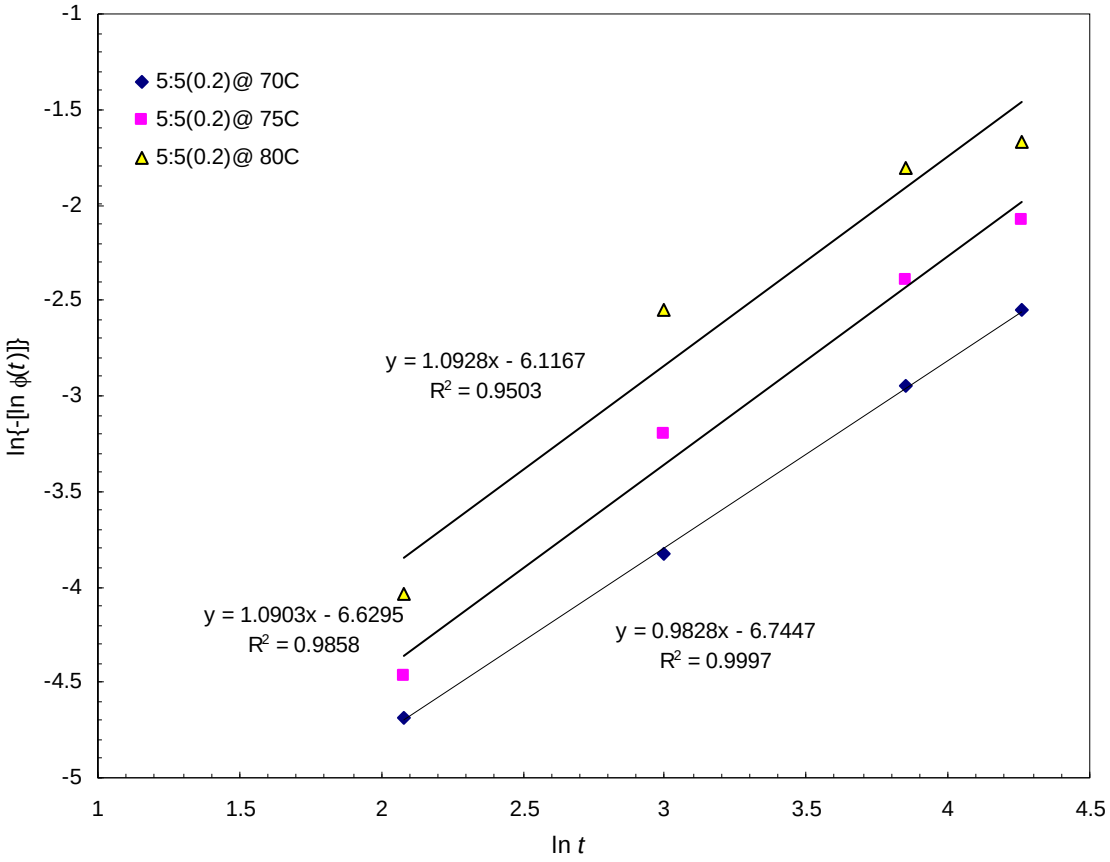

Figure A2.6.6 Plots for linear regression of the KWW parameters for sucrose-maltodextrin based bioglass samples with sucrose/maltodextrin ratio of 5:5, Na citrate/sucrose of 0.2.

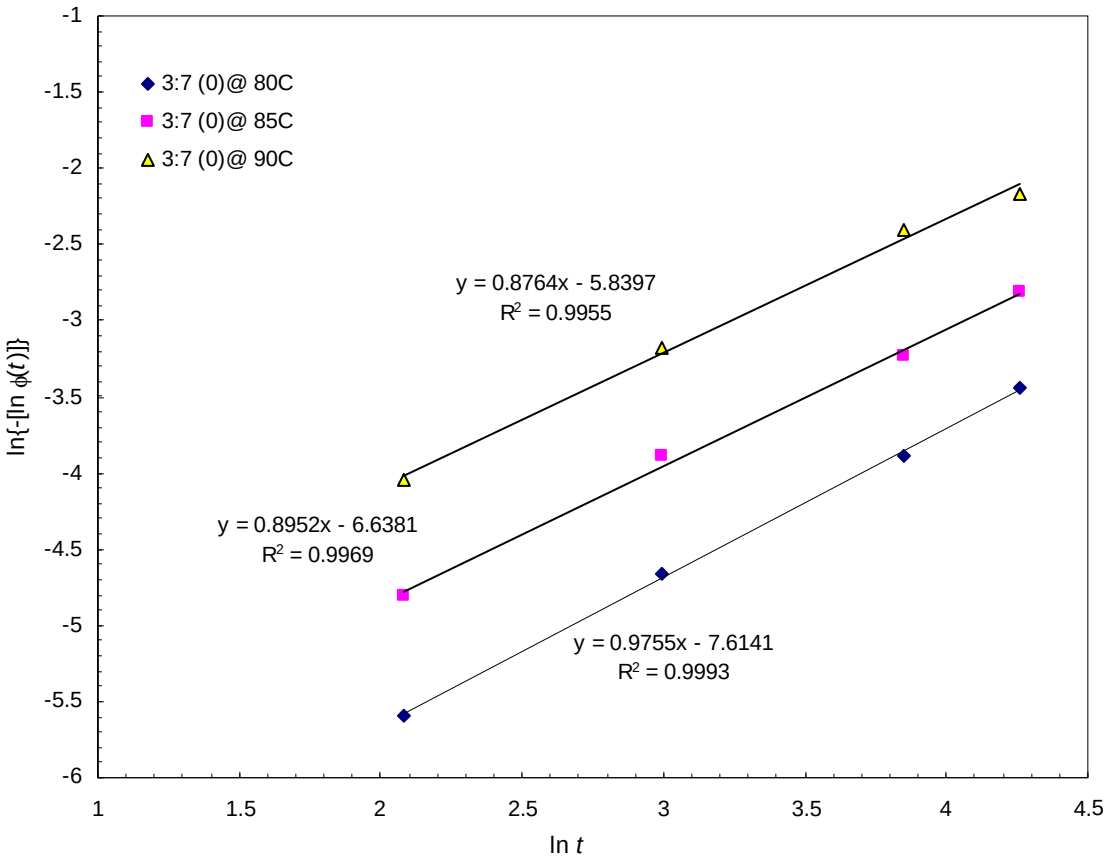

Figure A2.6.7 Plots for linear regression of the KWW parameters for sucrose-maltodextrin based bioglass samples with sucrose/maltodextrin ratio of 3:7, no Na citrate.

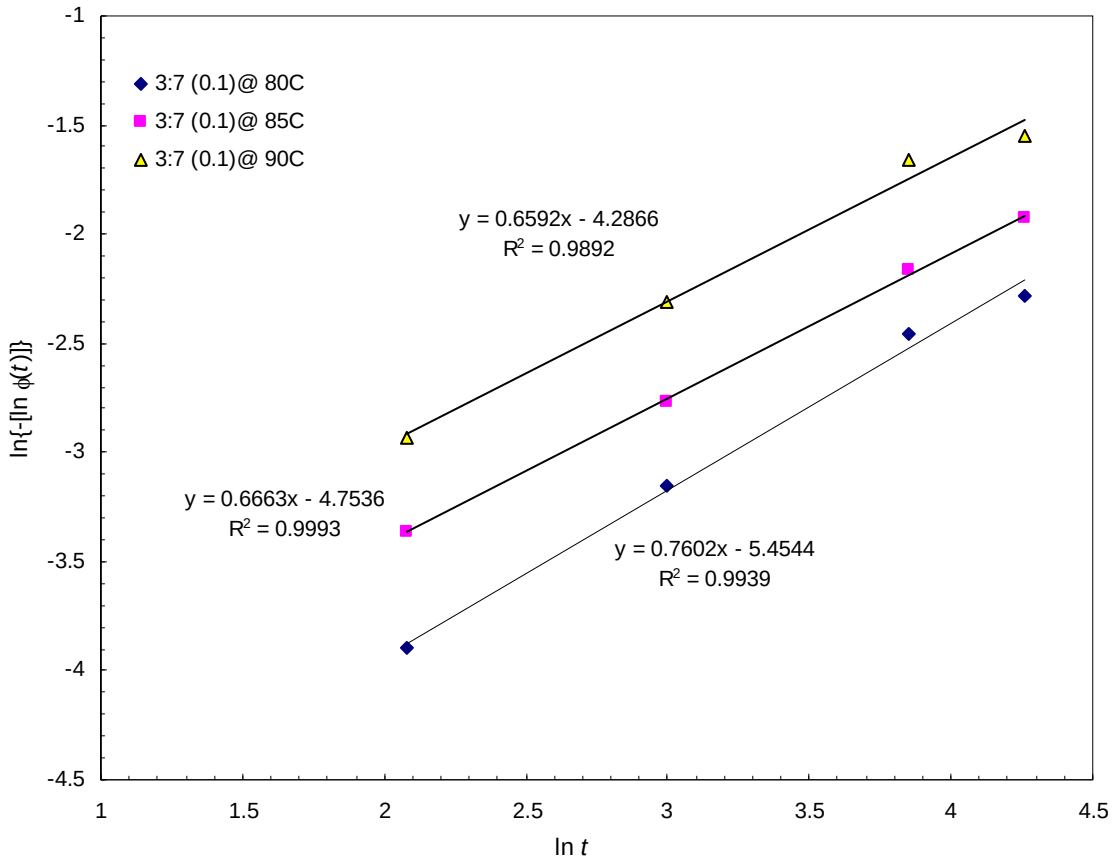

Figure A2.6.8 Plots for linear regression of the KWW parameters for sucrose-maltodextrin based bioglass samples with sucrose/maltodextrin ratio of 3:7, Na citrate/sucrose of 0.1.

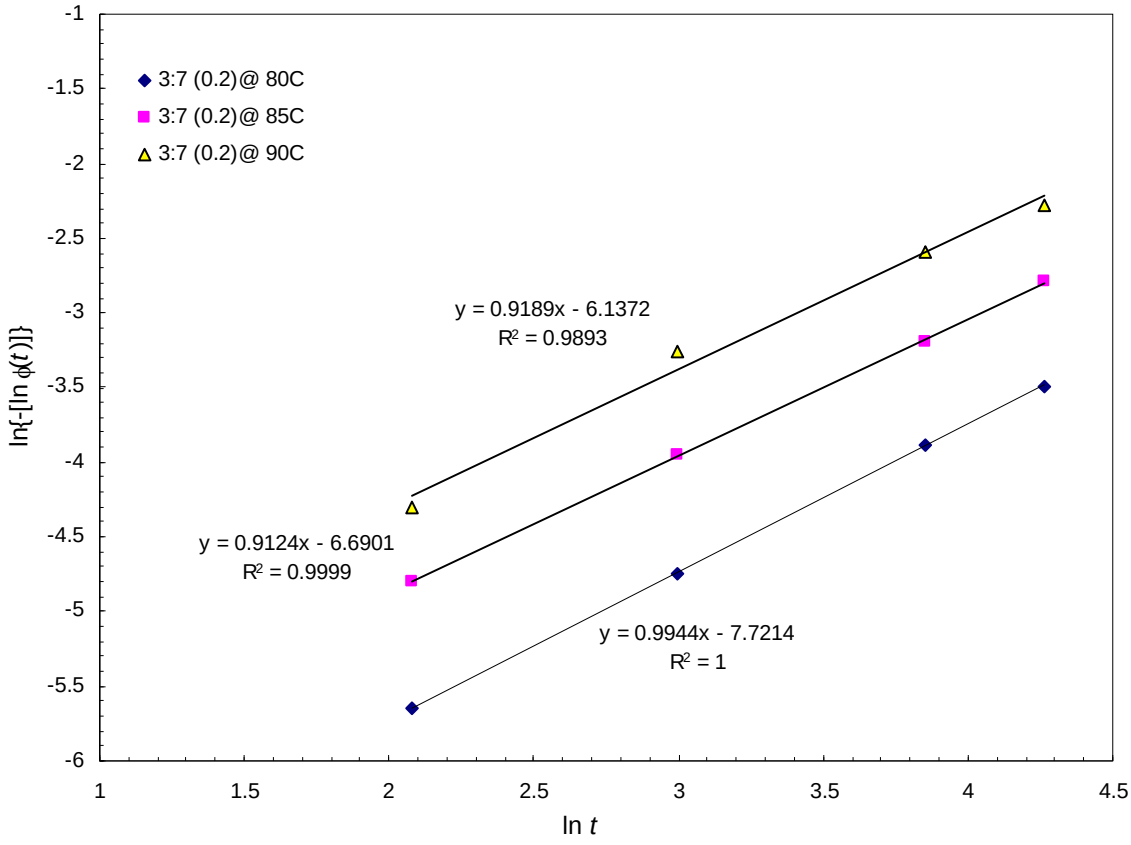

Figure A2.6.9 Plots for linear regression of the KWW parameters for sucrose-maltodextrin based bioglass samples with sucrose/maltodextrin ratio of 3:7, Na citrate/sucrose of 0.2.

Appendix 2.7 The Arrhenius plots of τ^{KWW} obtained with nonlinear regression

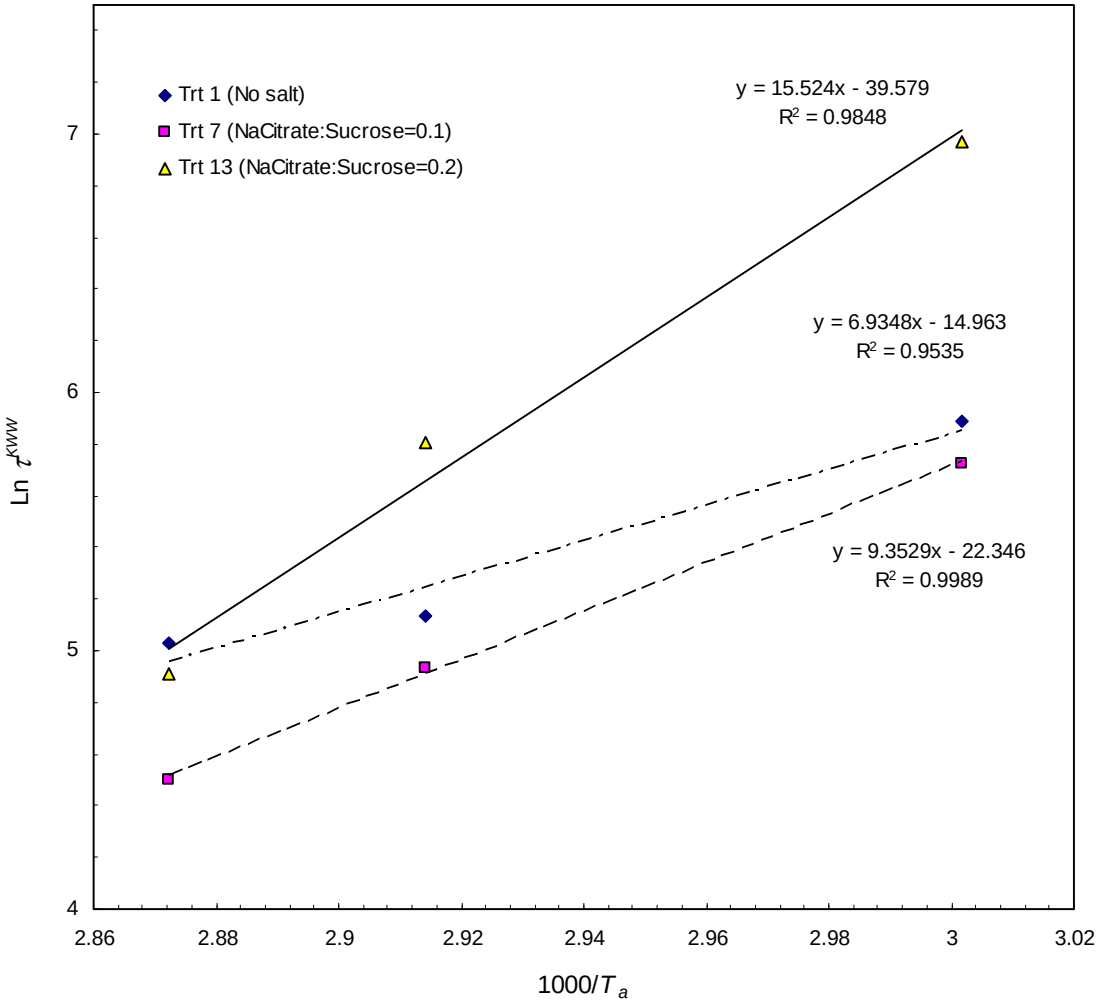

Figure A2.7.1 Arrhenius plots of τ^{KWW} (obtained with nonlinear regression) for sucrose-maltodextrin based bioglass samples with sucrose/maltodextrin ratio of 7:3.

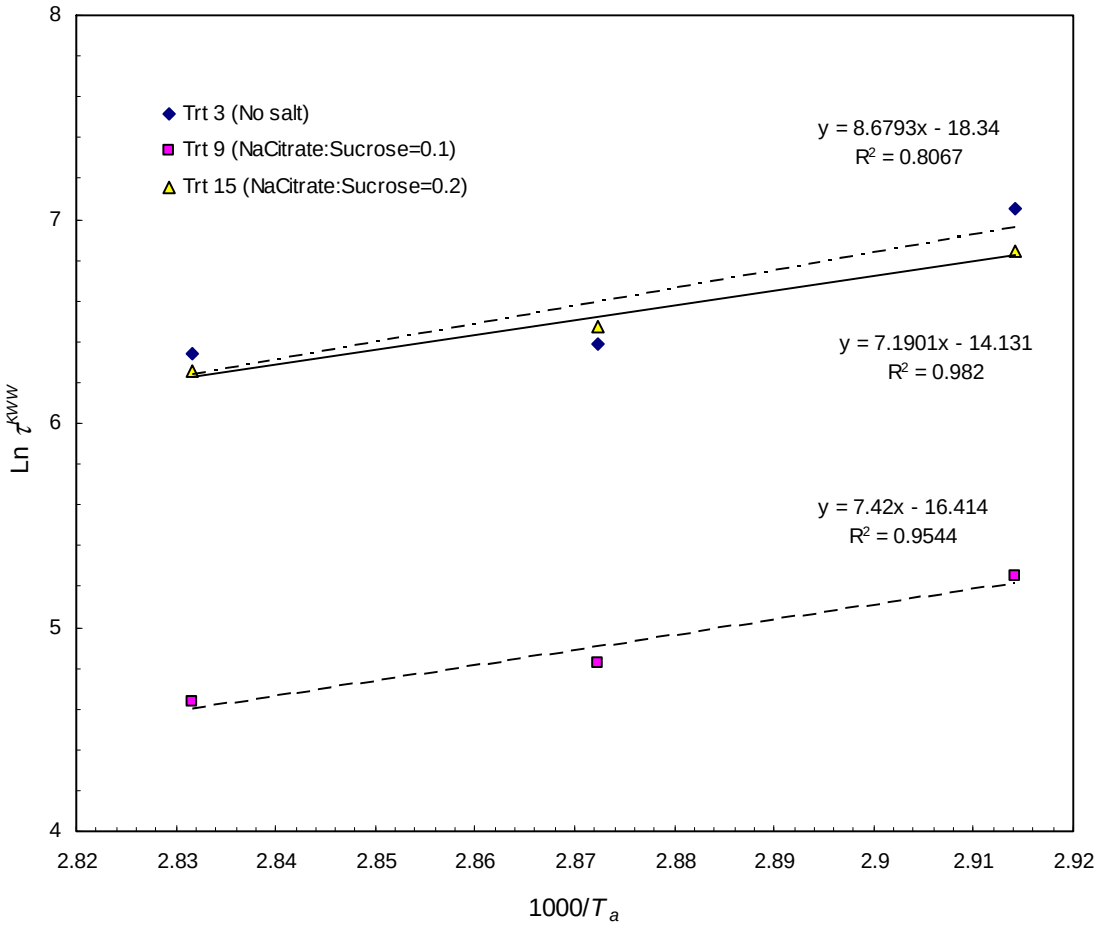

Figure A2.7.2 Arrhenius plots of τ^{KWW} (obtained with nonlinear regression) for sucrose-maltodextrin based bioglass samples with sucrose/maltodextrin of 5:5.

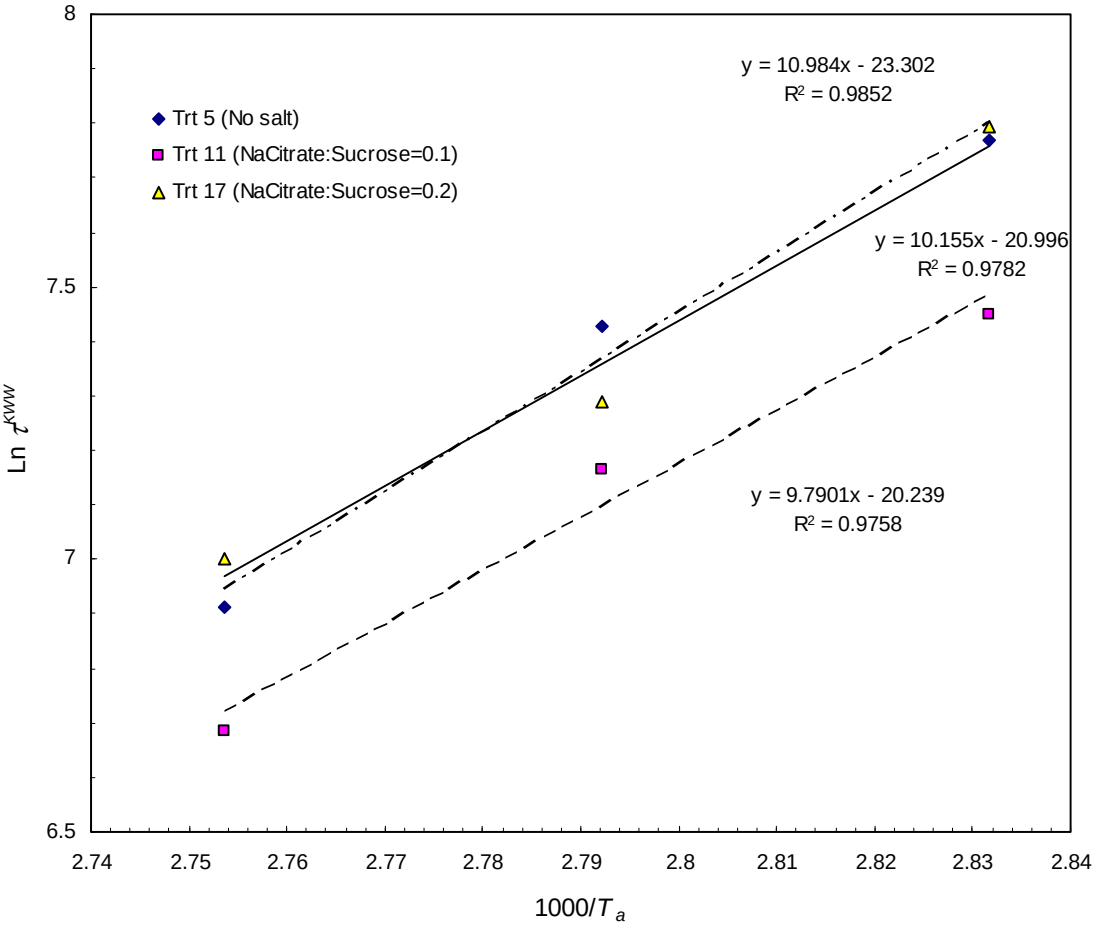

Figure A2.7.3 Arrhenius plots of τ^{KWW} (obtained with nonlinear regression) for sucrose-maltodextrin based bioglass samples with sucrose/maltodextrin ratio of 3:7.

Appendix 2.8 The Arrhenius plots of τ^{KWW} obtained with the linearised form of double logarithm of $\phi(t)$

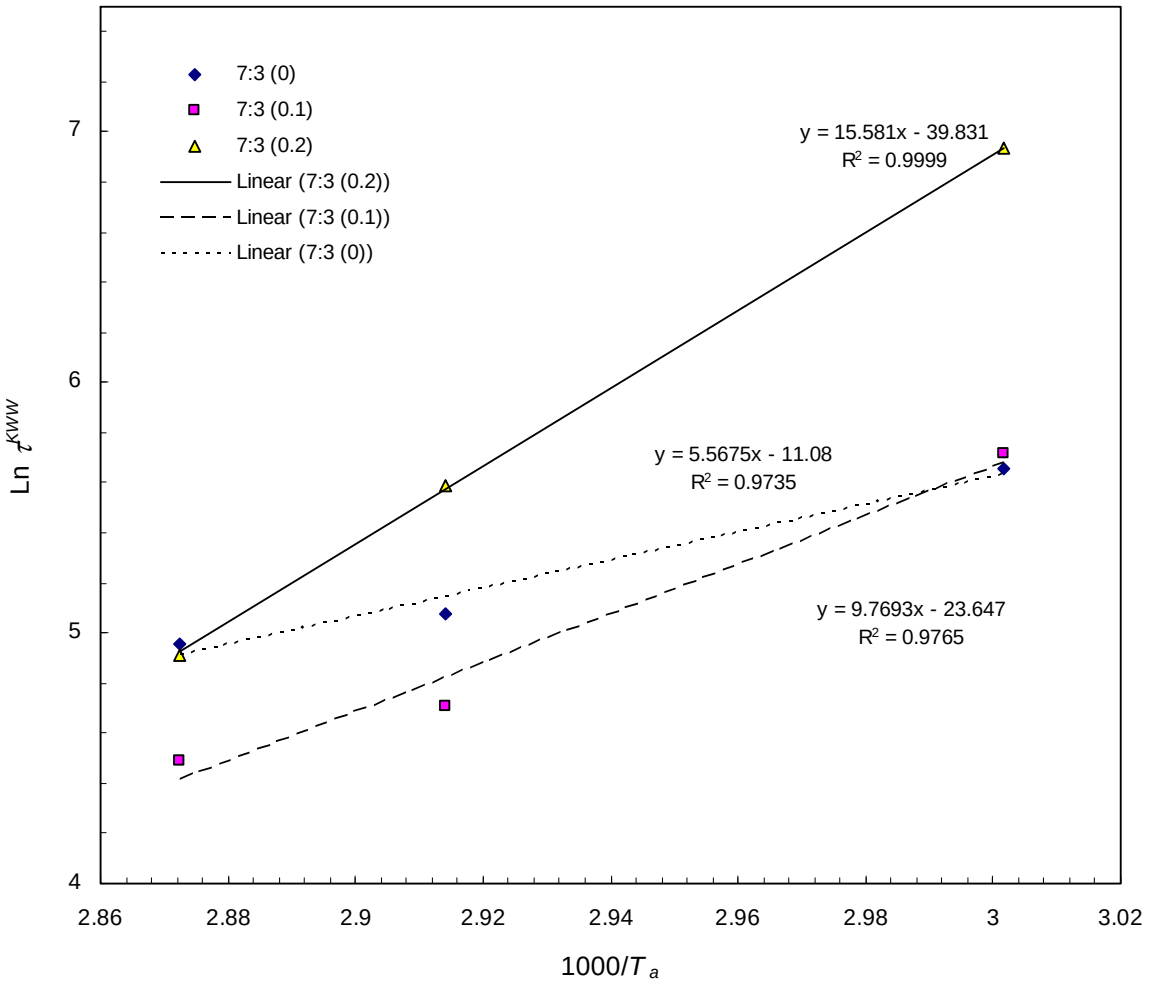

Figure A2.8.1 Arrhenius plots of τ^{KWW} (obtained with linearised technique) for sucrose-maltodextrin based bioglass samples with sucrose/maltodextrin ratio of 7:3. Figures in parenthesis shown in the legend are values of Na citrate/sucrose ratio.

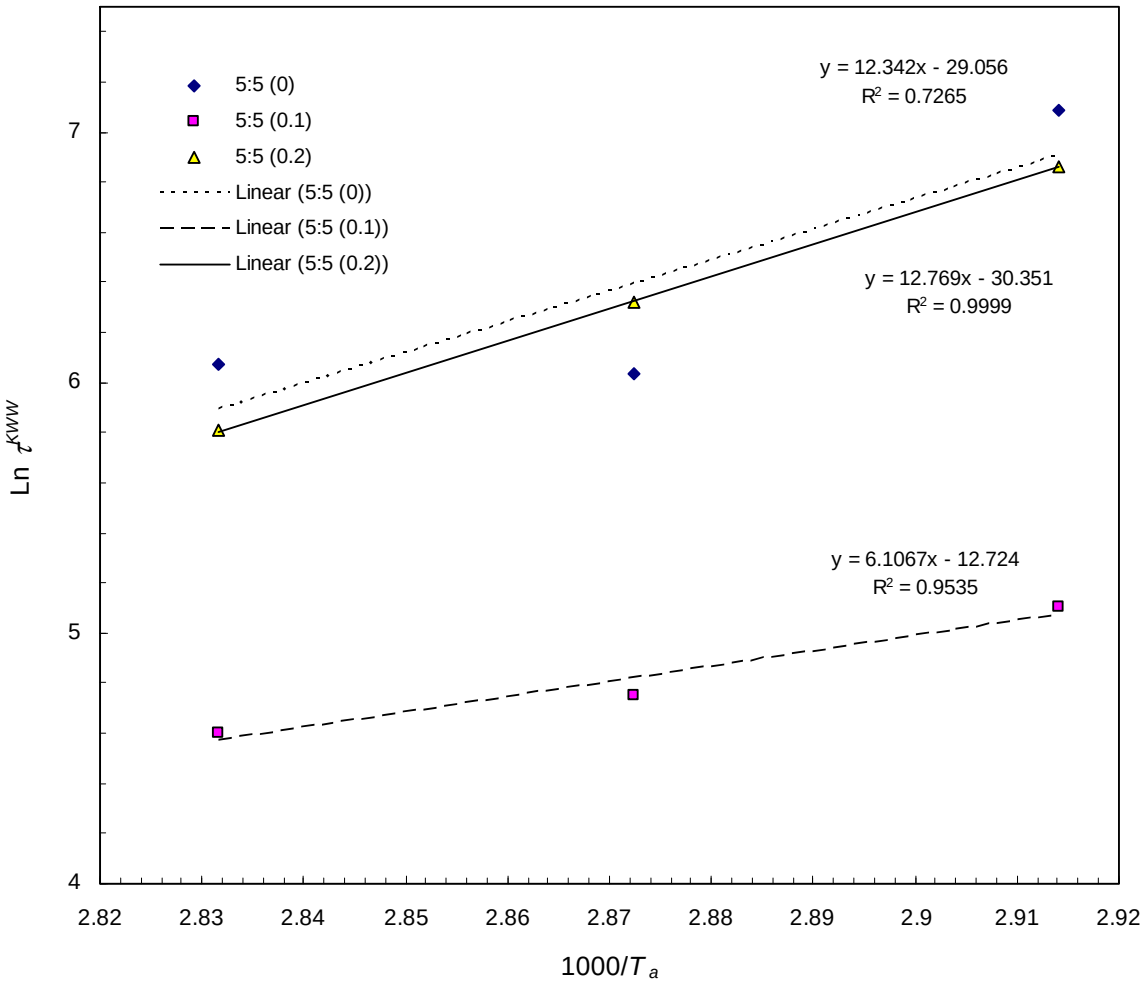

Figure A2.8.2 Arrhenius plots of τ^{KWW} (obtained with linearised technique) for sucrose-maltodextrin based bioglass samples with sucrose/maltodextrin ratio of 5:5. Figures in parenthesis shown in the legend are values of Na citrate/sucrose ratio.

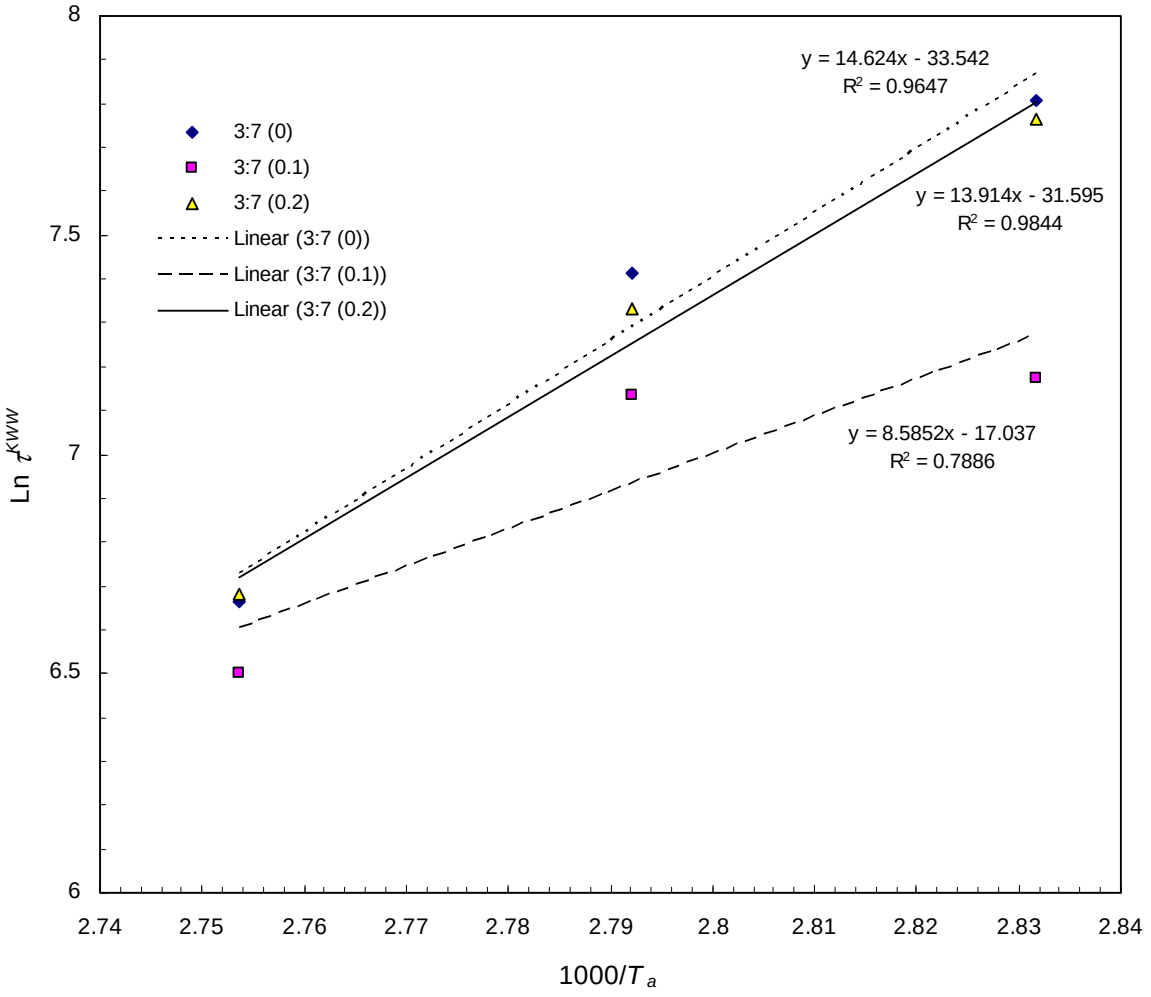

Figure A2.8.3 Arrhenius plots of τ^{KWW} (obtained with linearised technique) for sucrose-maltodextrin based bioglass samples with sucrose/maltodextrin ratio of 3:7. Figures in parenthesis shown in the legend are values of Na citrate/sucrose ratio.

CHAPTER 3

FTIR SPECTROSCOPIC EVALUATION OF SUCROSE-MALTODEXTRIN-Na CITRATE BIOGLASS

3.1 Abstract

Effects of sucrose, maltodextrin, Na citrate and moisture on their mixture—the bioglass model system—were study using the Fourier transform infrared spectroscopy (FTIR). Samples were formulated with different sucrose/maltodextrin ratios (SC/MD = 7:3, 5:5 and 3:7, by mass) and Na citrate/sucrose ratios (NaCit/SC = 0, 0.1 and 0.2, by mole) and two levels of moisture content, low (0.27 - 0.49 %wb) and high (2.83 to 4.4 %wb). Hydrogen bonding interactions were investigated by analyzing the OH-stretching absorption band in the FTIR spectra. There was no noticeable effect of moisture on the bioglass other than slight shift down of the OH-stretching band. The matrix of the system with high concentration of maltodextrin was loosely packed. Na citrate interacted with both sucrose and maltodextrin through carboxylic groups, as evidenced by the shifting of $\nu_{as}(COO^{-})$ and $\nu_{s}(COO^{-})$. However Na citrate tended to interact with sucrose rather than maltodextrin. The strongest

hydrogen-bonded network was observed in the system with highest concentration of sucrose (SC/MD = 7:3) and Na citrate (NaCit/SC = 0.2).

3.2 Introduction

Intermolecular network can be studied by indirectly observing the intramolecular mode of molecules since their oscillatory forces are sensitive to the level of molecular interaction with their surrounding. It is commonly observed that a change in oscillatory force of particular bond in a set of molecules induces some correlated changes in the oscillatory force of the neighboring bonds—intramolecular and intermolecular (Brubach et al., 2005). Molecular oscillation can be monitored using a number of techniques: differential scanning calorimetry (DSC), dynamic mechanical thermal analysis (DMTA), dielectric thermal analysis (DETA), nuclear magnetic resonance (NMR), and Fourier transform infrared spectroscopy (FTIR). Of these, the FTIR has been widely used to obtain information on molecular structure and intermolecular interactions in biological systems (Crowe et al., 1997; Wolkers et al., 1998; Ottenhof et al., 2003; Kets et al., 2004; Wolkers et al., 2004a; Wolkers et al., 2004b; Brubach et al., 2005; Chang et al., 2005; Oldenhof et al., 2005; Gallina et al., 2006; Gharsallaoui et al., 2008; Malsam and Aksan, 2009; Kadoya et al., 2010).

One of the important advantages of FTIR is that the information on chemical identity contained in FTIR spectra allows studying multiple component systems. Though Carbon-13 NMR (^{13}C NMR) technique is also capable of providing chemical identification of physical and chemical processes, it is time-consuming and lacks sensitivity (Ottenhof et al., 2003).

In carbohydrate research, the FTIR technique could provide insights into the nature of hydrogen-bonding network of the amorphous matrix, which otherwise could not be obtained using DSC, the most common technique. In addition, phase transitions of the system could also be detected from the thermotropic response of infrared absorption bands. The length and the strength of intermolecular hydrogen bonding could be respectively inferred from the band position and the shift in band position of the OH-stretching vibration from FTIR spectra (Wolkers et al., 2004b). FTIR spectra in the region of 1500 – 800 cm^{-1}, the so called a "fingerprint" region of sugar, can be used to differentiate types of sugar according to their molecular vibration sensitivity to the flexibility around the glycosidic bond. Vibrations in this region are mainly attributed to in-ring CO-stretching, inter-ring COC-, COH- and CCH-bending, and symmetrical deformations of CH_2 groups. The fingerprint region is sensitive to a physical state (amorphous/crystalline, glassy/rubbery) of sugar and hence could be used to monitor the transitions between states (Ottenhof et al., 2003). The spectra next from the fingerprint region, in a range of 1800 –1600 cm^{-1}, which usually arise from HOH-bending of water molecules, could provide important information about the effects of sugar on the hydrogen-bonded network of water (Gharsallaoui et al., 2008).

3.2.1 Infrared spectroscopy

Infrared spectroscopy deals with the infrared region of electromagnetic spectrum. The infrared region is usually divided into three sub-regions: the near-, mid- and far-infrared. The near-infrared, wavenumber of approximately 14000 – 4000 cm^{-1} (0.8 – 2.5 μm wavelength), possesses high energy which can excite overtone or harmonic vibrations. The mid-infrared, approximately 4000 – 400 cm^{-1} (2.5 – 25 μm), is generally used to study the fundamental

vibrations and associated rotational-vibrational structure. The low energy far-infrared region, approximately 400 – 10 cm^{-1} (25 – 1000 μm), which locates close to the microwave region, could be used for rotational spectroscopy (Anonymnous, 2010).

3.2.1.1 Theory

An infrared spectrum is formed as a consequence of absorbing electromagnetic radiation in the infrared region by a molecule at resonant frequencies of specific sets of chemical bonds within it. As a fundamental requirement for infrared activity, there must be a net change in dipole moment during the vibration of molecule or functional group (Atkins and Paula, 2009). Molecular bonds vibrate at different frequencies depending on the elements and types of bonds. Any chemical bond can vibrate at several frequencies including the ground state and several excited states. Besides, various modes of vibration, e.g., stretching, bending, and twisting about certain centers within a molecule, are simultaneously observed in an infrared spectrum. In the context of spectroscopy, frequency is commonly expressed as wavenumber which is inverse of wavelength given in reciprocal centimeter (cm^{-1}). Since it takes less energy to bend a bond than to stretch it, the stretching absorptions of a vibrating chemical bond occur at higher frequencies (wavenumbers) than do the corresponding bending absorptions. It can be then readily seen that energy and frequency are proportionally related. For covalent bond between two atoms, the stretching frequency can be estimated using the following equation (Coates, 2000):

$$\nu = \frac{1}{2\pi c}\sqrt{\frac{f(m_1 + m_2)}{m_1 \times m_2}} \qquad (3.1)$$

Where, ν is frequency (cm^{-1}),

c is velocity of light ($cm.s^{-1}$),

f is force constant for the bond, and

m_1, m_2 are atomic mass of the two atoms forming the bond.

Equation 3.1 indicates the significance of atomic mass on the stretching frequency of the bond. If one of the bonded atoms is hydrogen, then the mass ratio in the equation would be approximately unity. On the other hand, for the bonds of hydrogen with heavier atoms, this ratio would be much smaller. That is why the bonds of hydrogen with lightweight atoms, e.g., C-H, N-H, and O-H, exhibit much higher stretching frequencies than do the bonds of hydrogen with heavier atoms (Anonymnous, 2009).

3.2.1.2 FTIR measurement system

The infrared spectrometer employs a simple optical device called an interferometer which produces a unique type of signal containing all infrared frequencies encoded into it. The signal obtained from the interferometer is called interferogram. As the interferogram is measured, all frequencies are measured simultaneously and this is key to extremely fast FTIR measurements. However, a means to decode individual frequency is required since the measured interferogram cannot be interpreted directly (Thermo-Nicolet, 2001). FTIR refers to the manner in which infrared data are collected and converted from an interferogram to a spectrum via Fourier transformation. FTIR is a very useful tool for identifying chemicals in both organic and in organic materials. The ability to analyze materials in a variety of states—solid, liquid or gas—makes the technique highly versatile. FTIR spectra of pure compounds

are generally unique, like a molecular "fingerprint." For qualitative analysis, FTIR is probably the most powerful tool for indentifying types of chemical bonding or functional groups. The technique can be also used for quantitative analysis since the strength of absorption is proportional to concentration (Thermo-Nicolet, 2001; Exova, 2010).

3.2.1.3 Infrared sampling methods

The sampling method could have a profound impact on the final infrared spectrum and consequently the interpretation of FTIR data. Traditional transmission infrared spectroscopy suffers from the complicated and time-consuming sample preparation particularly for solid samples; besides, results obtained with this method are poorly reproducible. To address these issues, focus has been placed on the reflectance method of measurement, namely attenuated total reflectance (ATR), diffuse reflectance, specular reflectance and/or transflectance. The ATR and diffuse reflectance are favored due to the rapid sampling time and the excellent reproducibility they offer. The spectra obtained with these methods however suffer from distortion or aberration. The ATR spectra are simpler to handle as compared to those from the diffuse-reflectance method. In addition, the ATR is nondestructive, requires only minimum amount of sample, and provides excellent quality data with the best possible reproducibility. The downside is that the signal intensity across the spectrum increases as a function of wavelength. However, this issue could be handled via wavelength correction software algorithms (Coates, 2000; Perkin-Elmer, 2005).

3.2.2 Hydrogen bonding

Hydroxyl groups usually do not exist in isolation. They exhibit a high degree of association as a result of extensive hydrogen bonding. The interactions among these hydroxyl groups may be within the same molecule—intramolecular hydrogen bonding, or exist between neighboring molecules—intermolecular hydrogen bonding (Coates, 2000).

The network of hydrogen bonding is primarily responsible for holding up carbohydrate glass matrix (Wolkers et al., 1998; Imamura et al., 2006) leading to a significant broadening and lowering of the mean absorption frequency (Coates, 2000; Maréchal, 2011). The shift in the mean absorption frequency tends to be a function of the degree and strength of hydrogen bonding. A large shift to lower frequencies is observed in compounds which exhibit extremely strong hydrogen bonding (Coates, 2000). The change in the strength of hydrogen bonds was found to be in parallel with the changes in specific volume or density when a material transforms from one state to another. A larger density difference— a substantial change in the strength of hydrogen bonding—can be expected when a material changes from a rubbery state to a crystalline solid while there is a smaller difference of this property between the glassy and the rubbery states (Ottenhof et al., 2003).

3.2.3 FTIR spectroscopy in amorphous carbohydrates research

There has been controversy as to how carbohydrate glass could stabilize the macromolecules trapped within its matrix. On one side, it has been established that the stabilization effect of amorphous sugars on biomolecules encompasses two mechanisms: the formation of glassy state by sugars and the direct interaction between sugars and

biomolecules—the "water replacement" hypothesis (Crowe et al., 1998). Accordingly, a desirable amorphous sugar matrix in this regard should exhibit a high T_g and has the ability to bind with the target biomolecules. However, the water replacement concept is a thermodynamic stabilization mechanism and only applicable over the transition between equilibrium states, which is not the case for the thermodynamically non-equilibrium glassy systems. Alternatively, the concept of "dilution effect" has been later proposed. This effect does not require any particular interaction other than what is necessary for preventing phase separation. It is believed that the dilution effect is partly responsible for the stabilization of macromolecules in a glass matrix (Chang et al., 2005). Further evidences are still required for elucidating the related mechanisms.

FTIR spectroscopy is a powerful tool that facilitates the study of materials in amorphous state. The technique allows monitoring the changes in various chemical bonding species in the amorphous matrix. Many groups of researchers have employed the FTIR spectroscopy as a primary tool (Wolkers et al., 1998; Ottenhof et al., 2003; Wolkers et al., 2004b; Imamura et al., 2006) while others used the technique as a complementary measurement to help interpret the results along with other techniques (Kets et al., 2004; Kadoya et al., 2008).

In a carbohydrate-water system, where water significantly contributes to OH-stretching absorption band, clusters of water molecules could be categorized into three families according to their hydrogen bond organization. The first, originating from tetrahedrally bonded water molecules, namely networking water, locates in the region of around 3300 – 3314 cm^{-1}. The second is intermediate water, which is a weakly or distorted hydrogen-bonded family locates at around 3441 – 3470 cm^{-1}. The last family is free or

multimer water, which originates from water monomers and dimers and locates at around 3570 – 3610 cm^{-1} (Lerbret et al., 2005; Gallina et al., 2006; Malsam and Aksan, 2009). The OH-bending absorption band which locates in the region of 1500 – 1800 cm^{-1} does not contain any contribution from the hydroxyl groups of carbohydrates; the band solely originates from water (Lerbret et al., 2005; Gallina et al., 2006; Malsam and Aksan, 2009).

Among various absorption bands present in FTIR spectra, the OH-stretching vibration is the most useful for the study of amorphous carbohydrates. There exists a relationship between the rate of change of vibrational energy with temperature (wavenumber temperature coefficient, WTC) of OH-stretching vibration, and the glass transition of carbohydrate systems. The WTC is a parameter for determining the strength of hydrogen-bonded network. Typically, OH-stretching band falls in the range of 3200 – 3600 cm^{-1}, depending on temperature. As temperature rises, the band position of OH-stretching vibration shifts to the higher wavenumbers indicating the weakening of hydrogen bonds. An abrupt change in WTC of the OH-stretching mode has been observed during glass transition of carbohydrate systems. In fact, the OH-bending vibration also appears to relate to glass transition. However, this band falls in the fingerprint region of infrared spectrum, which is complex; many absorption bands with different temperature dependencies overlap in this region, and hence the assignment of this band becomes problematic. Another evidence to confirm the applicability of infrared spectroscopy for determining T_g is the plasticizing effect of water on a sugar glass in that the highest value of T_g determined with this technique was found in the sample with the lowest water content. There is however a limit for using the infrared spectroscopy for the analysis of T_g and WTC. As given above, the OH-stretching vibration

bands of water and sugar are superimposed leaving the technique applicable only to the systems with 0.3 g-H_2O/g (dry weight) or lower (Wolkers et al., 1998).

From the study on amorphous carbohydrates with different chain lengths, the result from FTIR analysis revealed interesting relationships among the characteristics of hydrogen bonding, T_g, and change in heat capacity during glass transition ($\Delta C_{p,GT}$). Wolkers et al. have reported a positive correlation between OH-stretching band position and T_g, which indicates that T_g increases with the average length of hydrogen bonds in amorphous sugars. The thermotropic response of OH-stretching vibration in the amorphous matrix revealed a relationship in which sugars with higher T_g exhibit the greater degree of freedom to rearrange hydrogen bonds. They suggested that this higher degree of freedom to rearrange the molecular packing during temperature change helps stabilizing the amorphous matrix. Even though T_g of disaccharides generally shows a positive correlation with molecular weight, predicting the T_g of disaccharides based solely on molecular weight is inaccurate. Disaccharides exhibit a broad range of T_g: 70 °C for dry sucrose, 95°C for dry maltose, and 110°C for trehalose. This wide distribution of T_g for disaccharides is believed to be an attribute of the differences in molecular packing which may be associated with the differences in intermolecular hydrogen bonding. These differences are reflected in the band position and the thermotropic response of OH-stretching vibration. As compared to sucrose, the wavenumber-temperature coefficient of OH-stretching vibration in a glassy state (WTC_g) of trehalose is higher. The higher WTC_g means the looser molecular packing. Thus carbohydrates that exhibit high T_g would possess a loose amorphous structure. Accordingly, the WTC_g is suggested as a measure for the degree of order or entropy in glassy state. It was also found that $\Delta C_{p,GT}$ decreased with the increasing T_g, and so the increasing WTC_g. The

finding indicates a direct association between $\Delta C_{p,GT}$ and the strength of hydrogen-bonded network of glassy systems (Wolkers et al., 2004b).

Wolkers et al. (2004a) studied the preservative property of sugars (glucose and sucrose) and phosphate systems on dried liposomes. FTIR measurements were carried out to investigate the interactions among phosphate, sugars and egg phosphatidylcholine (egg PC) liposomes through hydrogen bonding, and to determine the T_g of the mixtures. The result showed that the band position of OH-stretching vibration of sugars decreased with the increasing amount of phosphate and reached a minimum when phosphate/glucose ratio equal to unity. It was interpreted as phosphate increased, for a certain level, the T_g of amorphous sugar matrices by forming strong hydrogen bonding. This effect could help stabilize the liposomes during air drying. The observation on the response of OH-stretching vibration suggested that liposomes also interacted with sugar though hydrogen bonding, but with the less extent than that between phosphate and sugar. Besides, it was found phosphate decreased the WTC of OH-stretching vibration in the glassy state, which means there was less degree of freedom for hydrogen bonds to rearrange themselves. As a result, it was speculated that the effects of phosphate could explain the poor storage ability of liposomes in sugar-phosphate glass even with elevated T_g (Wolkers et al., 2004a).

The above results clearly demonstrate the significance of hydrogen bonding on the protective property of carbohydrate-glass systems. It should be however noted that the contribution of hydrogen bond networks to the amorphous matrix could be altered by a number of factors, e.g., molecular structure, molecular weight, and concentration of matrix components, and water content (Kadoya et al., 2008). In this study, we employed the FTIR

spectroscopy to elucidate effects of each of the components, sucrose, maltodextrin, Na citrate and moisture, on the bioglass model systems.

3.3 Materials and Methods

3.3.1 Materials and sample preparation

Materials and details on sample preparation are given in Chapter 2, sections 2.3.1 and 2.3.3, respectively.

3.3.2 Experimental design

Details about experimental design, and factors and their levels are given in Chapter 2, Tables 2.1 and 2.2.

3.3.3 Moisture determination

Moisture content of samples was determined using the Karl Fischer titration technique. Details of the measurements are given in Chapter 2, section 2.3.4.

3.3.4 FTIR spectroscopy

FTIR measurements were carried out at room temperature, approximately 25 °C, using a computer-controlled Spectrum 100 series FTIR spectrometer (Perkin Elmer, Inc., Norwalk, CT) equipped with universal ATR sampling unit. Prior to the measurements, a background signal was acquired by scanning an empty ATR sampling unit. A background spectrum is necessary for FTIR measurement due to the fact that the absorption intensity is in relative scale. This technique yields a spectrum which has all the instrument characteristics removed (Thermo-Nicolet, 2001). Samples were scanned over the wavenumber ranging from

4000 to 650 cm^{-1} for 25 scans per measurement with a resolution of 4 cm^{-1}. An additional sample holding plate was placed on the top of the diamond ATR sampling unit to aid the measurements since samples were in a form of fine powder. Two replicates of samples were measured with at least two measurements each.

Spectral analyses were carried out using the Spectrum software, version 6.2.0 (Perkin-Elmer, Inc., Norwalk, CT). Baseline correction was performed manually. In the analysis of OH-stretching band position, FTIR spectra in the wavenumber range of 3600 - 3000 cm^{-1} were selected, and normalized. The position of OH-stretching band was calculated as an average of spectral position at 8 0% of the peak height (Wolkers et al., 2004; Wolkers et al., 2004b; Oldenhof et al., 2005).

3.4 Results and Discussion

3.4.1 Characteristic of ATR-FTIR absorption spectra of individual component

Each component of bioglass model systems was subjected to infrared spectroscopy to acquire their mid-IR absorption characteristics. The results containing information on chemical identity of each component were expected to provide important elements for the investigation of molecular interactions in the mixtures. Thus a thorough understanding on characteristics of FTIR spectra obtained from individual component is crucial for comprehending the behaviors of bioglass model systems.

3.4.1.1 Water

The infrared absorption spectrum of deionized water as shown in Figure 3.1 apparently looks rather simple. There are two pronounced absorption bands at ~3300 and ~1630 cm^{-1}, which could be assigned as the OH-stretching and OH-bending (in plane) vibration, respectively.

In fact, water absorption spectrum is very complex and very little is known about its distinctive molecular-level features (Brubach et al., 2005; Maréchal, 2011). Water molecules are interconnected through both covalently and noncovalently bonded atoms. The first type of bonds gives rise to intramolecular vibrational modes while the later leads to intermolecular modes (Brubach et al., 2005). Water molecules may vibrate in a number of ways including symmetric stretch, asymmetric stretch, bending and liberations. Hidden in the vibrational spectra of water is much of structural information. The broad spectrum encompasses various absorption bands originating from the vibrations of water molecules, which have different degrees of connectivity. The cooperative/anti-cooperative nature of hydrogen bonds and the surrounding hydrogen bonds influences the strength of hydrogen bonding. The more weakened the hydrogen bonds, the more strengthened the covalent O-H bonds. And this results in the upshift of OH-stretching vibration frequency while the bending vibration frequency shifts down (Falk, 1984; Chaplin, 2012). Infrared spectroscopy revealed that almost all OH groups in liquid water establish hydrogen bonds in basic tetrahedral fashion but with less order than those in ice (Maréchal, 2011). These hydrogen bonds are highly versatile. They keep constantly rearranging while maintaining the cohesion of the whole water body (Brubach et al., 2005).

A close examination of OH-stretching band envelope (3700 – 2800 cm^{-1}) reveals that the envelope likely encompasses three sub-absorption bands, illustrated in Figure 3.2, which were also clearly observed from the infrared and Raman spectra of pure water reported in literature (Gallina et al., 2006). To resolve the underlying sub-absorption bands, Gallina and coworkers reproduced the spectra from infrared measurements by means of the Gaussian profiles where the experimental spectra of water at 25 °C were nicely reproduced by generating three curves centered at 3300, 3470 and 3610 cm^{-1}. Based on the literature data (Walrafen et al., 1986; Robinson et al., 1999; Freda et al., 2005)—considering the temperature, pressure and polarization behavior—three sub-absorption bands were constructed and assigned to the ordered tetrahedral hydrogen bonded structures (G1, at 3300 cm^{-1}), the distorted hydrogen bonded structures (G2, at 3470 cm^{-1}), and the water molecules with free hydroxyls (G3, at 3610 cm^{-1}) (Gallina et al., 2006). However, the OH-stretching band of de-ionized water obtained in this experiment (Figure 3.2) reveals that the locations of sub-absorption bands might be a little bit lower than those proposed values.

3.4.1.2 Crystalline sucrose

The absorption spectrum of crystalline sucrose is shown in Figure 3.3. It is characterized by very sharp absorption bands throughout the mid-infrared region, which are common for crystalline structure. In crystalline structure there exists a high degree of homogeneity of intermolecular interactions resulting in the less dispersion of vibrational levels (Wolkers et al., 2004b) and the increase in spectral resolution. There were two absorption peaks at ~3310 and ~3380 cm^{-1}, and one isolated sharp peak at 3560 cm^{-1} present in the region of OH-stretching band which centered around 3300 cm^{-1}. Crystallization causes

a decrease in the wavenumber (frequency) of OH-stretching vibration as a result of an increase in hydrogen-bond density and strength (Ottenhof et al., 2003; Wolkers et al., 2004b). The isolated peak has also been found in the spectra of other sugars (Lutz and Vandermaas, 1994; Wolkers et al., 2004b) and it is suggested that the peak arises from weakly bonded O-H···O system (Lutz and Vandermaas, 1994). There are approximately five absorption bands present in the CH-stretching region located between 3000 and 2800 cm^{-1}. The fingerprint region which covers the range of approximately 1500 – 800 cm^{-1} is complex showing a series of sharp overlapping absorption bands arising from CO-stretching, CC-stretching, and COH-bending vibrations (Kačuráková and Mathlouthi, 1996).

3.4.1.3 Maltodextrin powder

Maltodextrin spectrum exhibited a strong broad absorption band centered at ~3300 cm^{-1} and a weak band at ~1635 cm^{-1} which arise from OH-stretching and OH-bending (in plane) modes, respectively (Figure 3.4). CH-stretching absorption band was found at ~2900 cm^{-1}. As compared to the spectrum of crystalline sucrose, absorption bands in the region of carbohydrate fingerprint (1500 – 800 cm^{-1}) are broader showing extensive overlapping. In general, the spectrum of maltodextrin looks similar to that obtained from enzyme-hydrolyzed starch (Imam et al., 2006).

3.4.1.4 Crystalline Na citrate

The absorption spectrum of Na citrate—to be more precise, trisodium citrate dihydrate—is dominated by two major absorption bands as shown in Figure 3.5. These two bands with their peaks at around 1580 and 1385 cm^{-1}, which respectively correspond to the

antisymmetric ($\nu_{as}(COO^{-})$) and symmetric ($\nu_{s}(COO^{-})$) stretching bands of carboxyl groups of Na citrate (Kets et al., 2004; Max and Chapados, 2004). Water molecules apparently contributed to a small OH-bending absorption band located at ~1650 cm^{-1} which considerably overlapped with the $\nu_{as}(COO^{-})$ band. The OH-stretching absorption band was broad covering the range from 3600 to 2000 cm^{-1} causing overlap of many absorption bands. This broad band of OH-stretching vibration characteristic of carboxylic acids and their salts has also been reported (Max and Chapados, 2004). Besides, there are other two sharp absorption bands extending beyond the OH-stretching band envelop at approximately 2965 and 2920 cm^{-1}, which could be assigned to the CH-stretching vibrational modes. The absorption in the region of approximately 1320 cm^{-1} down to the lower wavenumbers are rather complex encompassing a number of bands.

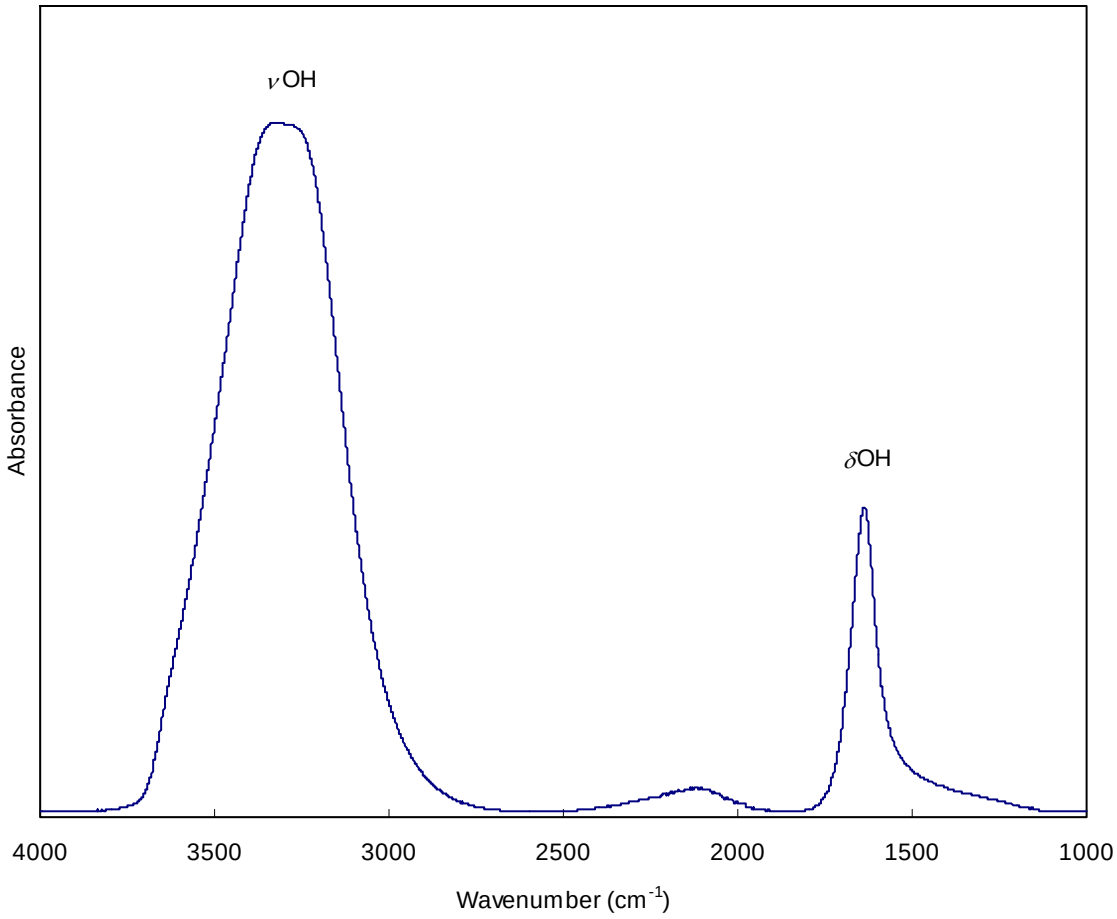

Figure 3.1 ATR-FTIR absorption spectrum of deionized water.

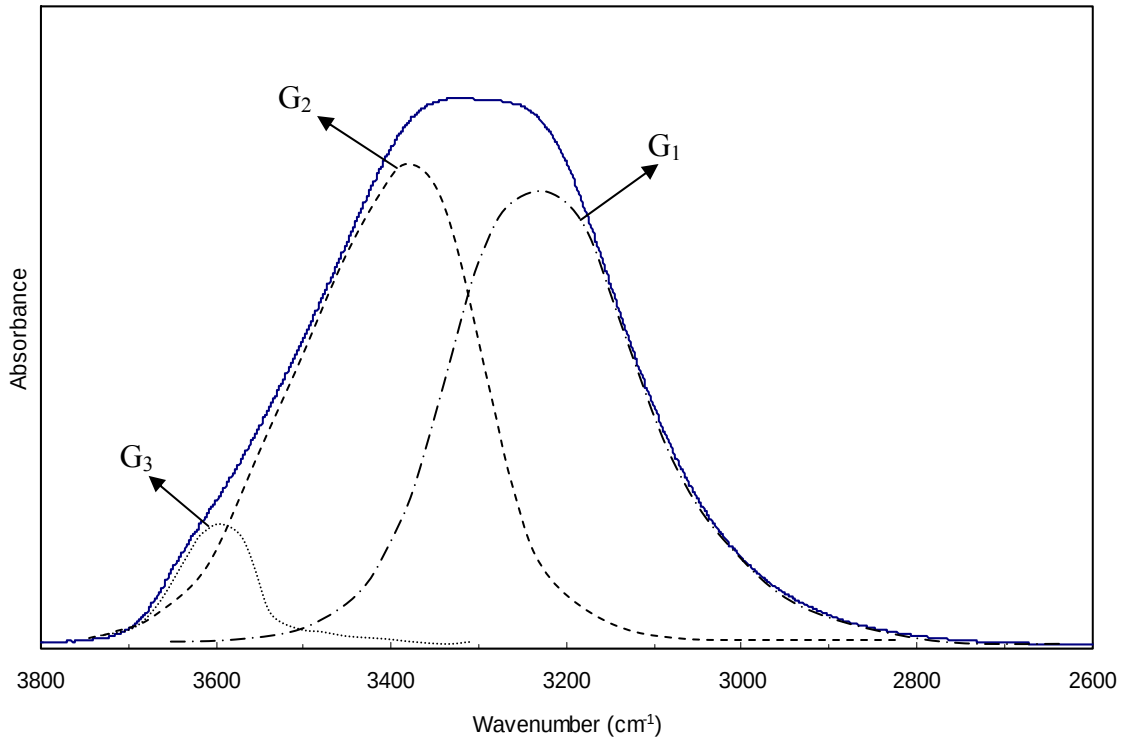

Figure 3.2 ATR-FTIR spectrum of deionized water in the region of OH-stretching absorption band obtained from this experiment. Three sub-absorption bands were manually sketched to represent the contribution from the ordered tetrahedral H-bonded structures (G_1), the distorted H-bonded structures (G_2), and water molecules having free hydroxyls (G_3) as proposed by Gallina et al. (2006).

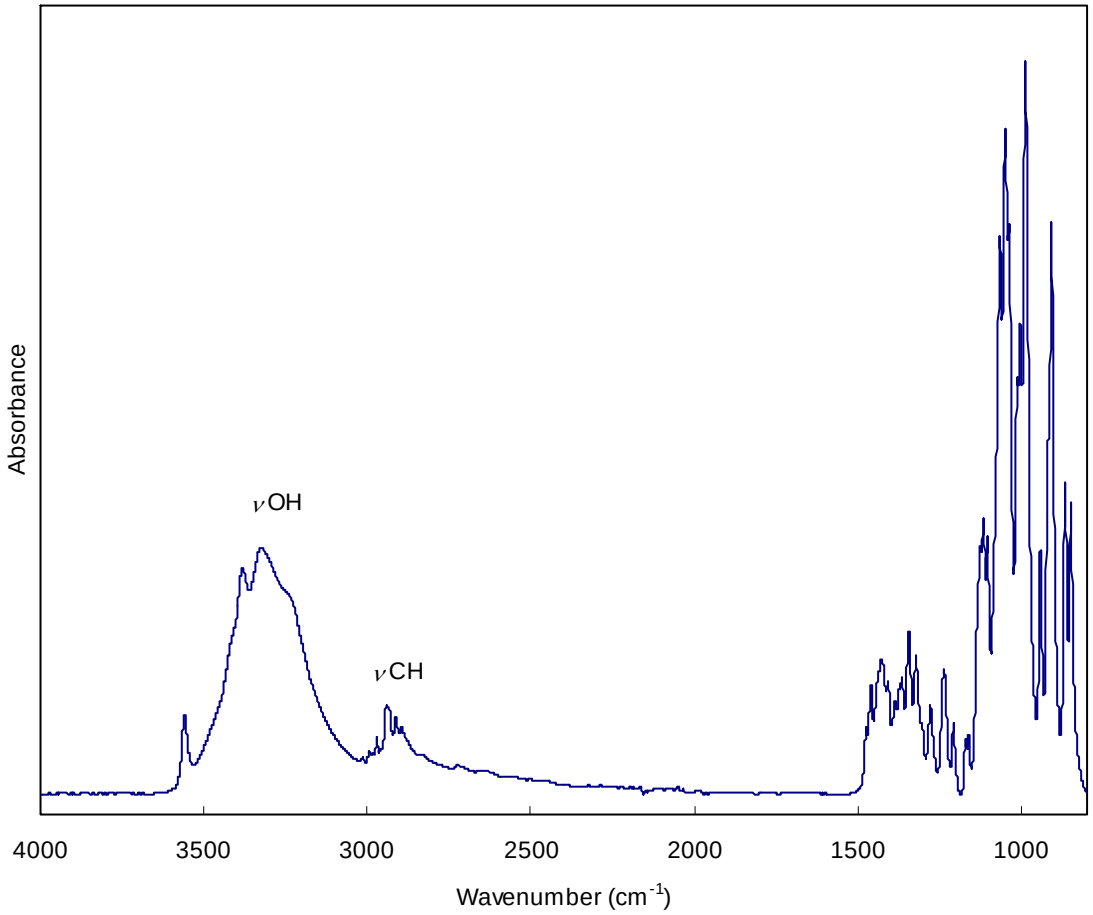

Figure 3.3 ATR-FTIR absorption spectrum of crystallize sucrose.

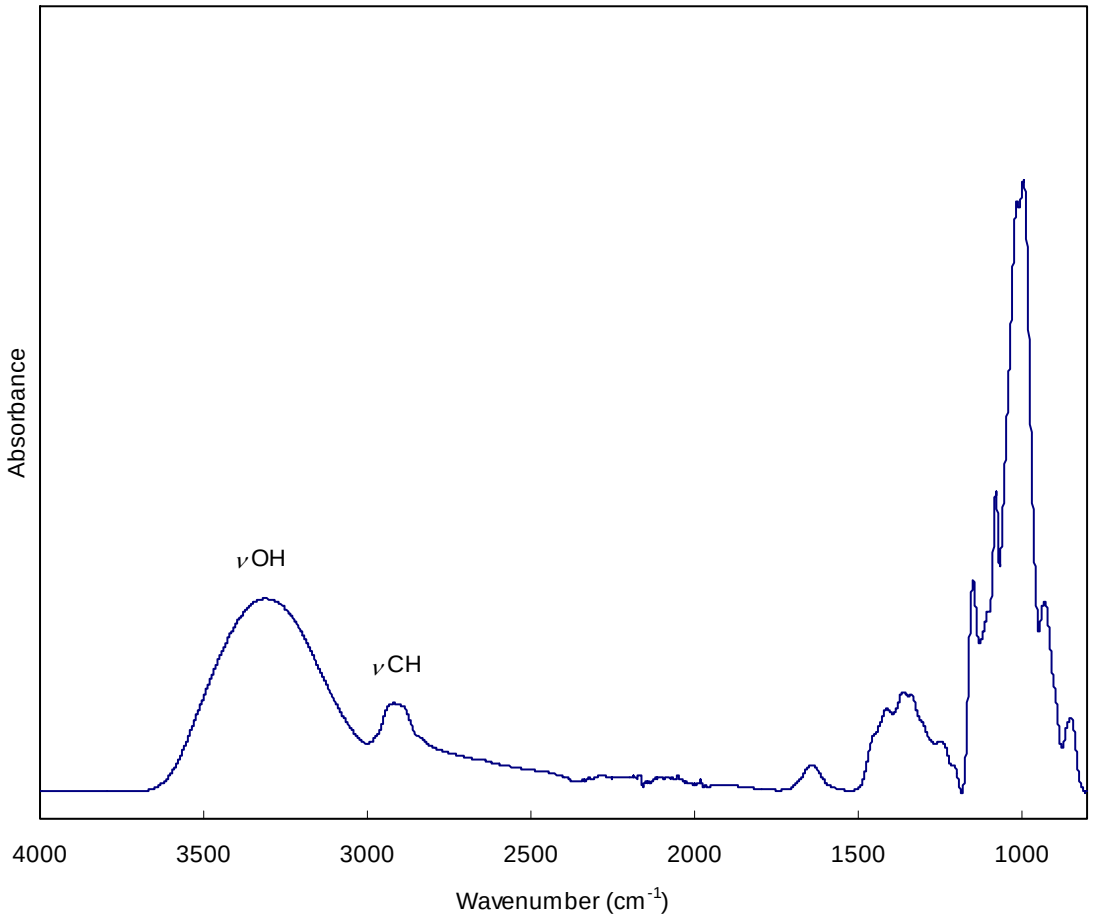

Figure 3.4 ATR-FTIR absorption spectrum of maltodextrin powder.

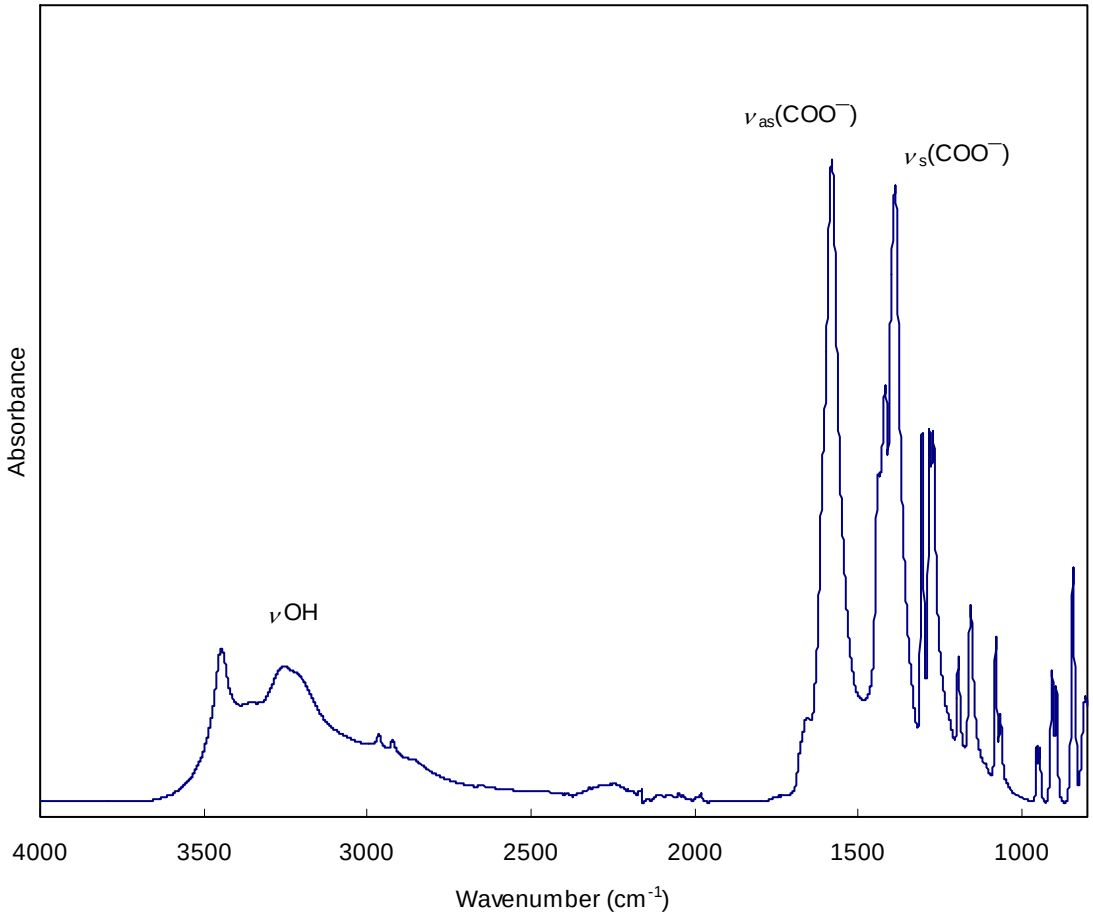

Figure 3.5 ATR-FTIR absorption spectrum of crystalline trisodium citrate dihydrate ($Na_3C_6H_5O_7$).

3.4.2 Effects of SC/MD on the characteristics of ATR-FTIR absorption spectra

Sucrose and maltodextrin are the principal components of the bioglass model system and hence it is plausible to expect much contribution from these materials to the characteristics of the system. In order to investigate the effect of SC/MD, absorption spectra of the systems without Na citrate were considered.

From mid-IR absorption spectra, the effect of SC/MD was observed in two regions: 1500 to 800 cm^{-1} and around 3300 cm^{-1}—the region of OH-stretching band. The first region encompasses the so called carbohydrate fingerprint region (1200 – 800 cm^{-1}). The absorption spectra in this region exhibit a number of broad overlapping bands. The representative absorption spectra of the systems without Na citrate are shown in Figures 3.6 and 3.7, for the systems with low (0.28 – 0.34 %wb) and high (2.83 – 4.04 %wb) levels of moisture, respectively. In general, the systems with different SC/MD exhibited quite similar features of absorption spectra in the range of 1500 – 1200 cm^{-1} which mainly arise from CH deformation vibrations (Kačuráková and Mathlouthi, 1996). However, the effect of SC/MD showed up on absorption spectra in the region of approximately 1200 – 950 cm^{-1}. The intensity of absorption band centered at around 1135, 1070, 1010 and 986 cm^{-1} increased with increasing SC/MD. These bands arise from the coupling of CO-stretching, CC-stretching and COH-bending vibrations. The two most interesting bands are those at around 1135 and 986 cm^{-1}, which are associated with the vibration of glycosidic linkages. The first one originates from the coupling of CO-stretching, CH-bending and COH-stretching vibrations, and the later solely arises from the CO-stretching vibration in the C-O-C glycosidic linkage (Kačuráková and Mathlouthi, 1996). A close examination reveals that as SC/MD decreased, there was a

noticeable upshift of the band at around 1135 cm^{-1}. This band shifted from approximately 1130 to 1142 cm^{-1} when SC/MD decreased from 7:3 to 3:7 suggesting the overall strengthening of glycosidic linkages due to more contribution from α-1,4 glycosidic linkages from maltodextrin which, as indicated by the result, are stronger than the α,β-1,2 glycosidic linkage in sucrose.

In a polymer system, T_g is mainly under the influence of chain flexibility which is governed by the nature of chemical groups constituting the main chain. Similarly, the melting temperature (T_m) is also controlled by the main chain stiffness; this is the reason why T_m and T_g are correlated (Young and Lovell, 1991). In amorphous saccharides, hydrogen bond and glycosidic linkage are primarily responsible to hold up the matrices by restricting the movement of pyranose rings (Imamura et al., 2006). According to their molecular structure, maltodextrin contains more glycosidic linkages than sucrose for the same number of pyranose rings. And so the increase in intensity of the bands originated from glycosidic linkages along with the decrease of SC/MD—the increase of maltodextrin concentration, was as expected. From the studies on various amorphous saccharides, it was found that T_g increased with the increasing number of pyranose rings, and so the number density of glycosidic linkages. The finding led to the conclusion that glycosidic linkage could restrict the ring segment of the pyranose ring more strongly than the hydrogen bond. Consequently, it was suggested that a larger oligomer could be held by fewer hydrogen bonds against glass transition. The degree of restriction by glycosidic linkage is dependent on the type of linkage—the linkage sites. For instance, the α-1,1 glycosidic linkage may restrict the movement of pyranose rings more than other types, whereas the α-1,6 glycosidic linkage was found to be the weakest type (Imamura et al., 2006). Results obtained from the calorimetric

measurements in Chapter 2 show a good agreement with those reported in the literature (Imamura et al., 2006). The T_g values of the bioglass model systems (without Na citrate) of SC/MD = 7:3, 5:5 and 3:7 were 86.6, 99.2 and 136.9 °C, respectively. As a result, it could be interpreted as T_g increases with the increasing glycosidic linkage density.

There was an upshift of OH-stretching band position with the decrease of SC/MD (Figure 3.8). Given in Figure 3.9 are the plots of OH-stretching band positions at 80% peak height against SC/MD. There was a clear positive correlation between OH-stretching band position and the concentration of maltodextrin. The shift of OH-stretching band position would be due to the alteration in the degree of hydrogen bonding. It was reported that the degree of hydrogen bonding formation decreased as the degree of polymerization increased up to 4 (Imamura et al., 2006). Wolkers and coworkers also reported the upshift of OH-stretching band position with T_g value of sugar glasses, which implies that the average length of the hydrogen bonds increases with increasing T_g (Wolkers et al., 2004b).

The finding suggests that the bioglass model system with higher concentration of maltodextrin forms a less dense amorphous structure, but with the higher T_g, as compared to the system with lower maltodextrin concentration. The higher T_g would be an attribute of the higher number density of glycosidic linkages, which restrict the pyranose ring segments more firmly than the hydrogen bonds.

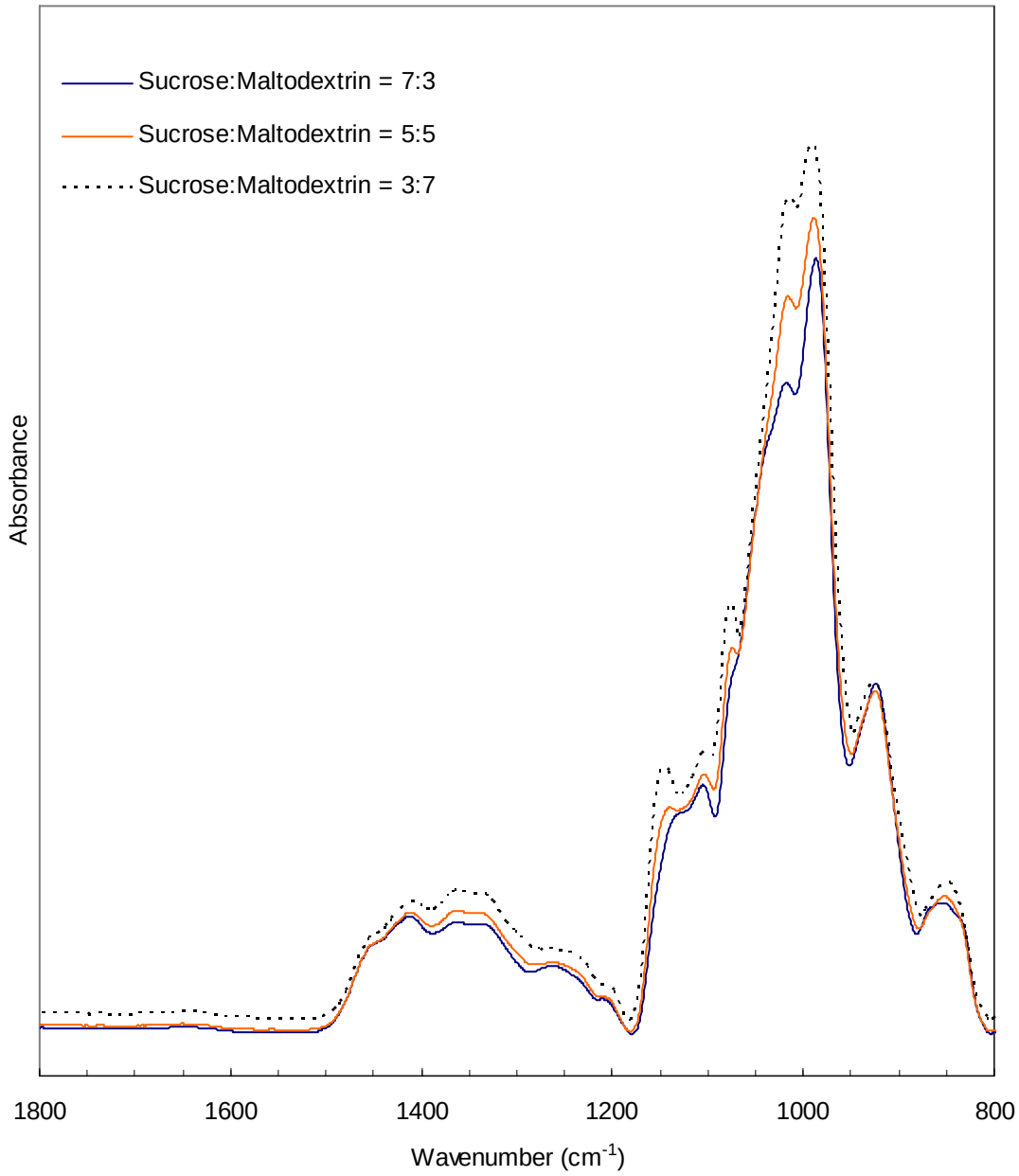

Figure 3.6 Representative ATR-FTIR absorption spectra in the fingerprint region of the bioglass systems without Na citrate equilibrated in the atmosphere of P_2O_5. Spectra were normalized to OH-stretching region (3500–3000 cm^{-1}).

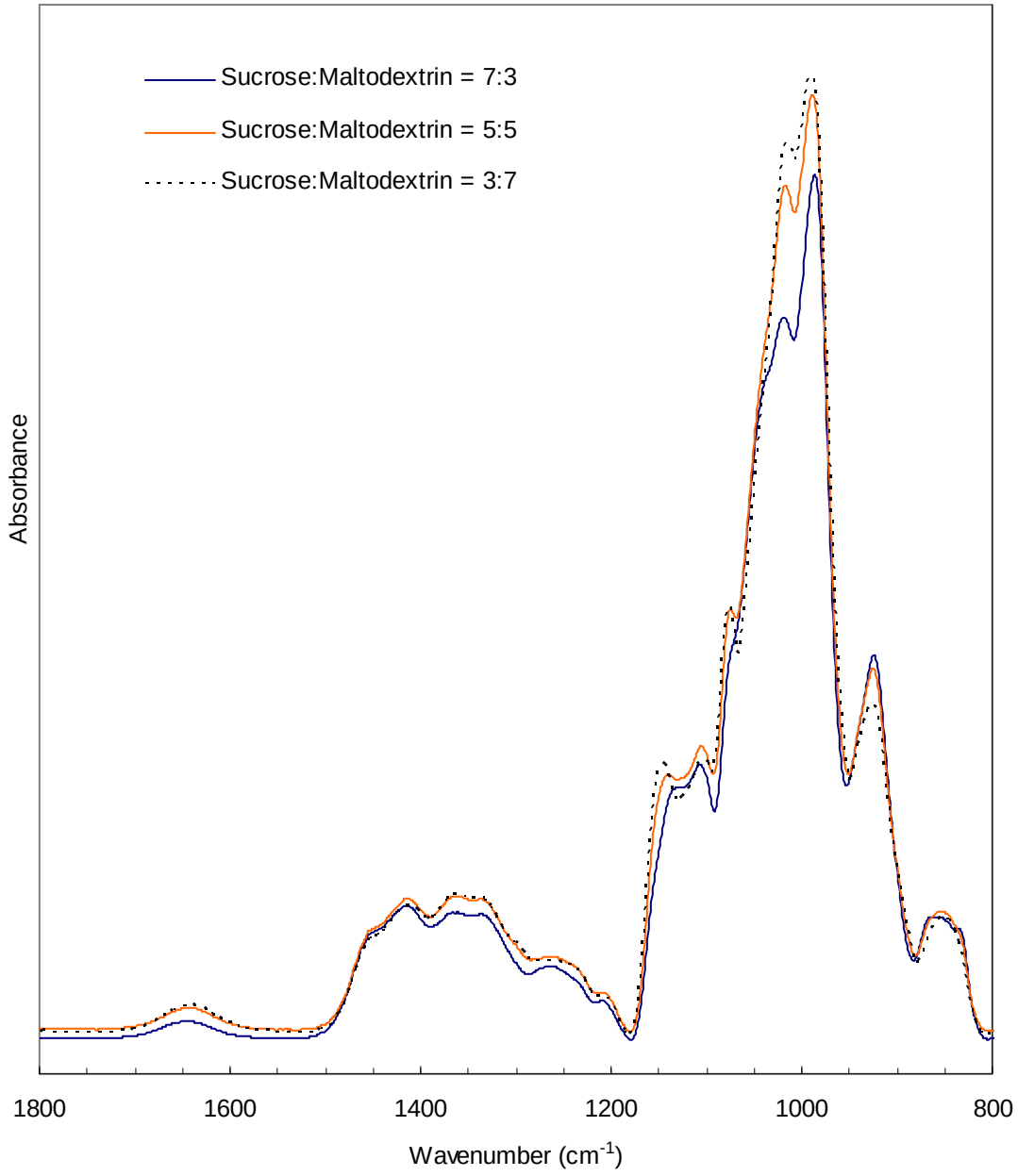

Figure 3.7 Representative ATR-FTIR absorption spectra in the fingerprint region of the bioglass systems without Na citrate, equilibrated in the atmosphere of saturated LiCl solution. Spectra were normalized to OH-stretching region (3500 – 3000 cm^{-1}).

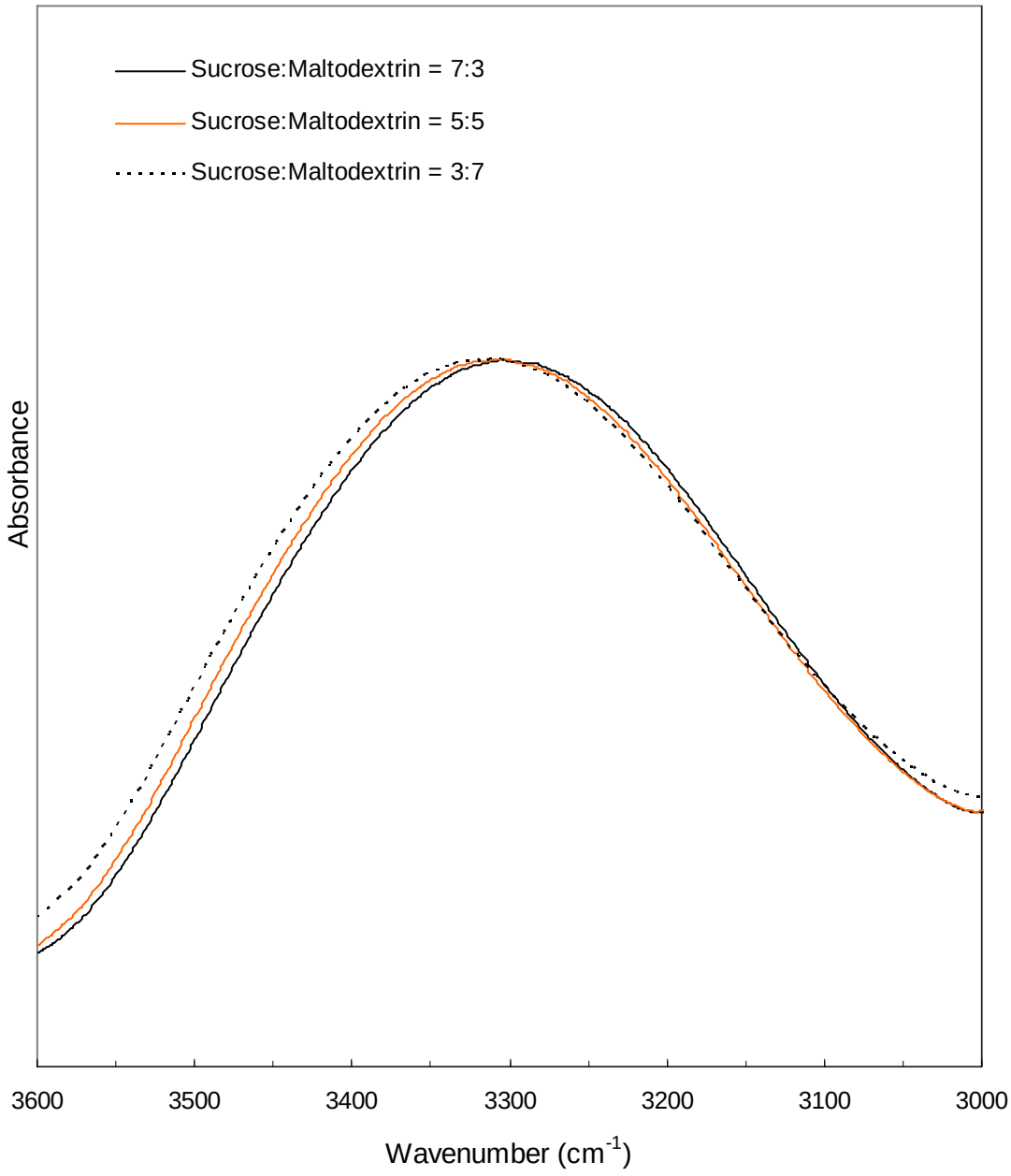

Figure 3.8 Representative ATR-FTIR absorption spectra (normalized) of the bioglass systems with different SC/MD in the region of OH-stretching vibration.

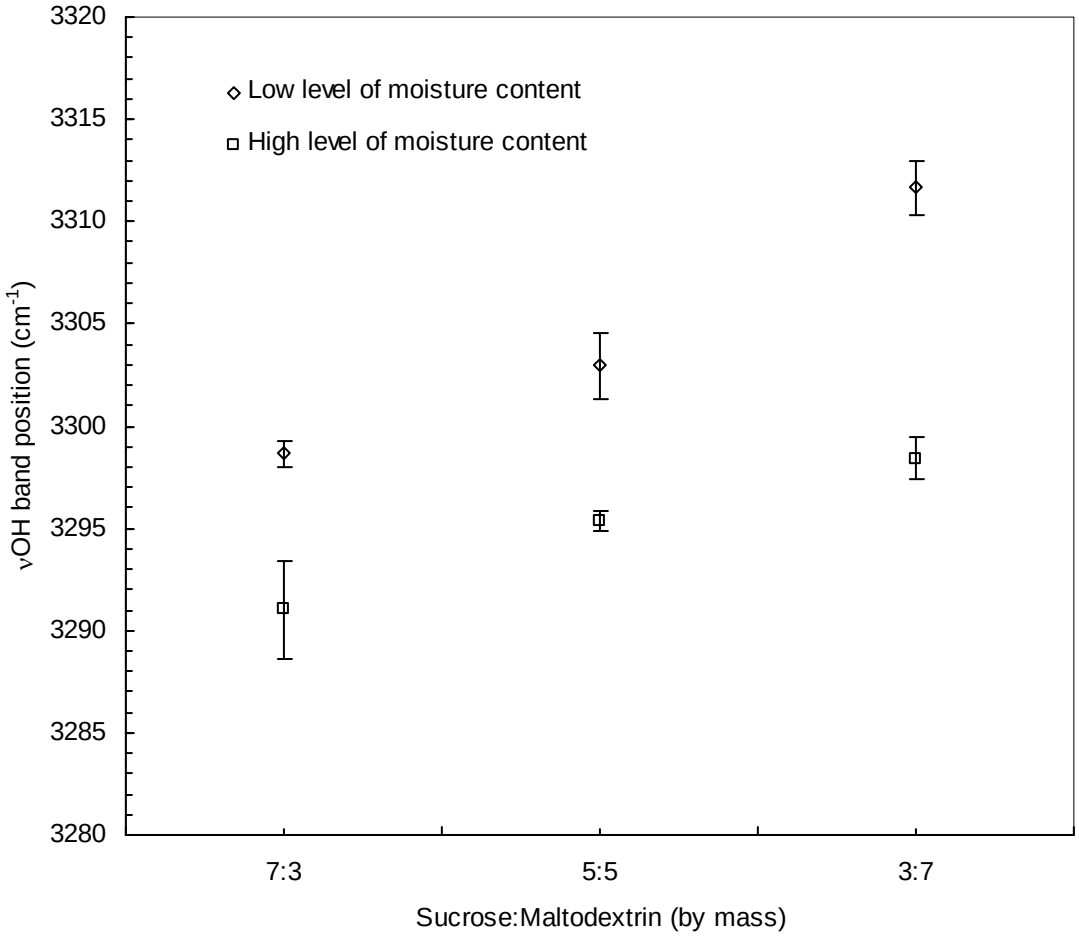

Figure 3.9 Band positions of OH-stretching vibration the bioglass model systems with different SC/MD. Data are means of two replicates and the error bars reflect standard deviations.

3.4.3 Effects of moisture on the characteristics of ATR-FTIR absorption spectra

Experimental data of moisture content for the bioglass model systems can be found in Chapter 2 (Tables 2.5 and 2.6). For the systems without Na citrate, the average moisture content of those equilibrated in P_2O_5 atmosphere and over saturated LiCl solution were 0.32±0.03 and 3.39±0.61 %wb, respectively.

FTIR spectroscopy is effective in elucidating the hydration and plasticization effects of water molecules on the conformational changes of oligosaccharides. Kačuráková and Mathlouthi, suggested that absorption spectra in the fingerprint region largely arises from the symmetrical deformation of CH_2 groups and the CO-stretching vibrations, and so it could provide rich structural information (Kačuráková and Mathlouthi, 1996).

However, within the range of moisture content in this experiment, there was no detectable effect of moisture content levels on the characteristic of IR absorption spectra in the fingerprint region (Figure 3.10). The range of moisture content in this experiment might be too low to observe any conformational change as a result hydration. The most noticeable difference between the spectra of systems with different levels of moisture content was the appearance of a weak band centered around 1640 cm^{-1} in the spectra obtained from the system with high-level moisture; this band is associated with the OH-bending vibrational mode. Though with low intensity, this band clearly indicated the presence of water in the systems since hydroxyl groups in carbohydrate do not contribute to this band (Lerbret et al., 2005; Gallina et al., 2006; Malsam and Aksan, 2009).

The effect of moisture was also found in the region of OH-stretching band where the downshift of wavenumber was observed, as shown in the inset in Figure 3.10. It is interesting that the downshift of OH-stretching band usually implies the stronger hydrogen bonding.

However, water would plasticize the amorphous saccharides, not strengthen. The DSC measurements also showed a decrease in T_g values as moisture increased. The possible reason for the downshift of OH-stretching band might be that water molecules appearing in the system were all in the ordered hydrogen-bonded structures. As discussed in section 3.4.1.1, the band position of the ordered hydrogen-bonded structures should be at wavenumbers slightly lower than 3300 cm^{-1}. However, the band position of OH-stretching vibration arises from saccharides is generally around 3300 cm^{-1} or higher. Consequently, the presence of water in a system would result in the downshift of wavenumber. The effect of moisture on the band position of OH-stretching vibration in the bioglass systems can be seen in Figure 3.9. Regardless of the SC/MD, it was clear that moisture caused the downshift of the OH-stretching band position in every system. The system with SC/MD of 3:7 was the most affected by moisture; the OH-stretching band position shifted down by approximately 13 cm^{-1}. The downshift of this band for the systems with SC/MD of 7:3 and 5:5 was quite similar in magnitude, approximately 7.6 cm^{-1}.

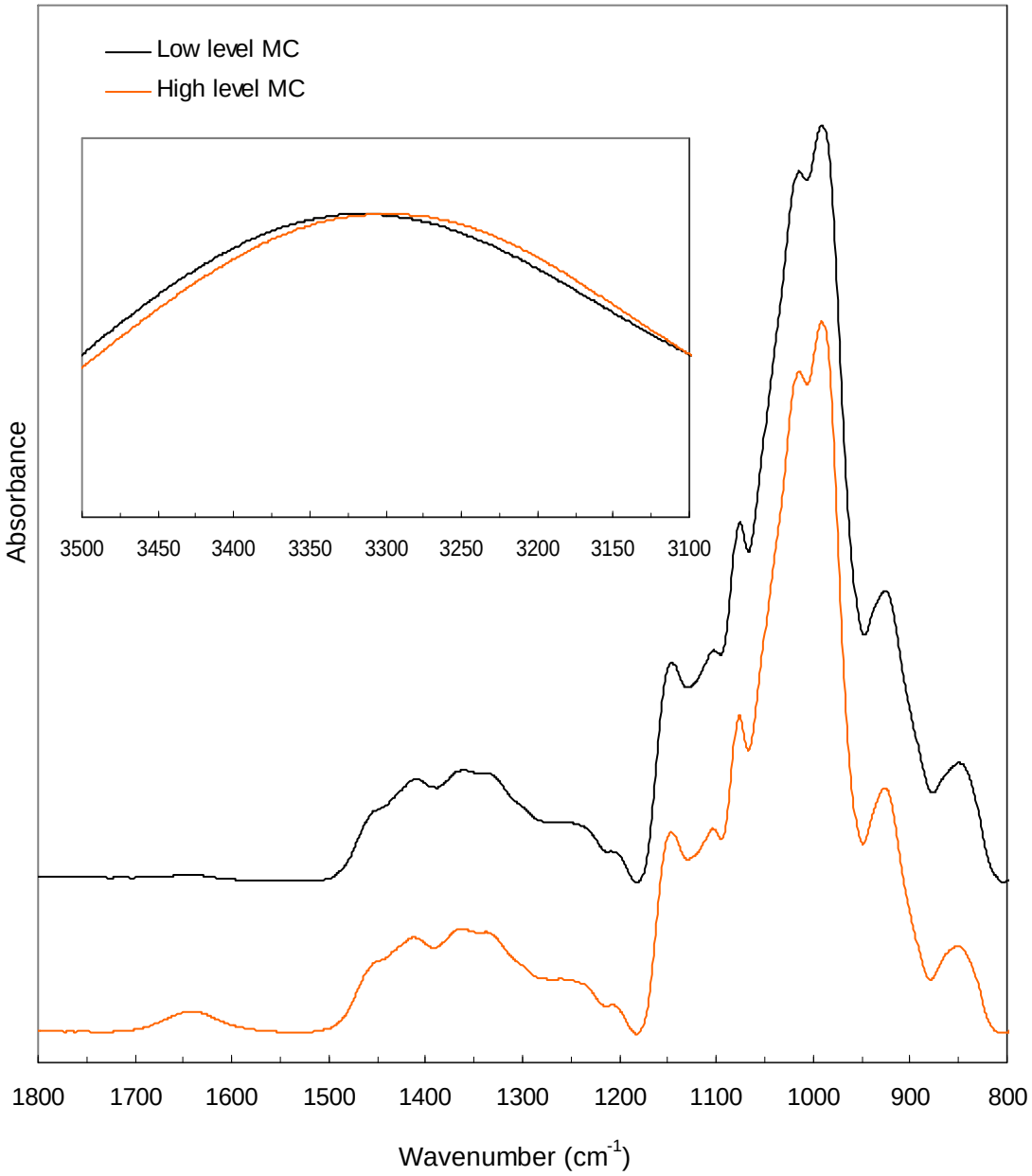

Figure 3.10 Representative ATR-FTIR absorption spectra (normalized) of the bioglass systems with high- and low-level of moisture content. The inset shows spectra in the region of OH-stretching vibration.

3.4.4 Evidences for the interaction between saccharides and Na citrate

There was no detectable effect of Na citrate on the absorption spectra in the region below 1200 cm^{-1}. However, in the region of approximately 1650 – 1300 cm^{-1}, there are antisymmetric ($\nu_{as}(COO^{-})$) and symmetric ($\nu_{s}(COO^{-})$) stretching vibrations of carboxyl group of Na citrate centered at around 1583 and 1375 cm^{-1}, respectively (Figures 3.11 and 3.12). While the band position of $\nu_{as}(COO^{-})$ stretching vibration was independent of SC/MD, its intensity decreased with increasing SC/MD. For the systems with high-level moisture content (Figure 3.12), this band partly overlapped with the OH-bending band which arises from water as illustrated in Figure 3.10. The $\nu_{s}(COO^{-})$ band completely overlapped with the absorption bands of saccharides rendering it difficult to precisely locate the band position. It appears that the intensity of this band slightly decreased with decreasing SC/MD—just as for the case of $\nu_{as}(COO^{-})$, but to a smaller extent.

Absorption spectra of the systems with different SC/MD were normalized to the range of 1500 – 1200 cm^{-1} and plotted along with that of Na citrate (Figure 3.13). As far as the shift in position is concerned, the $\nu_{s}(COO^{-})$ band clearly showed the downshift from around 1381 to 1367 cm^{-1} when SC/MD decreased from 7:3 to 3:7. It could be also seen that the $\nu_{s}(COO^{-})$ band position of the system with SC/MD of 7:3, or with lowest level of maltodextrin, was close to that of carboxyl group in Na citrate which was around 1385 cm^{-1}.

The inclusion of Na citrate in sucrose glass has reportedly helped strengthen hydrogen bonding and consequently increase the T_g. The interaction of Na citrate and sucrose was evidenced by an upshift (a few cm^{-1}) of $\nu_{as}(COO^{-})$ band position, while no change in $\nu_{s}(COO^{-})$ band position was detected (Kets et al., 2004). In this study, we further

investigated the band position of $\nu_{as}(COO^{-})$ obtained from the bioglass model systems as compared to that from Na citrate. The comparisons of normalized absorption spectra are given in Appendix 3.3. We found an upshift of $\nu_{as}(COO^{-})$ band for approximately 4 and 2 cm^{-1} for the systems with Na citrate/sucrose ratio (NaCit/SC) of 0.1 and 0.2, respectively, regardless of SC/MD and level of moisture content.

The findings suggest that the interactions between Na citrate and saccharides exist in the bioglass model system. It appears that citrate interacts with both sucrose and maltodextrin via carboxylic groups. The interaction of citrate and maltodextrin was evidenced by the continuing downshift of $\nu_{s}(COO^{-})$ band position with increasing maltodextrin concentration; this change was not found in amorphous sucrose system (Kets et al., 2004).

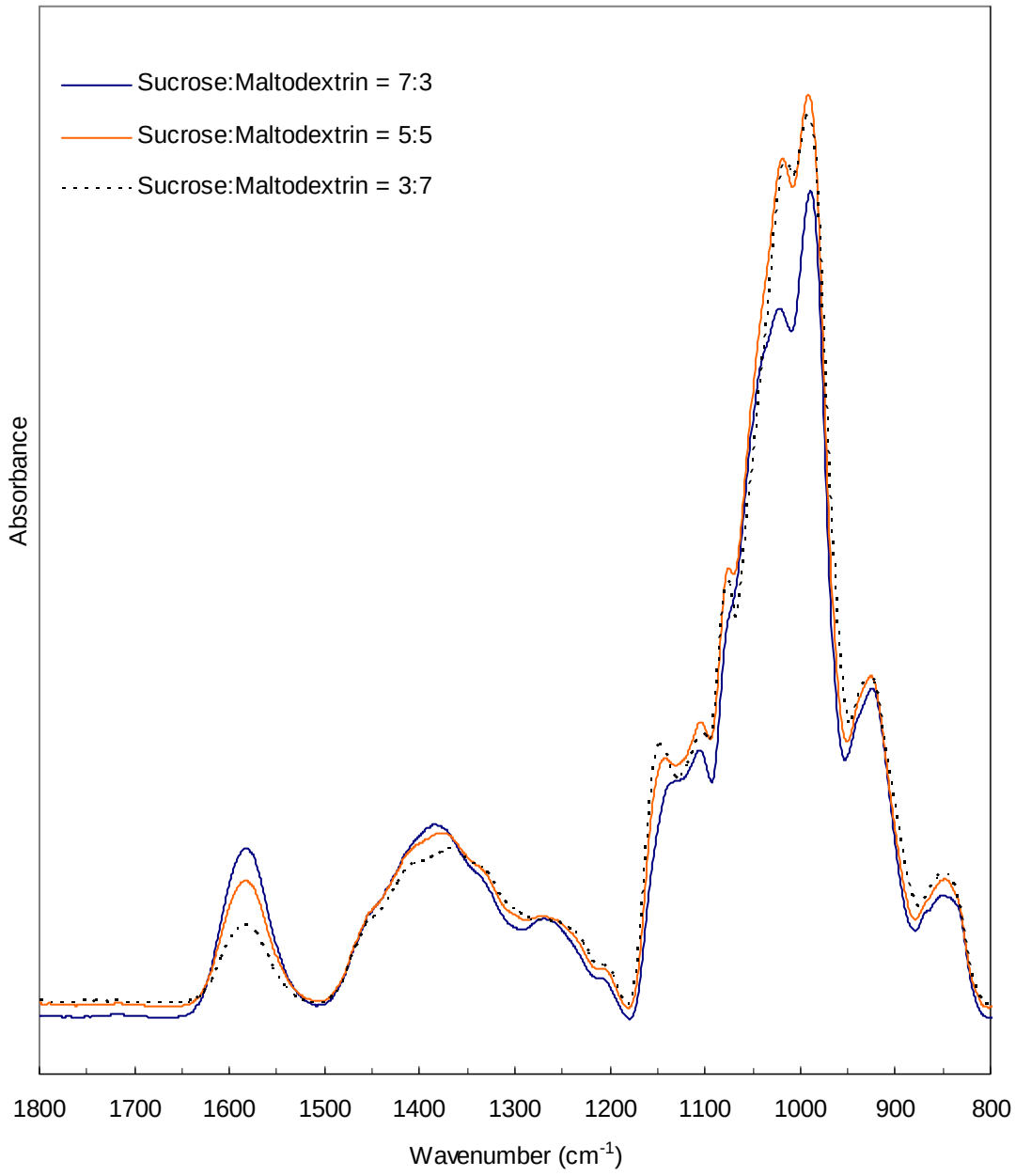

Figure 3.11 Representative ATR-FTIR absorption spectra in the fingerprint region of the bioglass model systems with NaCit/SC = 0.2 (by mole) equilibrated in the atmosphere of P_2O_5. Spectra were normalized to the OH-stretching region (3500 – 3000 cm^{-1}).

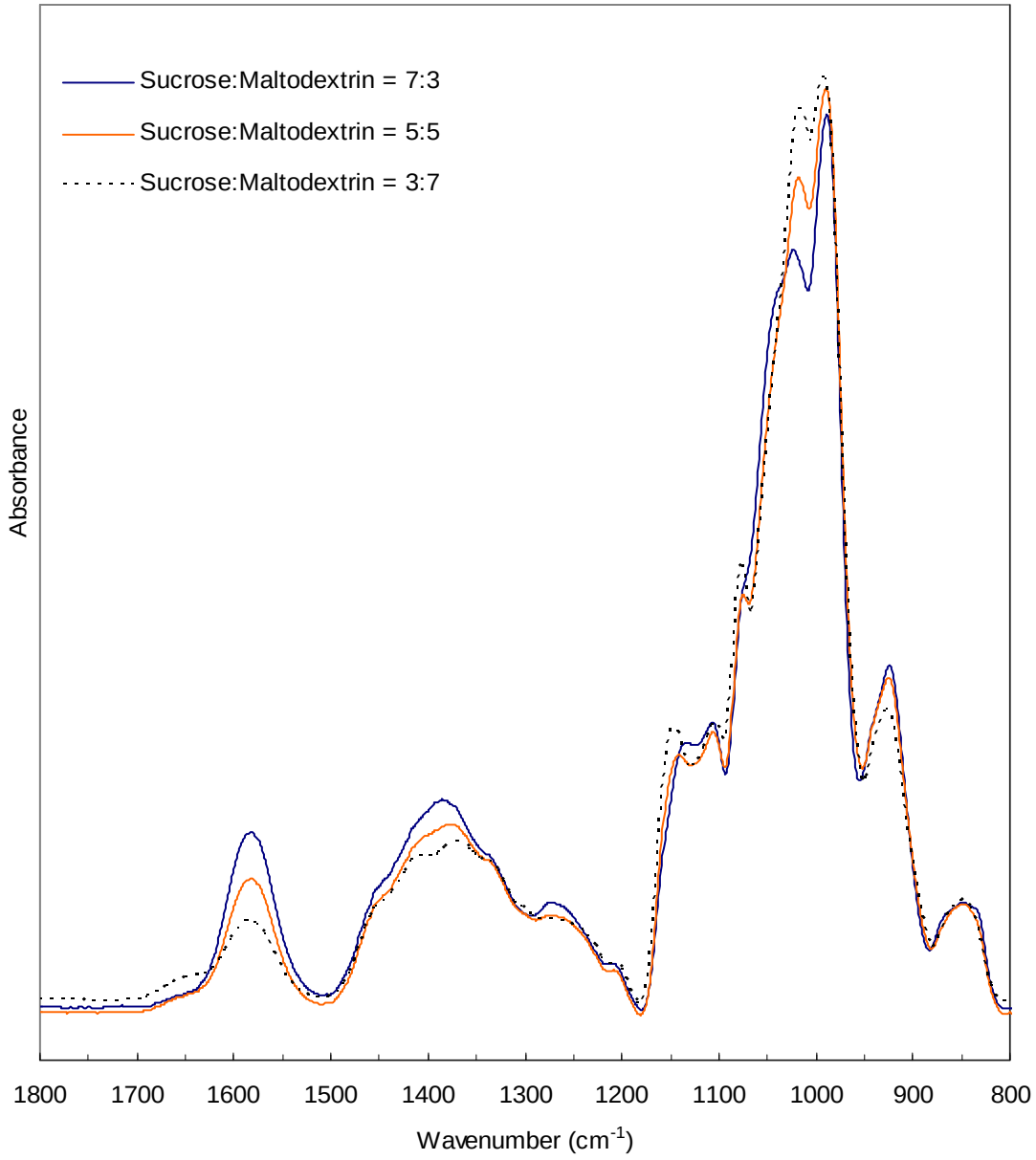

Figure 3.12 Representative ATR-FTIR absorption spectra in the fingerprint region of the bioglass model systems with NaCit/SC = 0.2 (by mole) equilibrated in the atmosphere of saturated LiCl solution. Spectra were normalized to OH-stretching region (3500 – 3000 cm^{-1})

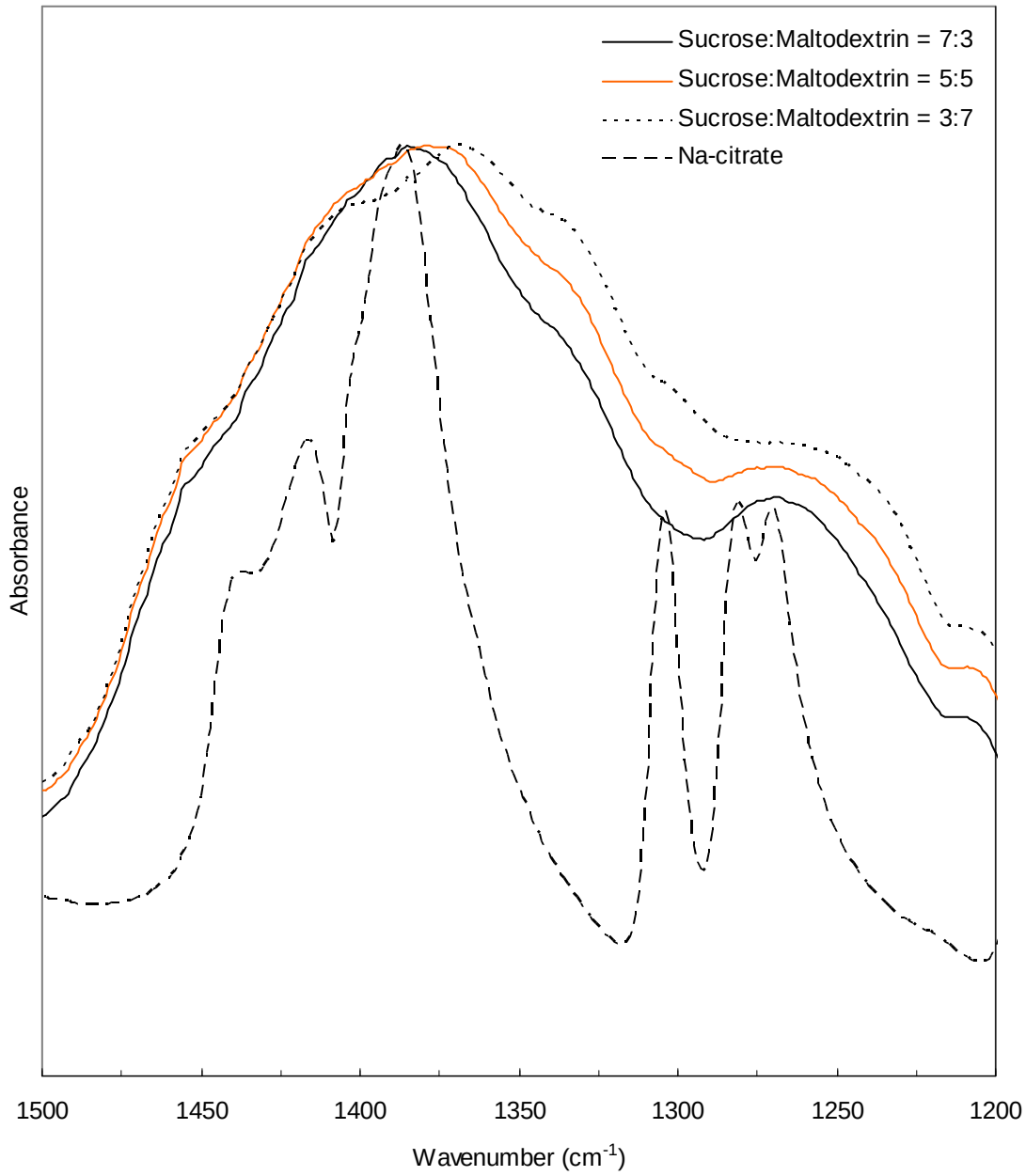

Figure 3.13 Representative ATR-FTIR absorption spectra of Na citrate and the bioglass model systems with NaCit/SC = 0.2 (by mole) equilibrated in the atmosphere of P_2O_5. Spectra were normalized to the region of 1500 – 1200 cm^{-1}.

3.4.5 Effects of Na citrate on characteristics of ATR-FTIR absorption spectra

Figures 3.14 – 3.19 show the representative ATR-FTIR absorption spectra of bioglass model systems without and with Na citrate at two different levels. The spectra clearly reveal the effects of Na citrate. The most noticeable change on the absorption spectra upon the addition of Na citrate was the increase in intensity of the $\nu_{as}(COO^{-})$ and $\nu_{s}(COO^{-})$ bands. Another observable change was the broadening of OH-stretching band, which reflects the alteration of hydrogen bonding network in the glass matrix. The higher the concentration of Na citrate, the more the broadening of OH-stretching band. The broad OH-stretching band could be interpreted as the more variations in the hydrogen bonding features—length and orientation (Wolkers et al., 2004b). A bit more details of this change is also given in the inset in each figure. It is noticeable that the band was broadened in a way that the band position shifted down indicating the weakening of OH bond since hydrogen bonding network in the glass matrix got stronger.

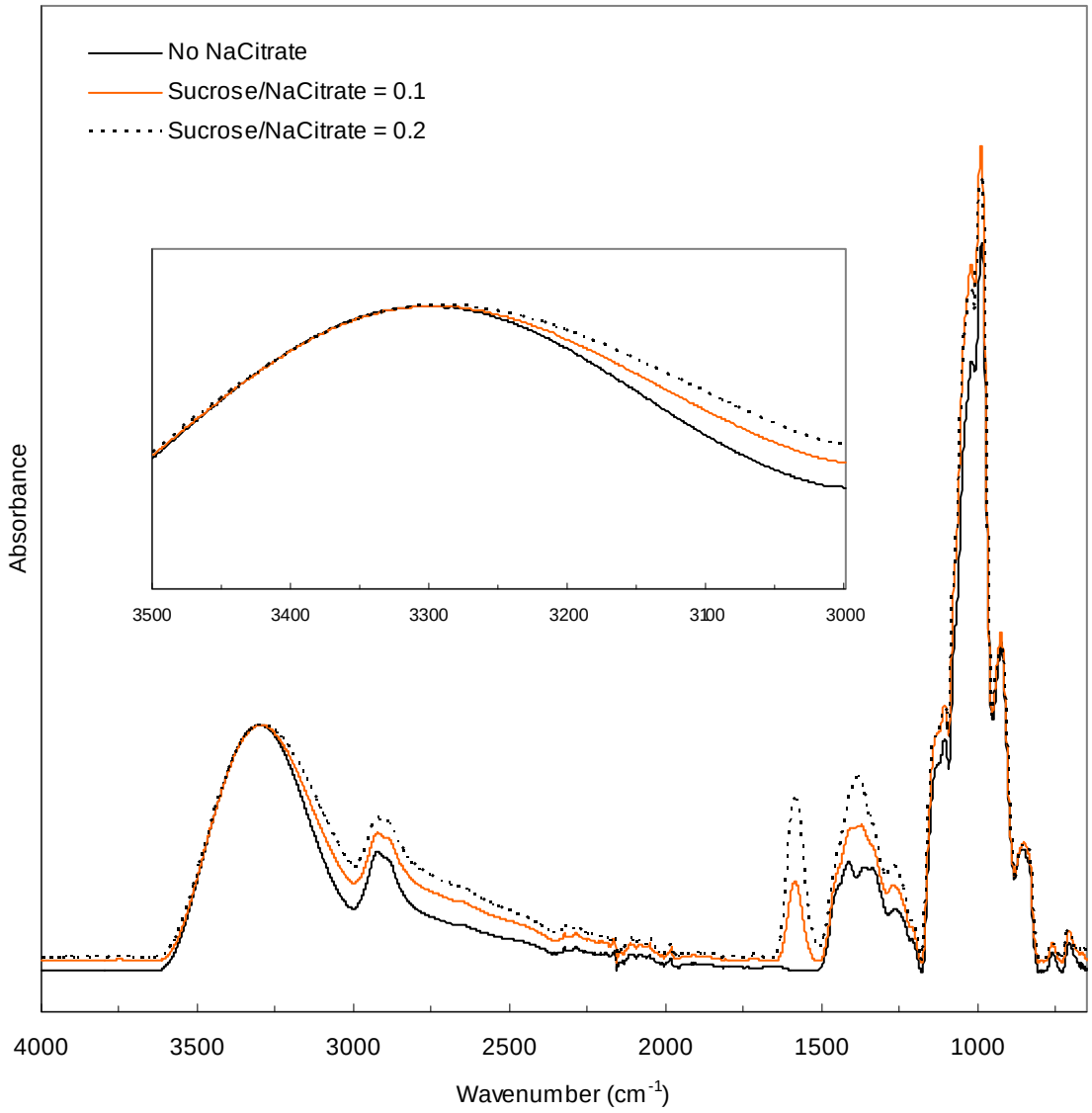

Figure 3.14 Representative normalized ATR-FTIR absorption spectra of the bioglass model systems with SC/MD = 7:3 (by mass) equilibrated in P_2O_5 atmosphere. The inset gives more detail on OH-stretching band.

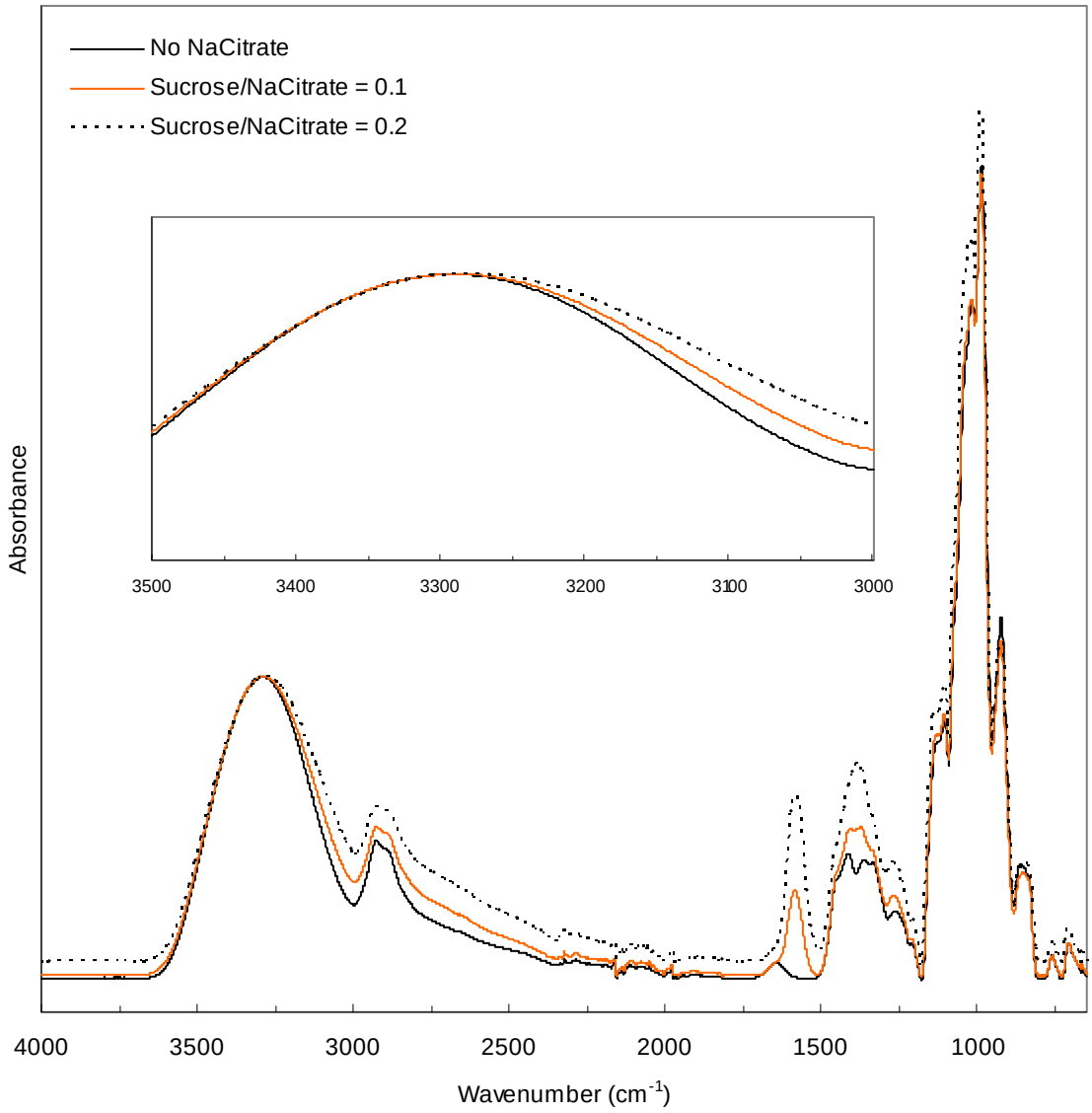

Figure 3.15 Representative normalized ATR-FTIR absorption spectra of the bioglass model systems with SC/MD = 7:3 (by mass) equilibrated in the atmosphere of saturated LiCl solution (high-level moisture content). The inset gives more detail on OH-stretching band.

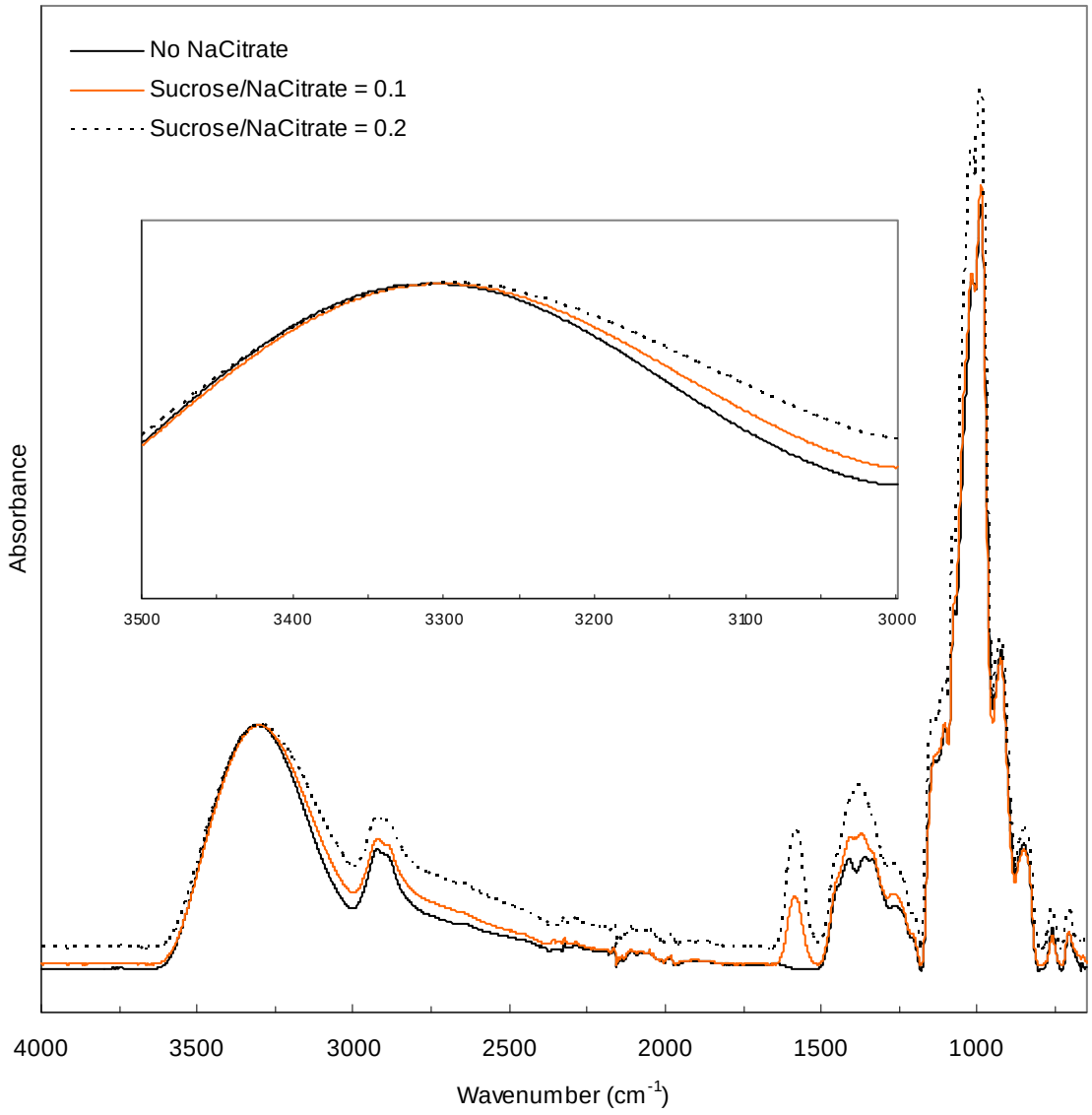

Figure 3.16 Representative normalized ATR-FTIR absorption spectra of the bioglass model systems with SC/MD = 5:5 (by mass) equilibrated in P_2O_5 atmosphere. The inset gives more detail on OH-stretching band.

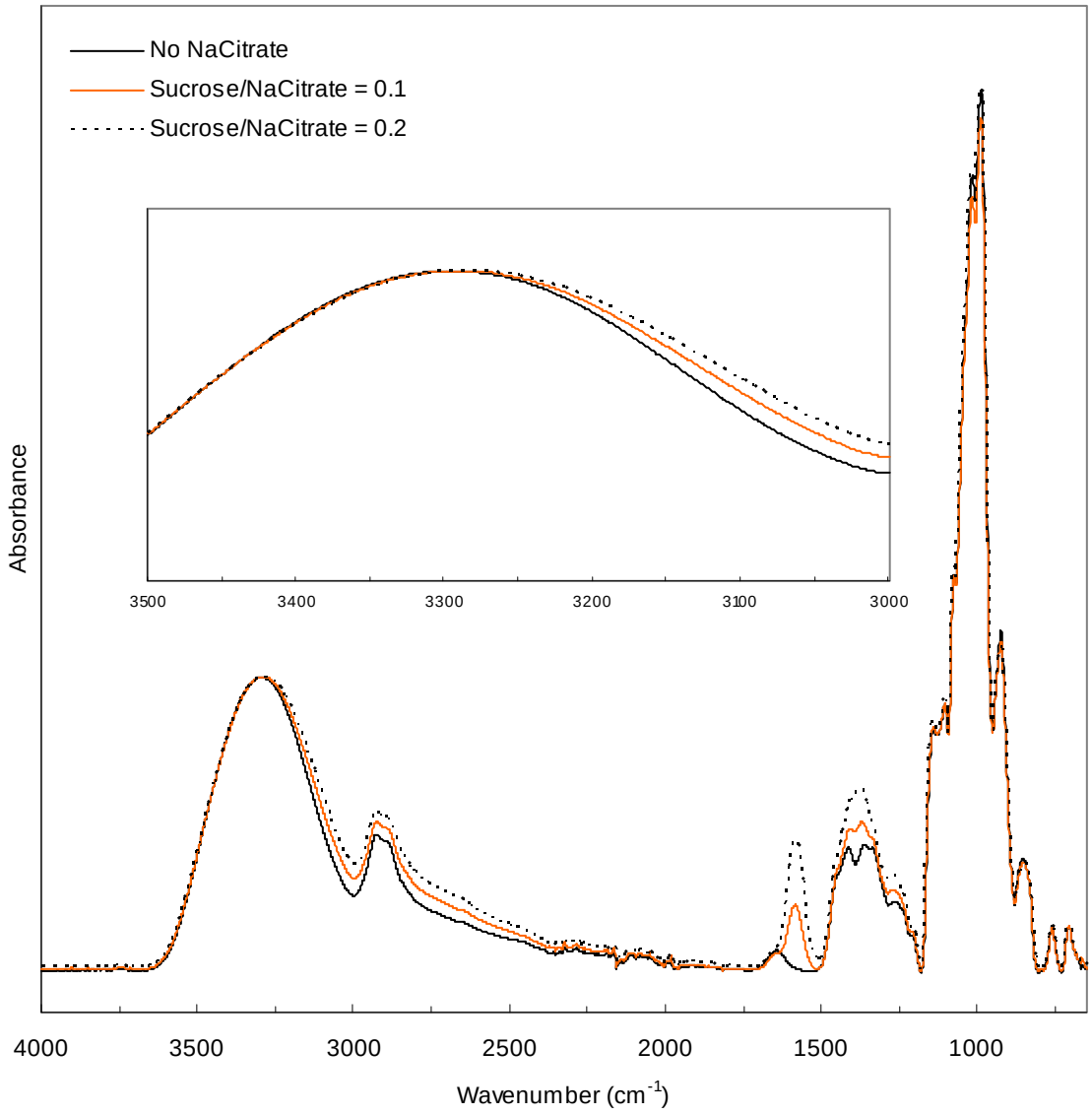

Figure 3.17 Representative normalized ATR-FTIR absorption spectra of the bioglass model systems with SC/MD of 5:5 (by mass) equilibrated in the atmosphere of saturated LiCl solution. The inset gives more detail on OH-stretching band.

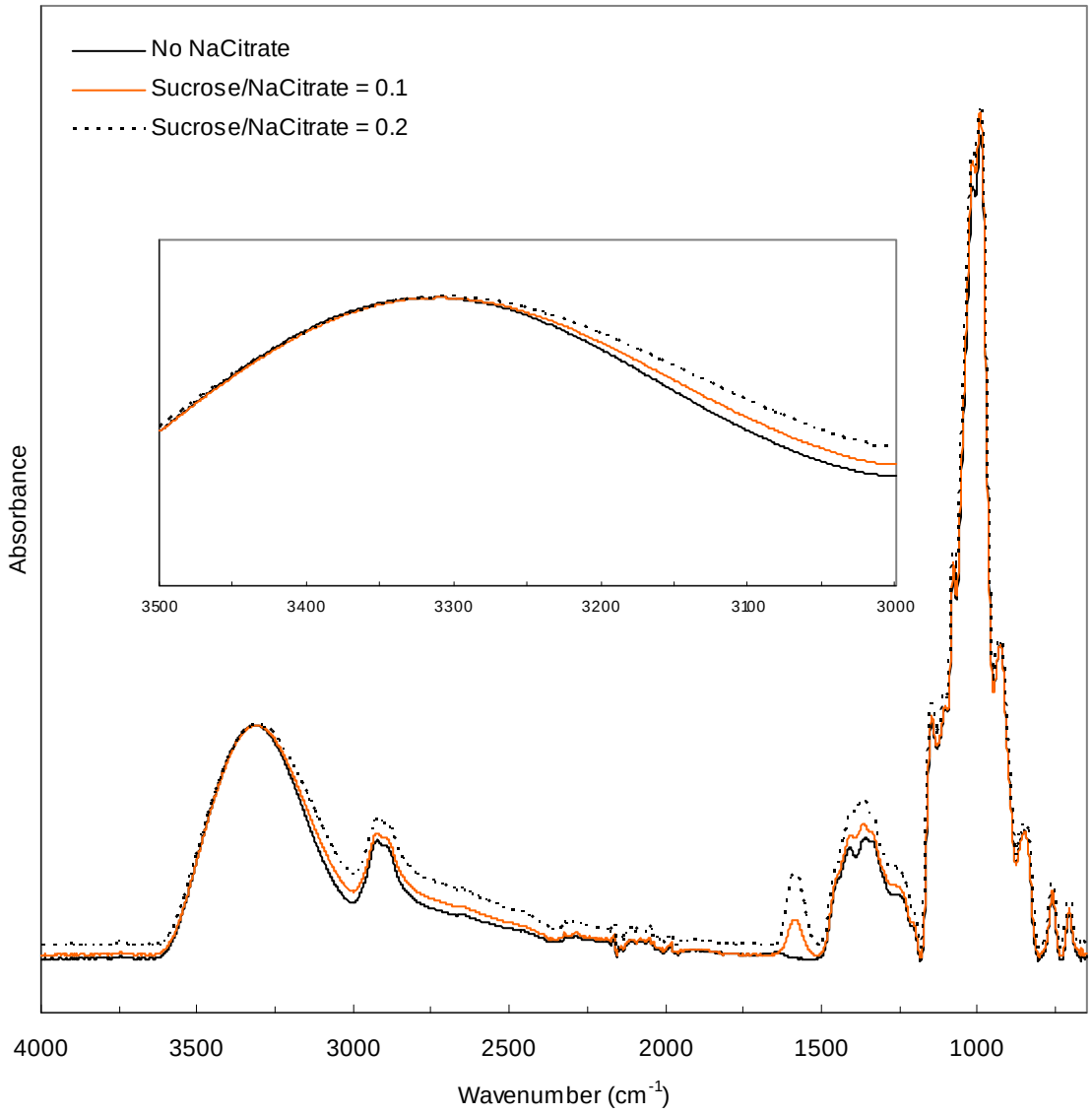

Figure 3.18 Representative normalized ATR-FTIR absorption spectra of the bioglass model systems with SC/MD = 3:7 (by mass) equilibrated in P_2O_5 atmosphere. The inset gives more detail on OH-stretching band.

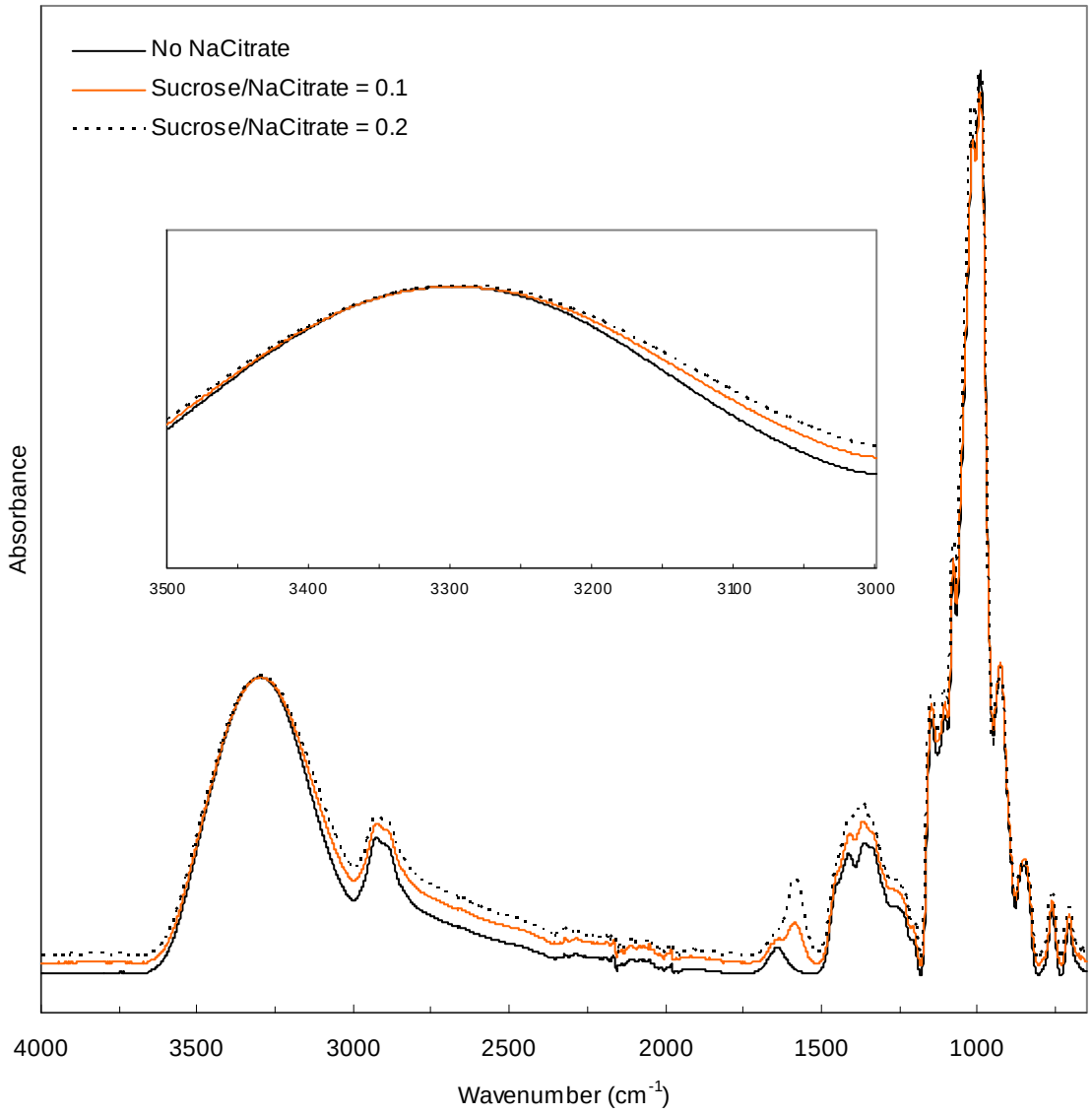

Figure 3.19 Representative normalized ATR-FTIR absorption spectra of the bioglass systems with SC/MD = 3:7 (by mass) equilibrated in the atmosphere of saturated LiCl solution. The inset gives more detail on OH-stretching band.

3.4.6 OH-stretching vibration

Hydrogen bonding between hydroxyl groups of sugar molecules are responsible to hold amorphous sugar matrices (Imamura et al., 2006). Information about hydrogen bonding could be inferred from the analysis of OH-stretching absorption band in FTIR spectra. Here, we consider two key features of OH-stretching band: band position and band width.

3.4.6.1 OH-stretching band position

Figures 3.20 and 3.21 show the effect of Na citrate on OH-stretching band position for the systems with low- and high-level of moisture content, respectively. In every system, regardless of SC/MD and moisture content levels, Na citrate resulted in a downshift of OH-stretching band position. Within a range of Na citrate concentration in this experiment, there was a positive correlation between the magnitude of the downshift and the concentration of Na citrate. On average, the OH-stretching band for the systems with NaCit/SC of 0.2 exhibited a larger downshift than that for the systems with NaCit/SC of 0.1 by approximately 9 and 5 cm^{-1} at low and high level of moisture content, respectively. It was also found that the effect of Na citrate is dependent on SC/MD and this held true regardless of moisture content level. The largest downshift of the OH-stretching band was found in the system with the highest sucrose content (SC/MD = 7:3) while the downshift was minimal in the system with the lowest sucrose content (SC/MD = 3:7).

The findings suggest that Na citrate interaction could help strengthen the hydrogen-bonded network in the matrix of amorphous sucrose-maltodextrin-Na citrate mixture, as manifested by the downshift of OH-stretching vibration wavenumber or frequency. Although Na citrate caused the downshift of OH-stretching band position in every system, but

apparently the system with the highest sucrose content was affected the most indicating greater interaction between Na citrate and sucrose than between Na citrate and maltodextrin. The less interaction between Na citrate and maltodextrin is likely due to spatial restrictions as maltodextrin molecules are bulkier than sucrose molecules. Similar behavior was reported in the literature on several sugar glasses. The hydrogen bonding interaction of macromolecules, the 1-Palmitoyl-2-oleoyl-*sn-glycero*-3-phosphocholine (POPC) vesicles, with small-molecule sugars including glucose, sucrose, and trehalose could be clearly observed from the downshift of OH-stretching band. On the other hand, this was not the case for dextran—the bulkier saccharides—and the POPC vesicles (Wolkers et al., 2004b).

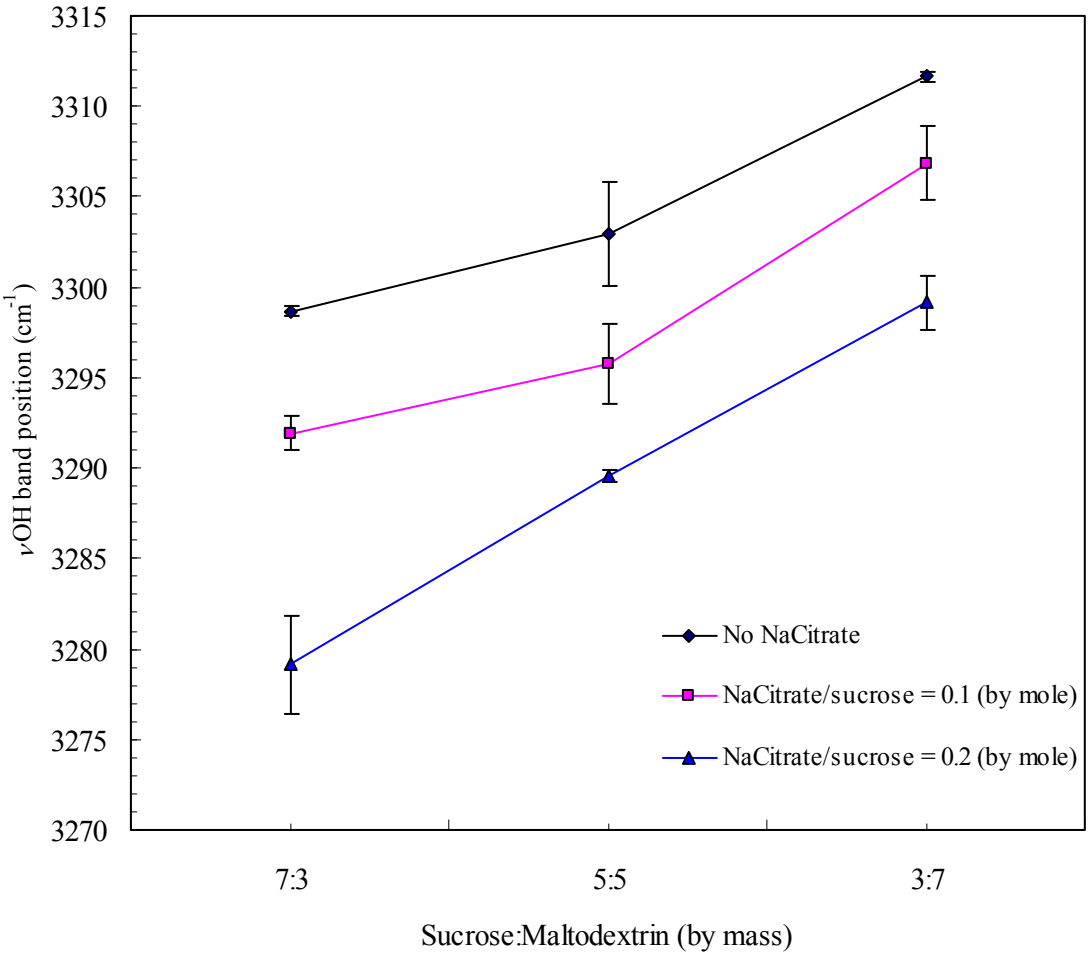

Figure 3.20 Effect of Na citrate on OH-stretching band position for samples with different SC/MD equilibrated in P_2O_5 atmosphere. Data are means of two replicates and the error bars reflect standard deviations.

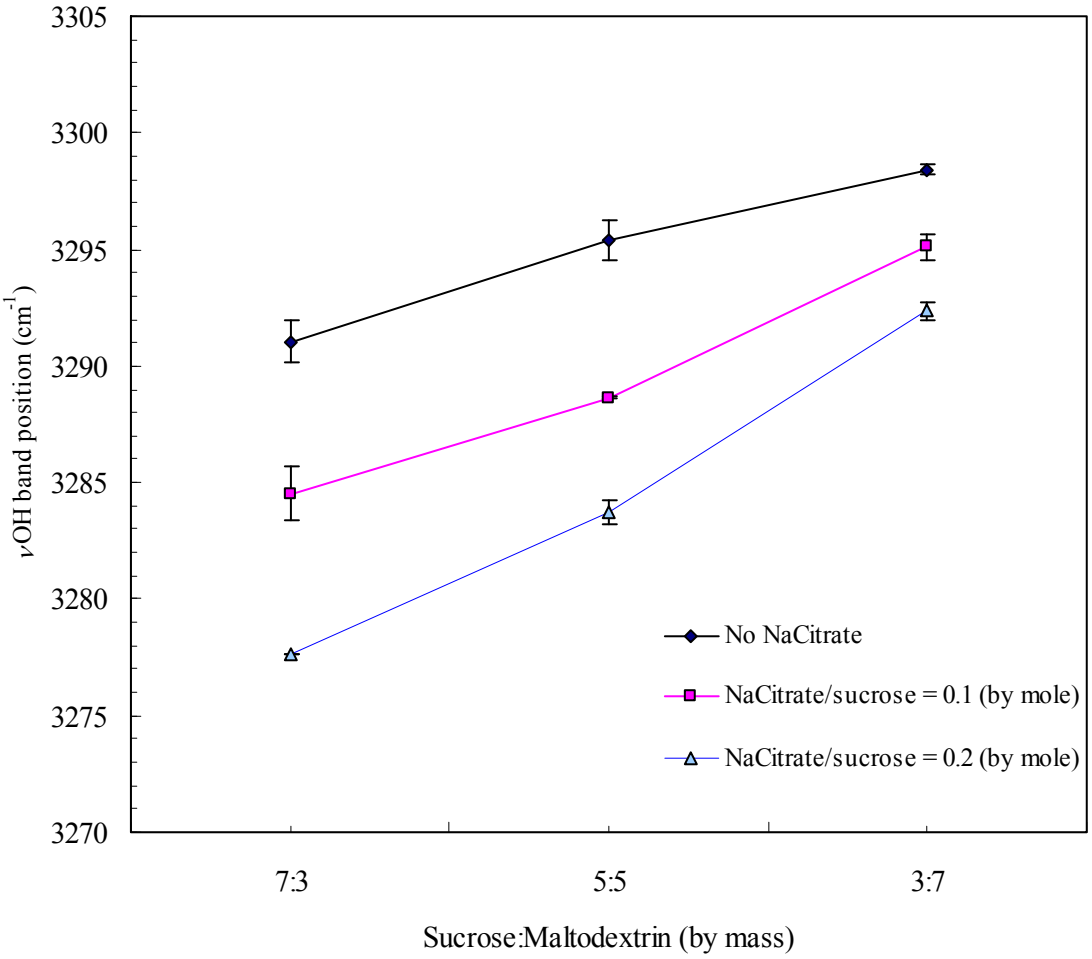

Figure 3.21 Effect of Na citrate on OH-stretching band position for samples with different SC/MD equilibrated in the atmosphere of saturated LiCl solution. Data are means of two replicates and the error bars reflect standard deviations.

3.4.6.2 The width of OH-stretching band

Other than the strength or length of hydrogen bond, the characteristics of OH-stretching absorption band could also provide information about the distribution of lengths and orientations of hydrogen bonding (Lutz and Vandermaas, 1994; Wolkers et al., 2004b). A narrow OH-stretching absorption band implies less distribution, while more distribution would be manifested by broadening of the band.

In this experiment the width of OH-stretching absorption band at 80% peak height was considered. The results are shown in Figures 3.22 and 3.23 for the bioglass model systems with low and high levels of moisture content, respectively. Without Na citrate, the widths of OH-stretching band in systems with different SC/MD were not much different in general. However, the systems with high-level moisture content exhibited a broader absorption band of approximately 220 cm^{-1} on average, as compared to 214 cm^{-1} seen in the systems with low-level moisture content, suggesting that water molecules contribute to larger distribution of hydrogen bonding features—lengths and orientations.

Regardless of moisture content levels within the range of this study, the introduction of Na citrate to sucrose-maltodextrin mixture resulted in the broadening of OH-stretching band in every system. The degree of band broadening correlated with both the concentrations of Na citrate and sucrose. The broadest OH-stretching band was found in the system with SC/MD of 7:3 while this band in the system with SC/MD of 3:7 showed minimal impact upon the addition of Na citrate. This could be interpreted as the interaction of Na citrate and bioglass model systems resulted in the wider spectrum of hydrogen bonding features. The result also suggests that Na citrate mainly interacted with sucrose.

An interesting observation could be made in the system with SC/MD of 7:3. Without Na citrate, the width of OH-stretching band in this system with high-level moisture content was larger than that of the system with low-level moisture content, 218.4 cm^{-1} compared to 212.6 cm^{-1}. However, the system with NaCit/SC of 0.2 at low-level moisture content exhibited a broader band, 240.2 cm^{-1} compared to 238.15 cm^{-1}. This is an important evidence to support that Na citrate could effectively interact with sucrose through hydrogen bonding in low moisture environment. The similar finding has been also reported by Kets and coworkers. They found that when residual water was 3.5% or higher, the presence of citrate reduced the T_g of sucrose-citrate mixture. However, removal of residual water lower than 3.5 % enabled the interaction between sucrose and citrate through hydrogen bonding leading to a firm glassy matrix, and consequently the T_g which exceeded individual T_g of pure sucrose and citrate was obtained (Kets et al., 2004).

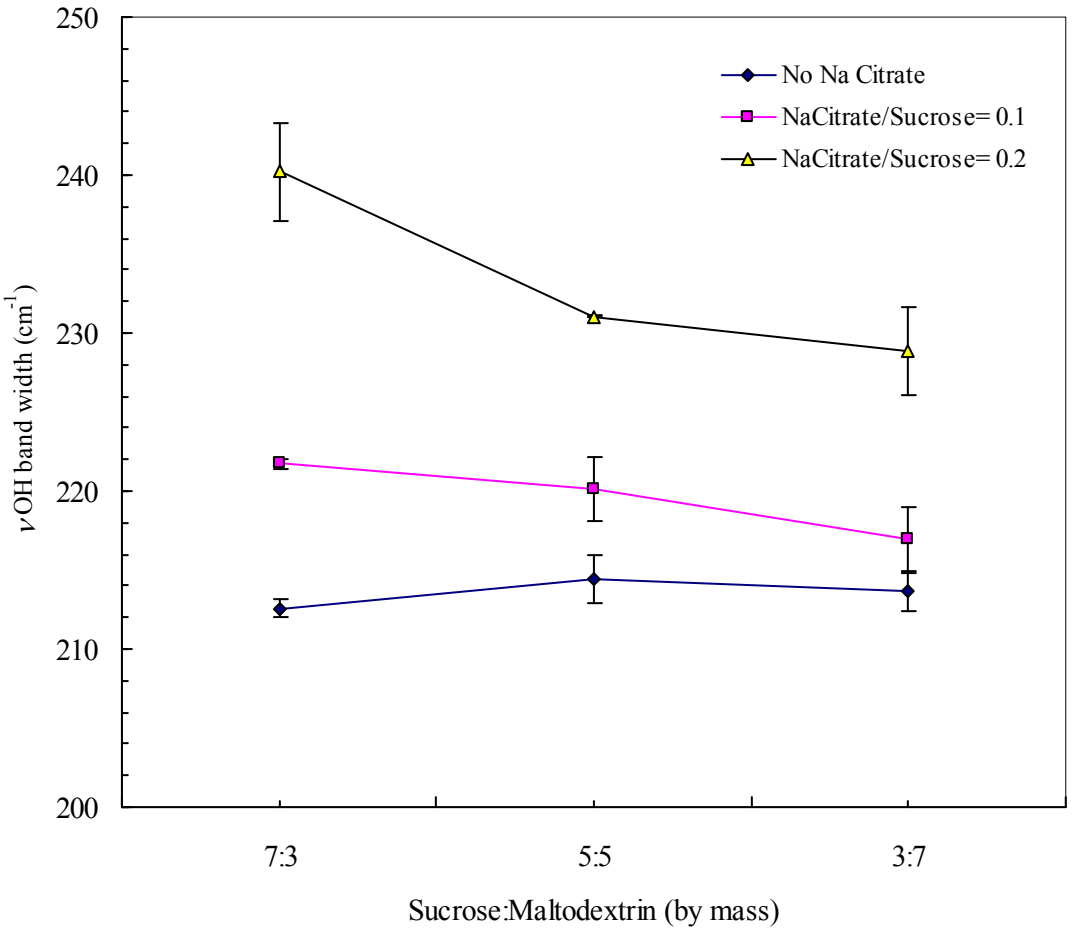

Figure 3.22 Effect of Na citrate on the width of OH-stretching band for samples with different SC/MD equilibrated in P_2O_5 atmosphere. Data are means of two replicates and the error bars reflect standard deviations.

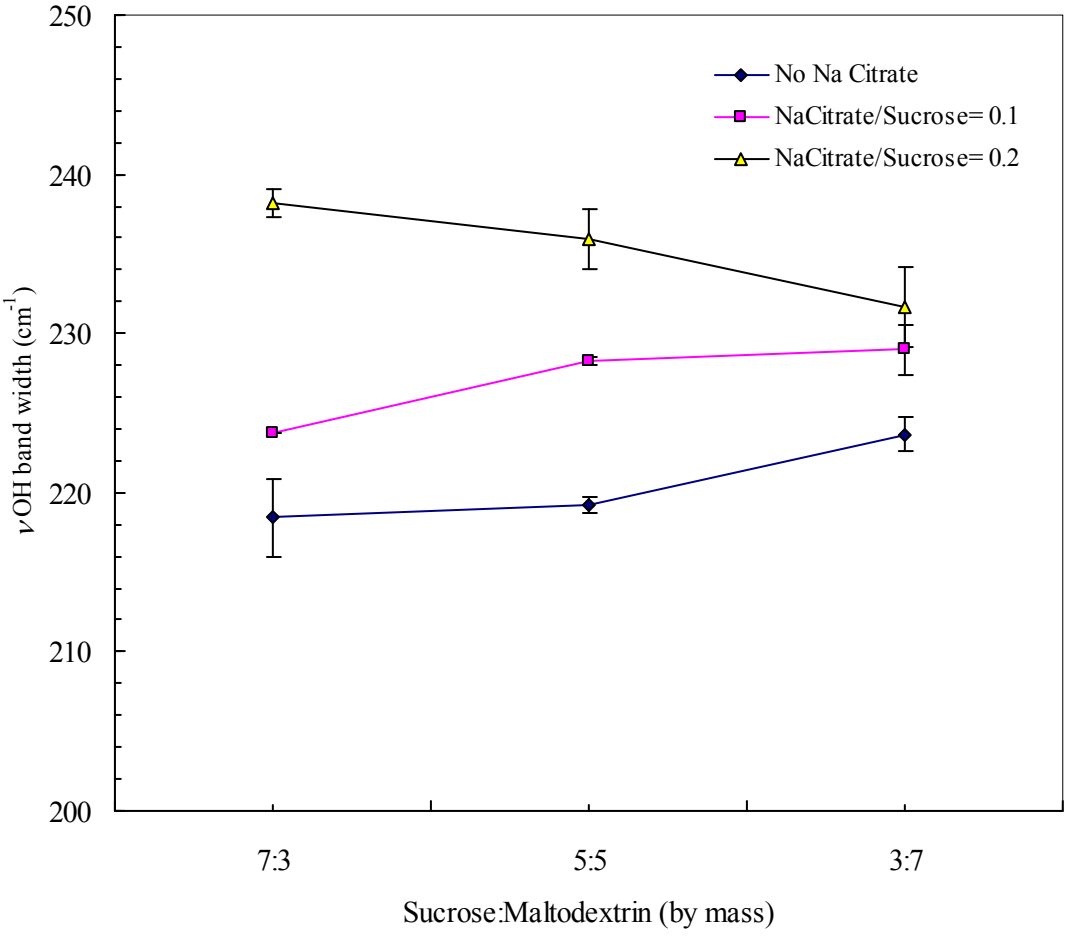

Figure 3.23 Effect of Na citrate on the width of OH-stretching band of the samples with different SC/MD equilibrated in the atmosphere of saturated LiCl solution. Data are means of two replicates and the error bars reflect standard deviations.

3.5 Conclusions

The composition of bioglass model system exhibited significant effects on its characteristic and molecular structure. The system with lower SC/MD showed the OH-stretching absorption band at higher wavenumber, in other words weaker hydrogen bonding. This observation suggests that molecular structure of the bioglass with high maltodextrin concentration, or low sucrose concentration is loosely packed. However, as can be seen in Chapter 2, the T_g of the system with lower SC/MD is greater than that of the system with higher SC/MD. Due to the fact that sucrose and maltodextrin molecules contain different types and number density of glycosidic linkages, the result would suggest that T_g is strongly under the influence of types and number density of glycosidic linkages, rather than the compactness of the glass structure.

Within the range of moisture contents studied (0.27 – 4.4 %wb), FTIR did not detect any plasticization effect of water on the bioglass. The only noticeable effect of water was to shift down the average wavenumber of OH-stretching band. This change might be because of water molecules were in the ordered hydrogen-bonded structure which exhibits the OH-stretching vibration at lower frequency/wavenumber than that of saccharides. As a result, the mean absorption frequency of OH-stretching vibration of the system with higher moisture content was lower than that of the system with lower moisture content.

Na citrate interacted with both sucrose and maltodextrin through carboxylic groups as evidenced by the shifting of $\nu_{as}(COO^{-})$ and $\nu_{s}(COO^{-})$ bands. The addition of Na citrate resulted in a broader and lower frequency of OH-stretching absorption band. The broadening

of the band suggests more varied hydrogen-bonding features—lengths and orientations while the downshift indicated the stronger hydrogen bonding. Na citrate tended to interact more with sucrose rather than with maltodextrin. The strongest hydrogen-bonded network was observed in the system with highest concentration of sucrose (SC/MD = 7:3) and Na citrate (NaCit/SC = 0.2).

3.6 References

Anonymnous. (2009). "The nature of vibrational spectroscopy." Retrieved Jan. 31, 2009, from http://www2.chemistry.msu.edu/faculty/reusch/virttxtjml/spectrpy/InfraRed/irspec1.htm.

Anonymnous. (2010). "Infrared spectroscopy." Retrieved Nov.7, 2010, from http://en.wikipedia.org/wiki/Infrared_spectroscopy.

Atkins, P. W. and Paula, J. D. (2009). Elements of physical chemistry. 5th ed. Oxford: Oxford University Press.

Brubach, J. B., Mermet, A., Filabozzi, A., Gerschel, A. and Roy, P. (2005). "Signatures of the hydrogen bonding in the infrared bands of water." The Journal of Chemical Physics **122**(18): 184509.

Chang, L., Shepherd, D., Sun, J., Ouellette, D., Grant, K. L., Tang, X. and Pikal, M. J. (2005). "Mechanism of protein stabilization by sugars during freeze-drying and storage: Native structure preservation, specific interaction, and/or immobilization in a glassy matrix?" Journal of Pharmaceutical Sciences **94**(7): 1427-1444.

Chaplin, M. (2012). "Water structure and science." Retrieved Jun. 5, 2012, from http://www.lsbu.ac.uk/water/vibrat.html.

Coates, J. (2000). Interpretation of infrared spectra, A practical approach. Encyclopedia of Analytical Chemistry. R. A. Meyers. Chichester, John Wiley & Sons**:** 10815-10837.

Crowe, J. H., Carpenter, J. F. and Crowe, L. M. (1998). "The role of vitrification in anhydrobiosis." Annual Review of Physiology **60**: 73-103.

Crowe, J. H., Oliver, A. E., Hoekstra, F. A. and Crowe, L. M. (1997). "Stabilization of dry membranes by mixtures of hydroxyethyl starch and glucose: The role of vitrification." Cryobiology **35**(1): 20-30.

Exova. (2010). "Fourier transform infrared spectroscopy." Technical Articles Retrieved Nov.5, 2010, from http:www.wcaslab.com/tech/tbftir.htm.

Falk, M. (1984). "The frequency of the H-O-H bending fundamental in solids and liquids." Spectrochimica Acta Part A: Molecular Spectroscopy **40**(1): 43-48.

Freda, M., Piluso, A., Santucci, A. and Sassi, P. (2005). "Transmittance Fourier transform infrared spectra of liquid water in the whole mid-infrared region: Temperature dependence and structural analysis." Applied Spectroscopy **59**(9): 1155-1159.

Gallina, M. E., Sassi, P., Paolantoni, M., Morresi, A. and Cataliotti, R. S. (2006). "Vibrational analysis of molecular interactions in aqueous glucose solutions. Temperature and concentration effects." The Journal of Physical Chemistry B **110**(17): 8856-8864.

Gharsallaoui, A., Rogé, B. and Mathlouthi, M. (2008). "Water-disaccharides interactions in saturated solution and the crystallisation conditions." Food Chemistry **106**(4): 1329-1339.

Imam, S. H., Gordon, S. H., Mohamed, A., Harry-O'kuru, R., Chiou, B. S., Glenn, G. M. and Orts, W. J. (2006). "Enzyme catalysis of insoluble cornstarch granules: Impact on surface morphology, properties and biodegradability." Polymer Degradation and Stability **91**(12): 2894-2900.

Imamura, K., Sakaura, K., Ohyama, K.-i., Fukushima, A., Imanaka, H., Sakiyama, T. and Nakanishi, K. (2006). "Temperature scanning FTIR analysis of hydrogen bonding states of various saccharides in amorphous matrixes below and above their glass transition temperatures." The Journal of Physical Chemistry B **110**(31): 15094-15099.

Kačuráková, M. and Mathlouthi, M. (1996). "FTIR and laser-Raman spectra of oligosaccharides in water: characterization of the glycosidic bond." Carbohydrate Research **284**(2): 145-157.

Kadoya, S., Fujii, K., Izutsu, K.-i., Yonemochi, E., Terada, K., Yomota, C. and Kawanishi, T. (2010). "Freeze-drying of proteins with glass-forming oligosaccharide-derived sugar alcohols." International Journal of Pharmaceutics **389**(1-2): 107-113.

Kadoya, S., Izutsu, K. I., Yonemochi, E., Terada, K., Yomota, C. and Kawanishi, T. (2008). "Glass-state amorphous salt solids formed by freeze-drying of amines and hydroxy carboxylic acids: Effect of hydrogen-bonding and electrostatic interactions." Chemical & Pharmaceutical Bulletin **56**(6): 821-826.

Kets, E. P. W., Ijpelaar, P. J., Hoekstra, F. A. and Vromans, H. (2004). "Citrate increases glass transition temperature of vitrified sucrose preparations." Cryobiology **48**(1): 46-54.

Lerbret, A., Bordat, P., Affouard, F., Guinet, Y., Hédoux, A., Paccou, L., Prévost, D. and Descamps, M. (2005). "Influence of homologous disaccharides on the hydrogen-bond network of water: complementary Raman scattering experiments and molecular dynamics simulations." Carbohydrate Research **340**(5): 881-887.

Lutz, E. T. G. and Vandermaas, J. H. (1994). "Hydrogen-bonds in crystalline carbohydrates - a variable-temperature FT-IR study." Journal of Molecular Structure **324**(1-2): 123-132.

Malsam, J. and Aksan, A. (2009). "Hydrogen bonding and kinetic/thermodynamic transitions of aqueous trehalose solutions at cryogenic temperatures." The Journal of Physical Chemistry B **113**(19): 6792-6799.

Maréchal, Y. (2011). "The molecular structure of liquid water delivered by absorption spectroscopy in the whole IR region completed with thermodynamics data." Journal of Molecular Structure **1004**(1-3): 146-155.

Max, J. J. and Chapados, C. (2004). "Infrared spectroscopy of aqueous carboxylic acids: Comparison between different acids and their salts." Journal of Physical Chemistry A **108**(16): 3324-3337.

Oldenhof, H., Wolkers, W. F., Fonseca, F., Passot, S. and Marin, M. (2005). "Effect of sucrose and maltodextrin on the physical properties and survival of air-dried *Lactobacillus bulgaricus*: An in situ Fourier transform infrared spectroscopy study." Biotechnology Progress **21**: 885-892.

Ottenhof, M.-A., MacNaughtan, W. and Farhat, I. A. (2003). "FTIR study of state and phase transitions of low moisture sucrose and lactose." Carbohydrate Research **338**(21): 2195-2202.

Perkin-Elmer. (2005). "FT-IR Spectroscopy: Attenuated Total Reflectance (ATR)." Technical Note 007024B_01 Retrieved Jul.4, 2012, from http://shop.perkinelmer.com/content/technicalinfo/tch_ftiratr.pdf.

Robinson, G. W., Chul Hee, C. and Urquidi, J. (1999). "Isosbestic points in liquid water: Further strong evidence for the two-state mixture model." Journal of Chemical Physics **111**(2): 698.

Thermo-Nicolet. (2001). "Introduction to Fourier transform infrared spectrometry." Retrieved Nov. 5, 2010, from http://mmrc.caltech.edu/FTIR/FTIRintro.pdf.

Walrafen, G. E., Hokmabadi, M. S. and Yang, W. H. (1986). "Raman isosbestic points from liquid water." Journal of Chemical Physics **85**(12): 6964.

Wolkers, W. F., Oldenhof, H., Alberda, M. and Hoekstra, F. A. (1998). "A Fourier transform infrared microspectroscopy study of sugar glasses: application to anhydrobiotic higher plant cells." Biochimica et Biophysica Acta (BBA) - General Subjects **1379**(1): 83-96.

Wolkers, W. F., Oldenhof, H., Tablin, F. and Crowe, J. H. (2004). "Preservation of Dried Liposomes in the Presence of Sugar and Phosphate." Biochimica et Biophysica Acta **1661**: 125-134.

Wolkers, W. F., Oldenhof, H., Tablin, F. and Crowe, J. H. (2004a). "Preservation of dried liposomes in the presence of sugar and phosphate." Biochimica et Biophysica Acta **1661**: 125-134.

Wolkers, W. F., Oliver, A. E., Tablin, F. and Crowe, J. H. (2004b). "A Fourier-transform infrared spectroscopy study of sugar glasses." Carbohydrate Research **339**(6): 1077-1085.

Young, R. J. and Lovell, P. A. (1991). Introduction to polymers. 2. Cheltenham: Stanley Thornes.

APPENDIX 3

Appendix 3.1 ATR-FTIR spectra of amorphous bioglass samples obtained in the mid infrared range

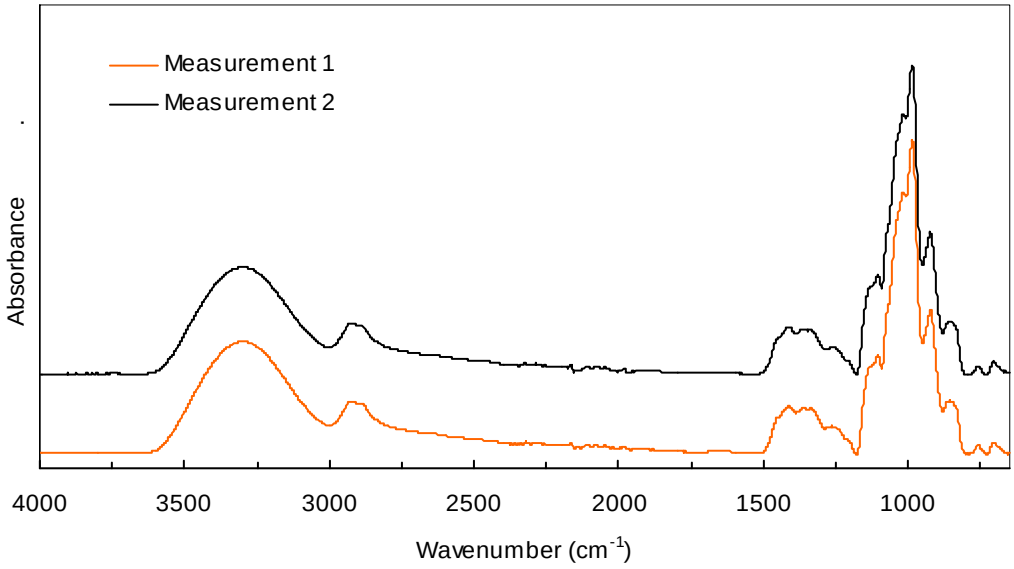

(a)

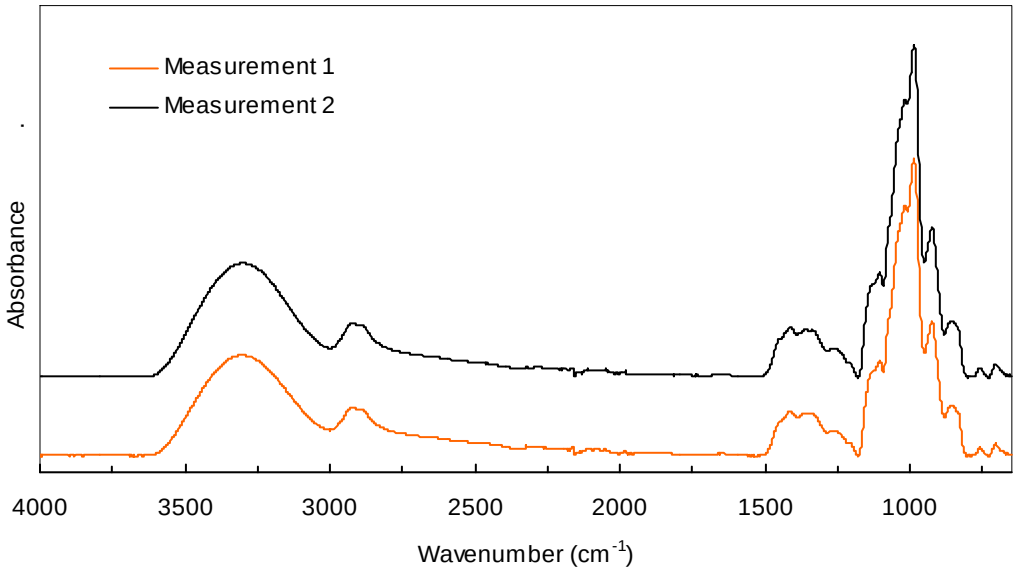

(b)

Figure A3.1.1 Absorption spectra of Treatment 1 (SC/MD = 7:3 (by mass), no Na citrate, equilibrated in P_2O_5 atmosphere), replication 1 (a) and 2 (b).

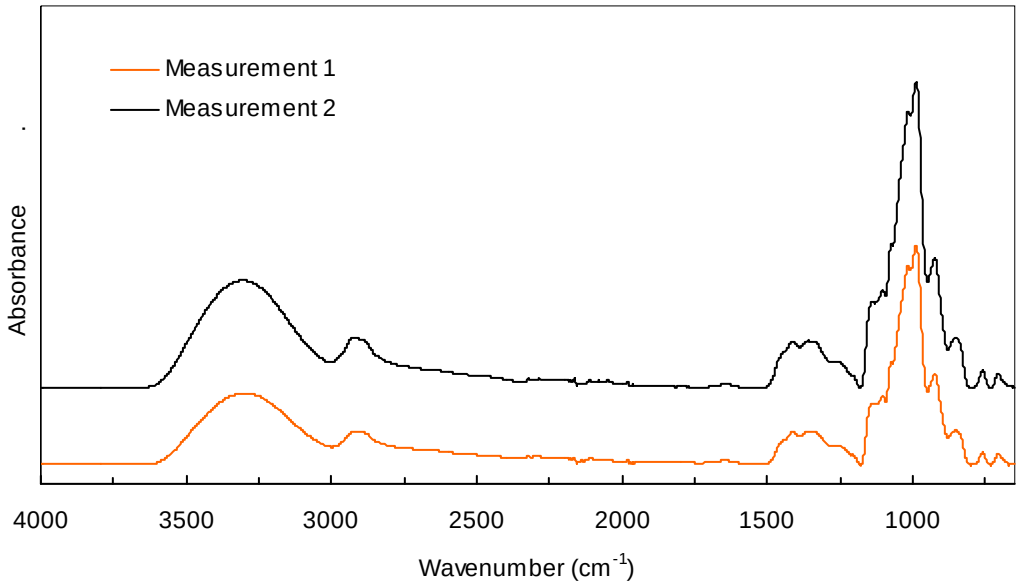

(a)

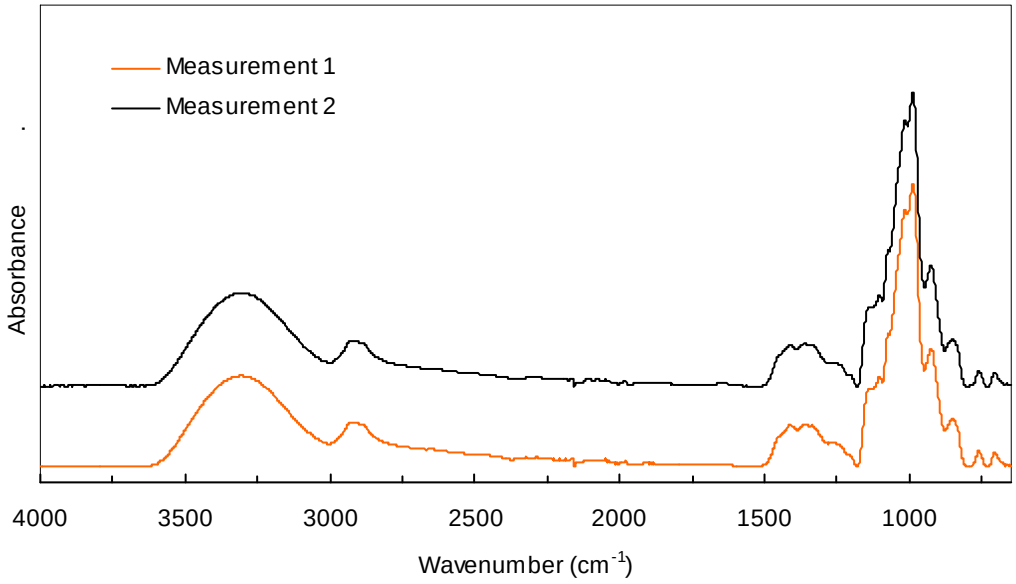

(b)

Figure A3.1.2 Absorption spectra of Treatment 3 (SC/MD = 5:5 (by mass), no Na citrate, equilibrated in P_2O_5 atmosphere), replication 1 (a) and 2 (b).

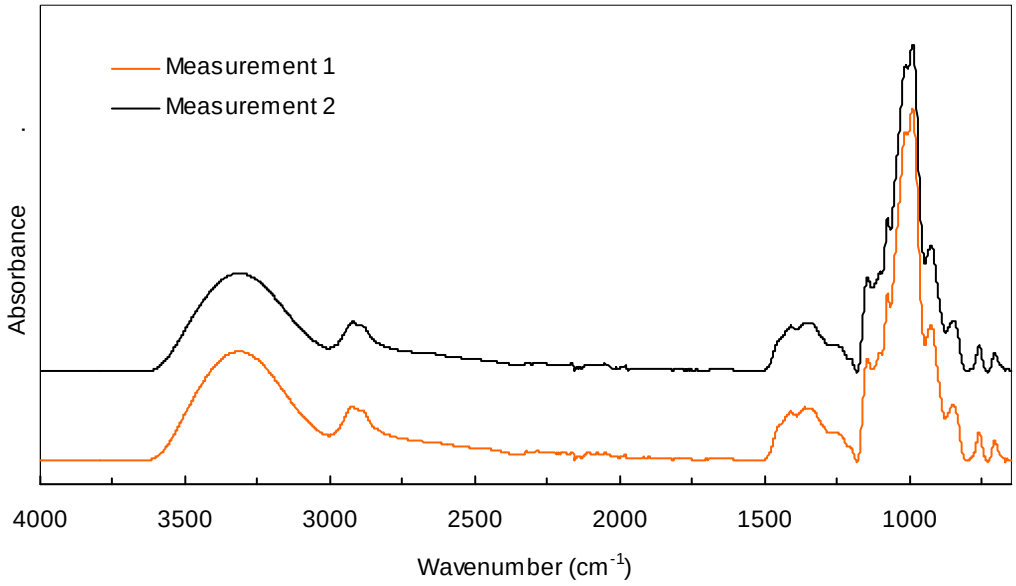

(a)

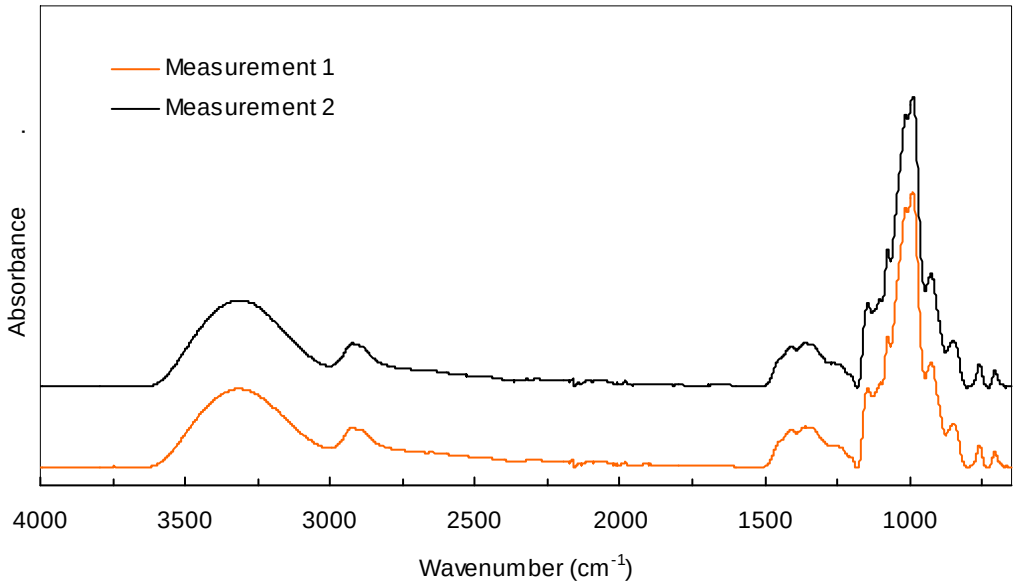

(b)

Figure A3.1.3 Absorption spectra of Treatment 5 (SC/MD = 3:7 (by mass), no Na citrate, equilibrated in P_2O_5 atmosphere), replication 1 (a) and 2 (b).

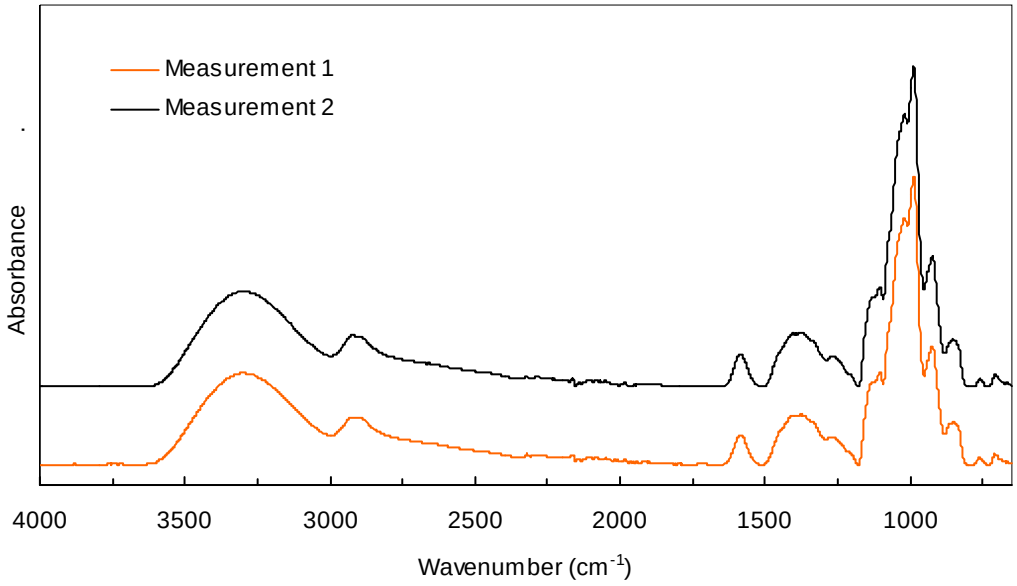

(a)

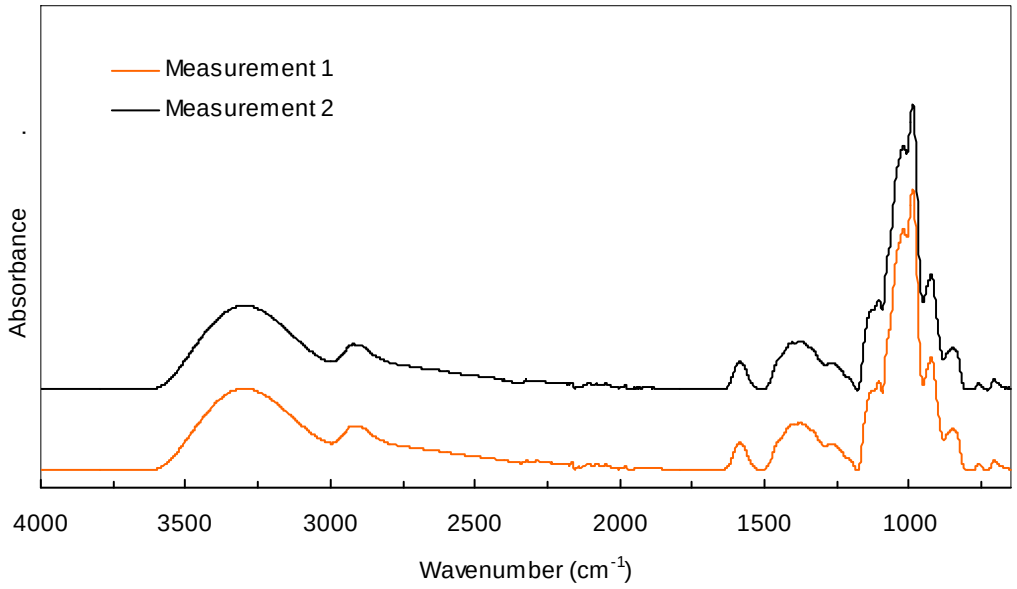

(b)

Figure A3.1.4 Absorption spectra of Treatment 7 (SC/MD = 7:3 (by mass), NaCit/SC = 0.1 (by mole), equilibrated in P_2O_5 atmosphere), replication 1 (a) and 2 (b).

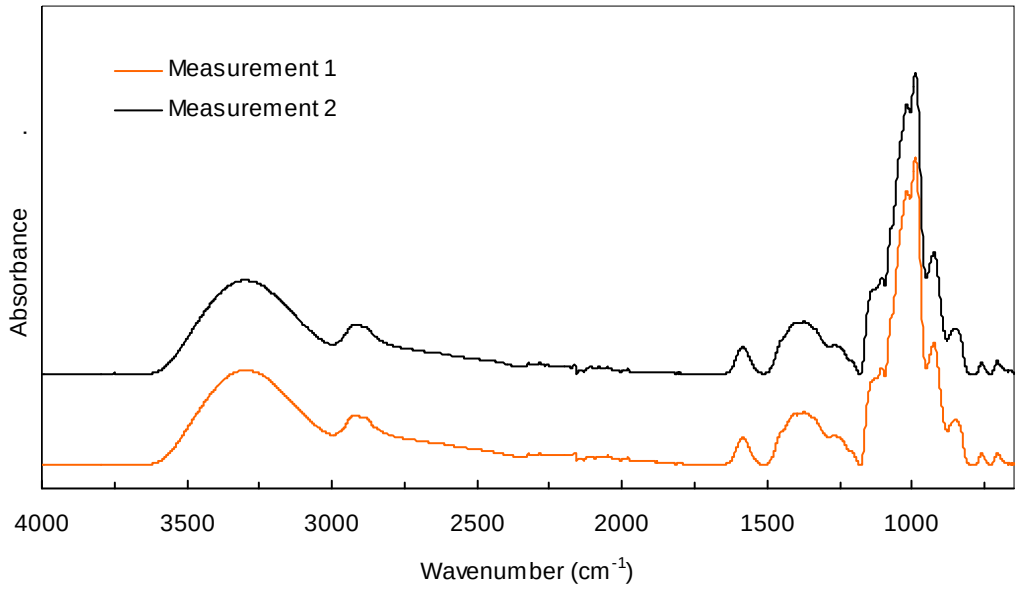

(a)

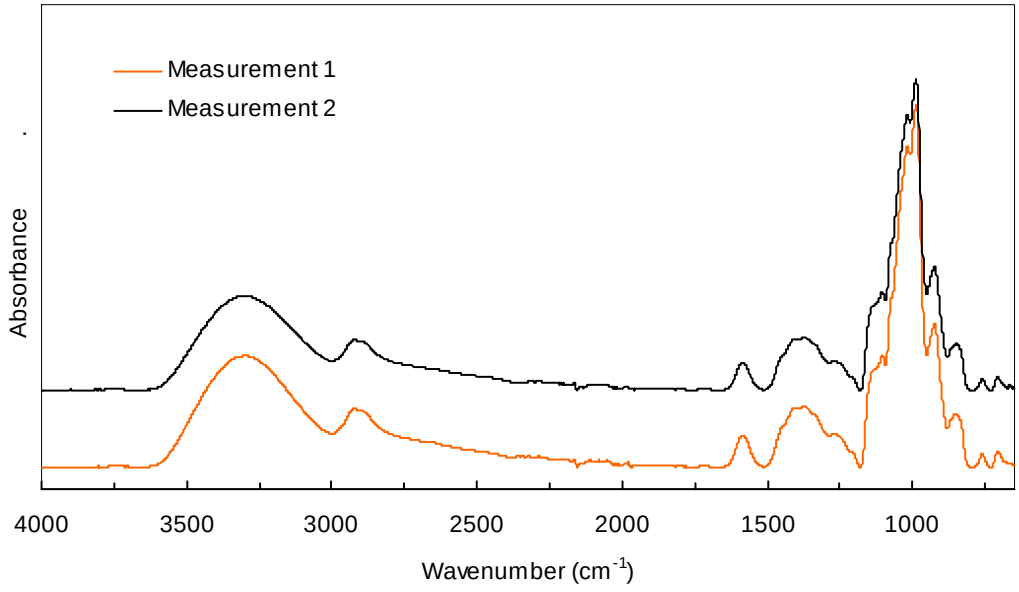

(b)

Figure A3.1.5 Absorption spectra of Treatment 9 (SC/MD = 5:5 (by mass), NaCit/SC = 0.1 (by mole), equilibrated in P_2O_5 atmosphere), replication 1 (a) and 2 (b).

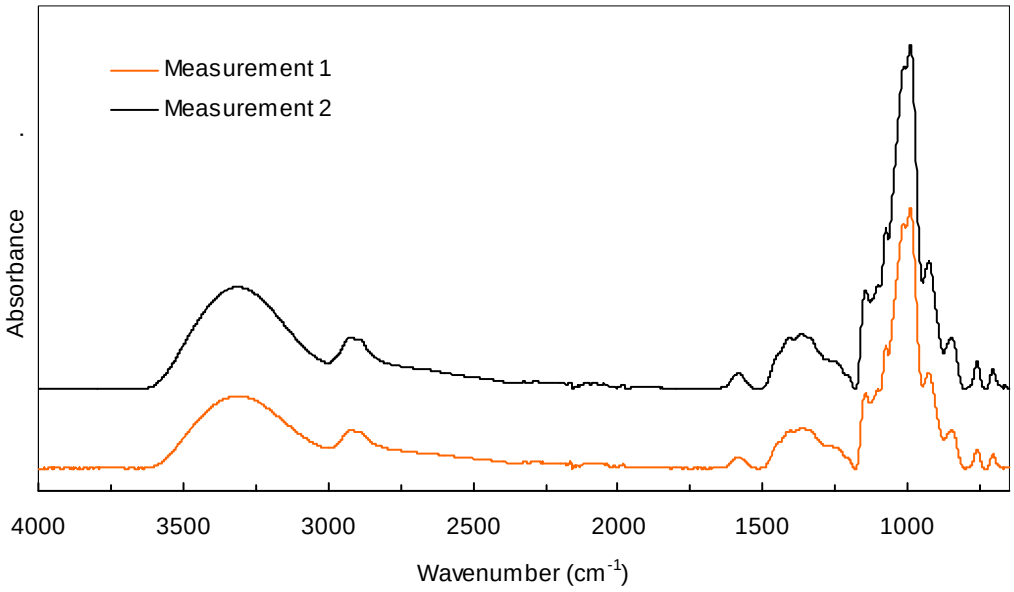

(a)

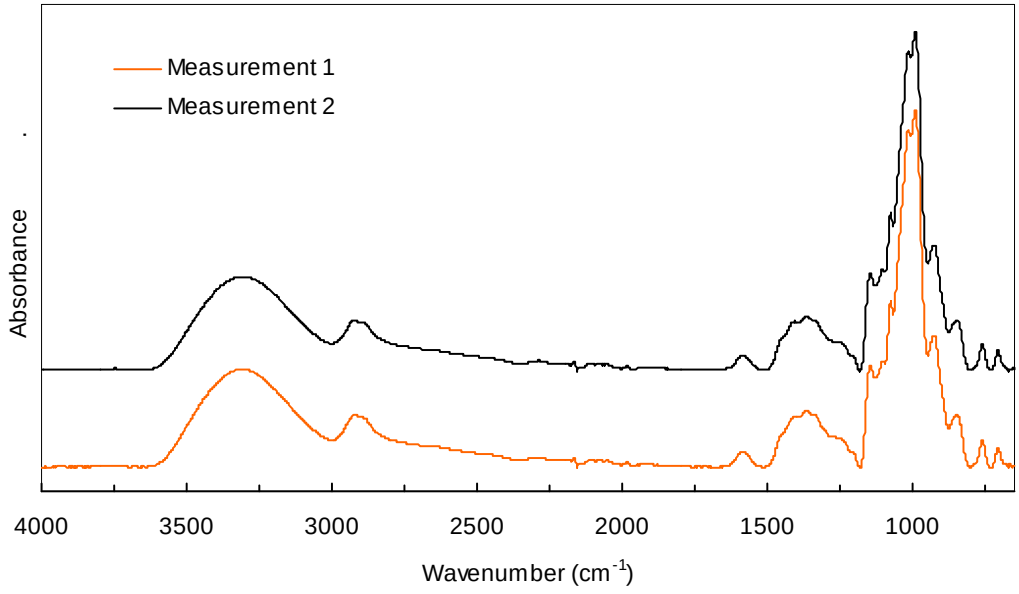

(b)

Figure A3.1.6 Absorption spectra of Treatment 11 (SC/MD = 3:7 (by mass), NaCit/SC = 0.1 (by mole), equilibrated in P_2O_5 atmosphere), replication 1 (a) and 2 (b).

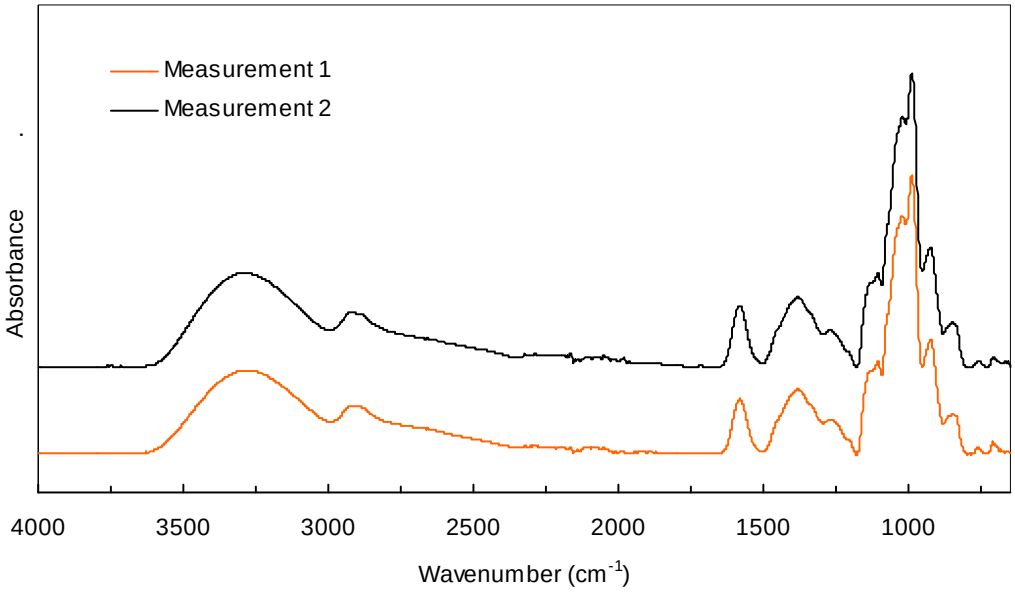

(a)

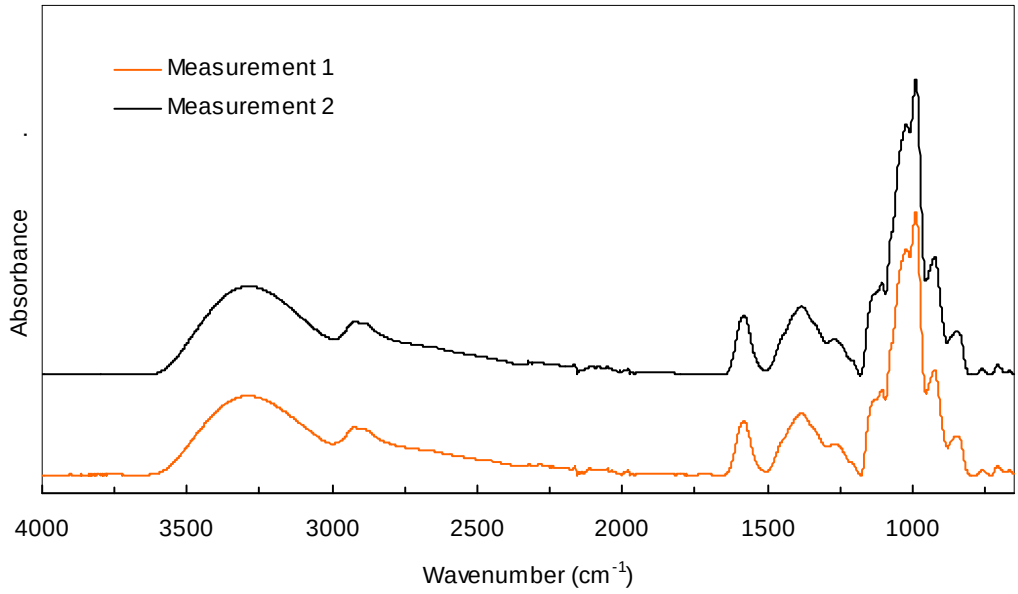

(b)

Figure A3.1.7 Absorption spectra of Treatment 13 (SC/MD = 7:3 (by mass), NaCit/SC = 0.2 (by mole), equilibrated in P_2O_5 atmosphere), replication 1 (a) and 2 (b).

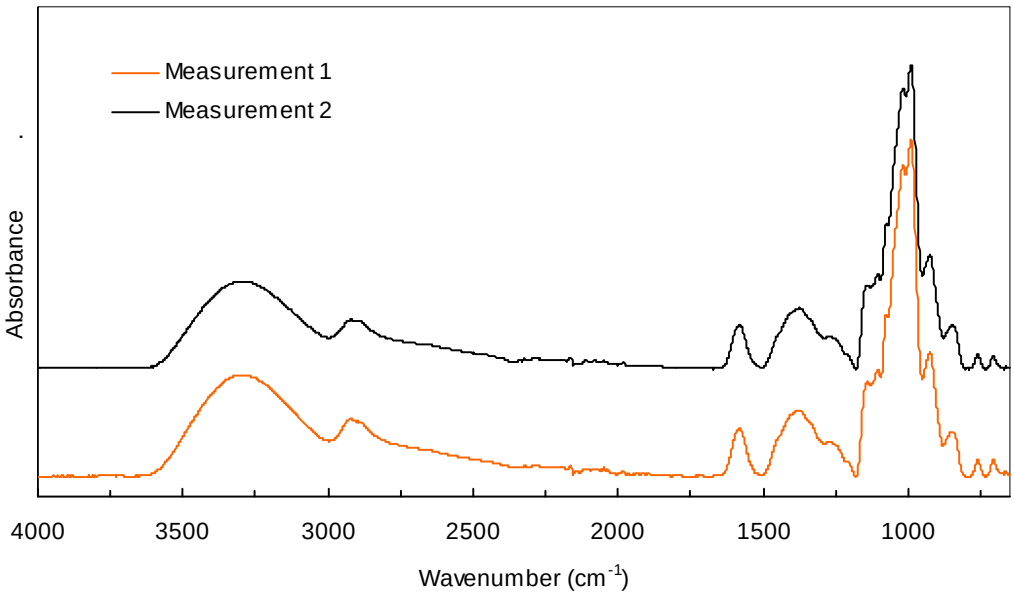

(a)

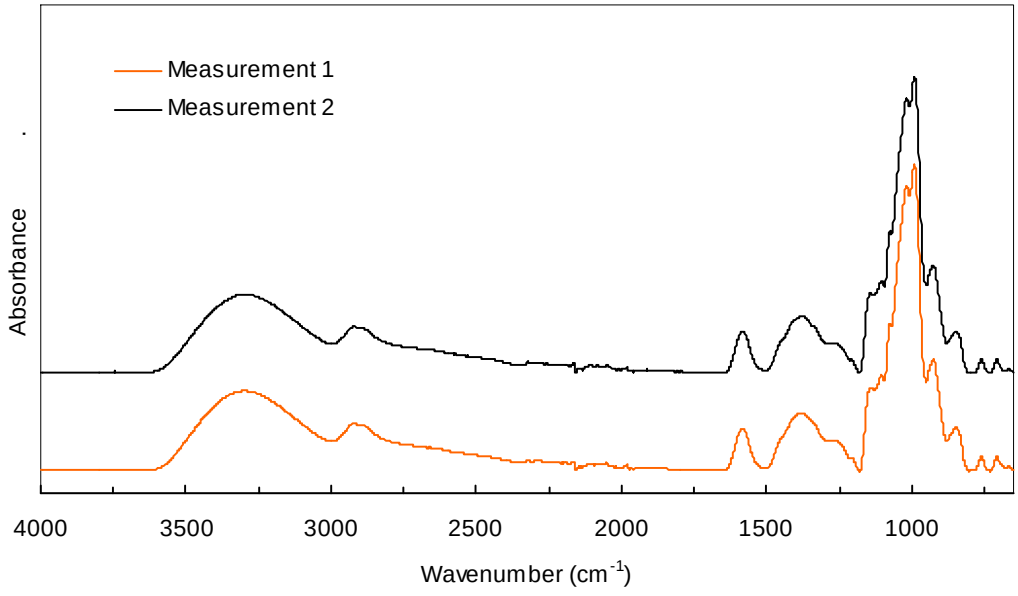

(b)

Figure A3.1.8 Absorption spectra of Treatment 15 (SC/MD = 5:5 (by mass), NaCit/SC = 0.2 (by mole), equilibrated in P_2O_5 atmosphere), replication 1 (a) and 2 (b).

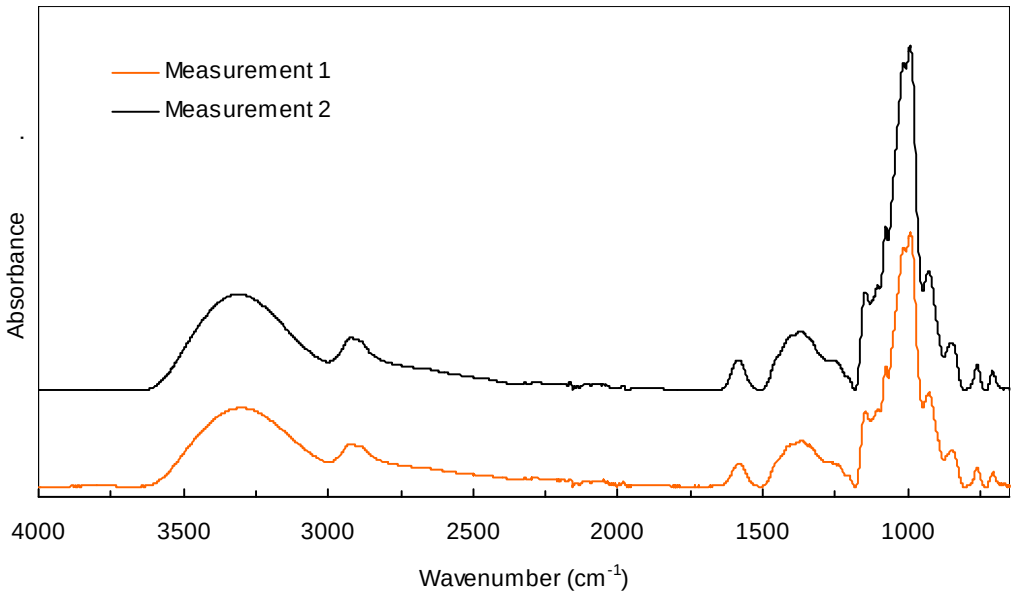

(a)

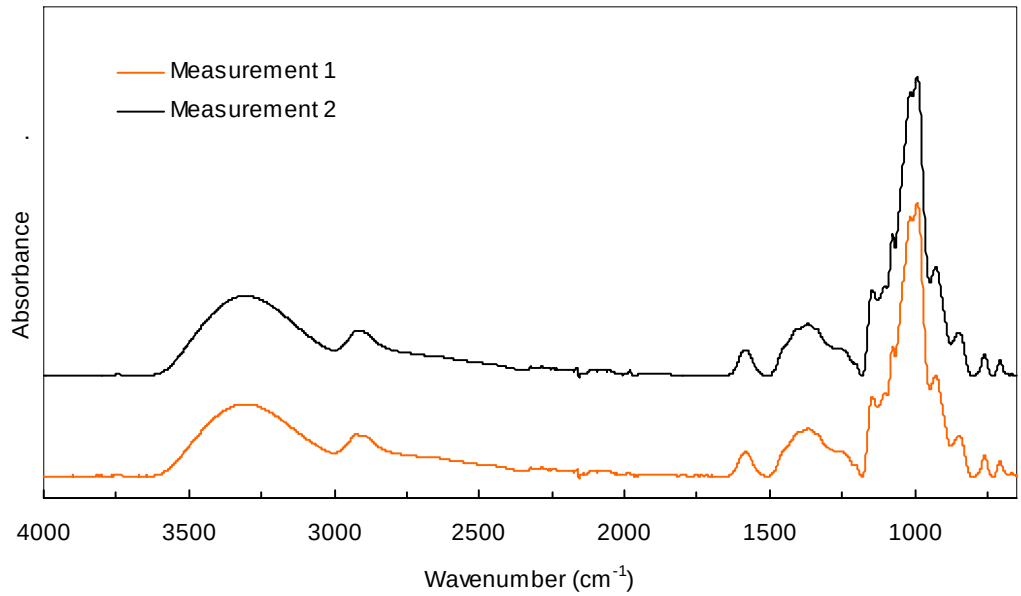

(b)

Figure A3.1.9 Absorption spectra of Treatment 17 (SC/MD = 3:7 (by mass), NaCit/SC = 0.2 (by mole), equilibrated in P_2O_5 atmosphere), replication 1 (a) and 2 (b).

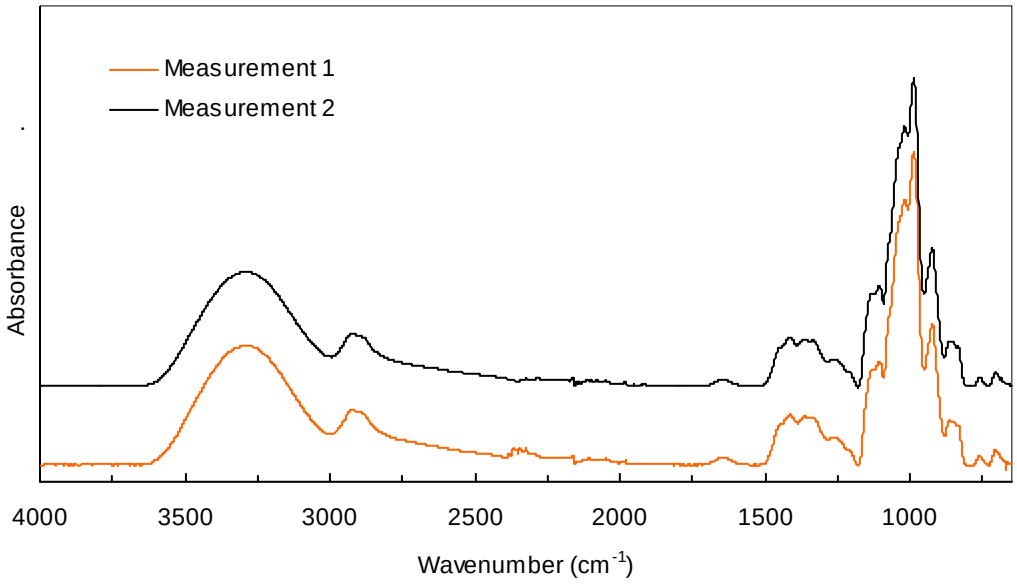

(a)

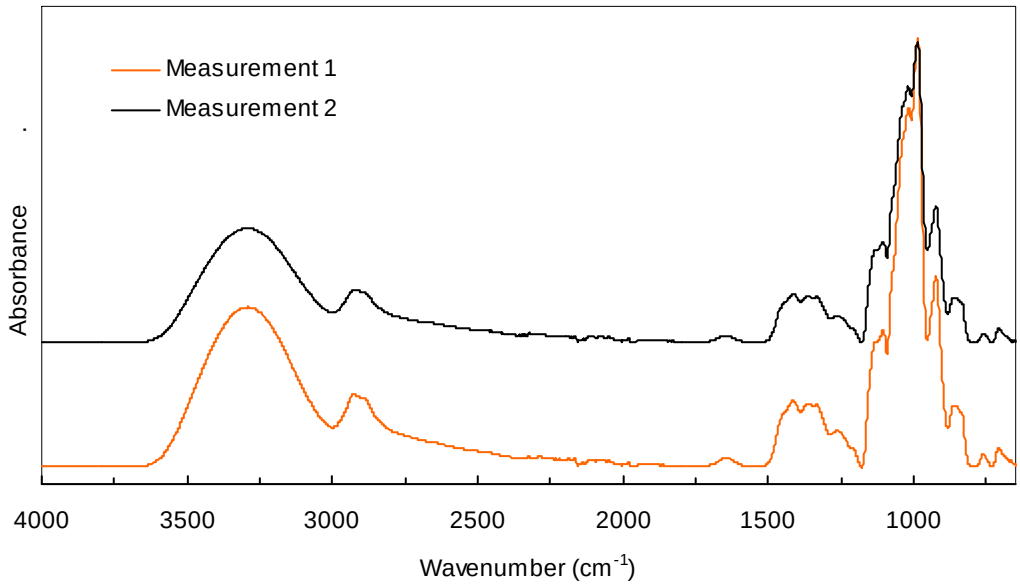

(b)

Figure A3.1.10 Absorption spectra of Treatment 2 (SC/MD = 7:3 (by mass), no Na citrate, equilibrated in saturated LiCl solution atmosphere), replication 1 (a) and 2 (b).

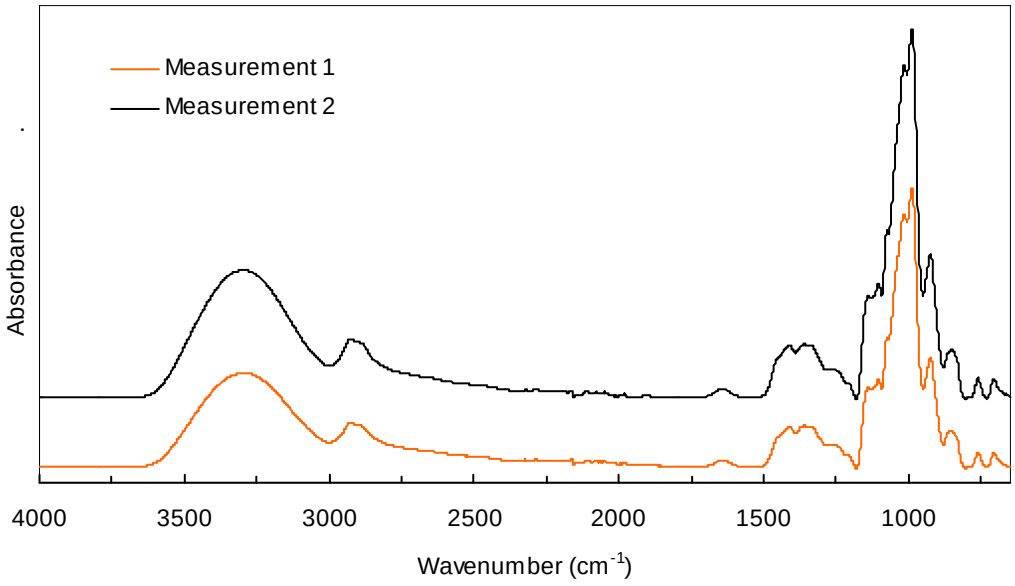

(a)

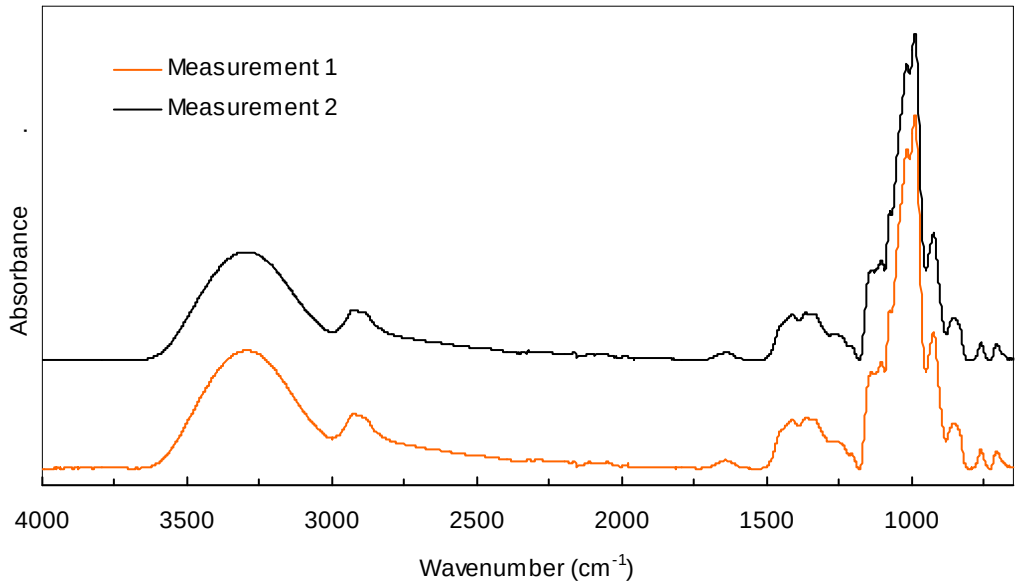

(b)

Figure A3.1.11 Absorption spectra of Treatment 4 (SC/MD = 5:5 (by mass), no Na citrate, equilibrated in saturated LiCl solution atmosphere), replication 1 (a) and 2 (b).

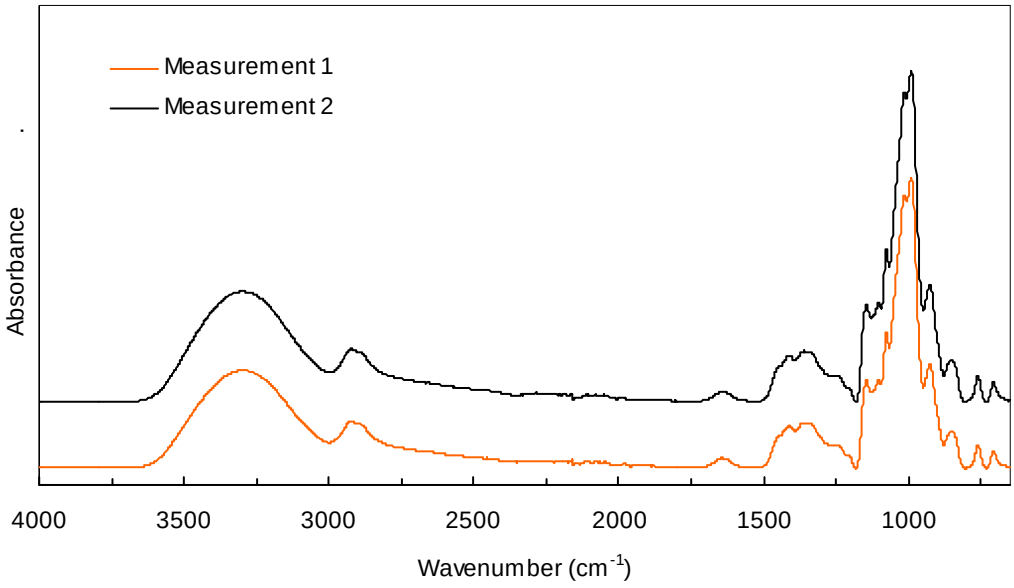

(a)

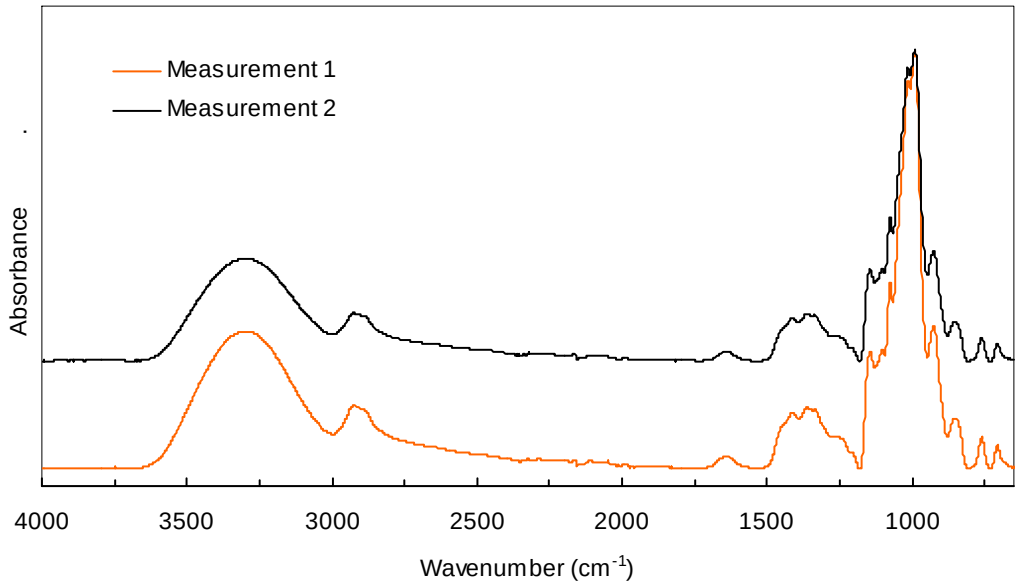

(b)

Figure A3.1.12 Absorption spectra of Treatment 6 (SC/MD = 3:7 (by mass), no Na citrate, equilibrated in saturated LiCl solution atmosphere), replication 1 (a) and 2 (b).

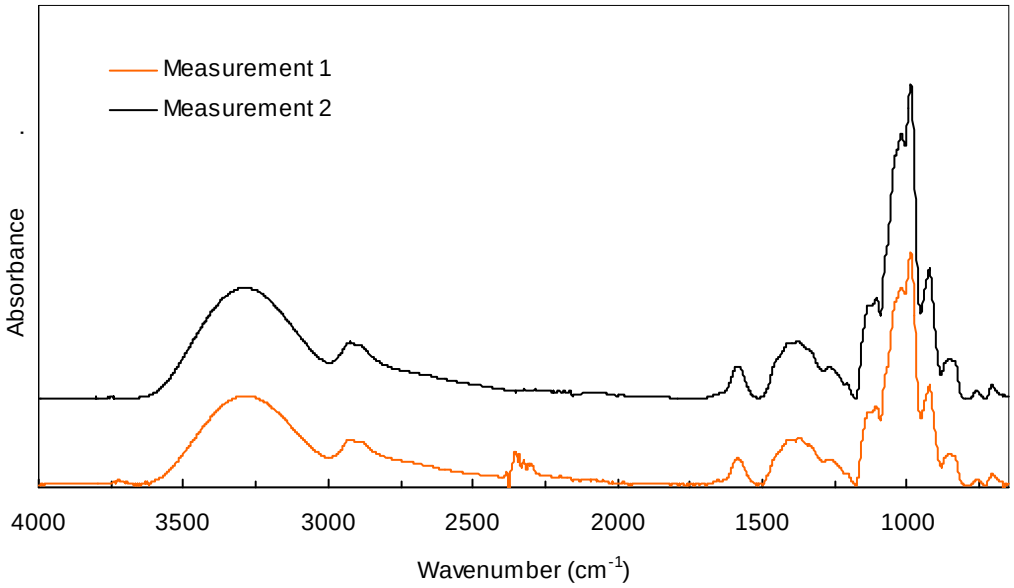

(a)

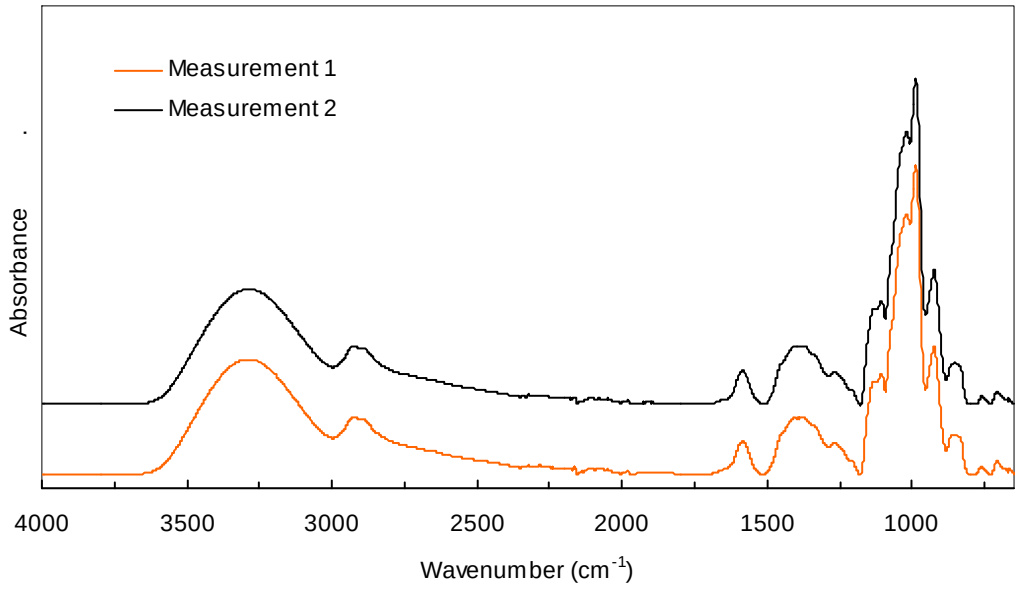

(b)

Figure A3.1.13 Absorption spectra of Treatment 8 (SC/MD = 7:3 (by mass), NaCit/SC = 0.1 (by mole), equilibrated in saturated LiCl solution atmosphere), replication 1 (a) and 2 (b).

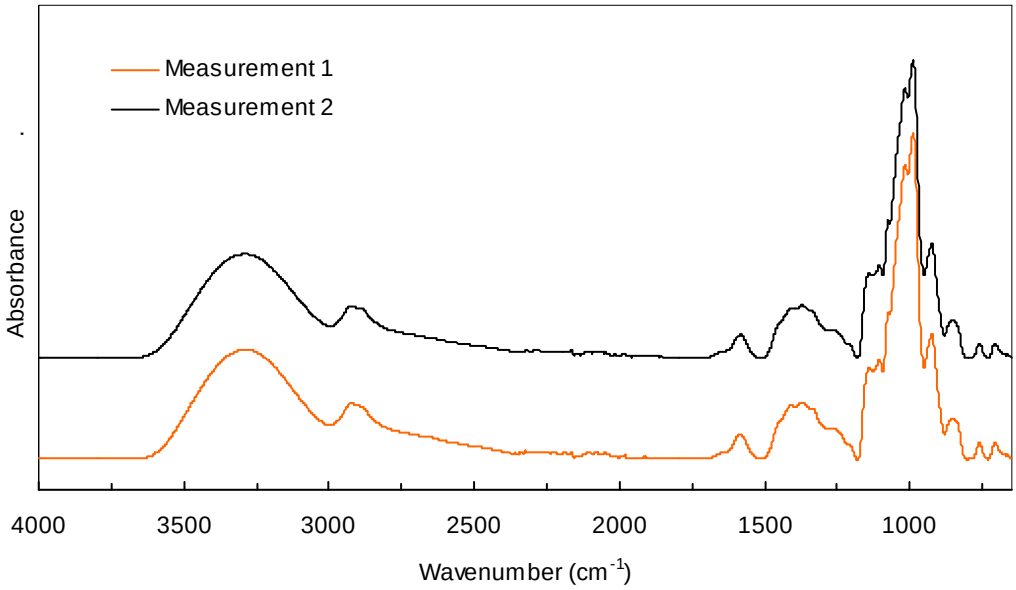

(a)

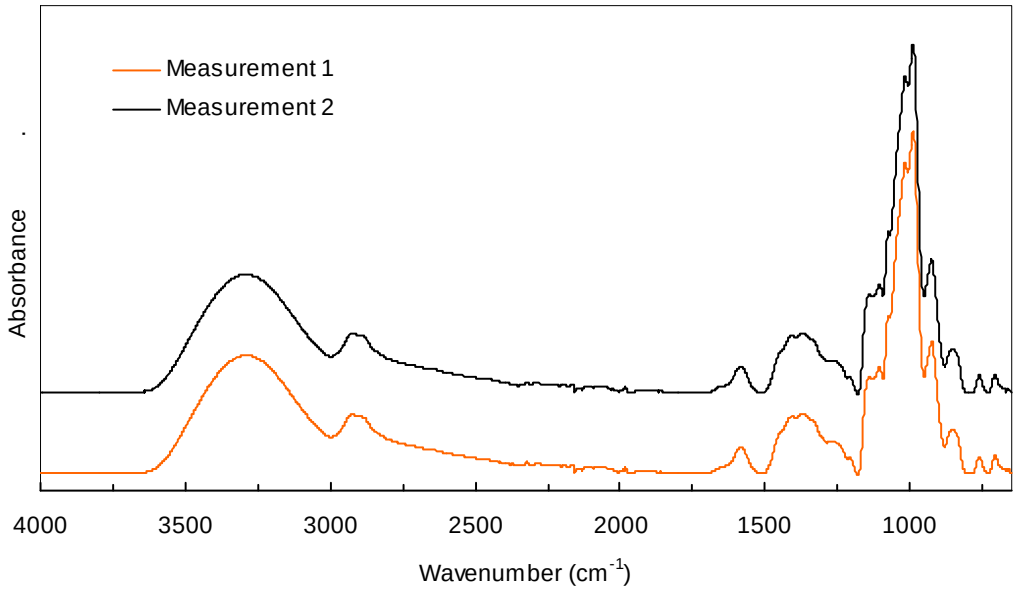

(b)

Figure A3.1.14 Absorption spectra of Treatment 10 (SC/MD = 5:5 (by mass), NaCit/SC = 0.1 (by mole), equilibrated in saturated LiCl solution atmosphere), replication 1 (a) and 2 (b).

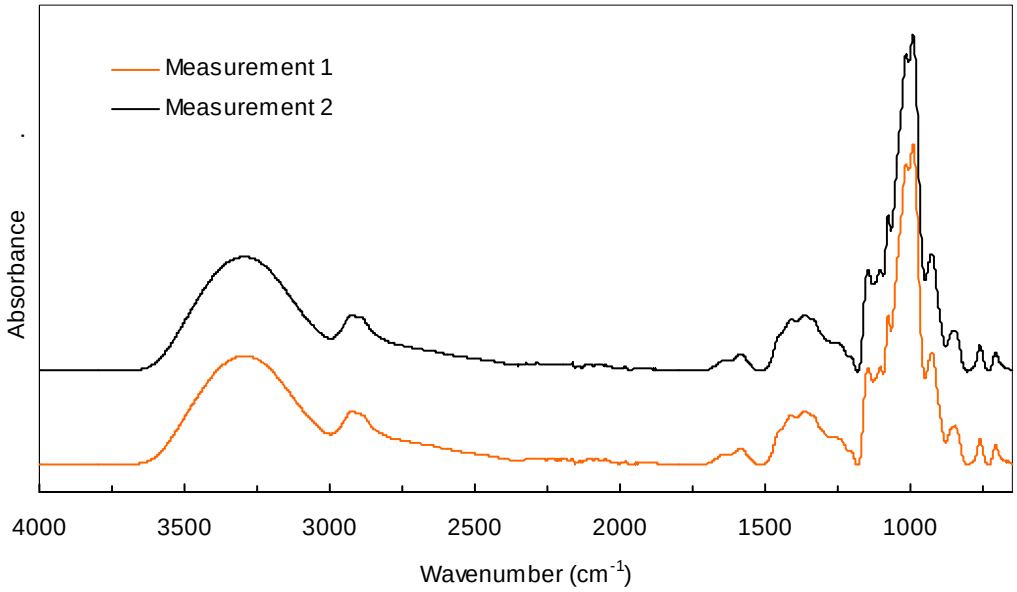

(a)

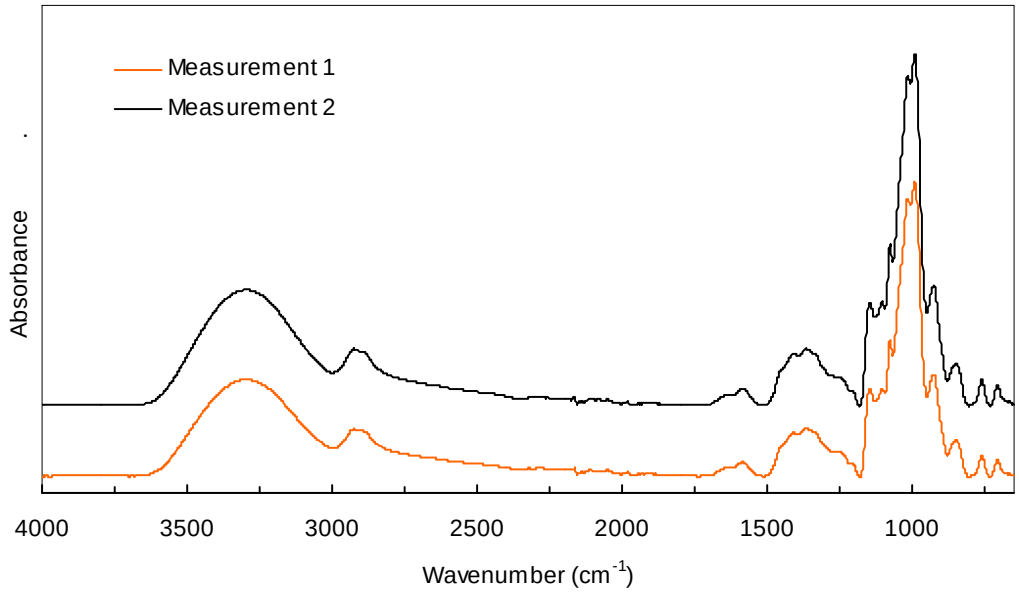

(b)

Figure A3.1.15 Absorption spectra of Treatment 12 (SC/MD = 3:7 (by mass), NaCit/SC = 0.1 (by mole), equilibrated in saturated LiCl solution atmosphere), replication 1 (a) and 2 (b).

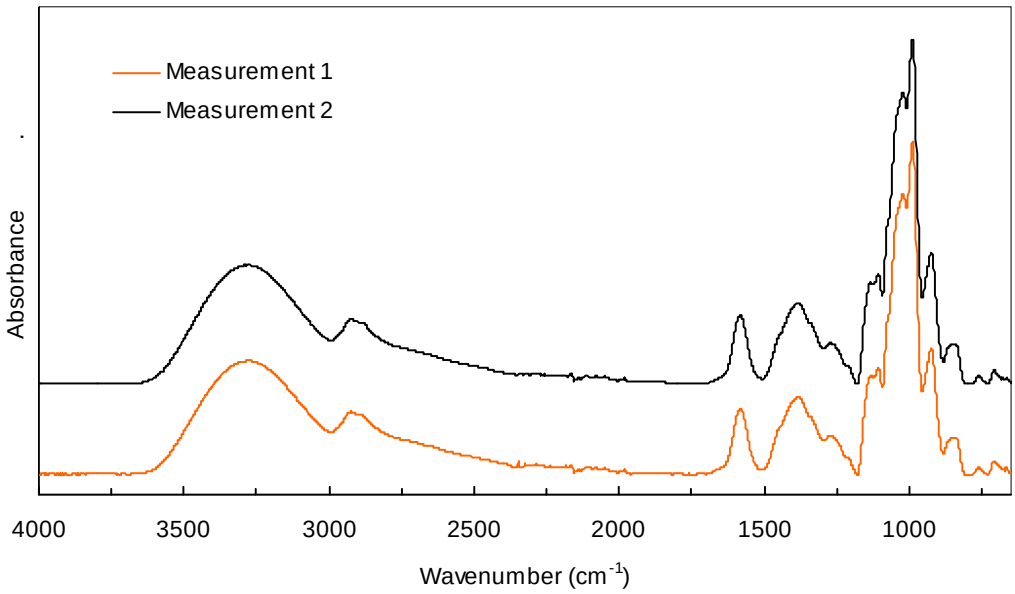

(a)

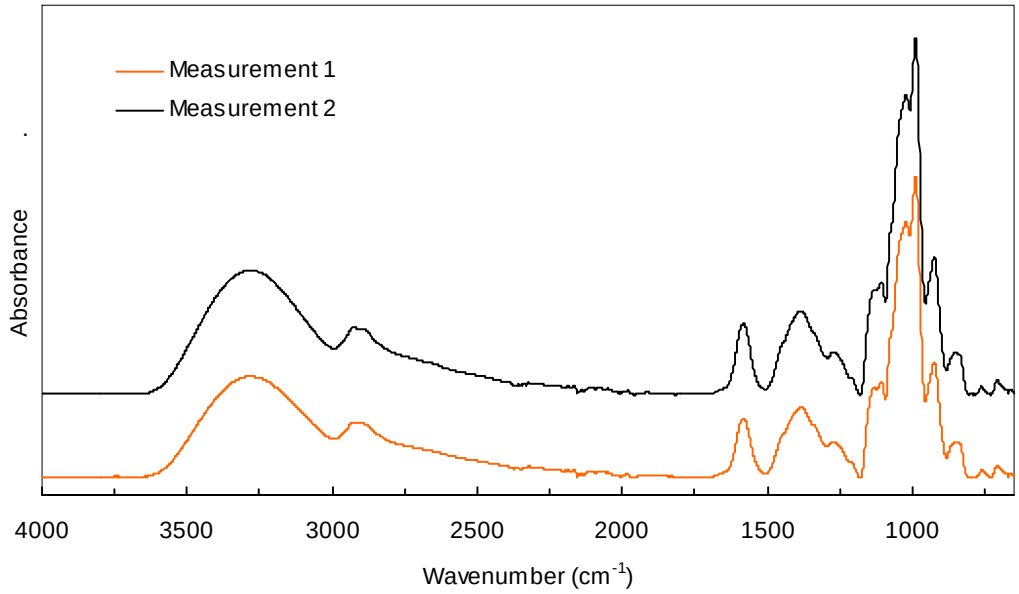

(b)

Figure A3.1.16 Absorption spectra of Treatment 14 (SC/MD = 7:3 (by mass), NaCit/SC = 0.2 (by mole), equilibrated in saturated LiCl solution atmosphere), replication 1 (a) and 2 (b).

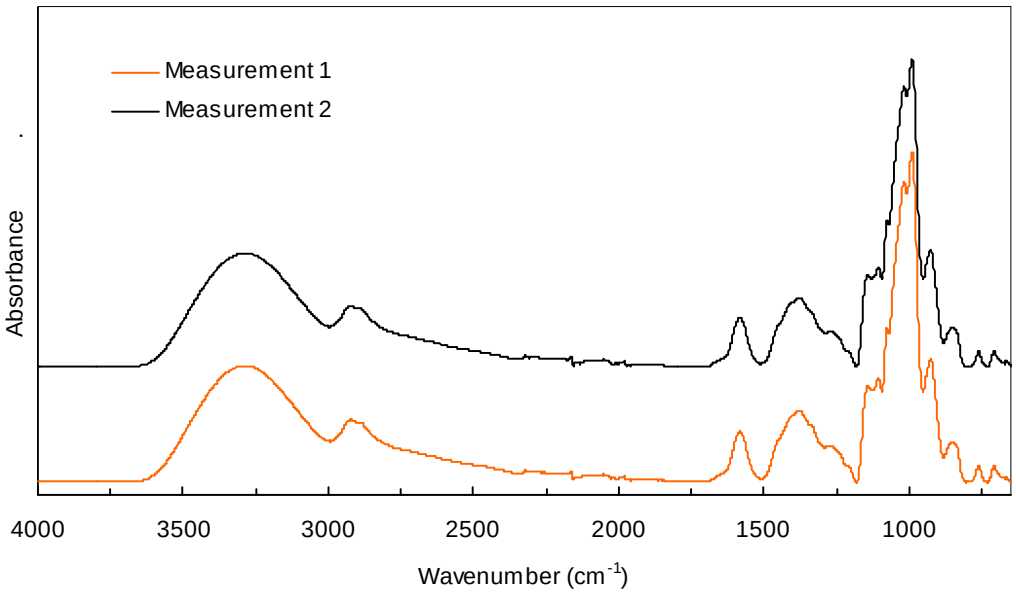

(a)

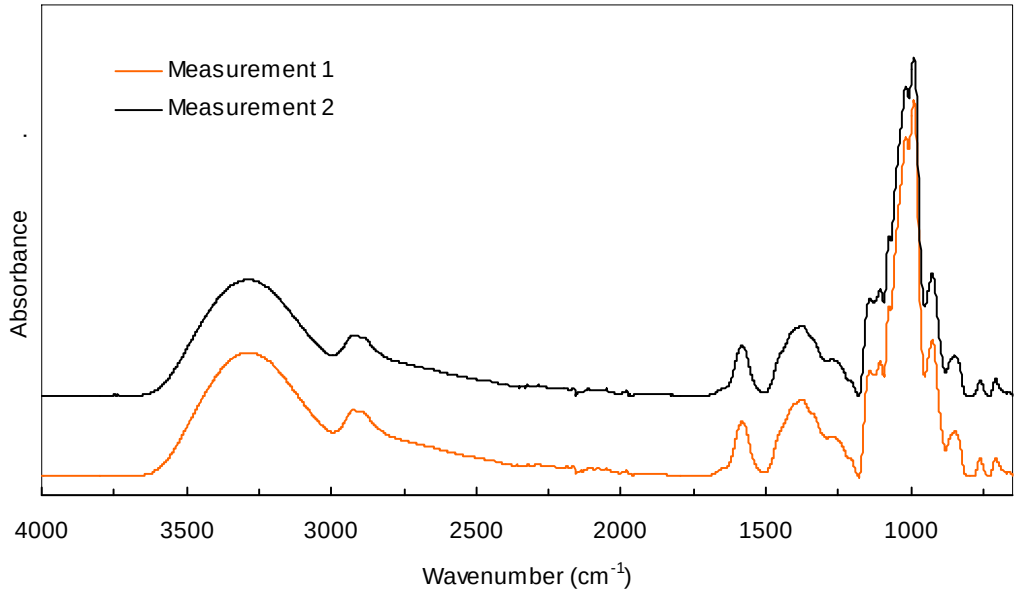

(b)

Figure A3.1.17 Absorption spectra of Treatment 16 (SC/MD = 5:5 (by mass), NaCit/SC = 0.2 (by mole), equilibrated in saturated LiCl solution atmosphere), replication 1 (a) and 2 (b).

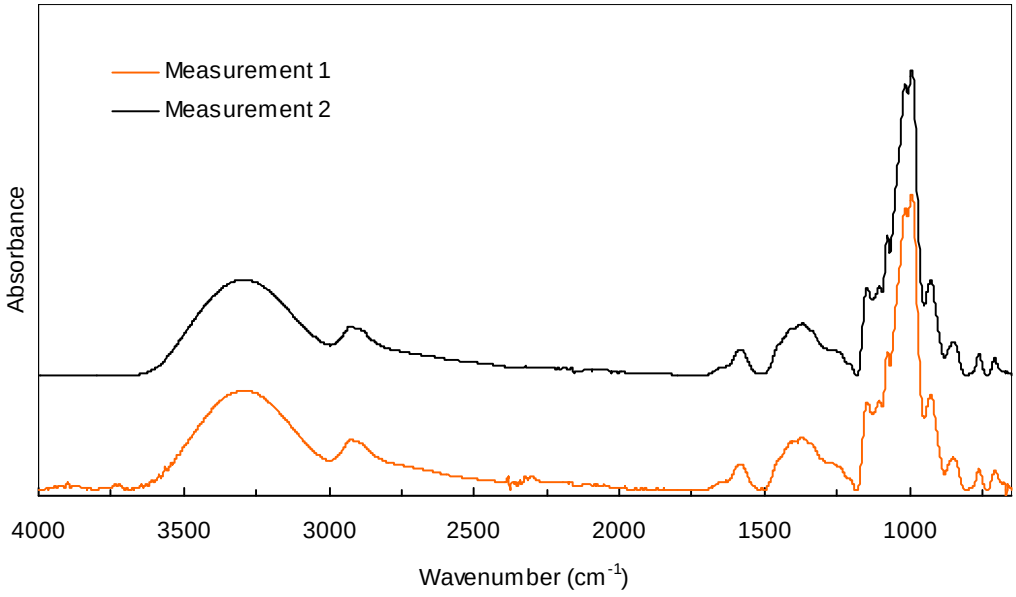

(a)

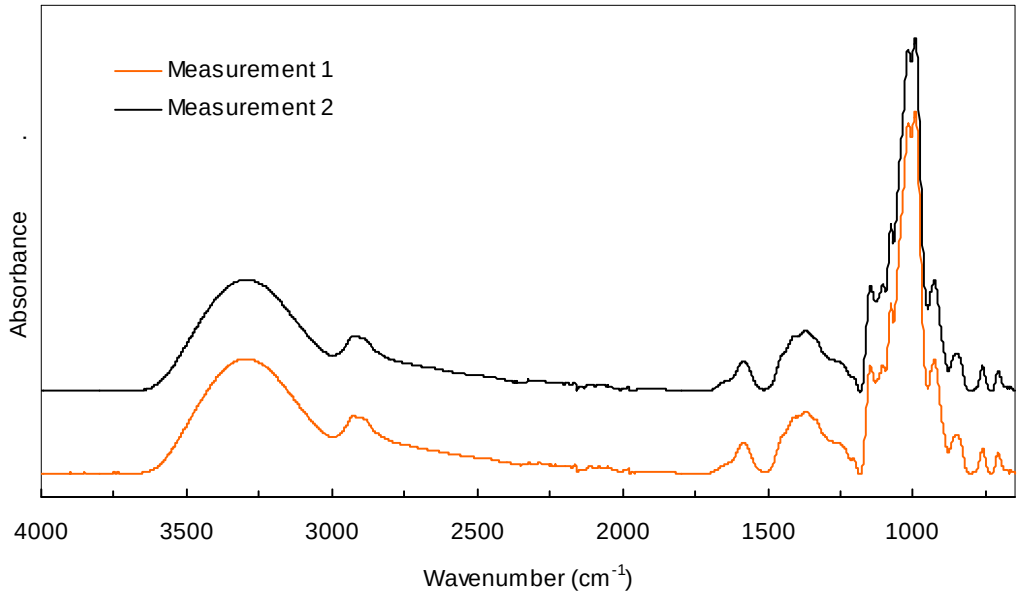

(b)

Figure A3.1.18 Absorption spectra of Treatment 18 (SC/MD = 3:7 (by mass), NaCit/SC = 0.2 (by mole), equilibrated in saturated LiCl solution atmosphere), replication 1 (a) and 2 (b).

Appendix 3.2 Representative ATR-FTIR absorption spectra in the region of antisymmetric ($\nu_{as}(COO^{-})$) stretching bands of crystalline trisodium citrate dihydrate as compared to those of amorphous bioglass samples. Spectra were normalized to the region of 1640 – 1540 cm^{-1}.

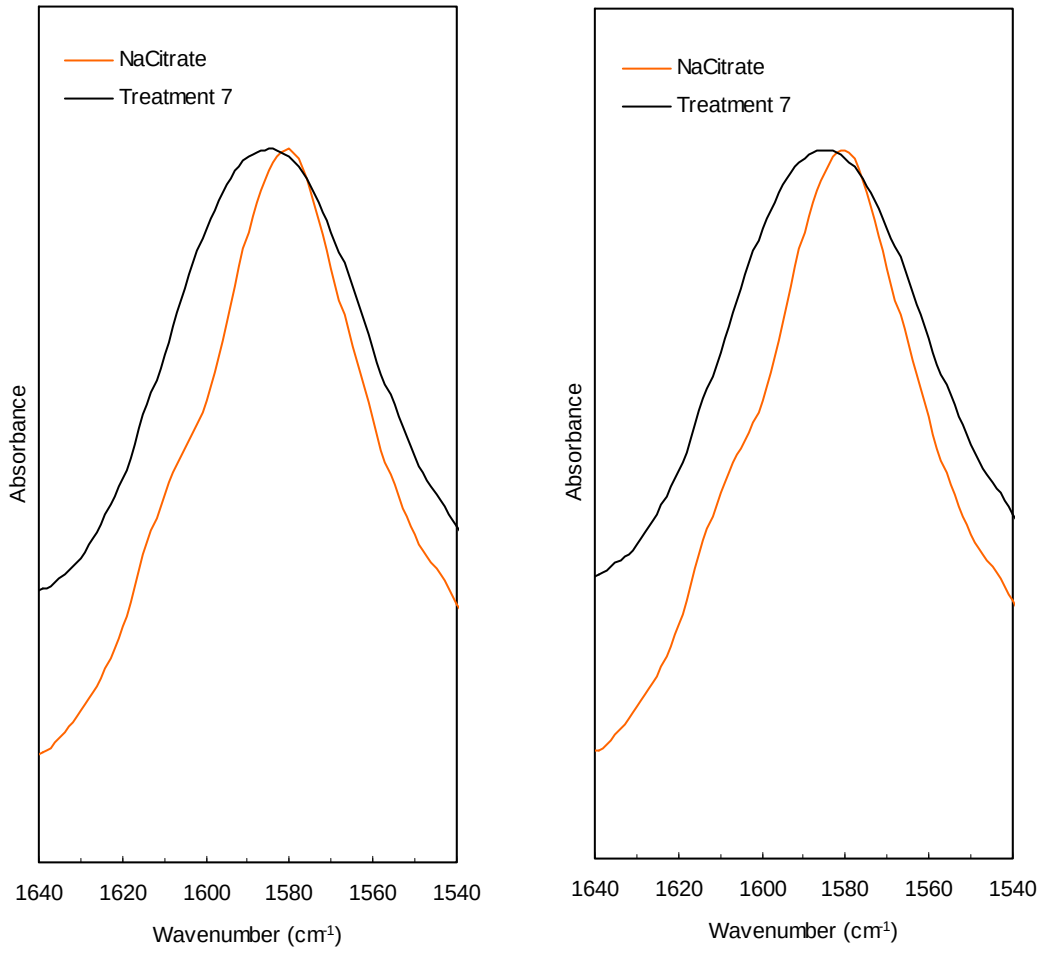

Figure A3.2.1 Absorption spectra of Na-citrate and Treatment 7 (SC/MD = 7:3 (by mass), NaCit/SC = 0.1 (by mole), equilibrated in P_2O_5 atmosphere), replication 1 (left) and 2 (right).

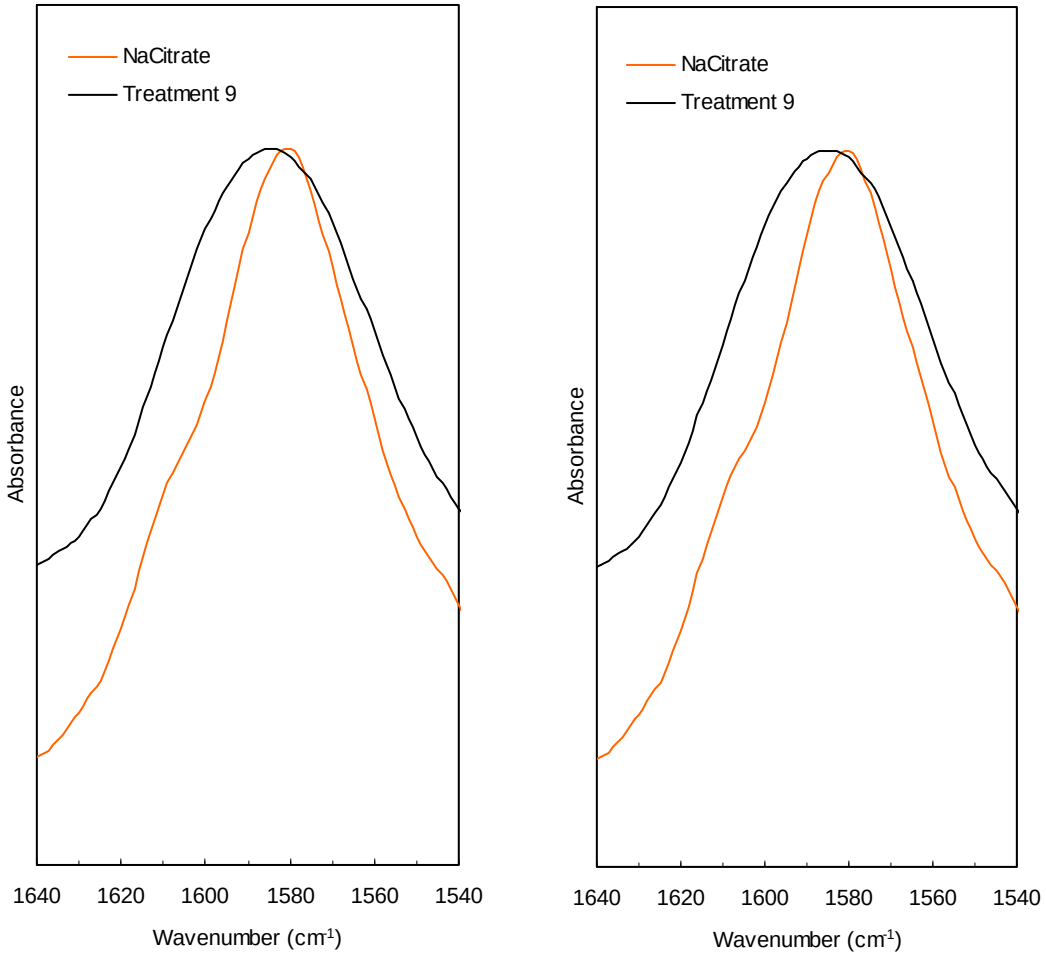

Figure A3.2.2 Absorption spectra of Na-citrate and Treatment 9 (SC/MD = 5:5 (by mass), NaCit/SC = 0.1 (by mole), equilibrated in P_2O_5 atmosphere), replication 1 (left) and 2 (right).

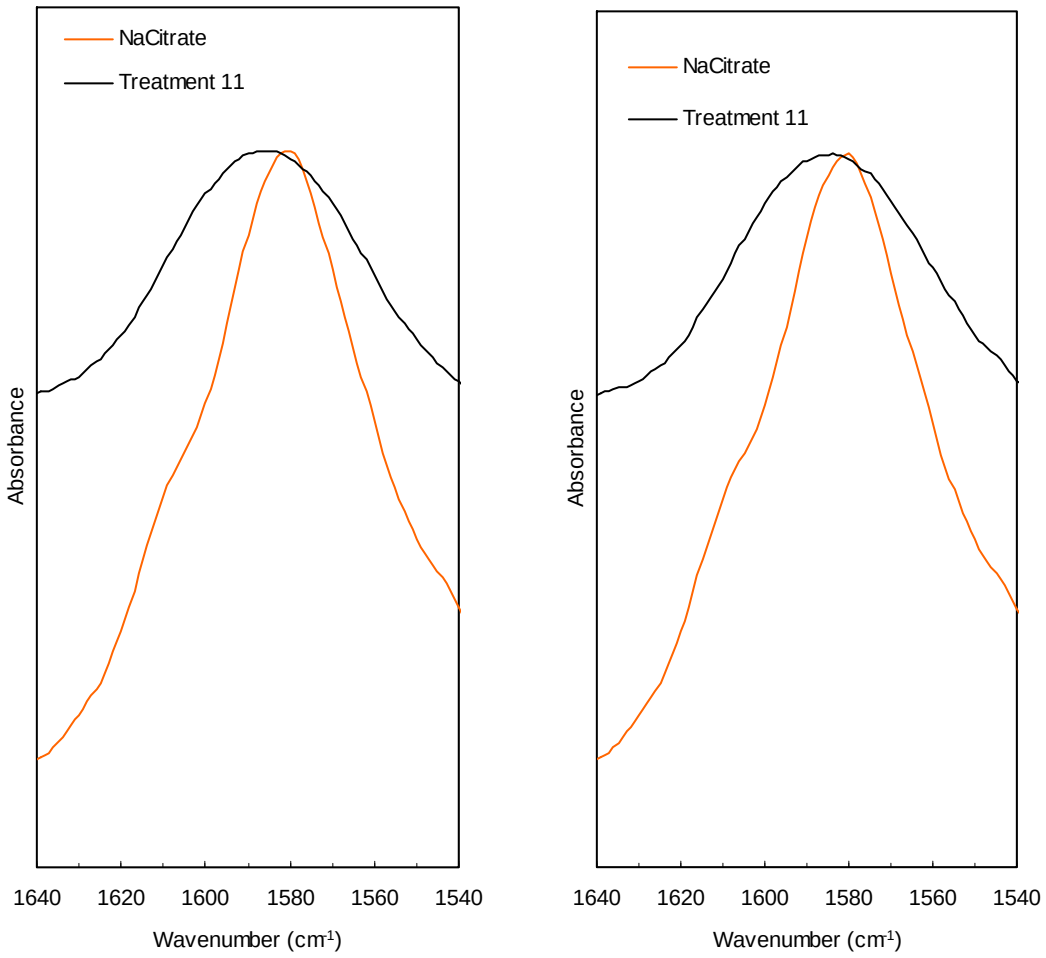

Figure A3.2.3 Absorption spectra of Na-citrate and Treatment 11 (SC/MD = 3:7 (by mass), NaCit/SC = 0.1 (by mole), equilibrated in P_2O_5 atmosphere), replication 1 (left) and 2 (right).

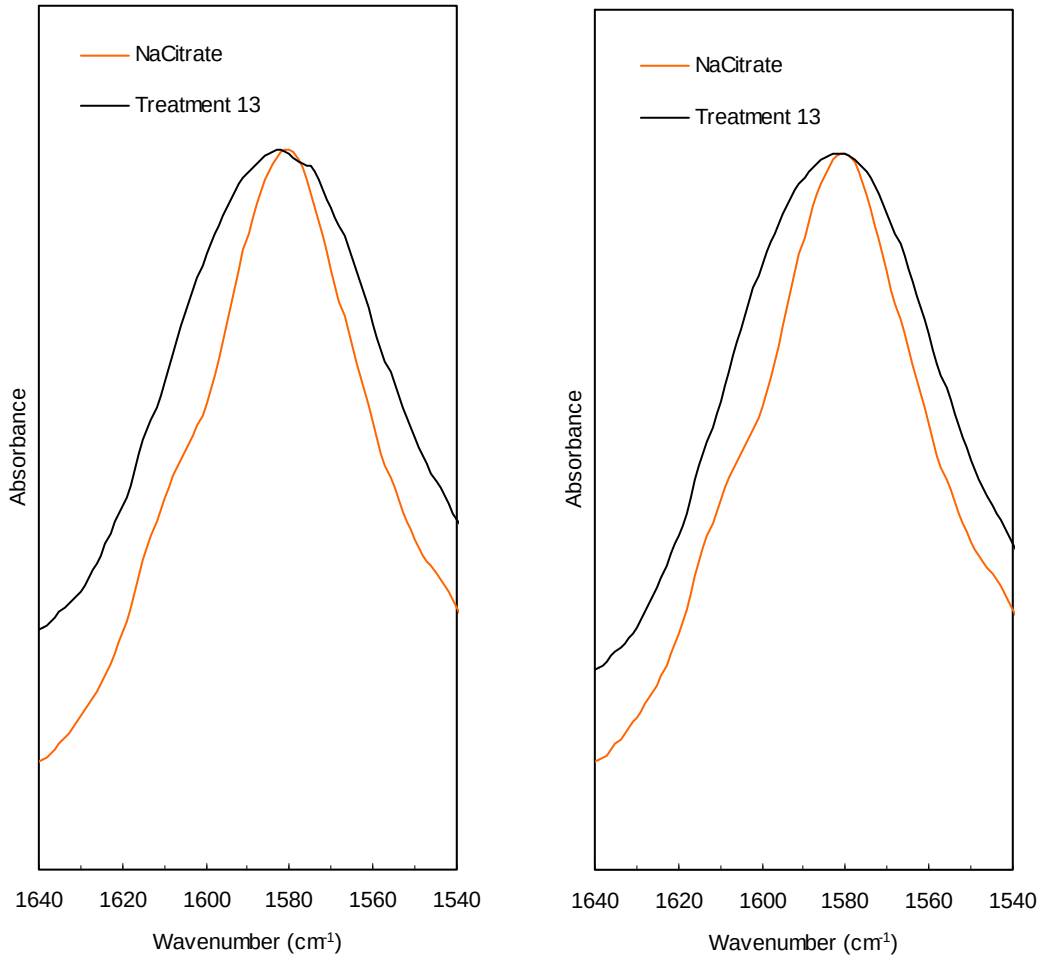

Figure A3.2.4 Absorption spectra of Na-citrate and Treatment 13 (SC/MD = 7:3 (by mass), NaCit/SC = 0.2 (by mole), equilibrated in P_2O_5 atmosphere), replication 1 (left) and 2 (right).

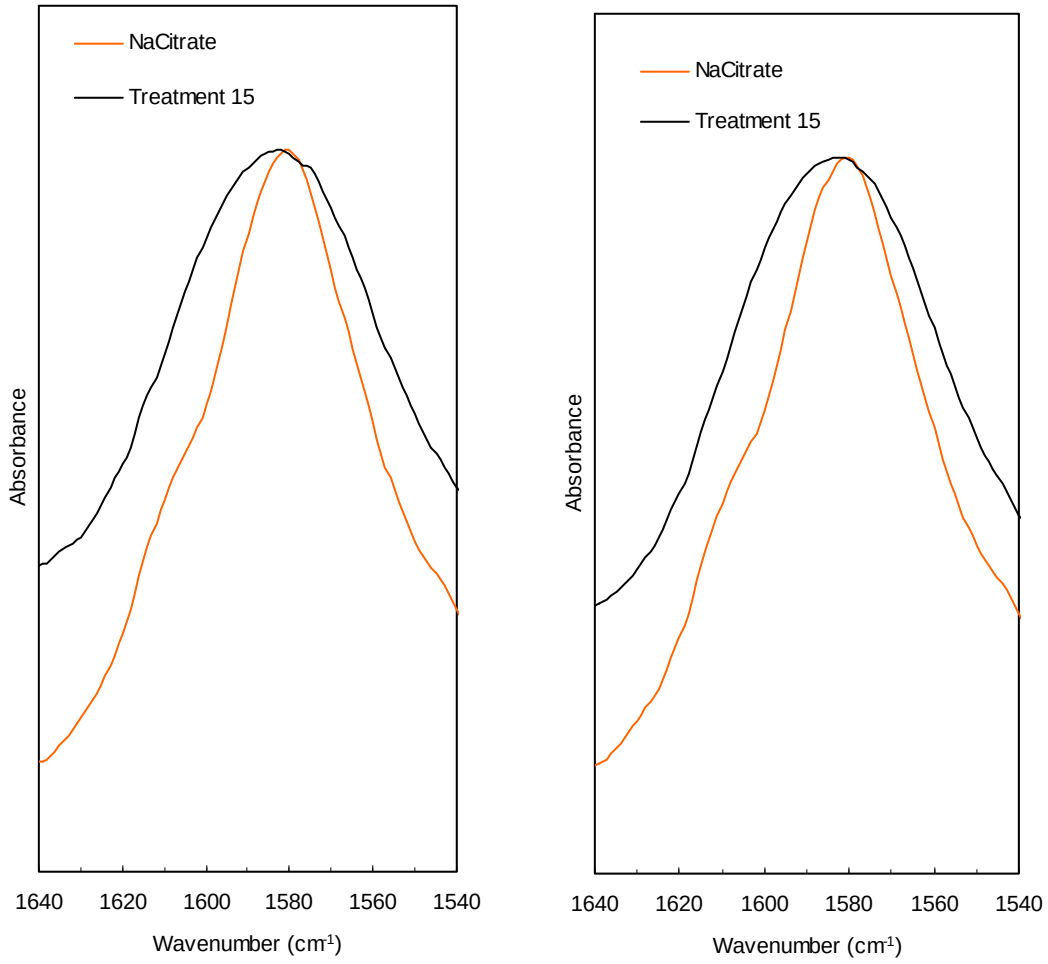

Figure A3.2.5 Absorption spectra of Na-citrate and Treatment 15 (SC/MD = 5:5 (by mass), NaCit/SC = 0.2 (by mole), equilibrated in P_2O_5 atmosphere), replication 1 (left) and 2 (right).

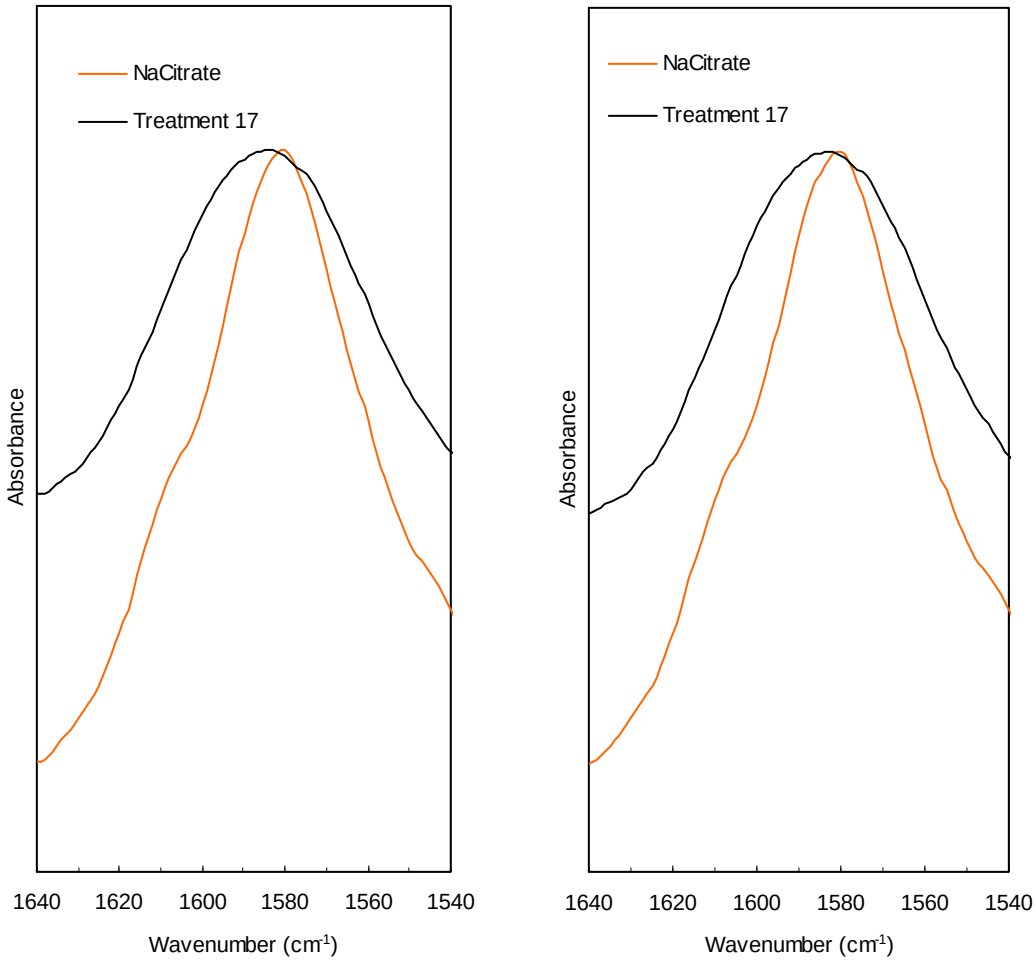

Figure A3.2.6 Absorption spectra of Na-citrate and Treatment 17 (SC/MD = 3:7 (by mass), NaCit/SC = 0.2 (by mole), equilibrated in P_2O_5 atmosphere), replication 1 (left) and 2 (right).

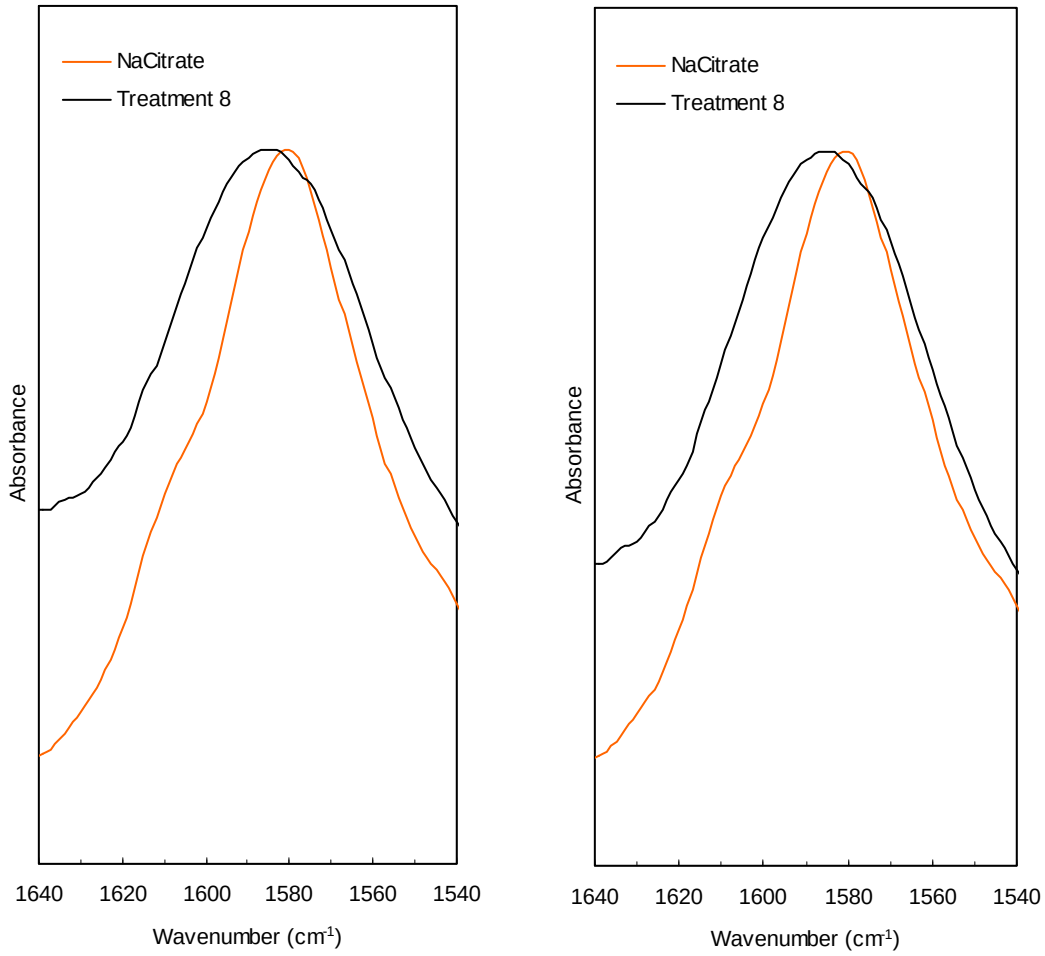

Figure A3.2.7 Absorption spectra of Na-citrate and Treatment 8 (SC/MD = 7:3 (by mass), NaCit/SC = 0.1 (by mole), equilibrated in saturated LiCl solution atmosphere), replication 1 (left) and 2 (right).

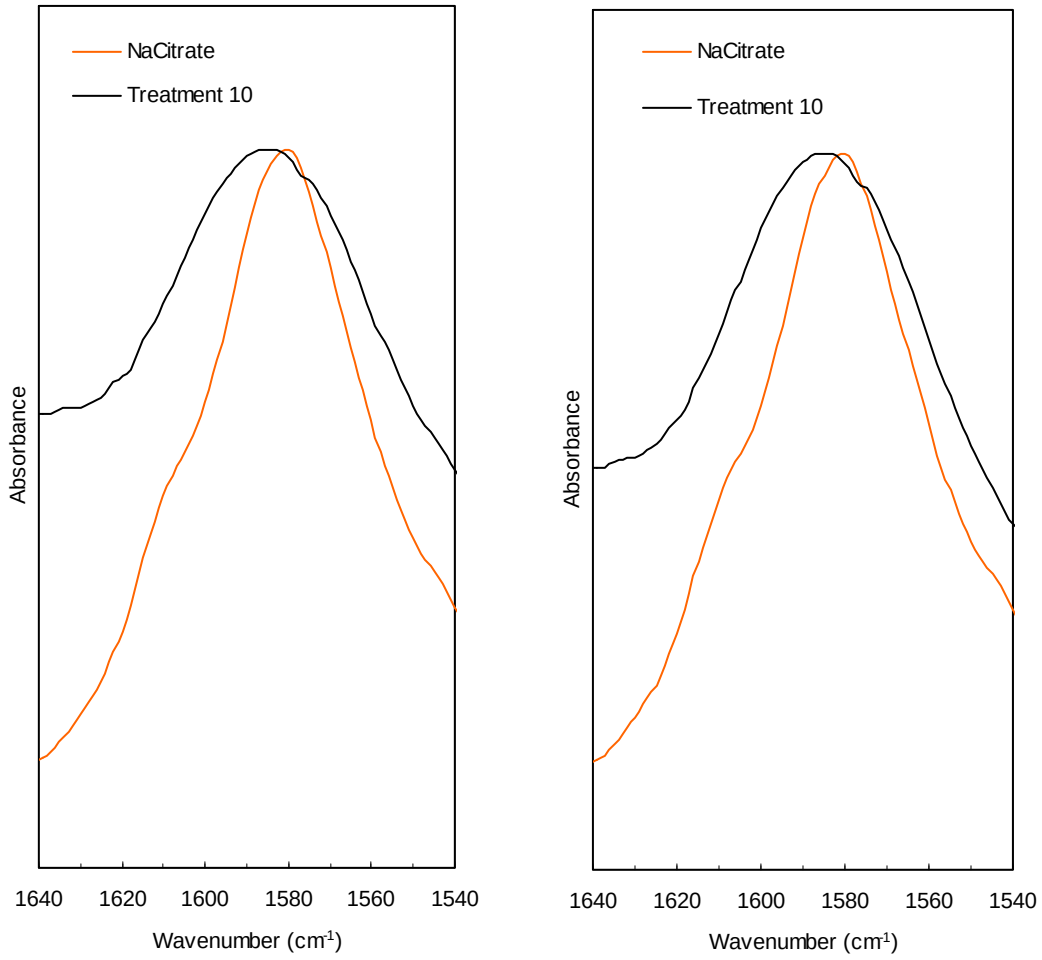

Figure A3.2.8 Absorption spectra of Na-citrate and Treatment 10 (SC/MD = 5:5 (by mass), NaCit/SC = 0.1 (by mole), equilibrated in saturated LiCl solution atmosphere), replication 1 (left) and 2 (right).

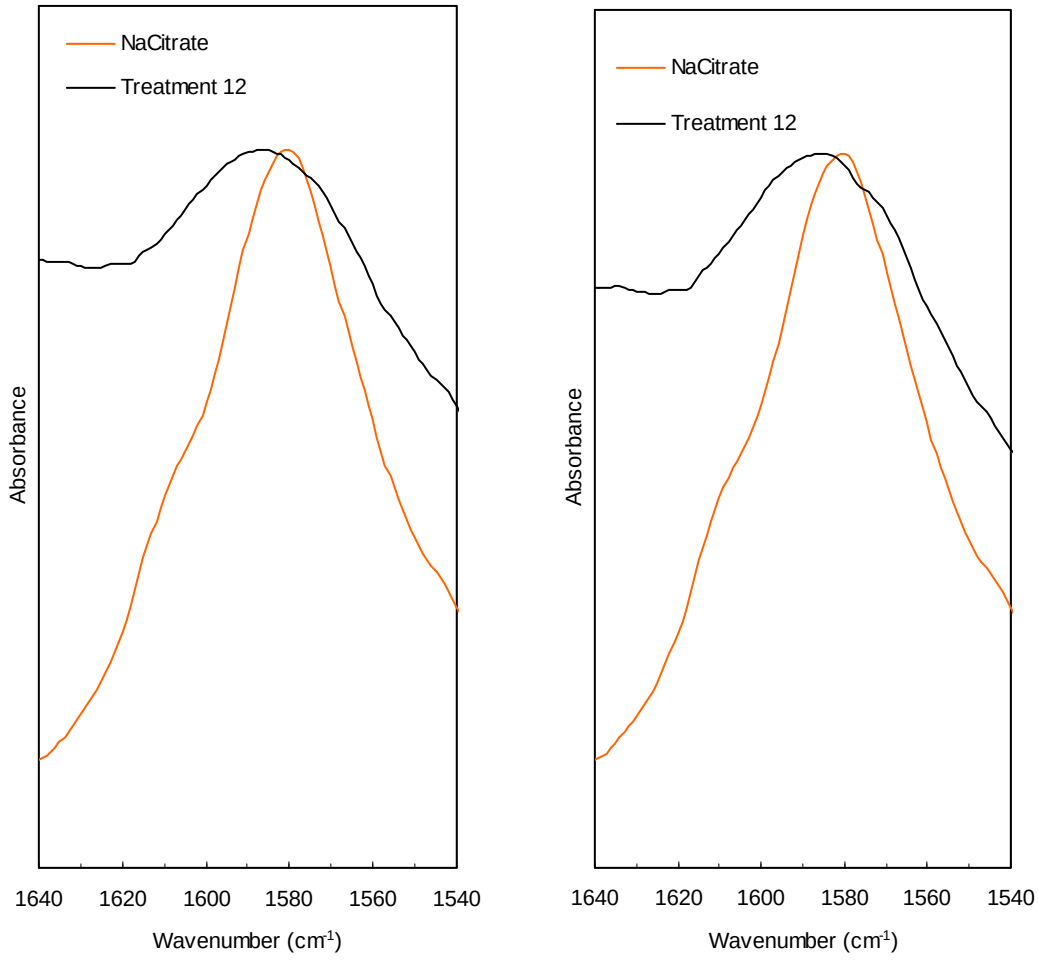

Figure A3.2.9 Absorption spectra of Na-citrate and Treatment 12 (SC/MD = 3:7 (by mass), NaCit/SC = 0.1 (by mole), equilibrated in saturated LiCl solution atmosphere), replication 1 (left) and 2 (right).

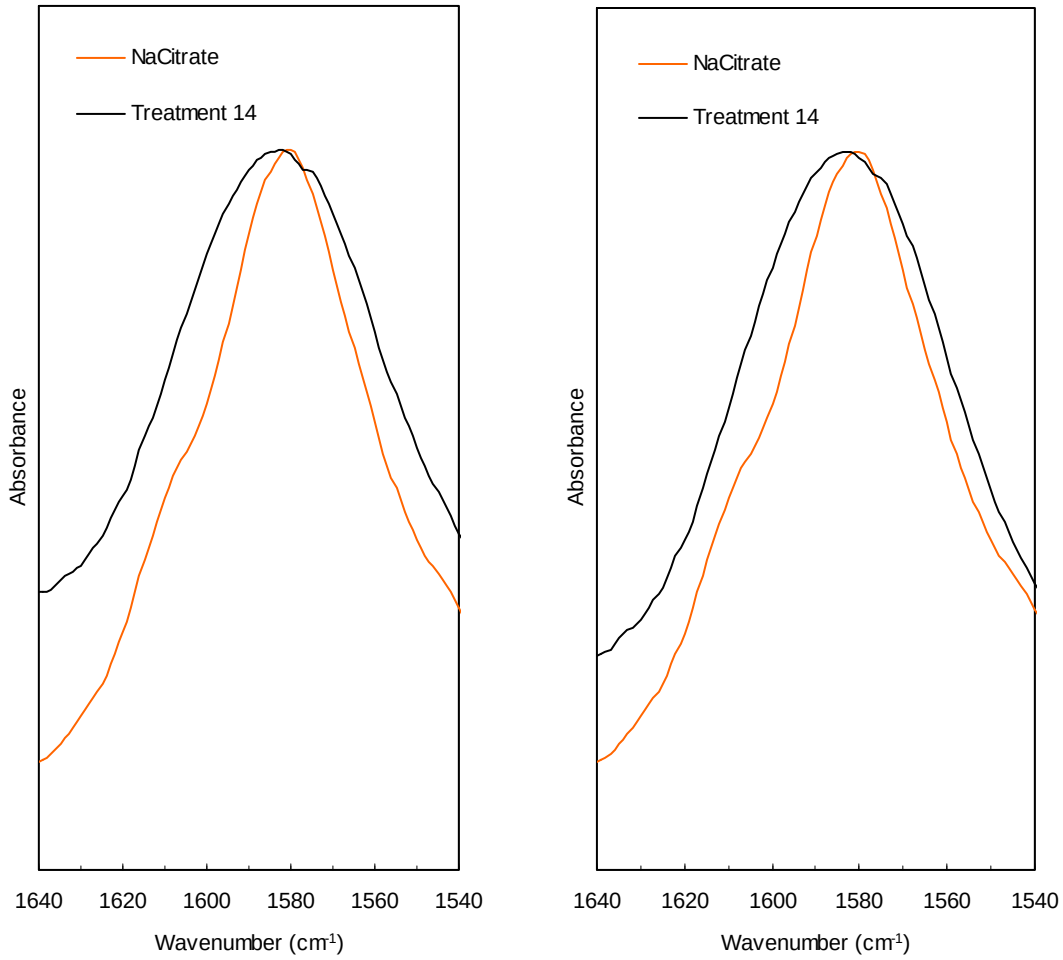

Figure A3.2.10 Absorption spectra of Na-citrate and Treatment 14 (SC/MD = 7:3 (by mass), NaCit/SC = 0.2 (by mole), equilibrated in saturated LiCl solution atmosphere), replication 1 (left) and 2 (right).

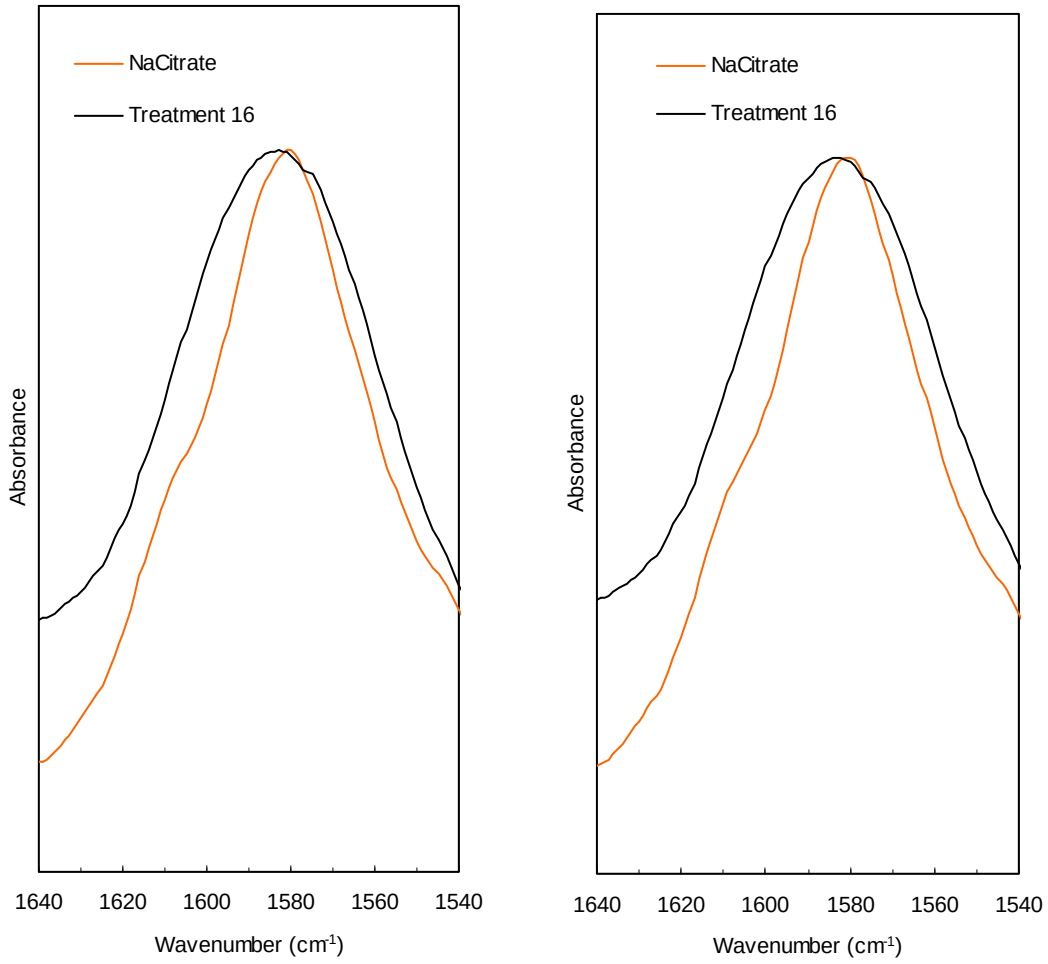

Figure A3.2.11 Absorption spectra of Na-citrate and Treatment 16 (SC/MD = 5:5 (by mass), NaCit/SC = 0.2 (by mole), equilibrated in saturated LiCl solution atmosphere), replication 1 (left) and 2 (right).

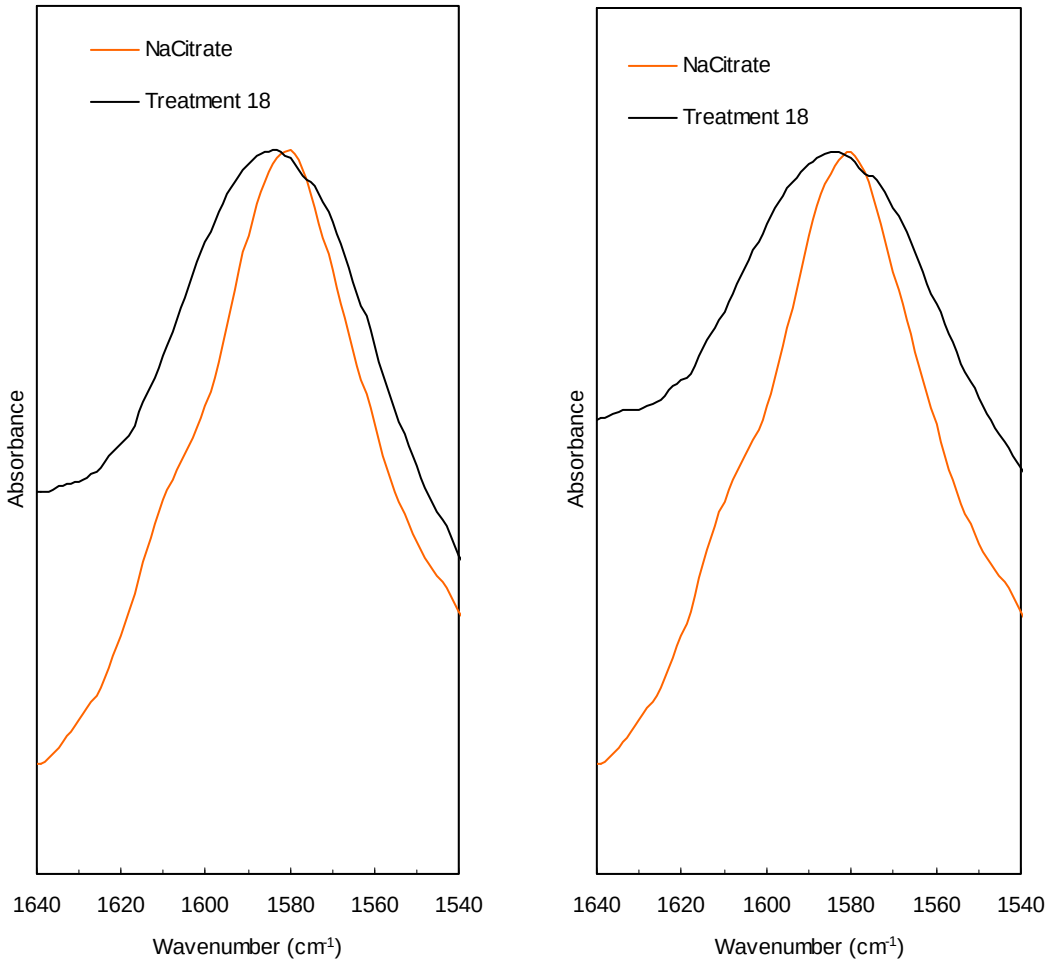

Figure A3.2.12 Absorption spectra of Na-citrate and Treatment 18 (SC/MD = 3:7 (by mass), NaCit/SC = 0.2 (by mole), equilibrated in saturated LiCl solution atmosphere), replication 1 (left) and 2 (right).

CHAPTER 4

RHEOLOGICAL AND MORPHOLOGICAL EVALUATIONS OF AMORPHOUS SUCROSE-MALTODEXTRIN-Na CITRATE MIXTURE

4.1 Abstract

Rheological properties and the mechanical relaxation behavior of rubbery amorphous sucrose-maltodextrin-Na citrate system were studied at room temperature using the small amplitude oscillatory shear (SAOS) test in the frequency range of 0.1 – 150 Hz. The system with high sucrose concentration exhibited viscous-dominant relaxation, while the system with high maltodextrin concentration exhibited elastic-dominant relaxation. The addition of Na citrate could retard molecular mobility presumably due to molecular interaction between Na citrate and sucrose rather than maltodextrin. The technique was capable to detect changes in molecular process even with a small variation in the matrix components. Evidences obtained with the scanning electron microscopy (SEM) imaging suggested the possible effect of Na citrate to interfere with molecular interactions in the system with high maltodextrin concentration; the system tended to be more brittle.

4.2 Introduction

The state of amorphous is thermodynamically nonequilibrium; molecular mobility becomes very important characteristic of amorphous materials. Molecular mobility has gained much of attention from food researchers since it is closely related to the physiochemical stability of food materials. In fact, the term “molecular mobility” encompasses a number of molecular movements, for instance the translational and rotational motions of molecules and the vibrational motions of side chains. Molecular mobility of amorphous carbohydrates can be studied using different techniques as previously discussed in Chapter 1. A common practice is to estimate the degree of molecular mobility from the relaxation process of material. Dynamic mechanical spectroscopy is known for its sensitivity to molecular relaxation process (Wetton, 1984). In polymer studies, the dynamic mechanical testing has proven useful for characterizing molecular structure since the test could provide information for both main chain and side group motions. Dynamic mechanical properties are frequency dependent; they could be related to particular types of molecular motion in polymers (Young and Lovell, 1991).

Microscopic structure is among important characteristics of food materials; it can be characterized using a number of techniques. Optical microscopy and electron microscopy have been very valuable tools for observing the physical state of components and microscopic structure (Morris and Miles, 1994). The techniques are particularly useful for observing microscopic changes that may occur in crystal size and crystallinity in foods during storage (Roos, 1995). Electron microscopy includes several techniques namely conventional transmission electron microscopy (CTEM), high resolution electron microscopy (HREM), and scanning electron microscopy (SEM) (Hermansson and Langton, 1994).

Among these, SEM has been commonly employed for characterizing the physical state and surface morphology of food materials and microstructure of polymers (Roos, 1995). For example, SEM has been used for examining spray-dried powder morphology (Alexander and King, 1985) and structural changes in other low-moisture amorphous foods (Gejl-Hansen and Flink, 1977).

This study was aimed at elucidating the effects of sucrose, maltodextrin, and Na citrate on the rheological behavior and morphological characteristics of the amorphous sucrose-maltodextrin-Na citrate system. The mixtures in the state of rubbery amorphous were characterized using SAOS test. SEM was used to obtain information on the morphology of the mixture in glassy state.

4.3 Materials and Methods

4.3.1 Materials

Details of materials are given in Chapter 2, section 2.3.1.

4.3.2 Experimental design

All samples used for SEM were from the set prepared for DSC measurements; so the experimental design is same as that in Chapter 2. For rheological measurements, the experimental design was also similar to that given in Chapter 2, section 2.3.2, except that there were only two factors in this part, i.e., sucrose/maltodextrin mass ratio (SC/MD) and Na citrate/sucrose mole ratio (NaCit/SC). The levels of each factor were also similar to that in Table 2.1.

4.3.3 Sample preparation for rheological measurements

Initially, the molten mixtures were prepared by heat evaporation similar to those in Chapter 2, section 2.3.3. After reaching the pre-determined moisture contents, they were molded into a 5-mm diameter cylindrical shape. The molding was done by injecting the molten mixture into a Teflon mold whose inner surface was coated with paraffin oil to prevent sticking. After removing from the mold, each sample was promptly transferred into small glass tubes, which were then vacuum-sealed in FoodSaver® plastic bags and stored in a desiccator. Treatments were prepared in duplicate.

Prior to rheological measurements, the FoodSaver® bags containing glass tubes with bioglass samples were transfer from the desiccator into a glove box flushed with Nitrogen gas which could bring down the relative humidity inside the glove box to approximately 5%. Samples were removed from the package and cut into about 7.56±0.11 mm long cylindrical specimens. The rest of samples were re-packed for moisture determination.

4.3.4 Moisture determination

Moisture content of samples was determined using the Karl Fisher titration technique as described in Chapter 2, section 2.3.4.

4.3.5 Rheological measurements

SAOS tests were conducted using the dynamic controlled stress rheometer (Bohlin C-VOR, Malvern Inc., Southhampton, MA) connected to a personal computer with Bohlin 6.40 software package. The measurements were performed using a 20-mm parallel-plate geometry (PP20) with slightly different gap heights according to the height of individual bioglass

specimen. Cyanoacrylate adhesive was applied to affix specimens to the parallel plates. A specially designed moisture solvent trap was used around the specimen and parallel plates to minimize moisture absorption. In addition, paraffin oil was applied on all of the contacts between the two halves of the trap, and between the trap and the bottom parallel plate Specimens were allowed to stand for approximately 15 min before starting for the adhesive to dry; the specimens were indeed stuck to the plates as observed while removing them. The tests were conducted isothermally at 25 °C in the frequency range of 0.01 – 150 Hz with the shear strain of 0.002%. Experimental data in rheological format were exported to MS Excel, corrected with the specimen geometry, and reported.

4.3.6 SEM measurements

4.3.6.1 Sample coating

Small amount of ground sample from each treatment was applied just enough to cover the surface of a 12-mm carbon adhesive tab glued on an aluminum mount. The aluminum mounts loaded with samples were transferred to a sputter-coater chamber. The chamber was flushed with argon gas for 5 cycles prior to subsequent coating with gold-palladium at 30 mA for 3 min. This procedure yields a coating thickness of approximately 30 nm. Coated samples were then immediately transferred into a desiccator for imaging.

4.3.6.2 SEM Imaging

Morphological study of glass samples were carried out using the Hitachi S-570 scanning electron microscope (SEM) at the Biological & Biomaterials Preparation, Imaging,

and Characterization(BBPIC) facility, Department of Animal Science, UW-Madison. The Hitachi S-570 SEM employs a crystal of Lanthanum Hexaboride (LaB_6) as an electron emitter allowing the utilization of low acceleration voltages, which helps prevent possible damage to samples as well as reduces charging artifacts, and provides considerable high resolution image. The instrument is robust and capable of imaging a wide range of biological samples. It delivers a magnification of about 10X to over 500,000X with great depth of field and resolution of a few nanometers to a few Angstroms.

Four aluminum mounts bearing coated samples were loaded into the SEM chamber at a time. Acceleration voltage was set to 10 kV. Focusing was fine-tuned at a magnification at least twice the actual image capturing magnification. From preliminary image capturing, we found that 1000X magnification provided much of topography with good depth of field and hence this level of magnification was applied throughout the entire experiments.

4.3.7 Statistical analysis

Moisture content of bioglass samples were statistically analyzed using the IBM SPSS Statistics 19 computer package. The analysis of variance (ANOVA F-test) was carried out with the general linear model (GLM). Tukey's range test was applied for simultaneous multiple comparisons. This comparison technique was chosen as it does control the experimentalwise error rate at the selected significance level (α) (Montgomery, 2005). All statistical analyses were conducted at $\alpha = 0.05$.

4.4 Results and Discussion

4.4.1 Moisture content

Moisture content of the samples used in rheological measurements ranged from 8.47 to 11.97 %wb which is comparable to the level found in cereal products stored at ambient temperature (Windham et al., 1997). These levels of moisture could substantially suppress the T_g of samples to be lower than room temperature, or the samples were in the state of rubbery amorphous. Graphical representation moisture content for the samples formulated with different recipes is given in Figure 4.1. It could be seen that moisture tended to in increase with the increasing concentration of maltodextrin. At the given SC/MD ratio, moisture content seemed to increase with the Na citrate concentration. Moisture content significantly increased with the increasing NaCit/SC or with the decreasing SC/MD. ANOVA confirmed the significant effects of NaCit/SC and SC/MD ratios on such trend of changes in moisture content (Appendix 4.1, Table A.4.1.2).

Direct interaction between Na^+ and water may be partly responsible for the elevated moisture content in bioglass samples upon the addition of Na citrate. Large glucose polymers with a broad spectrum of chain lengths and molecular weights in maltodextrin (McPherson and Seib, 1997; Chronakis, 1998) might be responsible for high viscosity of the molten mixture with high maltodextrin content. In turn, this high viscosity dictated the final moisture content that could be attained via heat evaporation. In addition, the three-dimensional network of glucose polymers in maltodextrin may contribute to a high degree of water holding capacity. Water existing in maltodextrin matrix could be either in the form of free or bound water. The polysaccharide-water interaction is significant under the influence of

polysaccharide molecular structure—linear or branched (Chronakis, 1998). However, water-maltodextrin interaction is weak and only approximately 4.5% of water (by mass) could be bound to maltodextrin molecules (Radosta et al., 1989; Radosta et al., 1989; Radosta and Schierbaum, 1990). The weak interaction permits high mobility of bound water and fast exchange with free water (Chronakis, 1998).

As there was no further adjustment on moisture content of the samples after quench cooling, the result would provide some perspective about the moisture content of products in practical situation for the similar processes, for instance, extrusion cooking.

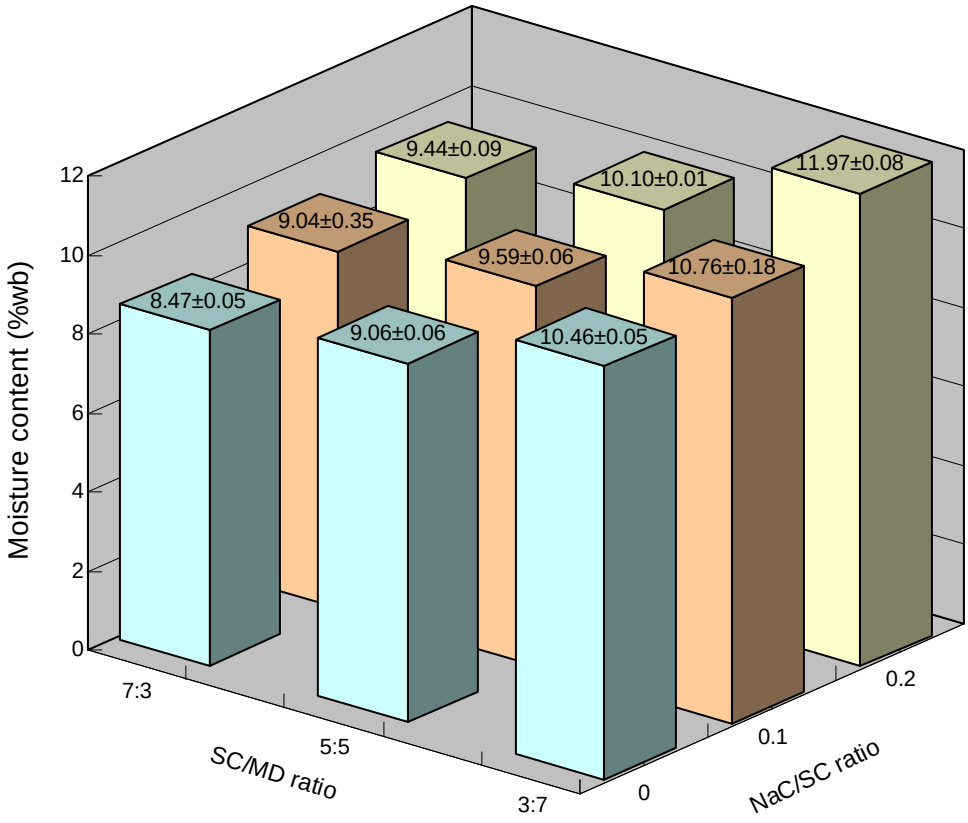

Figure 4.1 Moisture content of amorphous sucrose-maltodextrin-Na citrate systems having different compositions. Number on each bar represents mean ± standard deviation.

4.4.2 Rheological characteristics

4.4.2.1 Dynamic mechanical spectra

The SAOS data for the rubbery amorphous of sucrose-maltodextrin-Na citrate system (elastic modulus (G'), viscous modulus (G'') and loss tangent (tan δ)) as a function of frequency (f) in the range of 0.1 – 100 Hz at 25 °C are given in Appendix 4.2: Figures A4.2.1 – A4.2.18.

For the systems with the highest sucrose concentration (SC/MD of 7:3) as shown in Figures A4.2.1 – A4.2.6, it can be seen that in the range from low frequency limit (0.1 Hz) up to the frequency slightly higher than 10 Hz, samples exhibited liquid-like behavior (i.e., $G'' > G'$), the so called viscous region. In this region the energy generated by molecular motions dissipated as heat per cycle of sinusoidal deformation giving rise to the dominance of viscous component (Kasapis and Sablani, 2005). The dominance of G'' ceased at slightly different frequencies, which were approximately 50, 20, and 15 Hz for the systems with NaCit/SC of 0, 0.1, and 0.2, respectively. The change of viscoelasticity for approximately two orders of magnitude, from about 10 to 1000 MPa, was observed in the viscous region. At higher frequencies, G' started to exceed G'' and tan δ dropped to approximately one or lower; the systems behaved solid-like. The addition of Na citrate resulted in the greater shear moduli for the entire viscous region. The greatest moduli was observed in the system with the highest Na citrate concentration, with G'>1000 MPa at 100 Hz. This observation suggests that the modulation of molecular interaction by Na citrate results in a stronger amorphous matrix.

Mechanical spectra for the SC/MD = 5:5 system without Na citrate (Figures A4.2.7 and A4.2.8) show comparable magnitudes of G' and G'' in the frequency range of 0.1 – 3 Hz before G' began to take over afterwards. Once Na citrate was introduced to the systems, G'' became dominant up to approximately 3 Hz, i.e., the systems exhibited liquid-like behavior. A close examination reveals a slightly noticeable of G'' dominance in the system with higher Na citrate content (see also Figures A4.2.9 – A4.2.12). In other words, molecular motions developed a viscous rather than elastic character when Na citrate was added probably due to the plasticization effect of Na citrate on maltodextrin. However the effect of Na citrate on the magnitude of shear moduli or rigidity of the system was not clear.

For the systems with high maltodextrin concentration (SC/MD = 3:7; Figures A4.2.13 – A4.2.18), a solid-like behavior was observed over the entire range of applied frequencies. Apparently, the addition of Na citrate resulted in the decrease of rigidity; the higher the Na citrate concentration, the lower the shear moduli. This could be due to the interference of Na citrate with the hydrogen bonds in the amorphous matrix with high maltodextrin concentration.

The rigidity of the amorphous systems increased with the increasing concentration of large glass-forming molecules—maltodextrin, in this case. The matrices of amorphous saccharides are primarily hold up by hydrogen bonds and glycosidic linkages. The later was found experimentally that it could restrict the movement of pyranose rings more strongly than hydrogen bonds (Imamura et al., 2006). Since for the same number of pyranose rings maltodextrin possesses higher number glycosidic linkages than sucrose, this would explain the increase in the rigidity of systems when the maltodextrin concentration was increased.

4.4.2.2 Mechanical relaxation process

To provide a broader view for examining the mechanical relaxation process, tan δ values were plotted against angular frequency (ω) in a range of 0.01 to 1000 rad/s (Figures 4.2 – 4.10). Though mechanical relaxation process commonly extends over many decades of frequency, it could be seen that the majority of mechanical relaxation process of the samples were captured in the frequency range of this experiment.

The systems with highest sucrose concentration (SC/MD = 7:3; Figures 4.2 – 4.4) showed the strongest relaxation process with the maximum tan δ or the loss peak height of approximately 1.7 – 2.2. It should be noted that G' is dominant when tan δ is less than unity; if this value is greater than unity, G'' becomes dominant. From the plots it would be readily seen that the relaxation process is dominated by viscous component. The viscoelastic behavior in this region would be governed by the motions of small molecules—sucrose, and the configurational vibrations of segments (Ngai and Plazek, 1995; Kasapis and Sablani, 2005) of maltodextrin molecules. These motions would generate energy, which is dissipated during the sinusoidal deformation resulting in the dominantce of viscous component of relaxation process in the system with high sucrose concentration. The addition of Na citrate resulted in both the increase of loss peak height and the downshift of loss peak frequency (f_p). The loss peak heights of approximately 1.7, 2 and 2.2, and the f_p values of around 15, 5 and 3 rad/s, were observed in the systems with NaCit/SC of 0, 0.1 and 0.2, respectively. The most interesting change is the downshift of f_p, which suggests limited matrix mobility upon adding Na citrate; the higher the Na citrate concentration, the lower the molecular mobility within the matrix. The result agrees with the observations of enthalpy relaxation behavior (Chapter

2) and evidences from FTIR measurements (Chapter 3). Again, the reason for this change is probably be due to molecular interaction between sucrose and Na citrate, which would result in larger clusters with less mobility within the amorphous matrix.

Without Na citrate the relaxation process of the system with SC/MD of 5:5 was no longer dominated by viscous component. As compared to the relaxation process of the system with high sucrose concentration (SC/MD of 7:3), there was more contribution from elastic component to viscoelastic behavior; elastic and viscous components were equally significant. The motions involving bending and stretching of chemical bonds (Kasapis and Sablani, 2005) primarily contributed by glycosidic linkages in maltodextrin molecules might be responsible for the more significance of elastic component as maltodextrin concentration was increased. Unlike in the system with high sucrose concentration, the increase in the loss peak height and the downshift of f_p were barely observed when Na citrate was added. The relaxation process of the system without Na citrate (Figure 4.5) centered at around 3 rad/s, and slightly shifted to approximately 2 rad/s when Na citrate was added. Apparently, no significant difference in the downshift was observed between the systems with NaCit/SC of 0.1 and 0.2 (Figures 4.6 and 4.7). As a result, it would be legitimate to presume the high tendency of molecular interaction between Na citrate and sucrose rather than maltodextrin.

The relaxation process in the system with the highest maltodextrin concentration (SC/MD = 3:7; Figures 4.8 – 4.10) was dominated by elastic component ($\tan \delta < 1$) probably due to more contribution from stretching and bending of glycosidic linkages on maltodextrin molecules prevailing in this system. A slight increase in loss peak height was observed when Na citrate was added. Without a complete picture of the relaxation process, it was difficult to determine whether there was any change in f_p between the systems without Na citrate (Figure

4.8) and with NaCit/SC of 0.1 (Figure 4.9). It is interesting that in the system with NaCit/SC = 0.2, the relaxation peak shifted to higher frequency, approximately almost an order of magnitude as compared to the system without Na citrate indicating the higher mobility. This seemed to contradict the effect Na citrate in other systems. However, from Figure 4.1, when considering among the systems with high maltodextrin concentration, it could be seen that moisture content of the system with NaCit/SC = 0.2 was significantly higher than the rest; approximately 12 %wb as compared to approximately 10.5 –11 %wb in other systems. Water has a strong plasticization effect on amorphous carbohydrates (Champion et al., 2000; Noel et al., 2000; Shinyashiki et al., 2008); a difference of moisture content of only 1% could cause a significant difference in molecular mobility. A strong plasticization effect of water on sucrose-maltodextrin system was also observed in the DSC data (Chapter 2); the calorimetric glass transition temperature ($T_{g,DSC}$), denoted as T_g, was substantially suppressed by the increase of moisture by few percentage points. Two possible mechanisms have been proposed for plasticization of amorphous carbohydrate systems by water: 1) dynamically disrupt hydrogen bonding between carbohydrates (and then may also occupy the available sites (OH group), and 2) modulate the free volume in the system. These mechanisms increase the rate of relaxation and mobility of small permeants (Kilburn et al., 2005).

The relaxation processes commonly observed in mechanical or dielectric measurements exhibit different characteristics. The β-relaxation takes place at a higher frequency (or lower temperature) than α-relaxation. At the vicinity of glass transition, the strength of α-relaxation is usually much higher than that of β-relaxation (Shinyashiki et al., 2008). The α-relaxation is highly dependent on water content in that the process is shifted to lower temperature (or higher frequency), with increasing moisture content, which is not the

case for β-relaxation (Noel et al., 2000; Shinyashiki et al., 2008). It was also found that the temperature shift of α-relaxation is of the same order as the depression of the $T_{g,DSC}$ as a result of plasticization by water (Noel et al., 2000). In order to obtain glass transition temperature with the value comparable to $T_{g,DSC}$, the dielectric or mechanical glass transition temperature ($T_{g,\alpha}$) is conventionally defined as the temperature at which the characteristic time of α-relaxation process ($\tau_{,\alpha}$) is 100 s. According to Equation 1.15, the frequency that is equivalent to $\tau_{,\alpha}$ would be 0.01 rad/s, giving $\omega = 2\pi f$. In this study, the vibrational frequency of relaxation process (at 25 °C) was found in the range of approximately 1 – 10 rad/s. If the measurements had been carried out at temperatures lower than 25 °C, then the vibrational frequency of relaxation process would eventually reach 0.01 rad/s at $T_{g,\alpha}$, by definition. This expected $T_{g,\alpha}$ is much lower than the $T_{g,DSC}$ obtained from sucrose-maltodextrin-Na citrate system (see Chapter 2). However, this is not surprising since the moisture content was very different, approximately 10 % in this experiment compared to only within 4 % in DSC measurements. A moisture difference of just 1 % could give rise to a substantial difference in T_g, for instance $T_{g,DSC}$ of the system with SC/MD = 7:3 dropped from approximately 87 °C to 59 °C as the moisture contents was increased from around 0.3 % to 2.9 % (Table 2.5 and 2.6). A substantial $T_{g,DSC}$ reduction of dry amorphous D-Glucose for 56 °C when moisture content was increased to 10 % (w/w) was reported. The plasticization effect of water on carbohydrate systems appeared to be stronger in the system with more complex structure (Noel et al., 2000).

It might be difficult to relate mechanical relaxation with the primary relaxation (or enthalpy relaxation) without information about the temperature dependence of these

processes. However, in light of above discussion together with the fact that the relaxation process found in this experiment was sensitive to changes in moisture content and showed a loss peak with strong magnitude in the vicinity of the expected T_g, it is believed that this relaxation process is the primary or α category.

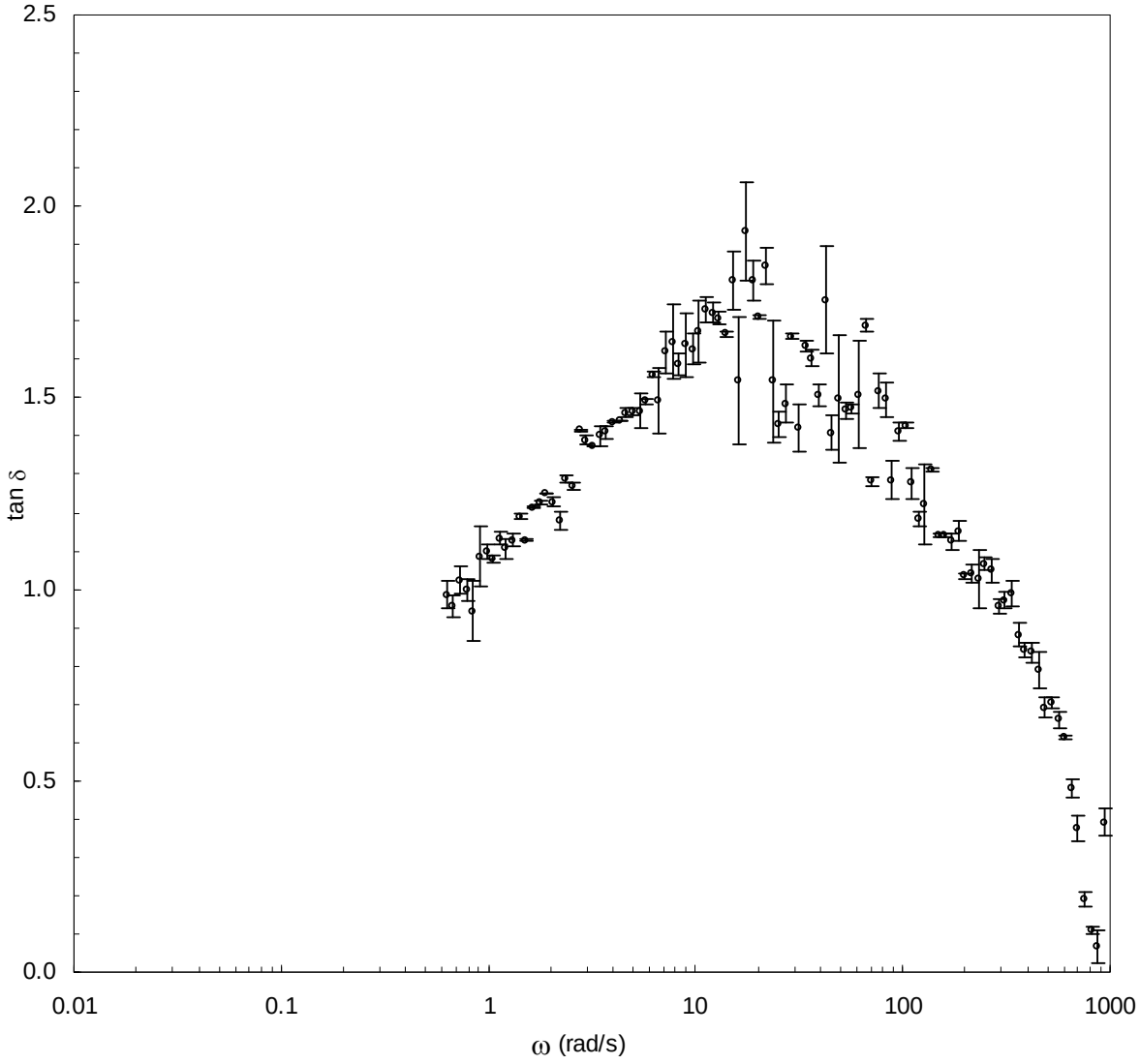

Figure 4.2 Frequency dependence of tan δ for the system with SC/MD = 7:3 without Na citrate. Data are means of two replicates and the error bars reflect standard deviations.

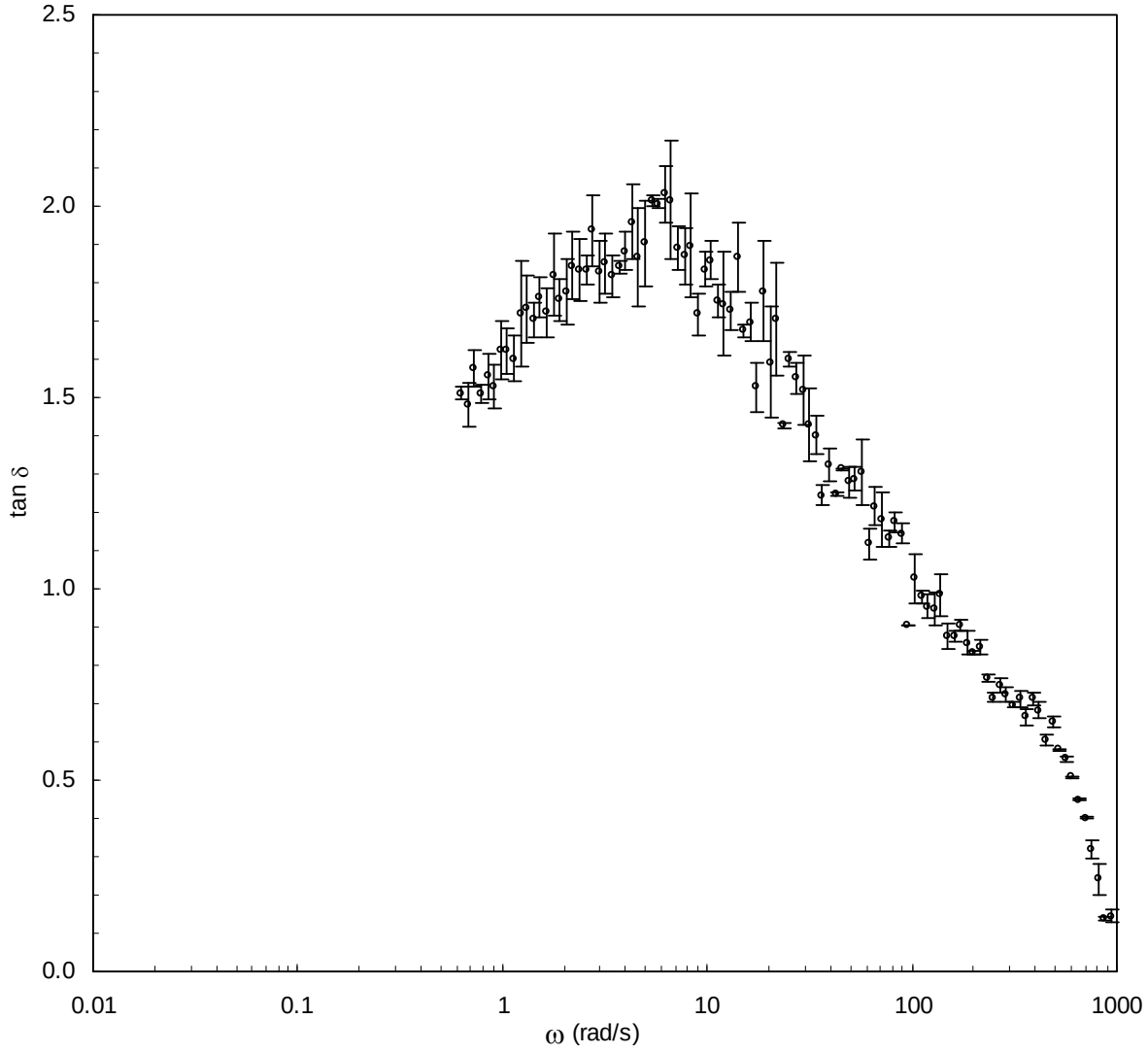

Figure 4.3 Frequency dependence of tan δ for the system with SC/MD = 7:3 and NaCit/SC = 0.1. Data are means of two replicates and the error bars reflect standard deviations.

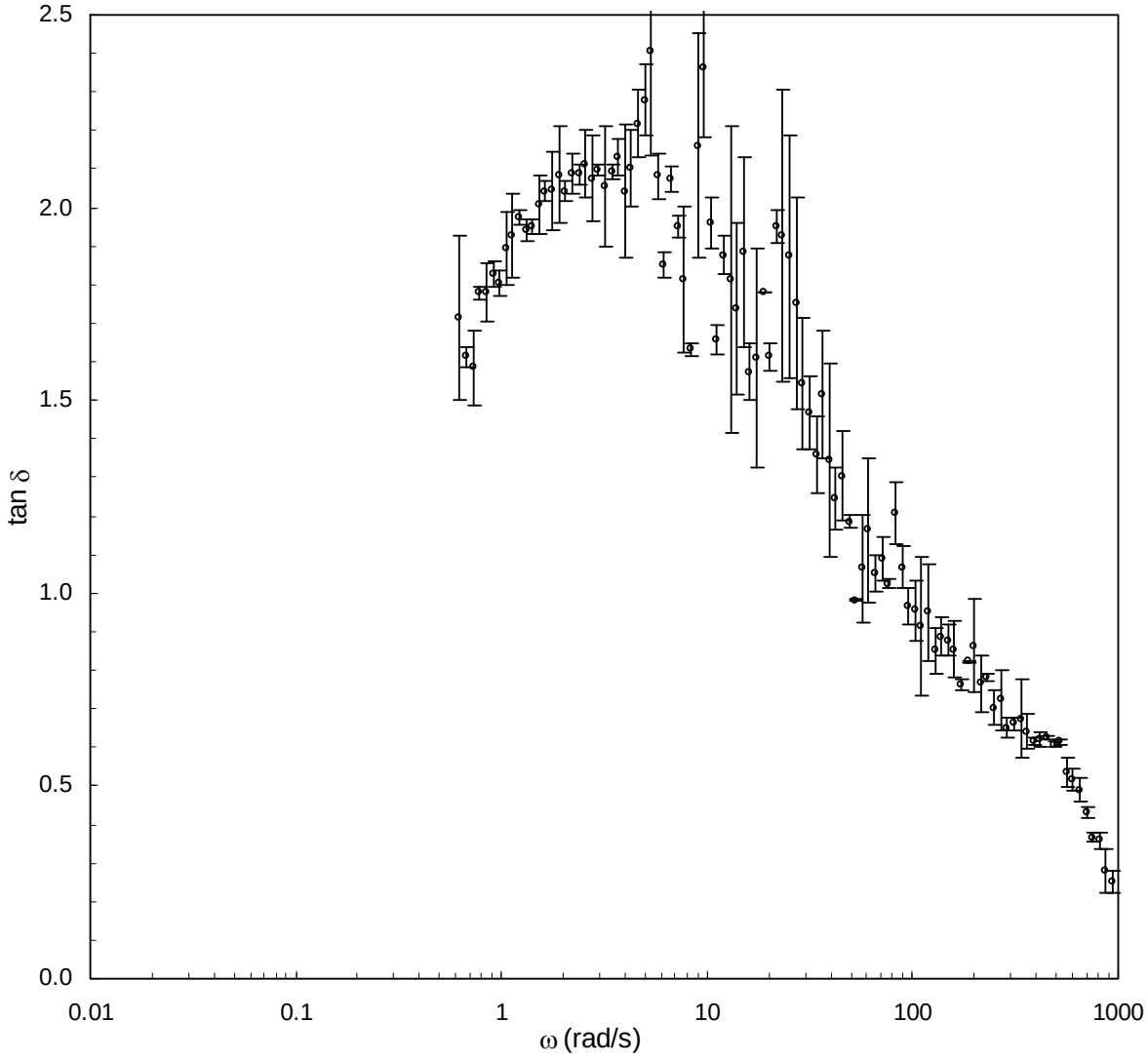

Figure 4.4 Frequency dependence of tan δ for the system with SC/MD = 7:3 and NaCit/SC = 0.2. Data are means of two replicates and the error bars reflect standard deviations.

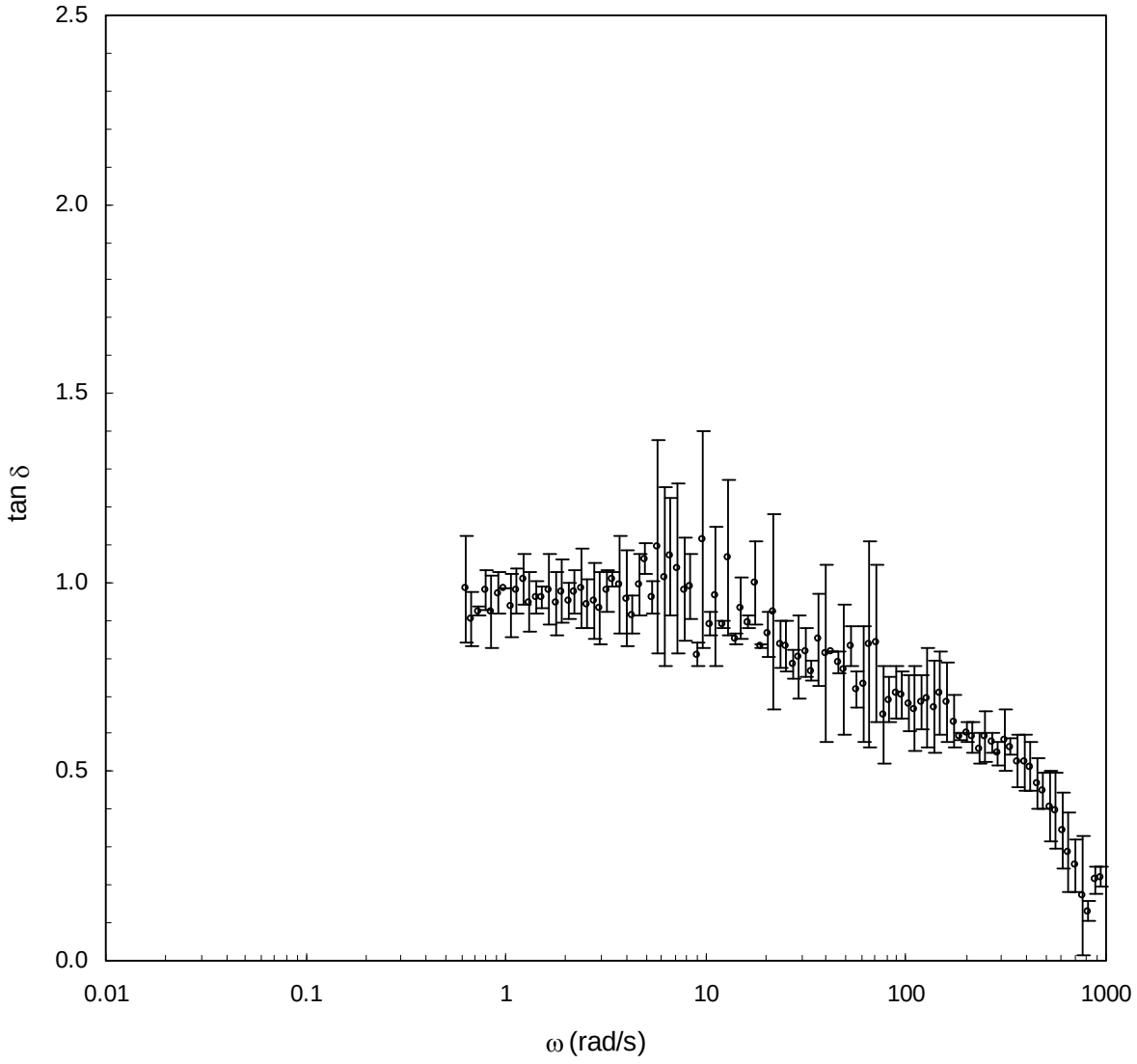

Figure 4.5 Frequency dependence of tan δ for the system with SC/MD = 5:5 without Na citrate. Data are means of two replicates and the error bars reflect standard deviations.

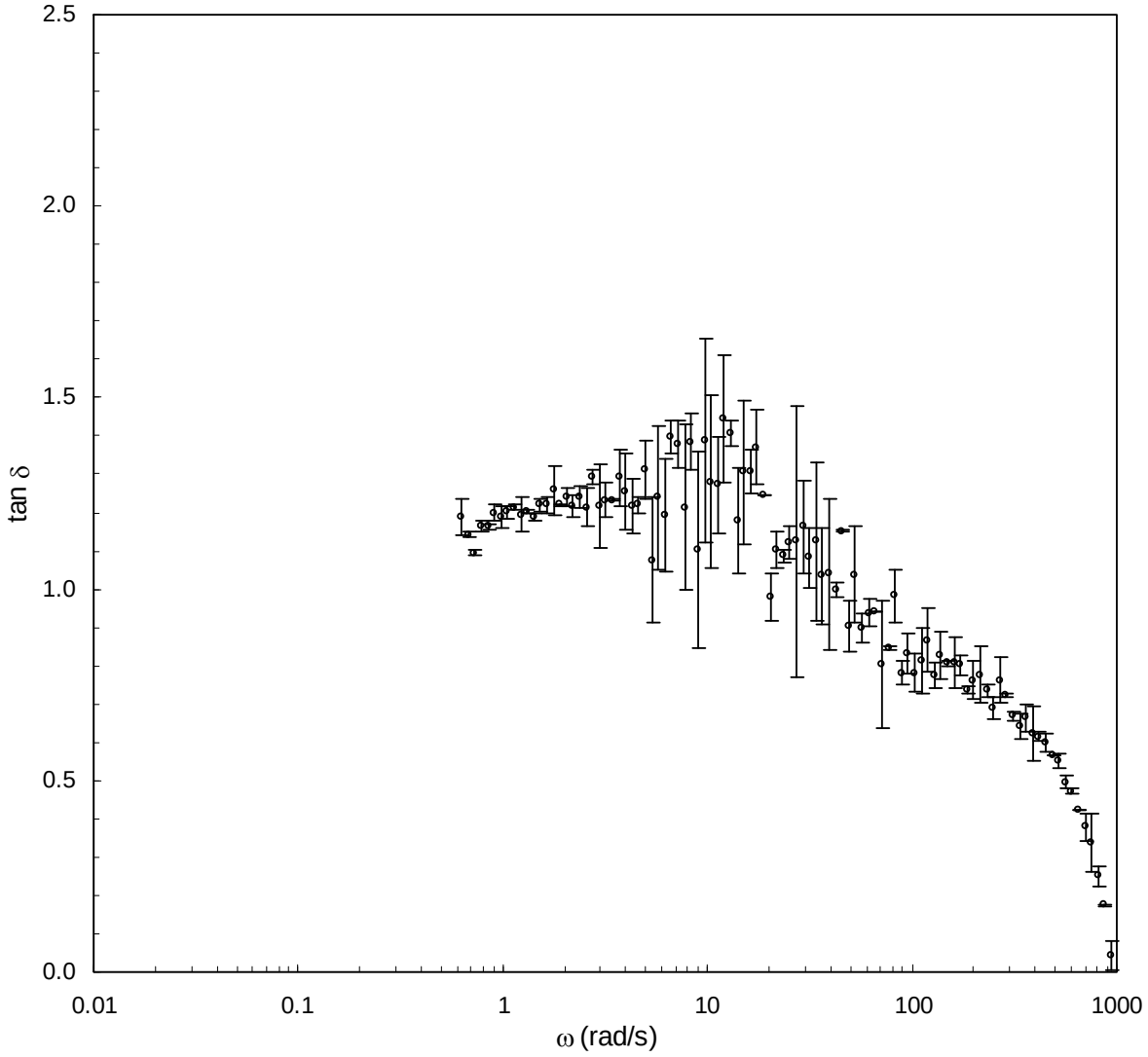

Figure 4.6 Frequency dependence of tan δ for the system with SC/MD = 5:5 and NaCit/SC = 0.1. Data are means of two replicates and the error bars reflect standard deviations.

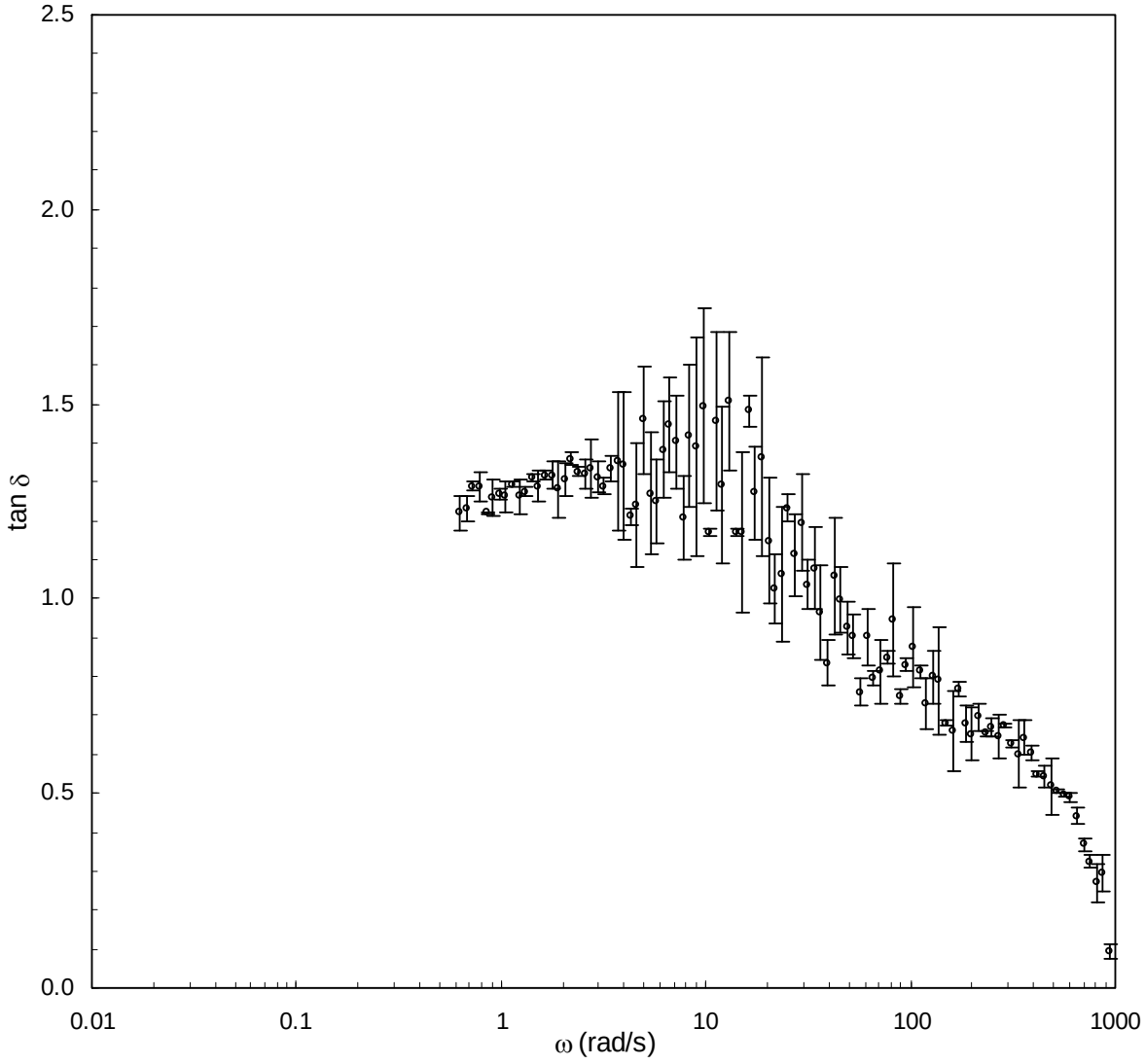

Figure 4.7 Frequency dependence of tan δ for the system with SC/MD = 5:5 and NaCit/SC = 0.2. Data are means of two replicates and the error bars reflect standard deviations.

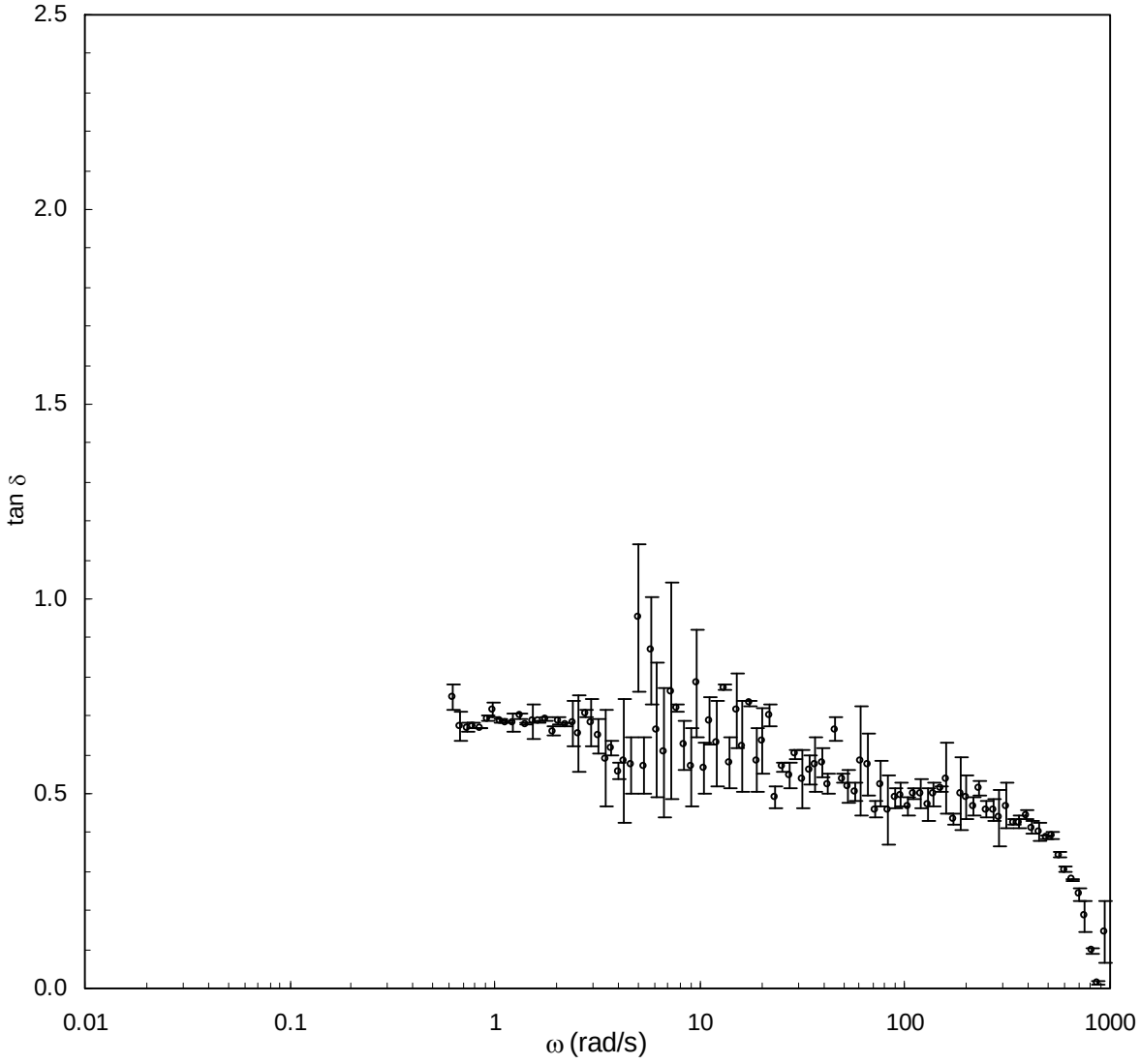

Figure 4.8 Frequency dependence of tan δ for the system with SC/MD = 3:7 without Na citrate. Data are means of two replicates and the error bars reflect standard deviations.

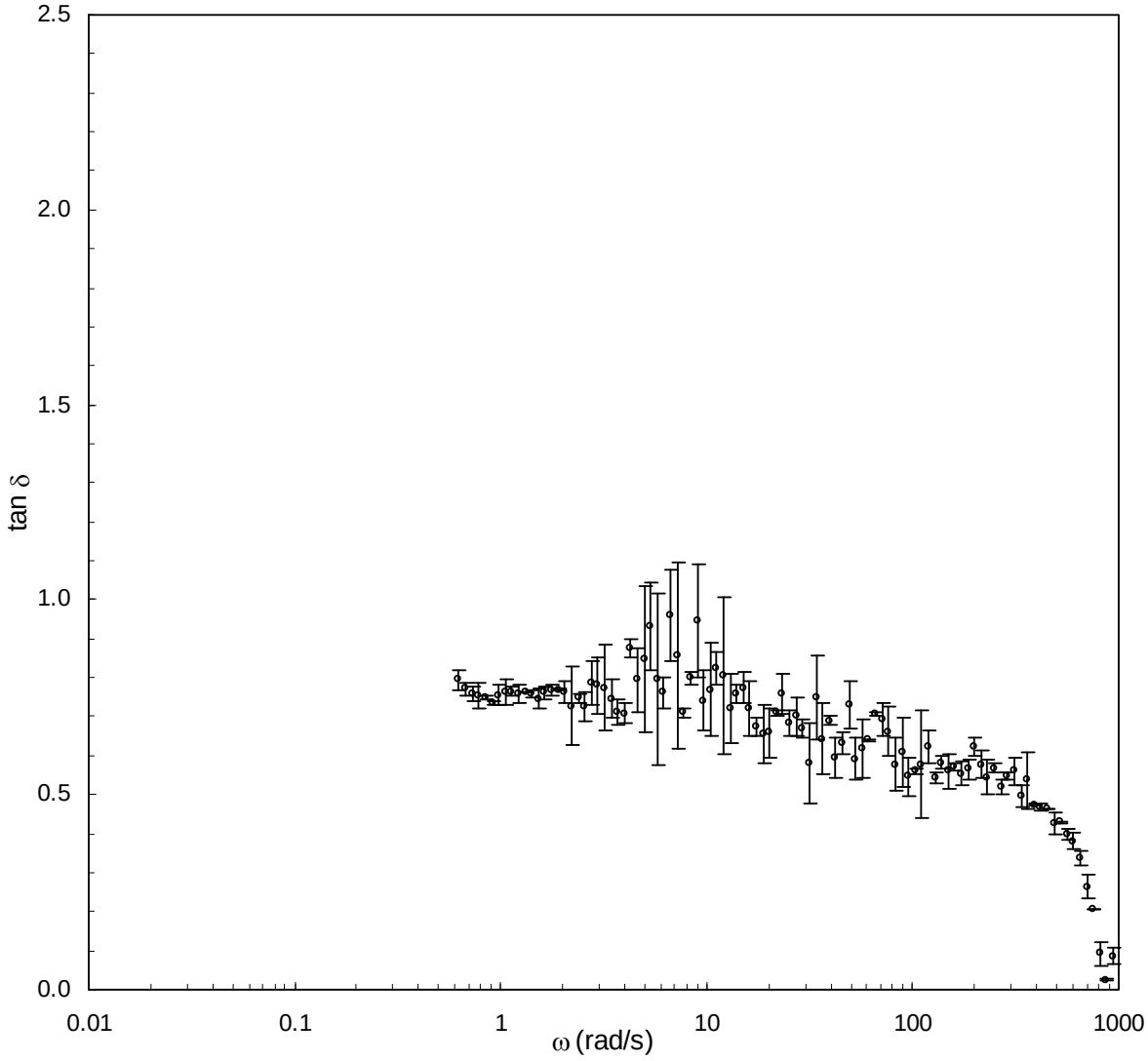

Figure 4.9 Frequency dependence of tan δ for the system with SC/MD = 3:7 and NaCit/SC = 0.1. Data are means of two replicates and the error bars reflect standard deviations.

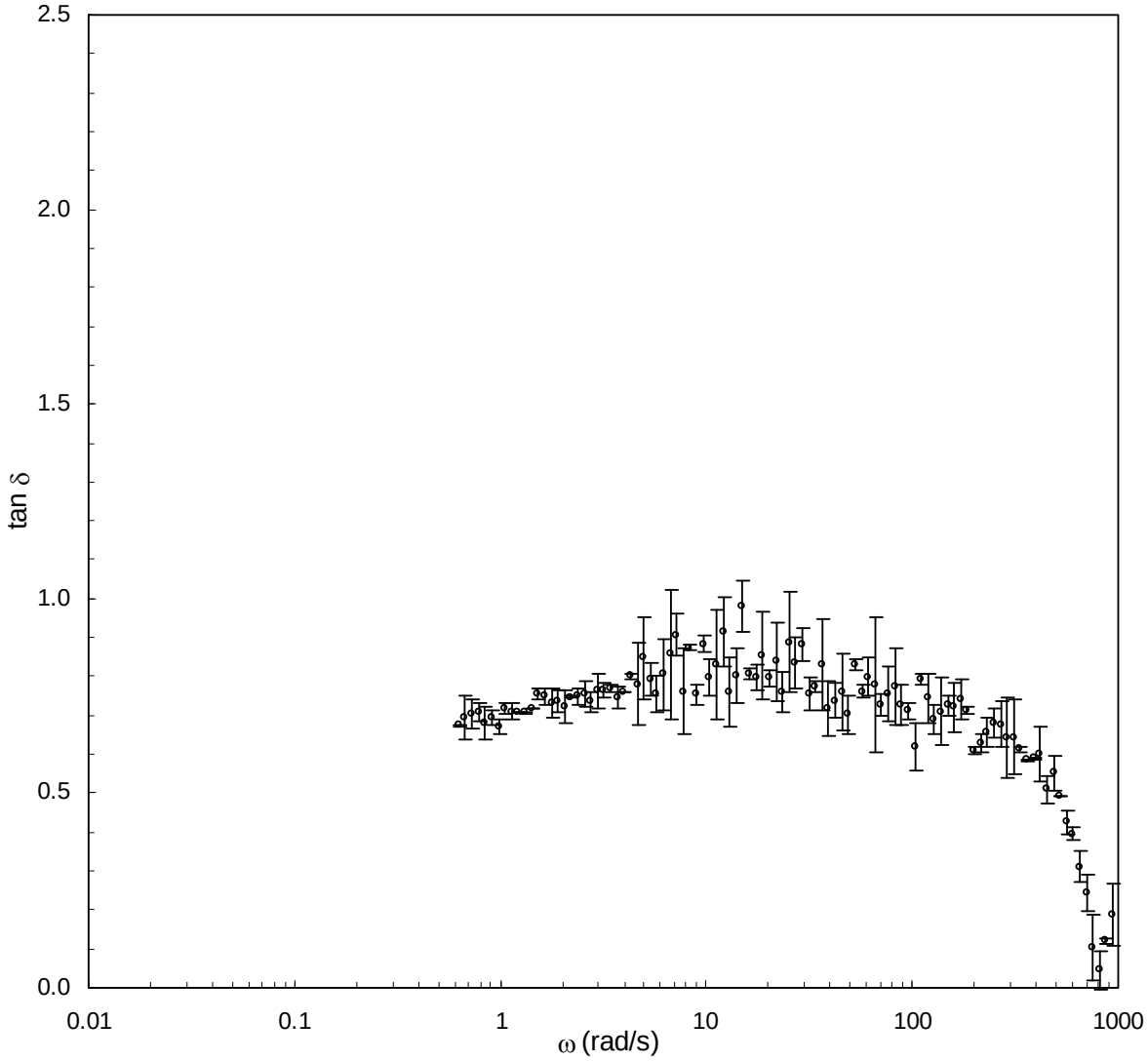

Figure 4.10 Frequency dependence of tan δ for the system with SC/MD = 7:3 and NaCit/SC = 0.2. Data are means of two replicates and the error bars reflect standard deviations.

4.4.3 Morphological characteristics

SEM images of glass-forming components—sucrose and maltodextrin powder—are given in Appendix 4.3. These images were expected to serve as references for the crystalline and amorphous states, respectively. Sucrose powder was obtained by grinding crystalline sucrose. Maltodextrin powder was imaged as received. Dry maltodextrin with DE value of around 20 exists in amorphous form due to the polydispersity of dextrose polymer chains inhibit crystallization (Fitzpatrick et al., 2010). The images of crystalline sucrose powder (Figure A4.3.1) show large particles with sharp edges and numerous small particles due to highly-brittle nature of sucrose crystal. In contrast, amorphous maltodextrin images (Figure A4.3.2) show particles with round edges and smooth-looking surface.

Given in Appendix 4.4 are the SEM images of the bioglass samples. It was difficult to determine the effect of matrix components from visual examination of the obtained images. In general, samples with high moisture content appeared smoother compared to samples of the same components at low moisture content. For the most part, the particles of samples with high sucrose concentration are smaller than those of the samples with high maltodextrin concentration suggesting brittle and ductile characters of the corresponding systems. Like synthetic polymers, intermolecular interactions and entanglements might contribute to the characteristic of maltodextrin. However, when Na citrate was added to the bioglass, there are more small particles as compared to in the system without Na citrate indicating increased brittleness. This could be due to the interference of Na citrate on intermolecular interaction of maltodextrin.

4.5 Conclusions

Using mechanical spectroscopy technique, it was possible to detect the changes in rheological properties and molecular process even with small variation in the composition of rubbery amorphous sucrose-maltodextrin-Na citrate system. Maltodextrin contributed to elastic or solid-like characteristic. The elastic-dominant nature of the system with high maltodextrin concentration suggests that molecular motions of maltodextrin primarily involve stretching and bending of glycosidic linkages. The large number of strong glycosidic linkages presenting in maltodextrin might be responsible for increasing the rigidity of the system as they could restrict the movement of pyranose rings more strongly than the hydrogen bonds (Imamura et al., 2006). In contrast, sucrose gave rise to viscous or liquid-like characteristic which suggests that the molecular motions of sucrose mainly result in the generation of heat which then dissipates during deformation. The addition of Na citrate to sucrose-maltodextrin mixture could reduce molecular mobility of the system in the state of rubbery amorphous. This finding suggests that Na citrate tended to interact more with sucrose than with maltodextrin. The molecular interaction between Na citrate and sucrose might result in the formation of large clusters which could hinder matrix mobility as manifested in the mechanical relaxation process. The plasticization effect due to the slight increase in moisture content was also observed from mechanical relaxation process.

It was difficult to determine the effects of individual components on the characteristic of sucrose-maltodextrin-Na citrate mixture from examining the SEM images. However, the appearance of smaller particle size in the system with high maltodextrin concentration suggests the possible effect of Na citrate in interfering with molecular interactions of maltodextrin.

4.6 References

Alexander, K. and King, C. J. (1985). "Factors governing surface morphology of spray-dried amorphous substances." Drying Technology **3**(3): 321 - 348.

Champion, D., Le Meste, M. and Simatos, D. (2000). "Towards an improved understanding of glass transition and relaxations in foods: molecular mobility in the glass transition range." Trends in Food Science & Technology **11**(2): 41-55.

Chronakis, I. S. (1998). "On the molecular characteristics, compositional properties, and structural-functional mechanisms of maltodextrins: A review." Critical Reviews in Food Science and Nutrition **38**(7): 599 - 637.

Fitzpatrick, J. J., Descamps, N., O'Meara, K., Jones, C., Walsh, D. and Spitere, M. (2010). "Comparing the caking behaviours of skim milk powder, amorphous maltodextrin and crystalline common salt." Powder Technology **204**(1): 131-137.

Gejl-Hansen, F. and Flink, J. M. (1977). "Freeze-dried carbohydrate containing oil-in-water emulsions: Microstructure and fat distribution." Journal of Food Science **42**(4): 1049-1055.

Hermansson, A. M. and Langton, M. (1994). Electron microscopy. Chpt. 6. Physical Techniques for the Study of Food Biopolymers S. B. Ross-Murphy. New York, Chapman & Hall**:** 277-341.

Imamura, K., Sakaura, K., Ohyama, K.-i., Fukushima, A., Imanaka, H., Sakiyama, T. and Nakanishi, K. (2006). "Temperature scanning FTIR analysis of hydrogen bonding states of various saccharides in amorphous matrixes below and above their glass transition temperatures." The Journal of Physical Chemistry B **110**(31): 15094-15099.

Kasapis, S. and Sablani, S. S. (2005). "A fundamental approach for the estimation of the mechanical glass transition temperature in gelatin." International Journal of Biological Macromolecules **36**(1-2): 71-78.

Kilburn, D., Claude, J., Schweizer, T., Alam, A. and Ubbink, J. (2005). "Carbohydrate polymers in amorphous states: An integrated thermodynamic and nanostructural investigation." Biomacromolecules **6**(2): 864-879.

McPherson, A. E. and Seib, P. A. (1997). "Preparation and properties of wheat and corn starch maltodextrins with a low dextrose equivalent." Cereal Chemistry **74**(4): 424-430.

Montgomery, D. C. (2005). Design and Analysis of Experiments. 6th. New Jersey: John Wiley & Sons, Inc.

Morris, V. J. and Miles, M. J. (1994). Birefringent techniques. Chpt. 5. Physical Techniques for the Study of Food Biopolymers. S. B. Rose-Murphy. New York, Chapman & Hall**:** 215-275.

Ngai, K. L. and Plazek, D. J. (1995). "Identification of different modes of molecular motion in polymers that cause thermorheological complexity." Rubber Chemistry and Technology **68**(3): 376-434.

Noel, T. R., Parker, R. and Ring, S. G. (2000). "Effect of molecular structure and water content on the dielectric relaxation behaviour of amorphous low molecular weight carbohydrates above and below their glass transition." Carbohydrate Research **329**(4): 839-845.

Radosta, S. and Schierbaum, F. (1990). "Polymer-water interaction of maltodextrins. Part III: Non-freezable water in maltodextrin solutions and gels." Starch - Stärke **42**(4): 142-147.

Radosta, S., Schierbaum, F., Reuther, F. and Anger, H. (1989). "Polymer-water interaction of maltodextrins. Part I: Water vapour sorption and desorption of maltodextrin powders." Starch - Stärke **41**(10): 395-401.

Radosta, S., Schierbaum, F. and Yuriev, W. P. (1989). "Polymer-water interaction of maltodextrins. Part II: NMR study of bound water in liquid maltodextrin-water systems." Starch - Stärke **41**(11): 428-430.

Roos, Y. (1995). Phase transitions in foods. San Diego: Academic Press.

Shinyashiki, N., Shinohara, M., Iwata, Y., Goto, T., Oyama, M., Suzuki, S., Yamamoto, W., Yagihara, S., Inoue, T., Oyaizu, S., Yamamoto, S., Ngai, K. L. and Capaccioli, S. (2008). "The glass transition and dielectric secondary relaxation of fructose-water mixtures." The Journal of Physical Chemistry B **112**(48): 15470-15477.

Wetton, R. E. (1984). "Dynamic mechanical method in the characterization of solid polymers." Polymer Testing **4**(2-4): 117-129.

Windham, W. R., Kays, S. E. and Barton, F. E. (1997). "Effect of cereal product residual moisture content on total dietary fiber determined by near-infrared reflectance spectroscopy." Journal of Agricultural and Food Chemistry **45**(1): 140-144.

Young, R. J. and Lovell, P. A. (1991). Introduction to polymers. 2. Cheltenham: Stanley Thornes.

APPENDIX 4

Appendix 4.1 Statistical analysis for the moisture content

Nomenclature for factors:

NaCit/SC: Na citrate/sucrose mole ratio.
SC/MD: Sucrose/maltodextrin mass ratio.
MC: Moisture content (%wb) of glass samples.

Table A4.1.1 Factors and levels for the analysis of moisture content

Between-Subjects Factors

		Value Label	N
NaCit/SC	1	0	6
	2	0.1	6
	3	0.2	6
SC/MD	1	7:3	6
	2	5:5	6
	3	3:7	6

Table A4.1.2 ANOVA table for the analysis of moisture content

Tests of Between-Subjects Effects

Dependent Variable:MC

Source	Type III Sum of Squares	df	Mean Square	F	Sig.
Corrected Model	18.390[a]	8	2.299	113.767	.000
Intercept	1754.886	1	1754.886	86851.671	.000
NaCit/SC	4.200	2	2.100	103.939	.000
SC/MD	13.789	2	6.895	341.227	.000
NaCit/SC * SC/MD	.400	4	.100	4.951	.022
Error	.182	9	.020		
Total	1773.458	18			
Corrected Total	18.572	17			

a. R Squared = .990 (Adjusted R Squared = .982)

Table A4.1.3 Effects of factors on moisture content

A: Effect of Citrate_SC (Tukey HSD[a,b])

NaCit/SC	N	MC: Subset		
		1	2	3
0	6	9.3267		
0.1	6		9.7933	
0.2	6			10.5017

Means for groups in homogeneous subsets are displayed.
Based on observed means. The error term is Mean Square(Error) = .020.
a) Uses Harmonic Mean Sample Size = 6. b) Alpha = .05.

B: Effect of SC/MD (Tukey HSD[a,b])

SC_MD	N	Subset		
		1	2	3
7:3	6	8.9783		
5:5	6		9.5817	
3:7	6			11.0617

Means for groups in homogeneous subsets are displayed.
Based on observed means. The error term is Mean Square(Error) = .020.
a) Uses Harmonic Mean Sample Size = 6. b) Alpha = .05.

C: Interaction effect between SC/MD and NaCit/SC (Tukey HSD[a,b])

SC_MD	Citrate_SC	N	Subset		
			1	2	3
7:3	0	2	8.465		
	0.1	2		9.035	
	0.2	2			9.435
5:5	0	2	9.060		
	0.1	2		9.585	
	0.2	2			10.100
3:7	0	2	10.455		
	0.1	2		10.760	
	0.2	2			11.970

Means for groups in homogeneous subsets are displayed.
Based on observed means. The error term is Mean Square(Error) = .020.
a) Uses Harmonic Mean Sample Size = 2. b) Alpha = .05.

Appendix 4.2 Rheological data obtained with the SAOS tests

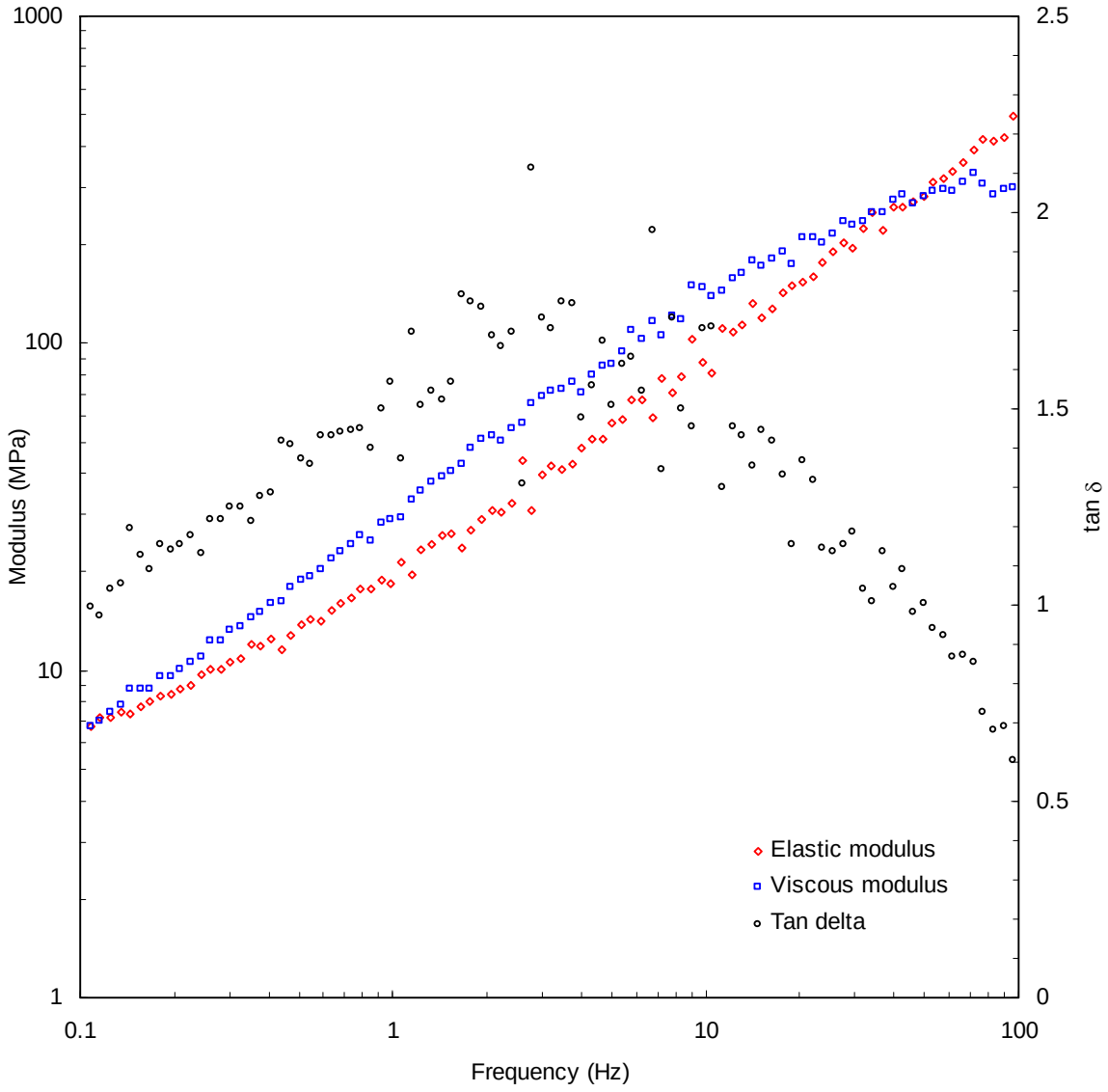

Figure A4.2.1. Dynamic moduli and tan δ as a function of frequency for the bioglass with SC/MD = 7:3, without Na citrate: Replicate 1.

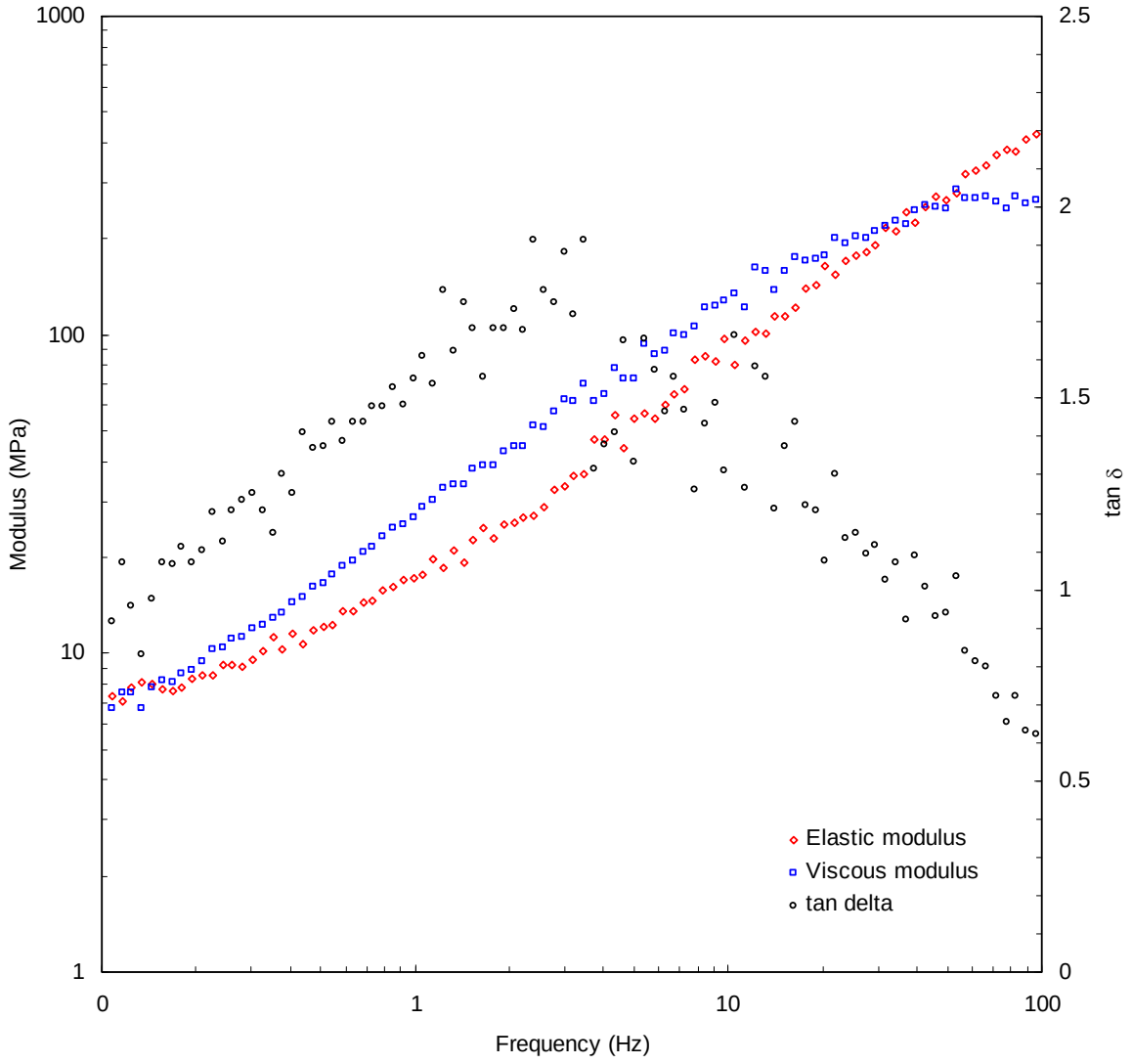

Figure A4.2.2. Dynamic shear moduli and tan δ as a function of frequency for the bioglass with SC/MD = 7:3, without Na citrate: Replicate 2.

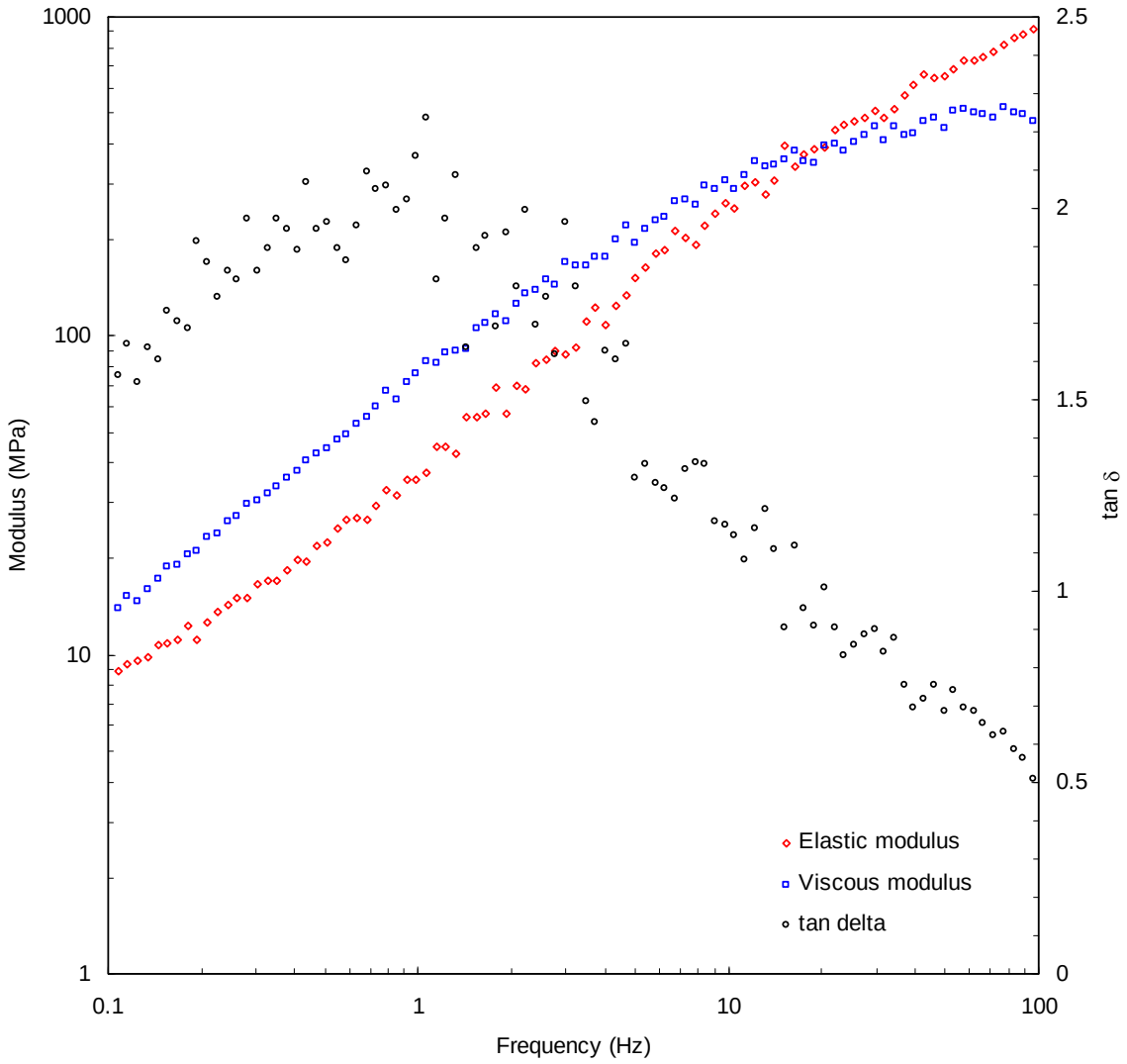

Figure A4.2.3. Dynamic shear moduli and tan δ as a function of frequency for the bioglass with SC/MD = 7:3 and NaCit/SC = 0.1: Replicate 1.

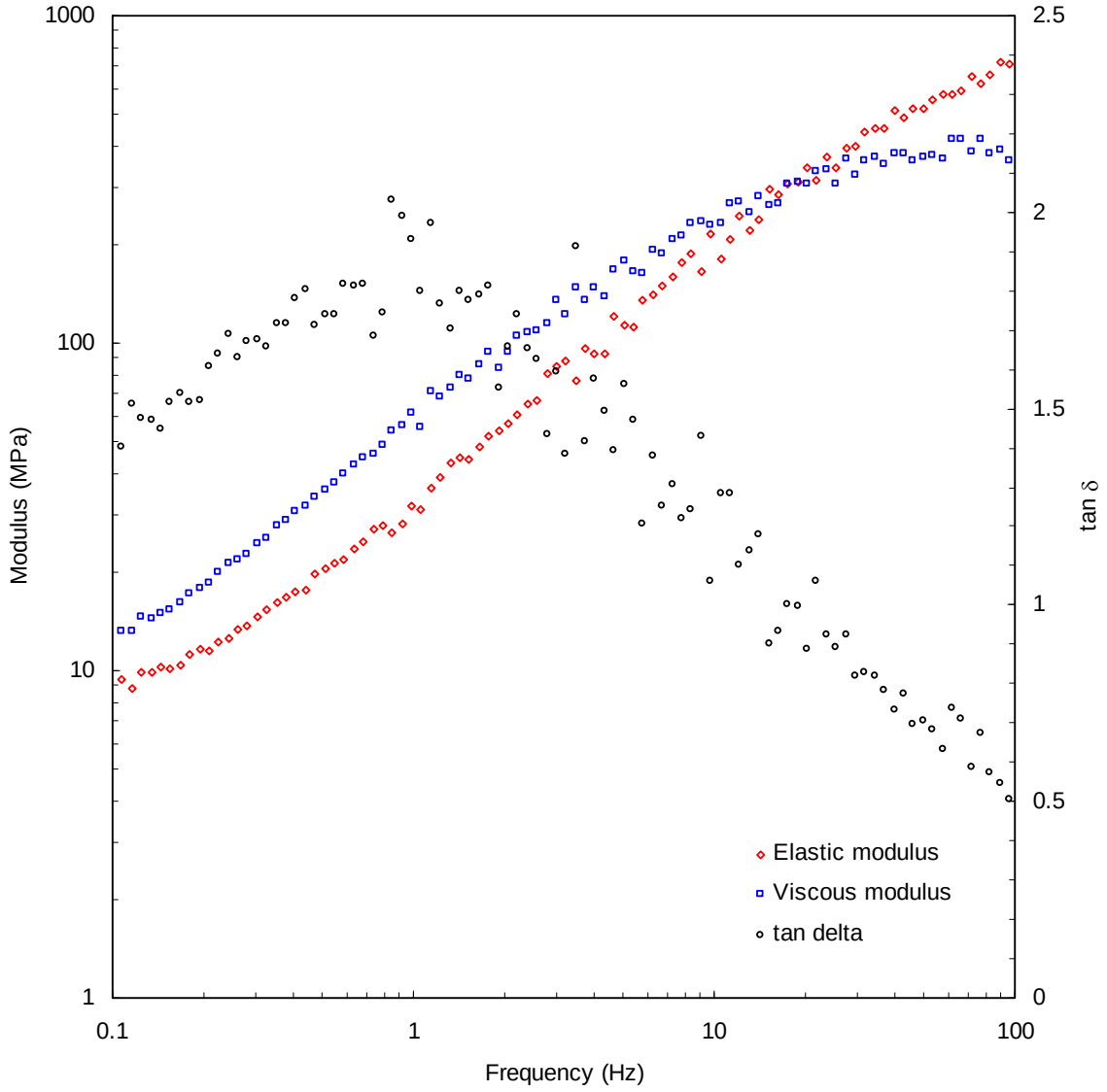

Figure A4.2.4. Dynamic shear moduli and tan δ as a function of frequency for the bioglass with SC/MD = 7:3 and NaCit/SC= 0.1: Replicate 2.

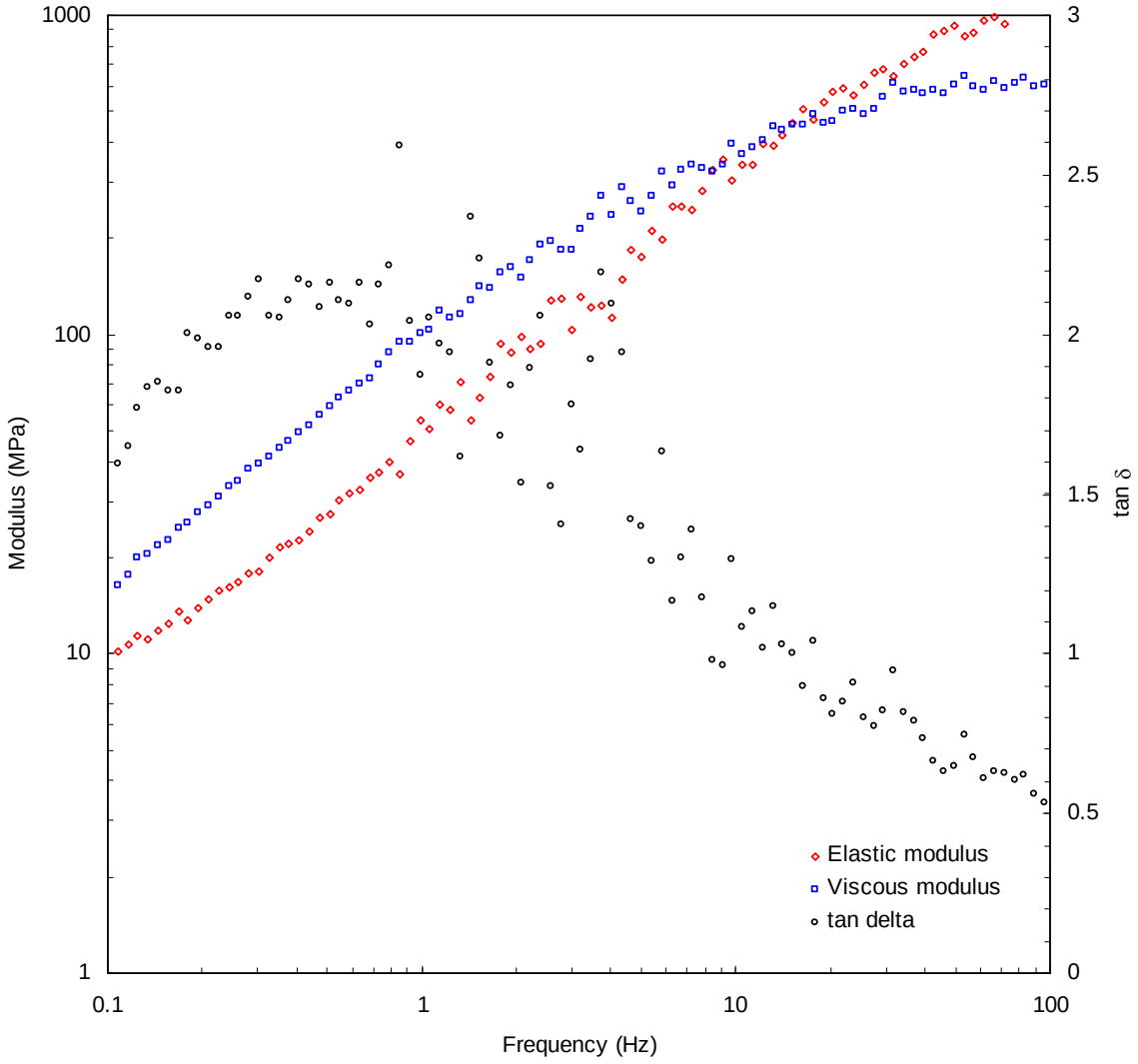

Figure A4.2.5. Dynamic shear moduli and tan δ as a function of frequency for the bioglass with SC/MD = 7:3 and NaCit/SC = 0.2: Replicate 1.

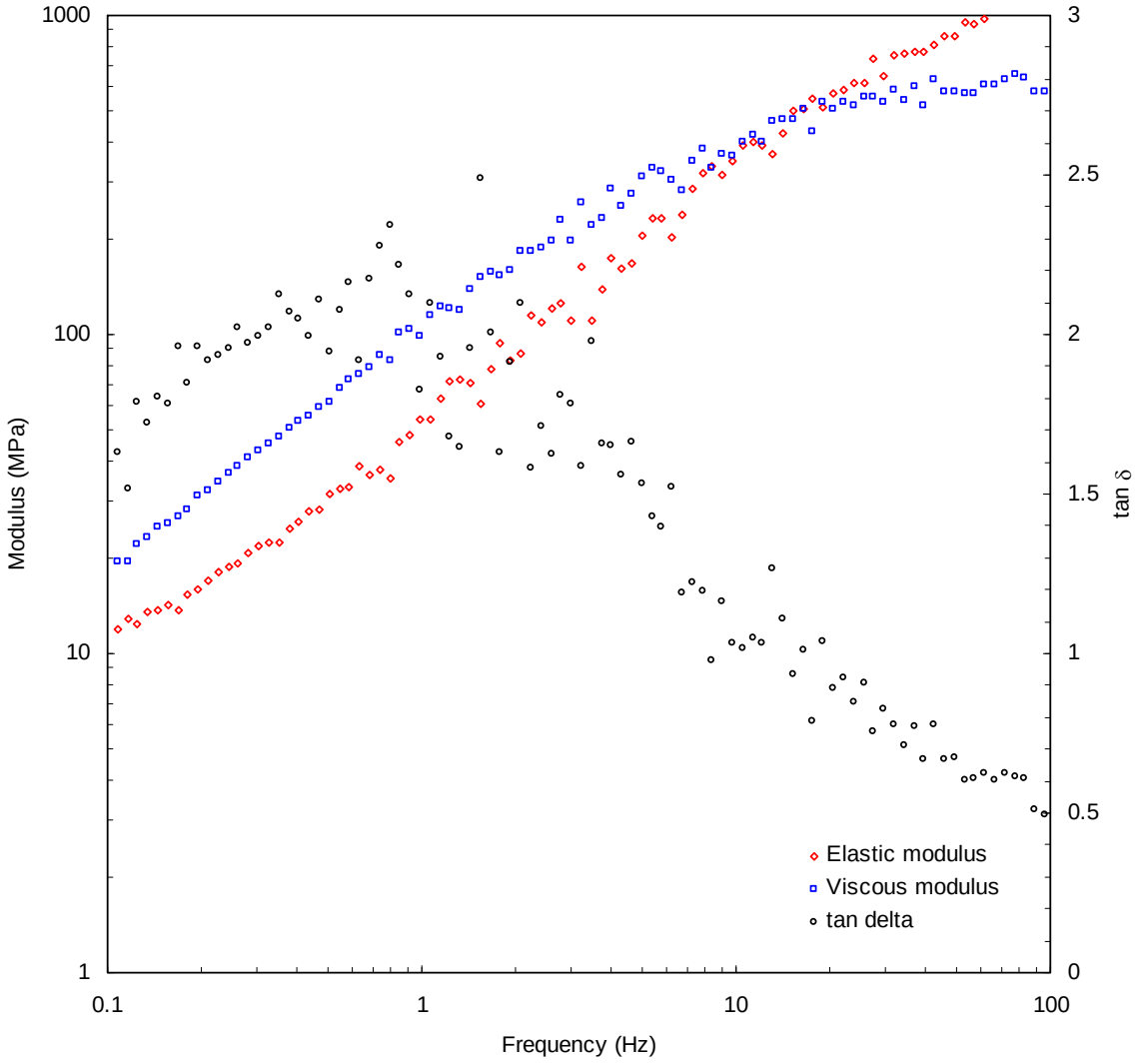

Figure A4.2.6. Dynamic shear moduli and tan δ as a function of frequency for the bioglass with SC/MD = 7:3 and NaCit/SC = 0.2: Replicate 2.

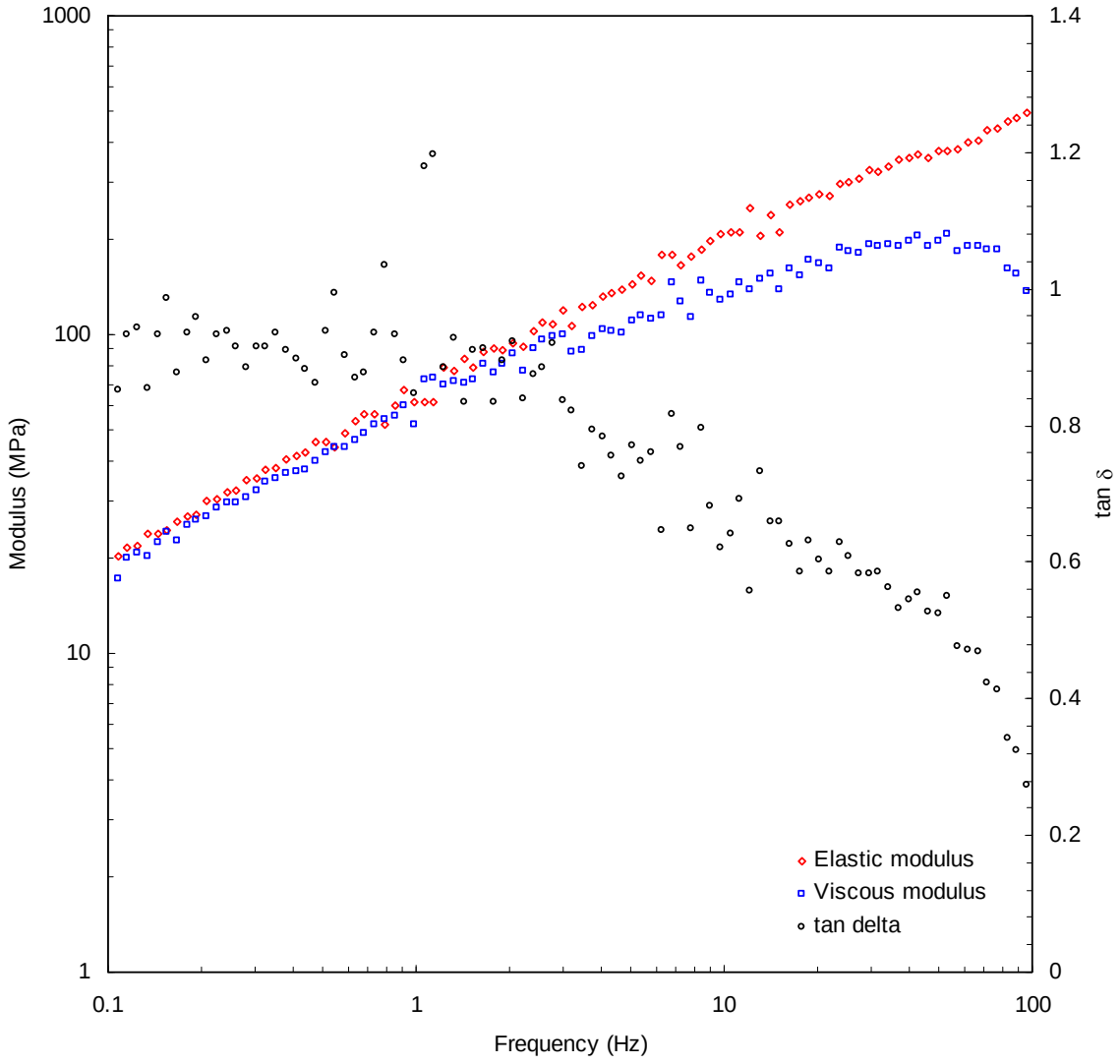

Figure A4.2.7. Dynamic shear moduli and tan δ as a function of frequency for the bioglass with SC/MD = 5:5, without Na citrate: Replicate 1.

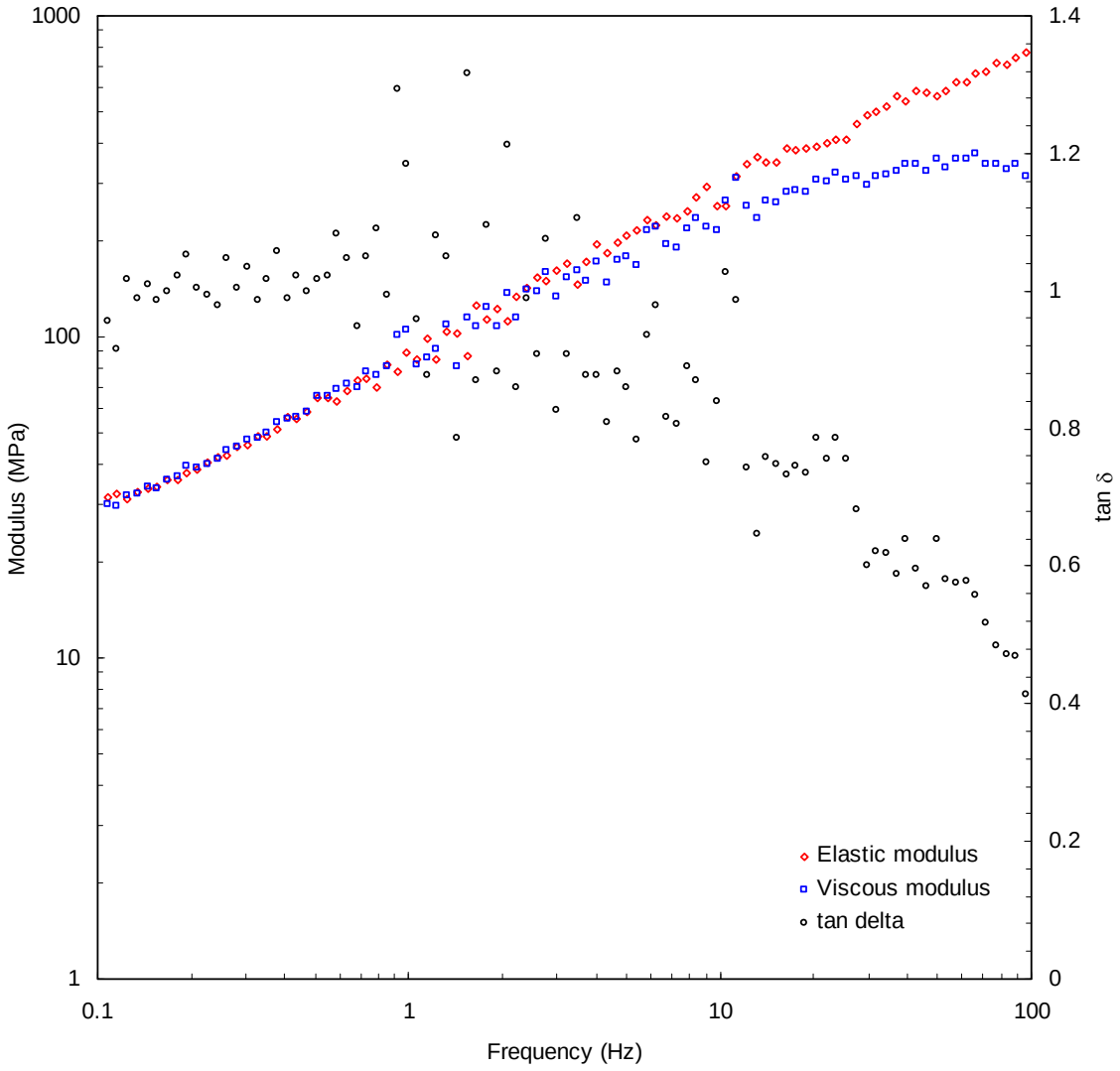

Figure A4.2.8. Dynamic shear moduli and tan δ as a function of frequency for the bioglass with SC/MD = 5:5, without Na citrate: Replicate 2.

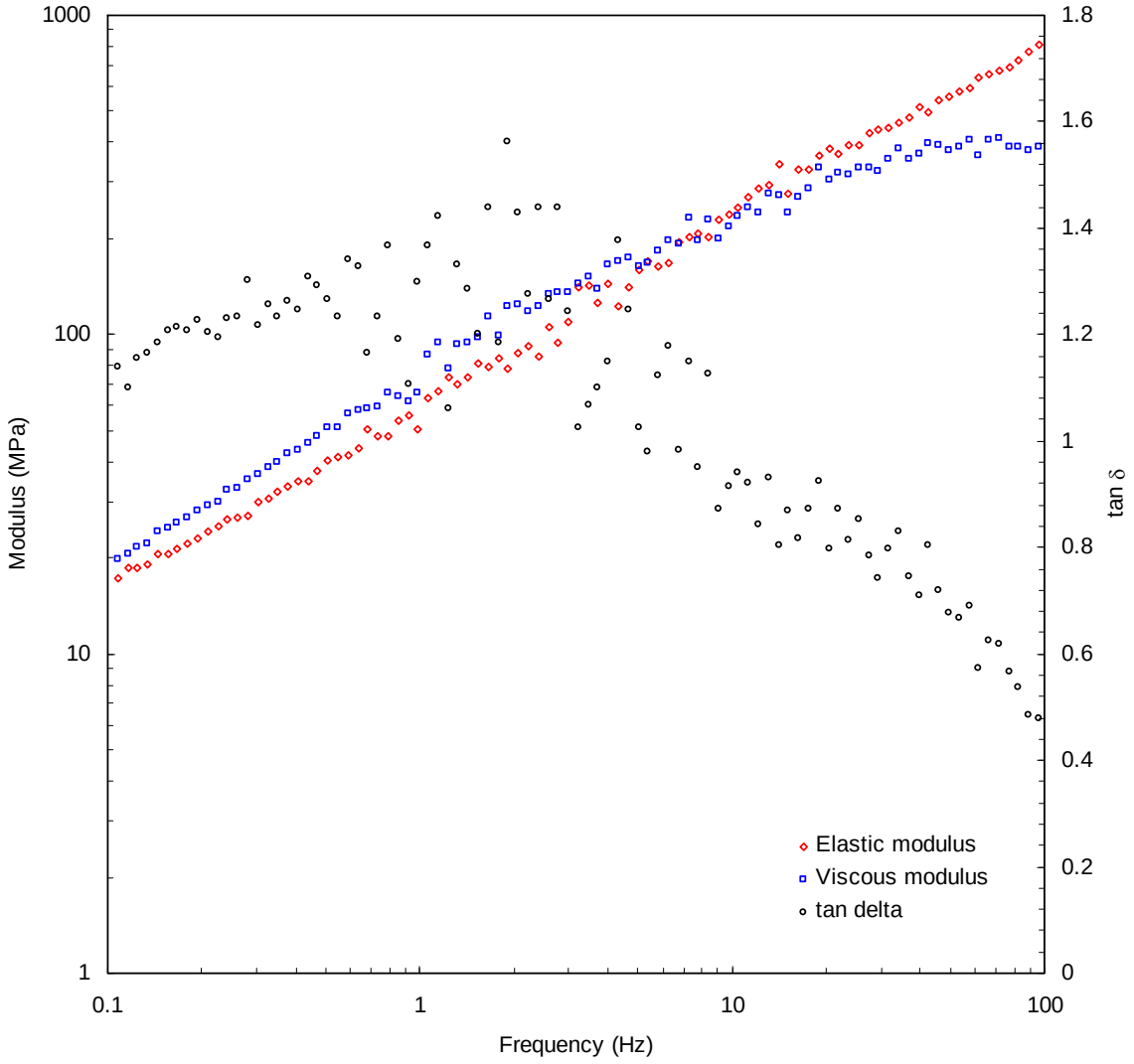

Figure A4.2.9. Dynamic shear moduli and tan δ as a function of frequency for the bioglass with SC/MD = 5:5 and NaCit/SC = 0.1: Replicate 1.

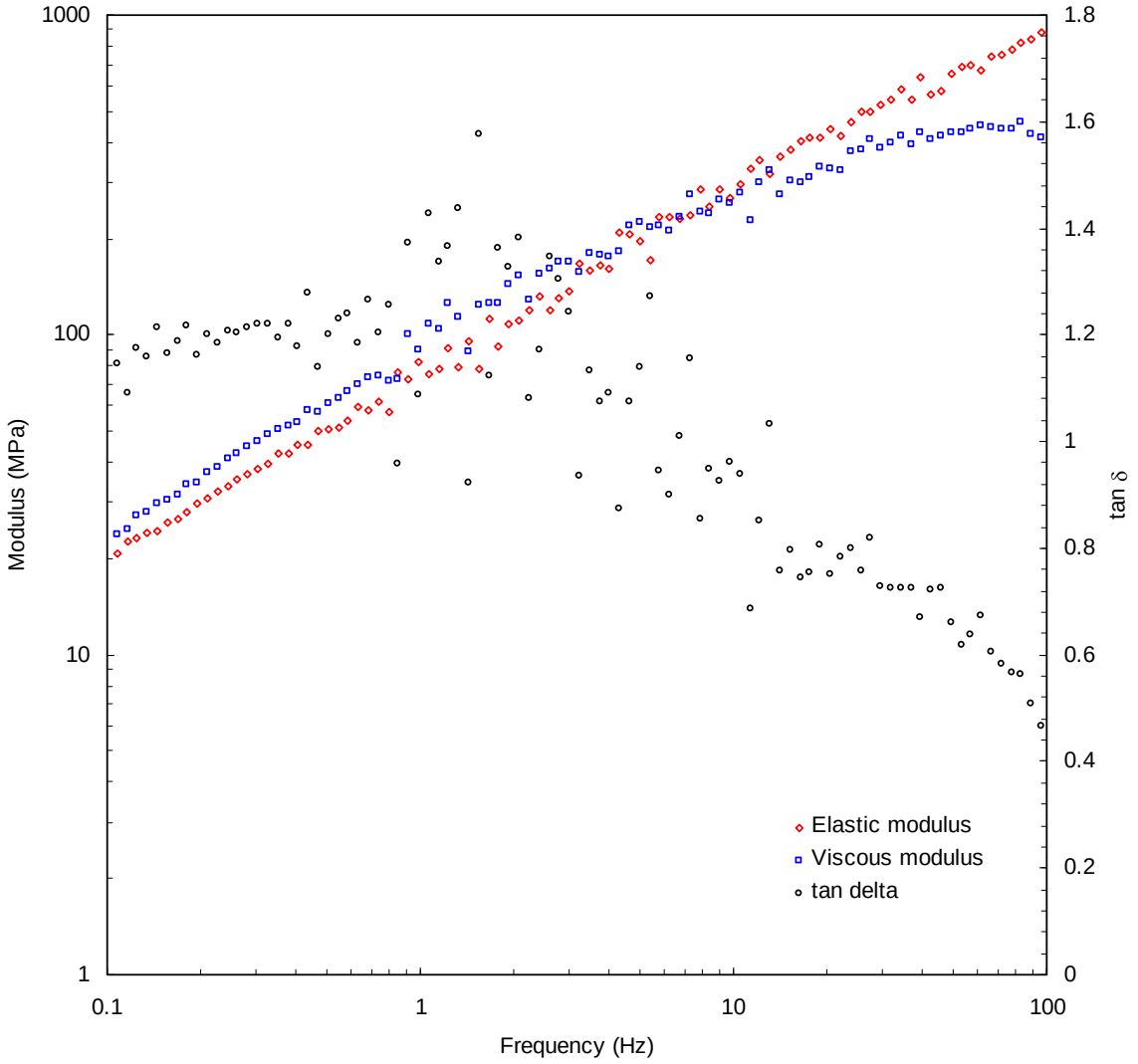

Figure A4.2.10. Dynamic shear moduli and tan δ as a function of frequency for the bioglass with SC/MD = 5:5 and NaCit/SC = 0.1: Replicate 2.

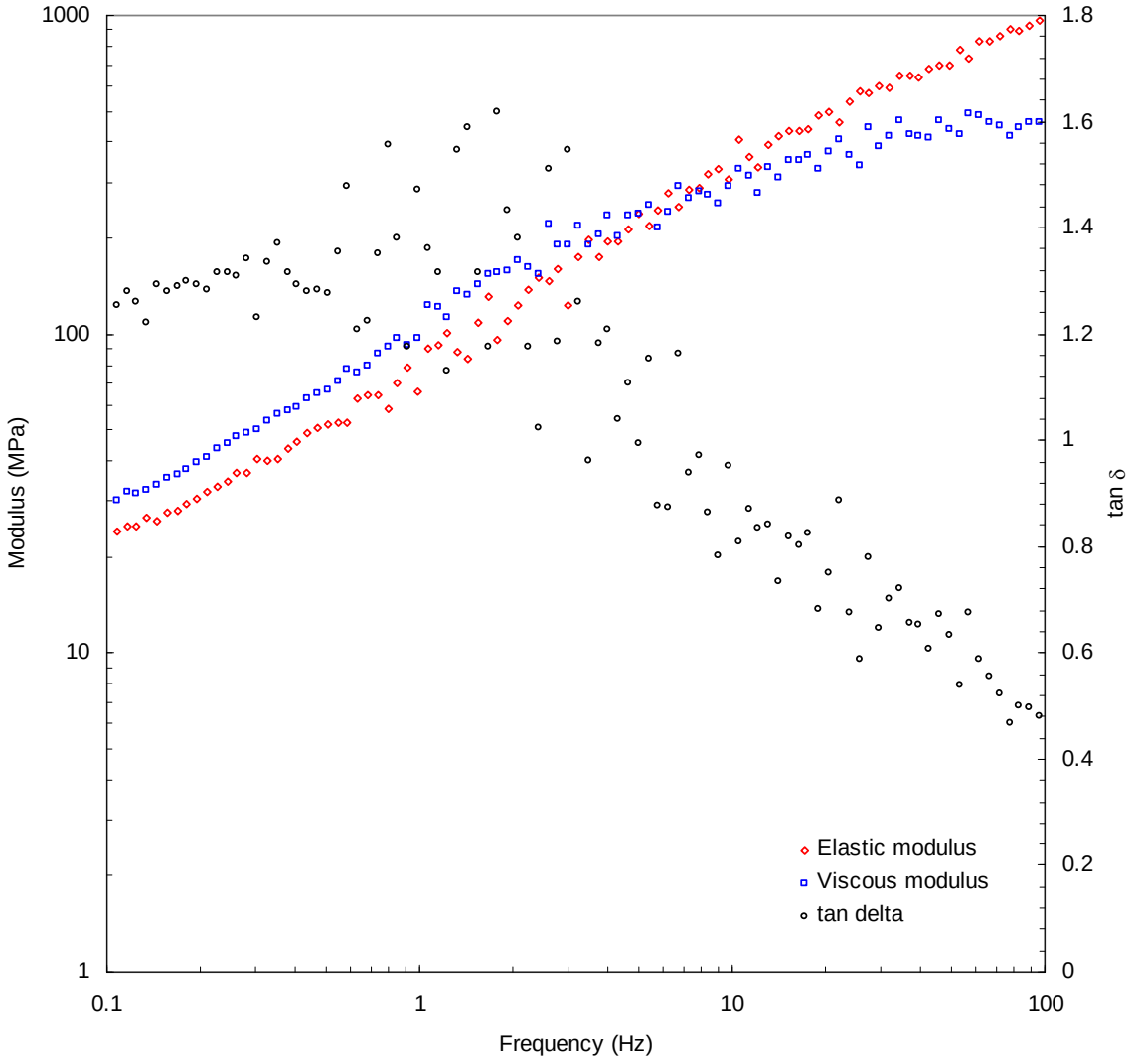

Figure A4.2.11. Dynamic shear moduli and tan δ as a function of frequency for the bioglass with SC/MD = 5:5 and NaCit/SC = 0.2: Replicate 1.

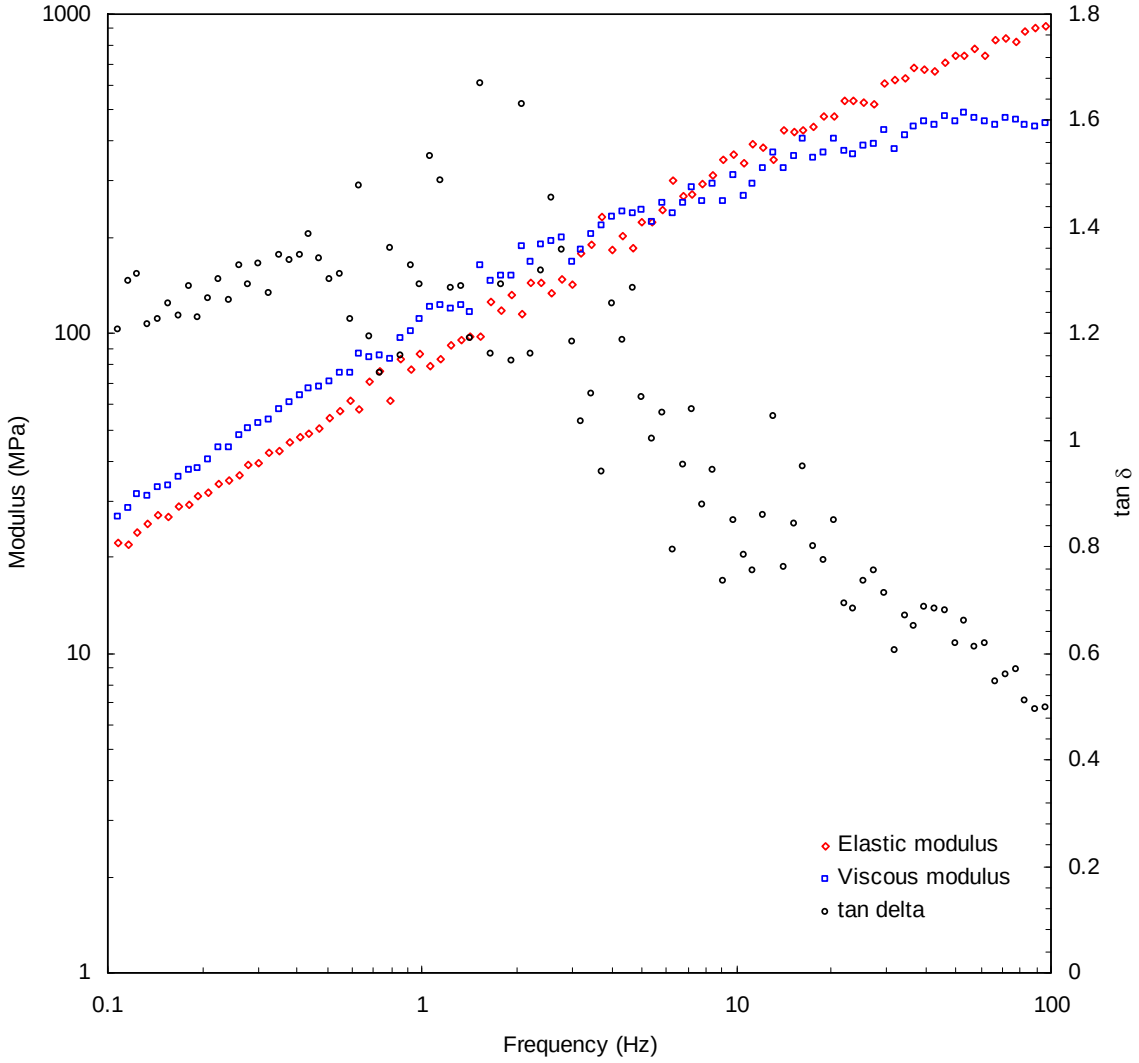

Figure A4.2.12. Dynamic shear moduli and tan δ as a function of frequency for the bioglass with SC/MD = 5:5 and NaCit/SC = 0.2: Replicate 2.

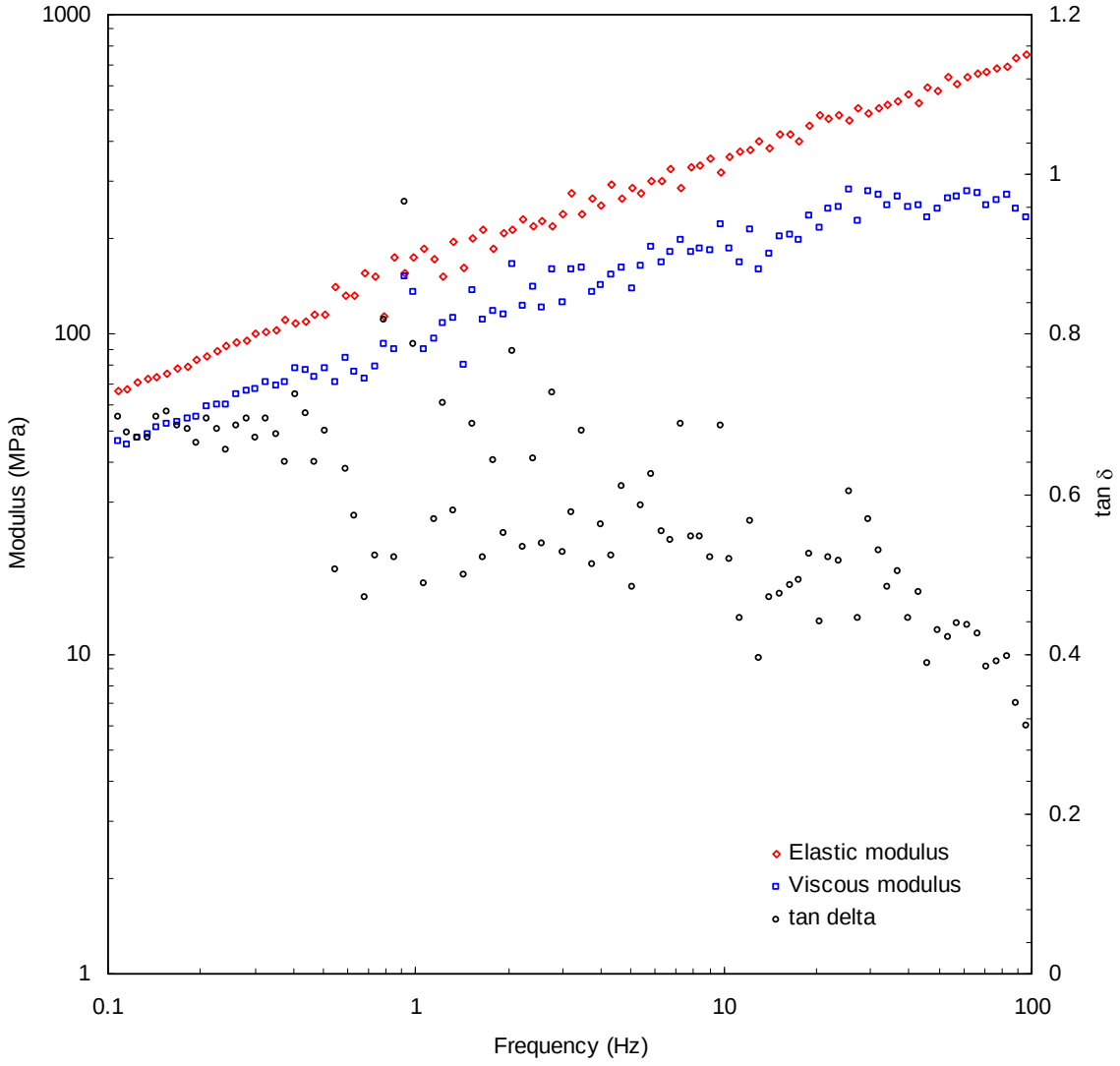

Figure A4.2.13. Dynamic shear moduli and tan δ as a function of frequency for the bioglass with SC/MD = 3:7, without Na citrate: Replicate 1.

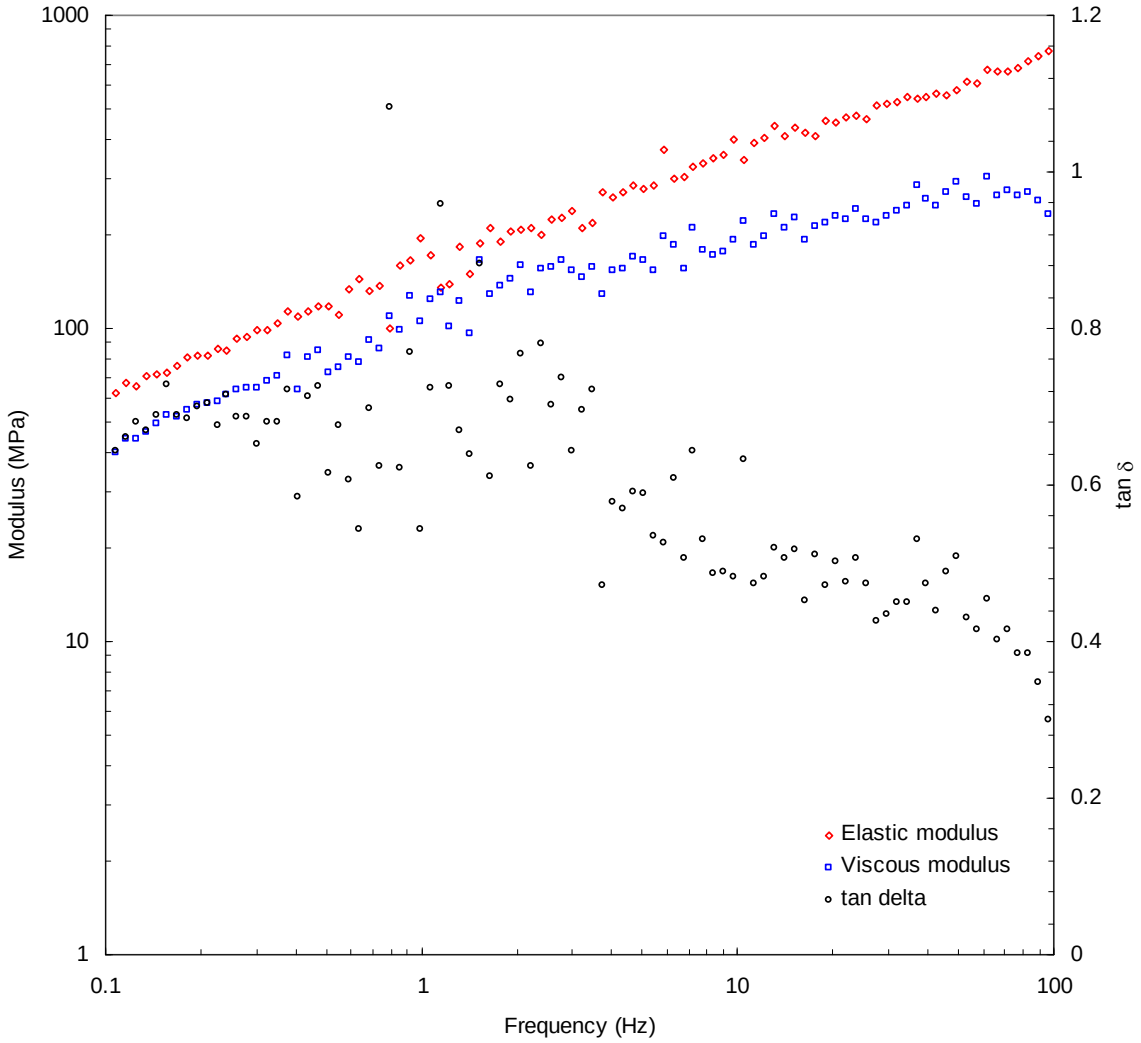

Figure A4.2.14. Dynamic shear moduli and tan δ as a function of frequency for the bioglass with SC/MD = 3:7, without Na citrate: Replicate 2.

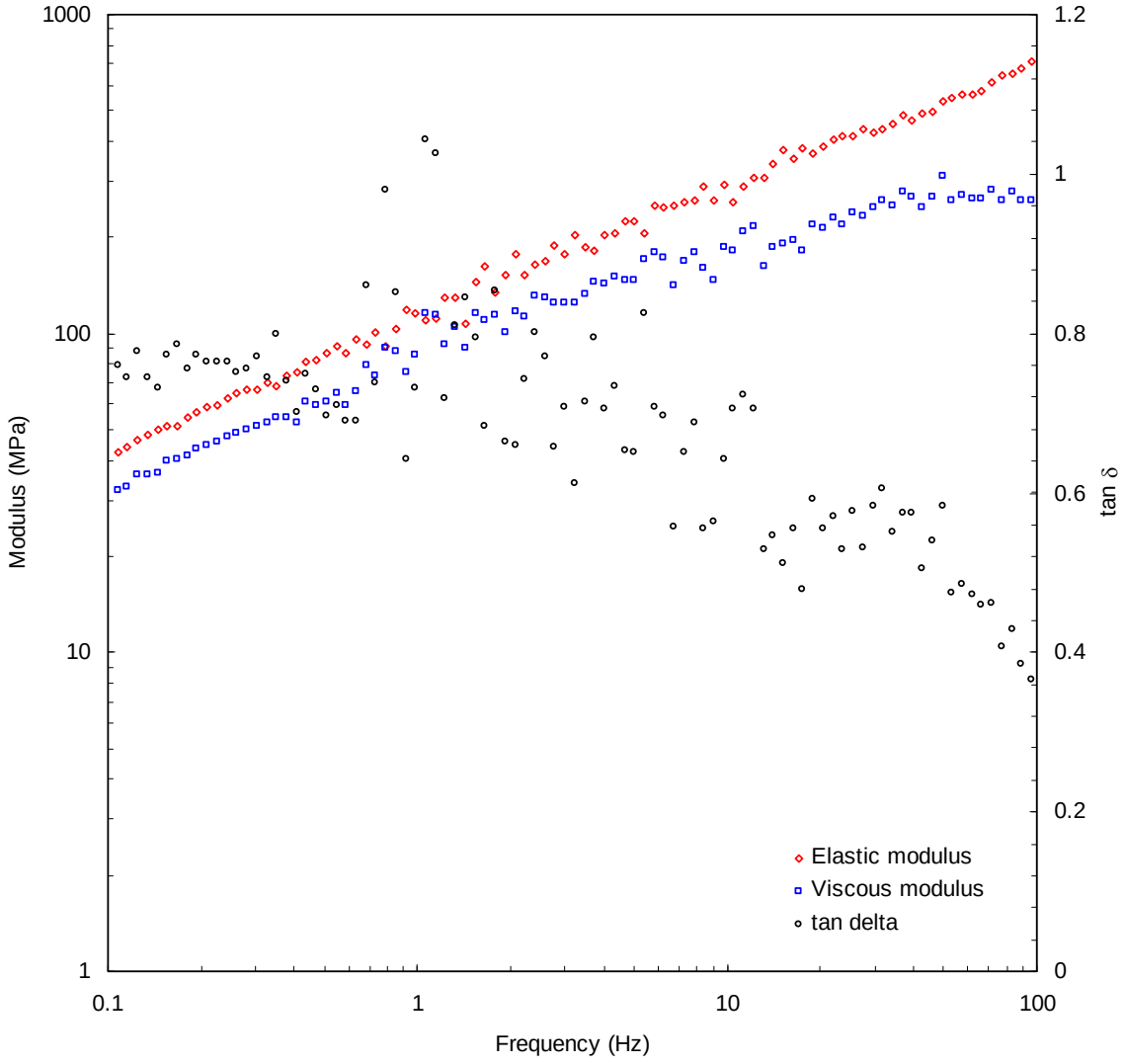

Figure A4.2.15. Dynamic shear moduli and tan δ as a function of frequency for the bioglass with SC/MD = 3:7 and NaCit/SC = 0.1: Replicate 1.

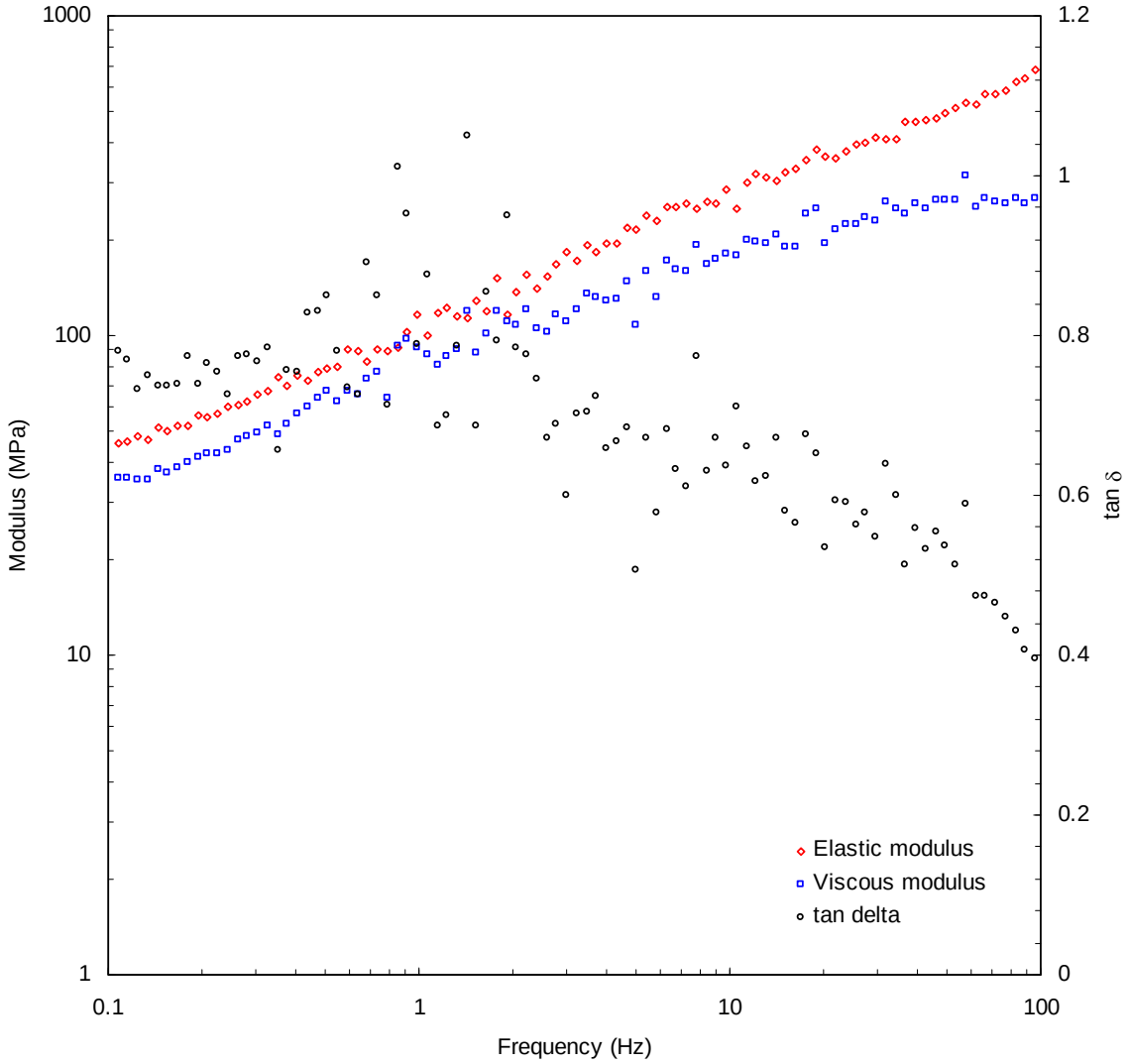

Figure A4.2.16. Dynamic shear moduli and tan δ as a function of frequency for the bioglass with SC/MD = 3:7 and NaCit/SC = 0.1: Replicate 2.

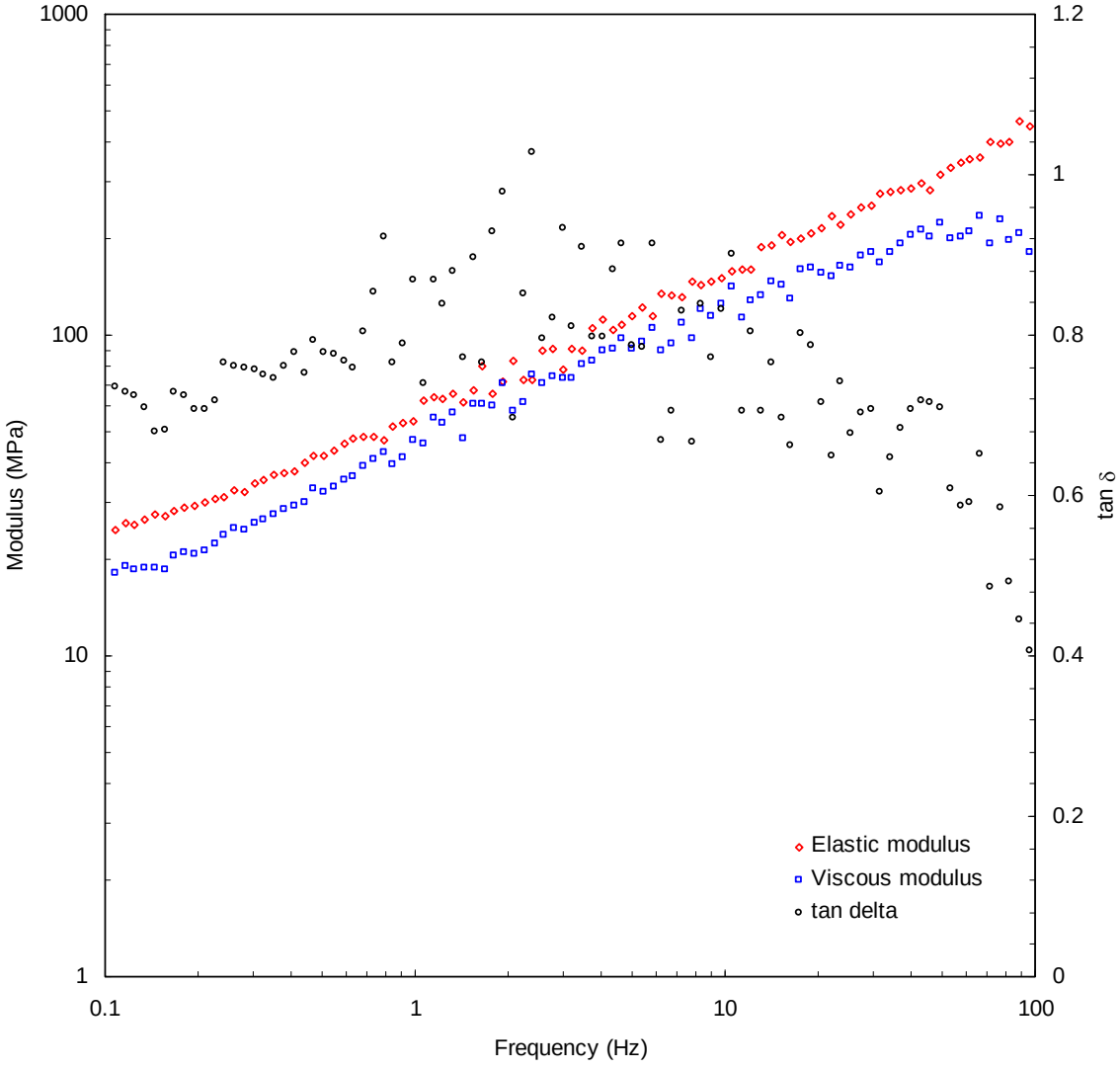

Figure A4.2.17. Dynamic shear moduli and tan δ as a function of frequency for the bioglass with SC/MD = 3:7 and NaCit/SC = 0.2: Replicate 1.

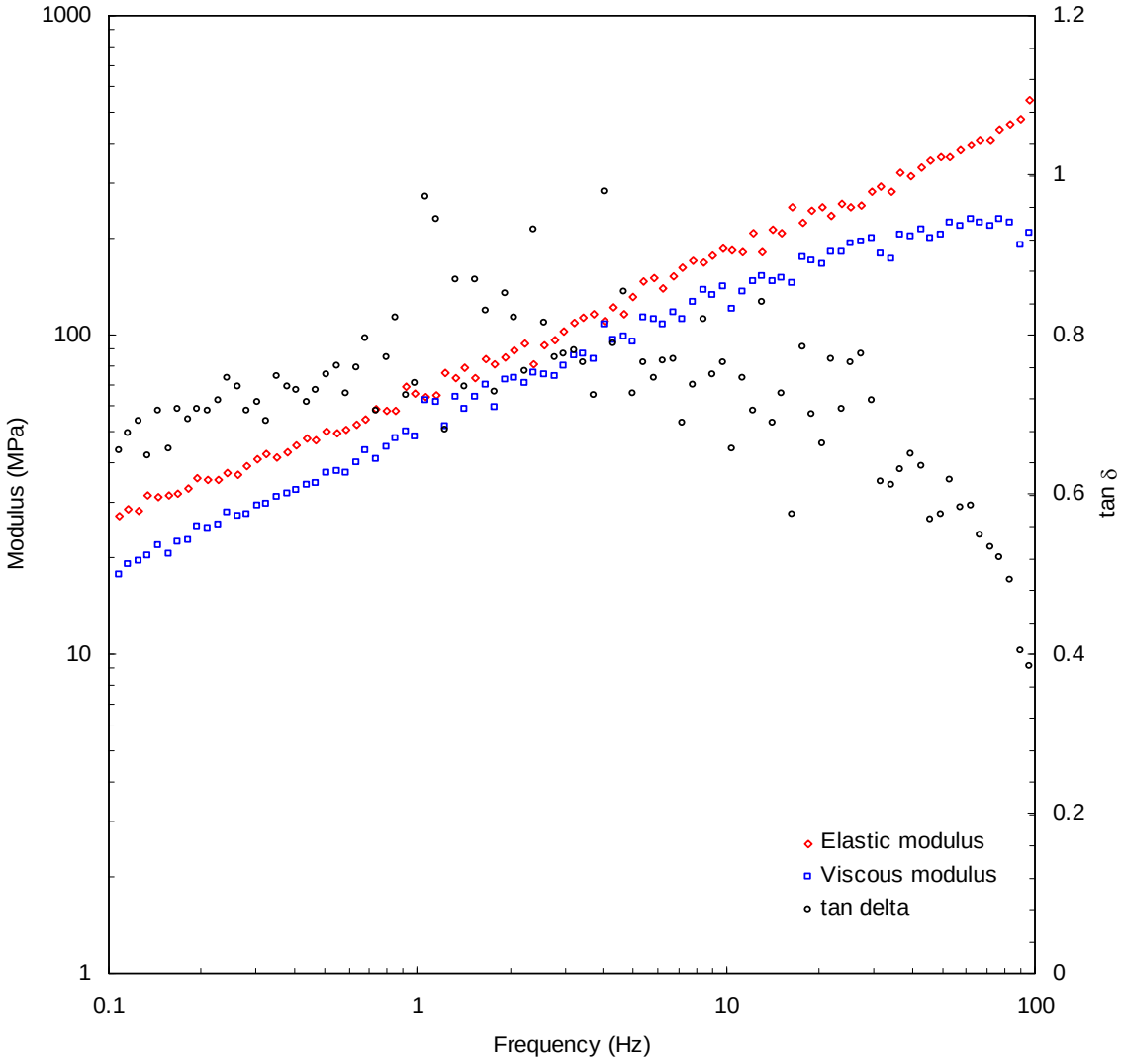

Figure A4.2.18. Dynamic shear moduli and tan δ as a function of frequency for the bioglass with SC/MD = 3:7 and NaCit/SC = 0.2: Replicate 2.

Appendix 4.3 SEM images of glass forming components for a bioglass model system

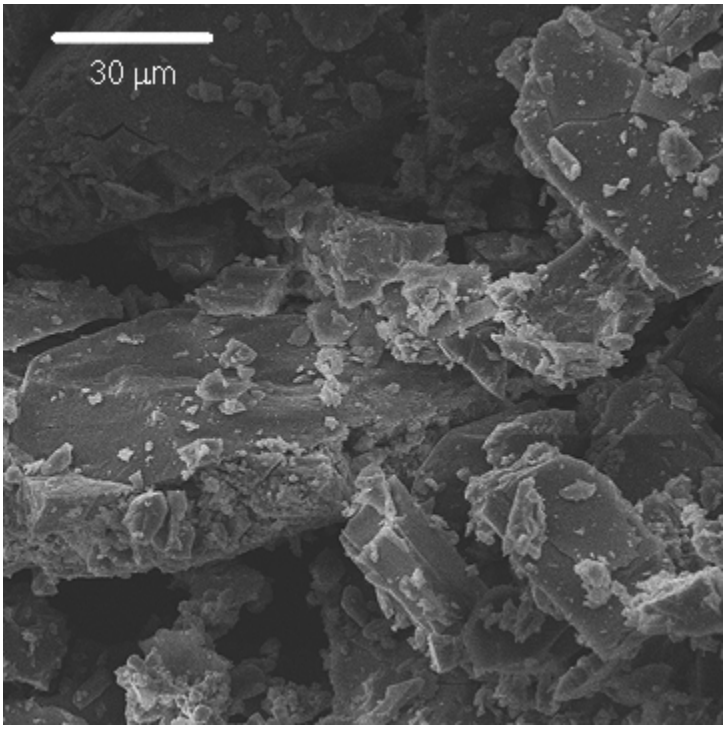

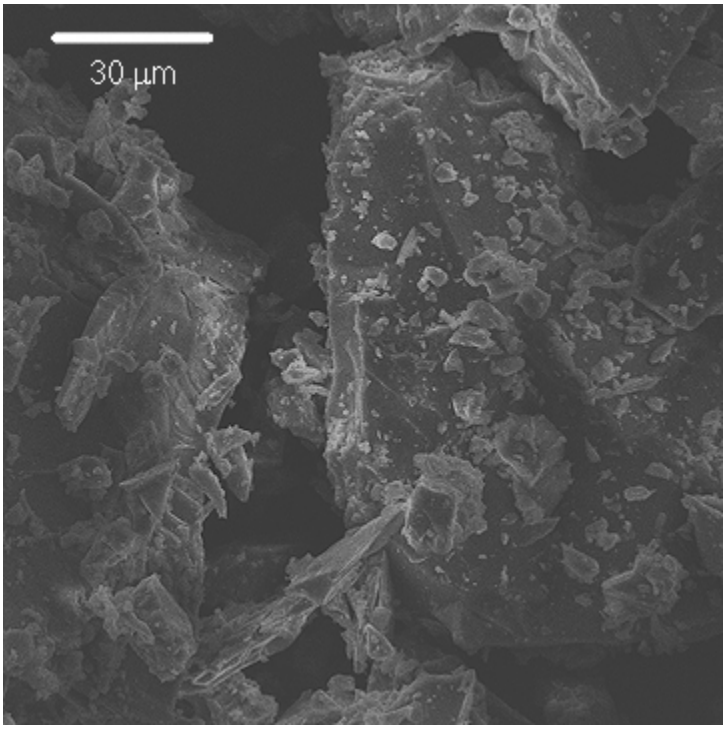

Figure A4.3.1 SEM images of crystallize sucrose (ground)—two measurements.

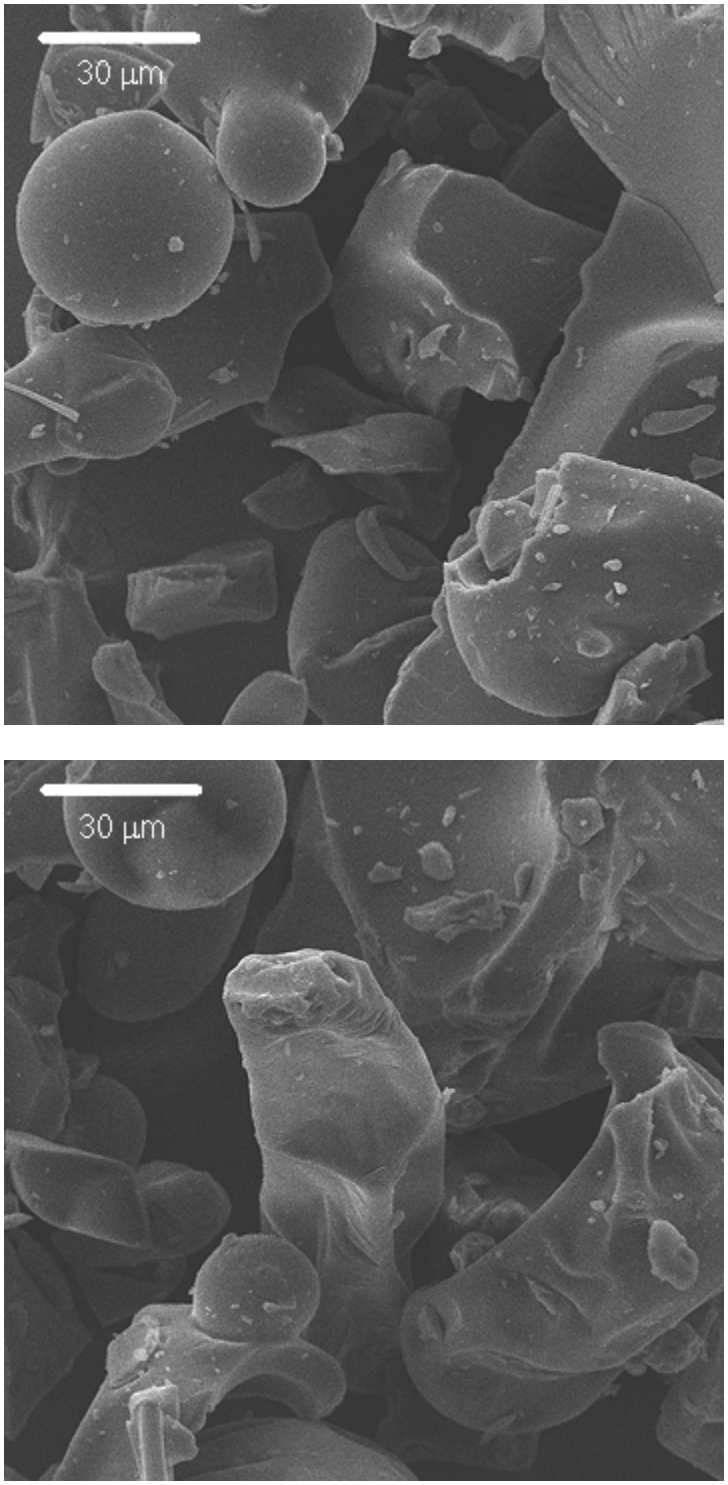

Figure A4.3.2 SEM images of maltodextrin powder—two measurements.

Appendix 4.4 SEM images of bioglass samples

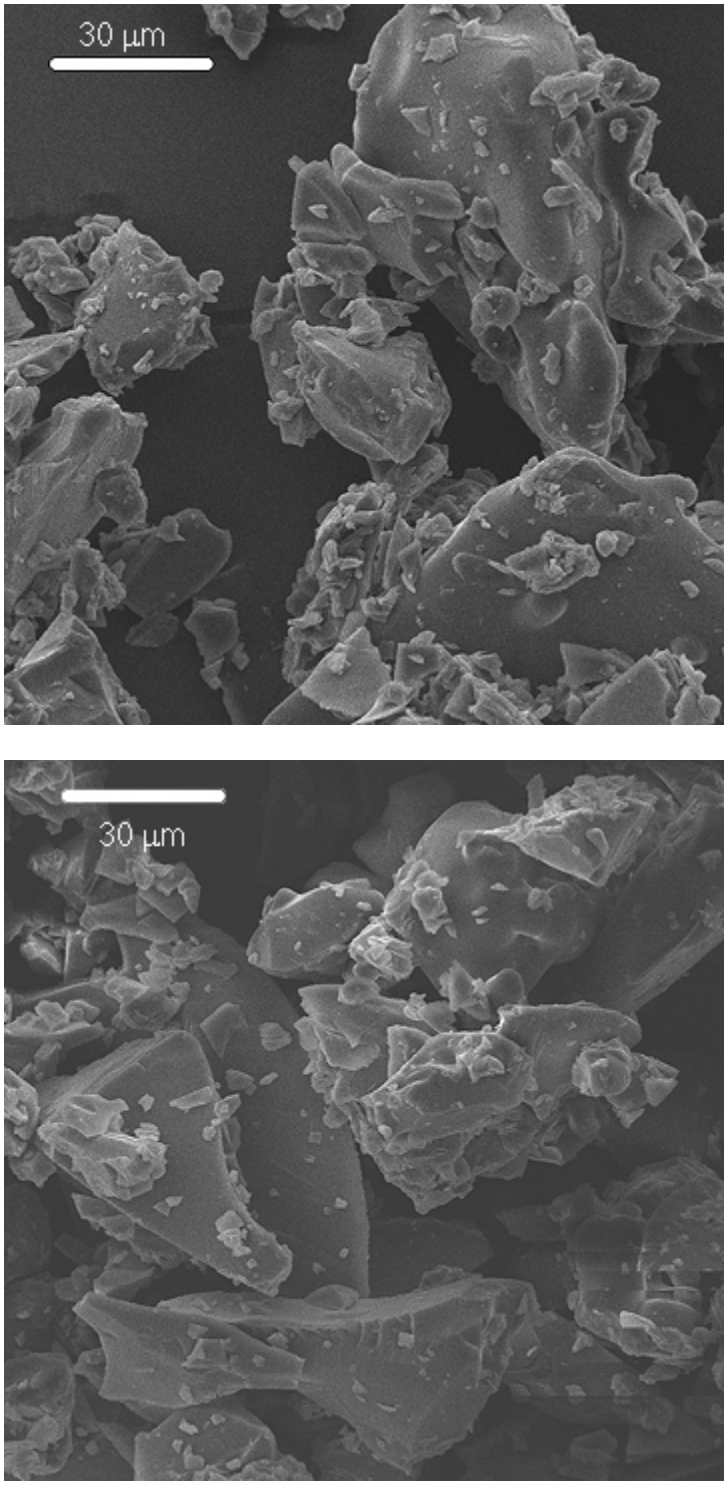

Figure A4.4.1 SEM images of the bioglass with SC/MD = 7:3, without Na citrate, equilibrated in the atmosphere over saturated LiCl solution (~11%RH).

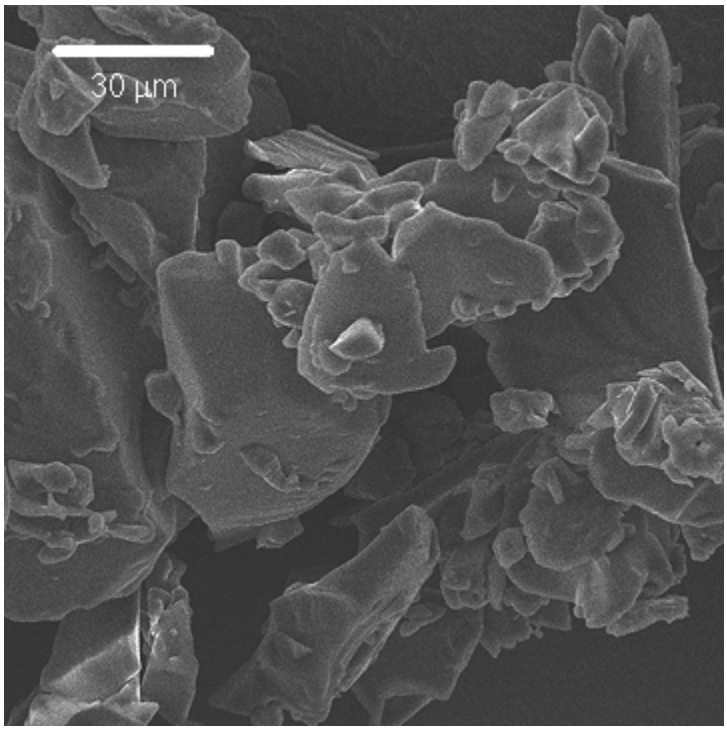

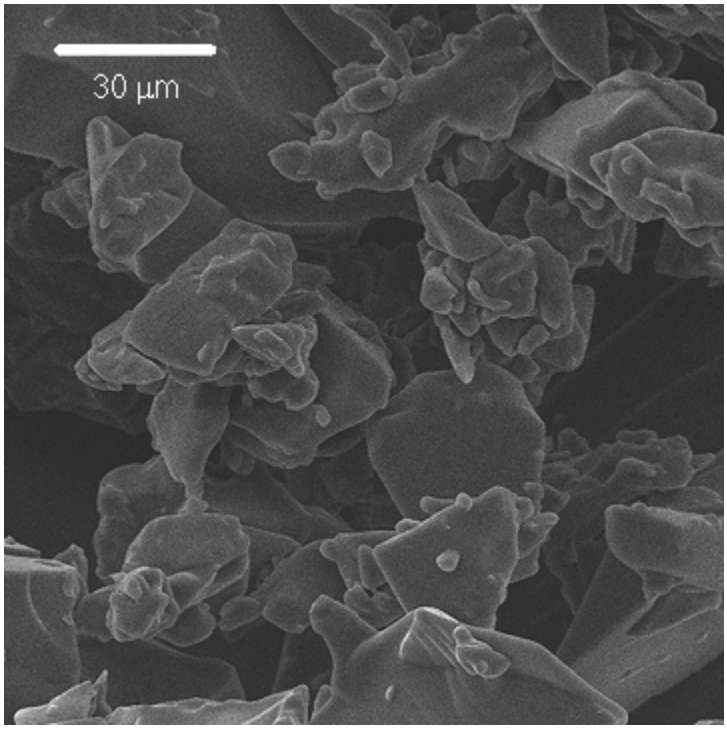

Figure A4.4.2 SEM images of the bioglass with SC/MD = 7:3, without Na citrate, equilibrated in the atmosphere over P_2O_5 powder (~1%RH).

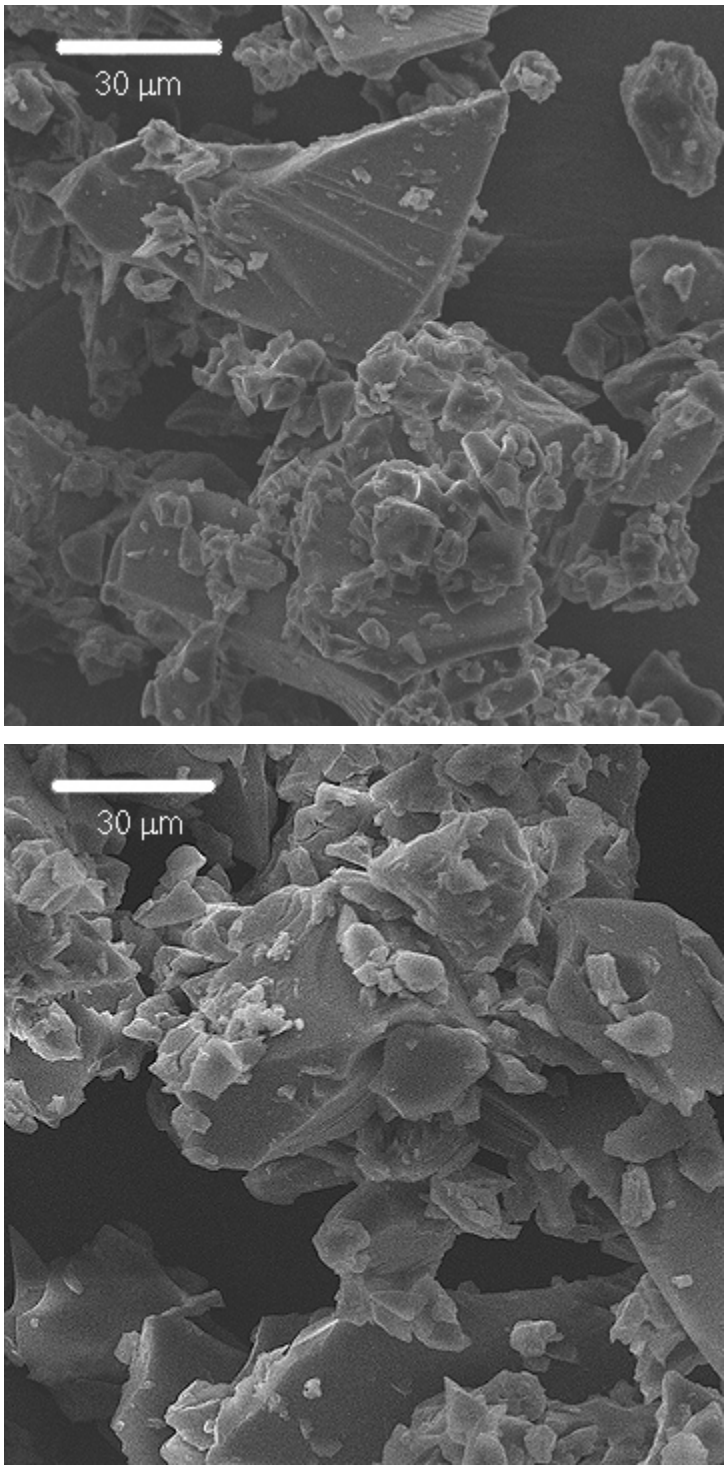

Figure A4.4.3 SEM images of the bioglass with SC/MD = 7:3 and NaCit/SC = 0.1, equilibrated in the atmosphere over saturated LiCl solution (~11%RH).

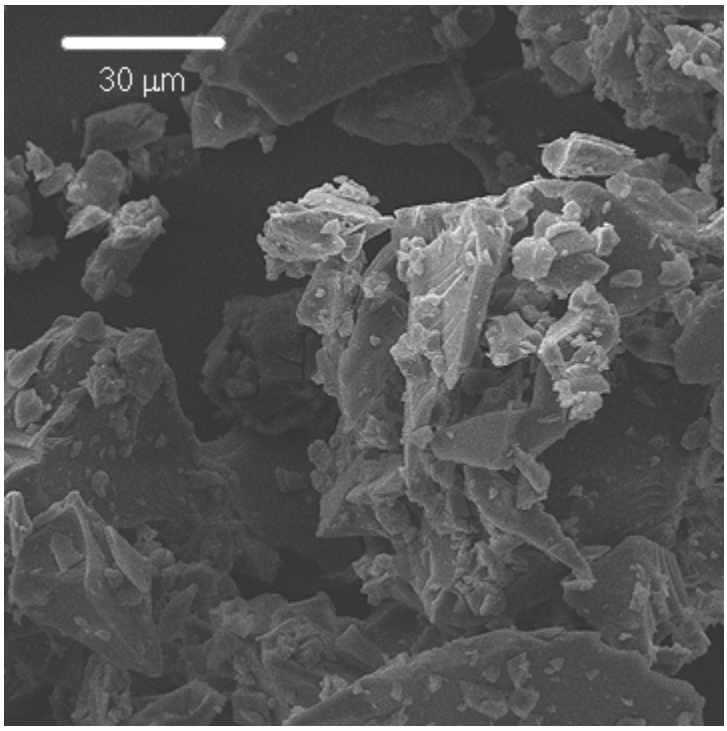

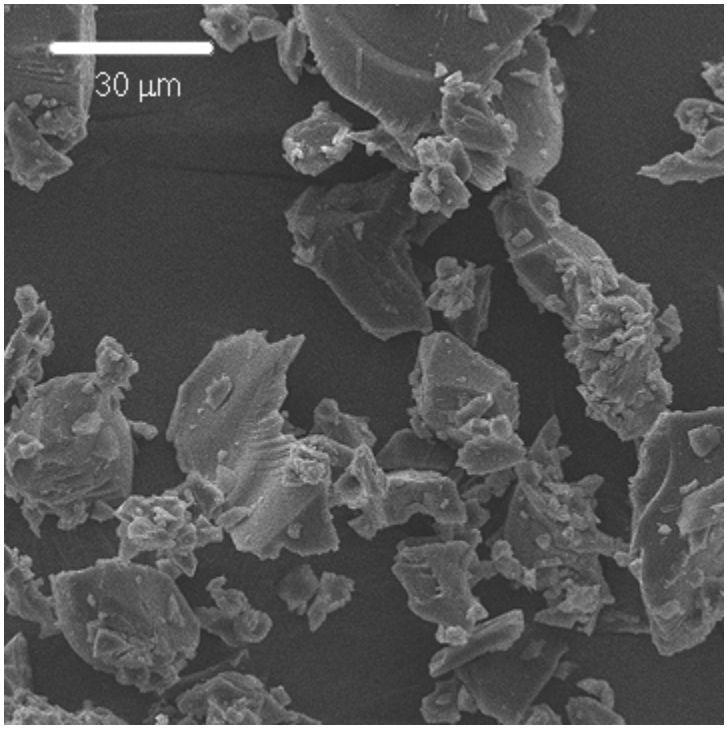

Figure A4.4.4 SEM images of the bioglass with SC/MD = 7:3, and NaCit/SC = 0.1, equilibrated in the atmosphere over P_2O_5 powder (~1%RH).

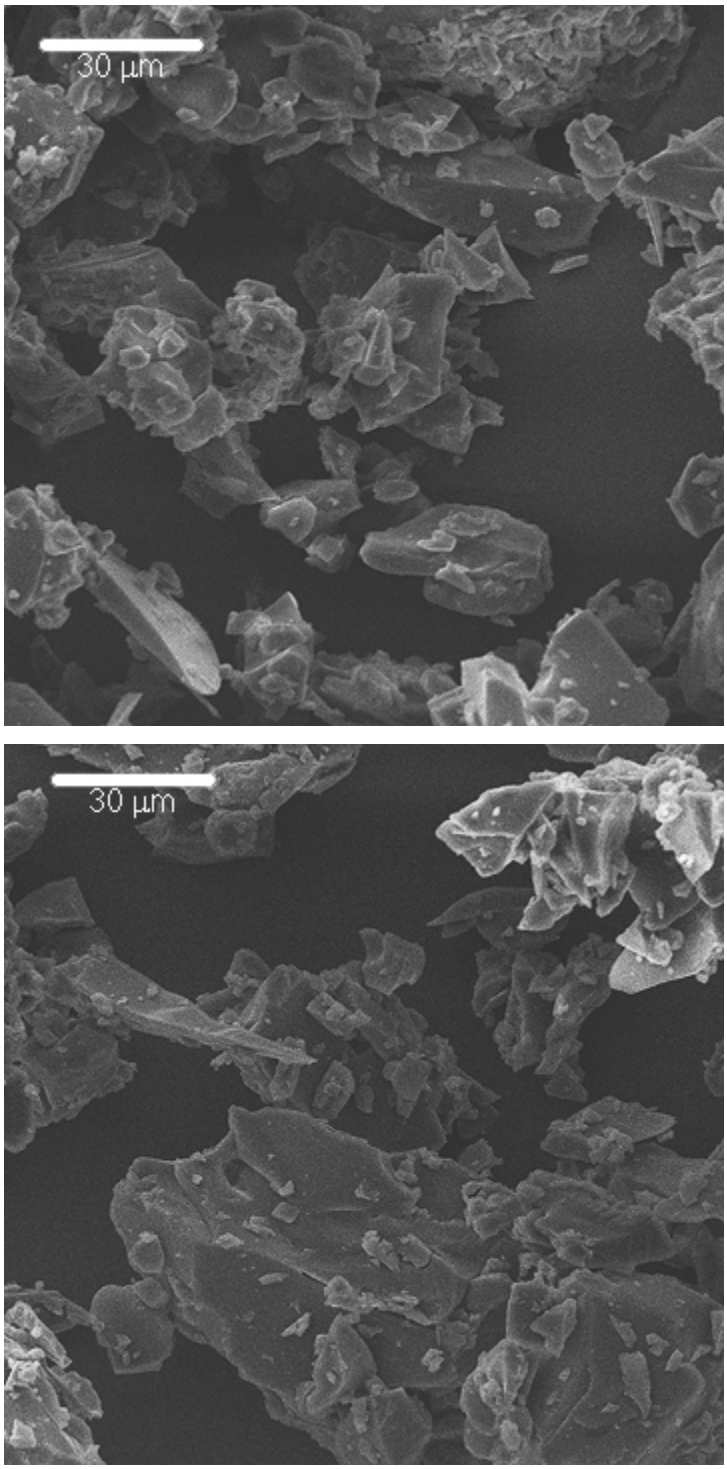

Figure A4.4.5 SEM images of the bioglass with SC/MD = 7:3 and NaCit/SC = 0.2, equilibrated in the atmosphere over saturated LiCl solution (~11%RH).

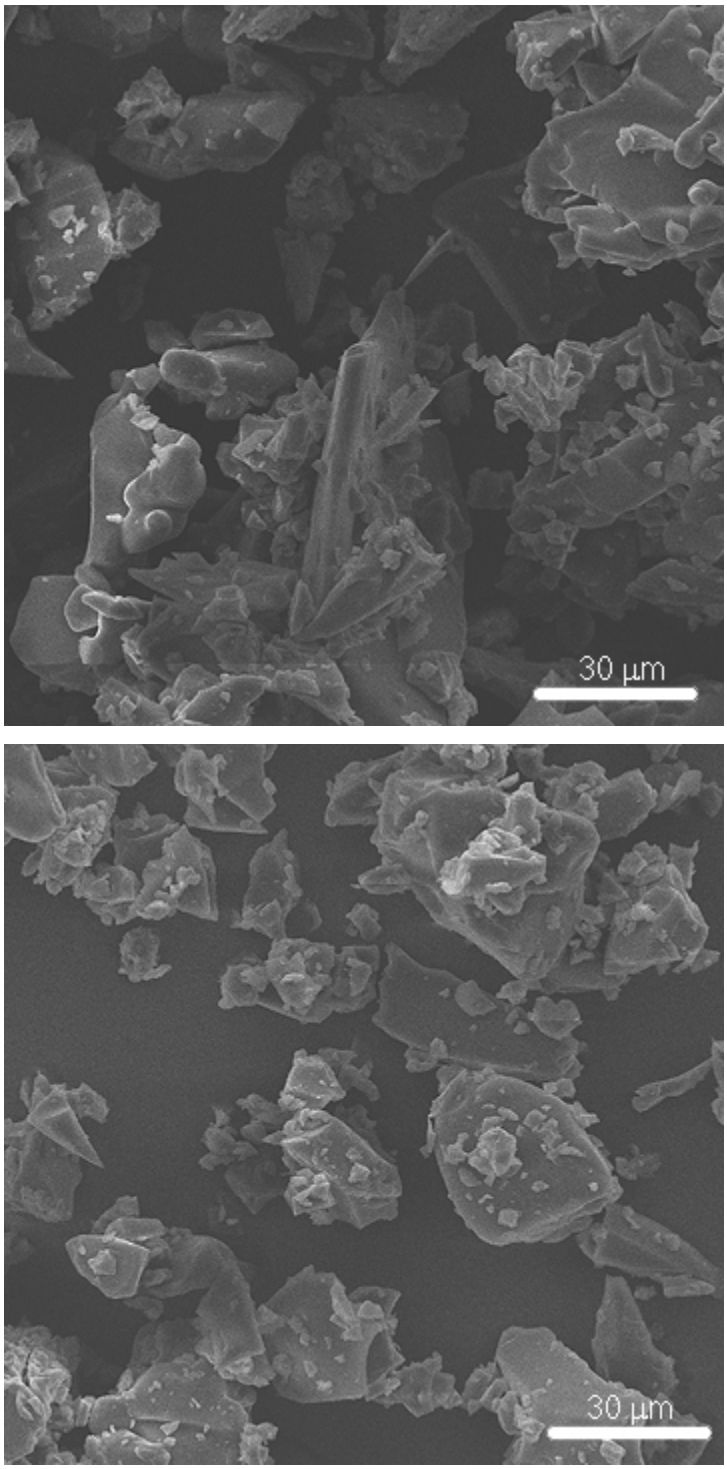

Figure A4.4.6 SEM images of the bioglass with SC/MD = 7:3 and NaCit/SC = 0.2, equilibrated in the atmosphere over P_2O_5 powder (~1%RH).

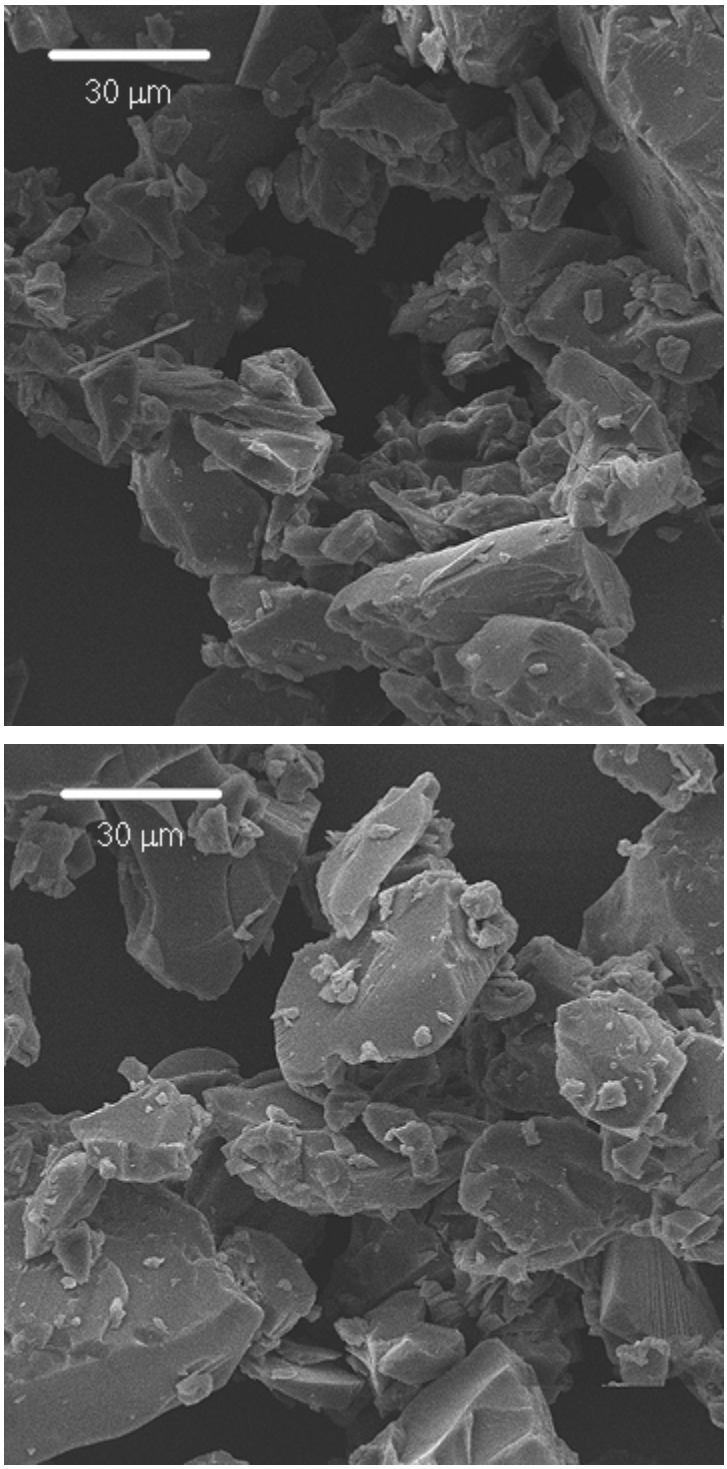

Figure A4.4.7 SEM images of the bioglass with SC/MD = 5:5, without Na citrate, equilibrated in the atmosphere over saturated LiCl solution (~11%RH).

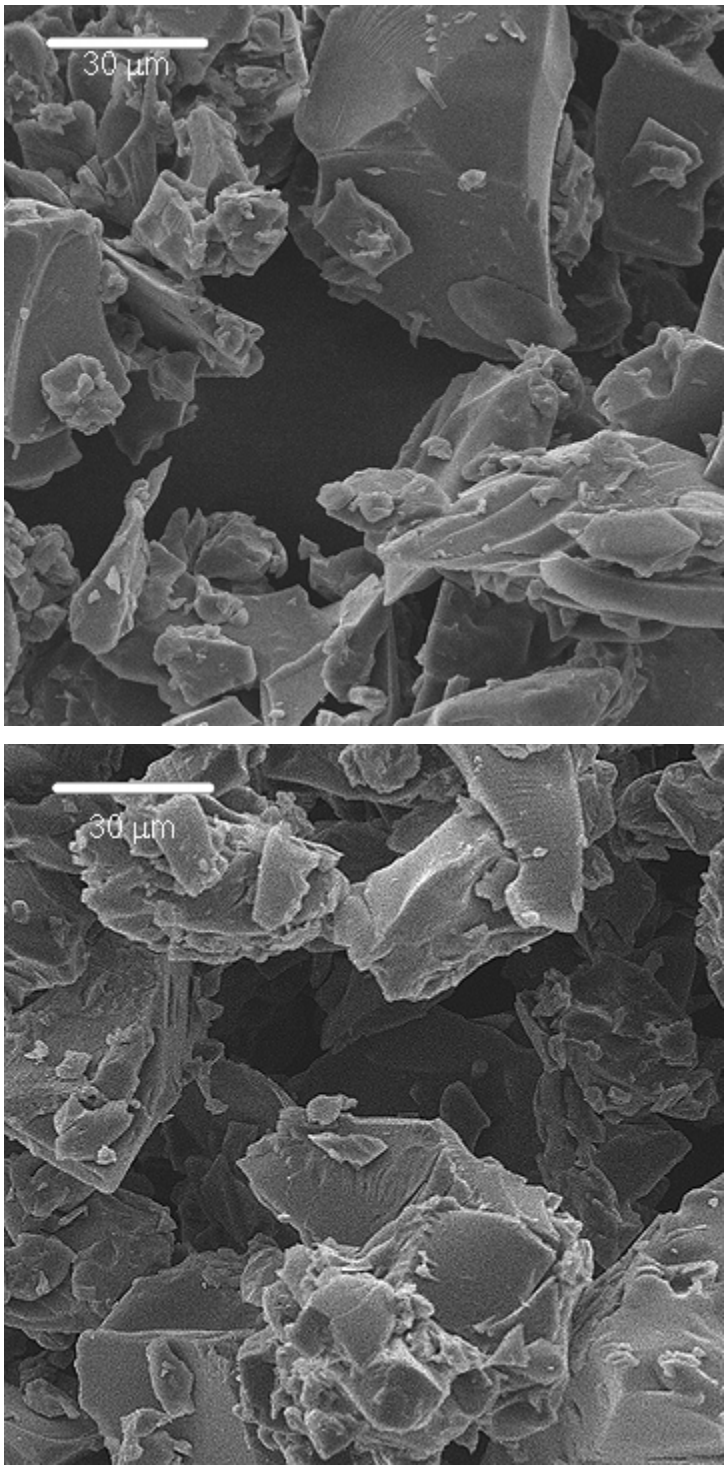

Figure A4.4.8 SEM images of the bioglass with SC/MD = 5:5, without Na citrate, equilibrated in the atmosphere over P_2O_5 powder (~1%RH).

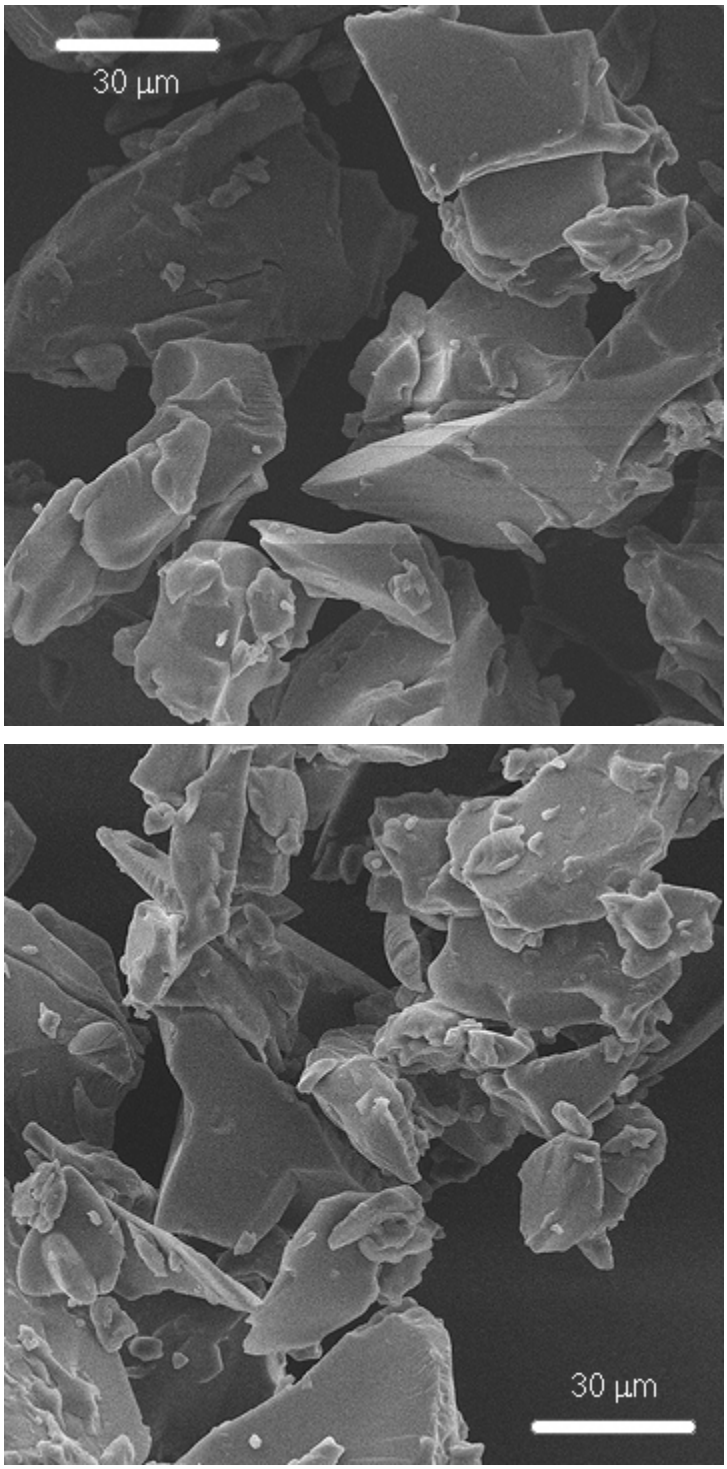

Figure A4.4.9 SEM images of the bioglass with SC/MD = 5:5 and NaCit/SC = 0.1, equilibrated in the atmosphere over saturated LiCl solution (~11%RH).

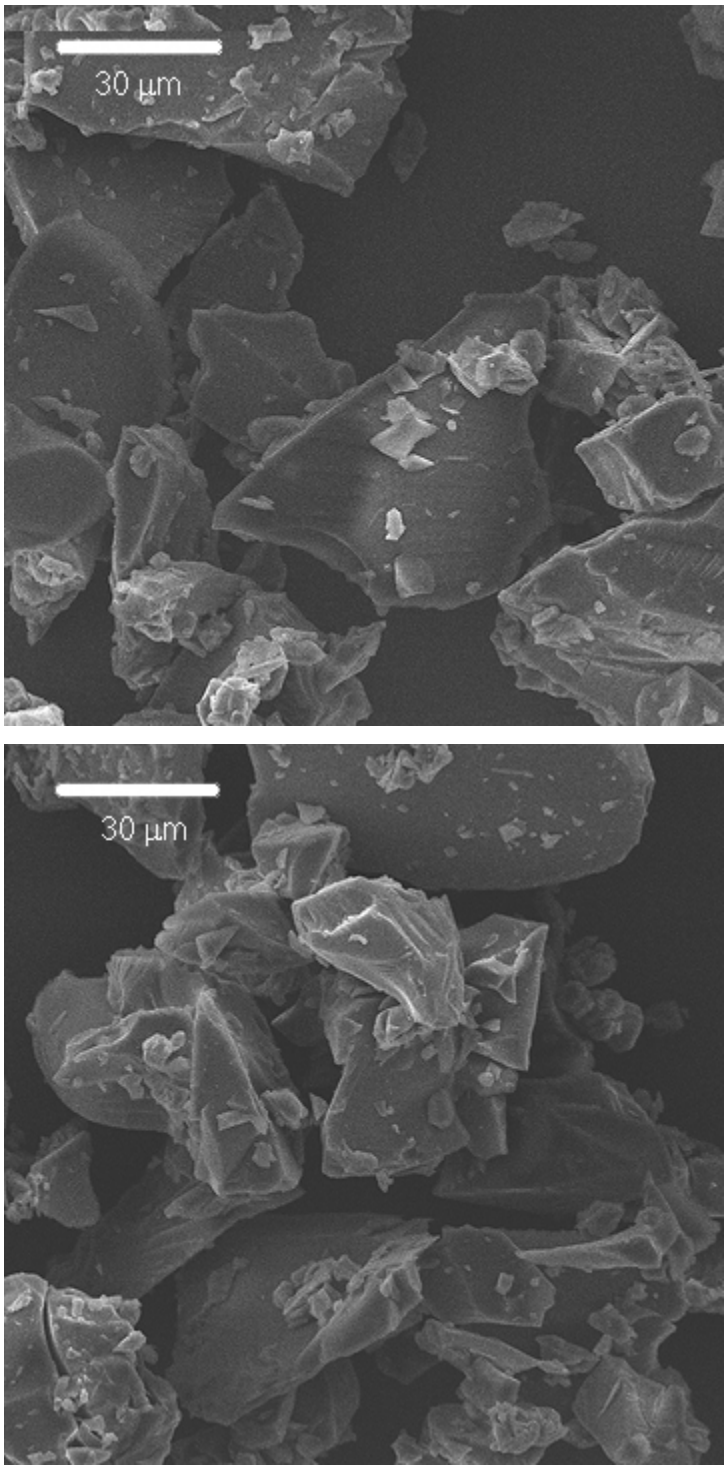

Figure A4.4.10 SEM images of the bioglass with SC/MD = 5:5 and NaCit/SC = 0.1, equilibrated in the atmosphere over P_2O_5 powder (~1%RH).

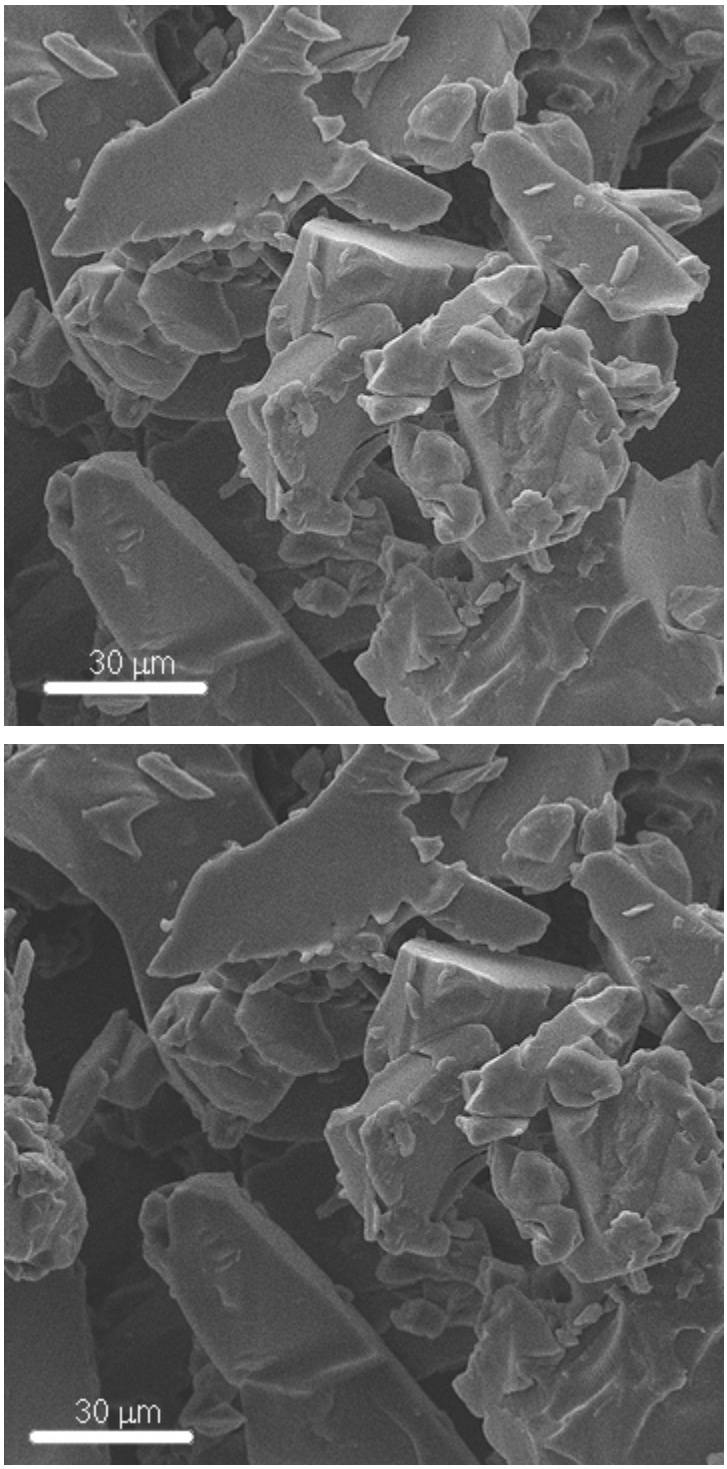

Figure A4.4.11 SEM images of the bioglass with SC/MD = 5:5 and NaCit/SC = 0.2, equilibrated in the atmosphere over saturated LiCl solution (~11%RH)

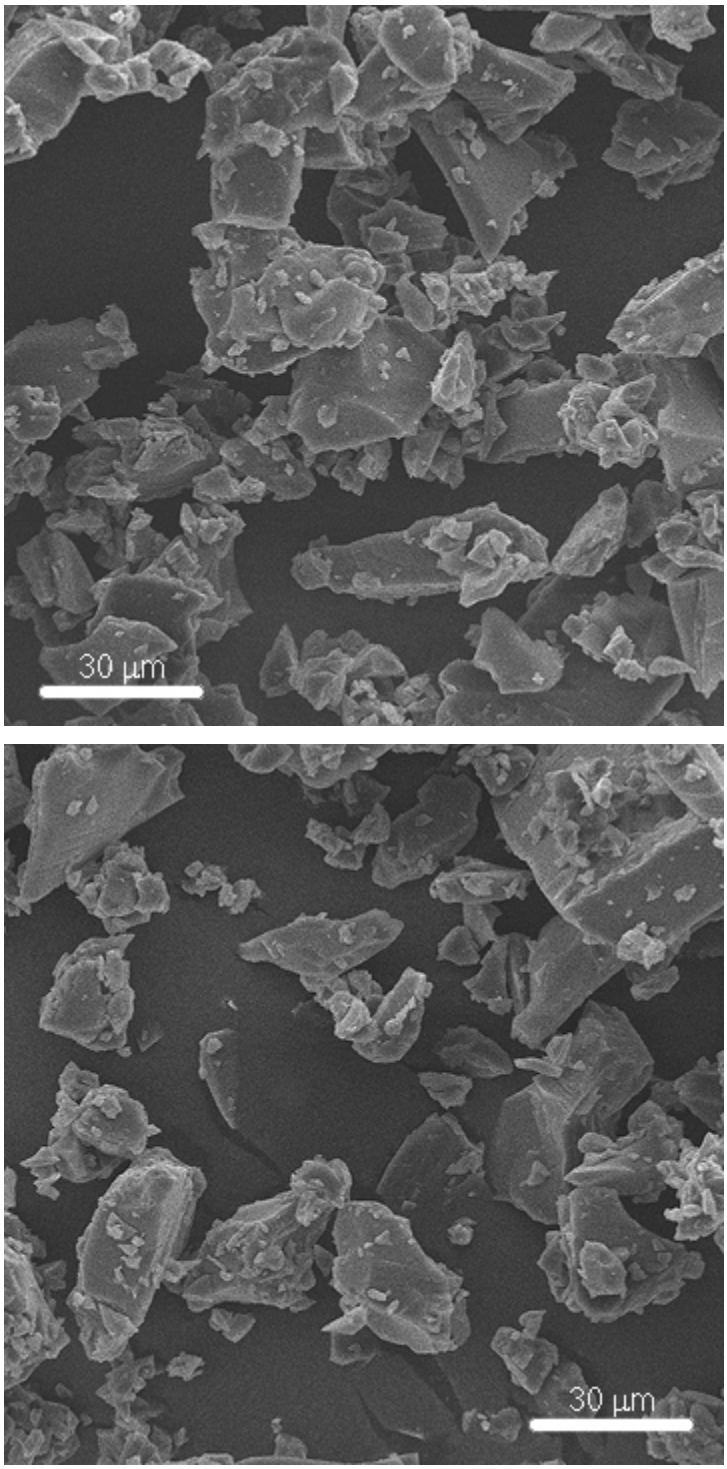

Figure A4.4.12 SEM images of the bioglass with SC/MD = 5:5 and NaCit/SC = 0.2, equilibrated in the atmosphere over P_2O_5 powder (~1%RH).

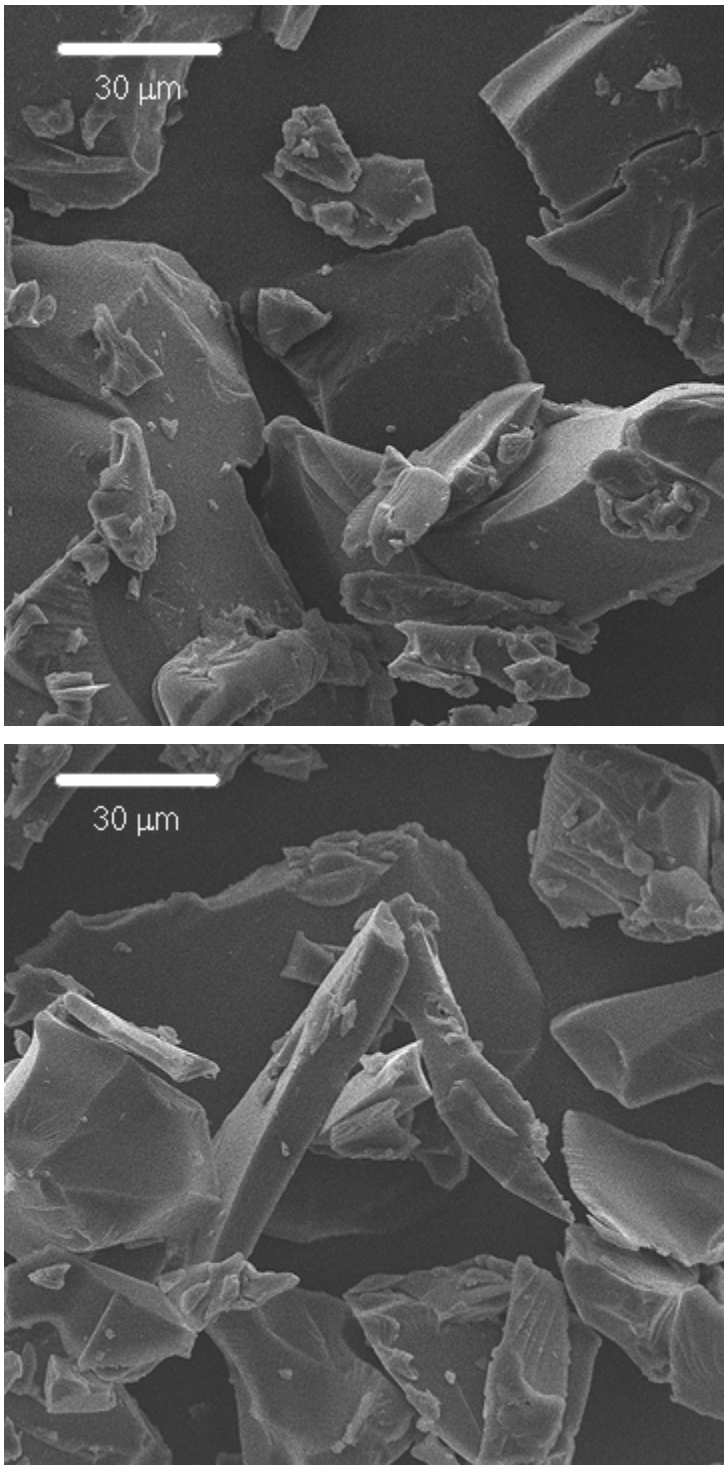

Figure A4.4.13 SEM images of the bioglass with SC/MD = 3:7, without Na citrate, equilibrated in the atmosphere over saturated LiCl solution (~11%RH).

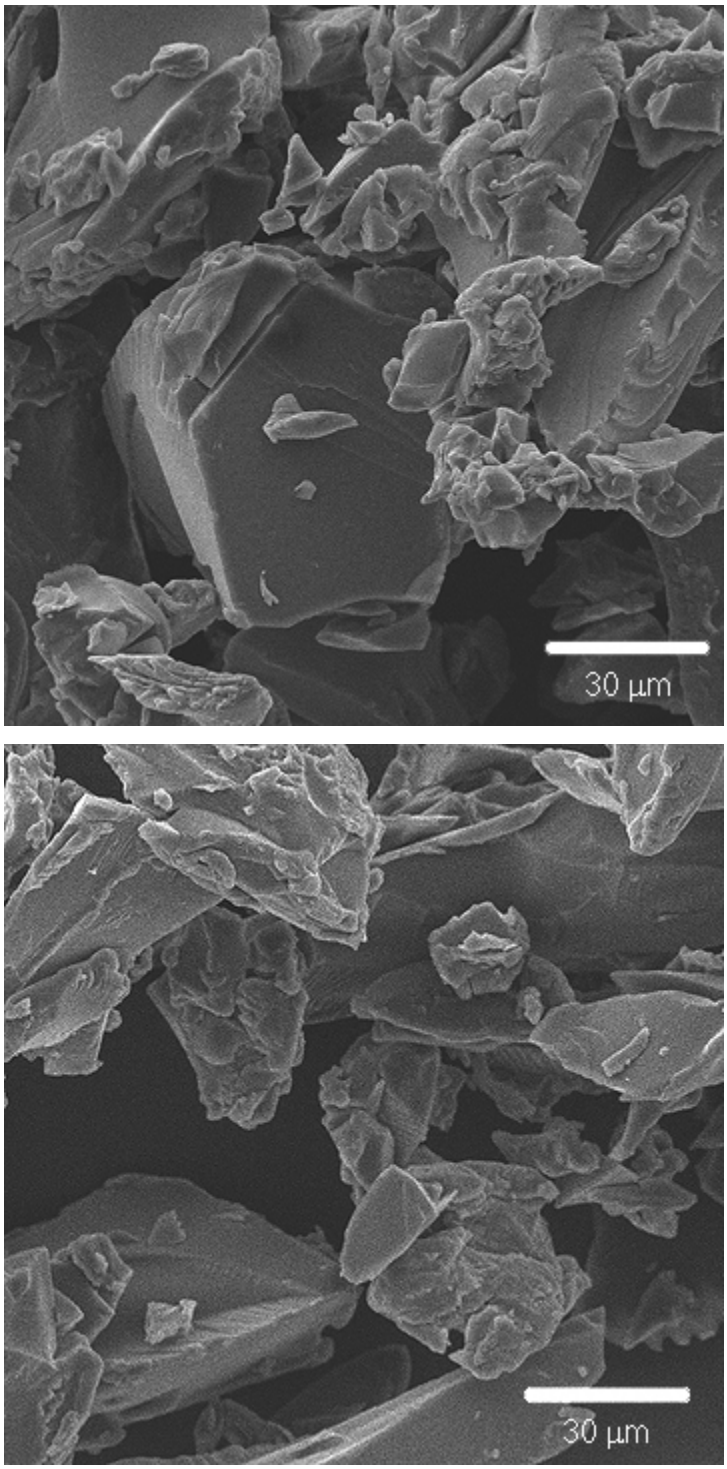

Figure A4.4.14 SEM images of the bioglass with SC/MD = 3:7, without Na citrate, equilibrated in the atmosphere over P_2O_5 powder (~1%RH).

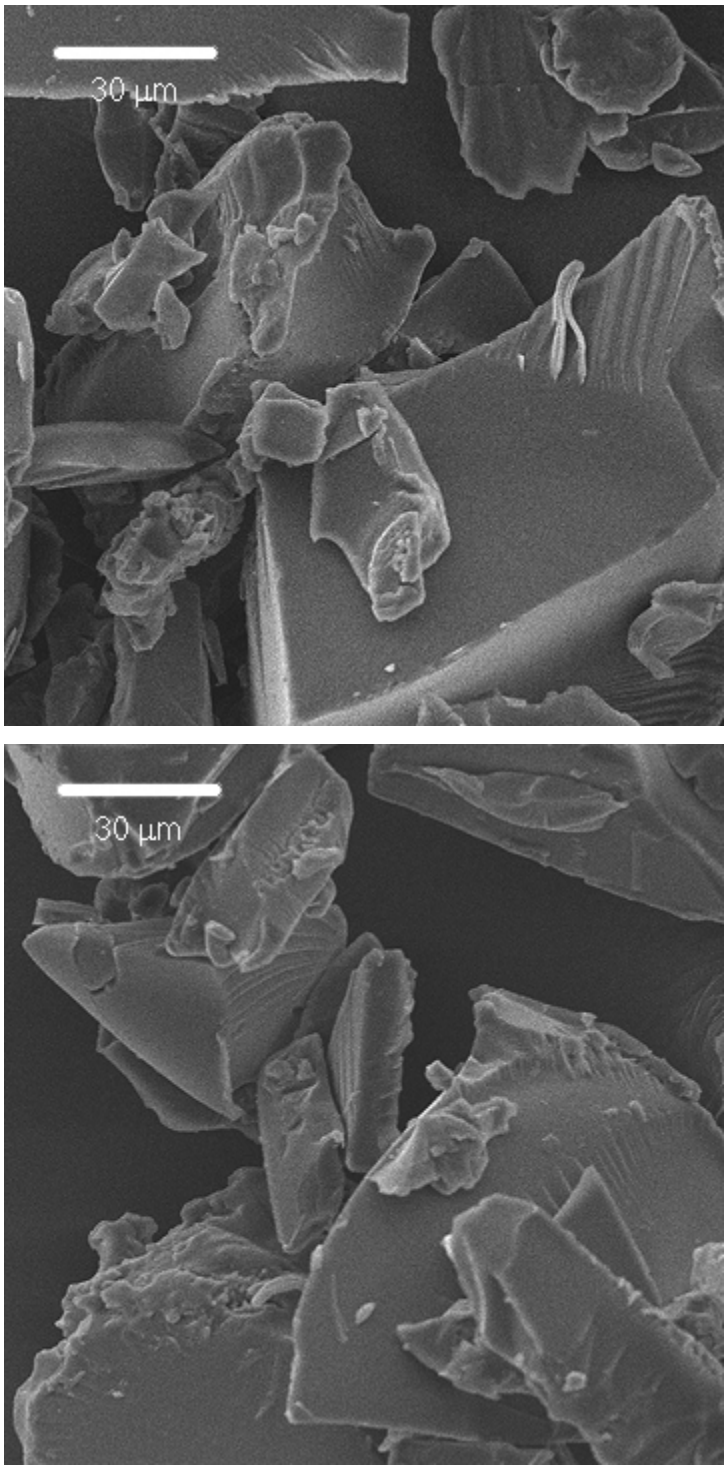

Figure A4.4.15 SEM images of the bioglass with SC/MD = 3:7 and NaCit/SC = 0.1, equilibrated in the atmosphere over saturated LiCl solution (~11%RH).

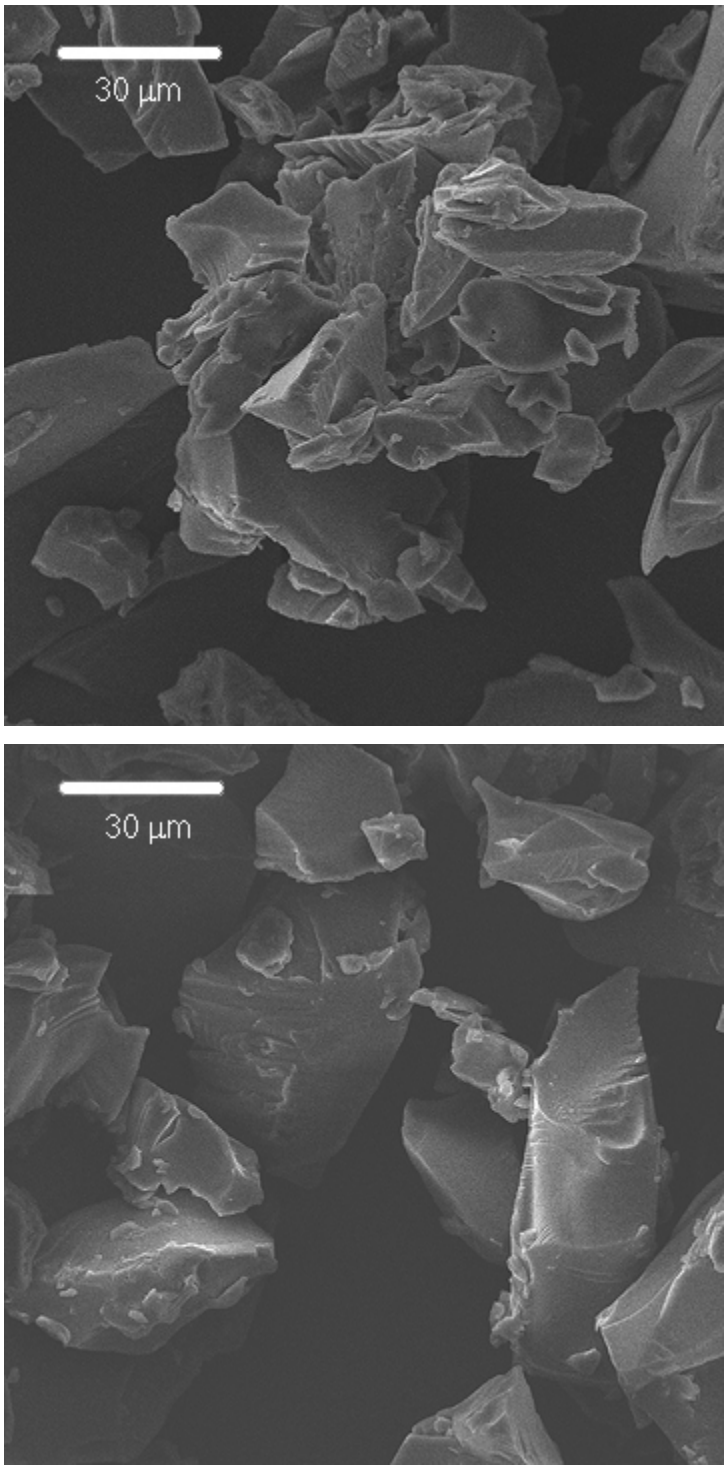

Figure A4.4.16 SEM images of the bioglass with SC/MD = 3:7 and NaCit/SC = 0.1, equilibrated in the atmosphere over P_2O_5 powder (~1%RH).

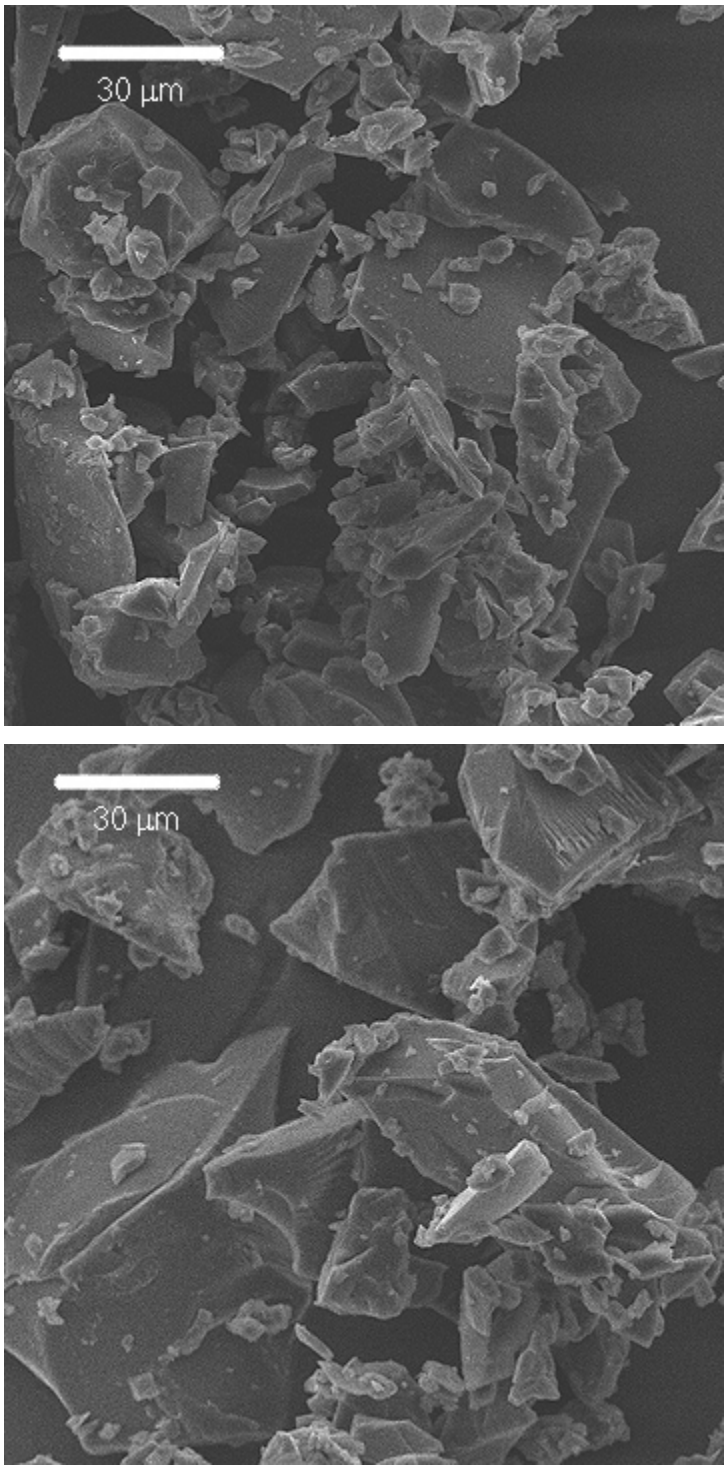

Figure A4.4.17 SEM images of the bioglass with SC/MD = 3:7, NaCit/SC = 0.2, equilibrated in the atmosphere over saturated LiCl solution (~11%RH).

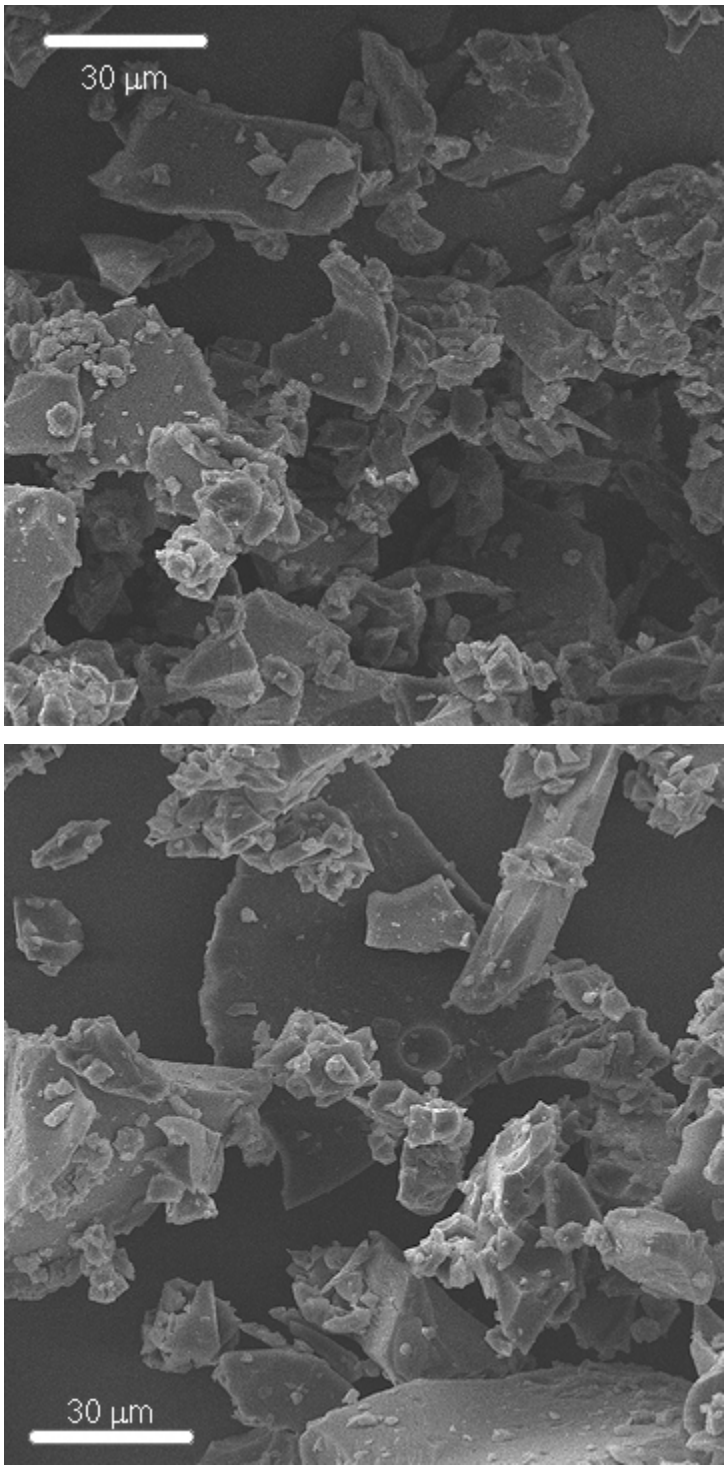

Figure A4.4.18 SEM images of the bioglass with SC/MD = 3:7 and NaCit/SC = 0.2, equilibrated in the atmosphere over P_2O_5 powder (~1%RH).

CHAPTER 5

SUMMARY AND RECOMMENDATIONS

5.1 General Summary

It has been well documented that amorphous sucrose possesses excellent protective property (Taylor and Zografi, 1998; Wolkers et al., 1998; Davidson and Sun, 2001). Though sucrose exhibits rather low $T_{g,}$ particularly when plasticized by just small amount of water, this property could be enhanced by mixing it with large glass-forming molecules such as maltodextrin (Bhandari and Hartel, 2005). Literature has also suggested the application of certain salts to increase T_g (Kets et al., 2004) and reduce molecular mobility of amorphous sucrose (You and Ludescher, 2008a; You and Ludescher, 2008b). Thus, a mixture of sucrose, maltodextrin and salt in amorphous state seems promising in that it might be potentially utilized as an encapsulation matrix for labile compounds. However amorphous materials are thermodynamically non-equilibrium; they evolve towards equilibrium over time. Besides water which usually presents in foods profoundly affects their T_g (Noel et al., 2000; Poirier-Brulez et al., 2006; Shinyashiki et al., 2008). Hence the thorough investigation on characteristics and behaviors of amorphous sucrose-maltodextrin-salt system would be indispensable prior to further applications.

In this study, the effects of sucrose, maltodextrin, Na citrate, and water on the glass transition characteristics, enthalpy relaxation, molecular aspects (in terms of the strength and length of hydrogen bonding), and rheological properties and behaviors of the amorphous sucrose-maltodextrin-Na citrate system were systematically investigated. Samples were formulated with sucrose/maltodextrin mass ratios (SC/MD) of 7:3, 5:5 and 3:7, and Na citrate/sucrose mole ratios (NaCit/SC) of 0, 0.1 and 0.2 at two different levels of moisture content: low (0.27 – 0.35 %wb) and high (2.83 – 4.40 %wb). Samples in the glassy state were studied using the modulated differential scanning calorimetry (MDSC), Fourier-transform infrared spectroscopy (FTIR), and scanning electron microscopy (SEM). The dynamic mechanical spectroscopy was used to evaluate samples in the rubbery-amorphous state (approximately 10 %wb moisture content).

MDSC data showed the dramatic plasticization effect of water in suppressing the T_g and increasing molecular mobility of the system. The T_g value of the system could be enhanced by increasing maltodextrin concentration. The enthalpy relaxation behavior obtained from isothermal aging experiments showed the opposite effects of water and maltodextrin; molecular mobility increased with the increasing moisture content while maltodextrin helped retard matrix mobility. The addition of Na citrate could increase T_g and reduce molecular mobility of the system presumably due to the molecular interaction between Na citrate and sucrose. The results confirm that enthalpy relaxation is a complex molecular process and using a simple expression like KWW equation to describe the relaxation has certain limitations. A large variation in β values reported in literature, including in this study, made a direct comparison of relaxation characteristic time (τ^{KWW}) less meaningful. The time required for 50 % completion of the theoretical possible maximum

enthalpy relaxation at a constant temperature below T_g ($t_{\phi(t)=0.5}$ w) was also used for data analysis. According to the $t_{\phi(t)=0.5}$ value, it was found that maltodextrin helps to improve the matrix stability. A substantial increase in stability could be achieved by slightly lowering the storage temperature. In addition, the $t_{\phi(t)=0.5}$ value suggests that Na citrate tends to interact with sucrose resulting in the less mobility of the bioglass system.

Additional insight about molecular interactions within the bioglass matrix was obtained from FTIR measurements. The system with high maltodextrin concentration formed loosely-packed amorphous structure. The glass matrix with stronger chemical bonds could be obtained when Na citrate was introduced to the sucrose-dominant system; the improved strength was primarily due to intermolecular hydrogen bonding between Na citrate and sucrose. Evidence obtained from SEM images suggested the possible effect of Na citrate to interfere with molecular interaction within the matrix of maltodextrin-dominant system; the interference likely made the system became more brittle.

It was found from rheological measurements that maltodextrin helped increase the rigidity of rubbery amorphous sucrose-maltodextrin system possibly due to the stronger glycosidic linkages in maltodextrin compared to those in sucrose. The system with high sucrose concentration exhibited a viscous-dominant mechanical relaxation. In contrast, elastic-dominant relaxation was observed in the system with high maltodextrin concentration. This difference in mechanical relaxation behavior might arise from different mechanisms of molecular motions. The energy generated by molecular motions of small molecules—sucrose—and the configurational vibrations of segments in large molecules—maltodextrin—may dissipate as heat per cycle of sinusoidal deformation giving rise to the dominance of viscous component (Ngai and Plazek, 1995; Kasapis and Sablani, 2005). Elastic component

may be contributed by the stretching and bending of glycosidic linkages in maltodextrin (Kasapis and Sablani, 2005). In the system with high sucrose concentration, the addition of Na citrate resulted in the downshift in frequency of relaxation process implying the slower molecular mobility. The molecular interactions between Na citrate and sucrose might lead to the formation of large clusters of these molecules that could retard the mechanical relaxation.

In summary, the results of this study confirm the strong plasticization effect of water on amorphous saccharides. Maltodextrin played significant role in T_g, molecular mobility and rigidity of the amorphous sucrose-maltodextrin based system, primarily due to the presence of strong glycosidic linkages. Though FTIR measurements revealed that Na citrate interacts with both maltodextrin and sucrose, the interactions yielded different effects. Na citrate interfered with the molecular interactions of maltodextrin decreasing T_g and possibly weakening the amorphous matrix as evidenced from the SEM images. On the other hand, the hydrogen bonding between Na citrate and sucrose resulted in the higher T_g and the lower molecular mobility as evidenced by the enthalpy and mechanical relaxation. The findings have shown that the stability of sucrose-maltodextrin amorphous system could be improved by the addition of Na citrate.

5.2 Recommendations for Future Research

Most studies on amorphous carbohydrates have been thus far dealing with binary or tertiary systems. Though it is of fundamental important to understand the behaviors of a simple amorphous system, real food products are far more complicated, generally containing many diverse ingredients. Certain molecular interactions between ingredients and glass-

forming molecules might significantly alter properties and behaviors of the system; the enthalpy relaxation, as a result of molecular mobility below T_g, could possibly be even more complex. In the worst case, such modulation may eventually impair the merits of amorphous matrix. Also, of now, theoretical understanding of glass transition phenomenon has not been firmly established. All of these reasons make investigating bioglass systems practically important. Further study may focus on model systems of complexity similar to that of end-use product of interest.

Most common applications of amorphous carbohydrate in literature relate to freeze drying. However the amorphous carbohydrate matrix may be incorporated in extruded foods, which are usually very low in moisture content. Extruded food products are considerably attractive delivery system for nutrients to address nutritional deficiencies. Also processing a food system containing glass-forming carbohydrates with the supercritical fluid extrusion, which requires only mild operating conditions, may allow high retention of flavors and nutrients (Paraman et al., 2012).

5.3 References

Bhandari, B. R. and Hartel, R. W. (2005). Phase transitions during food powder production and powder stability. Encapsulated and Food Powder. C. Onwulata and R. P. Konstance. New York, Marcel Dekker**:** 261-292.

Davidson, P. and Sun, W. Q. (2001). "Effect of sucrose/raffinose mass ratios on the stability of co-lyophilized protein during storage above the Tg." Pharmaceutical Research **18**(4): 474-479.

Kasapis, S. and Sablani, S. S. (2005). "A fundamental approach for the estimation of the mechanical glass transition temperature in gelatin." International Journal of Biological Macromolecules **36**(1-2): 71-78.

Kets, E. P. W., Ijpelaar, P. J., Hoekstra, F. A. and Vromans, H. (2004). "Citrate increases glass transition temperature of vitrified sucrose preparations." Cryobiology **48**(1): 46-54.

Ngai, K. L. and Plazek, D. J. (1995). "Identification of different modes of molecular motion in polymers that cause thermorheological complexity." Rubber Chemistry and Technology **68**(3): 376-434.

Noel, T. R., Parker, R. and Ring, S. G. (2000). "Effect of molecular structure and water content on the dielectric relaxation behaviour of amorphous low molecular weight carbohydrates above and below their glass transition." Carbohydrate Research **329**(4): 839-845.

Paraman, I., Wagner, M. E. and Rizvi, S. S. H. (2012). "Micronutrient and protein-fortified whole grain puffed rice made by supercritical fluid extrusion." Journal of Agricultural and Food Chemistry **60**(44): 11188-11194.

Poirier-Brulez, F., Roudaut, G., Champion, D., Tanguy, M. and Simatos, D. (2006). "Influence of sucrose and water content on molecular mobility in starch-based glasses as assessed through structure and secondary relaxation." Biopolymers **81**(2): 63-73.

Shinyashiki, N., Shinohara, M., Iwata, Y., Goto, T., Oyama, M., Suzuki, S., Yamamoto, W., Yagihara, S., Inoue, T., Oyaizu, S., Yamamoto, S., Ngai, K. L. and Capaccioli, S. (2008). "The glass transition and dielectric secondary relaxation of fructose-water mixtures." The Journal of Physical Chemistry B **112**(48): 15470-15477.

Taylor, L. S. and Zografi, G. (1998). "Sugar-polymer hydrogen bond interactions in lyophilized amorphous mixtures." Journal of Pharmaceutical Sciences **87**(12): 1615-1621.

Wolkers, W. F., Oldenhof, H., Alberda, M. and Hoekstra, F. A. (1998). "A Fourier transform infrared microspectroscopy study of sugar glasses: application to anhydrobiotic higher plant cells." Biochimica et Biophysica Acta (BBA) - General Subjects **1379**(1): 83-96.

You, Y. and Ludescher, R. D. (2008a). "The effect of salts on molecular mobility in amorphous sucrose monitored by erythrosin B phosphorescence." Carbohydrate Research **343**(15): 2641-2649.

You, Y. and Ludescher, R. D. (2008b). "The effect of sodium chloride on molecular mobility in amorphous sucrose detected by phosphorescence from the triplet probe erythrosin B." Carbohydrate Research **343**(2): 350-363.